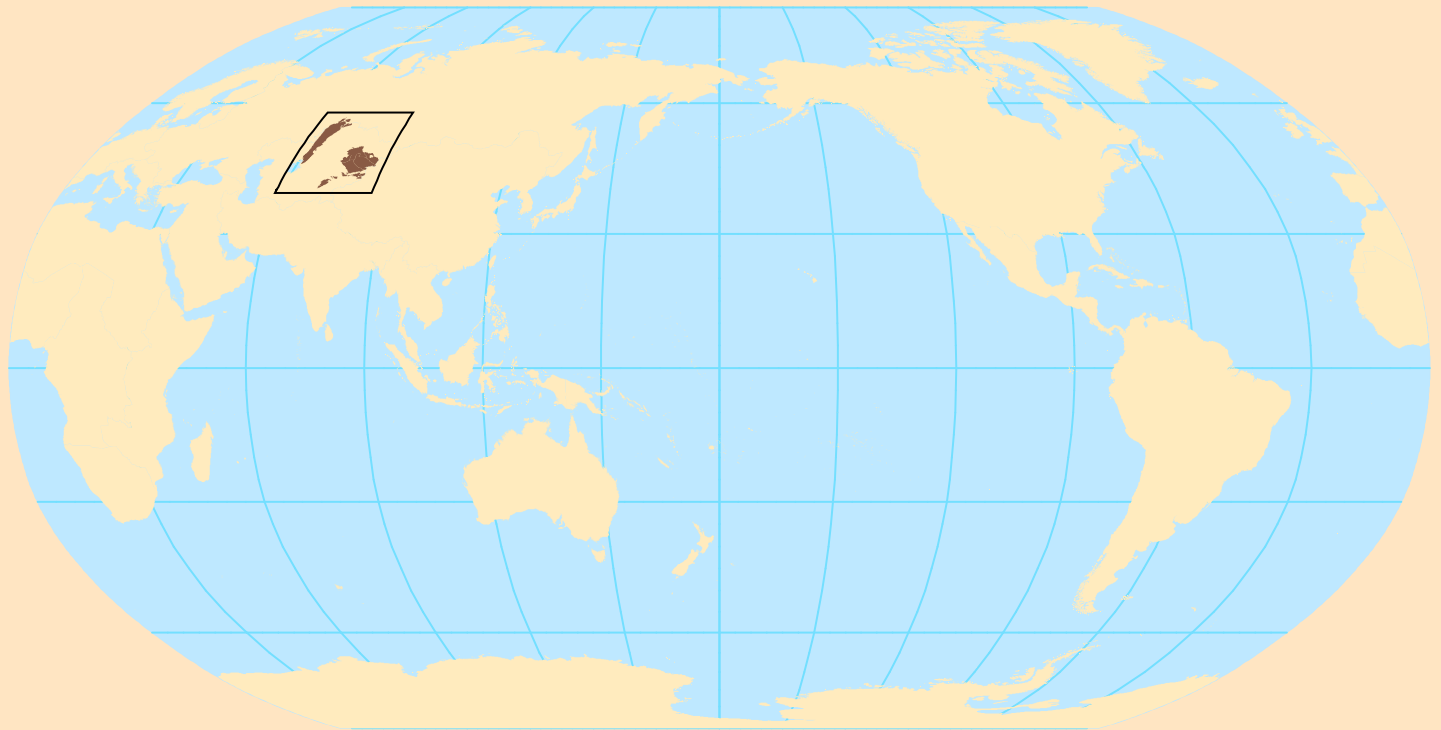


Porphyry Copper Assessment of Western Central Asia



Prepared in cooperation with the Centre for Russian and Central EurAsian Mineral Studies (CERCAMS), Natural History Museum, London

Scientific Investigations Report 2010–5090–N

This page intentionally left blank.

Global Mineral Resource Assessment

Michael L. Zientek, Jane M. Hammarstrom, Kathleen M. Johnson, editors

Porphyry Copper Assessment of Western Central Asia

By Byron R. Berger, John C. Mars, Paul D. Denning, Jeffrey D. Phillips, Jane M. Hammarstrom, Michael L. Zientek, Connie L. Dicken, and Lawrence J. Drew with contributions from Dmitriy Alexeiev, Reimar Seltmann, and Richard J. Herrington

Prepared in cooperation with the Centre for Russian and Central EurAsian Mineral Studies (CERCAMS), Natural History Museum, London

Scientific Investigations Report 2010–5090–N

U.S. Department of the Interior
U.S. Geological Survey

U.S. Department of the Interior
SALLY JEWELL, Secretary

U.S. Geological Survey
Suzette M. Kimball, Acting Director

U.S. Geological Survey, Reston, Virginia: 2014

For more information on the USGS—the Federal source for science about the Earth, its natural and living resources, natural hazards, and the environment, visit <http://www.usgs.gov> or call 1–888–ASK–USGS.

For an overview of USGS information products, including maps, imagery, and publications, visit <http://www.usgs.gov/pubprod>

To order this and other USGS information products, visit <http://store.usgs.gov>

Any use of trade, firm, or product names is for descriptive purposes only and does not imply endorsement by the U.S. Government.

Although this information product, for the most part, is in the public domain, it also may contain copyrighted materials as noted in the text. Permission to reproduce copyrighted items must be secured from the copyright owner.

Suggested citation:

Berger, B.R., Mars, J.C., Denning, P.D., Phillips, J.D., Hammarstrom, J.M., Zientek, M.L., Dicken, C.L., and Drew, L.J., with contributions from Alexeiev, D., Seltmann, R., and Herrington, R.J., 2014, Porphyry copper assessment of western Central Asia: U.S. Geological Survey Scientific Investigations Report 2010–5090–N, 219 p., 8 plates, and spatial data, <http://dx.doi.org/10.3133/sir20105090N>.

ISSN 2328-0328 (online)

Contents

Abstract.....	1
Introduction.....	2
Acknowledgments.....	4
References Cited.....	4
Chapter 1. Tectonic and Geologic Setting of Porphyry Copper Deposits in Western Central Asia.....	7
Introduction.....	7
Tectonic and Geologic Evolution of Western Central Asia and its Porphyry Copper Metallogeny.....	10
Geosyncline Tectonic Theory and Metallogeny.....	11
Historical Overview of Geosyncline Tectonic Theory.....	11
The Geosyncline Construct in Central Asia.....	12
Phanerozoic Evolution of Western Central Asia in a Plate-Tectonic Context.....	18
End Proterozoic.....	19
Lower Paleozoic: Cambrian-Silurian.....	21
The Kokchetav-North Tian Shan Magmatic-Arc Terrane.....	29
Southwestern Region.....	29
Northwestern Region.....	29
Northern Region.....	30
Implications of Mesothermal Gold Metallogeny to Porphyry Copper Deposit Potential in the Middle to Late Ordovician Stepnyak-North Tian Shan Magmatic Arc.....	31
The Bozshakol'-Chingiz Magmatic-Arc Terrane.....	34
Northwestern Segment.....	34
Southeastern Segment.....	34
The Chu-Ili Microcontinental Terrane.....	34
Aktau-Junggar Microcontinental Terrane.....	38
Zhaman-Sarysu Microcontinental Terrane.....	38
Baidalet-Akbastau Magmatic-Arc Terrane.....	38
Mid-Paleozoic: Devonian.....	40
Zharma-Saur Magmatic-Arc Terrane.....	40
Subduction of Junggar-Balkhash Ocean Plate.....	40
Devonian: North.....	47
Upper Paleozoic: Carboniferous-Permian.....	47
West Margin.....	52
Southwest to South Margins.....	54
Southeast to East Margins.....	55
Central Kazakhstan Orocline.....	55
Geologic Constraints on the Timing of Oroclinal Bending.....	55
Porphyry Copper Deposit Metallogeny of Western Central Asia and Potential for Undiscovered Deposits.....	64
Cambrian Period.....	64
Undiscovered Porphyry Copper Deposit Potential of Cambrian Magmatic-Arc Rocks.....	66

Contents—Continued

Ordovician Period	66
Western Kyrgyz Mountains and Kendyktas Ridge	66
Undiscovered Porphyry Copper Deposit Potential of Ordovician	
Magmatic-Arc Rocks	68
Tian Shan Ranges	68
Chu-Ili Ranges	68
Tengiz Basin-Kokchetav Region	68
Eastern Kazakhstan	71
Silurian Period	71
Devonian Period	71
Chatkal-Kurama Region, Uzbekistan	71
Kyrgyz Mountains, Kyrgyzstan-Southern Kazakhstan	72
Chu-Ili Ranges, Southern Kazakhstan	72
Central Kazakhstan: West and Northwest of Lake Balkhash	72
North and Eastern Central Kazakhstan	73
Eastern Kazakhstan	73
Carboniferous Period	75
Southwestern Tectonic Margin	75
Southeastern Tectonic Margin	77
Northeastern Tectonic Margin	77
Central Kazakhstan	79
East Limb of Orocline	79
North Limb of Orocline	79
West Limb of Orocline	81
Challenges to Quantitatively Assessing Undiscovered Porphyry Copper Deposits in	
Western Central Asia	83
Consistency with Descriptive Model	83
Additional Data Needed	86
Acknowledgments	86
References Cited	86
Chapter 2. Alteration Mapping of Potential Porphyry Copper Sites Using Advanced	
Spaceborne Thermal Emission and Reflection Radiometer (ASTER) Data in	
Central Asia	91
Introduction	91
Spectral Characteristics of Porphyry Copper Deposits	91
Data and Methods of Study	95
Logical Operator Mapping Results	98
Physical Characteristics of Potential Porphyry Copper Alteration Sites	105
Summary	110
References Cited	110

Contents—Continued

Chapter 3. Porphyry Copper Assessment of Western Central Asia—Kazakhstan, Uzbekistan, Kyrgyzstan, Tajikistan, and Parts of Russia	113
Introduction	113
Selecting Tracts for Assessment.....	113
Assessment Data.....	113
Known Deposits, Occurrences, and Linked Deposit Types.....	115
Spatial Rules for Grouping Deposits and Occurrences	115
Permissive Tracts	115
Chatkal and Kurama Arc	115
North Tian Shan Magmatic Arc	116
Balkhash-Ili Magmatic Arc.....	116
Valerianov Magmatic Arc, Southern Urals	116
Selection of Grade and Tonnage Models	118
The Assessment Process	118
Estimates of Numbers of Undiscovered Deposits	118
Summary of Probabilistic Assessment Results.....	119
Acknowledgments.....	125
References Cited.....	125
Appendix A. Porphyry Copper Assessment for Tract 142pCu8001, Chatkal and Kurama Ranges—Uzbekistan, Kyrgyzstan, and Tajikistan	128
Appendix B. Porphyry Copper Assessment for Tract 142pCu8002, Ordovician North Tian Shan Magmatic Arc—Kyrgyzstan and Kazakhstan.....	140
Appendix C. Porphyry Copper Assessment for Sub-tract 142pCu8003a, Late Paleozoic Balkhash-Ili Magmatic Arc (East)—Kazakhstan.....	153
Appendix D. Porphyry Copper Assessment for Sub-tract 142pCu8003b, Late Paleozoic Balkhash-Ili Magmatic Arc (North)—Kazakhstan	163
Appendix E. Porphyry Copper Assessment for Sub-tract 142pCu8003c, Late Paleozoic Balkhash-Ili Magmatic Arc (West)—Kazakhstan	173
Appendix F. Porphyry Copper Assessment for Sub-tract 142pCu8003d, Late Paleozoic Balkhash-Ili Magmatic Arc (Northwest)—Kazakhstan and Kyrgyzstan.....	182
Appendix G. Porphyry Copper Assessment for 142pCu8004, Late Paleozoic Central Balkhash-Ili Magmatic Arc—Kazakhstan.....	192
Appendix H. Porphyry Copper Assessment for 142pCu8005, Carboniferous Valerianov Arc—Kazakhstan and Russia	202
Appendix I. Description of Spatial Data Files	213
Appendix J. Assessment Participants.....	214
Appendix K. Geologic Time Charts.....	215

Plates

[Available online only at <http://pubs.usgs.gov/sir/2010/5090/n/>]

1. ASTER Hydrothermal Alteration Map of Northwestern Part of Study Area, Central Kazakhstan, Western Central Asia
2. ASTER Hydrothermal Alteration Map of Northeastern Part of Study Area, Eastern Kazakhstan and Western China, Western Central Asia
3. ASTER Hydrothermal Alteration Map of Southwestern Part of Study Area, Southern Kazakhstan, Uzbekistan, Tajikistan, Kyrgyzstan, and Western China, Western Central Asia
4. ASTER Hydrothermal Alteration Map of Southeastern Part of Study Area, Southeastern Kazakhstan, Kyrgyzstan, and Western China, Western Central Asia
5. ASTER Hydrothermal Alteration Map and Potential Porphyry Copper Sites of Northwestern Part of Study Area, Central Kazakhstan, Western Central Asia
6. ASTER Hydrothermal Alteration Map and Potential Porphyry Copper Sites of Northeastern Part of Study Area, Eastern Kazakhstan and Western China, Western Central Asia
7. ASTER Hydrothermal Alteration Map and Potential Porphyry Copper Sites of Southwestern Part of Study Area, Southern Kazakhstan, Uzbekistan, Tajikistan, Kyrgyzstan, and Western China, Western Central Asia
8. ASTER Hydrothermal Alteration Map and Potential Porphyry Copper Sites of Southeastern Part of Study Area, Southeastern Kazakhstan, Kyrgyzstan, and Western China, Western Central Asia

Figures

1.	Map of the western Central Asia study area	3
1-1.	Map showing location of the western Central Asia assessment area	7
1-2.	Maps showing geographic features and permissive tracts for porphyry copper deposits in western Central Asia	8
1-3.	Map showing the location of selected geosyncline complexes in central Kazakhstan.....	13
1-4.	Maps showing synopsis of model of stages of development of the Chingiz Meganticlinorium.....	14
1-5.	Block diagrams illustrating the tectonic evolution of the Chingiz Meganticlinorium	15
1-6.	Map of the Chingiz Meganticlinorium	16
1-7.	Lithotectonic terrane map of western Central Asia	17
1-8.	Map showing location of the East European, Siberian, and North China cratons and the Turan and Tarim tectonic blocks in relation to the Central Asian Orogenic Belt	19
1-9.	Map showing distribution of Precambrian rocks in western Central Asia.....	20
1-10.	Map of Cambrian stratified rocks in the western Central Asia study area	22
1-11.	Map of Cambrian intrusive rocks in the western Central Asia study area	23
1-12.	Map of Ordovician stratified rocks in the western Central Asia study area	24
1-13.	Map of Ordovician intrusive rocks in the western Central Asia study area.....	25
1-14.	Map of Silurian stratified rocks in the western Central Asia study area	26
1-15.	Map of Silurian intrusive rocks in the western Central Asia study area	27
1-16.	Modified lithotectonic terrane map.....	28

Figures—Continued

1-17.	Map of the distribution of mesothermal (orogenic) low-sulfide quartz-gold vein deposits and occurrences in the vicinity of the city of Kokchetav in north-central Kazakhstan.....	32
1-18.	Map of the distribution of mesothermal (orogenic) vein deposits and occurrences and major faults in the western Kyrgyz Range and vicinity, Kyrgyzstan and Kazakhstan.....	33
1-19.	Map showing the location of the Bozshakol' porphyry copper deposit.....	35
1-20.	Map showing the distribution of likely magmatic-arc rocks of Cambrian and Ordovician age in eastern Kazakhstan	36
1-21.	Map showing location of the Dzhair-Naiman shear zone, major faults, tectonic lineaments, and selected mineral deposits.....	37
1-22.	Modified lithotectonic terrane map of western Central Asia	39
1-23.	Map of Cambrian and Ordovician magmatic-arc rocks in northeastern Kazakhstan	41
1-24.	Map of Devonian stratified rocks in the western Central Asia study area.....	42
1-25.	Map of Devonian intrusive rocks in the western Central Asia study area	43
1-26.	Map of Upper Devonian (D ₃) rocks in the western Central Asia study area	44
1-27.	Map of selected geographic and tectonic features and mineral deposits in western Central Asia.....	45
1-28.	Map showing the principal tectonic units in the Tian Shan ranges of Kyrgyzstan and southern Kazakhstan.....	46
1-29.	Map of Carboniferous stratified rock types in the western Central Asia study area	48
1-30.	Map of Carboniferous intrusive rock types in the western Central Asia study area	49
1-31.	Map of Upper Carboniferous (C ₃) stratified rocks in the western Central Asia study area	50
1-32.	Map of Late Carboniferous to Early Permian rock types of western Central Asia.....	51
1-33.	Reduced-to-pole aeromagnetic map of the southeastern Ural Mountains and adjacent amalgamated Kazakhstan continent, Russia and Kazakhstan.....	53
1-34.	Map showing locations of Irtysh and Chara Fault Zones in eastern Kazakhstan	56
1-35.	Map of the North Balkhash region	57
1-36.	Map of the Spasski fold and thrust belt in north-central Kazakhstan	58
1-37.	Reduced-to-pole aeromagnetic map of the Spasski fold and thrust belt region, north-central Kazakhstan.....	60
1-38.	Generalized map of fold and fault structures within the hinge zone of the Devonian orocline in west-central Kazakhstan.....	61
1-39.	Maps showing the relation of mineralization to northwest-striking strike-slip faulting in the North Balkhash region	62
1-40.	Location map of the Cambrian Bozshakol' porphyry copper deposit.....	65
1-41.	Location map of Ordovician porphyry copper deposits and occurrences in the Kyrgyz Range and on Kandyktas Ridge.....	67
1-42.	Location map of Ordovician porphyry copper occurrences in northern-most Central Kazakhstan.....	70
1-43.	Location map of Devonian porphyry copper deposits and occurrences in the North Balkhash region	74
1-44.	Location map of Carboniferous porphyry copper deposits and occurrences in the Trans-Urals zone in Russia and adjacent Kazakhstan	76
1-45.	Location map of Carboniferous porphyry copper deposits and occurrences in the Chatkal-Kurama region of eastern Uzbekistan.....	78

Figures—Continued

1-46.	Location map of Carboniferous porphyry copper deposits and occurrences in Central Kazakhstan.....	80
1-47.	Geologic map from Seltmann and others (2009) for an area to the west of Lake Balkhash in central Kazakhstan.....	82
1-48.	Geologic maps of a part of the Kyrgyz Range in northwest Kyrgyzstan and adjacent Kazakhstan in the western Tian Shan ranges.....	84
2-1.	Location map of permissive porphyry copper tracts in western Central Asia.....	92
2-2.	Advanced Spaceborne Thermal Emission and Reflection Radiometer (ASTER) alteration map coverage of permissive tracts in western Central Asia.....	93
2-3.	Illustrated deposit model of a porphyry copper deposit.....	94
2-4.	Visible near-infrared (VNIR) through the short-wave infrared (SWIR) reflectance sample spectra and Advanced Spaceborne Thermal Emission and Reflection Radiometer (ASTER) resampled sample spectra of kaolinite, alunite, and sericite.....	96
2-5.	Thermal infrared radiation (TIR) emissivity sample spectra and Advanced Spaceborne Thermal Emission and Reflection Radiometer (ASTER) resampled sample spectra of opal and quartz.....	97
2-6.	Visible near-infrared (VNIR) through the short-wave infrared (SWIR) reflectance sample spectra and Advanced Spaceborne Thermal Emission and Reflection Radiometer (ASTER) resampled sample spectra of green vegetation.....	99
2-7.	Sample spectra from Cuprite and Gemfield, Nevada.....	100
2-8.	Comparison of mapped altered rock and Advanced Spaceborne Thermal Emission and Reflection Radiometer (ASTER) data for Cuprite, Nevada.....	102
2-9.	Alteration map of the Kounrad mine, Kazakhstan.....	103
2-10.	Advanced Spaceborne Thermal Emission and Reflection Radiometer (ASTER) alteration map of the Kounrad mine, Kazakhstan.....	104
2-11.	Advanced Spaceborne Thermal Emission and Reflection Radiometer (ASTER) alteration map and potential porphyry copper sites of the Kounrad mine area in Kazakhstan.....	106
2-12.	Permissive tracts and potential deposit sites in western Central Asia.....	107
2-13.	Advanced Spaceborne Thermal Emission and Reflection Radiometer (ASTER) low-pass filter map compiled from argillic and phyllic alteration in the Kounrad mine area in Kazakhstan used to determine alteration density of each potential porphyry copper site in western Central Asia.....	108
2-14.	Landsat TM false color composite image of southeastern Kazakhstan and permissive tracts.....	109
3-1.	Map of permissive tracts for porphyry copper deposits in western Central Asia.....	114
3-2.	Distribution of log tonnage and log grade data for porphyry copper deposits in western Central Asia.....	120
3-3.	Bar charts comparing identified copper and gold resources in known deposits with mean and median estimates of undiscovered resources for each tract in western Central Asia.....	122
A1.	Map showing the location, known deposits, and significant prospects and occurrences for tract 142pCu8001, Chatkal and Kurama Ranges—Uzbekistan, Kyrgyzstan, and Tajikistan.....	129
A2.	Map of permissive Carboniferous volcanic and volcanoclastic rocks and intrusive rocks in tract 142pCu8001, Chatkal and Kurama Ranges—Uzbekistan, Kyrgyzstan, and Tajikistan, on a digital elevation base.....	130

Figures—Continued

A3.	Cumulative frequency plot showing the results of Monte Carlo computer simulation of undiscovered resources, tract 142pCu8001, Chatkal and Kurama Ranges—Uzbekistan, Kyrgyzstan, and Tajikistan	137
B1.	Map showing the location, known deposits, and significant prospects and occurrences for permissive tract 142pCu8002, Ordovician North Tian Shan magmatic arc—Kyrgyzstan and Kazakhstan.....	141
B2.	Map showing the distribution of permissive Ordovician volcanic and volcanoclastic and intrusive rocks in tract 142pCu8002, Ordovician North Tian Shan magmatic arc—Kyrgyzstan and Kazakhstan, on a digital elevation base.....	143
B3.	Cumulative frequency plot showing the results of Monte Carlo computer simulation of undiscovered resources in permissive tract 142pCu8002, Ordovician North Tian Shan magmatic arc—Kyrgyzstan and Kazakhstan.....	150
C1.	Map showing the location, known deposits, and significant prospects and occurrences for sub-tract 142pCu8003a, Late Paleozoic Balkhash-Ili magmatic arc (east)—Kazakhstan.....	154
C2.	Map of permissive Carboniferous volcanic and volcanoclastic rocks and intrusive rocks in sub-tract 142pCu8003a, Late Paleozoic Balkhash-Ili magmatic arc (east)—Kazakhstan, on a digital elevation base.....	155
C3.	Cumulative frequency plot showing the results of Monte Carlo computer simulation of undiscovered resources in sub-tract 142pCu8003a, Late Paleozoic Balkhash-Ili magmatic arc (east)—Kazakhstan.....	160
D1.	Map showing the location, known deposits, and significant prospects and occurrences for permissive sub-tract 142pCu8003b, Late Paleozoic Balkhash-Ili magmatic arc (north)—Kazakhstan	164
D2.	Map of permissive Carboniferous volcanic and volcanoclastic rocks and intrusive rocks in sub-tract 142pCu8003b, Late Paleozoic Balkhash-Ili magmatic arc (north)—Kazakhstan, on a digital elevation base	166
D3.	Cumulative frequency plot showing the results of Monte Carlo computer simulation of undiscovered resources in sub-tract 142pCu8003b, Late Paleozoic Balkhash-Ili magmatic arc (north)—Kazakhstan.	171
E1.	Map showing the location, known deposits, and significant occurrences for sub-tract 142pCu8003c, Late Paleozoic Balkhash-Ili magmatic arc (west)—Kazakhstan.....	174
E2.	Map of permissive Carboniferous volcanic and volcanoclastic rocks and intrusive rocks in sub-tract 142pCu8003c, Late Paleozoic Balkhash-Ili magmatic arc (west)—Kazakhstan, on a digital elevation base.....	176
E3.	Cumulative frequency plot showing the results of Monte Carlo computer simulation of undiscovered resources in sub-tract 142pCu8003c, Late Paleozoic Balkhash-Ili magmatic arc (west)—Kazakhstan	180
F1.	Map showing the location, known deposits, and significant occurrences for sub-tract 142pCu8003d, Late Paleozoic Balkhash-Ili magmatic arc (northwest)—Kazakhstan and Kyrgyzstan.....	183
F2.	Map showing the distribution of permissive Carboniferous volcanic and volcanoclastic rocks and intrusive rocks in sub-tract 142pCu8003d, Late Paleozoic Balkhash-Ili magmatic arc (northwest)—Kazakhstan and Kyrgyzstan, on a digital elevation base	185
F3.	Cumulative frequency plot showing the results of Monte Carlo computer simulation of undiscovered resources for sub-tract 142pCu8003d, Late Paleozoic Balkhash-Ili magmatic arc (northwest)—Kazakhstan and Kyrgyzstan.....	189

Figures—Continued

G1.	Map showing the location, known deposits, and significant occurrences for tract 142pCu8004, Late Paleozoic Central Balkhash-Ili magmatic arc—Kazakhstan.....	193
G2.	Map showing distribution of permissive Carboniferous volcanic and volcanoclastic rocks and intrusive rocks in tract 142pCu8004, Late Paleozoic Central Balkhash-Ili magmatic arc—Kazakhstan, on a digital elevation base	195
G3.	Map showing the extent of permissive rock, Quaternary and Neogene cover, copper deposits and occurrences from Seltmann and others (2009), and ASTER alteration sites in tract 142pCu8004, Late Paleozoic Central Balkhash-Ili magmatic arc—Kazakhstan	196
G4.	Cumulative frequency plot showing the results of Monte Carlo computer simulation of undiscovered resources in tract 142pCu8004, Late Paleozoic Central Balkhash-Ili magmatic arc—Kazakhstan	200
H1.	Map showing the location, known deposits, and significant occurrences for tract 142pCu8005, Carboniferous Valerianov Arc—Kazakhstan and Russia	203
H2.	Distribution of permissive Carboniferous volcanic and volcanoclastic rocks and intrusive rocks in part of tract 142pCu8005, Carboniferous Valerianov Arc—Kazakhstan and Russia, on a digital elevation base	205
H3.	Cumulative frequency plot showing the results of Monte Carlo computer simulation of undiscovered resources, tract 142pCu8005, Carboniferous Valerianov Arc—Kazakhstan and Russia.....	210
K1.	Geologic time correlations among Series-Epoch map symbols and durations for Phanerozoic Eons as used in Russia	217
K2.	Geologic time correlations among Series-Epoch map symbols and durations for Precambrian Eons as used in Russia	218

Tables

2-1.	Physical characteristics and locations of potential porphyry copper sites, western Central Asia [available online only as a .xlsx file at http://pubs.usgs.gov/sir/2010/5090/n/]	
3-1.	Porphyry copper deposits of western Central Asia	116
3-2.	Permissive tracts for porphyry copper deposits in western Central Asia	117
3-3.	Statistical test results, porphyry copper assessment, western Central Asia	119
3-4.	Summary of estimates of numbers of undiscovered deposits, numbers of known deposits, tract areas, and deposit densities for the porphyry copper assessment of western Central Asia.....	124
3-5.	Summary of simulations of undiscovered resources in porphyry copper deposits and comparison with identified copper and gold resources in porphyry copper deposits within each permissive tract, western Central Asia	124
A1.	Summary of selected resource assessment results for tract 142pCu8001, Chatkal and Kurama Ranges—Uzbekistan, Kyrgyzstan, and Tajikistan	128
A2.	Porphyry copper deposits in tract 142pCu8001, Chatkal and Kurama Ranges—Uzbekistan, Kyrgyzstan, and Tajikistan	133
A3.	Significant occurrences of porphyry copper and copper-gold skarn in tract 142pCu8001, Chatkal and Kurama Ranges—Uzbekistan, Kyrgyzstan, and Tajikistan.....	135
A4.	Principal sources of information used in the assessment of tract 142pCu8001, Chatkal and Kurama Ranges—Kazakhstan, Uzbekistan, Kyrgyzstan, and Tajikistan.....	135

Tables—Continued

A5. Undiscovered deposit estimates, deposit numbers, tract area, and deposit density for tract 142pCu8001, Chatkal and Kurama Ranges—Uzbekistan, Kyrgyzstan, and Tajikistan.....	136
A6. Results of Monte Carlo simulations of undiscovered resources for tract 142pCu8001, Chatkal and Kurama Ranges—Uzbekistan, Kyrgyzstan, and Tajikistan.....	136
B1. Summary of selected resource assessment results for tract 142pCu8002, Ordovician North Tian Shan magmatic arc—Kyrgyzstan and Kazakhstan	140
B2. Identified porphyry copper resources in tract 142pCu8002, Ordovician North Tian Shan magmatic arc—Kyrgyzstan and Kazakhstan	147
B3. Significant occurrences of porphyry-style and copper skarn prospects in tract 142pCu8002, Ordovician North Tian Shan magmatic arc—Kyrgyzstan and Kazakhstan.....	147
B4. Principal sources of information used for the delineation of tract 142pCu8002, Ordovician North Tian Shan magmatic arc—Kyrgyzstan and Kazakhstan	149
B5. Undiscovered deposit estimates, deposit numbers, tract area, and deposit density for tract 142pCu8002, Ordovician North Tian Shan magmatic arc—Kyrgyzstan and Kazakhstan	149
B6. Results of Monte Carlo simulations of undiscovered resources for tract 142pCu8002, Ordovician North Tian Shan magmatic arc—Kyrgyzstan and Kazakhstan.....	149
C1. Summary of selected resource assessment results for sub-tract 142pCu8003a, Late Paleozoic Balkhash-Ili magmatic arc (east)—Kazakhstan	153
C2. Porphyry copper deposits in sub-tract 142pCu8003a, Late Paleozoic Balkhash-Ili magmatic arc (east)—Kazakhstan	157
C3. Significant porphyry copper occurrences in sub-tract 142pCu8003a, Late Paleozoic Balkhash-Ili magmatic arc (east)—Kazakhstan.....	158
C4. Principal sources of information used for delineation of sub-tract 142pCu8003a, Late Paleozoic Balkhash-Ili magmatic arc (east)—Kazakhstan	159
C5. Undiscovered deposit estimates, deposit numbers, tract area, and deposit density for tract 142pCu8003a, Late Paleozoic Balkhash-Ili magmatic arc (east)—Kazakhstan.....	159
C6. Results of Monte Carlo simulations of undiscovered resources for sub-tract 142pCu8003a, Late Paleozoic Balkhash-Ili magmatic arc (east)—Kazakhstan	160
D1. Summary of selected resource assessment results for sub-tract 142pCu8003b, Late Paleozoic Balkhash-Ili magmatic arc (north)—Kazakhstan.....	163
D2. Porphyry copper deposits in sub-tract 142pCu8003b, Late Paleozoic Balkhash-Ili magmatic arc (north)—Kazakhstan	167
D3. Significant occurrences of porphyry-style copper in sub-tract 142pCu8003b, Late Paleozoic Balkhash-Ili magmatic arc (north)—Kazakhstan.....	168
D4. Principal sources of information used for the delineation of sub-tract 142pCu8003b, Late Paleozoic Balkhash-Ili magmatic arc (north)—Kazakhstan	169
D5. Undiscovered deposit estimates, deposit numbers, tract area, and deposit density for sub-tract 142pCu8003b, Late Paleozoic Balkhash-Ili magmatic arc (north)—Kazakhstan	170
D6. Results of Monte Carlo simulations of undiscovered resources for sub-tract 142pCu8003b, Late Paleozoic Balkhash-Ili magmatic arc (north)—Kazakhstan	170
E1. Summary of selected resource assessment results for sub-tract 142pCu8003c, Late Paleozoic Balkhash-Ili magmatic arc (west)—Kazakhstan	173

Tables—Continued

E2.	Porphyry copper deposits in sub-tract 142pCu8003c, Late Paleozoic Balkhash-Ili magmatic arc (west)—Kazakhstan	175
E3.	Significant porphyry copper occurrences in sub-tract 142pCu8003c Late Paleozoic Balkhash-Ili magmatic arc (west)—Kazakhstan	178
E4.	Principal sources of information used for the delineation of sub-tract 142pCu8003c, Late Paleozoic Balkhash-Ili magmatic arc (west)—Kazakhstan	179
E5.	Undiscovered deposit estimates, deposit numbers, area, and deposit density for sub-tract 142pCu8003c, Late Paleozoic Balkhash-Ili magmatic arc (west)—Kazakhstan	179
E6.	Results of Monte Carlo simulations of undiscovered resources for sub-tract 142pCu8003c, Late Paleozoic Balkhash-Ili magmatic arc (west)—Kazakhstan	180
F1.	Summary of selected resource assessment results for sub-tract 142pCu8003d, Late Paleozoic Balkhash-Ili magmatic arc (northwest)—Kazakhstan and Kyrgyzstan.....	182
F2.	Porphyry copper deposits in sub-tract 142pCu8003d, Late Paleozoic Balkhash-Ili magmatic arc (northwest)—Kazakhstan and Kyrgyzstan	186
F3.	Significant porphyry copper occurrences in sub-tract 142pCu8003d, Late Paleozoic Balkhash-Ili magmatic arc (northwest)—Kazakhstan and Kyrgyzstan	187
F4.	Principal sources of information used for the delineation of sub-tract 142pCu8003d, Late Paleozoic Balkhash-Ili magmatic arc (northwest)—Kazakhstan and Kyrgyzstan.....	188
F5.	Undiscovered deposit estimates, deposit numbers, sub-tract area, and deposit density for sub-tract 142pCu8003d, Late Paleozoic Balkhash-Ili magmatic arc (northwest)—Kazakhstan and Kyrgyzstan.....	188
F6.	Results of Monte Carlo simulations of undiscovered resources for sub-tract 142pCu8003d, Late Paleozoic Balkhash-Ili magmatic arc (northwest)—Kazakhstan and Kyrgyzstan	189
G1.	Summary of selected resource assessment results for tract 142pCu8004, Late Paleozoic Central Balkhash-Ili magmatic arc—Kazakhstan.....	192
G2.	Principal sources of information used to delineate tract 142pCu8004, Late Paleozoic Central Balkhash-Ili magmatic arc—Kazakhstan.....	198
G3.	Undiscovered deposit estimates, deposit numbers, tract area, and deposit density for tract 142pCu8004, Late Paleozoic Central Balkhash-Ili magmatic arc—Kazakhstan	199
G4.	Results of Monte Carlo simulations of undiscovered resources for tract 142pCu8004, Late Paleozoic Central Balkhash-Ili magmatic arc—Kazakhstan.....	199
H1.	Summary of selected resource assessment results for tract 142pCu8005, Carboniferous Valerianov Arc—Kazakhstan and Russia	202
H2.	Porphyry copper deposits in tract 142pCu8005, Carboniferous Valerianov Arc—Kazakhstan and Russia	207
H3.	Significant porphyry copper-related occurrences in tract 142pCu8005, Carboniferous Valerianov Arc—Kazakhstan and Russia	207
H4.	Principal sources of information used for tract 142pCu8005, Carboniferous Valerianov Arc—Kazakhstan and Russia	208
H5.	Undiscovered deposit estimates, deposit numbers, tract area, and deposit density for tract 142pCu8005, Carboniferous Valerianov Arc—Kazakhstan and Russia.....	209
H6.	Results of Monte Carlo simulations of undiscovered resources for tract 142pCu8005, Carboniferous Valerianov Arc—Kazakhstan and Russia	209

Conversion Factors, Abbreviations and Acronymns, and Chemical Symbols

Conversion Factors

Inch/Pound to SI

Multiply	By	To obtain
Length		
foot (ft)	0.3048	meter (m)
mile (mi)	1.609	kilometer (km)
yard (yd)	0.9144	meter (m)
Area		
acre	0.4047	hectare (ha)
acre	0.004047	square kilometer (km ²)
square mile (mi ²)	259.0	hectare (ha)
square mile (mi ²)	2.590	square kilometer (km ²)
Mass		
ounce, troy (troy oz)	31.015	gram (g)
ounce, troy (troy oz)	0.0000311	megagram (Mg)
ton, short (2,000 lb)	0.9072	megagram (Mg)

SI to Inch/Pound

Multiply	By	To obtain
Length		
meter (m)	3.281	foot (ft)
kilometer (km)	0.6214	mile (mi)
meter (m)	1.094	yard (yd)
Area		
hectare (ha)	2.471	acre
hectare (ha)	0.003861	square mile (mi ²)
square kilometer (km ²)	247.1	acre
square kilometer (km ²)	0.3861	square mile (mi ²)
Mass		
gram (g)	0.03527	ounce, avoirdupois (oz)
megagram (Mg)	1.102	ton, short (2,000 lb)
megagram (Mg)	0.9842	ton, long (2,240 lb)

Other conversions used in this report

metric ton (t)	1	megagram (Mg)
troy ounce per short ton	34.2857	gram per metric ton (g/t)
percent (%)	10,000	parts per million (ppm) or grams per metric ton (g/t)
percent metal	0.01 × metal grade, percent × ore tonnage, metric tons	metric tons of metal

Acronyms and Abbreviations Used

ANOVA	analysis of variance
ASTER	Advanced Spaceborne Thermal Emission and Reflection Radiometer
GIS	geographic information system
lat	latitude
long	longitude
Ma	million of years before the present
Mt	million metric tons
SSIB	small-scale digital international boundaries
t	metric ton
USGS	U.S. Geological Survey

Chemical Symbols Used

Ag	silver
Au	gold
Bi	bismuth
Co	cobalt
Cu	copper
Fe	iron
In	indium
Mo	molybdenum
Pb	lead
Re	rhenium
Se	selenium
Te	tellurium

Porphyry Copper Assessment of Western Central Asia

By Byron R. Berger¹, John C. Mars², Paul D. Denning¹, Jeffrey D. Phillips¹, Jane M. Hammarstrom², Michael L. Zientek³, Connie L. Dicken², and Lawrence J. Drew² with contributions from Dmitriy Alexeiev⁴, Reimar Seltmann⁵, and Richard J. Herrington⁵

Abstract

The U.S. Geological Survey conducted an assessment of resources associated with porphyry copper deposits in the western Central Asia countries of Kyrgyzstan, Uzbekistan, Kazakhstan, and Tajikistan and the southern Urals of Kazakhstan and Russia as part of a global mineral resource assessment. The purpose of the study was to (1) delineate permissive areas (tracts) for undiscovered porphyry copper deposits; (2) compile a database of known porphyry copper deposits and significant prospects; (3) where data permit, estimate numbers of undiscovered deposits within those permissive tracts; and (4) provide probabilistic estimates the amounts of copper (Cu), molybdenum (Mo), gold (Au), and silver (Ag) that could be contained in those undiscovered deposits.

Western Central Asia, a region diverse in its geologic complexity, is situated north of the Tarim and North China tectonic blocks and sandwiched between the East European and Siberian cratons. The Ural Mountains form the western margin of the region; the southern margin is formed by the high-standing ranges that make up the Tian Shan mountain range in the border regions of Kazakhstan, Kyrgyzstan, and western China, where the effects of collisional tectonics are well displayed. The tectonic collage that makes up the core of western Central Asia is perhaps the geologically least understood part of the region. There is broad agreement that the early Paleozoic is made up of tectonically juxtaposed blocks that vary from Precambrian-cored microcontinents to magmatic arc and related complexes to subduction-related accretionary complexes. The rudiments of an incipient, contiguous single Kazakhstan block were formed by the end of the Silurian. In the middle to late Paleozoic, the block was unconformably superposed by two large, nested magmatic-arc belts, one Devonian, the other Carboniferous. Both magmatic-arc complexes were folded into a horseshoe-shaped, southeast-opening orocline in response to the final collisions of the various surrounding cratonic blocks with the Kazakhstan block. Additional deformation in the upper Cenozoic derived from the collision of India and China

significantly redistributed fragments of the various mosaicked blocks, particularly in the central and southern parts of the western Central Asian region. Porphyry copper deposits are associated with many of the magmatic-arc fragments and belts throughout the geologically complex region, and economically important deposits are found in arc sequences of all Paleozoic Periods. The economically most productive arcs are Carboniferous.

The assessment includes a discussion of the tectonic and geologic setting of porphyry copper deposits in western Central Asia (chapter 1), an application of remote sensing data for hydrothermal alteration mapping as a tool for porphyry copper assessment in the region (chapter 2), and a probabilistic assessment of undiscovered porphyry copper resources in four areas that represent Ordovician and Late Paleozoic (Carboniferous-Permian) magmatic arcs (chapter 3). The principal litho-tectonic terrane concept used to delineate permissive tracts was that of a magmatic arc that formed in the subduction boundary zone above a subducting plate. Eight permissive tracts are delineated on the basis of mapped and inferred subsurface distributions of igneous rocks assigned to magmatic arcs of specified age ranges that define areas where the occurrence of porphyry copper deposits within 1 kilometer of the Earth's surface is possible. These tracts range in area from about 8,000 to 200,000 square kilometers and host 18 known porphyry copper deposits that contain about 54 million metric tons of copper. Available data included geologic maps, the distribution of significant porphyry copper occurrences and potentially related deposit types, the distribution of hydrothermal alteration patterns that are consistent with porphyry copper mineralization, and information on possible subsurface extensions of permissive rocks. On the basis of analyses of these data, the assessment team estimated a mean of 25 undiscovered porphyry copper deposits for the study area. Estimates of numbers of undiscovered deposits were combined with grade and tonnage models in a Monte Carlo simulation to yield a mean estimate of 95 million metric tons of copper in undiscovered porphyry copper deposits; this represents about twice the amount of identified porphyry copper resources (54 million metric tons).

¹U.S. Geological Survey, Denver, Colorado, United States.

²U.S. Geological Survey, Reston, Virginia, United States.

³U.S. Geological Survey, Spokane, Washington, United States.

⁴Russian Academy of Science, Moscow, Russia.

⁵Centre for Russian and Central EurAsian Mineral Studies (CERCAMS), Natural History Museum, London, United Kingdom.

Detailed descriptions of each permissive tract, including the rationales for delineation and assessment, are given in appendixes, along with a geographic information system (GIS) that includes permissive tract boundaries, point locations of known porphyry copper deposits and significant occurrences, and hydrothermal alteration data based on analysis of remote sensing data.

Introduction

By Jane M. Hammarstrom

Porphyry copper deposits represent large volumes of hydrothermally altered granitoid porphyry rocks that contain relatively evenly distributed copper sulfide minerals as disseminations, veins, and breccias (Berger and others, 2008; John and others, 2010). Deposits typically have large tonnages (greater than 100 million metric tons), low to moderate grade (average about 0.44 percent copper), and are amenable to large-scale, open-pit mining. Porphyry copper deposits provide approximately 60 percent of the world copper supply and may contain significant resources of gold, silver, and molybdenum (Singer, 1995). Central Asia hosts a number of significant porphyry copper deposits of Paleozoic age, including the supergiant Almalyk deposit in Uzbekistan, which contains about 24 million metric tons of copper, and world class deposits at Aktogai-Aidarly, Bozshakol', and Kounrad in Kazakhstan (fig. 1), each of which contains 2 million metric tons or more copper (Singer, 1995; Singer and others, 2008).

An assessment of undiscovered resources in porphyry copper deposits in western Central Asia was done as part of a global mineral resource assessment. The study area includes the countries of Kyrgyzstan, Uzbekistan, Kazakhstan, and Tajikistan and the southern Urals of Kazakhstan and Russia (fig. 1). Contiguous geologic areas in eastern Kazakhstan and China are assessed in a report on the Central Asia Orogenic Belt. The purpose of the study was to (1) delineate permissive areas (tracts) for undiscovered porphyry copper deposits at a scale of 1:1,000,000; (2) compile a database of known porphyry copper deposits and significant prospects; (3) where data permit, estimate numbers of undiscovered deposits within those permissive tracts, and (4) provide probabilistic estimates the amounts of copper (Cu), molybdenum (Mo), gold (Au), and silver (Ag) that could be contained in those undiscovered deposits.

The assessment followed the three-part form of mineral resource assessment described by Singer (1993; 2007a,b) and Singer and Menzie (2010). In applying the three-part form of mineral resource assessment, geographic areas (permissive tracts) are delineated on the basis of available

data on geologic features typically associated with the type of deposit under consideration, as reported in descriptive mineral deposit models. The amount of metal contained in undiscovered deposits is estimated by using grade and tonnage models combined with probabilistic estimates of numbers of undiscovered deposits. Estimates of numbers of undiscovered deposits are made at different confidence levels using a variety of estimation strategies. The estimates express the degree of belief that some fixed but unknown number of deposits exists within the tract; these estimates represent a measure of the favorability of the permissive tract and uncertainty about what may exist (Singer, 2007a). Monte Carlo methods (Root and others, 1992) are used to combine estimates of numbers of undiscovered deposit from three-part assessments with grade and tonnage models to produce a probabilistic estimate of undiscovered resources. For the probabilistic assessment of undiscovered resources associated with porphyry copper deposits in selected areas western Central Asia, the global porphyry copper grade and tonnage models of Singer and others (2008) were combined with estimates of numbers of undiscovered deposits in the EMINERS computer program (Bawiec and Spanski, 2012; Duval, 2012).

The starting point for the assessment is the delineation of the permissive tracts. A permissive tract is defined as the surface projection of a volume of rock in which the geology permits the existence of a mineral deposit of a specified type. Permissive tracts for porphyry copper deposits are based on subduction-related magmatic arcs or postsubduction or postcollisional magmatic belts of a given age range. Permissive tracts for porphyry copper deposits are geographic areas that include volcanic and intrusive rocks of a specified age range that typically can be related to a particular tectonic setting (magmatic arc). Therefore, tracts are based primarily on geologic map units that define the magmatic arc or belt and any data that allows the tract to be projected under shallow (less than 1 kilometer, km) cover. A depth limit of 1 km to the top of a porphyry system was adopted for the global porphyry copper assessment.

The geologic complexity of western Central Asia posed challenges for assessment relative to assessments of younger, less-deformed magmatic arc terrains in other parts of the world. This complexity necessitated a detailed analysis of the geodynamic framework of the region as a prelude to defining the permissive tracts for assessment. Chapter 1 of this report provides the tectonic, geologic, and metallogenic context for porphyry copper deposits in western Central Asia along with a discussion of the resource potential of early Paleozoic magmatic arcs, such as the fragmented arc system that hosts the Bozshakol' deposit. Chapter 1 also establishes the geologic framework for permissive tracts for the four arc systems that were assessed quantitatively (fig. 1) and includes an analysis of regional-scale magnetic data, as well as a discussion of cross sections shown on 1:200,000-scale geologic maps.

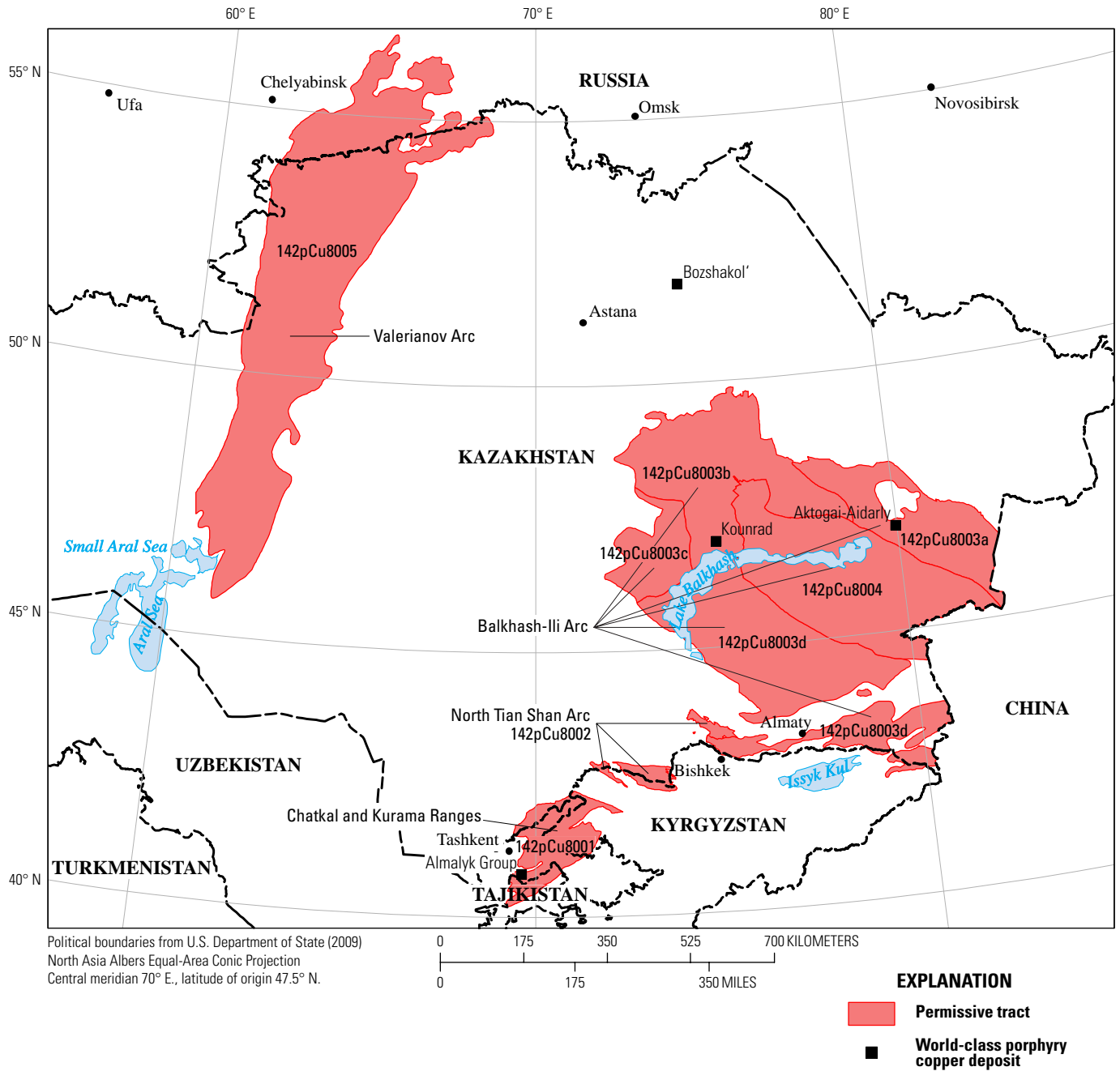


Figure 1. Map of the western Central Asia study area showing permissive tracts for porphyry copper deposits and locations of world-class porphyry copper deposits.

4 Porphyry Copper Assessment of Western Central Asia

These detailed geologic maps show drill sites that provided constraints for extending permissive areas under younger cover. The areas selected for quantitative assessment are: (1) the Late Carboniferous to Permian Chatkal and Karama Ranges (tract 142pCu8001) in Kazakhstan, Kyrgyzstan, Tajikistan, and Uzbekistan, (2) the Ordovician North Tian Shan⁶ magmatic arc (tract 142pCu8002) in Kazakhstan and Kyrgyzstan, (3) the Late Paleozoic (Carboniferous-Permian) Balkhash-Ili magmatic arc (tracts 142pCu8003a–d and 142pCu8004) in Kazakhstan and Kyrgyzstan, and (4) the Carboniferous Valerianov Arc in Kazakhstan, Uzbekistan, and Russia. Separate tracts or sub-tracts are delineated within an area based on differences in expected distributions of undiscovered deposits or differences in available data. Each permissive tract is assigned a unique identifier (Coded_Id) as well as a geographic/geologic name. Identifiers are based on United Nations regions (142 for Asia), deposit type (pCu), and a 4-digit number. Informal tract identifiers also were used by the assessment team (for example, CA01PC). Political boundaries are based on data maintained by the U.S. Department of State (2009).

Chapter 2 describes the application of satellite data for mapping of hydrothermal alteration and the results of the remote sensing data analysis for the study area. The lack of heavy vegetative cover throughout much of western Central Asia allowed use of spectral reflectance remote sensing (ASTER⁷) data to map hydrothermal alteration at the surface as an assessment tool.

Chapter 3 summarizes the quantitative mineral resource assessment. The assessment data, rationales for delineation of individual permissive tracts and estimates, and results are included in appendixes A through H. Spatial data (GIS files) for permissive tracts for undiscovered porphyry copper deposits, locations of deposits and significant occurrences in the permissive tracts, and ASTER alteration data accompany this report (appendix I). Assessment workshop participants are listed in appendix J.

Geologic time scales used on geologic maps for former Soviet Union countries as well as for China and Mongolia differ slightly from the International Stratigraphic Chart (International Commission on Stratigraphy, 2010) and from each other. Appendix K includes correlation tables to clarify geologic age terms used in this report.

Permissive tracts are based on geology, irrespective of political boundaries. Therefore, tracts may cross country boundaries or include lands that have already been developed for other uses or been withdrawn from mineral development as protected areas. The tracts are presented at a scale of 1:1,000,000 and are not intended for use at larger scales.

⁶Also spelled as Tien Shan.

⁷Advanced Spaceborne Thermal Emission and Reflection Radiometer.

Readers should note that this assessment was done in 2009 and 2010. A number of relevant papers have been published since that time (for example, Seltmann and others, 2011; Wilhelm and others 2012). In addition, mineral properties frequently change hands, and more recent information on deposits and occurrences may be available.

Commodity terms are spelled out in the text but abbreviated in the tables and in reference to porphyry deposit subtypes: Cu, copper; Mo, molybdenum; Au, gold; Ag, silver.

Acknowledgments

The assessment was facilitated by a close working relationship of the U.S. Geological Survey (USGS) with the Centre for Russian and Central EurAsian Mineral Studies (CERCAMS) at the Natural History Museum, London. In particular, Dr. Reimar Seltmann, Director of CERCAMS, and Dr. Richard Herrington facilitated project workshops, participated in project meetings, and provided invaluable data and guidance, as well as contacts for the geology of Central Asia. CERCAMS hosted project workshops organized by Dr. Reimar Seltmann in Almaty, Kazakhstan, and at the Natural History Museum. Dr. Dmitriy Alexeiev of the Russian Academy of Sciences shared his extensive knowledge of the geology of Kazakhstan. Drs. Vitaly Shatov, Victor Popov, and Andrei Chitalin attended workshops and graciously provided data and expertise on the geology and resources of the region. USGS colleague Walter Bawiec participated in early workshops and assisted with the geographic information system (GIS). Dr. Alla Dolgoplova, CERCAMS, assisted with translation and contacts and was an organizer of the Almaty workshop. Jeff Doebrich, USGS, facilitated the working relationship between CERCAMS and the USGS. Heather Parks, USGS Spokane office, greatly facilitated completion of the project by editing final figures and assisting with manuscript proofreading and editing.

References Cited

- Bawiec, W.J., and Spanski, G.T., 2012, Quick-start guide for version 3.0 of EMINERS—Economic Mineral Resource Simulator: U.S. Geological Survey Open-File Report 2009–1057, 26 p., accessed June 30, 2012, at <http://pubs.usgs.gov/of/2009/1057/>. (This report supplements USGS OFR 2004–1344.)
- Berger, B.R., Ayuso, R.A., Wynn, J.C., and Seal, R.R., 2008, Preliminary model of porphyry copper deposits: U.S. Geological Survey Open-File Report 2008–1321, 55 p., accessed May 15, 2009, at <http://pubs.usgs.gov/of/2008/1321/>.

- Drew, L.J., Singer, D.A., Menzie, W.D., and Berger, B.R., 1999, Mineral-resource assessment—State of the art: *Geologica Hungarica Series Geologica*, v. 24, p. 31–40.
- Duval, J.S., 2012, Version 3.0 of EMINERS—Economic Mineral Resource Simulator: U.S. Geological Survey Open-File Report 2004–1344, accessed July 15, 2012, at <http://pubs.usgs.gov/of/2004/1344/>.
- International Committee on Stratigraphy, 2010, International Stratigraphic Chart: accessed October 1, 2011, at [http://www.stratigraphy.org/column.php?id=Chart/Time Scale](http://www.stratigraphy.org/column.php?id=Chart/Time%20Scale).
- John, D.A., Ayuso, R.A., Barton, M.D., Blakely, R.J., Bodnar, R.J., Dilles, J.H., Gray, Floyd, Graybeal, F.T., Mars, J.C., McPhee, D.K., Seal, R.R., Taylor, R.D., and Vikre, P.G., 2010, Porphyry copper deposit model, chapter B of Mineral deposit models for resource assessment: U.S. Geological Survey Scientific Investigations Report 2010–5070–B, 169 p., accessed January 15, 2011, at <http://pubs.usgs.gov/sir/2010/5070/b/>.
- Root, D.H., Menzie, W.D., and Scott, W.A., 1992, Computer Monte Carlo simulation in quantitative resource estimation: *Natural Resources Research*, v. 1, no. 2, p. 125–138.
- Seltmann, R., Konopelko, D., Biske, G., Divaev, F.D., and Sergeev, S., 2011, Hercynian post-collisional magmatism in the context of Paleozoic magmatic evolution of the Tianshan orogenic belt: *Journal of Asian Earth Sciences*, v. 42, p. 821–838.
- Singer, D.A., 1993, Basic concepts in three-part quantitative assessments of undiscovered mineral resources: *Nonrenewable Resources*, v. 2, no. 2, p. 69–81.
- Singer, D.A., 1995, World class base and precious metal deposits—A quantitative analysis: *Economic Geology*, v. 90, no.1, p. 88–104.
- Singer, D.A., 2007a, Short course introduction to quantitative mineral resource assessments: U.S. Geological Survey Open-File Report 2007–1434, accessed May 15, 2009, at <http://pubs.usgs.gov/of/2007/1434/>.
- Singer, D.A., 2007b, Estimating amounts of undiscovered resources, in Briskey, J.A., and Schulz, K.J., eds., *Proceedings for a workshop on deposit modeling, mineral resource assessment, and their role in sustainable development*, 31st International Geological Congress, Rio de Janeiro, Brazil, August 18–19, 2000: U.S. Geological Survey Circular 1294, p. 79–84. (Also available online at <http://pubs.usgs.gov/circ/2007/1294/>.)
- Singer, D.A., Berger, V.I., and Moring, B.C., 2008, Porphyry copper deposits of the World; database and grade and tonnage models: U.S. Geological Survey Open-File Report 2008–1155, accessed June 10, 2010, at <http://pubs.usgs.gov/of/2008/1155/>.
- Singer, D.A., and Menzie, W.D., 2010, *Quantitative mineral resource assessments—An integrated approach*: New York, Oxford University Press, 219 p.
- U.S. Department of State, 2009, Small-scale digital international land boundaries (SSIB)—Lines, edition 10, and polygons, beta edition 1, in *Boundaries and sovereignty encyclopedia (B.A.S.E.)*: U.S. Department of State, Office of the Geographer and Global Issues.
- Wilhem, C., Windley, B.F., and Stampfli, G.M., 2012, The Altaids of Central Asia—A tectonic and evolutionary innovative review: *Earth-Science Reviews* v. 113, p. 303–341.

This page intentionally left blank.

Chapter 1. Tectonic and Geologic Setting of Porphyry Copper Deposits in Western Central Asia

By Byron R. Berger¹, Paul D. Denning¹, and Jeffrey D. Phillips¹

Introduction

Western Central Asia is a region of diverse geologic complexity situated north of the North China tectonic block and sandwiched between the East European and Siberian cratons (fig. 1-1). The Ural Mountains, a region with sets of fold belts and imbricated thrust faults, are along the western margin, the southern margin is the high-standing ranges that make up the Tian Shan wherein the effects of collisional tectonics are well displayed, the Altai Mountains arbitrarily separate western from eastern Central Asia, and the Siberian Basin is the northern margin (fig. 1-2A).

Variouly known as the “Central Asian Fold Belt” (for example, Zonenshain and others, 1990) or the “Altaids” (for example, Sengör and others, 1993), the Central Asia Orogenic Belt in its broadest sense (fig. 1-1) is a region of complex geologic relations, oftentimes characterized as a “collage” of numerous tectonic, structural, and stratigraphic parts that were assembled and intermittently deformed beginning about 1 billion years ago (giga-annum, Ga) (Windley and others, 2007). Although accretion was essentially complete by about 250 million years ago (mega-annum, Ma) (Windley and others, 2007), the region is still tectonically active. As a consequence of its long and varied tectonic history, Central Asia is home to many types and styles of mineral deposits, a large number of which are of current or historical economic importance. From volcanogenic polymetallic kuroko-style deposits (for example, Rudnyi Altai, Russia) to sedimentary rock-hosted copper deposits (for example, Dzhezkazgan, Kazakhstan) to “orogenic” low-sulfide gold deposits (for example, Kumtor, Kyrgyzstan) to numerous porphyry copper deposits (for example, Kal’makyr at Almalyk, Uzbekistan, and Bayan Obo, Mongolia), it is one of Earth’s most richly mineralized regions.

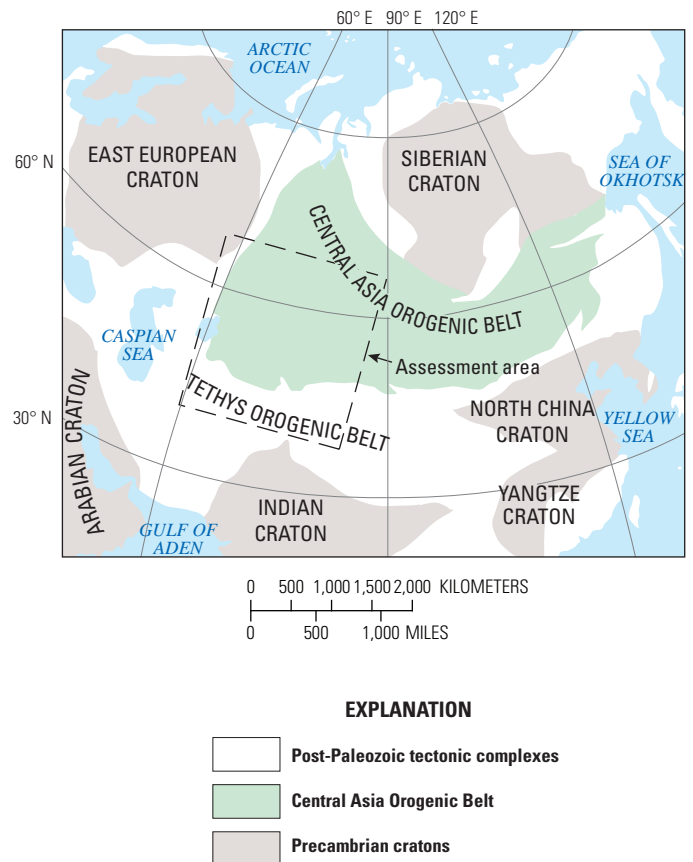


Figure 1-1. Map showing location of the western Central Asia assessment area (dashed outline) within the Central Asian Orogenic Belt with respect to surrounding cratons and the Tethys Orogenic Belt.

Central Asia has long been recognized as a locus of orogenic activity (see, for example, Suess, 1908), and an understanding of its tectonic and structural history is essential to interpreting its metallogenic evolution and the assumptions and data underpinning our assessment of undiscovered porphyry copper deposits in the region (fig. 1-2B).

¹U.S. Geological Survey, Denver, Colorado.



Figure 1-2. Location maps. *A*, Map of western Central Asia showing countries, country boundaries, selected cities and lakes, and locations of selected geographic features pertinent to the text on a digital elevation base for reference purposes. *B*, Locations of assessment tracts within the study area. Detailed discussion of each tract is given in the appendixes.



Figure 1-2.—Continued

Although the predominating belief structure regarding the tectonic evolution of Central Asia has changed in the past one to two decades from a “fixist” geosyncline-based theory of tectonics to a “dynamic” plate-tectonics-based theory, the predominance of geosyncline theory in the former Soviet Union for most of the 20th century means that this theory served as a context for much of the available geologic mapping, tectonic and structural interpretations, and mineral-deposit descriptions and models. Consequently, post-Soviet era regional literature on the geology and metallogeny of the focus of this report, western Central Asia (fig. 1-2A), often consists of a hybridization of terminology and ideas derived in the geosynclinal context integrated with terminology derived from a plate-tectonic context. Thus, an understanding of the premises on which the geosyncline theory was built is helpful to anyone undertaking a mineral-resource assessment of undiscovered mineral deposits in this region.

Owing to the remoteness, the oftentimes harsh terrain conditions of western Central Asia, and political barriers to access, the temporal and spatial relations of porphyry-style copper deposits to their tectonic and geologic settings are known primarily through Russian-language publications (for example, Abdulin and others, 1978), as well as the mostly recent English synopses of those publications (for example, Kudryavtsev, 1996; Yakubchuk, 2004; Seltmann and Porter, 2005). The Centre for Russian and Central EurAsian Mineral Studies (CERCAMS), headquartered at The Natural History Museum, London (<http://naturalhistorymuseum.ac.uk>), has the most comprehensive English-language geologic and metallogenic data bases available on the region. Although no Precambrian porphyry-style copper deposits have been reported in Central Asia, deposits in magmatic-arc rocks dating from the Middle Cambrian through the Late Carboniferous have been reported (see Kudryavtsev, 1996). Owing to the complex tectonic and structural history of western Central Asia, the older Paleozoic magmatic arcs have been highly fragmented as well as largely covered by younger deposits. Consequently, the number of preserved deposits formed during any particular Paleozoic Epoch increases through time and the geologic coherence of the arcs similarly improves as the arcs become more recent.

Mining in western Central Asia dates back more than three millennia, when the region became a minor source of copper and tin during the Bronze Age as well as a region of gold, silver, and lead production (Cierny and Weisgerber, 2003). Although Tsarist Russia looked to Central Asia for copper resources during the second half of the 19th century, it was during the Soviet era that the most extensive and intensive mapping and exploration expeditions were undertaken, and for these, the footprints of the ancient miners were good guides to mineralization (N. Kurbanov, 1991, oral commun.). Significant deposits were discovered in the late 1920s to early 1930s in the region north of Lake Balkhash (fig. 1-2A), for example the Kounrad deposit about 15 kilometers (km) north of Balkhash City, Kazakhstan, and at Almalyk, Uzbekistan (Nekrasoff, 1935). Because of the

paucity of published data and uncertainty regarding the extent of Soviet-era minerals exploration, the historical difficulty of access for non-Soviet block exploration companies, as well as the geographic remoteness of much of western Central Asia and the rugged topography in some areas, we supplemented publically available geological information with interpretations of ASTER and Thematic Mapper satellite data to (1) correlate the interpreted remotely sensed data with hydrothermal alteration shown on Soviet era 1:200,000-scale geologic maps, (2) correlate the interpreted remotely sensed data with mineral occurrence locality data in Seltmann and others (2009), (3) develop a mineral assemblage model for selected porphyry-style deposits in western Central Asia and apply the model in areas deemed to be permissive and quantitatively assessable for the occurrence of undiscovered porphyry copper deposits (fig. 1-2B), and (4) use alteration data to identify hydrothermal fluid flow-controlling faults and fractures identifiable on satellite imagery.

This chapter provides a tectonic, geologic, and metallogenic context for the U.S. Geological Survey’s (USGS) quantitative mineral-resource assessment of undiscovered porphyry copper-style deposits of selected ages and regions in western Central Asia. The tectonic and geologic evolution discussions are divided into sections on (1) geosyncline tectonic theory and metallogeny, (2) Phanerozoic evolution of western Central Asia in a plate-tectonic context, (3) porphyry copper deposit metallogeny of western Central Asia, and (4) challenges in quantitatively assessing undiscovered deposits in highly deformed geologic terranes. The application of satellite data in western Central Asia is discussed in chapter 2 of this report. The quantitative assessment is summarized in chapter 3, along with appendixes that document the rationale for the assessment. Figures 1-2A and 1-2B show selected geographic features and place names for reference purposes.

Tectonic and Geologic Evolution of Western Central Asia and its Porphyry Copper Metallogeny

The large number of published maps and extensive literature on the geology, tectonics, and structure of western Central Asia (fig. 1-2A) represents decades of work. Furthermore, the body of work reflects different schools of thought regarding the fundamental processes that drive tectonic activity as well as ore-forming processes. Although for the purposes of this report plate-tectonic theory is accepted as a context for interpreting the tectonic evolution and metallogeny of Central Asia, much of the available information on the region presumed a very different tectonic construct, principally the geosynclinal tectonic theory that prevailed in the former Soviet Union for most of the 20th century, as well as a different scheme for classifying mineral deposits and one that is closely tied to the structure and igneous history embedded in geosyncline theory.

Geosyncline Tectonic Theory and Metallogeny

A general understanding of the history and tenets of the geosyncline theory and metallogeny in a theoretical context are helpful when reading former Soviet Union literature and necessary when interpreting Eurasian literature in a North American tectonic context. The following paragraphs provide a brief summary of selected aspects of geosyncline theory and metallogeny in this context.

Historical Overview of Geosyncline Tectonic Theory

During the 19th century, the desire to interpret and understand mobile belts and their origin led to the development of the geosyncline tectonic theory. The intellectual roots of this theory are in North America where, principally, Hall (1859) and Dana (1873) first established the basic tenets of the theory. The driving mechanism was widely believed to be an expanding earth. Haug (1900) imported and popularized the theory in Europe from where it was brought into the Russian literature by Bogdanovich (1906). With time, the concept grew from one of two basins—one oceanic (eugeosyncline) the other shallow water (miogeosyncline)—separated by an uplifted barrier with deep crustal rocks in its core, to a theory with considerable scope and complexity to account for multiple intrusive and deformation events over a period of time. Nevertheless, the dominance of vertical, not horizontal, motion of Earth's crust remained a core assumption underlying the theoretical model (compare Khain and Ryabukhin, 2002).

By the 1930s, principally under the leadership of Soviet scientist V.V. Belousov, it was recognized that mobile belts are part of an orogenic cycle with many different parts, that igneous rocks are a part of geosyncline development, and that faults, some of which are deep-seated, bound mobile belts. Working in the Greater Caucasus, Belousov (for example, 1970) drew on technical approaches being used at that time in the western Mediterranean region by the German paleotectonicist H. Stille (Khain and Sheynmann, 1962). These techniques are seen as having put the Russian geosyncline model on a sounder theoretical base as debates ensued about how geosynclines develop and how the various parts, from fold belts to marginal troughs to platforms, are related.

During the 1940s, the “formations method,” which includes the juxtaposition of epochs of folding (for example, Caledonian, Hercynian, and Alpine; see Bertrand, 1887), created an evolutionary theory of geosynclines wherein first-cycle troughs eventually developed axial uplifts that then could transform the geosyncline into a geanticline (Khain and

Sheynmann, 1962). Folding accompanies axial uplift, and the folding, in turn, facilitates the rise of magma in the crust. In this way, magmatic activity became coupled to the stages of evolution of mobile belts. Away from the axial uplifts, the secondary cycle troughs further evolve to the point at which, eventually, one secondary trough merges with another secondary trough to form an intermontane trough, whereas another may roll onto an adjoining platform, thereby forming a foredeep.

Although Obruchev (1926) recognized that faults bound geosynclines, it was in the 1940s that regional-scale, deep-seated faults were recognized to bound geosynclinal regions (Khain and Sheynmann, 1962), and such fault zones were found to correlate with a variety of geologic processes including metamorphism, the distribution of rock facies, and stratigraphic thicknesses (Peive, 1945).

What forces drove geosyncline development was widely debated throughout the reign of geosyncline tectonic theory (Khain and Sheynmann, 1962). Whereas 19th century mechanistic explanations attributed the driving force for geosynclinal evolution to contractional forces as a consequence of a cooling Earth in which thrust faults played a central role in deformation, in mid-20th century Russia the principal driving mechanism was considered to be vertical, oscillatory movements (Khain and Ryabukhin, 2002) and that long-distance, horizontal tectonic transport did not occur. Ironically, the vertical forces premise effectively denies the existence of the large nappe structures that had been well mapped during the 1930s at several localities, including the northern and central Ural Mountains, the Greater Caucasus, and Transbaikalia (Khain and Ryabukhin, 2002).

During the 1950s and 1960s, a period that includes a considerable proportion of the geologic quadrangle mapping done in Central Asia, careful field observations led to the inexorable fact that thrust and large strike-slip fault systems were widespread here and elsewhere. By the early 1960s, the interpretation and tectonic significance of ophiolite complexes became broadly known and their occurrences in Central Asia recognized (Khain and Ryabukhin, 2002). All of these elements were recorded on the geologic maps of western Central Asia, but the state-of-understanding was largely in the context of geosyncline theory.

Although Alfred Wegener's continental drift hypothesis was first published in Russian during the 1920s (Khain and Ryabukhin, 2002), it did not gain widespread traction until the advent of plate tectonics. Belousov (1970), who had refuted Wegener's hypothesis in an earlier era, opposed the idea of plate tectonics and continued to do so for the duration of his career. Khain (1970), in discussing the fixist versus mobilist controversy, was the first to state the basic postulates of plate-tectonic theory in the Russian literature (Khain and Ryabukhin, 2002). From this point on, the battle between the geosyncline and plate-tectonic theorists gained intensity, to a great extent divided along generational lines.

The Geosyncline Construct in Central Asia

A geosyncline is a region within which the initial stage is a continuum of sedimentation accompanied by considerable downwarping. The concurrent infilling was predominantly by marine sedimentary and volcanic formations (Nalivkin, 1973). The second stage of geosyncline development consists of folding and emergence into mountainous regions; that is, a system of folded and uplifted mountain ranges. Erosion accompanies uplift and results in the formation of adjacent basins, each containing sedimentary deposits. Where deformation is most intense, generally the deepest parts of geosynclines, intrusive masses originate. The third stage of geosyncline development is marked by the termination of fold deformation and an increase in the rate of erosion. Thus, the relief diminishes and the geosyncline becomes a platform, a tectonic unit that was formerly folded and compacted, had become rigid, and on which later rock formations set unconformably with little or no fold deformation.

A second cycle of geosyncline development may then ensue, and the above stages are repeated. Thus, the order of a geosyncline is defined by its ages of folding, which are constrained using paleontological assemblages and the geochronology of igneous rocks. In most of the former Soviet Union, the first-order geosynclines are Precambrian. The Precambrian basement in western Central Asia is heterogeneous and the boundary of the Precambrian geosyncline is somewhat arbitrary (Nalivkin, 1973). That is, it is made up of many “massifs” and includes, for example, rocks that correlate with rocks in the Urals Geosyncline to the west (East European craton in fig. 1-1) and Siberia to the north.

In western Central Asia, the oldest geosyncline was known as the Angara Geosyncline (Siberian craton in fig. 1-1). Although Archean rocks occur, Proterozoic rocks predominate. The Angara Geosyncline is situated between the European Platform on the west and, more specifically the Urals Geosyncline, the Siberian Platform on the east to northeast (Sayan Altai and Baikal regions in Russia), and the Tarim and North China platforms on the south (the Tian Shan ranges and adjoining areas in fig. 1-2A). Nalivkin (1973) considers it diagnostic and a distinguishing characteristic of the Angara Platform that the Hercynian orogeny is strongly manifested and that Cambrian and Jurassic tectonics differ from neighboring first-order geosynclines. The Angara Geosyncline region is an aggregation of several Precambrian microcontinental blocks that differ in terms of age, geologic environment, petrology, petrochemistry, and types of structures. Nalivkin (1973) shows Angara and its posterosional tectonic successor, the Angara Platform, to be roughly comparable to Suess' (1908) “Altaids,” a name derived from the Altai Mountains, but it is not the same as Şengör and Natal'in's (1996) “Angara Craton,” which is correlative with the Siberian Platform.

The break between the Precambrian and the Cambrian marks the beginning of a new, second geosynclinal tectonic

cycle in western Central Asia. For the Paleozoic as a whole, most literature discusses two distinct geosynclinal cycles, one that includes the Late Precambrian (Zonenshain, 1973) together with the Cambrian to the Late Silurian to earliest Devonian and the ensuing one including the Middle Devonian through the Permian. Each geosynclinal phase consists of a lower ophiolitic assemblage followed by a flysch-graywacke sequence and ends with volcanic rocks in its upper part. The fold deformation phases of the first and second cycles are called the Caledonian Orogeny and the Variscan or Hercynian Orogeny, respectively. Variability in the ages of ophiolite is significant—for example, as old as Early Silurian or Late Ordovician in one region of the Variscan geosyncline to as young as Late Devonian to Early Carboniferous in another region (Zonenshain, 1973)—and shows that these orogenic episodes did not occur concurrently across the whole of its respective geosyncline; rather, they varied spatially and temporally. Consequently, each of these two Paleozoic geosynclines is a system within which there are a series of alternating anticlinoria and synclinoria. Each of the individual tectonic units has a long history of development and each differs significantly in its structural elements (Bakhteyev and Filatova, 1969).

To illustrate how a complex geosynclinal system may develop, we use a model published by Markova (1948) for the Chingiz, Akbastau, and Arkalyk ranges northeast of Lake Balkhash, Kazakhstan (refer to “Chingiz Range” on fig. 1-2A). Figure 1-3 is a reference figure for the anticlinoria (that is, uplifts) and synclinoria (that is, troughs) in this region. The base map shows the faults and Carboniferous magmatic-arc-related layered and intrusive rock units (after Seltmann and others, 2009) to assist in contrasting the mapping according to a geosynclinal model and a plate-tectonic unit, which is herein interpreted as a once continuous magmatic arc. In the course of modeling geosyncline development, most investigators tried to distinguish the stages of development based on the sequences of sedimentary and igneous rocks and their deformation in conjunction with regional, deep-seated faults (see Khain and Sheynmann, 1962). In the Chingiz Meganticlinorium example here (fig. 1-3), the earliest Phanerozoic basinal rocks on the deformed Proterozoic basement are deep ocean-floor basin deposits, including cherts and spilitic volcanic rocks; the distribution of these rocks defines the Phanerozoic geosyncline. They are Lower to Middle Cambrian in the Chingiz and Arkalyk ranges and Middle to Upper Cambrian in the Akbastau Range (fig. 1-4). This age variation led Markova (1948) to model the geosyncline as developing initially in the Chingiz Range (fig. 1-4A) and expanding to include the Akbastau and Arkalyk ridges by the Upper Cambrian (fig. 1-4B). Because shallow water and continental sedimentary rocks define the locations of basins, in the Chingiz Range and Arkalyk Ridge it is Upper Cambrian sedimentary rocks and Lower Ordovician in the Akbastau Ridge that required the portrayal of basins or synclinoria flanking a central core anticlinorium (the Chingiz Range) with boundary anticlinoria and deep faults delimiting the margin of the geosyncline. Figure 1-5A is a block diagram model of the stage shown in figure 1-4B.

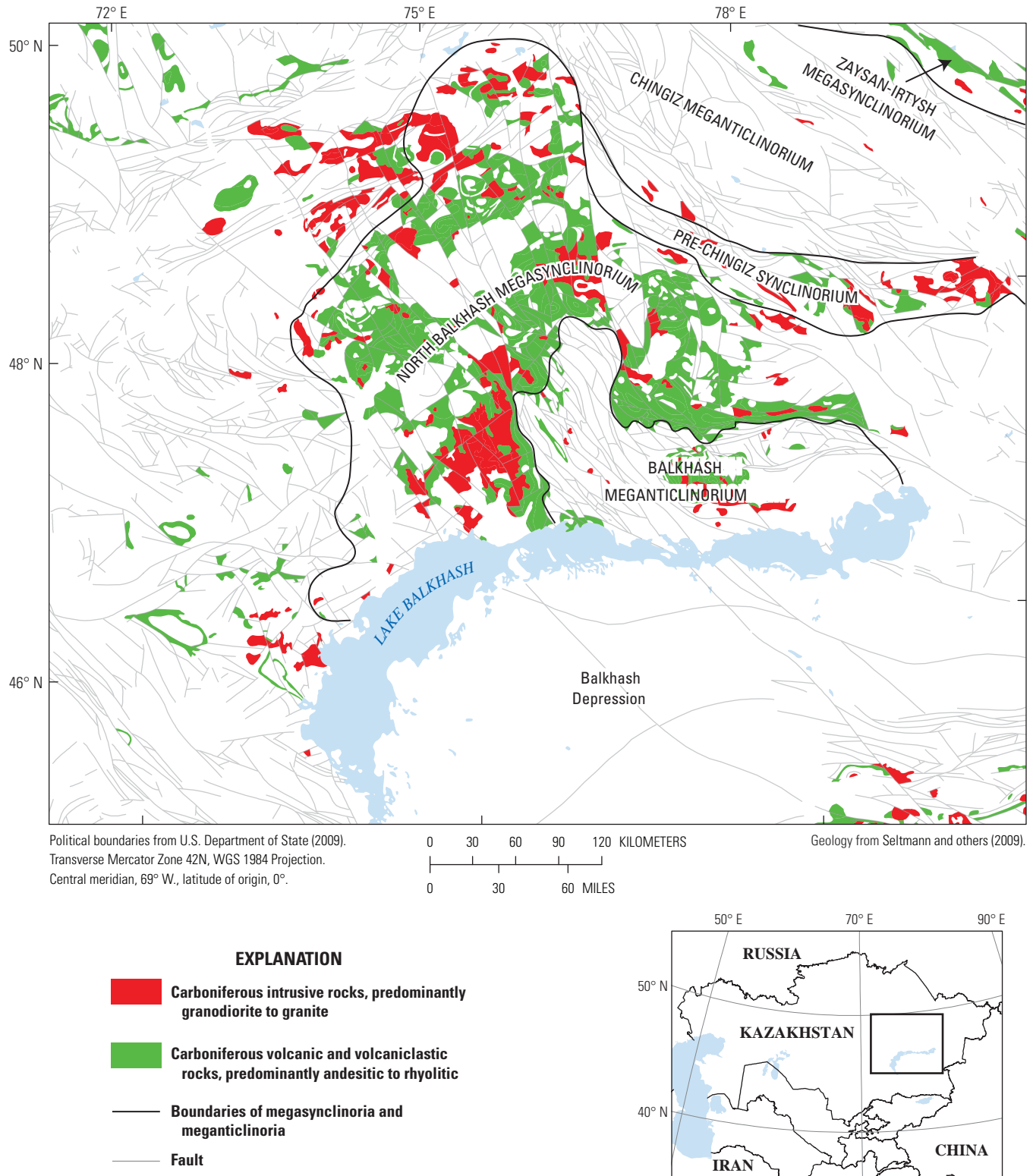


Figure 1-3. Map showing the location of selected geosyncline complexes to the north and northeast of Lake Balkhash in central Kazakhstan, after Orlov and others (1981), plotted on a base showing faults and structural lineaments and geologic map units that include Carboniferous arc volcanic and volcanoclastic rocks (green) and intrusive rocks (red). Base map derived from Seltmann and others (2009). Location of map area shown on inset.

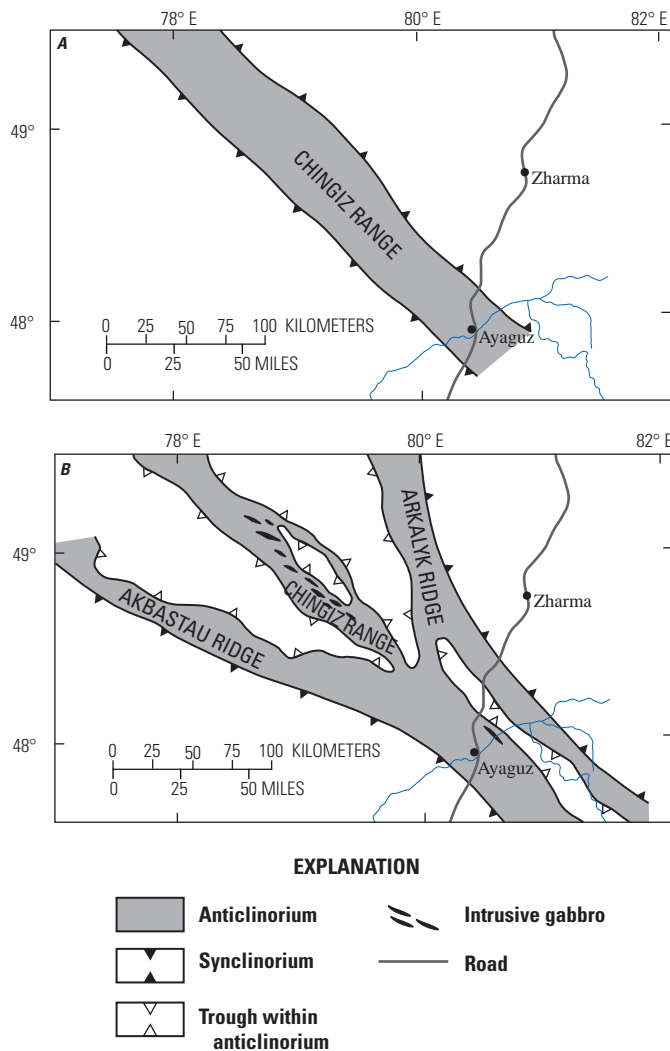


Figure 1-4. Maps showing synopsis of model of stages of development of the Chingiz Meganticlinorium of Markova (1948). Location of meganticlinorium is shown in figure 1.3. *A*, The initial stage of development was the formation of an anticlinorium beginning in the Middle Cambrian in the Chingiz Mountains northeast of Lake Balkhash, Kazakhstan (see Markova, 1948). The geanticline formed on an erosional platform of deformed Precambrian rocks. *B*, Following a period of deformation and subsequent erosion during the Upper Cambrian, the geanticline expanded to take in the region between the Akbastau Ridge on the west of the Chingiz Range and the Arkalyk Ridge on the east. Locations of the cities of Ayaguz and Zharna are shown for reference. Location of map area shown on inset.

To account for discontinuities in the stratigraphic sections, such as unconformities and other planar contacts, erosion was invoked. Thus, between each period of central and boundary anticlinoria development and the beginning of synclinoria development, there would be a major episode of denudation (fig. 1-5*B*). Magmas play an integral role in the development of a geosyncline, and their compositions reflect the stage of evolution of a geosyncline. Mafic to ultramafic magmas, now recognized as pieces of ophiolite complexes, are emplaced in the early development of a geosyncline and drive its uplift, which, in turn, causes deformation. In subsequent uplift and folding events, the melts become more and more siliceous. Thus, gabbros and peridotites are early and dacites and rhyolites are later. In figures 1-4 and 1-5, gabbro is emplaced into the core of the Chingiz Range uplift and was the driver for the initial development of the geanticline, whereas later deformation events involved intermediate to siliceous plutons (fig. 1-5*C*).

The Seltmann and others (2009) geologic map, used in our resource assessment (see appendixes), was compiled from underlying geologic studies that include map data drawn upon by Markova (1948). Thus, the logical foundations for

Markova's (1948) Chingiz Meganticlinorium interpretation are recognizable on Seltmann and others' (2009) geology of the Chingiz-Akbastau-Arkalyk geanticlinal area. Figure 1-6 is a map derived from the Seltmann and others' (2009) map using ArcGIS to highlight Cambrian and mixed Cambrian–Ordovician map units we have classified as to whether they are likely or unlikely to have been deposited in a magmatic-arc environment. Overlaying this base are the approximate geotectonic terrane boundaries of Windley and others (2007) and the anticlinorial ridge areas of Akbastau, Chingiz, and Arkalyk shown on figure 1-5*A*. Although the logic of the geosyncline interpretation is evident in figure 1-5, by bringing paleogeographic constraints as required by fossil assemblage latitudinal affinities, paleomagnetic data interpretations, and thrust and fold belt tectonics to bear on the interpretation of the Seltmann and others' (2009) map units, Windley and others (2007) portray a significantly different interpretation. The lithotectonic terranes of Windley and others (2007) are shown on figure 1-6, and the entire tectonic context of western Central Asia is shown in figure 1-7. In the plate-tectonic context of Windley and others (2007), the three arms of the Chingiz Meganticlinorium have no genetic relation.

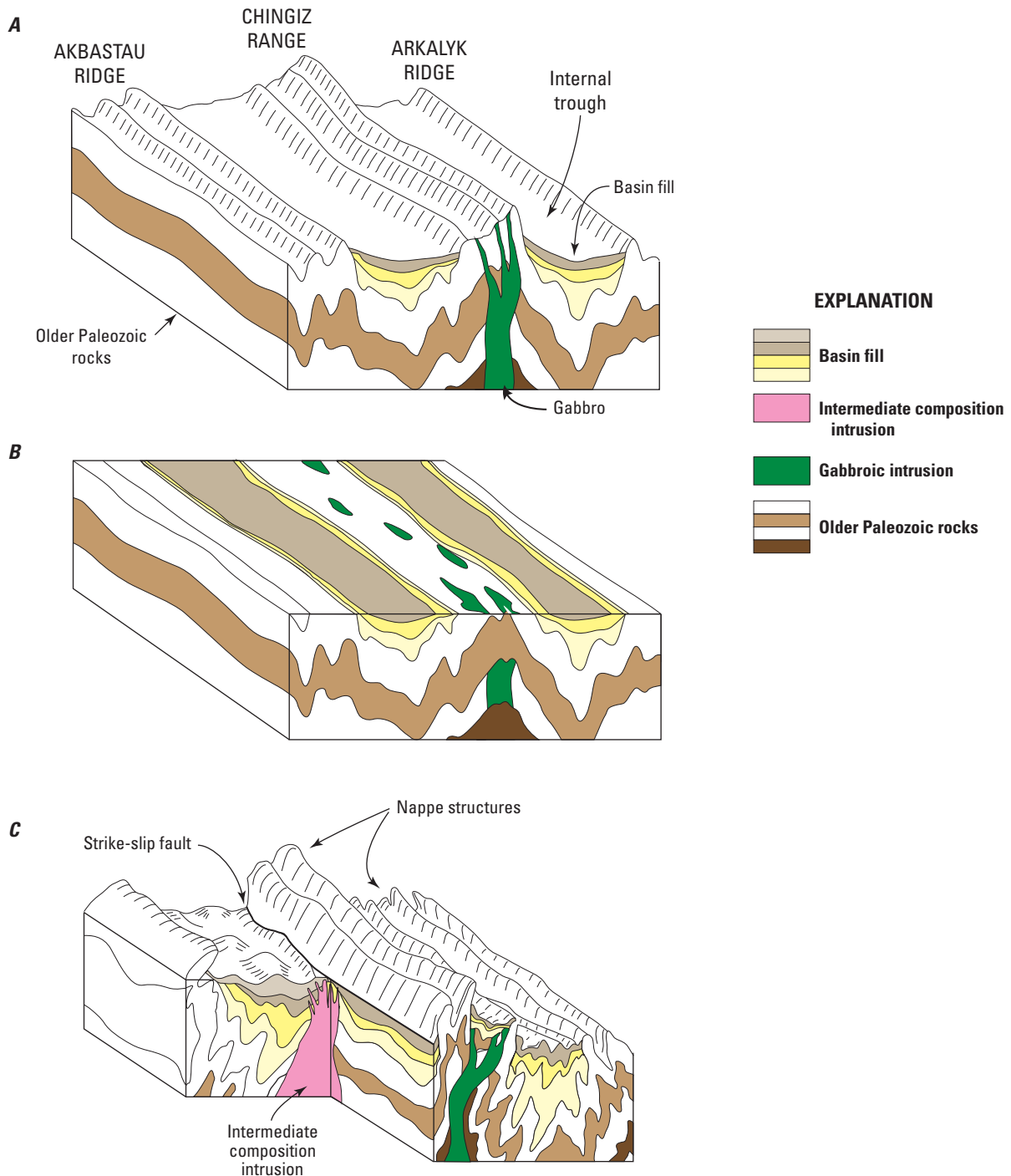


Figure 1-5. Block diagrams illustrating the tectonic evolution of the Chingiz Meganticlinorium (after Markova, 1948) shown in figure 1-4. *A*, Cartoon showing the three prongs of the Chingiz Meganticlinorium at the end of the Cambrian. The geanticlines are separated by synformal troughs within which volcanic and sedimentary rocks were deposited. *B*, Cartoon depicting the erosional event in the meganticlinorium during the Lower Silurian. *C*, Long-lived meganticlinoriums go through multiple cycles of deposition, uplift, deformation, and erosion. With each such cycle, the structural complexity of the geanticline increases, with eventual uplift resulting in nappe structures that can lay out onto the topography to form short displacement thrust faults. Long distance thrust fault displacement does not occur because vertical tectonics are considered the driving mechanism for deformation in the geosynclinal tectonic model. However, large displacement strike-slip faults may occur.

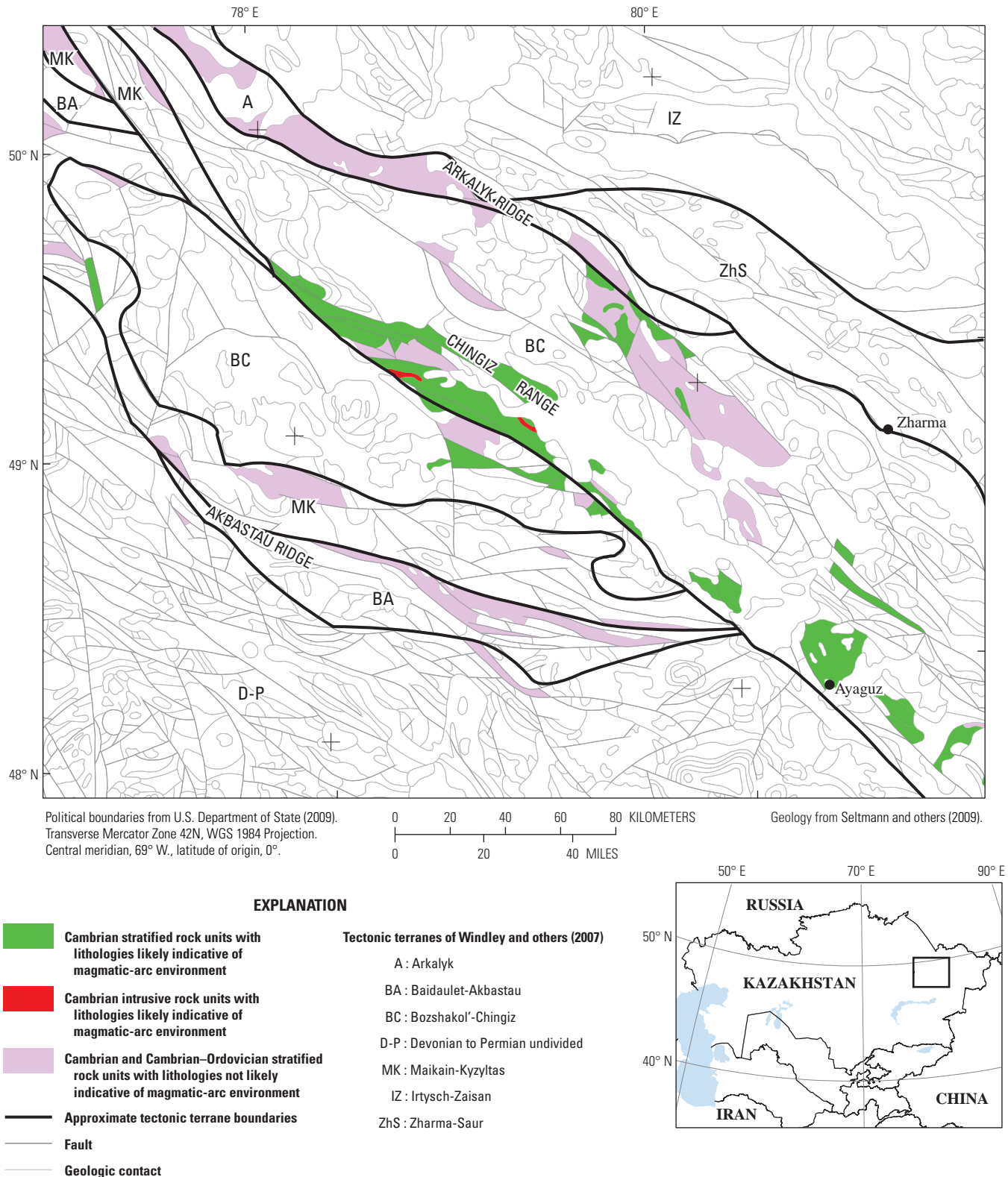


Figure 1-6. Map showing the relation of the Chingiz Meganticlinorium (see fig. 1-3 for location) to the lithotectonic terranes of Windley and others (2007) plotted on a fault and geologic base derived after Seltmann and others (2009). Those Cambrian to Cambrian-Ordovician geologic map units interpreted as likely to have been deposited in a magmatic-arc environment are shown in green and red; rocks of the same ages deposited in some other tectonic environment are color coded in lavender. The lithotectonic boundaries of Windley and others (2007) are approximately located and illustrate the lack of correspondence between a geosyncline tectonic model of the region and a plate-tectonic model. The cities of Ayaguz and Zharma are shown for reference with regard to the geosyncline model in figure 1-4. Location of map area shown on inset.

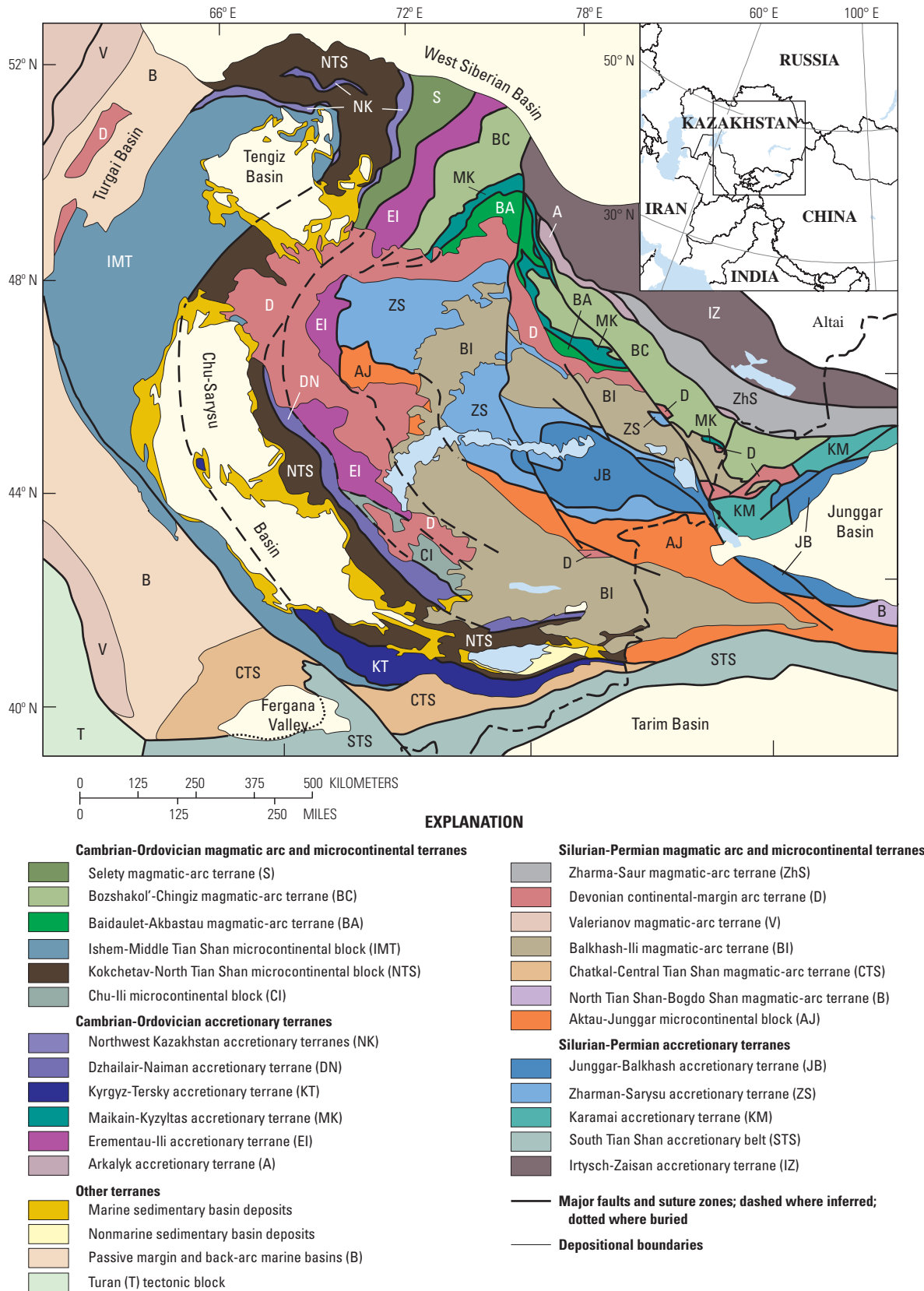


Figure 1-7. Lithotectonic terrane map of western Central Asia after Windley and others (2007), with modifications based on the models of Heubeck (2001) and Alexeiev and others (2010). Location of map area shown on inset.

Historically, a major emphasis in metallogenic studies has been on the relation in space and time of mineral deposits to regional tectonic and structural features as well as to petrochemistry. This was also the case in the Soviet Union (Safonov and others, 2007), except that the unifying structural and tectonic framework context in the Soviet Union was geosynclinal theory. Along with the rapid development of geosyncline tectonic theory during the 1930s and 1940s in the Soviet Union, the field of mineral deposits and their classification and tectonic settings evolved in parallel, thereby inextricably linking them in Soviet-era literature. Because Central Asia was deemed a priority area for resource development during the mid-twentieth century, many exploration expeditions were organized and extensive databases were assembled regarding the structural control of ore deposits in this region. The importance of geosyncline theory to economic geology in the Soviet Union lay in the context of (1) the definition of ore districts, ore fields, and ore deposits; (2) the structural position of ore districts and fields in the tectonic framework; (3) the typing of ore-hosting rocks and structures; and (4) the typing of favorable environments.

Terms such as ore districts and ore fields are based on geological attributes, but meanings are not the same for all ore deposit types and may vary, even in an ore deposit class, from author to author, as well as through time (Safonov and others, 2007). Because the regular arrangement of mineral deposits in space and time is useful in exploration, the nature of an ore field, a collection of spatially associated and presumed genetically linked deposits, is based primarily on the internal and external structure of the ore field in the context of its host-rock lithology. For example, for porphyry copper deposits its immediate association with a presumed genetically linked igneous rock sequence is important. If this ore-related complex is part of a larger grouping of associated igneous rocks, such as a large stock or batholith, the larger associated igneous domain constitutes an ore district. Kreiter (1956), who studied magmatic-hydrothermal nonferrous metal and gold deposits, regarded the structure of an ore field as a combination of faults that control the localization of closely spaced deposits of a particular type (for example, porphyry copper-molybdenum) associated with an intrusive complex, whereas Wolfson (1962), who studied lower temperature deposits (for example, roll-front uranium), defined the structure of an ore field analogously but in the context of regional faults (Safonov and others, 2007).

Within an ore field, the priority for classification of deposits was ore mineral or ore metal assemblages. These schemes were used because of the importance to the state of mineral economic considerations. A further subclassification of deposits was based on form such as veins, stockworks and disseminations, massive, and replacements (for example, skarn). This manner of classifying deposits can lead to confusion in interpreting former Soviet Union maps and reports. For example, base-metal deposits that in North America are classified as Kuroko-type volcanogenic massive sulfide deposits might in the Russian language literature be

classified in a variety of ways. For example, an aforesaid “Kuroko-type” deposit might, in the Russian-language literature, could be called chalcopyritic (pyrite-chalcopyrite-sphalerite±pyrrhotite-galena-tetrahedrite) and elsewhere in the ore field be called pyritic-polymetallic. This latter class might be further broken down into copper-zinc, lead-zinc, and gold-bearing deposit types. Either chalcopyritic or pyritic-polymetallic might be further broken down into massive, segregated, and stockwork-type deposits with the further complication that stockworks may be subdivided into “meshed” and “subparallel” types (see Smirnov, 1977). On metallogenic maps, the symbols and colors used usually designate the metal or metal suite (color) and form (symbol shape) such as vein or stockwork. Therefore, a copper-gold stockwork with disseminations that is in a North American context the feeder zone to a Kuroko-type massive sulfide deposit cannot be distinguished on symbol alone from a stockwork and disseminated copper-gold porphyry deposit. Consequently, the combination of stockwork and disseminated ores can apply to a large variety of deposit types in the context of American literature, including volcanogenic massive sulfide, orogenic (mesothermal), and porphyry styles.

In the former Soviet Union, the supplanting of the geosyncline tectonic theory by plate-tectonic concepts during the late 20th century did not lead to the wholesale reclassification of ore deposits or the abandonment of names pertaining to geosynclinal tectonic blocks and units. Rather, the literature typically contains a hybridization of North American/western European terms and terms that reference the former Soviet systematics. Thus, the authors of that literature may use terminology familiar to North American geologists but, in fact, retain in their discussions of mineral deposits a structural characterization of ore fields that is based on their position in a tectonic block as defined by geosynclinal theory and some theory, say, regarding the relation of ore fields to nonlinear structural features originally germane to a geosynclinal construct.

Phanerozoic Evolution of Western Central Asia in a Plate-Tectonic Context

The Central Asian Orogenic Belt (fig. 1-8) is one of the largest and most geologically heterogeneous accretionary orogens on Earth. Its evolution is important to understanding the metallogeny of the western Central Asia assessment region, but its longevity, structural complexity, and paucity of modern detailed studies present challenges to deciphering its assembly and assessing its undiscovered mineral-resource potential. As a consequence, although many compilations regarding the tectonic evolution of western Central Asia in a plate-tectonic context have been published (for example, Mossakovsky and others, 1993; Şengör and Natal'in, 1996;

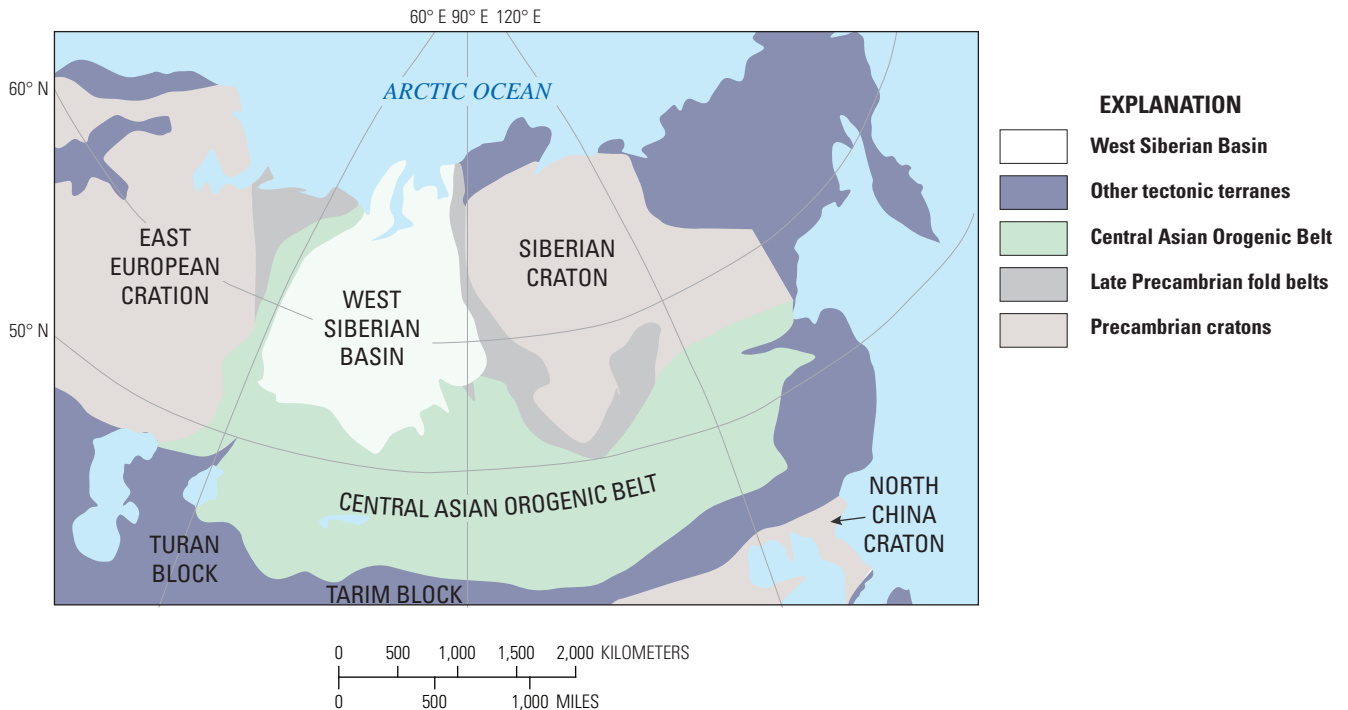


Figure 1-8. Map showing location of the East European, Siberian, and North China cratons and the Turan and Tarim tectonic blocks in relation to the Central Asian Orogenic Belt. Terrane areas covered by the West Siberian Basin shown for reference purposes.

Filippova and others, 2001; Yakubchuk and others, 2002; Windley and others, 2007), reconstructions are commonly mutually exclusive, and there is little in the way of a consistent use of terminology (Levashova and others, 2008). Consequently, in this overview it is only possible to provide a broad brush summary of tectonic events that necessarily makes generalizations and oversimplifies a story that is much more complicated in actuality and which will, more than likely, be revised as more data are acquired. In the discussions that follow, the central organizing principle of the discussions is first, time and second, accretionary complex.

End Proterozoic

The Precambrian basement of western Central Asia in its broadest geographic context (for example, Şengör and others, 1993; Windley and others, 2007) consists of the East European (Baltica) craton in the northwest, the Siberian craton in the northeast, the Turan and Tarim tectonic blocks to the south, the North China craton to the southeast (fig. 1-8), and a collage of Proterozoic cored microcontinental fragments in between (Windley and others, 2007). The Precambrian masses were stitched together through multiple collision events and over a considerable period of time.

At the end of the Proterozoic, western Central Asia consisted of oceanic and various microcontinental masses between the eastern margin of the East European craton, the western margin of the Siberian craton, and the northern

margins of the Turan, Tarim and North China terranes. Windley and others (2007) characterize the microcontinental masses as consisting of Paleoproterozoic basement with Neoproterozoic to Early Paleozoic cover (fig. 1-9), although Seltmann and others (2009) also show Archean rocks predominantly in the southern Ural Mountains, in the Kokchetav massif, and in scattered occurrences in the Tian Shan. Ophiolites generally bound the microcontinental fragments, and differences in the ophiolite complexes indicate that the fragments formed in different geologic environments and experienced different geologic histories during the Late Precambrian, implying that they were isolated, allochthonous blocks (Windley and others, 2007).

According to lithologies and mineral occurrences in Seltmann and others (2009), some of the Precambrian massifs contain remnants of magmatic-arc environments. For example, the Kokchetav-North Tian Shan tectonic block of Windley and others (2007) (fig. 1-7) is sutured on its east margin to the Dzhailair-Naiman tectonic block. Riphean and Vendian rocks along the suture zone include calc-alkaline metavolcanic rocks as do Vendian-Early Cambrian rocks. Across a Mesozoic to Tertiary basin to the west is the Ulutau Range (fig. 1-9), where analogous Precambrian metavolcanic rocks crop out. There, also, the arc environment continued into the Early Cambrian. In the Ulutau Range, Seltmann and others (2009) show a symbol for a porphyry-style prospect with copper in Vendian-Early Cambrian rocks. Although the actual age of the copper prospect is unknown, it is assumed here to be Cambrian.

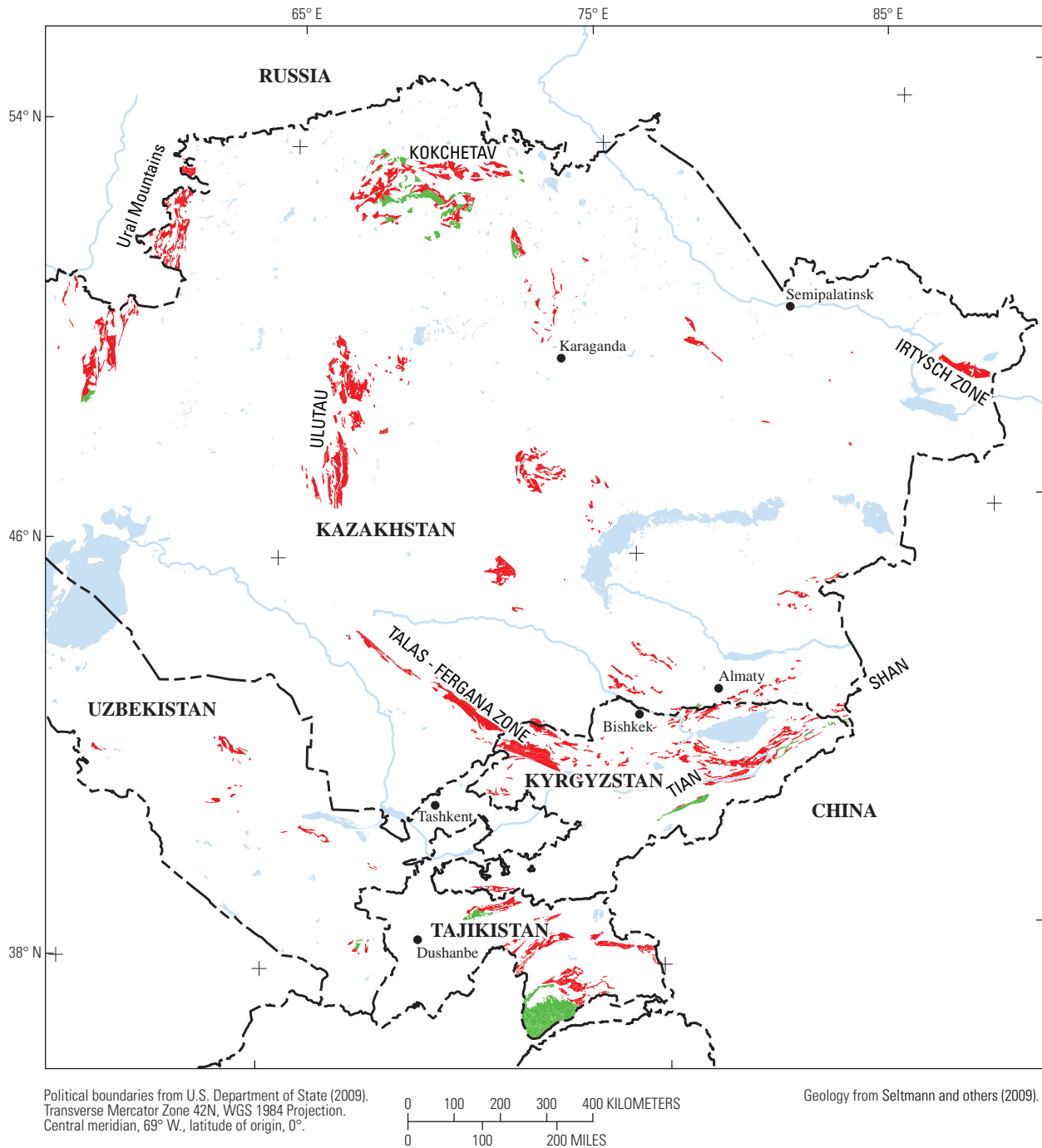


Figure 1-9. Map showing distribution of Precambrian rocks in western Central Asia (after Seltmann and others, 2009). Proterozoic rocks are colored red, and Archean rocks are colored green. Selected terrane names are shown for reference purposes.

Lower Paleozoic: Cambrian-Silurian

Lower Paleozoic rocks, Cambrian- through Silurian-age, are widespread in the southern Urals, central Kazakhstan, eastern Kazakhstan, and in the Tian Shan ranges along the southern border of the study area. Cambrian rocks (figs. 1-10 and 1-11) occur in relatively small blocks and widely spaced areas and are the volumetrically least common of the Paleozoic rocks. Overall, the mapped outcrops describe a ring-like zone around central Kazakhstan consisting of fragmented slivers of Cambrian magmatic arcs that are tectonically interleaved with other age rocks. The greatest number of map units is in north-central Kazakhstan (fig. 1-10) and constitute the Bozshakol'-Chingiz magmatic-arc terrane of Windley and others (2007) (fig. 1-7). As is evident from figure 1-11, very few of the Cambrian magmatic-arc outcrops consist of intrusive rocks. By comparison, Ordovician rocks are more abundant and widespread (figs. 1-12 and 1-13) than Cambrian rocks. Favorable volcanic and volcanoclastic rocks (fig. 1-12) are most abundant in north-central and eastern Kazakhstan and in the Ulutau area, with scattered outcrops along major fault zones in west-central Kazakhstan and in western Kyrgyzstan, whereas favorable Ordovician intrusive rocks (fig. 1-13) are most abundant in north-central Kazakhstan and in the Tian Shan ranges. As with the Cambrian arcs, the Ordovician arc rocks occur as tectonic fragments structurally juxtaposed with rocks of other ages including Cambrian. Silurian magmatic-arc rocks (figs. 1-14 and 1-15) are less common than Ordovician and more akin to the Cambrian arc fragments. They occur in greatest abundance in east-central Kazakhstan. The favorable lithologies in central Uzbekistan are metamorphosed to greenschist facies, contain marine lithologies, and are not known to host any porphyry copper deposits.

The Phanerozoic assembly of western Central Asia, in a present-day geographic context, began in the west during the late Cambrian to Early Ordovician. The following sequencing of events is that described principally by Windley and others (2007) and Alexeiev and others (2011) (fig. 1-16). The earliest event occurred during the Early to Middle Cambrian in the North Tian Shan (NTS) when the Kokchetav microcontinental mass collided along the Kumdykol suture zone in northernmost Kazakhstan with the North Tian Shan block (see Buslov and others, 2010). This local closure was followed during the Early Ordovician by south to north closure of the oceanic terrane between the Ishim-Middle Tian Shan (IMT) microcontinent on the west and the Kokchetav-North Tian Shan² (NTS) microcontinent on its east forming the intervening Kyrgyz-Tersky (KT) accretionary wedge

(fig. 1-16). Final closure in the north between IMT and NTS occurred during the Middle Ordovician, forming the South Kokchetav (unit SK in fig. 1-16) accretionary wedge between the main microcontinental masses.

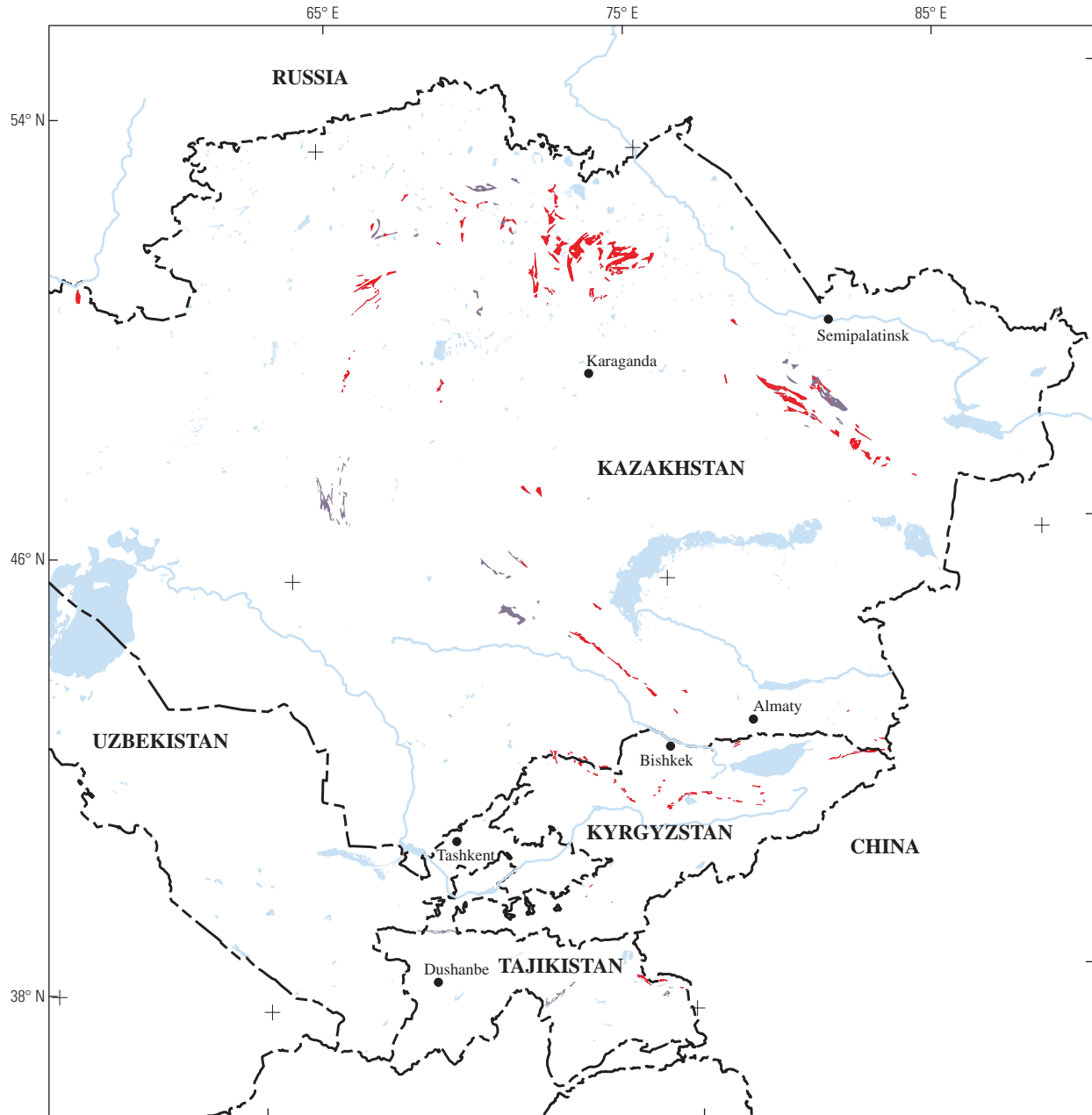
On its northeastern margin in northern Kazakhstan, the amalgamated IMT-NTS mass collided with the Selety (S) volcanic-arc assemblage, forming the intervening Urumbai accretionary wedge (unit U in fig. 1-16). This collision may have occurred concurrently with the final closure of the intervening IMT-KNT ocean but before the Late Ordovician, owing to the fact that the Late Ordovician Kokchetav-North Tian Shan magmatic arc was built out onto the Urumbai accretionary wedge with a fore-arc basin formed on the Selety terrane (Alexeiev, 2008).

Eastward and across some span of ocean from the IMT and NTS microcontinental terranes, there was a concurrent, complex array of small, Precambrian-cored microcontinental terranes. Magmatic arcs, as well as oceanic island-arc terranes, are associated with these terranes (for example, Yakubchuk, 1990).

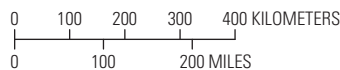
Stratigraphic sections with Cambrian to Late Silurian magmatic-arc assemblage rocks occur predominantly in the west, north, and northeast to east of western Central Asia. Some of these arcs, for example the Ordovician Baidalet-Akbastau Arc in the north (unit BA in fig. 1-16), formed on oceanic crust whereas others, for example the Cambrian to Silurian Bozshakol'-Chingiz Arc (unit BC in fig. 1-16) in the northeast and east, formed on continental fragments, and yet others, for example the Ordovician Kokchetav-North Tian Shan Arc (unit NTS in fig. 1-16) in the west, formed on microcontinental and accreted rocks. Except for the Bozshakol'-Chingiz Arc, the Early Paleozoic arcs were characteristically short lived, and faunal evidence implies that the arcs of a given period were not all active at the same time (Windley and others, 2007).

The occurrence of a Vendian-Early Cambrian arc terrane beneath the Ordovician Kokchetav-North Tian Shan arc terrane in western central Kazakhstan was noted above. Although the classification of a porphyry-style copper occurrence by Seltmann and others (2009) in the Vendian-Early Cambrian rocks of the Ulutau Range (fig. 1-2A) has not been independently verified, a valid occurrence would support the presence of an active arc along the margin of a Precambrian microcontinent that pre-dates the beginning of the assembly in the Middle Cambrian of the central Kazakhstan tectonic collage (see Degtyarev and Ryazantsev, 2007). Furthermore, this supports the supposition of Windley and others (2007) that Paleozoic Kazakhstan was assembled through the accretion of several isolated and independent microcontinental masses.

²Alexeiev (2008) introduced the term Kokchetav-North Tian Shan (KNT) domain in a CERCAMS 12 oral update as a replacement of the Stepnyak-North Tian Shan (NTS) domain of Windley and others (2007). The boundaries of KNT differ in small, but significant, ways from NTS. Alexeiev (2008) retains use of the term Stepnyak-North Tian Shan in reference to the Late Ordovician magmatic arc that developed across several microcontinental masses following Early Ordovician accretion in westernmost west Central Asia.



Political boundaries from U.S. Department of State (2009).
 Transverse Mercator Zone 42N, WGS 1984 Projection.
 Central meridian, 69° W., latitude of origin, 0°.



Geology from Seltmann and others (2009).

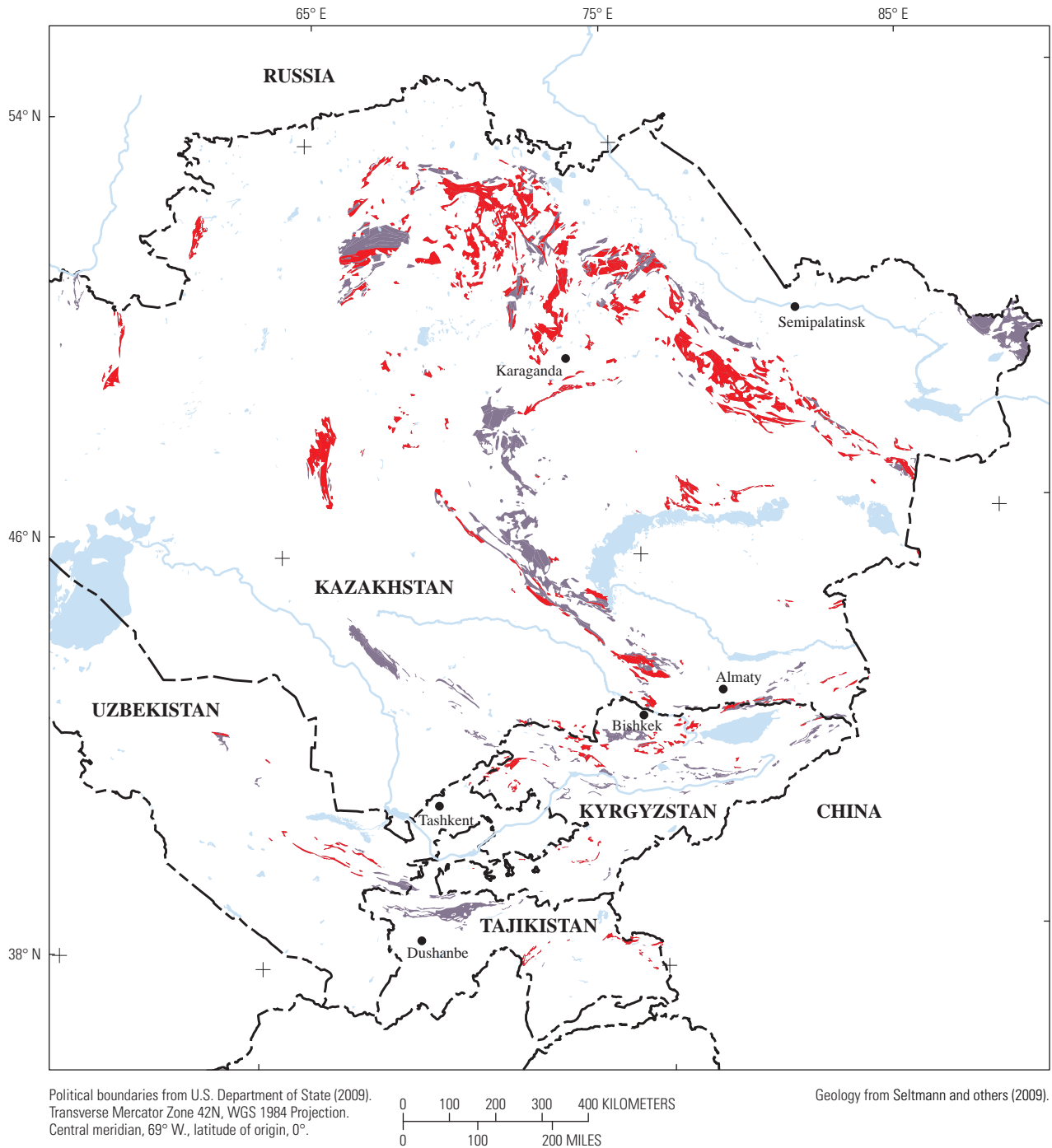
EXPLANATION

- Cambrian stratified rocks deposited in magmatic-arc terranes
- Cambrian stratified rocks not associated with magmatic-arc terranes

Figure 1-10. Map showing distribution of Cambrian stratified rocks in the western Central Asia study area based on lithologies in the map units in Seltmann and others (2009). Those map units containing lithologies likely to have been deposited in magmatic-arc terranes are shown in red; map units with lithologies unlikely to have been deposited in a magmatic-arc terrane are shown in lavender.



Figure 1-11. Map showing distribution of Cambrian intrusive rocks in the western Central Asia study area based on lithologies in the map units in Seltmann and others (2009). Those map units likely to have been emplaced in a magmatic-arc terrane are shown in red; intrusive rocks unlikely to have been deposited in a magmatic-arc terrane are shown in lavender.



EXPLANATION

- Ordovician stratified rocks deposited in magmatic-arc terranes
- Ordovician stratified rocks not associated with magmatic-arc terranes

Figure 1-12. Map showing distribution of Ordovician stratified rocks in the western Central Asia study area based on lithologies in the map units in Seltmann and others (2009). Those map units containing lithologies likely to have been deposited in magmatic-arc terranes are shown in red; map units with lithologies unlikely to have been deposited in a magmatic-arc terrane are shown in lavender.

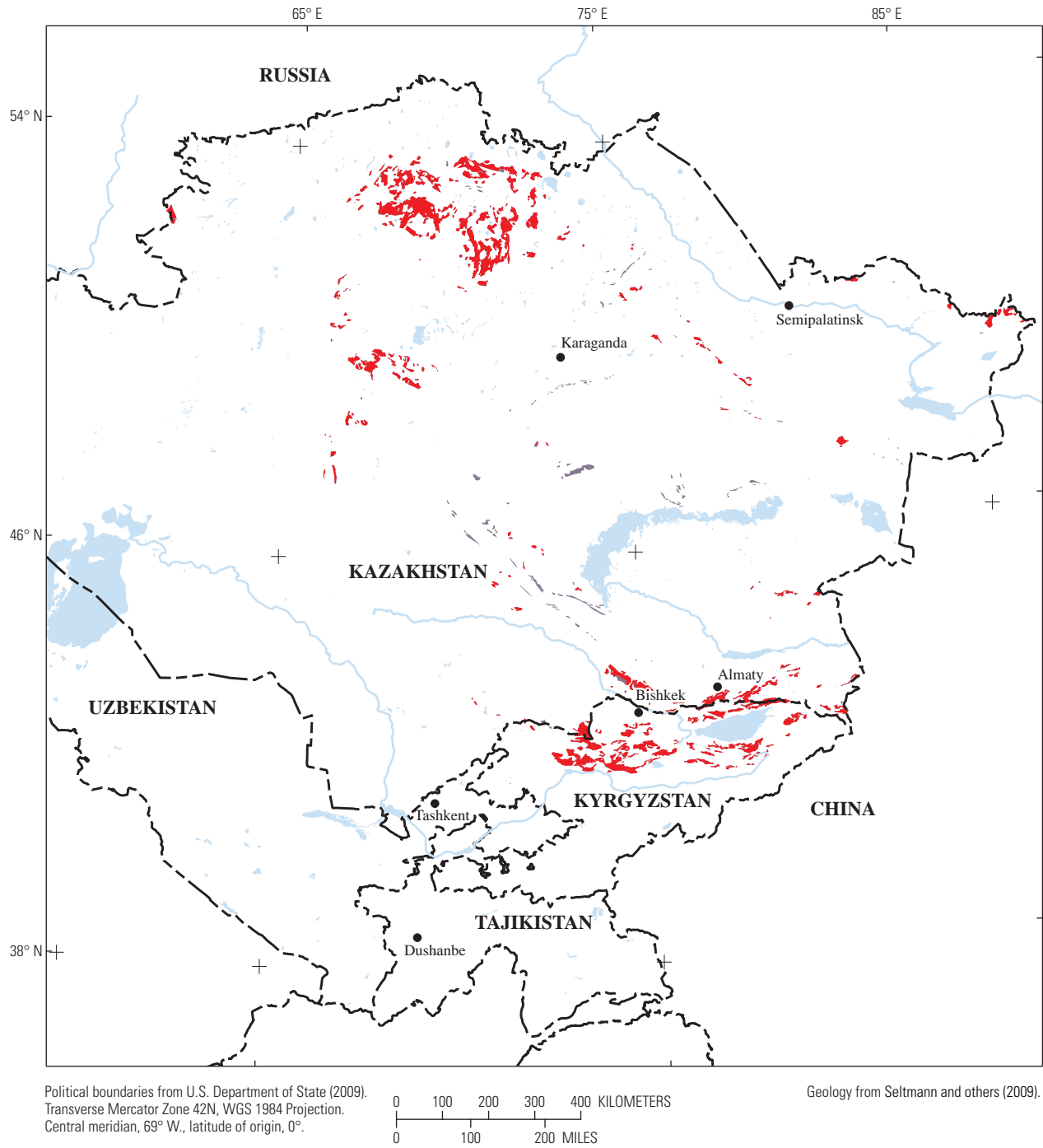


Figure 1-13. Map showing distribution of Ordovician intrusive rocks in the western Central Asia study area based on lithologies in the map units in Seltmann and others (2009). Those map units likely to have been emplaced in a magmatic-arc terrane are shown in red; intrusive rocks unlikely to have been emplaced in a magmatic-arc terrane are shown in lavender.



Figure 1-14. Map showing distribution of Silurian stratified rocks in the western Central Asia study area based on lithologies in the map units in Seltmann and others (2009). Those map units containing lithologies likely to have been deposited in magmatic-arc terranes are shown in red; map units with lithologies unlikely to have been deposited in a magmatic-arc terrane are shown in lavender.



Figure 1-15. Map showing distribution of Silurian intrusive rocks in the western Central Asia study area base based on lithologies in the map units in Seltmann and others (2009). Those map units likely to have been emplaced in a magmatic-arc terrane are shown in red; intrusive rocks unlikely to have been emplaced in a magmatic-arc terrane are shown in lavender.

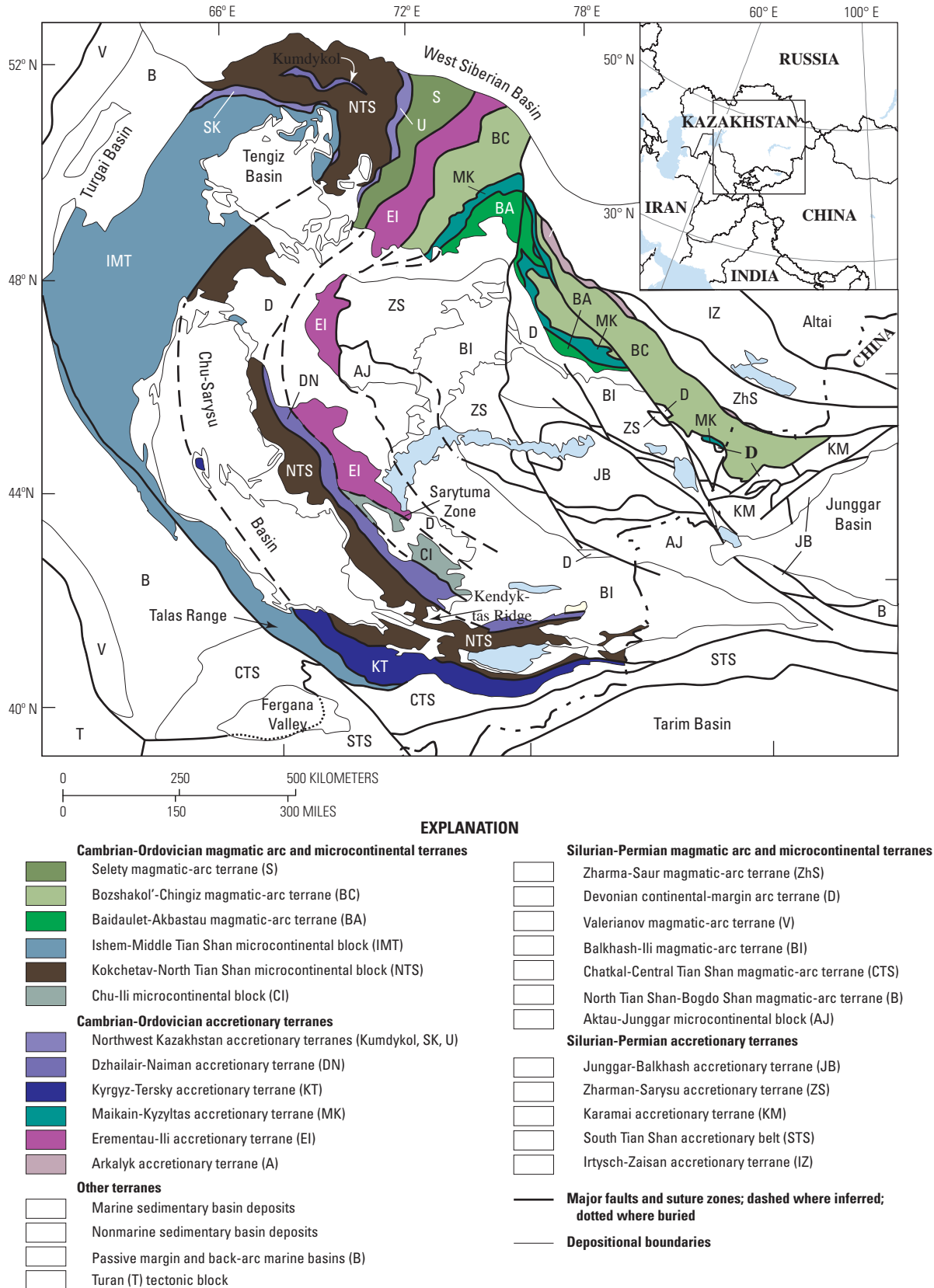


Figure 1-16. Modified lithotectonic terrane map (after Windley and others, 2007) of western Central Asia (refer to figure 1-7), highlighting Cambrian and Ordovician magmatic-arc and accreted terranes. Location of map area shown on inset.

The Kokchetav-North Tian Shan Magmatic-Arc Terrane

Southwestern Region

The heterogeneous Cambrian and Ordovician lithologies in the western Kyrgyz Range of northwestern Kyrgyzstan and south-central Kazakhstan (fig. 1-2A) suggest a complex tectonic history. On the north side of the Talas-Fergana Fault Zone (Talas-Fergana Zone in fig. 1-9) in the Talas Range that parallels the fault zone in Kyrgyzstan, Cambrian to Middle Ordovician rocks consist of limestone and dolomite. They are stratigraphically above Vendian and older Precambrian rocks that are predominantly continental in character but include some Vendian acidic tuffs (see Seltnann and others, 2009). Windley and others (2007) assign these rocks to the Ishim-Middle Tian Shan (IMT) microcontinent (fig. 1-16). To the north, this block is in tectonic contact with the Kyrgyz-Tersky (KT) accretionary wedge block of Windley and others (2007) and caught up in a suture zone that includes continental-like Riphean rocks, but Seltnann and others (2009) show no Vendian rocks. Early Cambrian ocean-floor siliceous sedimentary and mafic volcanic rocks occur in KT together with Lower Cambrian gabbroic to dioritic intrusions and masses of serpentinite. These ocean-floor rocks persist in the KT terrane to its eastern terminus south of Lake Issyk-Kul (fig. 1-16) in the Tian Shan ranges (fig. 1-2A). Although some Cambrian sections have an assemblage of rocks suggestive of a deep-water to slope-rise transition including tuffs and scattered remnants of Late Cambrian to Lower Ordovician rocks, they also contain probable arc-related volcanic-rock assemblages.

Upper Cambrian to Lower Ordovician rocks in the KT block (fig. 1-16) are predominantly continental to shallow marine but include andesitic tuff (see Seltnann and others, 2009). Windley and others (2007) show that the Kokchetav-North Tian Shan (NTS) microcontinental block makes up the westernmost end of the Kyrgyz Range. However, the Cambrian and Riphean sections do not differ lithologically from their time-stratigraphic equivalents in the KT block. The principal stratigraphic difference between the western KT and adjacent NTS block is that Early Devonian rocks are widespread in NTS, but sparse in the western part of KT. As one proceeds east in the Kyrgyz Range in the NTS terrane (fig. 1-16) towards Lake Issyk-Kul, Cambrian rocks are absent to sparse, whereas they are common in the KT immediately south, and younger Paleozoic rocks become widespread. Thus, what may be inferred from the stratigraphy is that the Cambrian platform to extensional basin environment of the IMT is accreted to the NTS block on which the Cambrian consists of a deep, ocean-floor environment on a Precambrian continental crust, and the KT block is merely a structurally deeper view into the orogen owing to Late Paleozoic and younger strike-slip and reverse faulting.

The faults separating the IMT, KT, and NTS structural blocks localize mesothermal-style low-sulfide gold-bearing quartz vein deposits. These deposits, which typically form at depths of 5 or more kilometers, provide direct evidence of significant vertical uplift on the localizing fault zones. In conjunction with the increasingly younger stratigraphic horizons from south to north, the lithology of the lower Paleozoic rocks, and the presence of porphyry copper-gold deposits in the north and their absence to the south, this supports the interpretation that the Kyrgyz-Tersky “accretionary wedge” of Windley and others (2007) is a more deeply eroded part of the Kokchetav-North Tian Shan block.

North and east of the Kyrgyz Range, Cambrian rocks are absent from the Kandyktas Ridge (fig. 1-16) in south-central Kazakhstan. Here, Early Ordovician continental assemblages, including some volcanic rocks, lie directly on Precambrian Riphean basement. A suture-related fault on the northern margin of the ridge juxtaposes Upper Cambrian to Lower Ordovician rocks of continental affinity. Windley and others (2007) assign these rocks to the Dzhalaïr-Naiman tectonic block (DN), not the NTS. Degtyarev and Ryazantsev (2007) interpret these same Middle to Upper Cambrian sequences to mark the completion of collision along the suture zone. However, there is no map evidence of Ordovician arc-related intrusions or mineralization in the Cambrian-Ordovician rocks along Kandyktas Ridge or in DN rocks to the east. Further, lithologic descriptions in Seltnann and others (2009) describe the Middle Ordovician rocks on the fault contact with the DN Cambrian-Ordovician rocks as schistose, a description not given to the adjacent DN rocks, which indicates that the high-strain fault juxtaposition postdates arc magmatism.

There are no lithologic or mineral occurrence data indicating the likelihood of Cambrian arc magmatism in the southwestern NTS. However, the presence of andesitic volcanic rocks in Lower Ordovician units and their prevalence along with dacites and intermediate composition intrusions in Middle to Late Ordovician units imply that magmatic-arc volcanism may have begun in the Lower Ordovician and at least intermittently spanned the duration of the Ordovician in the southwestern NTS region. The most prospective part of this arc, once quite extensive, is now restricted to the western Kyrgyz Range.

Northwestern Region

Approximately 275 km northwest of the Kandyktas Ridge along the Dzhalaïr-Naiman structural zone (DN-NTS boundary in fig. 1-16) in the NTS terrane are exposures of Early to Middle Cambrian rocks, but they have continental affinities, not those of magmatic arcs. Seltnann and others (2009) show some map exposures of favorable stratified Ordovician rocks in this region; Devonian rocks often set directly on Cambrian rocks. Fifty to sixty kilometers farther northwest, Middle to Late Cambrian rocks have marine

slope to deeper water affinities, whereas Vendian to Lower Cambrian rocks have magmatic-arc affinities. The occurrence of greenstone and metamorphosed stratiform base-metal deposits suggests that the arc may have been submarine.

West ~190 km across the northern end of the Chu-Sarysu Basin (fig. 1-2A) from the north end of the exposed Dzhalaïr-Naiman structural zone is the Ulutau (“tau” implies range or mountains). On the east side of the range, Vendian to Lower Cambrian rocks include intermediate to siliceous volcanic rocks along with shallow marine sedimentary rocks. This is the same section noted above wherein Seltmann and others (2009) report an unverified porphyry-style copper prospect. Volcanogenic massive sulfide occurrences in this same map unit imply that at least some parts of the arc were submarine. As to the east along the Dzhalaïr-Naiman structural zone, the Devonian, not the Ordovician, tectonically overlies the Cambrian rocks.

A major reactivated Precambrian shear zone trends north-south along the center of the Ulutau separating two distinct Precambrian tectonic terranes (see Strokin and Filatova, 1977). West of the suture and on the west side of the Ulutau, the Cambrian consists of euxinic marine basin sedimentary rocks overlain by deep-water siliceous Early Ordovician rocks. Above these units are Middle to Late Ordovician magmatic-arc rocks (see Seltmann and others, 2009); no prospects or occurrences are known in these Ordovician rocks that could help further characterize them. The contrast in Cambrian lithologies across the Ulutau shear zone, as well as overlying deep-water Lower Ordovician sedimentary rocks, are suggestive of a likely collision of the two different basement terranes during the Early Ordovician. However, Windley and others (2009) consider the Middle to Upper Ordovician magmatic-arc rocks on the west side of the Ulutau to be postcollisional and position the IMT-NTS tectonic boundary well to the east, in the vicinity of Dzhezkazgan (fig. 1-2A) beneath the Chu-Sarysu Basin, where Seltmann and others (2009) show the trace of a geophysically inferred shear zone. Whether the suture zone is in the Ulutau or farther east, the geologic relations support the conclusion that accretion occurred during the Early Ordovician and prior to magmatic-arc activity.

Early Cambrian (?) arc-related volcanic rocks persist north in the Ulutau to the southwest margin of the Tengiz Basin (fig. 1-2A). They are in contact with Riphean Precambrian rocks (Seltmann and others, 2009). Seltmann and others (2009) show only cobalt and mesothermal low-sulfide gold occurrences associated with these Cambrian rocks. About 70+ km to the east, but still adjoining the southwestern part of the Tengiz Basin, the Cambrian is missing and Early Ordovician magmatic-arc rocks (fig. 1-13) intrude Precambrian rocks. Associated Ordovician

volcanogenic massive sulfide deposits imply that this arc segment was submarine. Late Ordovician magmatic-arc intrusions that border the southeastern Tengiz Basin contain porphyry copper prospects, as well as bismuth-copper porphyry prospects (Seltmann and others, 2009). This Ordovician arc segment occurs in a northwest-southeast trend that is about 60 km wide and 160 km long, although all documented porphyry-style deposits are at the northwest end and mineral occurrences are sparse elsewhere (Seltmann and others, 2009). At its southeast end, the Late Ordovician arc-related intrusions are lost beneath a cover of Devonian and Carboniferous rocks. At this same southeast end, however, the Cambrian reappears. Early to Late Cambrian rocks are mixtures of magmatic-arc volcanic rocks and marine sedimentary rocks. The Cambrian rocks are in contact with Early Ordovician sedimentary rocks, a contrast to the same age rocks to the northwest, and Middle to Late Ordovician magmatic-arc volcanic rocks and Late Ordovician magmatic-arc intrusions. Windley and others (2007) include the Middle to Upper Ordovician magmatic-arc rocks in the IMT terrane, whereas Alexeiev and others (2010) include them in the NTS terrane. Early Silurian sedimentary rocks, which make their first appearance in this part of the NTS terrane, indicate that NTS Ordovician arc activity had ended by the beginning of the Silurian.

Northern Region

Lower Paleozoic rocks occur around the Precambrian Kokchetav massif (Kokchetav Region in fig. 1-2A) as well as, in part, across it. Cambrian rocks on the northwest margin of the Tengiz Basin reflect two different environments. One unit, age undifferentiated, consists of euxinic sedimentary rocks analogous to those on the west side of the Ulutau. The other unit, Upper Cambrian to Lower Ordovician in age, consists of ocean-floor basalts and spilites. The Early to Middle and Middle to Late Ordovician sequences consist of sedimentary rocks, as well as intermediate to siliceous volcanic rocks. The volcanic rocks are referred to as the Stepnyak Arc. However, Late Ordovician (460–440 Ma; Letnikov and others, 2009) intrusions, which Windley and others (2007) correlate with other NTS magmatic-arc segments, are widespread and intrude all older rock units. The intrusions are abundant in and around the Kokchetav massif and to the east. Most mineral deposits in the Kokchetav area are molybdenum-bearing and include porphyry-style molybdenum occurrences as well as molybdenum- and molybdenum-uranium bearing veins. Although present, copper is a minor constituent within and adjacent to the Kokchetav massif. In this region, however, copper is an important commodity in volcanogenic massive sulfide occurrences in Late Ordovician magmatic-arc

rocks, suggesting that the NTS arc was to some extent submarine. Nevertheless, southeast of the Kokchetav massif in the NTS arc, as well as farther east in the Urumbai (U) accretionary complex (fig. 1-16), the suture zone with the Selety (S) tectonic block to the east (Windley and others, 2007), a number of porphyry-style copper and copper-gold, and copper-bearing skarn occurrences are associated with intrusive rock complexes (Seltmann and others, 2009), implying that these parts of the Late Ordovician arc were terrestrial. A Middle Ordovician flysch sequence that occurs in the S terrane is considered a Stepnyak fore-arc basin by Alexeiev (2008) and Spiridonov (1995). The occurrence of Late Ordovician arc rocks in the accreted U terrane with a complementary Middle to Late Ordovician fore arc underlain by Early Ordovician slope and Late Cambrian to Lower Ordovician ocean-floor deposits in the S terrane (Seltmann and others, 2009) imply an Early Ordovician docking of the S terrane.

In the U terrane (fig. 1-16), there are slices of Early to Middle Cambrian tholeiitic island-arc basalt, as well as Middle to Late Cambrian chert-bearing complexes (Degtyarev and Ryazantsev, 2007). Pre-accretion, the U terrane was oceanic in character and proximal to a magmatic arc, probably the Selety Arc.

According to Degtyarev and Ryazantsev (2007), the precollision rocks in the S terrane consist of Early to Middle Cambrian tholeiitic island-arc type pillow basalts, tuffs, and carbonaceous sedimentary rocks. Andesite, tuff, and dacite were deposited on the more mafic island-arc volcanic rock foundation. There are apparently small volcanogenic massive sulfide deposits in the Selety Arc rocks, implying that the arc was, at least in part, submarine.

Silurian rocks are not abundant in the Kokchetav region. Earliest Silurian gabbroic to quartz dioritic intrusions are considered postarc (Spiridonov, 1995; Letnikov and others, 2009), and there are also complexes of Silurian alkaline granites, granites, and quartz monzonites (Seltmann and others, 2009). Later Silurian to Devonian rocks in the Kokchetav region are discussed elsewhere in this report. In the U terrane, there are some Silurian sections (unassigned age) of siliciclastic rocks.

Generally, collision-related, mesothermal low-sulfide quartz-gold deposits are widespread around and across the eastern half of the Precambrian Kokchetav massif, extending over to the S terrane. Most, but not all, are associated with Ordovician rock complexes. Letnikov and others (2009) obtained a very early Silurian U-Pb date (~441 Ma) for the postmagmatic arc host igneous complex in the Stepnyak mining district. This implies a collision event terminated magmatic-arc activity at the beginning of the Silurian, most likely with the Bozshakol'-Chingiz terrane (D. Alexeiev, Russian Academy of Sciences, written commun., 2010).

Implications of Mesothermal Gold Metallogeny to Porphyry Copper Deposit Potential in the Middle to Late Ordovician Stepnyak-North Tian Shan Magmatic Arc

Because mesothermal, low-sulfide quartz-gold deposits are widespread in the north and south of the North Tian Shan terrane, those that are well studied provide insights regarding the timing of collisional events and depths of exposure along ore-controlling structural zones. This information, in turn, is useful in assessing the potential for undiscovered porphyry copper deposits in this arc terrane.

Spiridonov (1995) describes low-sulfide quartz-gold deposits in north-central Kazakhstan as being along fault structures with reverse-sense displacement and hosted by greenschist-grade metamorphosed and deformed rocks. Associated alteration assemblages include sericite, mariposite, biotite, potassium feldspar (K-feldspar), albite, carbonate (ferrodolomite and siderite), and kaolinite or pyrophyllite. On the basis of trace and minor element zoning (Sb-Hg-Tl shallow to W-Te deep), relation of crack-seal veins to large-magnitude reverse faults, and mineral barometric estimates from associated igneous rocks, Spiridonov (1995) estimates the depths of formation of selected gold deposits in the Kokchetav region (fig. 1-17) to range from less than 1 to 3 km at the Bestobe deposits to 3–7 km at the Stepnyak deposit to 7–12 km at the Tsentral'nyi Dzhelambet deposit. These estimates imply a large amount of regional variation in uplift and erosion to depths below the level of formation of most porphyry copper deposits. As is evident from the distribution of orogenic gold deposits in the Kokchetav region (fig. 1-17), there has been significant vertical displacement on many tectonic boundaries.

Pressure-depth estimates comparable to those of Spiridonov (1995) are not available for the northern Tian Shan region of Kyrgyzstan. Although there are low-sulfide quartz-gold occurrences along most major fault zones in the western Tian Shan, the best available information pertinent to the Stepnyak-North Tian Shan magmatic arc is that regarding the Jerooy mesothermal gold deposit (fig. 1-18). At Jerooy, the paragenetic sequence is quartz-molybdenite-scheelite with tetradymite and bismuthinite altering molybdenite, quartz-pyrrhotite±pyrite-chalcopyrite-marcasite, quartz-pyrite±arsenopyrite, gold-bismuthinite-quartz±tetradymite, quartz-carbonate-boulangerite-jamesonite, and quartz-galena-carbonate (Davis, 2002). The molybdenite and scheelite are more typical of deeper and higher temperature deposits, whereas the antimony mineralization is more typical of generally shallower deposits. R. Goldfarb (USGS, oral commun., 2011) suggests that the Jerooy deposit may have formed as shallow as 3–7 km. Because the deposit-localizing shear zone, the Ichkelitau-Susamyr Fault Zone has a reverse-slip displacement component with south side up, porphyry copper deposits are more likely to occur to the north than to the south of this fault zone.

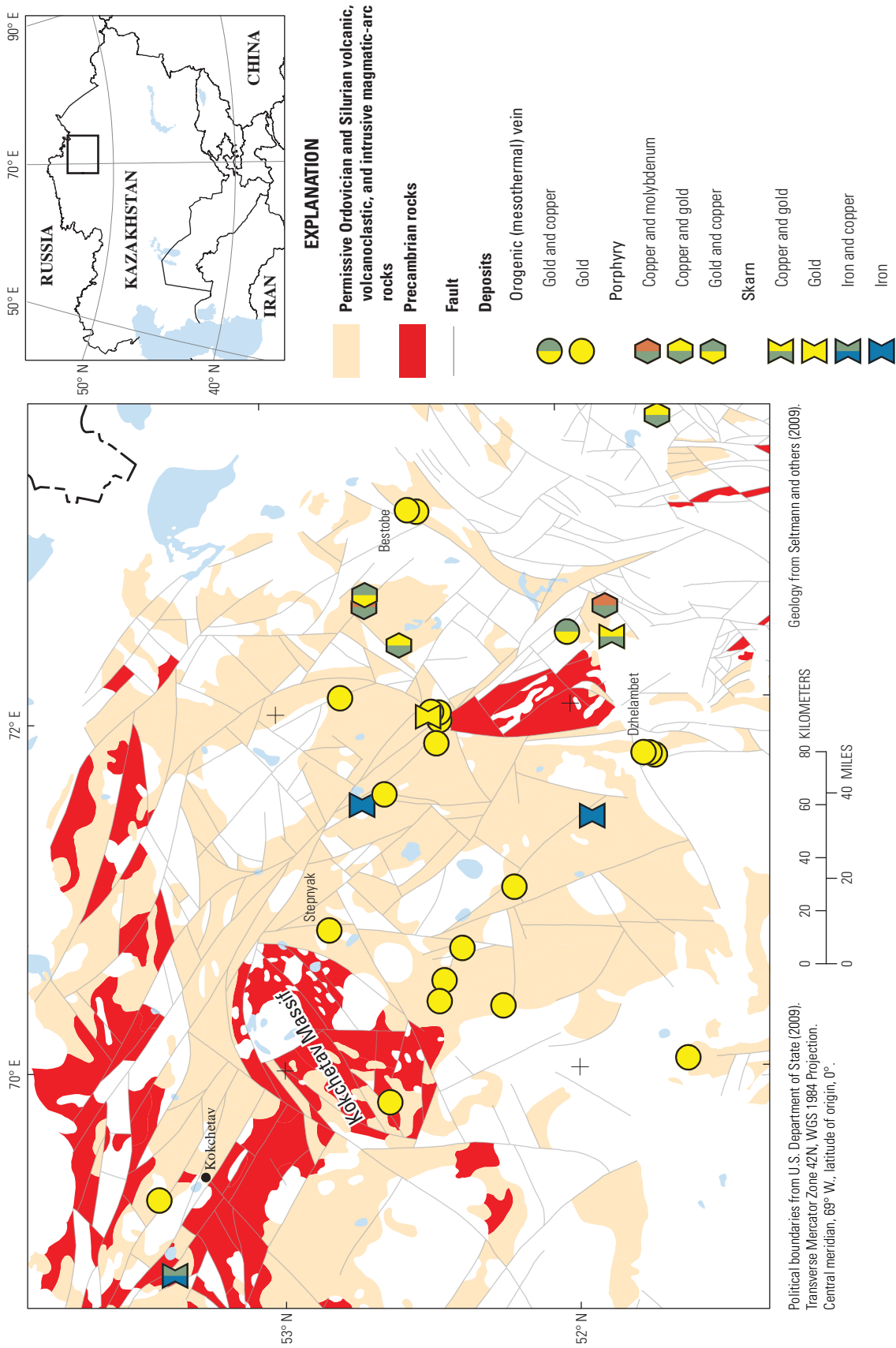


Figure 1-17. Map of the distribution of mesothermal (orogenic) low-sulfide quartz-gold vein deposits and occurrences, other selected occurrence types, and major faults in the vicinity of the city of Kokchetav in north-central Kazakhstan on a base showing Ordovician and Silurian map units likely to have been deposited in a magmatic-arc terrane (tan) and Precambrian rock outcrops (red). The Kokchetav Massif and selected mines are shown for reference. Location of map area shown on inset. (After Seltmann and others, 2009.)

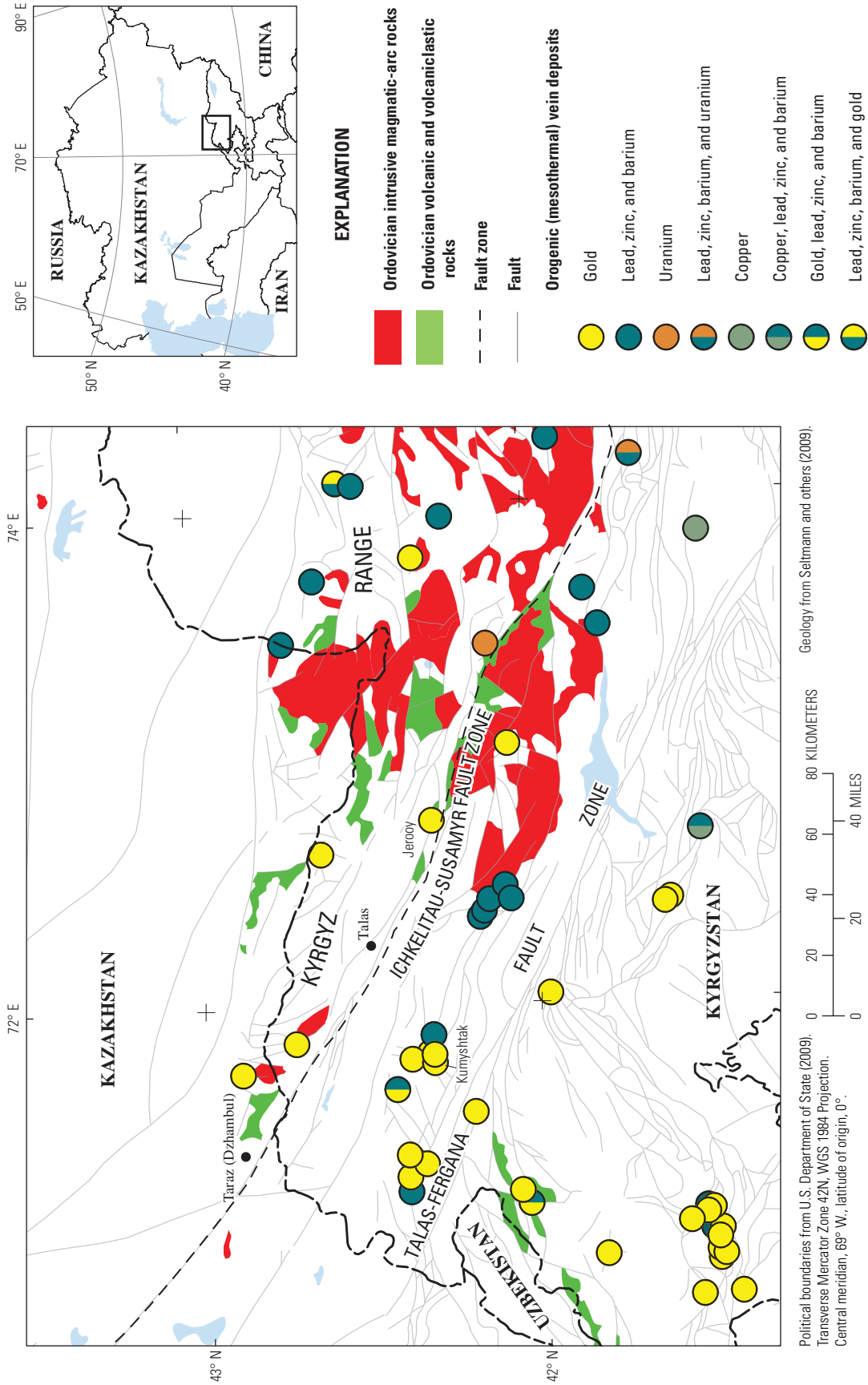


Figure 1-18. Map of the distribution of mesothermal (orogenic) vein deposits and occurrences and major faults in the western Kyrgyz Range and vicinity, Kyrgyzstan and Kazakhstan. Volcanic and volcaniclastic rocks likely to have been deposited in a magmatic-arc environment are shown in green. Intrusive rocks likely to have been emplaced in a magmatic-arc environment are shown in red. Selected mine names and towns are shown for reference. Location of map area shown on inset. (After Seltmann and others, 2009.)

The Bozshakol'-Chingiz Magmatic-Arc Terrane

The Bozshakol'-Chingiz (BC) magmatic-arc terrane is a hooked staff-shaped (present-day geography) area that has been separated into two parts, northwestern (the hook) and southeastern (the staff), by Late Paleozoic strike-slip faulting (fig. 1-16). The northwest segment is separated on the northwest from the Selety (S) terrane by the Erementau-Ili (EI) accretionary wedge and from the Baidaulat-Akbastau (BA) terrane by the Maikain-Kyzyltas (MK) terrane on the southeast (Windley and others, 2007).

The Cambrian of the northern EI terrane consists of a deformed Early to Middle Cambrian ocean-floor sequence with some arc-type rocks, a Middle Cambrian magmatic-arc sequence with porphyry-style copper mineralization, and a Late Cambrian to Middle Ordovician slope sequence with some arc-affinity volcanic rocks (Seltmann and others, 2009).

Northwestern Segment

The Middle Cambrian Bozshakol' magmatic arc (fig. 1-16) in which the Bozshakol' porphyry copper deposit (fig. 1-19) formed was built on an Early to Middle Cambrian ocean-floor sequence (Seltmann and others, 2009) consisting of tholeiitic basalt, basalt, and volcanogenic sedimentary rocks (Kheraskova and others, 2003). Ocean-floor deposits continue into the Early Ordovician, but the Middle to Late Ordovician consists of more continental, shallow-water sedimentary rocks (VMS deposits in fig. 1-19). The oceanic-arc rocks are exposed only in the northwestern corner of the northeast end of this segment of the BC terrane. Elsewhere in the domain, Cambrian outcrops are sparse and consist of ocean-floor rocks with only hints that intermediate to siliceous volcanic centers might have once been nearby but are now either covered by younger rocks or eroded away. Early Silurian rocks are widespread in the northwest BC terrane, consisting of terrestrial to perhaps shallow marine sandstones, siltstones, and conglomerates (Seltmann and others, 2009).

Windley and others (2007) show the northwestern hook of the BC terrane to pinch out to the southwest against a major northeast-trending suture zone (fig. 1-16). Before reaching the shear zone, however, the BC terrane becomes covered by Devonian rocks. The EI accretionary wedge similarly is buried beneath the Devonian to the southwest, but Windley and others (2007) correlate this unit with accretionary complexes to the south and thus show it to persist to the western end of Lake Balkhash, where it is tectonically truncated. The segments of the inferred correlative EI terrane are described elsewhere below.

Southeastern Segment

The southeastern segment of the BC terrane (fig. 1-16) is much like the northwestern segment in that the Cambrian magmatic arc, here known as the Chingiz Arc, was built on Cambrian deep-water marine rocks. These arc rocks crop out predominantly along the southwestern part of this terrane segment and are strongly deformed in proximity to

regional-scale faults. Numerous volcanogenic massive sulfide occurrences (Seltmann and others, 2009) (fig. 1-20) are suggestive that this arc section was submarine.

Remnants of a Middle Ordovician magmatic arc occur in the southern part of this segment. Copper-bearing volcanogenic massive sulfide occurrences (Seltmann and others, 2009) (fig. 1-20) indicate that the arc was submarine. A stockwork-style copper occurrence in proximity to a massive sulfide occurrence in the BC arc could be a remnant feeder zone to a submarine vent zone.

Lower Silurian rocks are siliciclastics, but late Early to Late Silurian mafic, intermediate to siliceous, and alkalic intrusions are likely remnants of a Silurian magmatic arc that was built across the BC, MK, and BA terranes (fig. 1-16). In the southern part of the combined terranes, Seltmann and others (2009) show some submarine volcanogenic massive sulfide occurrences with arc-related rock suites, particularly in the southern BA terrane, as well as subaerial porphyry copper, copper skarn, and porphyry-style copper-tungsten deposits associated with Early and Late Silurian rocks in all three terranes.

The Chu-Ili Microcontinental Terrane

The Kokchetav-North Tian Shan microcontinental block (NTS) was sutured to the Chu-Ili (CI) microcontinental block (fig. 1-16) along the Dzhair-Naiman shear zone, which is well delineated by strings of orogenic gold deposits (fig. 1-21). The Dzhair-Naiman (DN) accretionary wedge separates the two continental masses. Windley and others (2007) show the suturing to have occurred during the interval Late Cambrian to Early Ordovician based on the interpretation of Ordovician sedimentary rocks in the DN terrane as a fore-arc basin to the NTS arc. The fore-arc deposits are largely siliciclastic slope-rise deposits, and siliciclastic rocks characteristic of submarine fan and slope environments as young as Late Ordovician persist to the north along the fault zone (Popov and others, 2009). With the exception of a few tuffs, Popov and others (2009) record no Ordovician magmatic-arc or volcanoclastic rocks through the Middle Ordovician.

The oldest dated Cambrian rocks in the DN block are pillow lavas and chert underlain by gabbro that is intruded by Middle Cambrian dikes (Popov and others, 2009). The next younger rocks above this ocean-floor sequence, probably along a tectonic contact, are Late Cambrian to Early Ordovician, predominantly siliciclastic rocks, although some carbonate and mafic volcanic and intrusive rocks are present (Seltmann and others, 2009). Seltmann and others (2009) show volcanogenic massive sulfide occurrences in association with these ocean-floor rocks (fig. 1-21). Elsewhere, some Middle Ordovician sections contain tuffs, and there is a relatively small exposure of Early to Middle Ordovician basaltic and andesitic volcanic rocks associated with marine carbonate rocks (Popov and others, 2009) within the Dzhair-Naiman Fault Zone. These sections are intermingled with Lower Ordovician ophiolite fragments.

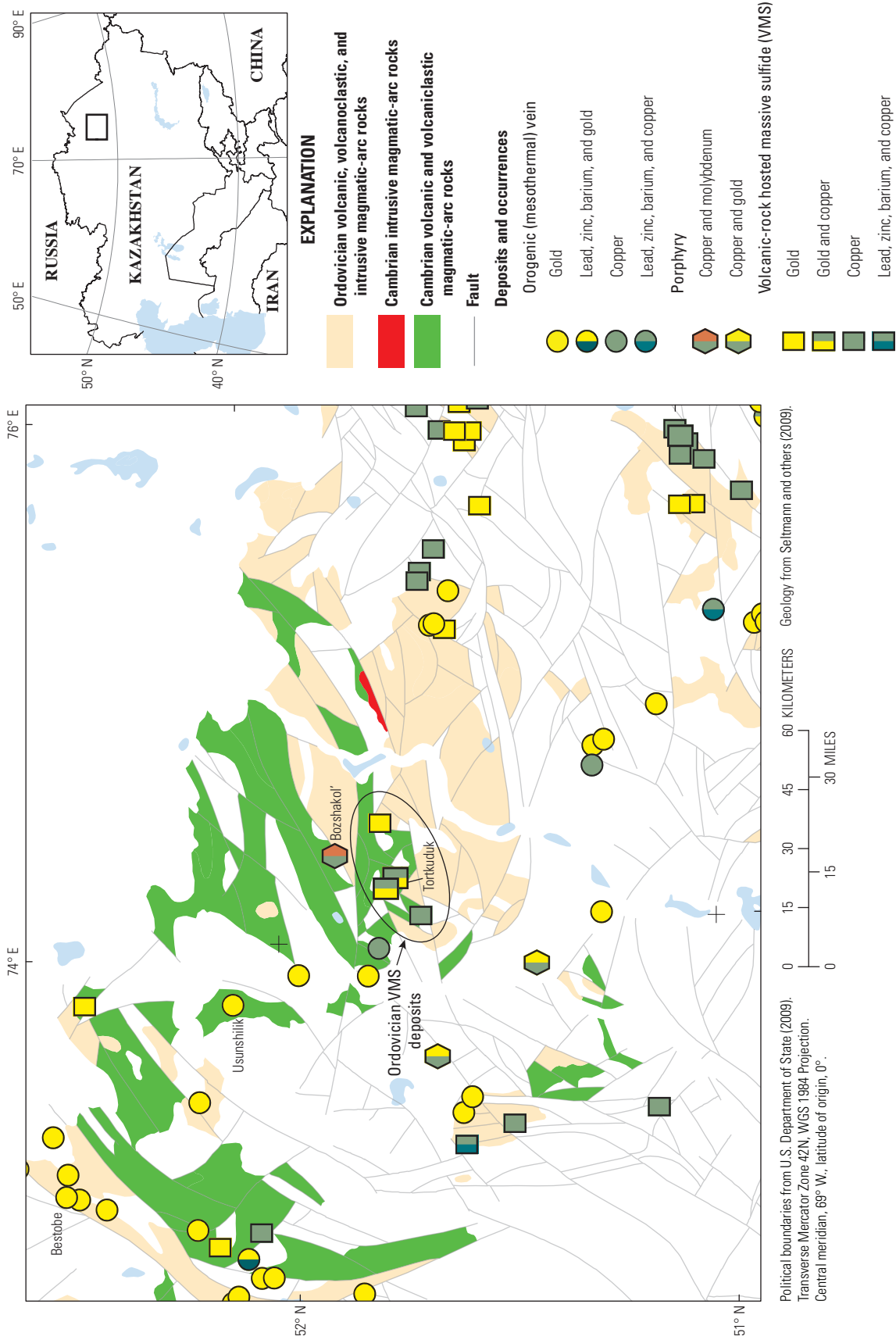


Figure 1-19. Map showing the location of the Bozshakol' porphyry copper deposit on a geographic base showing Cambrian stratified rocks likely to have been deposited in a magmatic-arc environment shown in green, Cambrian intrusive rocks likely to have been employed in a magmatic-arc environment in red, and Ordovician probable magmatic-arc rocks (undivided) in tan. The locations of porphyry copper occurrences and massive sulfide occurrences formed in a submarine arc environment are shown. Selected mine names are given for reference. Location of map area shown on inset. (After Seitmann and others, 2009.)

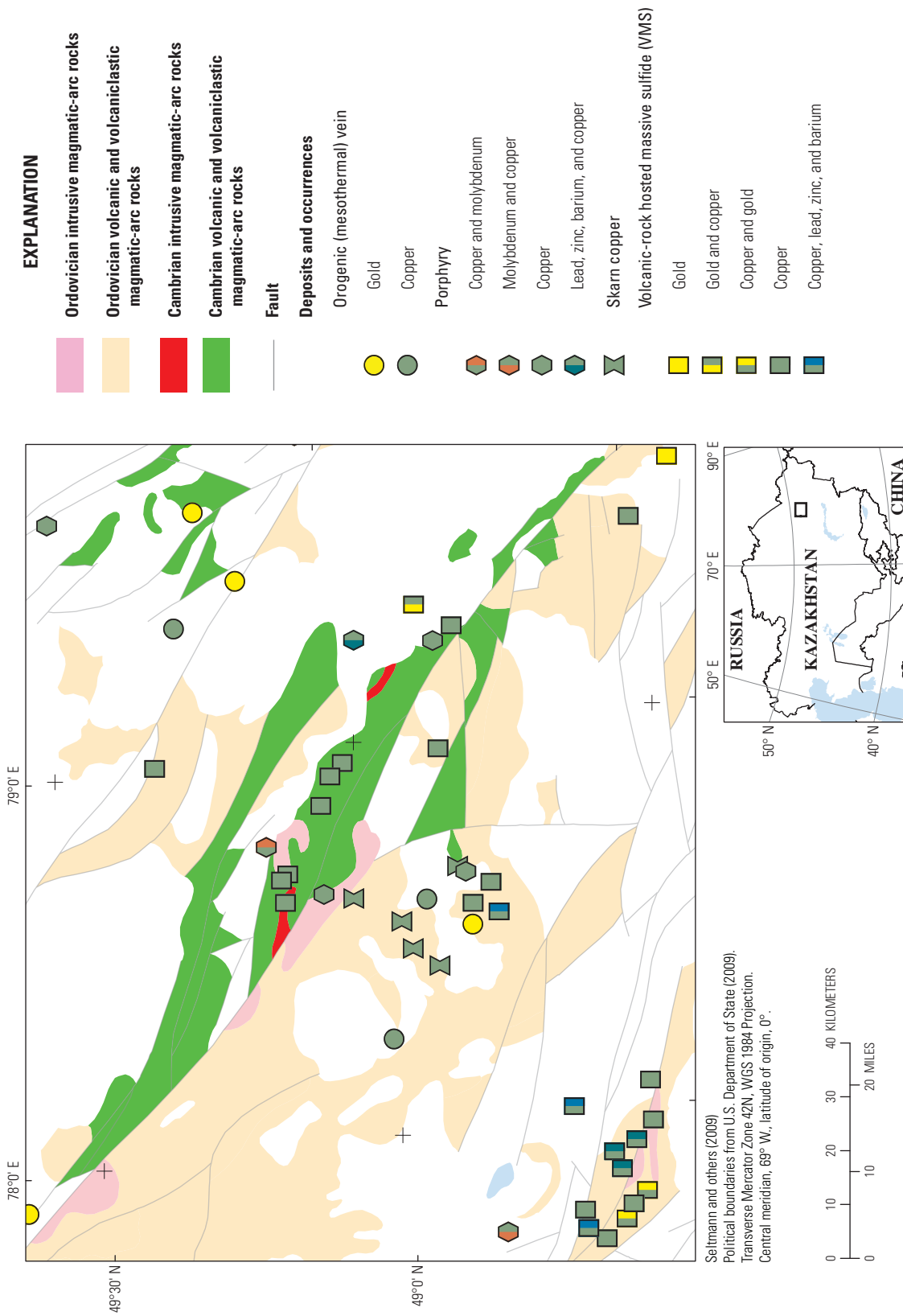


Figure 1-20. Map showing the distribution of likely magmatic-arc rocks of Cambrian and Ordovician age in eastern Kazakhstan. The locations of numerous massive sulfide, mesothermal (orogenic) vein, and porphyry-type occurrences shown. Orogenic occurrences imply strong deformation and uplift; volcanicogenic massive sulfide occurrences imply submarine arc conditions. Location of map area shown on inset. (After Seltmann and others, 2009.)

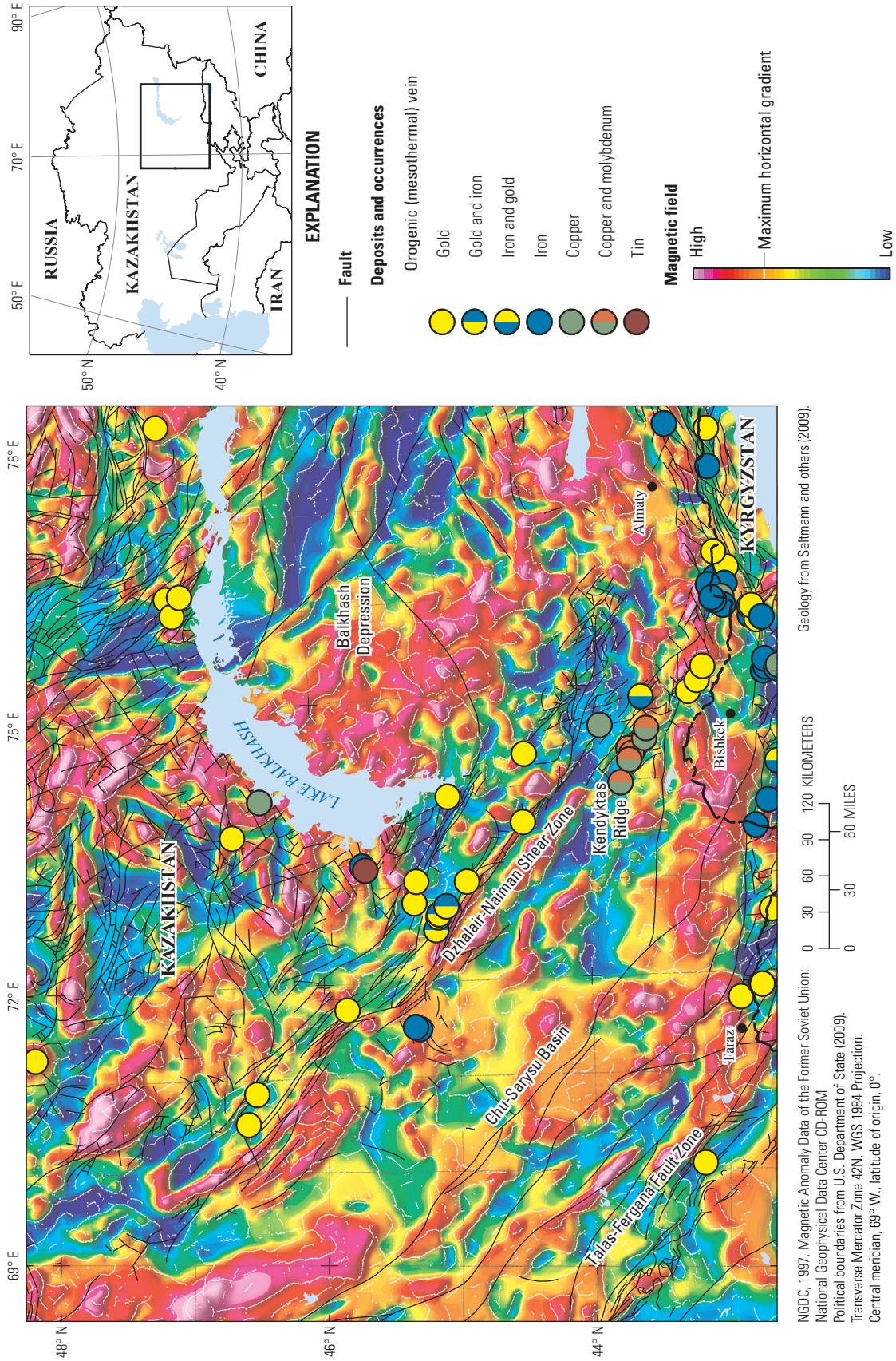


Figure 1-21. Map showing location of the Dzhalaïr-Naiman shear zone, major faults, tectonic lineaments, and selected mineral deposits (from Seltmann and others, 2009) in south-central Kazakhstan on a reduced-to-pole aeromagnetic base. Mesothermal (orogenic) vein deposits and occurrences indicate where tectonic uplift has been the greatest. Location of map area shown on inset. Selected cities and geographic features shown for reference.

Cambrian rocks in the CI terrane to the northeast of its structural boundary with the DN terrane (fig. 1-16) consist primarily of mixtures of deep-ocean siliciclastic rocks, cherts and shales, and submarine fan and slope deposits (Popov and others, 2009; Seltmann and others, 2009). Farther north in the CI terrane, exposures are of Lower to Upper Ordovician suites that are mixtures of marine siliciclastic and carbonate rocks. On the western and eastern margins of the CI terrane are mélanges with remnants of Late Cambrian to Early Ordovician arc-related basalts and andesites. These mélanges are part of the DZ terrane on the southwestern margin of CI and the EI terrane on the northeastern margin. The fault zone juxtaposing the CI and EI terranes (fig. 1-16) is known as the Sarytuma zone. In the EI mélange southeast along the Sarytuma zone, a part of the terrane shown by Popov and others (2009) but not shown on Windley and others (2007), Seltmann and others (2009) show stockwork-style mineral occurrences in the Early to Middle Ordovician rocks. To the northwest along the Sarytuma Fault Zone, Seltmann and others (2009) show volcanogenic massive-sulfide occurrences in the mélange, implying that these arc remnants were submarine.

Few Silurian rocks are preserved in the CI and adjacent DZ and EI terranes. Where found, they consist predominantly of siliciclastic rocks.

Toward its northern end, directly to the west of Lake Balkhash (fig. 1-2C), the DZ accreted wedge is in tectonic contact with the EI accreted wedge (fig. 1-16). This relation persists for at least 200 km to the northwest, where both tectonic blocks are covered by younger rocks. The eastern margin of the EI terrane is not exposed; its easternmost exposure forms the margin of Lake Balkhash at its southwesternmost end.

Aktau-Junggar Microcontinental Terrane

About 155 km northwest of the northwest margin of Lake Balkhash is a Precambrian microcontinental mass known as Aktau-Junggar (AJ) (fig. 1-22). In the north, the exposed part of this terrane is small and triangular shaped, but, beneath Devonian and Carboniferous magmatic-arc sequences, it is widespread. Windley and others (2007) show it to be the basement to not just a region from Lake Balkhash to the northwest but also to much of the Balkhash Depression region (fig. 1-2C) to the south of Lake Balkhash. The western boundary of the AJ terrane for most of its extent is a tectonic zone that juxtaposes the EI terrane. In the exposed part of the terrane, Vendian to Early Cambrian suites consist of mixtures of siliciclastic and carbonate rocks (Seltmann and others, 2009). Early to Middle Ordovician suites consist of predominantly siliciclastic rocks but also contain some limestone. There are a few Late Ordovician granodiorite intrusions, one of which may be related to a porphyry copper occurrence in an adjoining ultramafic intrusive complex (see Seltmann and others, 2009). Early to Middle Silurian suites consist of siliciclastic, carbonate, and magmatic arc-type volcanic rocks. Porphyry copper and skarn-type copper-zinc-lead deposits are shown by Seltmann and others (2009)

in association with the Silurian rocks, but their age is equivocal owing to the widespread overlap of Devonian and Carboniferous magmatic-arc rocks in this region. To the north, the AJ terrane is tectonically juxtaposed to the Zhaman-Sarysu (ZS) microcontinental block (fig. 1-22).

Zhaman-Sarysu Microcontinental Terrane

Cambrian rocks are absent in the ZS terrane (fig. 1-22). The oldest Paleozoic rocks are Late Ordovician to Early Silurian magmatic-arc rocks found primarily in the west-southwest of the exposed part of this terrane. Volcanogenic massive sulfide deposits indicate that most of this arc segment was submarine, although Seltmann and others (2009) show there to be a few porphyry-style copper occurrences associated with these rocks. Nevertheless, the predominance of sedimentary rocks in most Silurian units, together with widespread overlap of Devonian and Carboniferous magmatic-arc rocks, puts in question a Silurian age of any of the identified porphyry copper occurrences.

Upper Cambrian to Early Ordovician rocks in the EI terrane on the west of the ZS consist predominantly of siliciclastic rocks, including deep-water cherts and shales, but the occurrence of tuffaceous sandstones indicates proximity to volcanic centers. Volcanogenic massive sulfide occurrences suggest that the volcanic sequence was submarine.

The northern boundary of the ZS terrane is buried beneath Devonian magmatic-arc rocks, but Windley and others (2007) link it into a suture zone between the Maikain-Kyzyltas (MK) accretionary wedge and the Baidaulet-Akbastau (BA) magmatic arc.

Baidaulet-Akbastau Magmatic-Arc Terrane

The Baidaulet-Akbastau (BA) terrane is accreted to the BC terrane across the MK accretionary wedge (fig. 1-16) (Windley and others, 2007). Alexeiev (2008) suggests that the BA-MK suture is middle Late Ordovician. There are only a few areas within the BA terrane where remnants of a Late Cambrian to Early Ordovician magmatic arc are exposed. Descriptions in Seltmann and others (2009) are suggestive that an andesitic arc was built on Cambrian-age deep-water sedimentary and mafic volcanic rocks. Submarine volcanogenic deposits, valuable primarily for their contained gold, indicate that the Cambrian to Ordovician BA arc was submarine. Volcanogenic massive sulfide deposits, of importance for copper and other base metals as well as gold, indicate that submarine magmatic-arc volcanism persisted, likely intermittently, throughout the extent of the BA arc into the Late Ordovician. One or two stockwork-style copper-gold occurrences in the southeastern part of the BA terrane are associated with volcanogenic massive sulfide occurrences and are likely exposures of stringer zones that formerly underlay massive sulfide occurrences rather than being porphyry-style deposits.

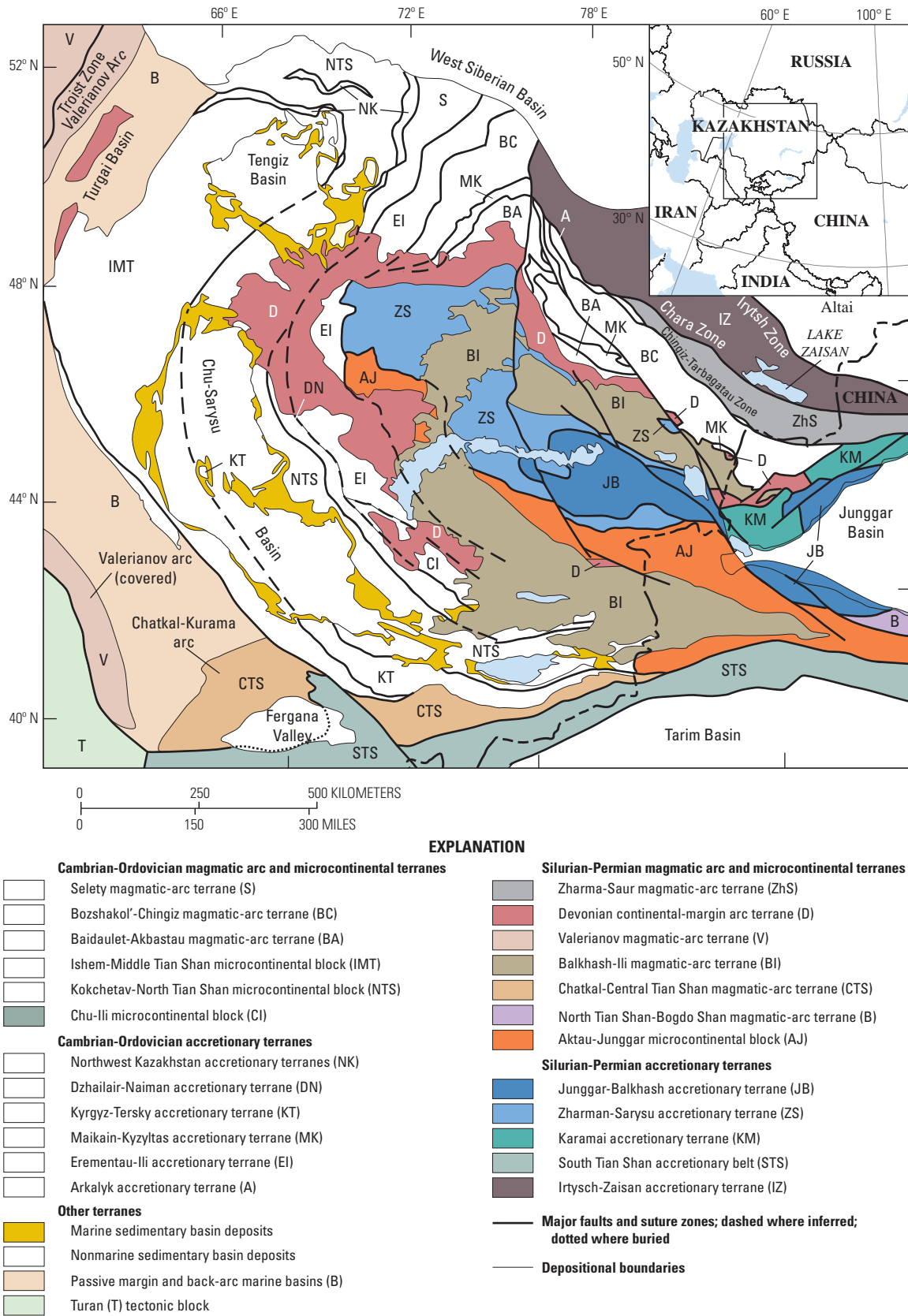


Figure 1-22. Modified lithotectonic terrane map of western Central Asia (refer figure 1-7) after Windley and others (2007), highlighting Devonian and Carboniferous magmatic-arc and accreted terranes. Location of map area shown on inset.

Early Silurian outcrops of siliciclastic rocks are widespread across the MK and BA terranes. The Early Silurian is not prospective for porphyry copper deposits, and it is likely that the scattered epizonal mineral occurrences, including epithermal and porphyry styles shown by Seltmann and others (2009) within the Silurian rocks, are related to Devonian and younger arc-related suites that intrude the Silurian.

A string of ophiolite blocks delineate the suture zone between the BA and MK accretionary wedge terranes. In the MK terrane, a tectonic mixture of Late Ordovician siliciclastic rock suites and volcanic-arc suites suggests that the middle Late Ordovician collision terminated subduction in the Late Ordovician BA arc.

Postsuturing strike-slip faulting (fig. 1-16) has lent the BA, MK, and BC terranes a composite, tightly hooked shape around a regional-scale north-south, right-lateral strike-slip fault (fig. 1-23). Alexeiev (2008) suggests that this small orocline-like bend developed during the Late Carboniferous to Early Permian.

Mid-Paleozoic: Devonian

By the Early Devonian, the many microcontinental blocks, accretionary wedges, and Cambrian to Silurian magmatic arcs across central and southern Kazakhstan had been assembled into a single mass, the Kazakhstan continent marginal to which Devonian subduction and associated magmatic-arc volcanism occurred. However, it was still not the completed landmass of today because the new Kazakhstan continent was still separated by oceans from the Siberian, East European (Baltica), and Tarim cratonic masses (fig. 1-8).

In a palinspastic reconstruction of the new Kazakhstan continent in the Early Devonian by Windley and others (2007), the Uralian Ocean separated Kazakhstan from the Magnitogorsk and Khanty-Mansi oceanic arcs to the southwest off the East European craton coast, the Turkestan Ocean separated then eastern Kazakhstan from the Tarim cratonic mass farther to the east, the Junggar-Balkhash Ocean bordered Kazakhstan on the north, and the Ob-Zaisan Ocean separated Kazakhstan from Siberia to the northwest.

Devonian magmatic-arc rocks are scattered across the whole of the assessed region (figs. 1-24–1-26) and reflect a renewal of subduction following the amalgamation of the Early Devonian Kazakhstan continent. The most continuous and conspicuous belt of Devonian rocks forms a tight, 1,600-km long, southeast-opening, horseshoe-shaped domain in Central Kazakhstan (figs. 1-22 and 1-24). From the vicinity of the city of Ayaguz (fig. 1-27) near the end of its southeast limb to the southwestmost limb in the Chu-Ili Range along the west side of the Balkhash Depression, the chain of volcanoes represents a once, slightly arcuate northwest-trending arc (Abrajevitch and others, 2007) that was oroclinally bent owing to the convergence of the Baltica, Siberia, and Tarim cratonic blocks (fig. 1-8) on the evolving Kazakhstan continent. The

orocline can be no older than Middle Devonian (Abrajevitch and others, 2007) nor younger than Late Permian (Abrajevitch and others, 2008). Abrajevitch and others (2008) suggest that oroclinal bending might have begun during the Late Devonian as a consequence of the initial collision of the Tarim craton with the new Kazakhstan continental assemblage, which Heubeck (2001) interpreted to have occurred in a scissor-like fashion and was completed by middle Early Carboniferous. In the discussions below, it is assumed that scattered pieces of the Devonian magmatic arc in the northern Tian Shan ranges, North Tian Shan tectonic block (fig. 1-28), and the oroclinally bent arc once were parts of a once more or less continuous arc that developed in a northwest-southeast orientation owing to southwest-directed subduction of the Junggar-Balkhash lithosphere off the Devonian northeast Kazakhstan coastline (see Windley and others, 2007).

Zharma-Saur Magmatic-Arc Terrane

The terrane on which the Devonian to Carboniferous Zharma-Saur (ZhS) magmatic-arc was built (fig. 1-22) is accreted across the Arkalyk (A) accretionary wedge to the southeastern southeast segment of the BC terrane (Windley and others, 2007). Alexeiev (2008) shows the time of accretion to be Cambrian to Ordovician, but the occurrence of Silurian magmatic-arc rocks on both sides of the suture zone are indicative that the time of docking was no later than Late Ordovician. Owing to extensive cover by younger rocks, including the ZhS arc rocks, there is only a relatively small region near the Kazakhstan-China border where Early Silurian arc-related rocks are exposed.

Subduction of Junggar-Balkhash Ocean Plate

Subduction beneath mid-Paleozoic Kazakhstan began during the Early Devonian (see Seltmann and others, 2009). Using paleomagnetic data, Abrajevitch and others (2007) reconstructed the Devonian arc of Central Kazakhstan and determined it was generally a northeast-facing, northwest-southeast trending arc (Devonian coordinates) with subduction occurring beneath Kazakhstan along its boundary with the Junggar-Balkhash plate to the northeast. The southeastern end (Devonian coordinates) crops out in present-day southernmost Kazakhstan in the North Tian Shan tectonic block (fig. 1-28), but tectonically has been severely fragmented and interleaved with stratigraphic sections deposited in non-arc environments. Farther south and to the west, two Early and Middle Devonian suites were combined by Seltmann and others (2009) in a single map unit, one consisting of andesite, basalt, and mafic tuff (ocean floor), the second of dacite and rhyolite (magmatic arc) (Seltmann and others, 2009). Base-metal vein occurrences are shown by Seltmann and others (2009), as well as a volcanogenic massive sulfide (VMS) occurrence.

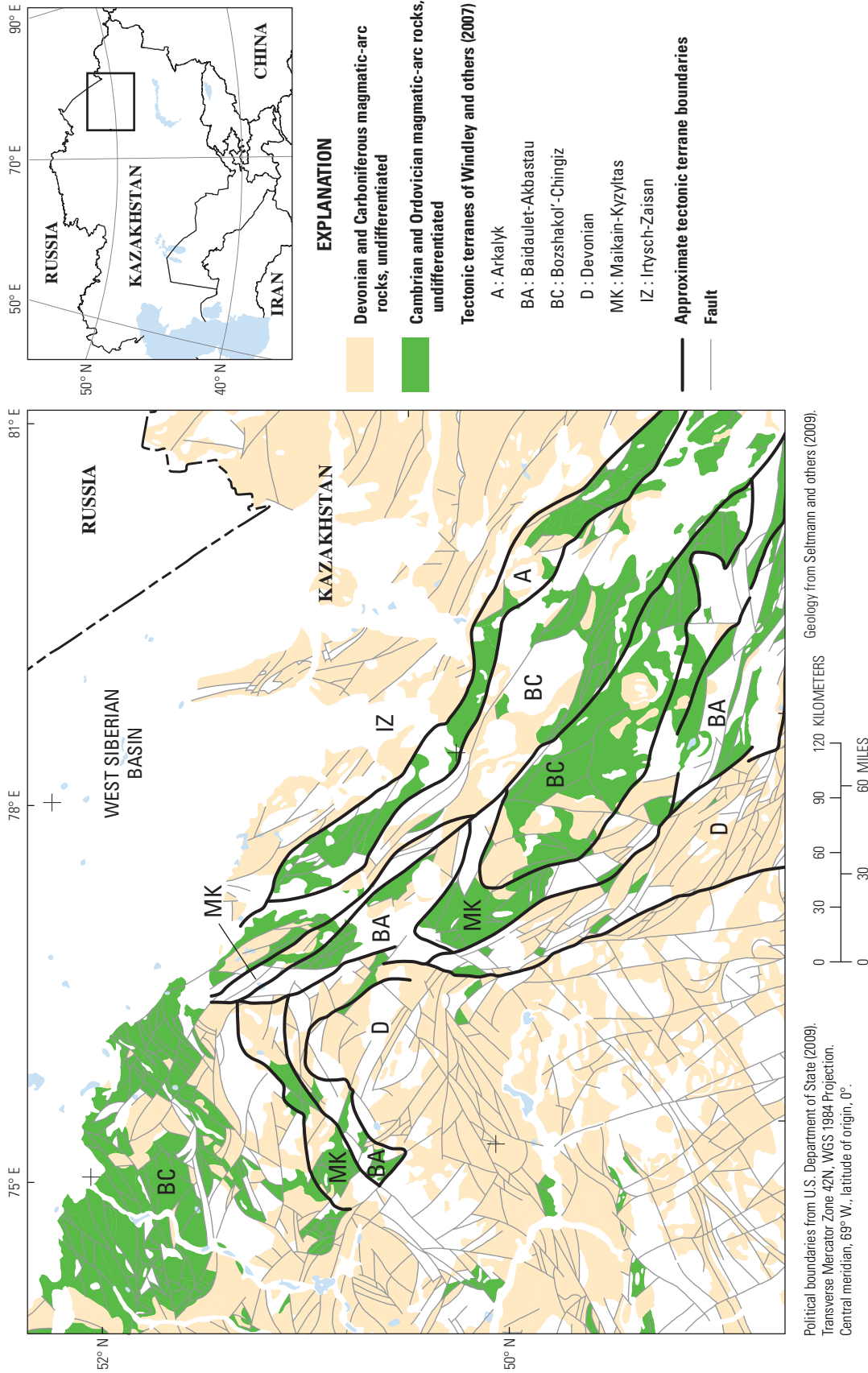
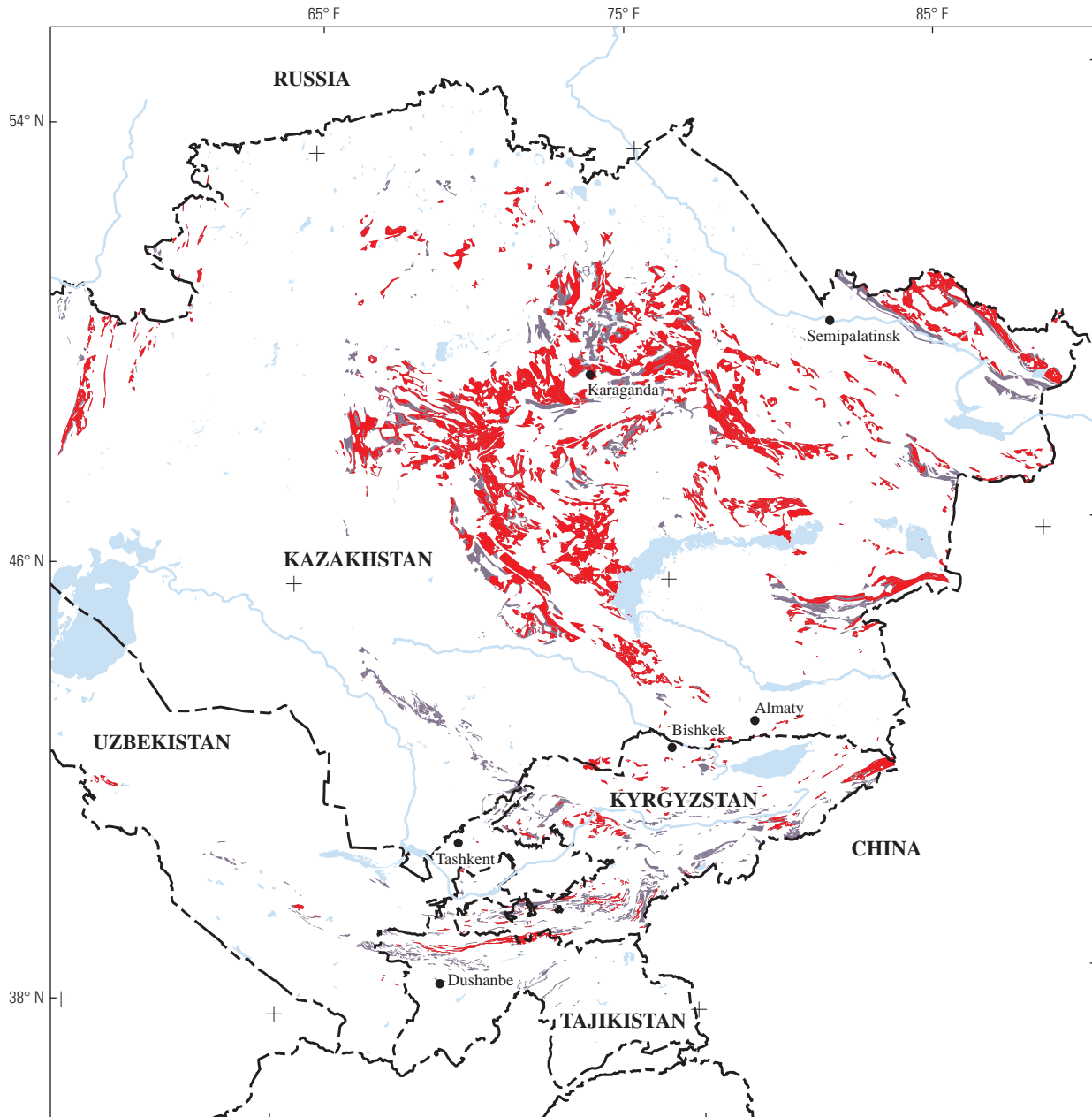


Figure 1-23. Map showing distribution of Cambrian and Ordovician magmatic-arc rocks in relation to Devonian and Carboniferous magmatic-arc rocks on a fault base (light gray lines) (after Seltmann and others, 2009) in northeastern Kazakhstan. The lithotectonic terranes of Windley and others (2009) are shown for reference; the terrane boundaries (dark lines) are approximately located. The map pattern of the Cambrian and Ordovician rocks is hook-shaped (oroclinal bend?) in response to regional-scale strike-slip faulting. Location of map area shown on inset.



Political boundaries from U.S. Department of State (2009).
 Transverse Mercator Zone 42N, WGS 1984 Projection.
 Central meridian, 69° W., latitude of origin, 0°.

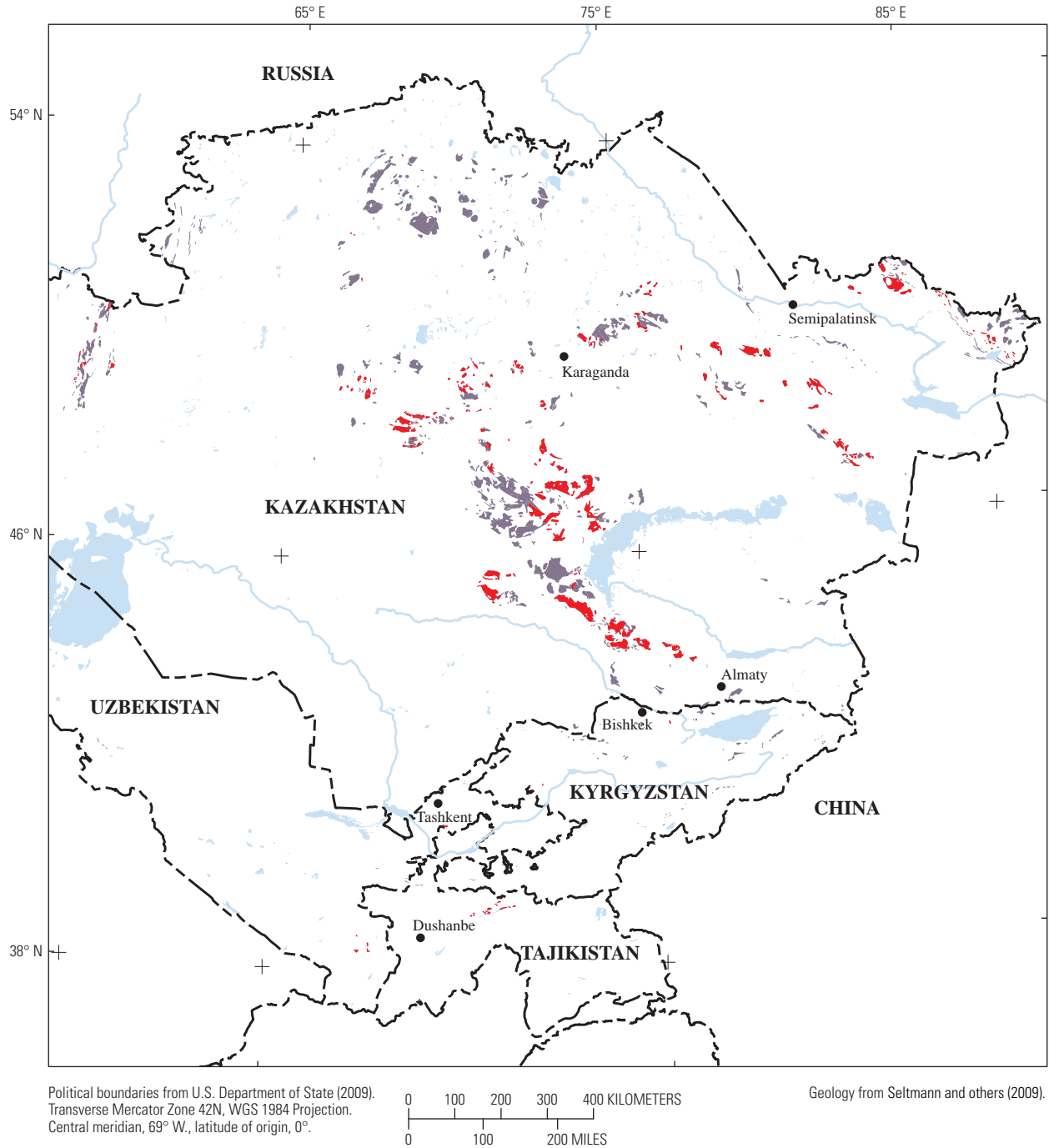


Geology from Seltmann and others (2009).

EXPLANATION

- Devonian stratified rocks deposited in magmatic-arc terranes
- Devonian stratified rocks not associated with magmatic-arc terranes

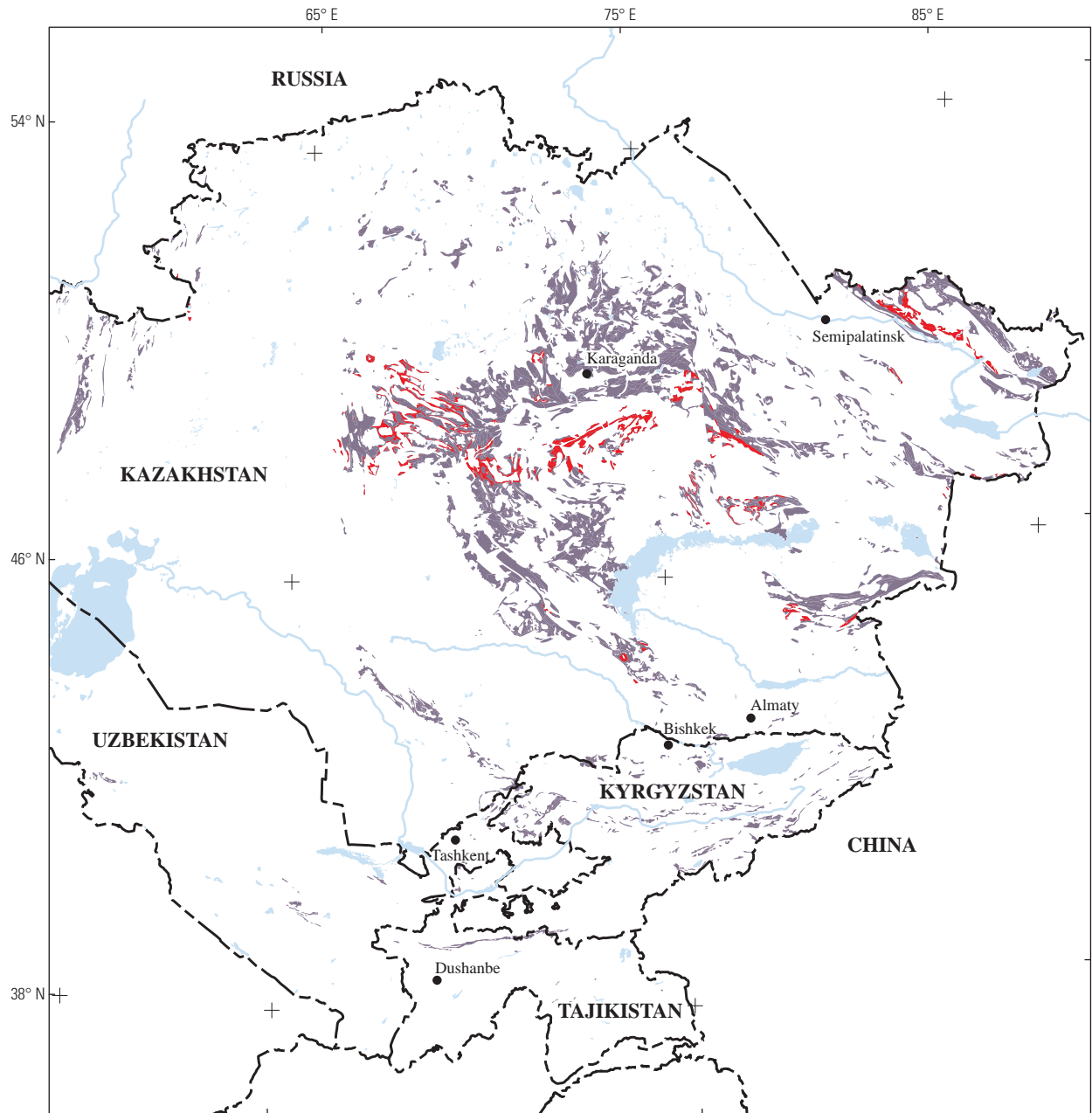
Figure 1-24. Map showing the distribution of Devonian stratified rocks in the western Central Asia study area likely to have been deposited in a magmatic-arc environment (red). Those map units containing rock types not likely to have been deposited in magmatic-arc terranes are shown in lavender. (After Seltmann and others, 2009.)



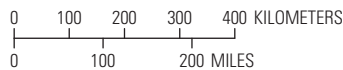
EXPLANATION

- Devonian intrusive rocks emplaced in magmatic-arc terranes
- Devonian intrusive rocks not associated with magmatic-arc terranes

Figure 1-25. Map showing the distribution of Devonian intrusive rocks in the western Central Asia study area likely to have been emplaced in a magmatic-arc environment (red). Those intrusive rocks not likely to have been emplaced in magmatic-arc terranes are shown in lavender. (After Seltmann and others, 2009.)



Political boundaries from U.S. Department of State (2009).
 Transverse Mercator Zone 42N, WGS 1984 Projection.
 Central meridian, 69° W, latitude of origin, 0°.



Geology from Seltmann and others (2009).

EXPLANATION

- Upper Devonian stratified rocks deposited in magmatic-arc terranes
- Devonian stratified rocks not associated with magmatic-arc terranes

Figure 1-26. Map showing the distribution of Upper Devonian (D_3) rocks in the western Central Asia study area likely to have been deposited in magmatic-arc environments shown in red (after Seltmann and others, 2009). Those map units containing Upper Devonian rock types not likely to have been deposited in magmatic-arc terranes are shown in lavender. The Late Devonian magmatic-arc rocks indicate the locations of the last stages of Devonian subduction in western Central Asia prior to widespread Carboniferous magmatic-arc volcanism.

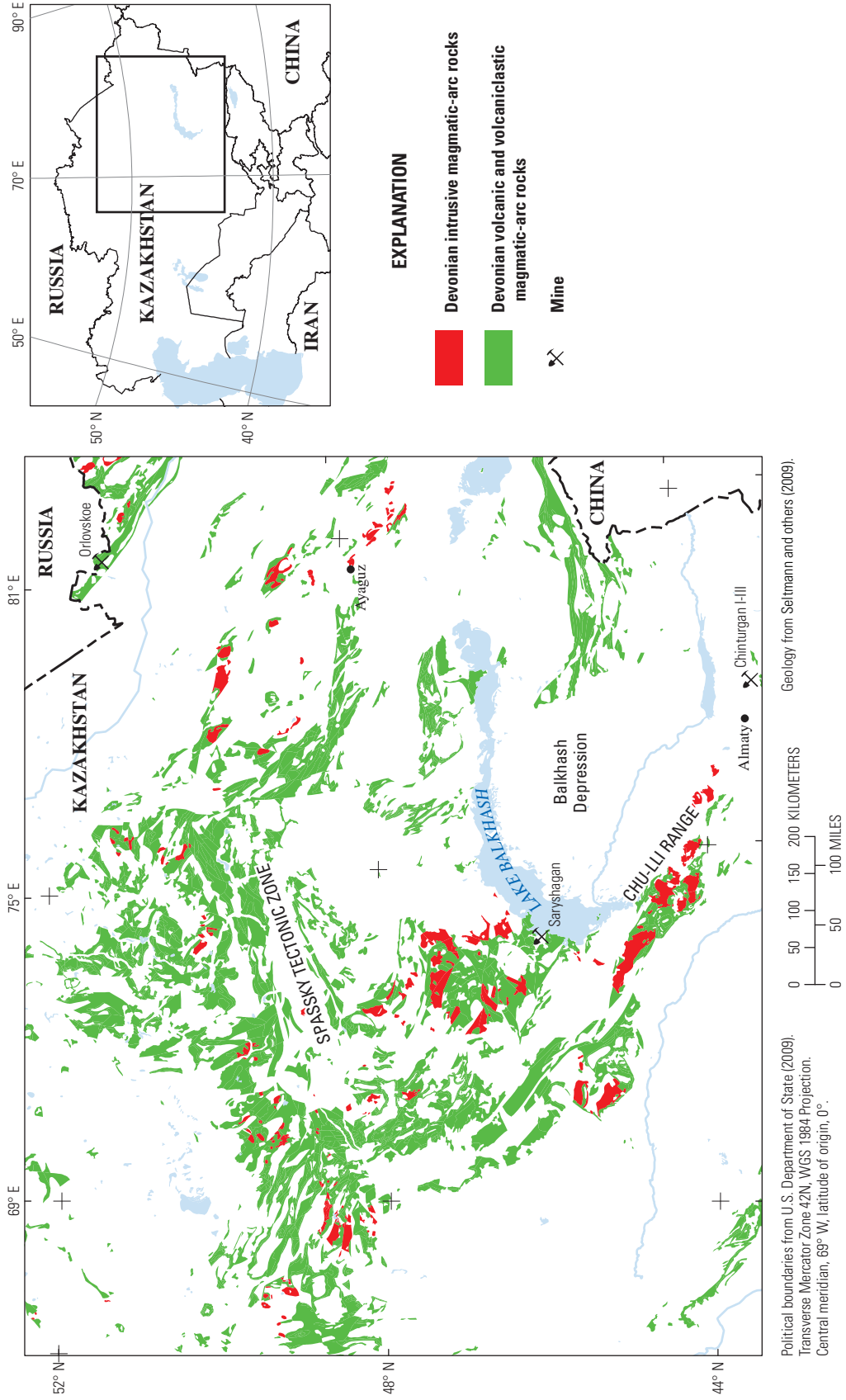


Figure 1-27. Map of selected geographic and tectonic features and mineral deposits showing the distribution of Devonian stratified (green) and intrusive (red) rocks in western Central Asia. Location of map area shown on inset. (After Seltmann and others, 2009.)

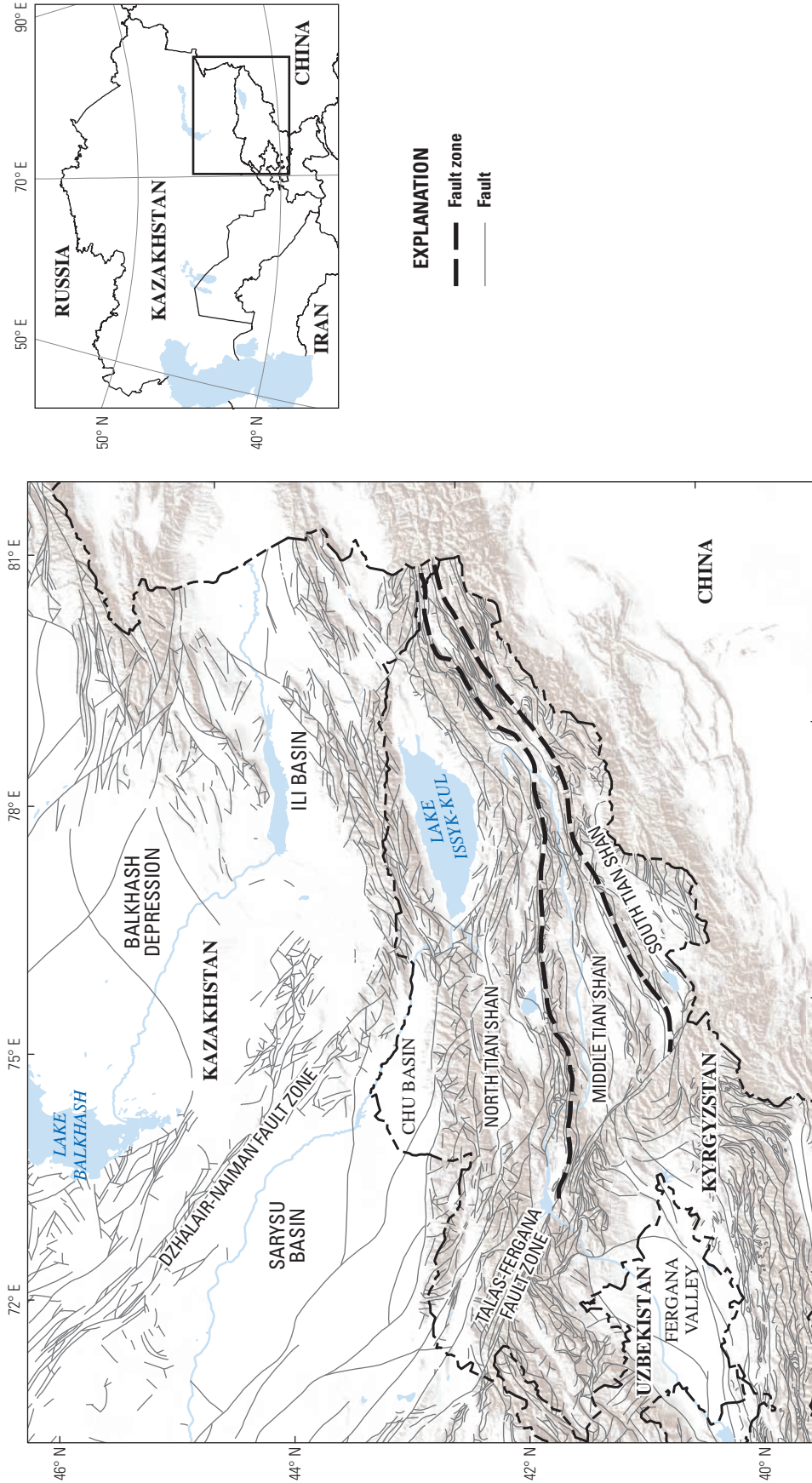


Figure 1-28. Map showing the principal tectonic units (black, dashed boundaries) in the Tian Shan ranges of Kyrgyzstan and southern Kazakhstan on a fault and digital elevation base. Selected geographic locations and fault zones labeled for reference. Location of map area shown on inset. (After Seltmann and others, 2009.)

Seltmann and others (2009) describe one of the veins as a small polymetallic mesothermal occurrence known as the Chinturgen I-III (fig. 1-27), implying a syndeformation genesis. A lack of descriptive information precludes knowing how the VMS occurrence relates to either of the two lithologic suites, but it is suggestive of a submarine volcanic back-arc or mid-ocean ridge environment. Widely separated outcrops of Early to Middle Devonian suites with arc-type volcanic rocks persist to the tectonic boundary between the North Tian Shan and Middle Tian Shan tectonic blocks. Early Devonian basalt-andesite-rhyolite arc-type volcanic rocks crop out in the western Kyrgyz Range (fig. 1-2A) of Kyrgyzstan and directly overlie copper-gold porphyry mineralized Late Ordovician Kokchetav-North Tian Shan magmatic-arc rocks (fig. 1-18). Seltmann and others (2009) show no significant mineral occurrences in the Devonian rocks. Two intrusive rock suites are associated with the volcanic rocks, one consisting of granophyres and granite, the second of syenites. Immediately south in the Kyrgyz-Tersky (KT) accretionary wedge (fig. 1-16), Early to Middle Devonian rocks include siliciclastic rocks assemblages, as well as magmatic-arc assemblages. South across the suture zone between the KT and Ishim-Middle Tian Shan (IMT) terranes, Middle to Late Devonian rocks consist of passive margin sedimentary rock sequences (see Seltmann and others, 2009).

In the central Tian Shan to the south of the North Tian Shan–Middle Tian Shan tectonic block suture (fig. 1-28), Middle to Late Devonian rocks are sedimentary analogs to the IMT rocks noted above. Yet farther south, the Early to Middle Devonian rocks in the South Tian Shan tectonic block are sedimentary, whereas Middle to Late Devonian rocks include mafic volcanic to tuffaceous rocks. Seltmann and others (2009) report no mineral occurrences in South Tian Shan volcanic rocks. Several small massive sulfide deposits occur in ophiolite fragments along the Middle Tian Shan–South Tian Shan suture zone.

Devonian: North

A more than 350-km long, northwest-southeast-trending belt of Early to early Middle Devonian magmatic-arc and associated gabbroic to granitic intrusive rocks are exposed, although granodioritic intrusions are most abundant, in easternmost present-day Kazakhstan, where they are tectonically juxtaposed across the Irtysh suture zone (location in fig. 1-22) to the east margin of the Irtysh-Zaisan accretionary wedge terrane (fig. 1-22, IZ) of Windley and others (2007). Numerous copper-bearing volcanogenic massive sulfides occur in this region (Seltmann and others, 2009), implying that this part of an arc along the Devonian southeast margin of the Junggar-Balkhash Ocean was submarine. The large Orlovskoe massive sulfide deposit (fig. 1-27) is described by Seltmann and others (2009) to be stratigraphically conformable with Middle to Late Devonian

volcanogenic sedimentary rocks and associated with plagiogranite porphyritic intrusions.

To the northwest of Lake Zaisan (location in fig. 1-2A), Early Devonian arc rocks are caught up in a suture zone with Middle to Late Devonian ophiolites (Seltmann and others, 2007). These may be part of an arc sequence to the southwest that Windley and others (2007) call the Devonian to Carboniferous Zharma-Saur magmatic-arc terrane (fig. 1-22). Early to Middle Devonian andesitic to dacitic arc-related rocks are exposed in relatively small structural blocks (for example, 40 by 10 km or so) within this terrane that consist primarily of Carboniferous rocks. Small exposures of Devonian (?) ophiolite (Seltmann and others, 2009) are suggestive that the Zharma-Saur arc was built on the Arkalyk accretionary wedge terrane (fig. 1-16) of Windley and others (2007), which also hosts remnants of Early to Middle Silurian magmatic-arc rocks.

Across present-day Central Kazakhstan, west of the Chingiz-Tarbagatay shear zone (location in fig. 1-22), the Devonian arc rocks are more continuously exposed (fig. 1-24). This is the northeast (present-day) end of the southeast-opening, horseshoe-shaped orocline of Central Kazakhstan. Over all, the tightly bent orocline is generally bilaterally symmetric and on the order of 1,600 km from tip to tip.

Seltmann and others (2009) show a number of porphyry-style copper, copper-gold, and copper-tungsten deposits in association with the Early to Middle Devonian arc-related rocks. Unlike the Devonian arc to the east of the Irtysh suture zone (fig. 1-22), however, the Zharma-Saur Arc was subaerial.

Upper Paleozoic: Carboniferous-Permian

Depending on which paleogeographic reconstruction one presumes, perhaps three Carboniferous magmatic arcs were active around the margin of the Kazakhstan block immediately preceding the final completion of the tectonic collage known today as western Central Asia. The distribution of these arc rocks is shown in figures 1-29 through 1-32. In western Kazakhstan, the Valerianov arc (fig. 1-22) formed above an east-dipping subduction zone into which the Uralian Ocean was closing. Concurrently, volcanism was active in southern Kazakhstan, Kyrgyzstan, and eastern Uzbekistan above north-dipping subduction that was closing the remnants of the Turkestan Ocean, as well as in present-day central Kazakhstan where the Balkhash-Ili Arc marks the final closing of the Junggar-Balkhash Ocean. In some syntheses (for example, Windley and others, 2007), the Chatkal-Kurama Arc (fig. 1-22) in eastern Uzbekistan is linked to the Valerianov Arc as the Uralian Ocean closed, whereas in others (for example, Herrington and others, 2005) the Chatkal-Kurama Arc is linked to subduction of the Tarim Plate as the Turkestan Ocean closed. The Balkhash-Ili Arc formed above the subduction zone as the Junggar-Balkhash Ocean closed.

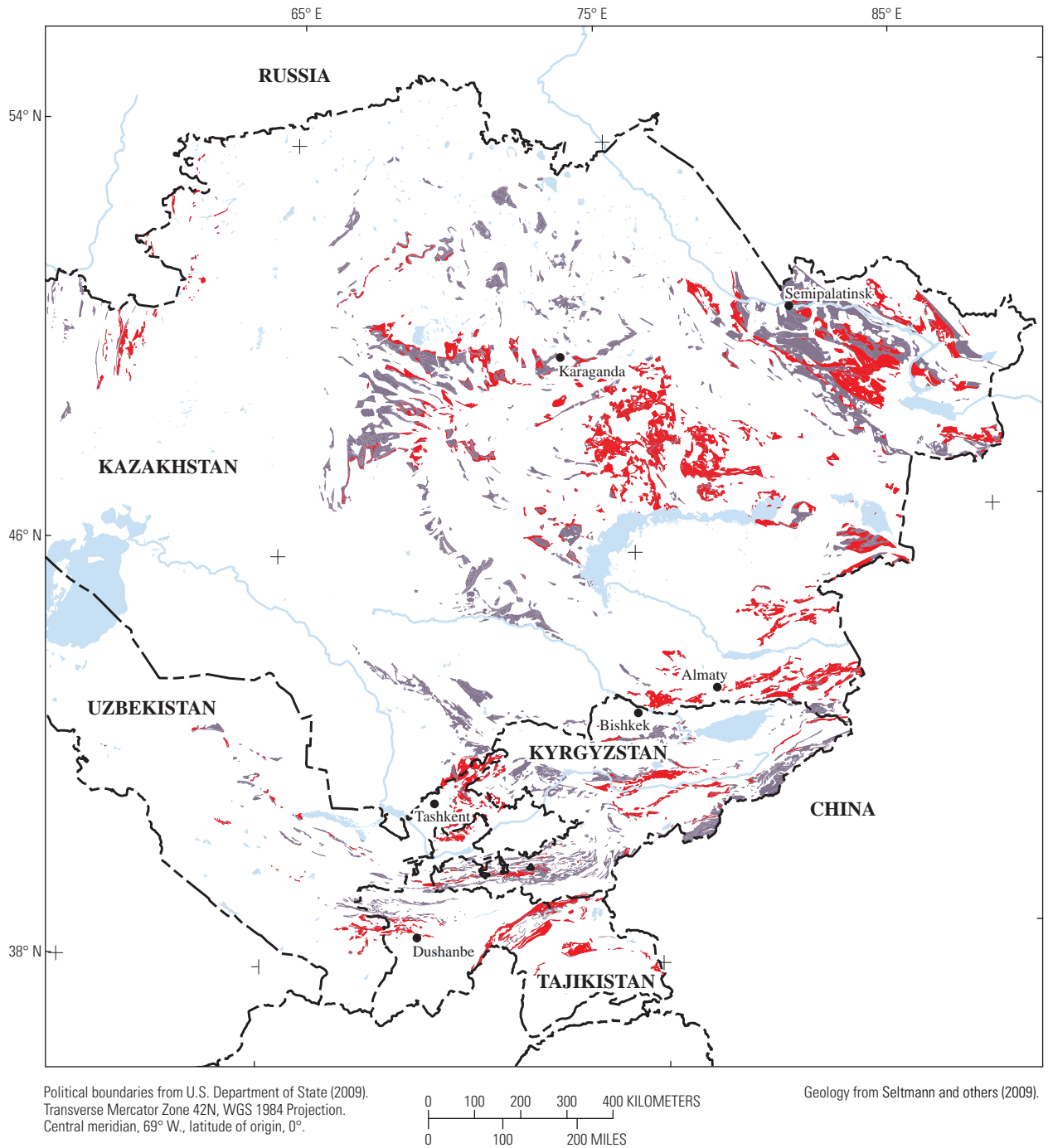
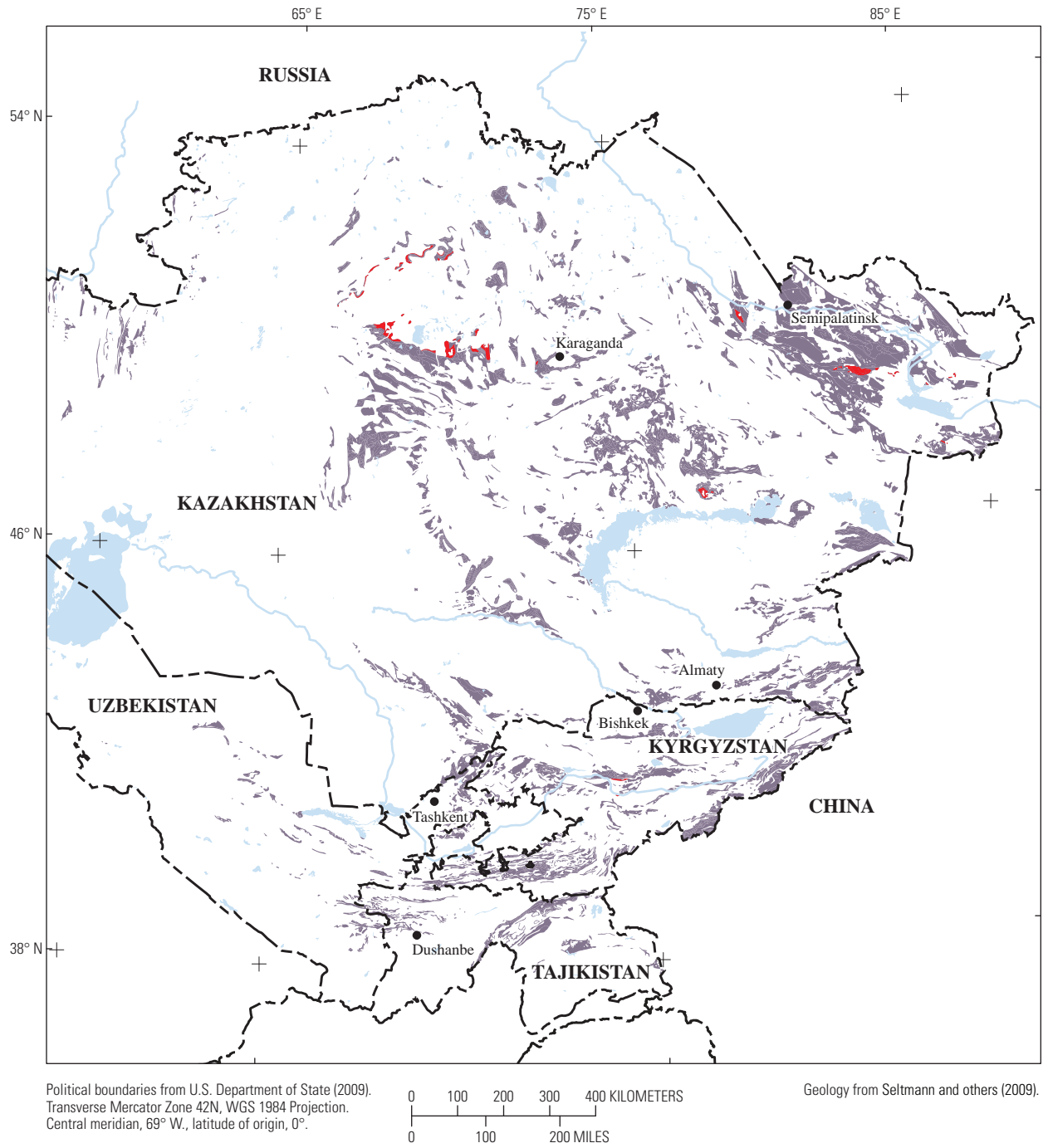


Figure 1-29. Map showing distribution of Carboniferous stratified rock types in the western Central Asia study area likely to have been deposited in a magmatic-arc environment (red) and those not likely to have been deposited in a magmatic-arc environment (lavender). (After Seltmann and others, 2009.)



Figure 1-30. Map showing distribution of Carboniferous intrusive rock types in the western Central Asia study area likely to have been emplaced in a magmatic-arc environment (red) and those not likely to have been deposited in a magmatic-arc environment (lavender). (After Seltmann and others, 2009.)



EXPLANATION

- Upper Carboniferous stratified rocks deposited in magmatic-arc terranes**
- Carboniferous stratified rocks not associated with magmatic-arc terranes**

Figure 1-31. Map of distribution of Upper Carboniferous (C₃) stratified rocks in the western Central Asia study area likely to have been deposited in magmatic-arc environments (red). Those map units containing Upper Carboniferous rock types not likely to have been deposited in magmatic-arc environments are shown in lavender. (After Seltmann and others, 2009.)



EXPLANATION

- Carboniferous-Permian stratified rocks deposited in magmatic-arc terranes
- Carboniferous-Permian stratified rocks not associated with magmatic-arc terranes

Figure 1-32. Map of distribution of Late Carboniferous to Early Permian rock types likely to have been deposited in magmatic-arc environments (red) and those not likely to have been deposited in magmatic-arc environments (lavender). This magmatic-arc activity marks the end of Paleozoic subduction and the final amalgamation of western Central Asia. (After Seltmann and others, 2009.)

West Margin

The present-day western boundary of the amalgamated Kazakhstan plate is marked by what is referred to as the Ural-Turkestan suture zone (Thomas and others, 1999), a zone that juxtaposes the main Uralian tectonic zone along the eastern margin of the Eastern European craton (fig. 1-8) and the present-day western margin of the Kazakhstan block on which the Carboniferous Valerianov magmatic arc in the southeast Urals formed. However, the paleotectonics of the southwestern Kazakhstan block just prior to the onset of Valerianov Arc activity is equivocal. Filippova and others (2001) and Windley and others (2007) interpret the Early to Middle Devonian magmatic arc in central Kazakhstan (Ubagan Arc of Filippova and others, 2001) to have formed above an inferred subduction zone that must be buried beneath the Turgai and Chu-Sarysu basins (fig. 1-22) in present-day west-central Kazakhstan. Filippova and others (2001) show Late Devonian passive-margin rocks west of the older Devonian arc assemblages, so the Valerianov Arc must represent the shift of subduction from the southwest of the Magnitogorsk Arc to the northeast. Herrington and others (2005) surmise that subduction beneath Kazakhstan northeast of Late Devonian postcollisional Magnitogorsk magmatism began before end-Devonian on the basis of the ages of subduction-related granitic rocks in the eastern Urals.

The tectonic zones between the East European craton on the west and the amalgamated Kazakhstan block to the east (fig. 1-33), an orogenic zone known as the Uralides (see Herrington and others, 2005) record the time-space history of the closure of the oceans separating these two Precambrian-cored masses. The Uralide tectonic zones trend north-south in present-day coordinates, and the most important to interpreting the mineral-resource potential along the southwestern margin of Kazakhstan during the Carboniferous are, from west to east, the Magnitogorsk, East Uralian, and Trans-Uralian zones (Brown and others, 2008). Now adjoined to the East European craton along the main Uralian Fault suture, during the late Early to Middle Devonian the Magnitogorsk Arc was active above northeast-directed subduction of an ocean basin that separated it from the East European plate margin. Arc magmatism persisted along the Magnitogorsk Arc into the Late Devonian. The youngest dated episode is uppermost Devonian (Bea and others, 2002) along the eastern tectonic margin of the Magnitogorsk zone. Early Carboniferous alkali-calcic gabbro-granite complexes that intrude ophiolitic rocks along the Main Uralian Fault Zone and form a meridional lineament within the Magnitogorsk zone likely herald the last vestiges of subduction zone magmas and the switch to wholly postcollisional magmatism within the zone.

The Magnitogorsk zone is structurally juxtaposed to the East Uralian zone along the East Magnitogorsk Fault Zone (Ayarza and others, 2000) along which ophiolite masses occur. Brown and others (2008) note a significant change to the occurrence of higher metamorphic grade rocks (for example, upper greenschist to granulite) east of this fault zone from

low-grades in the Magnitogorsk zone as well as an increase in the intensity of deformation in the East Uralian zone. The high grade of metamorphism and subparallel, major north-trending regional fault zones with intermittent ophiolites along them are characteristics of the 60–80 kilometer-wide East Uralian zone. Brown and others (2008) refer to the entirety of the zone as a suture in a broad use of the term. However, uppermost Devonian to Early Carboniferous subduction-related igneous complexes with a distinct continental isotopic signature (see Bea and others, 2002) intruded an already amalgamated terrane. Bea and others (2002) interpret these superposed volcano-plutonic centers as Valerianov Arc-related magmatism. Soviet-era geologic maps and Seltmann and others (2009) show that the regional-scale, north-trending fault zones with ophiolite fragments along them continue to the east of the structural boundary, the Troisk Fault Zone (fig. 1-33), between the East Uralian and the Trans-Uralian zones, implying that the original east margin of this amalgamated basement for the Valerianov Arc is located east of the tectonic boundary now separating the two zones. An interpretation of the crustal structure along a seismic line that crosses the Ural Mountains by Tryggvason and others (2001) shows the East Uralian zone to form the upper plate of a west-dipping reverse fault with the Trans-Uralian block in the footwall and the high-angle Troisk Fault largely breaching the Trans-Uralian block in the subsurface, itself with buried, east-verging reverse faults, but coinciding at the surface with the terrane-bounding master west-dipping reverse fault.

Where studied in the southeastern East Uralian zone, as well as farther north (about lat 52° 33' N., long 6° 4' E.) in the zone in the Denisov eugeosyncline, as defined by geosyncline theory, Savelieva and others (2002) suggest that the ophiolite fragments are remnants of spreading ridge magmatism. Savelieva and Nesbitt (1996) interpret these Silurian to Devonian East Uralian ophiolite remnants as having been deformed initially into regional-scale nappe structures, perhaps during destruction of the spreading centers, and deformed again by the regional faults in the East Uralian and Trans-Uralian zones, as well as by Late Paleozoic intrusions and Precambrian-cored metamorphic complexes in the East Uralian zone. Porphyry copper deposits that postdate ophiolite fragment emplacement in the Denisov eugeosynclinal domain (for example, Mikheyev; location on fig. 1-33), as well as east of the Troisk Fault Zone (for example, Spiridonov; location on fig. 1-33), and the commonality of the basement terrane east and west of the Troisk Fault Zone suggest that the interpretation of Bea and others (2002) that Late Devonian to Carboniferous intrusive complexes in both the East Uralian and Trans-Uralian zones were part of the Valerianov magmatic arc is the most likely interpretation, given available data.

Within the regionally broad interpretation of the Valerianov magmatic arc (East Uralian and Trans-Uralian zones), magnetic data show the arc to be relatively continuous in the Trans-Uralian zone, where it is mostly covered, but geologic maps show it to be disaggregated in the East Uralian zone. Nevertheless, there are Carboniferous magmatic-arc

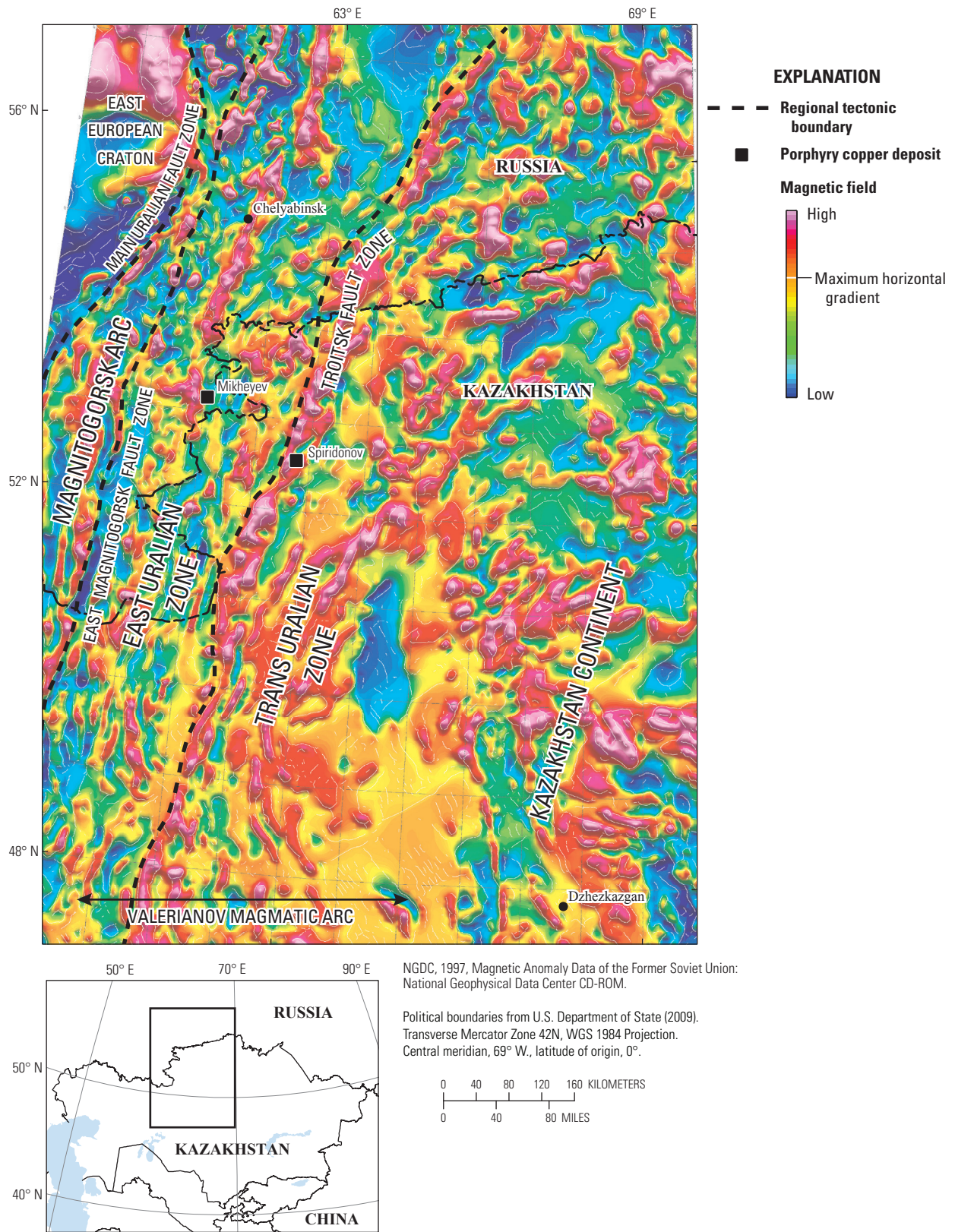


Figure 1-33. Reduced-to-pole aeromagnetic map of the southeastern Ural Mountains and adjacent amalgamated Kazakhstan continent, Russia and Kazakhstan, showing the approximate tectonic boundaries (black dashed lines) separating the East European craton, Magnitogorsk magmatic arc, East Uralian tectonic zone, and the Trans Uralian tectonic zone. For reference, the approximate original breadth of the Valerianov magmatic arc is shown, as are selected cities and porphyry copper deposits. Location of map area shown on inset.

intrusive complexes in the East Uralian zone with associated porphyry copper occurrences (for example, Ageyeva and others, 1984; Petrov and others, 2006; Seltmann and others, 2009). Important to an assessment of undiscovered porphyry copper deposits in the East Uralian part of the Valerianov Arc is the extent to which the arc rocks can be reassembled. Therefore, the nature and extent of post-Carboniferous deformation in the East Uralian zone is important. Several lines of evidence suggest that the East Uralian zone should not be quantitatively assessed for undiscovered porphyry copper deposits at its current state of understanding. Gerdes and others (2002) and Görz and others (2009) document the onset of high-strain deformation in the East Uralian zone at the beginning of the Permian and extending into the Triassic. Compressional and transpressional strains dominated in the zone with significant strike-slip and strike-slip-reverse displacements on north-trending structures (present-day coordinates). Kolb and others (2005) established that the Valerianov Arc-related Borizov and Plast intrusive complexes (Early Carboniferous) have gneissic fabrics linked to high-temperature and 2–3 kilobars pressure metamorphism during the late Early Permian. Economically important mesothermal (orogenic) low-sulfide gold deposits were formed within these complexes following peak metamorphism, implying that these arc complexes have been uplifted 6–10 km. Herrington and others (2005) show there to be a large number of such mesothermal (orogenic) type gold-bearing quartz deposits along the major north-trending shear zones, including near the East Uralian zone-bounding East Magnitogorsk and Troisk Fault Zones. Thus, the Valerianov Arc was disaggregated along major regional strike-slip fault zones to an unknown but ostensibly major extent, and most of the permissive rocks have been uplifted and the depths in the arc where porphyry copper deposits are most likely to form has been eroded to an unknown extent throughout the East Uralian zone.

Filippova and others (2001) and Windley and others (2007) link the Valerianov Arc in the present-day southeastern Urals south to the Aral Sea and then infer that it turns southeast towards present-day eastern Uzbekistan and the Chatkal-Kurama region, although direct evidence for the Aral Sea to the Chatkal-Kurama connection is buried beneath Mesozoic and Cenozoic cover. Further, a tectonic explanation for the east bend is not given. Heubeck (2001) provides an explanation for the apparent bend by terminating the Valerianov Arc above a northeast-dipping subduction zone at a triple junction where the Valerianov Arc zone intersects a separate, northwest-dipping subduction zone along the southeastern margin of the Kazakhstan block (fig. 1-22). Herrington and others (2005) place the Chatkal-Kurama magmatic arc along the southeastern margin of Carboniferous Kazakhstan, consistent with Heubeck's (2001) model, thereby implying that it was not directly linked into the Valerianov Arc. Görz and Hielscher (2010) present a kinematic model for the southern Uralides and Valerianov arc terrane that serves to highlight the significant differences between the tectonic histories of the magmatic-arc terrane in the East

Uralian and Trans-Uralian and the contemporaneous Chatkal-Kurama Arc and adjacent area. In this report, the Chatkal-Kurama is discussed as part of an arc associated with the closure of the Turkestan Ocean off the southeast coast of Carboniferous Kazakhstan.

Southwest to South Margins

In this report, the generalities of the Heubeck (2001) model and the interpretation of Herrington and others (2005) are accepted, and the Carboniferous Chatkal-Kurama magmatic arc (fig. 1-22) is considered a consequence of the subduction of the Turkestan Ocean beneath Kazakhstan. In this regard, it differs from the interpretation of Windley and others (2007). A further difference with Windley and others (2007) is that the arc is continued to the Talas-Fergana Fault (location on fig. 1-28), because there are diorite to granodiorite intrusions against the fault zone that cannot be excluded from permissivity for the occurrence of porphyry copper deposits.

The basement for the Carboniferous Chatkal-Kurama magmatic arc consists of Ordovician and Silurian nonmarine rocks overlain by Early Devonian volcanic rocks. These, in turn, are overlain by Late Devonian to Early Carboniferous carbonate rocks. Andesitic to dacitic arc volcanism began during the Early Carboniferous. Despite how one reconstructs the northwest margin of the Paleotethys Ocean to the southeast of the Turkestan Ocean, paleotectonic models show the Turkestan Ocean to have closed from southwest to northeast (for example, Heubeck, 2001) and likely impacted the Chatkal-Kurama region by the upper Late Carboniferous. Subduction-related magmatism lingered into the Lower Permian when it was supplanted by postcollisional magmatism.

Remnants of the Chatkal-Kurama magmatic arc are present in the southern Tian Shan ranges (see Windley and others, 2007), but there is little geologic and no structural continuity preserved owing to the complex Paleozoic to Recent collisional history in this region. From its western tip in Uzbekistan east to the border with China, the Tian Shan ranges are a strongly and multiply deformed region. In the study area, the ranges make up three tectonic units—North Tian Shan, Central Tian Shan, and South Tian Shan—separated by suture zones with the whole complex of ranges bound north and south by major strike-slip and strike-slip-reverse fault zones. This same nomenclature is not used across the border in China. In China, the North Tian Shan tectonic block of southeastern Kazakhstan and eastern Kyrgyzstan is known as the Yili Block (Wang and others, 2007), and in China the North Tian Shan Block is situated to the north of the Yili Block along the southern margin of the Junggar Basin.

The juxtaposition of the North and Central Tian Shan tectonic units in the study area took place along the Nikolaev Line (fig. 1-28), which resulted from the closing of an ocean basin to the southeast of the Kazakhstan block. Along the southern margin of the Central Tian Shan is the Late Devonian to Early Carboniferous Balkhash-Ili magmatic arc

(see Heubeck, 2001). Heubeck (2001) modeled the North Tian Shan-Central Tian Shan collision to have taken place in a scissor-like fashion from east to west; accretion was completed by the middle Early Carboniferous. Collision of the amalgamated North Tian Shan-Central Tian Shan tectonic unit with the South Tian Shan tectonic unit occurred during the Late Carboniferous to Early Permian (Heubeck, 2007). Xiao and others (2009) argue that the biostratigraphic data of Chen and Shi (2003) preclude a final accretion before mid-Early Permian, but this final closure was well to the east in the present-day Tian Shan ranges to the south of the Junggar Basin (fig. 1-22).

Southeast to East Margins

The Carboniferous tectonic setting of present-day eastern Kazakhstan reflects the rotations and translations that occurred during the final closing of the ocean basins adjoining the Siberia, North China, and Tarim cratons. As the Devonian came to an end, the Ob-Zaisan Ocean still separated Siberia from the north to northwest passive margin of Kazakhstan, but it was narrowing through subduction on the east side of the ocean beneath a narrow, northeast-trending array of small continental masses that, at its south end, were colliding with Kazakhstan (Bykadorov and others, 2003). On the east margin of this narrow continental mass, the also-narrowing Junggar-Balkhash ocean floor was subducting both to the west beneath Siberia and to the east beneath the Tarim block (see Windley and others, 2007). The Carboniferous arcs active as these two oceans closed are now an arc sequence continuous to the southeast into the Chinese Altai north of the Junggar Basin and bounded on the present-day southwest by the Irtysh (Erqis) suture zone and the Zharma-Saur volcanic arc south of Lake Zaisan (fig. 1-22). The Zharma-Saur magmatic arc formed on a narrow continental mass on the north of Kazakhstan as the Ob-Zaisan Ocean was closing.

The nature and timing of final assembly remain controversial (see Xiao and others, 2009). From studies in northwest China, Xiao and others (2009) argue that the presence of subduction-related constituents in Permian accretionary units precludes a final docking of Tarim and Siberia before end-Permian. Buslov and others (2010) discuss the complex arrangement of collisional and accretionary complexes in eastern Kazakhstan and conclude that the collage of terranes in the Altai region (fig. 1-2C) are the consequence of two main collisional events, one the Late Devonian to Early Carboniferous collision between the Mongolian Altai and Siberian craton and the Late Carboniferous to Permian collision of the Siberian and Kazakhstan tectonic blocks during which the Chara and Irtysh suture/strike-slip fault zones (fig. 1-22) in eastern Kazakhstan were formed. The Irtysh suture separates the Kalba-Narym and Rudny Altai terranes of Buslov and others (2010) (fig. 1-34) and forms the east boundary of Windley and others' (2007) Irtysh-Zaisan tectonic terrane (fig. 1-22) against what is known as the Gorny Altai in Russia. Buslov and others (2010) describe Late Carboniferous

to Early Permian mélanges separating thrust sheets along the Chara Fault Zone and show Permian postcollisional granites truncating Chara strike-slip faults. Early Permian dates on metamorphic rocks along the Irtysh zone are considered to date the time of strike-slip displacement along the suture zone. All told, available data from central Uzbekistan east to North Xinjiang, China, suggest that the final closure of the southern margin of present-day western Central Asia took place in the latest Carboniferous to Early Permian in the west and latest Permian to Triassic farther east.

Central Kazakhstan Orocline

Just as the Devonian arc of central Kazakhstan, the Carboniferous magmatic-arc rocks form a horseshoe-shaped outcrop distribution pattern (unit BI in fig. 1-22) (see Windley and others, 2007) and are part of the Central Kazakhstan orocline. As portrayed by Windley and others (2007) (fig. 1-22) and may be inferred from Seltmann and others (2009), the axis of the Carboniferous oroclinal fold is not colinear with the axis of the Devonian orocline (fig. 1-24). A fanning outward swarm of $\sim 320^\circ$ – 325° faults (see Seltmann and others, 2009) (fig. 1-35) demarcate the Carboniferous axial trace, a difference of 20° – 30° from the current position of the more westerly striking Devonian axis. Using paleomagnetic data, Abrajevitch and others (2007) confirmed the oroclinal nature of the Devonian outcrop pattern and, by inference, the Carboniferous pattern, and showed that the original Devonian arc trend was linear and northwest-southeast. Although the timing of onset of oroclinal bending is controversial (for example, Alexeiev, 2008), Abrajevitch and others (2008) suggest that rotation began as early as the Late Devonian to Early Carboniferous in response to the initial collision of Kazakhstan and the Tarim Plate. Because there are implications regarding the timing of oroclinal bending to the mineral-resource potential in the region, a short review of pertinent data is presented below. Whenever the onset of oroclinal bending began, paleomagnetic data show the process to have been largely completed by early Permian (see Abrajevitch and others, 2007, 2008; Levashova and others, 2008).

Geologic Constraints on the Timing of Oroclinal Bending

Chitalin (1996) summarizes the evolution of the Variscan orogeny in Central Kazakhstan, thereby documenting the tectonic events that affected the oroclinally bent Devonian and Carboniferous magmatic-arc terranes across the core of western Central Asia. Figure 1-36A shows a sketch tectonic map of the region to the north and northwest of the North Balkhash region; figure 1-36B shows the geology in cross section. These maps document north and west transport directions across what is known as the Spassky tectonic zone (fig. 1-2A) as well as to west and southwest-transport around the west margin of the North Balkhash accretionary wedge of Windley and others (2007). Windley and others (2007)

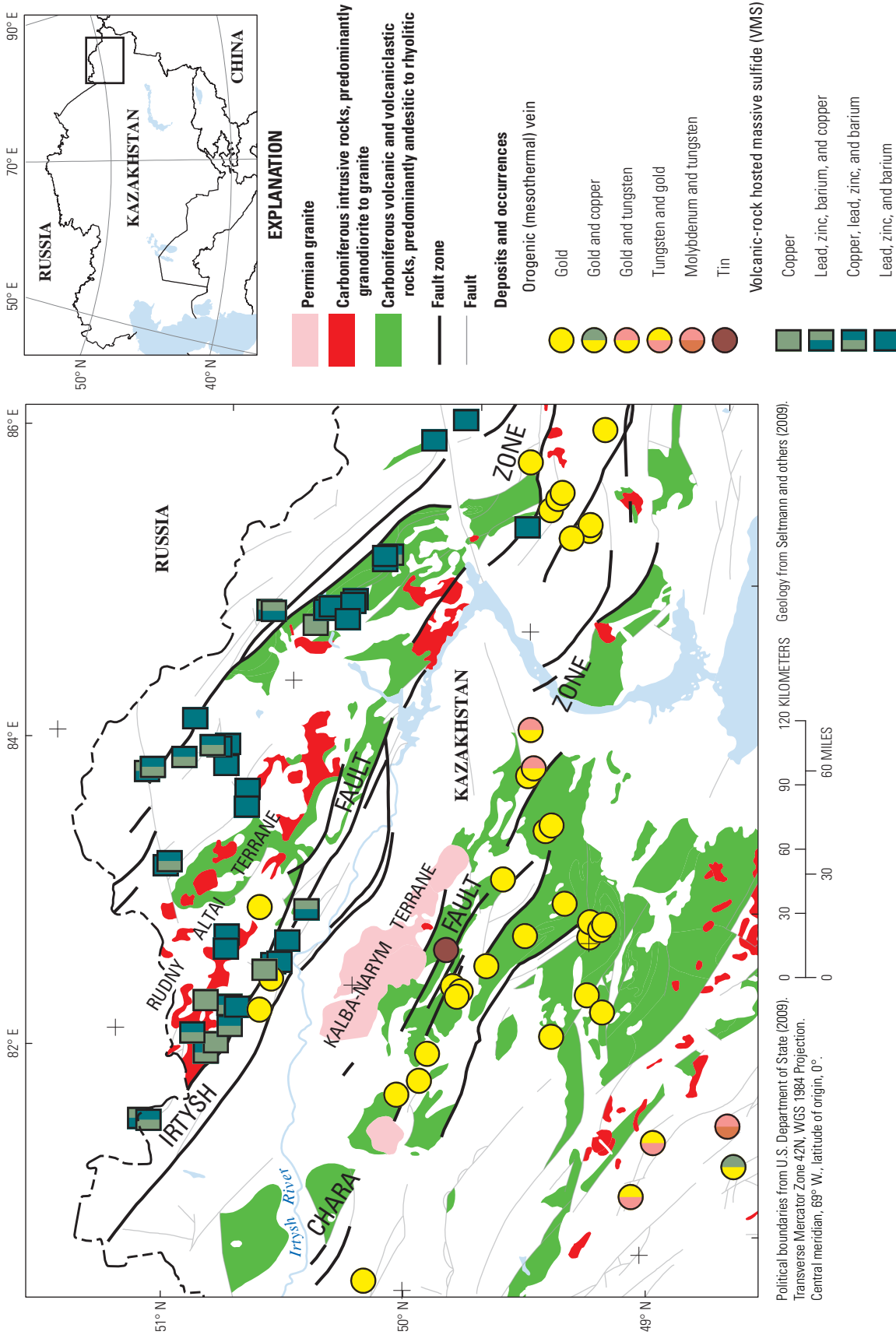
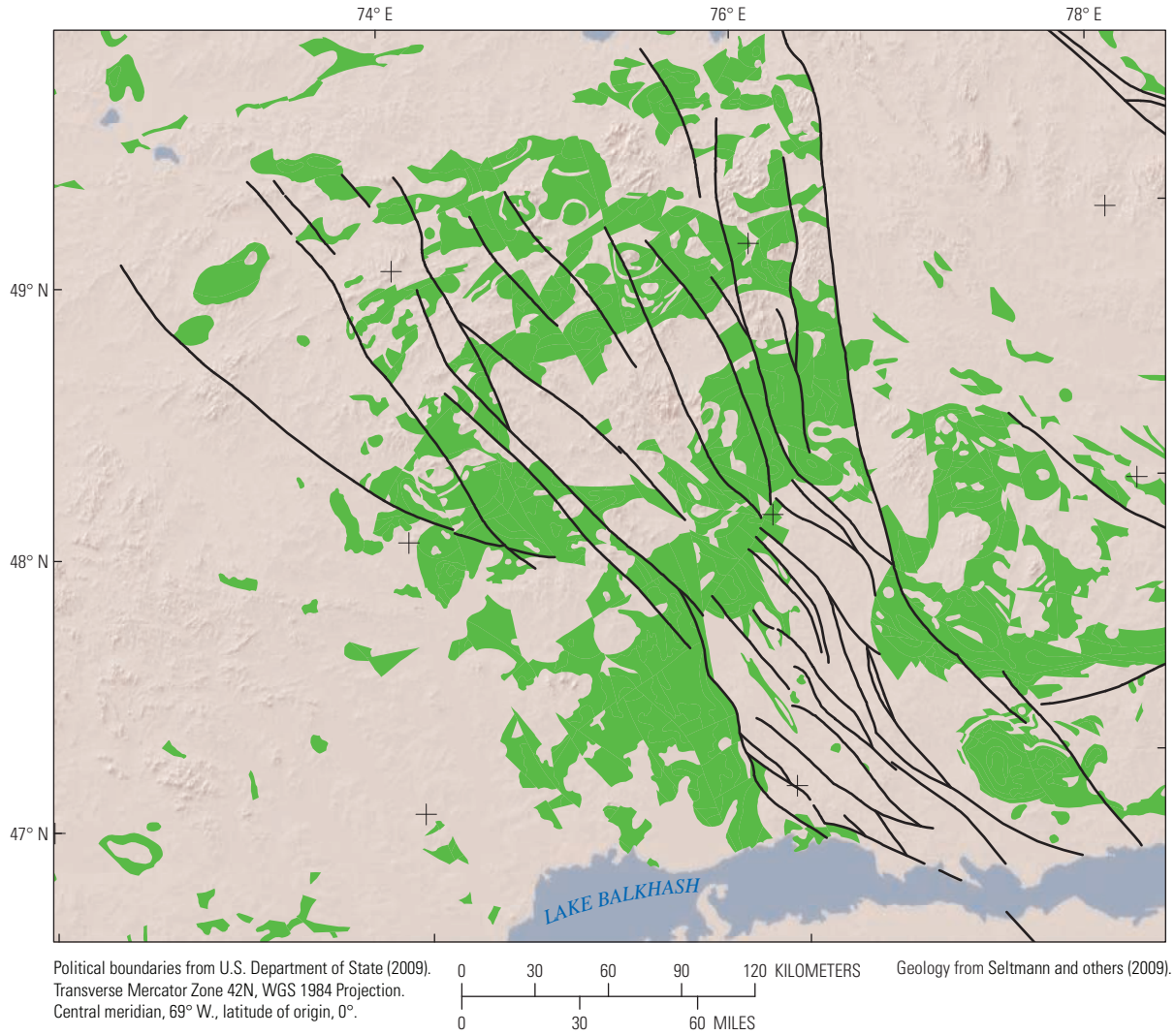


Figure 1-34. Map showing locations of Irtysch and Chara Fault Zones in eastern Kazakhstan. Shown are the Carboniferous stratified (green) and intrusive (red) rocks (after Seitmann and others, 2009) interpreted to have been deposited in a magmatic-arc environment. Postcollisional Permian granites in dark pink. The Irtysch and Chara Fault Zones are ophiolite-bearing suture zones related to the final assembly of western Central Asia at the end of the Paleozoic. The Irtysch Fault Zone separates the Rudny Altai terrane on the northeast, a submarine magmatic-arc sequence formed along the margin of the Siberian craton, and the Kalba-Narym terrane of Buslov and others (2004), which is within the Irtysch-Zaisan tectonic terrane of Windley and others (2007). Buslov and others (2004) correlate rocks in the Chara zone with a complex of rocks in the west Junggar region of China and thus represent a tectonized accretionary complex formed during the collision of the Tarim block with Siberia. The Permian intrusions indicate that strike-slip deformation along the Chara zone had ended before the end of the Paleozoic. Submarine volcanogenic massive sulfide deposits imply a submarine volcanic arc environment. The yellow circles show the locations of mesothermal (orogenic) vein deposits that indicate there has been several kilometers of uplift along many of the faults. Location of map area shown on inset.



- EXPLANATION**
- Carboniferous volcanic, volcanoclastic, and intrusive magmatic-arc rocks
 - Strike-slip fault

Figure 1-35. Map of the North Balkhash region showing the fan-like splaying of strike-slip faults (dark lines) in the hinge zone of the Carboniferous orocline (after Seltmann and others, 2009). Also shown are Carboniferous rocks interpreted to have been deposited in a magmatic-arc environment (from Seltmann and others, 2009). Location of map area shown on inset.

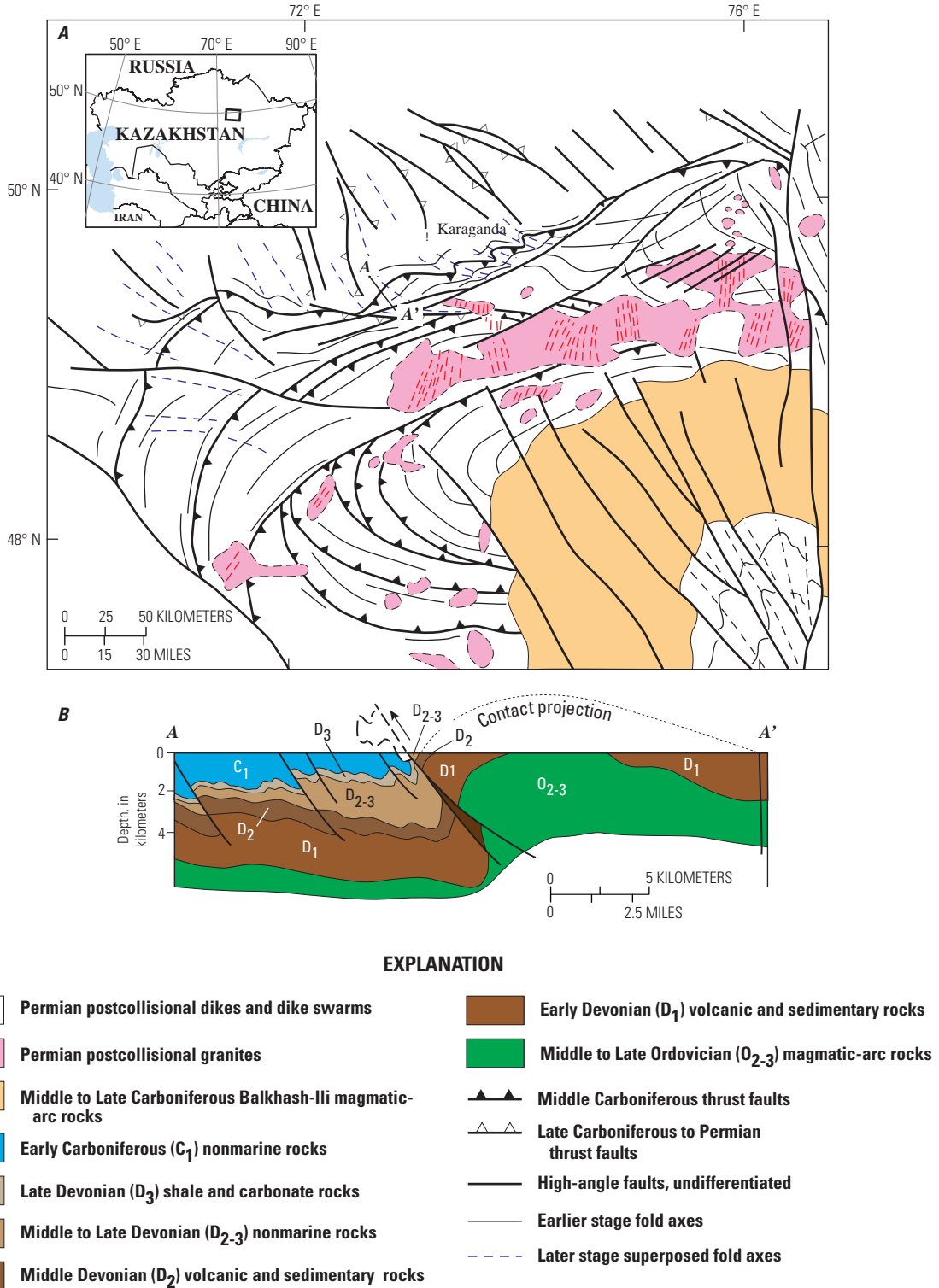


Figure 1-36. Map of the Spasski fold and thrust belt. *A*, Generalized tectonic map of the Spasski fold and thrust belt along the north and northwest margins of the North Balkhash region in north-central Kazakhstan. The latitude, longitude, and location of the city of Karaganda were approximated using Google Earth and are shown for reference purposes. *B*, Schematic cross section A-A' (location in fig. 1-36A) of the frontal part of the Spasski fold and thrust belt. Carboniferous Balkhash-Ili magmatic arc rocks are shown in orange and postcollisional Permian intrusions are shown in pink. Both map and cross section are after Chitalin (1996). Location of map area shown on inset.

interpret the accretion of the North Balkhash accretionary wedge (ZS and AJ terranes in fig. 1-22) to have been completed by Late Devonian, thereby setting a maximum age for deformation along the Spassky zone owing to the fact that deformation along the southern margin of the Spassky zone appears to track the EI-ZS-AJ tectonic contact (fig. 1-22). The north margin of the Spassky zone is a series of north-verging nappe structures that involve Early Carboniferous Visean rocks (fig. 1-36B). Figure 1-37 shows the reduced-to-pole aeromagnetic patterns for the map area in figure 1-36A and some of the fault zones mapped by Chitalin (1996) and Seltmann and others (2009), as well as the boundaries of the tectonic terranes of Windley and others (2007). The Devonian and Carboniferous magmatic arcs overlap and are generally in unconformable contact with underlying basement rocks. There is little correlation of the arc terrane boundaries and tectonic and structural elements as interpreted from the aeromagnetic data. The geologic evidence is that thrust and associated strike-slip faulting postdate the beginning of the Carboniferous. The axis of the oroclinally bent Devonian arc sequences is west of the westernmost, escape-related thrust faults and axial faults indicate north-south shortening within the Devonian oroclinal hinge zone (fig. 1-38). The axial reverse faults involve Early Carboniferous Tournasian and Visean rocks, from which it can be inferred that the axial faults as currently defined formed concurrently and progressively with deformation along the Spassky zone. North-south shortening in the axial zone involves younger Carboniferous rocks and indicates that shortening strains continued well into the time of Balkhash-Ili magmatic-arc volcanism.

Heubeck (2001) digitally reconstructed the southeast margin (northern Tian Shan) of the amalgamated Kazakhstan block during the period of closure of the Turkestan Ocean. His model implies initial collision sometime after the Tournasian (359–345 Ma) in the Early Carboniferous in the southwest part of figure 1-22—that is, southwest of the triple junction at the south end of the Valerianov Arc. This window of timing is consistent with the post-Visean (345–328 Ma) timing for nappe development shown by Chitalin (1996) in the Spassky zone.

Chitalin (1996) shows Carboniferous Balkhash-Ili magmatic arc rocks to overlap the fold and fault structures of the Spassky zone (fig. 1-36A). Chitalin (1996) also shows fold axial traces trending north-northwest, as well as northwest-striking strike-slip faults within the Balkhash-Ili arc terrane and crosscutting the Spassky zone nappes implying generally east-west shortening in the Balkhash-Ili Arc concurrent with volcanism. Dikes, joint swarms, and mineralized faults are common in Carboniferous and younger plutons in the North Balkhash region and corroborate the syntectonic emplacement of arc and postarc intrusions. Figure 1-39A shows the interpreted Carboniferous oroclinal hinge faults in the North Balkhash region on the backdrop of Carboniferous magmatic-arc rocks after Seltmann and others' (2009). Figure 1-39B is an annotated Landsat 5 (band 7) image of a Carboniferous arc-related pluton in the North Balkhash region illustrating

the tectonic control on faulting, dike emplacement, and hydrothermal alteration east of the hinge zone. Figure 1-39C is an annotated Landsat 5 (band 7) image of a Permian pluton within the hinge zone. Although northwest-striking strike-slip faults east of the hinge zone appear to localize hydrothermal alteration to the west of the pluton, dikes and mineralization within the pluton (fig. 1-39B) strike northeast. This northeast trend is interpreted to be a response of the interaction of the northwest-striking faults with east-west-striking faults that locally perturb the regional strain field where east-west faults mechanically link with the northwest-striking faults. Within the hinge zone (fig. 1-39C), both dikes and faults strike northwest, as do the most continuous zones of hydrothermal alteration. In general, hydrothermal alteration, major regional faults, and pluton related dikes within the hinge zone strike northwest. The inference drawn from these relations is that hinge-zone faults were active synhydrothermally during the Late Carboniferous. Although there has been displacement on some of the northwest-striking faults since the Paleozoic, as a group, they formed concurrently with Carboniferous magmatic-arc volcanism and should be considered prospective for the occurrence of undiscovered mineral resources.

The implication of the geologic data is that oroclinal bending was progressive and began during the Early to early Late Carboniferous but prior to the onset of Balkhash-Ili Arc activity. Bending was mostly complete in the North Balkhash region and to the north and west by the latest Carboniferous. The implication to mineral-resource potential in the Devonian and Carboniferous arc terranes is that the Devonian arc was significantly deformed prior to the onset of Carboniferous arc volcanism and any mineralization associated with Devonian intrusive-rock centers was likely affected by the deformation. In the Devonian oroclinal axis zone, Late Devonian magmatic bodies intrude folded older Devonian stratified rocks, deformation that precedes Spassky zone deformation. In contrast, throughout this region, the Carboniferous intrusive centers are mostly intact, and related mineralized zones are likely to be less deformed than Devonian ones except, perhaps, to the west and southwest of Lake Balkhash.

Consistent with the inference that tectonic rotation occurred concurrently with arc volcanism is the fact that, in the north Balkhash Lake region, remotely sensed data analyzed in this investigation show polymetallic mineralization along some of the hinge faults is spatially associated with Carboniferous intrusions. Confirmative pluton ages are few in this region. Perhaps as a guide to the general timing of North Balkhash mineralization, the Kounrad porphyry copper deposit is associated with a ~330 Ma stock (Seltmann and Porter, 2005) and late- to postsubduction magmatism purportedly persisted into the earliest Permian. Intrusive rock dates in the Sayak ore district are similar, ~347 to ~304 Ma (Seltmann and Porter, 2005). By the latter part of this time interval, most magmatism was postcollisional, resulting in the formation of molybdenum, tungsten, and rare earth element enriched deposits and not porphyry-style copper deposits.

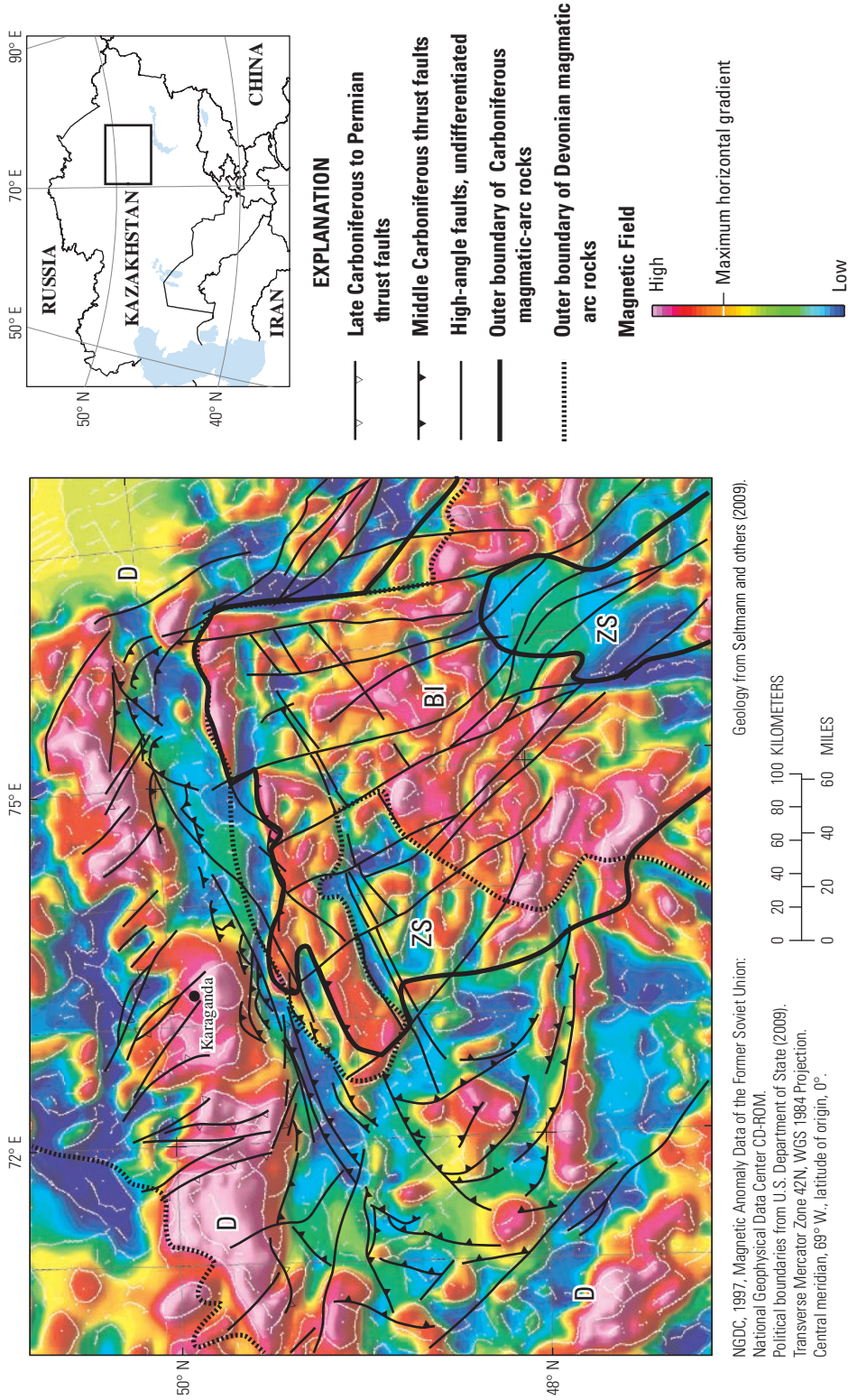


Figure 1-37. Reduced-to-pole aeromagnetic map of the Spasski fold and thrust belt region, north-central Kazakhstan, shown in figure 1-36, with selected faults from Seltmann and others (2009) and the approximated boundaries of the lithotectonic terranes of Windley and others (2007). The Devonian magmatic arc overlaps the Carboniferous Balkhash-Ili magmatic arc on its west margin and forms a horseshoe-shaped band of Devonian arc rocks around the Carboniferous arc rocks. The location of Karaganda city is approximately located from Seltmann and others (2009). Location of map area shown on inset. D, Devonian active continental margin; ZS, Ordoevician-Devonian Zhaman-Sarysu subduction-accretion complex; BI, Late Devonian-Permian Balkhash-Ili active continental margin.

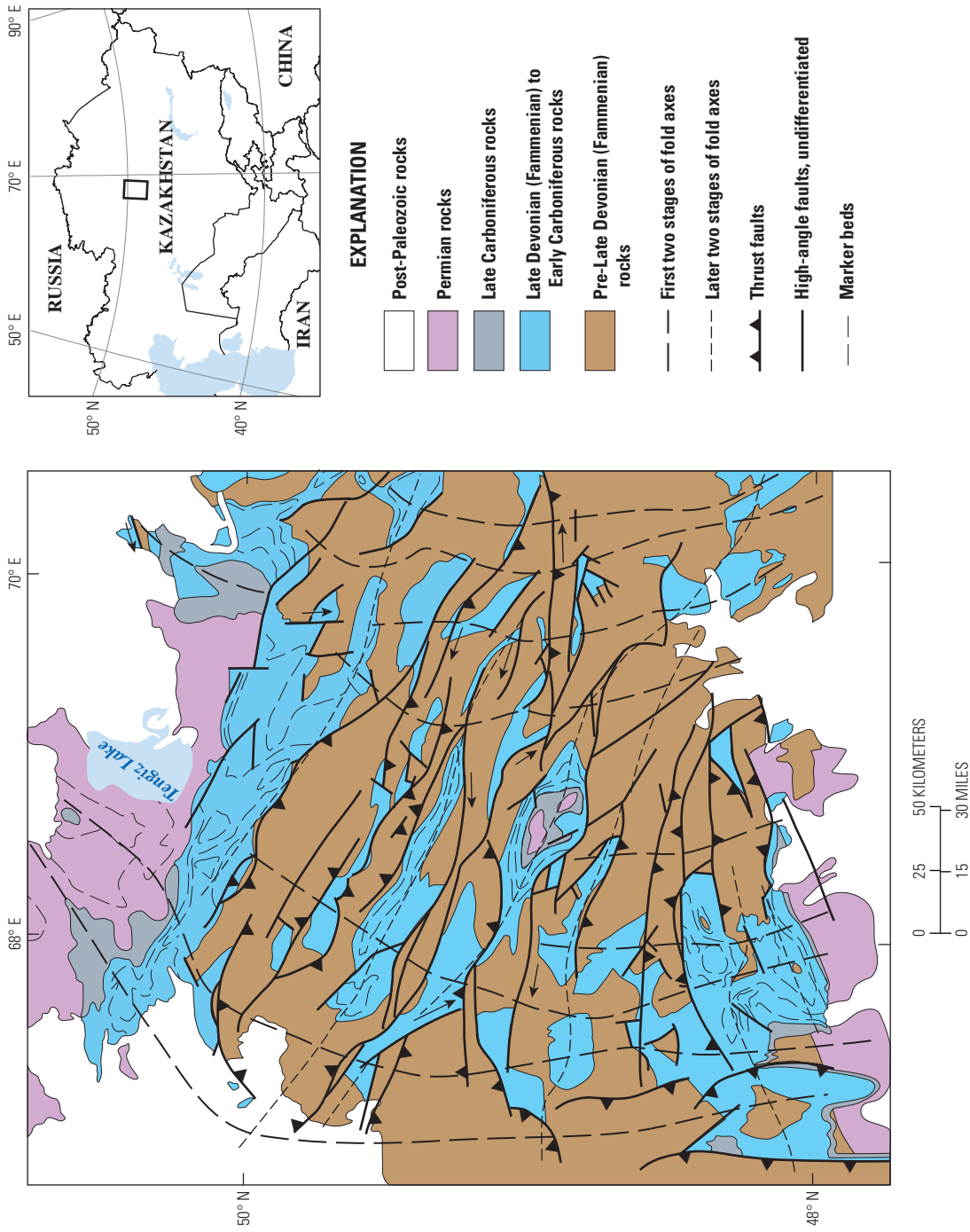


Figure 1-38. Generalized map of fold and fault structures within the hinge zone of the Devonian orocline in west-central Kazakhstan (after Chitalin, 1996, and Seltmann and others, 2009). The latitude and longitude are approximately located from Seltmann and others (2009). Location of map area shown on inset.

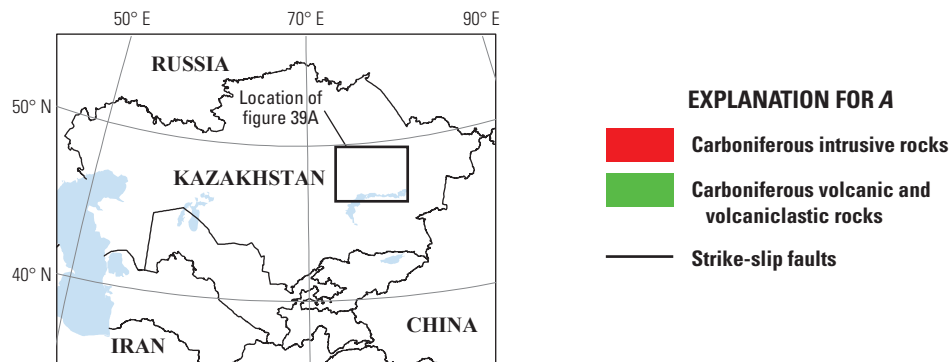
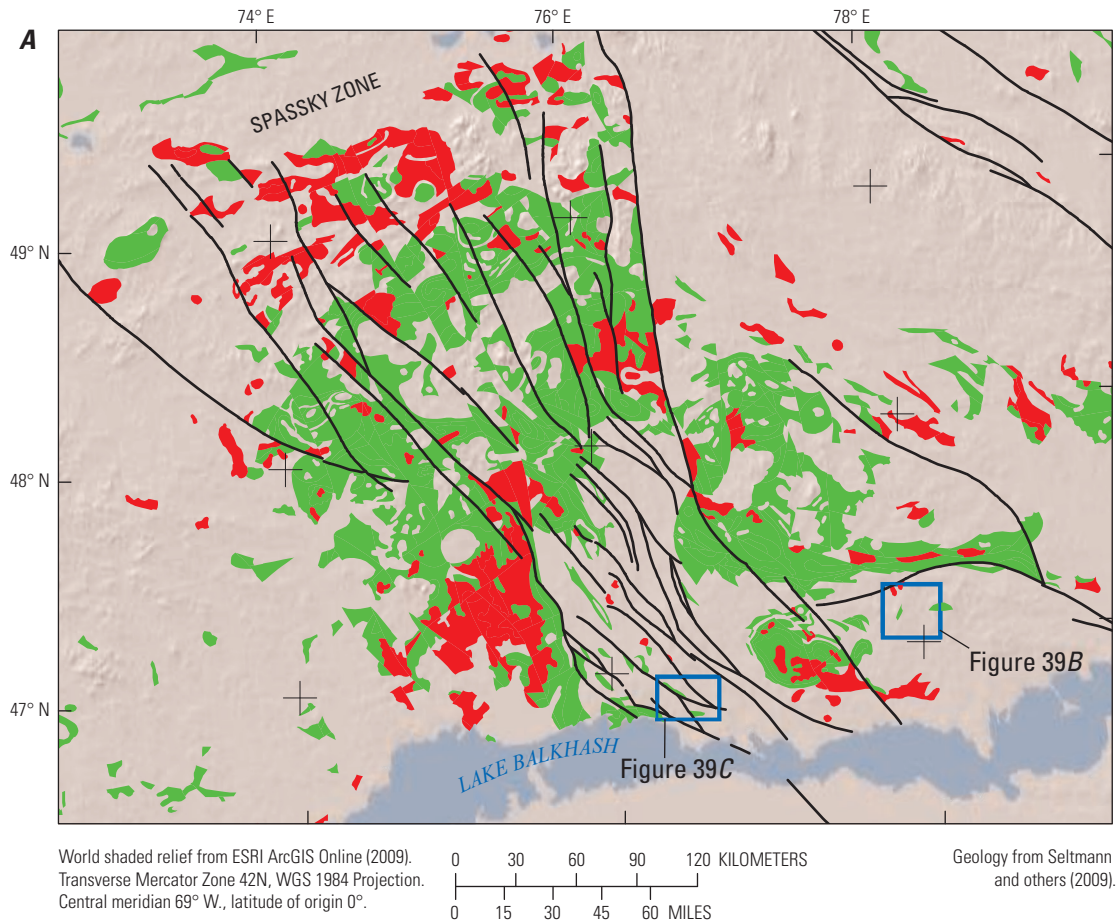


Figure 1-39. Maps showing the relation of mineralization to northwest-striking strike-slip faulting in the North Balkhash region in the hinge zone of the Carboniferous orocline. *A*, Generalized map of the North Balkhash region showing the principal strike-slip faults in the hinge zone and magmatic-arc Carboniferous intrusions (red) and stratified rocks (green) (from Seltmann and others, 2009). The locations of figs. 1-39*B* and 1-39*C* are shown. *B*, Landsat 5 (band 7) satellite image of a stock near the east margin of the Carboniferous oroclinal hinge zone. Major faults (white lines) on this side of the hinge zone strike northwest, generally east-west (after Seltmann and others, 2009). Dikes (purple lines) in the stock strike predominantly northeast. Seltmann and others (2009) show a porphyry copper occurrence to the east of the center of the stock. Hydrothermal alteration, interpreted from Advanced Spaceborne Thermal Emission and Reflection Radiometer (ASTER) satellite data by J.C. Mars and considered Carboniferous, occurs along northwest-striking faults to the west of the stock and along northeast-striking zones within the stock. *C*, Landsat 5 (Band 7) satellite image of a stock within the hinge zone of the Carboniferous oroclinal bend. Major faults (white lines) within the hinge zone strike northwest. Dikes (purple lines) in the stock strike predominantly northwest. Hydrothermal alteration, interpreted from ASTER satellite data by J.C. Mars, occurs along northwest and some northeast (not mapped) striking faults to the west of the stock. The fault towards the upper right-hand corner of the image offsets the stock and is likely post-Carboniferous. Location of map area shown on inset.

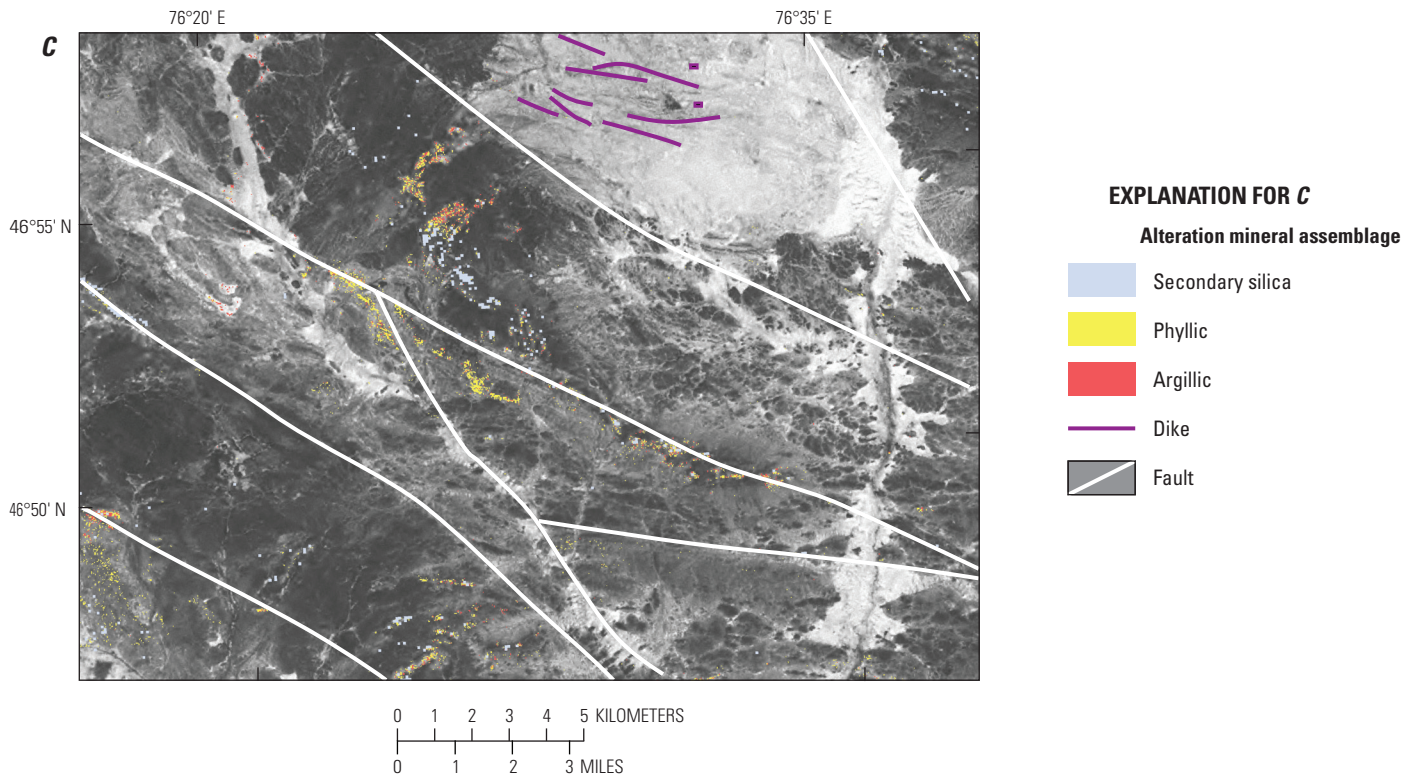
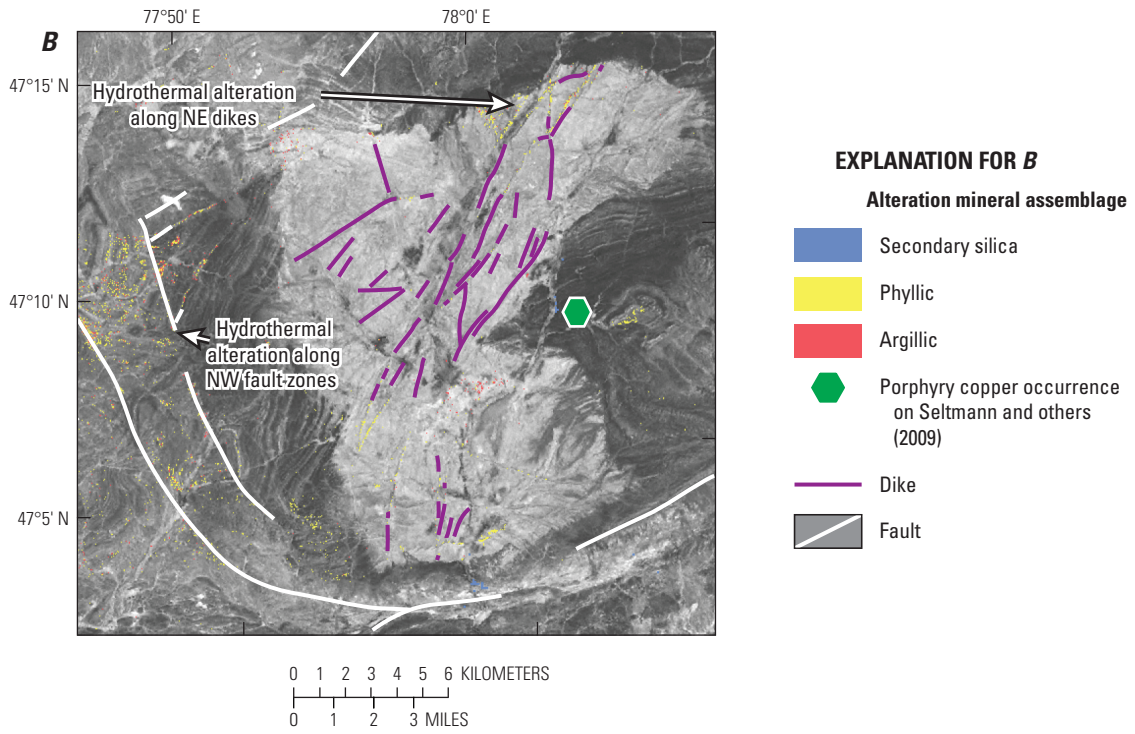


Figure 1-39.—Continued

Porphyry Copper Deposit Metallogeny of Western Central Asia and Potential for Undiscovered Deposits

The following discussion of porphyry copper deposit metallogeny is organized in terms of magmatic arc development in western Central Asia through time. Known porphyry copper deposits and occurrences are described, along with an evaluation of the potential for undiscovered porphyry copper deposits and the rationale for selecting some magmatic arc terrains (fig. 1-2B) for quantitative assessment (see chapter 3).

Cambrian Period

Western Central Asian Cambrian magmatic arcs, wherein porphyry copper-type deposits are expected to occur, were once widespread but are now to varying degrees structurally deformed and tectonically dismembered. The degree of tectonic preservation varies from a resemblance of partial coherence, as in the Bozshakol' Arc in the Bozshakol'-Chingiz magmatic arc terrane (fig. 1-19) of Windley and others (2007) in northern Kazakhstan, to small, isolated and highly deformed blocks only 5–10 km on a side in the central Tian Shan ranges in Kyrgyzstan (for example, fig. 1-18).

Seltmann and others (2009) show some Cambrian arcs to have few or no documented mineral occurrences, whereas others have several arc-related mineral occurrences. Nevertheless, few Cambrian occurrences have had economic significance. In some Cambrian magmatic-arc terranes, at the time scale of Periods, both porphyry copper-type (PPY Cu) and volcanogenic massive sulfide-type (VMS) deposit types occur within the same grouping of arc-type rocks considered permissive for the occurrence of an undiscovered porphyry copper deposit. For example, in the Cambrian Bozshakol'-Chingiz Arc (BC terrane in fig. 1-16), VMS occurrences associated with arc-type andesite-dacite rocks occur, including a few PPY Cu occurrences in close proximity to VMS deposits (fig. 1-20). In the Bozshakol' deposit area, Seltmann and others (2009) show a VMS occurrence in Middle Cambrian rocks. However, the actual age of the VMS occurrence is equivocal, because Tortkuduk is described by Seltmann and others (2009) as Ordovician (undifferentiated).

The economically most significant Cambrian porphyry copper occurrence found to date is the Bozshakol' deposit in the northwest segment of the Bozshakol'-Chingiz magmatic-arc terrane in northern Kazakhstan (fig. 1-40). Discovered in 1929 (Kudryavtsev, 1996), mineralization occurs in an igneous complex of quartz diorite and tonalite, part of a magmatic-arc built on Early to Middle Cambrian ocean-floor deposits. The deposit is located along a regional, northeast- to east-northeast-trending zone of thrust faulting along which the Late Cambrian arc rocks are overthrust by a folded sequence of Middle to Late

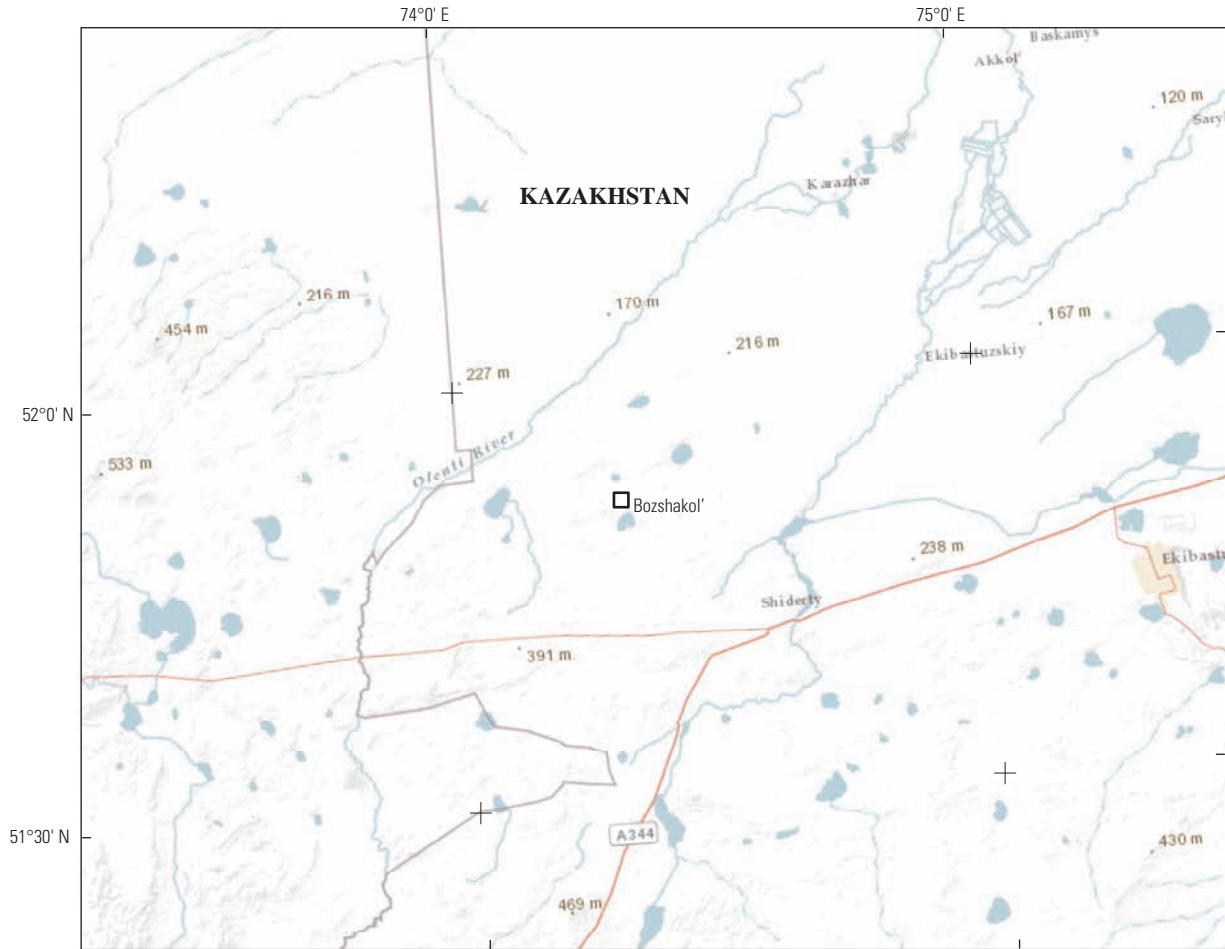
Ordovician carbonate and siliciclastic rocks, intermediate composition tuffs, and rhyolite sills and dikes (Seltmann and Porter, 2005). Late Ordovician gabbro bodies occur along the structural contact between the Ordovician suites and the Cambrian suites.

Within the Bozshakol' deposit, the principal igneous rocks are small diorite and quartz diorite stocks and premineralization Late Cambrian dikes of porphyritic tonalite and tonalite porphyry. These intrude the older Cambrian formations. They strike east-northeast to east (Seltmann and Porter, 2005) along a structural zone, slightly oblique to the present-day exposure of the thrust front such that the mineralization-controlling deformation zone becomes buried beneath the Ordovician (?) allochthon to the east. The economic mineralization occurs in altered volcanic rocks, both ocean-floor mafic and intermediate-composition arc rocks, around the porphyritic dikes.

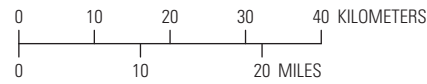
The ore bodies consist of linear stockwork zones that strike northeast and dip steeply to the north (Kudryavtsev, 1996). The principal ore minerals are pyrite and chalcopyrite with accessory magnetite, molybdenite, and sphalerite. Less common ore minerals include bornite, cubanite, and galena. Near the surface, the ore zone is more or less a continuous body on the order of 3 km along the strike of the controlling fault system with an average width of about 500 m. The continuity of the ore bodies decreases with depth, that is it segments, and the width of each segment narrows. Thus, the overall geometry of the Bozshakol' deposit is one of downward branching ore shoots that plunge to the northeast (see Seltmann and Porter, 2005). At all levels, the somewhat sinuous shape of the ore bodies in plan view (see Kudryavtsev, 1996) together with the unusual length/width ratio of the ore geometry suggest that the deposit has undergone postdepositional deformation. Fold structures (Seltmann and Porter, 2005) in the Cambrian volcanic rocks are consistent with this interpretation.

Bozshakol' is unusual in that it contains local concentrations of pentlandite along with the platinum group elements, principally palladium, along with tellurides. Cobalt, nickel, and platinum group elements are related to the vein assemblage pyrrhotite-chalcopyrite-pyrite and are abundant in the western part of the deposit, where oceanic basalts are most common (see Kudryavtsev, 1996).

Hydrothermal alteration (Kudryavtsev, 1996) is zoned from a potassic core through a phyllic zone to an outer zone of propylitic alteration. Quartz, K-feldspar, biotite, magnetite, and pyrrhotite are common in the potassically altered rocks. Phyllic alteration is typically quartz, sericite, carbonate, and chlorite in the volcanic rocks and quartz-sericite in intrusive rocks (Seltmann and Porter, 2005). The propylitic assemblage includes chlorite, epidote, actinolite, calcite, and prehnite and is quite extensive (Kudryavtsev, 1996). Propylitization extends for more than 6 km along the fault zone and is 400 m to more than 2 km wide.



World topographic base from ESRI ArcGIS Online (2009).
 Political boundaries from U.S. Department of State (2009).
 Transverse Mercator Zone 42N, WGS 1984 Projection.
 Central meridian, 69° W., latitude of origin, 0°.



EXPLANATION

□ Porphyry copper occurrence

Figure 1-40. Location map of the Cambrian Bozshakol' porphyry copper deposit in north-central Kazakhstan on a geographic base. Location of map area shown on inset.

Undiscovered Porphyry Copper Deposit Potential of Cambrian Magmatic-Arc Rocks

All of the Cambrian magmatic-arc terranes in Central Asia have undergone more than one significant deformation event and in addition have been affected by the Late Devonian and younger oroclinal bending of western Central Asia. In many instances, quite different lithotectonic terranes have been interleaved structurally, for example, terranes as diverse as ones representative of passive margins with ones reflective of magmatic-arc rocks. Through time, once coherent Cambrian arc terranes have been distended and fragmented into small blocks of unknown dimensions. Even in arcs where near-economic occurrences such as the Bozshakol' deposit have been discovered, it's likely the initial geometry has been distorted owing to postmineralization deformation events and in a manner that cannot be predicted across the whole of the permissive Bozshakol'-Chingiz arc terrane. In addition, much of this arc is tectonically masked by large overthrust nappes. Consequently, a quantitative, probabilistic estimation of the undiscovered porphyry copper deposits in Cambrian arc terranes based on existing geologic descriptive models was not done.

Ordovician Period

Remnants of Central Asian Ordovician magmatic arcs, wherein porphyry copper-type deposits are expected to occur, are more extensive than the Cambrian arc terranes (figs. 1-12 and 1-13). Similar to the Cambrian terranes, the Ordovician magmatic arcs have been structurally deformed and tectonically dismembered. Seltmann and others (2009) show porphyry copper occurrences to be common in several areas, most notably in the western Tian Shan and immediately north on Kendyktas Ridge, in the Kokchetav region in northern Kazakhstan, and in eastern Central Kazakhstan. All of the known deposits are low-grade copper occurrences, but deposits (fig. 1-41) in the western Kyrgyz Mountains and on Kendyktas Ridge along the Chu-Sarysu Basin margin are of economic interest owing to their gold contents.

Western Kyrgyz Mountains and Kendyktas Ridge

Ordovician magmatic-arc rocks extend for several hundred kilometers along the length of the Tian Shan ranges of Kyrgyzstan. In the western Kyrgyz Range in the west of the Tian Shan, there are a number of porphyry copper-gold deposits (fig. 1-41) and occurrences in a 60-km-long, east-west-trending belt, the most extensively explored occurrence of which is the Taldy Bulak (Talas)³ deposit. Occurrences in the general vicinity include Chonur, Dzhangyzstal, Kentash, Andash, and Aktash.

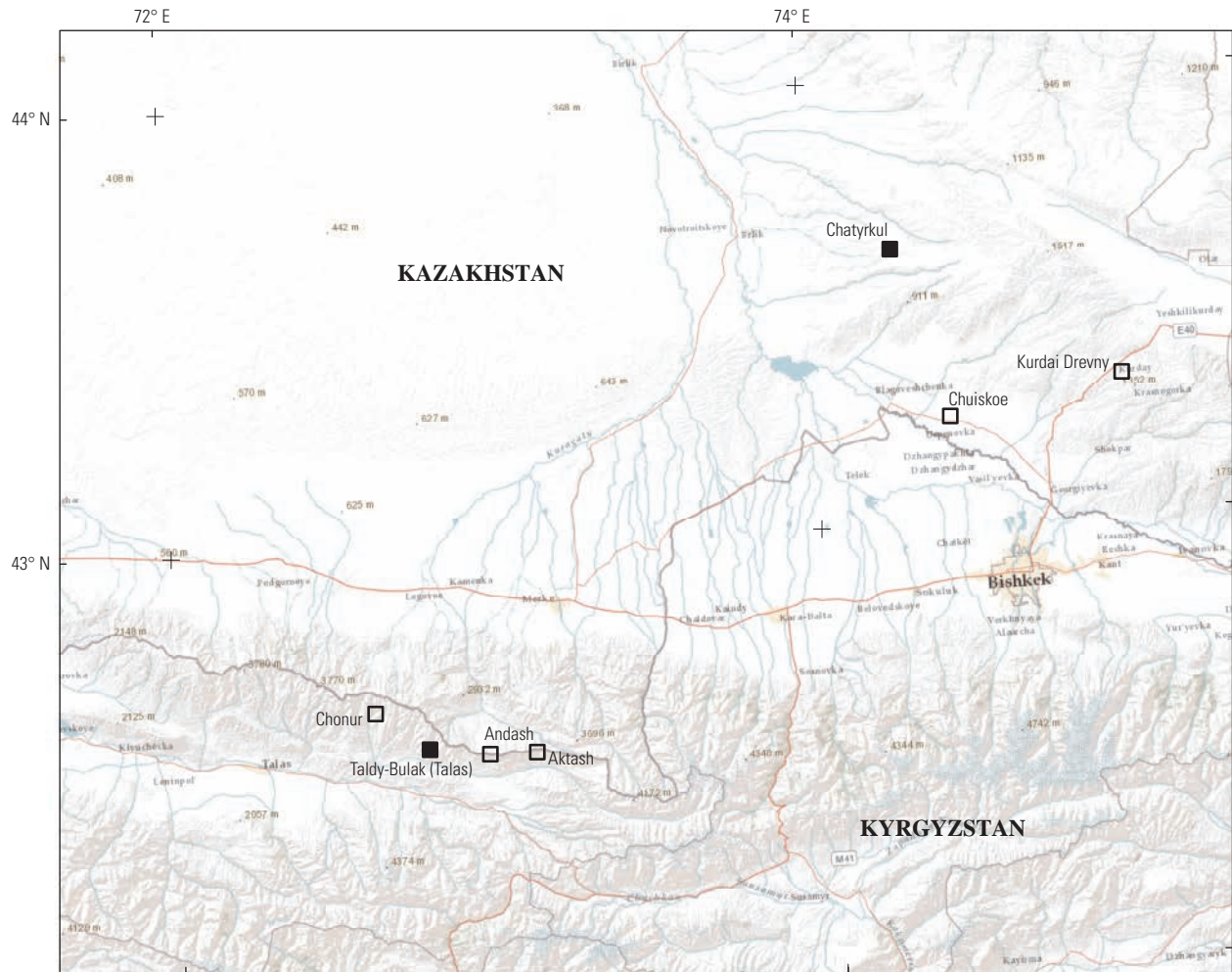
³Talas is used herein to distinguish this Taldy-Bulak porphyry copper deposit from an occurrence of the same type and name a few kilometers north in Kazakhstan (compare Seltmann and others, 2009).

Taldy Bulak (Talas) is located on the northern slope of the Talas River valley drainage basin, Kyrgyzstan. Singer and others (2008) report the deposit to consist of 540 million metric tons (Mt) at 0.24 percent copper, 0.008 percent molybdenum, and 0.5 grams per ton (g/t) gold. An alternative resource consisting of 446 Mt of indicated mineral resource at 0.15 percent copper, 0.0081 percent molybdenum, and 0.31 g/t gold and an inferred resource of 384 Mt at 0.12 percent copper, 0.0099 percent molybdenum, and 0.35 g/t gold (at 0.0 g/t gold cutoffs) was published on <http://www.sedar.com> by Wardell Armstrong International (2010) on behalf of Orsu Metals Corporation.

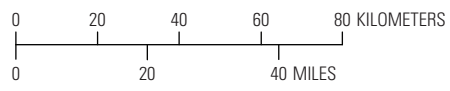
Taldy Bulak (Talas) is related to a latest Ordovician granodioritic intrusive complex for which Jenchuraeva (1997) reports a date of 444±8 Ma. The geology of the Taldy Bulak (Talas) area is complex. The oldest rocks in the immediate vicinity are Early Cambrian spilite, chert, and andesite that elsewhere in the western Kyrgyz Mountains unconformably overlie strongly deformed Precambrian basement (Stepanenko, 1959). The Early Cambrian rocks are tectonically overlain by Late Cambrian to Early Ordovician fine- to coarse-grained siliciclastic rocks, limestone, and tuff. These rocks are, in turn, overlain by Late Ordovician andesite, dacite, and tuffaceous magmatic-arc rocks and sandstone (Seltmann and others, 2009) that are intruded by synvolcanic granodioritic plutons and dikes.

The mineralization occurs predominantly in stockwork quartz veins with the best grades occurring in lens-form east-west zones (Seltmann and Porter, 2005). Hydrothermal alteration consists of quartz, K-feldspar, tourmaline, sericite, and chlorite. Ore minerals include pyrite, chalcopyrite, magnetite, and hematite, and minor sphalerite, tetrahedrite, and pyrrhotite (Seltmann and Porter, 2005).

The Taldy Bulak (Talas) deposit sets in a 50–60 km-long stretch of the western Kyrgyz Mountains wherein there are a large number of mineral occurrences, principally copper-gold and gold, and hydrothermal alteration associated with Ordovician intrusive rocks. In the west is Chonur, a porphyry copper-molybdenum-gold occurrence (Seltmann and others, 2009) about 15–20 km northwest of Taldy Bulak (Talas). It is associated with an Ordovician intrusion emplaced into Ordovician volcanic rocks. Jenchuraeva (1997) reports an age of 460 Ma on galena in a quartz vein with surrounding sericitic alteration 15–20 km east of Taldy Bulak (Talas) at the Andash porphyry copper-gold occurrence (fig. 1-41). Seltmann and others (2009) describe Andash as a large deposit with ~0.4 percent copper and as much as grams per ton gold. It is associated with Late Ordovician diorite to granodiorite porphyries intrusive into Ordovician volcanic and sedimentary rocks. The principal ore minerals are pyrite and chalcopyrite with minor sphalerite, and galena gangue minerals include quartz, K-feldspar, sericite, chlorite, magnetite, hematite, and tourmaline (Seltmann and others, 2009). About 10 km farther east are several gold and copper-gold skarn occurrences, one of which, Aktash, has been historically mined (fig. 1-41).



World topographic base from ESRI ArcGIS Online (2009). Political boundaries from U.S. Department of State (2009). Transverse Mercator Zone 42N, WGS 1984 Projection. Central meridian, 69° W., latitude of origin, 0°.



- EXPLANATION**
- Porphyry copper deposit
 - Porphyry copper occurrence

Figure 1-41. Location map of Ordovician porphyry copper deposits and occurrences in the Kyrgyz Range and on Kandyktas Ridge on a geographic base. Location of map area shown on inset.

Aktash consists of several skarn deposits associated with a Late Ordovician granodiorite intrusion. The skarns consist primarily of garnet and diopsidic pyroxene with magnetite. Ore minerals include pyrite, chalcocopyrite, galena, sphalerite, arsenopyrite, bismuthinite, molybdenite, and gold.

About 170 km northeast of Taldy Bulak (Talas) is the Chatyrkul deposit (fig. 1-41) on Kendyktas Ridge in Kazakhstan. Singer and others (2008) report a tonnage and grade of 90.7 Mt at 0.6 percent copper. The deposit occurs in Late Ordovician biotite-amphibole granodiorite porphyry (Seltmann and others, 2009). Although stockwork-style veins occur at Chatyrkul, most of the mined ore came from through-going veins that crosscut the stockwork zones and have open-space filling and breccia textures (Zhukov and others, 1998). The ore-controlling faults strike north to northeast. The principal ore mineral is chalcocopyrite with associated magnetite, pyrite, molybdenite, and galena. Less common are sphalerite, bornite, cassiterite, and native gold. The principal gangue minerals include quartz, K-feldspar, sericite, chlorite, fluorite, calcite, and zeolites. Copper, copper-gold, and copper-molybdenum vein deposits are widespread along the Kendyktas Ridge. About 170 km southeast of the Chatyrkul deposit is the Kurdai Drevny (fig. 1-41) porphyry copper-molybdenum occurrence. There is little information available regarding this deposit, but the nearby Kurdai porphyry molybdenum deposit has been mined. Seltmann and others (2008) show other scattered porphyry copper style occurrences on Kendyktas Ridge, including the small Chuiskoe porphyry molybdenum-copper occurrence on the edge of the Chu-Sarysu Basin, but none have been described in any detail.

Undiscovered Porphyry Copper Deposit Potential of Ordovician Magmatic-Arc Rocks

Aside from the moderately well-preserved Late Ordovician magmatic arc in the westernmost northern Kyrgyz Mountains of Kyrgyzstan and adjacent Kazakhstan and the Kendyktas Ridge in Kazakhstan, elsewhere Ordovician arc terranes have been subjected either to repeated episodes of deformation that preclude reconstruction of the terranes with currently available geologic information or have been eroded to depths greater than those at which porphyry-style deposits are likely to have formed. Therefore, these terranes were not quantitatively assessed. Nevertheless, they constitute permissive magmatic-arc terranes and their copper metallogeny is briefly discussed below.

Tian Shan Ranges

The tectonic boundary between the Kokchetav-North Tian Shan (NTS) block and the Kyrgyz-Tersky (KT) accreted terrane complex of Windley and others (2007) (fig. 1-16) strikes northwest in the western Kyrgyz Range and roughly describes a line between the cities of Taraz (Dzhambul), Kazakhstan, at the westernmost tip of the Kyrgyz Range and the city of Talas, Kyrgyzstan (city locations shown in

fig. 1-2A). Northeast of this boundary, the surficial deposits and porphyritic intrusions of the Late Ordovician Stepnyak-North Tian Shan magmatic arc crop out (see Windley and others, 2007), but to the southwest of this deformation zone, although arc-related intrusions are widespread, the volcanic cover and its shallow roots have been eroded away. Orogenic, low-sulfide quartz-gold occurrences are within the shear zone as well as on either side of it (fig. 1-18). When classic, crack-seal ribbon veins are observed, that is, the deposit is truly “orogenic,” then it may be reasonably assumed that the occurrence formed at 5–10+ km depth, a depth that is generally below depths at which porphyry copper deposits are known to form. Jerooy, the most prominent of the orogenic occurrences along the SNT-KT boundary fault zone, lies about 50 km to the southeast of the town of Talas (fig. 1-18) and about 30 km south of the Taldy Bulak (Talas) deposit.

Chu-Ili Ranges

Seltmann and others (2009) show stockwork-style copper and copper-molybdenum occurrences associated with Late Cambrian to Early Ordovician and Middle Ordovician rocks in the Chu-Ili region to the east of the Dzhalaïr-Naiman shear zone (fig. 1-21) over to the southwesternmost shore of Lake Balkhash. Within the Dzhalaïr-Naiman Fault Zone, the occurrences are shown by Seltmann and others (2009) in Late Cambrian to Early Ordovician stratigraphic units that do not contain magmatic-arc-related rocks.

To the east near Lake Balkhash, porphyry copper occurrences are in groupings of Late Cambrian to Early Ordovician composited map units at least one of which includes arc-related volcanic rocks. However, the stratigraphic groupings on the geologic map of Seltmann and others (2009) appear to include lithologies deposited in non-arc environments, but neither the proportions of each mapped unit nor the structural relations between the grouped lithologic units are specified.

Tengiz Basin-Kokchetav Region

The Tengiz Basin (figs. 1-2A) borders the Devonian orocline hinge zone (fig. 1-38) on the north and is bounded itself to the north by the Kokchetav region (fig. 1-2A). Seltmann and others (2009) show a porphyry copper occurrence about 110 km due southwest of the shore of Tengiz Lake in an Ordovician intrusive complex. Fewer than 15 km east-southeast of this occurrence, Seltmann and others (2009) show another porphyry copper occurrence in an area mapped as Middle to Late Devonian red beds and near Late Devonian siliciclastic and carbonate rocks with some tuff beds. The nearest mapped Devonian intrusion is about 25 km distant and consists of Middle Devonian leucocratic granite and alaskite, the same as a Late Devonian granite about 40 km distant. Middle Devonian magmatic-arc-related rocks crop out within 15 km of the second occurrence, but they are older than the supposed host rock of the second occurrence. The proximity of these occurrences may be fortuitous, but the possibility

that both are the same age and one mislocated if they are Ordovician cannot be ruled out, and both being Devonian is also a possibility. No other or even possibly linked deposit types occur in this region. Therefore, owing to a paucity of deposit-occurrence evidence and equivocal as to age and occurrence locations in this region, no attempt was made to quantitatively assess this Ordovician arc segment for any undiscovered porphyry copper deposits.

To the north of the Tengiz Basin, Late Ordovician intrusions are widespread. West of the Kokchetav Precambrian massif (fig. 1-17), only a few porphyry copper occurrences are documented. Zhukov and others (1998) provide a brief description of the Baksy porphyry-type copper occurrence (fig. 1-42) located adjacent to the Ishym River on a narrow spur of older rocks between the west margin of the Tengiz Basin and the east margin of the Turgai Trough (fig. 1-2A). This occurrence is in Lower to Middle Ordovician fine-grained siliciclastic rocks intruded by Late Ordovician granodiorite porphyries (Seltmann and others, 2009; Zhukov and others, 1998). Zhukov and others (1998) describe pyrite, chalcopyrite, and gold (\pm molybdenum) to occur in relatively small (to 140 m on strike, 20 m wide and 100 m tall) ore bodies within quartz-tourmaline-calcite veins. The mineralization is confined to the hornfelsic contact zone of the intrusive rocks. Tourmaline-epidote-garnet altered mafic tuffaceous rocks (Cambrian?) and massive and vein magnetite also are present.

Far more common north and west of the Tengiz Basin are molybdenum and tungsten porphyry-style occurrences. Although many of the molybdenum occurrences are shown by Seltmann and others (2009) to occur in Ordovician rocks, they also occur in large Silurian to Devonian leucocratic granites and may all be post-Ordovician. Also in this general region, Ordovician bedded rocks contain some volcanogenic massive sulfide occurrences suggestive of the predominance of marine conditions for the Ordovician arc in this region.

East of the Precambrian Kokchetav massif, porphyry copper occurrences are more common than farther west (Seltmann and others, 2009) as are possibly related copper and copper-gold skarn occurrences. Descriptive information is available for only a few porphyry copper occurrences in this region. Four described here (fig. 1-42) are the Osennee occurrence, the Mongol and Seletinsky ore fields, and the Kyzyltu occurrence. The Osennee porphyry copper-gold occurrence is located about 200 km east-southeast of Kokchetav city (Zhukov and others, 1998). It is associated with a small (4 by 2 km) Late Ordovician intrusive complex consisting of diorite, quartz diorite, granodiorite, and plagiogranite intrusive into an Early to Middle Cambrian ocean-floor volcanic rock sequence that is unconformably overlain by Middle Ordovician magmatic-arc volcanic rocks. Stockwork and disseminated copper mineralization is associated with quartz-sericite altered and propylitized granodiorite porphyry (Zhukov and others, 1998). Sulfide minerals include pyrite, chalcopyrite, and molybdenite with associated hematite. Zhukov and others (1998) note that

stockwork vein densities vary from 1–10 per meter of core. A zone of secondary enrichment has not been identified.

The Mongol ore field is about 50–60 km northeast of Aksu city, a center of orogenic gold production. The ore field is in what is known locally as the Arkalyk intrusive complex (Zhukov and others, 1998), an assemblage of diorite, quartz diorite, granodiorite, and granite. Zhukov and others (1998) list five mineralized areas in the ore field, Mongol I, II, III, IV, and V. Each is localized in a zone of faulting in quartz diorite, granodiorite, and dacite, and consists of vein-form bodies of tourmaline and quartz. Mongol V has been the most completely explored of the mineralized areas. Sulfide mineralization occurs in quartz-tourmaline veinlets with K-feldspar selvages. Mongol V consists of groupings of stockwork zones with dimensions of as much as 600 m long by as much as 20 m wide within which multiple ore bodies have been delineated. The ore bodies strike northeast and terminate against uneconomic andesite dikes and a dacite intrusion. The principal sulfide minerals are pyrite, chalcopyrite, and molybdenite with some bornite, chalcocite, and covellite. Gangue minerals include quartz, tourmaline, K-feldspar, chlorite, epidote, and sericite. Zhukov and others (1998) report a “small” tonnage of ore reserves averaging 0.57 percent copper and 0.09 percent molybdenum to have been delineated to a depth of 200 m with additional reserve potential at depth. Seltmann and others (2009) show Mongol to be only one of many occurrences in the intrusive complex, most of which were apparently prospected in prehistoric times (Zhukov and others, 1998).

The Seletinsky intrusive complex ore district is 70–80 km southeast of Aksu city. Seltmann and others (2009) show five occurrences associated with this intrusive complex. Descriptive information is available for two, Seletinskoe and Kyzyltu (spelled “Kyzyltau” in Seltmann and others, 2009). The intrusive complex consists of diorite, quartz diorite, granodiorite, granodiorite porphyry, quartz monzonite, and granite porphyry. Monzodiorite and leucocratic granite are widespread (Zhukov and others, 1998). The complex is intrusive into Middle to Late Cambrian and Early to Late Ordovician suites. The Seletinskoe occurrence is in the central part of the intrusive complex, principally in a zone of brecciation affected by K-feldspar, silica, sericite, and propylitic alteration. Sulfide minerals include pyrite, chalcopyrite, bornite, molybdenite, and chalcocite. Secondary enrichment is not extensive. In plan view (Zhukov and others, 1998), the ore zones are vein-form and separated by from just a few meters to more than 100 m. Postmineralization faults offset many of the ore zones. In cross section, Zhukov and others (1998) show the ore bodies to be very irregular, varying from rectangular bodies to relatively thin sheets. The mineralized zone is truncated at depth by a flat fault. Kyzyltu is in the southeastern part of the Seletinsky complex along the contact of the Late Ordovician Seletinsky plutonic complex with Middle Devonian volcanic and sedimentary rocks cut by Late Devonian granodiorite porphyry. Zhukov and others (1998) show the mineralization to crosscut Ordovician and

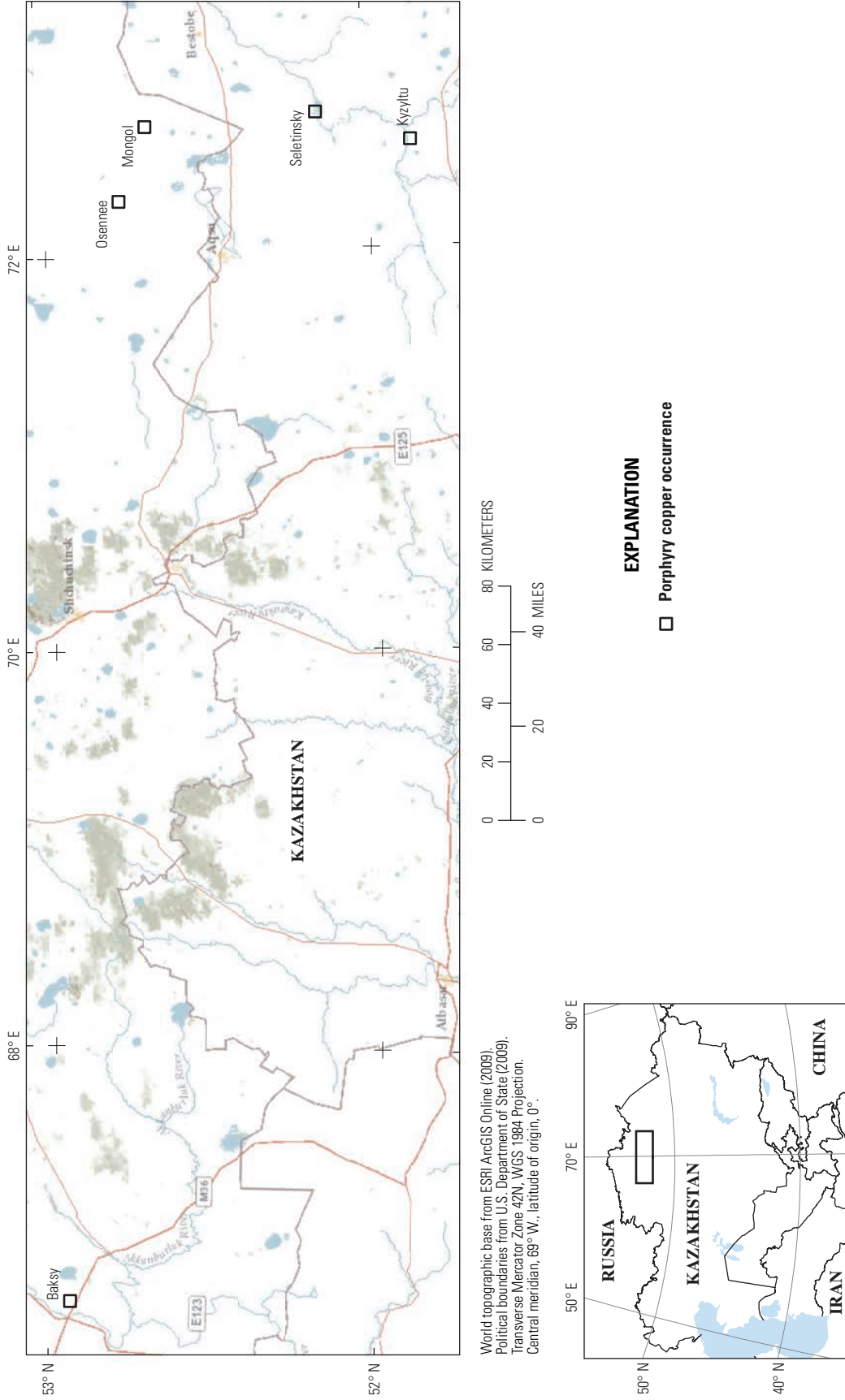


Figure 1-42. Location map of Ordovician porphyry copper occurrences in northern-most Central Kazakhstan east and west of the Kokchetav Precambrian massif on a geographic base. Location of map area shown on inset.

Devonian rocks. This relation raises the question as to the age of all porphyry copper occurrences in the Seletinsky intrusive complex and, perhaps, elsewhere in this region that might have been overlapped by Devonian or younger magmatic-arc activity.

Widespread to the north and east of the Kokchetav massif are structurally controlled orogenic gold deposits (fig. 1-17), some occurring in proximity to porphyry copper occurrences. The orogenic gold deposits are indicative of a fair amount of erosion down into the Late Ordovician magmatic-arc terrane thereby delimiting the potential for viable porphyry copper deposits. Multiple collision events have also modified the Ordovician geologic landscape where the porphyry-style occurrences are found. Seltmann and others (2009) show arc volcanic and near-arc tuffaceous rocks to be primarily Middle Ordovician map units and mixed on the geologic map (presumably owing to tectonics) with non-arc-related marine sedimentary rocks. Furthermore, Late Ordovician fore-arc sedimentary rocks were thrust back across the arc terrane and now are intermingled with the permissive rock units. Due to the lack of any known deposits, a paucity of descriptive information on occurrences, and some question as to the accuracy of age assignments, and the degree and repetition of collision-related tectonics, no quantitative assessment of this Late Ordovician magmatic-arc terrain was done.

Eastern Kazakhstan

A swath of Ordovician magmatic-arc rocks trends northwest-southeast for 500–600 km in eastern Kazakhstan (figs. 1-12). Seltmann and others (2009) show a porphyry gold-copper occurrence in Middle to Late Ordovician siliciclastic sedimentary rocks that are in close proximity to magmatic-arc volcanic rocks. However, most mineral occurrences in the Late Ordovician arc-related rocks of eastern Kazakhstan, excepting some copper skarn occurrences, are volcanogenic massive sulfide occurrences. This suggests that the arc was submarine throughout this region. Owing to the arc being submarine, its strongly deformed nature, and the lack of any known porphyry copper deposits, a quantitative assessment of this region of Ordovician magmatic-arc activity for undiscovered porphyry copper deposits was not undertaken.

Silurian Period

Outcrops of Silurian rocks (figs. 1-14 and 1-15) are less abundant than Ordovician rocks, and most of the mapped outcrops consist of rocks not typical of magmatic-arc environments. Seltmann and others (2009) show a porphyry copper-molybdenum occurrence that may be within a small fault-bounded block of Early Silurian magmatic-arc rocks near the southwest shoreline of Lake Balkhash. However, the mapped location is on or near a structural boundary with Middle Silurian to Early Devonian rocks that include

andesite and dacite volcanic rocks, so the age of the deposit is equivocal. No descriptive information is available for this occurrence. Other fault-bounded exposures of Early Silurian magmatic-arc rock suites occur along a 40 km-long trend to the northwest from Lake Balkhash, each block being 2–4 km wide and 10–15 km long, but there is no evidence of a porphyry-style copper occurrence cited (Seltmann and others, 2009). Farther northwest are Early Silurian rock suites, but they do not include rock types indicative of a magmatic-arc environment. Copper-molybdenum and copper-tungsten occurrences in this area are likely Devonian or younger. Eighty to 125 km due north, several small exposures of Early to Middle Silurian rocks include rhyolite. One map unit includes a stockwork tungsten occurrence, another porphyry copper-gold occurrence (Seltmann and others, 2009), but all of the Silurian rocks are surrounded by Devonian to Carboniferous magmatic-arc rocks, and the ages of occurrences in the Silurian rocks are subject to question.

The most regionally extensive zone of Silurian magmatic-arc rocks is east of Lake Balkhash (fig. 1-14) in a trend that extends northwest from the Chinese border for more than 500 km. Seltmann and others (2009) show an occurrence here and there in the mapped Silurian suites, but most occurrences are volcanogenic massive sulfides and indicative that much, perhaps all, of the arc was submarine.

Devonian Period

On the amalgamation in the Early Devonian of the Kazakhstan continent, the formation and accretion of relatively short magmatic-arc segments, as characterized the earlier Paleozoic subduction zones, ended. Subduction along the whole of northeastern Kazakhstan resulted in a long, continuous Devonian arc. Thus, as may be seen in figures 1-24, 1-25, and 1-26, Devonian magmatic-arc rocks are widespread and abundant in western Central Asia. Commensurately, together with better geologic and tectonic preservation of magmatic-arc rock assemblages, this resulted in a greater number of porphyry copper-type occurrences than during previous Periods. In the discussion that follows, the Devonian porphyry copper metallogeny is discussed in terms of present-day geography.

Chatkal-Kurama Region, Uzbekistan

Remnants of an Early to Middle Devonian magmatic-arc assemblage are present throughout the Chatkal-Kurama region (fig. 1-22) of southwest Kyrgyzstan and adjacent Uzbekistan and Tajikistan. However, Seltmann and others (2009) do not show any porphyry copper or possibly linked occurrence types within Devonian magmatic-arc rocks. Owing to the paucity of magmatic-arc rock assemblages in this region and their wide spacing and the lack of identified occurrences, the area was not quantitatively assessed for undiscovered deposits.

Kyrgyz Mountains, Kyrgyzstan-Southern Kazakhstan

Devonian magmatic-arc rocks crop out in the western Kyrgyz Mountains and directly overlie mineralized Late Ordovician magmatic-arc rocks. Early Devonian rock suites are similar to those found in the Chatkal-Kurama region, but the later Devonian suites are more siliceous and Middle to Late Devonian intrusions are alkalic or granites. Most mineral occurrences shown by Seltmann and others (2009) in association with western Kyrgyz Mountains Devonian magmatic-arc rock suites are orogenic gold or a polymetallic variant and a few epithermal copper to copper-gold occurrences. Many of the mapped units (Seltmann and others, 2009) in the Kyrgyz Mountains are mixtures of magmatic arc and non-arc-related rocks that have been tectonically juxtaposed. There are no reported Devonian porphyry-type copper deposits nor reported zones of alteration suggestive of these deposits. These factors, together with the overlap of Devonian magmatic-arc rocks over mineralized Ordovician rocks and, in turn, the overlap of mineralized Carboniferous rocks onto Devonian rocks, led to the decision to not make a quantitative assessment for undiscovered Devonian porphyry copper deposits in the Kyrgyz Mountains.

Chu-Ili Ranges, Southern Kazakhstan

Devonian magmatic-arc rocks are exposed in the Chu-Ili region east of the Dzhailair-Naiman tectonic zone and west of the Balkhash Depression (fig. 1-27). Early to Middle Devonian volcanic-rock assemblages tend to include a large proportion of andesite and dacite whereas Late Devonian assemblages include more rhyolite. This change in igneous chemistry appears to be reflected in the types of mineral deposits that occur in the region. In Seltmann and others (2009), porphyry copper and porphyry copper-molybdenum occurrences are more commonly associated with Early and Middle Devonian rocks than Late Devonian rocks. In contrast, epithermal uranium occurrences are found in Late Devonian volcanic rocks with associated rhyolitic intrusions. Most of the Devonian intrusions are Late Devonian and the map units are mixtures of the higher silica granite suites and more intermediate granodiorite (Seltmann and others, 2009). At the south end of the Chu-Ili region near the Tian Shan ranges, the Devonian magmatic-arc rocks are overlapped by Carboniferous magmatic-arc rocks, as is apparently also the case to the east in the Balkhash Depression (D. Alexeiev, oral commun., 2009). On the order of 60–70 km west of the main regional-scale fault displacement, there is a ~3,500 km² Middle Devonian diorite-granodiorite complex wherein Seltmann and others (2009) show 5 porphyry molybdenum-copper and 2 porphyry copper-bismuth occurrences. Given the number of known occurrences, the predominance of molybdenum over copper and lack of descriptive information, this small area was not quantitatively assessed.

Owing to the occurrence in the Chu-Ili region of older magmatic-arc sequences with known porphyry copper occurrences, the structural complexity of this region and lack of clear definition of the proportion of intrusive and volcanic rock suites that consist of andesitic to dacitic rocks, and the overlap of Carboniferous magmatic-arc rocks, this approximately 300 km-long region of Devonian magmatic-arc rocks was not quantitatively assessed for undiscovered porphyry copper deposits.

Central Kazakhstan: West and Northwest of Lake Balkhash

How far to the east the Devonian magmatic arc in the Chu-Ili ranges extends beneath the Balkhash Depression sediments is unknown, but it crops out along the southwestern north-shore margin of Lake Balkhash to approximately 74° E. longitude (fig. 1-27). Seltmann and others (2009) show a number of porphyry copper occurrences in this area, some ostensibly associated with Devonian rocks, others clearly associated with Carboniferous rocks. A porphyry copper deposit shown in Seltmann and others (2009), Saryshagan (location in fig. 1-27), as occurring in Middle to Late Devonian magmatic-arc volcanic rocks has a reported age of Late Carboniferous (Singer and others, 2008). Thus, the Devonian arc was overlapped by Carboniferous magmatic-arc activity in this region, thereby making equivocal the ages of identified porphyry copper occurrences irrespective of their host-rock ages.

Those Carboniferous volcanic-arc rocks present in the region immediately north of Lake Balkhash are lower Early Carboniferous, perhaps indicative of Devonian arc activity lingering into the Carboniferous. However, between about 47° N. and 48° N. latitude, a shallow water carbonate reef-type environment succeeded the Late Devonian arc magmatism. In this gap, porphyry-style copper occurrences spatially associated with Late Devonian intrusions and volcanic formations are likely Devonian. Both porphyry copper-molybdenum and molybdenum-copper occurrences are recorded by Seltmann and others (2009) as being associated with Late Devonian leucogranites and granite porphyries. From about 48° N. latitude and farther north, the Early Devonian igneous complexes include some intermediate composition intrusions whereas the Late Devonian volcanic rocks are bimodal and the intrusions granitic. The siliceous igneous activity at this latitude persisted into the earliest Early Carboniferous (Seltmann and others, 2009). Sedimentary exhalative lead-zinc deposits and occurrences are found in the Late Devonian to Early Carboniferous bedded rocks over a wide area in this region and tin is associated with some Late Devonian intrusions. Porphyry copper occurrences shown by Seltmann and others (2009) appear to be associated wholly with Early to Middle Devonian intrusive rock complexes. Akmola and Batembai are two occurrences in these older Devonian rocks listed in Seltmann and others (2009), but no descriptive information is available.

North and Eastern Central Kazakhstan

North of about 49.5° N. latitude and east of about 72° E. longitude, Devonian volcanic rocks (fig. 1-24) are widespread and are not co-mingled with Carboniferous arc-related formations. In this region, andesitic to dacitic magmatic-arc rocks are Early to Middle Devonian. Seltmann and others (2009) show porphyry copper occurrences associated these rock complexes (fig. 1-43), including the large, low-grade Nurkazgan (Samarsk) deposit (~lat 73° E., long 50.2° N.) in the Karaganda province about 380 km north-northwest of the Carboniferous open-pit mine in the Kounrad porphyry copper deposit near Lake Balkhash. Nurkazgan is associated with the Tukulamsky plutonic complex (Zhukov and others, 1998) that is intrusive into a suite of Devonian volcanic and volcanoclastic rocks of generally andesitic composition (Seltmann and others, 2009). The intrusive rocks are predominantly granodiorites. Mineralization is associated with granodiorite microporphyrries and magmatic breccias (Zhukov and others, 1998). Three varieties of mineralization occur in the ore field—gold-polymetallic, gold-copper, and gold-copper-molybdenum. In map view, Zhukov and others (1998) show the deposit to consist of two large areas of outcropping stockwork veins separated by about 2 km. The northern of these two is considered a low-grade gold-copper-molybdenum occurrence, whereas the more southern area has associated breccias and gold-copper mineralization. Hydrothermal alteration minerals include quartz, K-feldspar, biotite, sericite, pyrite, tourmaline, chlorite, epidote, and carbonate. Ore minerals include chalcopyrite, tetrahedrite, and molybdenite with accessory bornite, sphalerite, galena, native gold. In the southeastern part of the ore field are areas of silica-alunite alteration.

Northeast of the Nurkazgan deposit is a prospect interpreted to be the Shaitandy occurrence in the Karaganda province. This occurrence is in Devonian andesitic lavas, volcanoclastic sedimentary rocks, and sandstones intruded by diorite porphyry and trachyandesite porphyry. Thin lenses of copper mineralization are associated with zones of silicification and propylitization (Zhukov and others, 1998). Shaitandy, where malachite is observed at the surface, lies within the historical Spassky copper ore field, which was trenched and drilled in the 1960s and 1970s and is part of Great Western Exploration Limited's (2012) Spasskaya copper belt project. About 100 km southeast of the Nurkazgan deposit is an occurrence interpreted to be Khadzhikongan (fig. 1-43) based on its geology and location vis-à-vis the railroad. Khadzhikongan is in Karaganda province (lat ~74.4° E., long 50.0° N.). The occurrence is in Middle Devonian andesitic volcanic rocks and conglomerates and subvolcanic andesitic intrusions (Zhukov and others, 1998). Hydrothermal alteration includes quartz, sericite, pyrite, magnetite, chlorite, epidote, barite, and fluorite. Ore minerals include chalcopyrite with bornite, sphalerite, and galena. Zhukov and others (1998) describe the mineralization as commonly very fine grained disseminations or nodular zones in volcanic rocks.

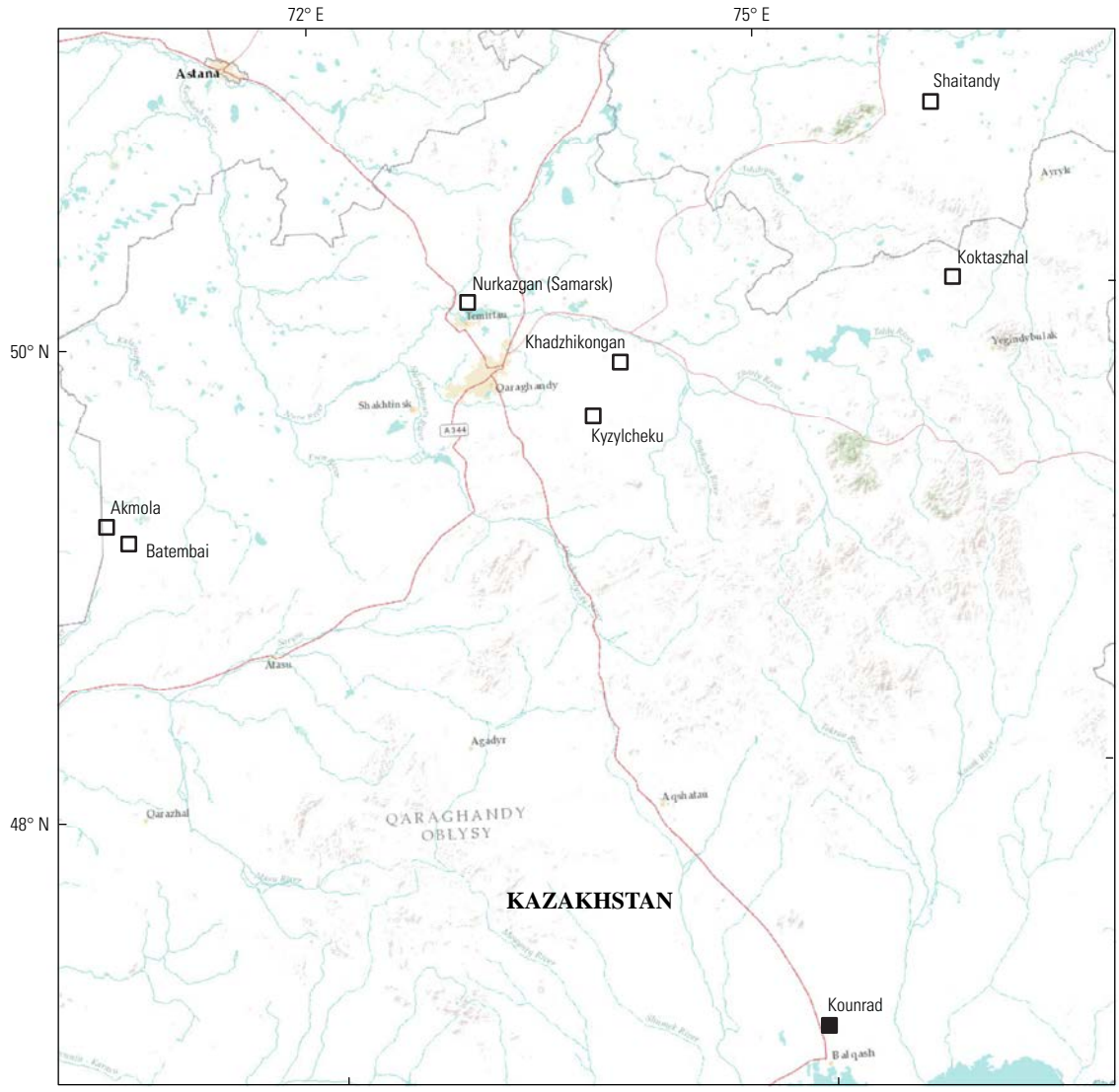
Also south-southeast of the Nurkazgan porphyry copper deposit is an occurrence categorized as a porphyry copper by Zhukov and others (1998) and known as Kyzylcheku (lat ~73.7° N., long 49.6° E.) (fig. 1-43). Seltmann and others (2009) show no porphyry copper occurrence in this region, but a large number of epithermal-style deposits are present in this sequence of Devonian rocks. The Kyzylcheku occurrence is associated with brecciated limestones and porphyritic lavas with quartz-sericite-kaolinite alteration. Also present is an advanced argillic alteration assemblage that includes quartz and andalusite. No primary sulfide minerals are reported by Zhukov and others (1998), and the level of exploration reported by them does not seem sufficient to establish the presence of a porphyry copper occurrence.

Farther east (for example, lat 75.6° E., long 50.2° N.), Seltmann and others (2009) show stockwork-type copper occurrences spatially associated with volcanogenic massive sulfide deposits, suggesting that the Devonian arc in this part of Kazakhstan was submarine. Red beds become common throughout this region in the Middle to Late Devonian and are associated with bimodal basalt-rhyolite volcanic rocks. There are numerous copper-bearing epithermal occurrences in the bimodal assemblage rocks along with some sedimentary-rock hosted copper deposits (Seltmann and others, 2009).

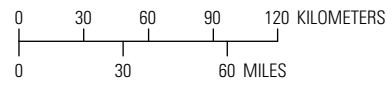
Early to Middle Devonian arc-related rocks at about latitude 50° N. terminate east at about longitude 76° E. against a major fault zone. Porphyry copper occurrences (for example, Koktaszhal) near this fault zone intrude highly deformed Devonian rocks and mineralization is, in part, controlled by schistosity. The Koktaszhal occurrence (lat ~76.2° E., long 50.1° N.) is located in Karaganda province (fig. 1-43). It is associated with a Middle Devonian sequence of dacites, siliceous tuffs, sandstones, and limestone intruded by tonalite and granodiorite of the Koktaszhal'sky igneous complex (Zhukov and others, 1998). Mineralization is most closely associated with plagiogranite porphyries. The host rocks have been strongly deformed and mineralization is in a series of en echelon, steeply dipping quartz vein zones that are localized along planes of schistosity with intervening alteration of chlorite-sericite. In these quartz veins, copper minerals occur in thin gaps and nodular accumulations (Zhukov and others, 1998). Hydrothermal alteration includes quartz, sericite, chlorite, pyrite, magnetite, and ilmenite. Ore minerals include chalcopyrite and bornite, with accessory molybdenite and tetrahedrite. Seltmann and others (2009) show other occurrences in the immediate vicinity and an additional group 40–30 km west.

Eastern Kazakhstan

The Early to Middle Devonian arc assemblages persist to the east of 76° E. longitude along the southeast-trending arm of the Devonian orocline (fig. 1-27), but the structural blocks are less contiguous than in Central Kazakhstan, and the occurrence of Carboniferous intrusions in the Devonian units obscure the age of mineral deposits. As was the case



World topographic base from ESRI ArcGIS Online (2009).
 Political boundaries from U.S. Department of State (2009).
 Transverse Mercator Zone 42N, WGS 1984 Projection.
 Central meridian, 69° W., latitude of origin, 0°.



EXPLANATION

- Porphyry copper deposit
- Porphyry copper occurrence

Figure 1-43. Location map of Devonian porphyry copper deposits and occurrences in the North Balkhash region on a geographic base. The location of the Carboniferous Kounrad porphyry copper deposit and mine is shown for reference purposes. Location of map area shown on inset.

in easternmost Central Kazakhstan, the occurrence of volcanogenic massive sulfide deposits in some parts of the Early Devonian sections suggests that parts of the arc were submarine. Arc activity appears to have persisted into the Late Devonian in Eastern Kazakhstan.

Carboniferous Period

The Carboniferous is the economically most important period for porphyry copper deposits in western Central Asia with the Kal'makyr (Almalyk), Uzbekistan, and Kounrad (near Balkhash City), Kazakhstan, deposits (fig. 1-2A) as prominent examples that are counted amongst the world's best of this class of deposits. The Carboniferous has also received a great deal of geologic and tectonic scrutiny, and, therefore, its history is arguably the best understood of the Paleozoic periods.

As noted above, by the Late Devonian the amalgamation of a Kazakhstan continental mass made up of many Precambrian massifs and Cambrian to Devonian magmatic arcs was underway. Except for eastern and southern Kazakhstan, by the upper Late Devonian active subduction had ended and the semblance of the single Kazakhstan Plate formed. Thus, by the beginning of the Carboniferous, the progressive collisional sandwiching of Kazakhstan between the East European craton, Siberian craton, and Turkestan-Tarim-North China Plates was underway. The final closure of all of the ocean basins did not occur until the latest Carboniferous and into the Permian. Subduction-related magmatism and collision-related tectonics continued well into the Permian and, perhaps, into younger Periods in the southeast of Kazakhstan and into China. Although the spatial progression of the amalgamation and the relation of porphyry copper metallogeny to this progressive event is still being unraveled, detailed studies around the southwestern, southern, and southeastern margins of western Central Asia help to set constraints on the history. The following sections discuss Carboniferous tectonics and porphyry copper metallogeny beginning in the region to the southwest of the Kazakhstan tectonic block in Paleozoic coordinates, as per Filippova and others (2001) and Windley and others (2007).

Southwestern Tectonic Margin

The Valerianov Arc in west-central Kazakhstan and adjacent Russia (fig. 1-22) is within 1 km of Earth's surface over an area that is on the order of 190,000 km². Of this vast area, only about 5 percent consists of outcrop and all of the known porphyry copper occurrences and potentially related deposit types are within or near these outcropping Paleozoic rocks, all of which are located near the suture zone on the west side of the arc. Seltmann and others (2009) show there to be 35–40 porphyry copper occurrences in the exposed to near-exposed part of the arc, but descriptive information is not available for most of them. Zhukov and others (1998)

describe three of the occurrences—Bataly, Benkala North, and Spiridonovskoe (fig. 1-44). Varvarinskoe, listed as a porphyry copper deposit by Singer and others (2008), is classified as a gold-copper skarn deposit by Zhukov and others (1998).

The Benkala North porphyry copper deposit (fig. 1-44) is located near the west margin of the arc in upper Early Carboniferous volcanogenic and sedimentary rocks intruded by the middle Carboniferous Sokolov-Sarbai diorite-granite complex (Zhukov and others, 1998). The volcanogenic rocks are basalt, andesitic basalt, andesite, dacite, tuffs tuffaceous sandstone, and tuffaceous shales. Ore is associated with a suite of dikes that are apophyses off a mass of porphyritic quartz diorite and granodiorite. Mineralization occurs primarily in stockwork quartz veins and consists of pyrite, chalcopyrite, and magnetite with associated molybdenite, bornite, chalcocite, and digenite. Associated alteration includes biotite, K-feldspar, chlorite, sericite, carbonate, and tourmaline. Postore quartz-carbonate veins contain pyrite, barite, and anhydrite (now gypsum). Oxide ore is present, but tonnages are not economically significant, and there is a small chalcocite enrichment blanket overlying the primary ore body.

Spiridonovskoe (fig. 1-44) represents a group of occurrences located about 150 km north-northeast of the Benkala North deposit. The mineralization occurs as separate bodies in discrete fault-bounded blocks (Zhukov and others, 1998). The west side of the largest, middle mineralized zone is tectonic, probably part of the regional-scale Olshansky Fault Zone along the west side of which are large serpentinite bodies. According to Zhukov and others (1998), Spiridonovskoe occurs in Silurian mafic tuffs and porphyries and the Devonian Denisov diorite-granodiorite complex. Seltmann and others (2009) show late Early Carboniferous volcanic and sedimentary rocks immediately northwest of the Spiridonovskoe group in the position of rocks mapped as Middle Devonian in Zhukov and others (1998). Because the Denisov magmatic arc was active to the present-day west of the Valerianov Arc (Herrington and others, 2005) and there are ophiolite fragments along the Olshansky Fault Zone adjacent to the occurrences, it is possible that Spiridonovskoe formed in an accreted block that has subsequently been structurally comingled with Valerianov Arc rocks. Until additional information is available, Spiridonovskoe should be considered of uncertain age. Mineralization at Spiridonovskoe consists of vein and disseminated pyrite, chalcopyrite, molybdenite, bornite and cubanite with some primary chalcocite and covellite. Alteration minerals include quartz, chlorite, sericite, K-feldspar, and carbonate.

The Bataly porphyry copper occurrence (fig. 1-44) lies 50–60 km northwest of the Spiridonovskoe group of occurrences (Seltmann and others, 2009). The occurrence is associated with Krasnoarmeisk-Bataly volcanic center wherein Carboniferous diorite porphyries, granodiorite, and quartz diorite stocks and mafic and acidic dikes intrude volcanoclastic breccias and late Early Carboniferous andesitic lavas (Zhukov and others, 1998). Copper-molybdenum stockwork and disseminated mineralization occurs in the Bataly

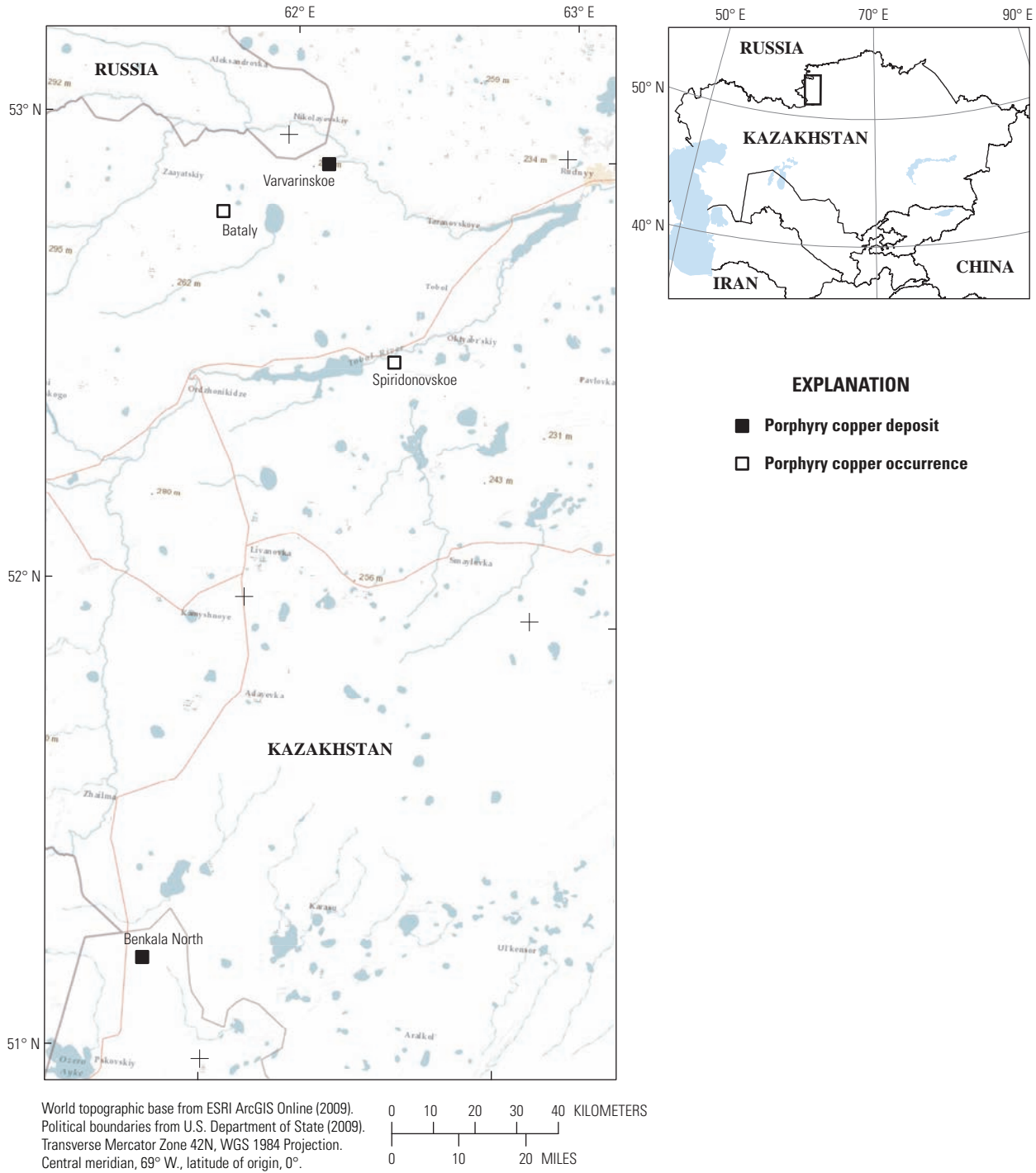


Figure 1-44. Location map of Carboniferous porphyry copper deposits and occurrences in the Trans-Urals zone in Russia and adjacent Kazakhstan on a geographic base. Location of map area shown on inset.

granodiorite-granodiorite porphyry-plagiogranite complex in a zone of northwest- to west-northwest-trending faults that both bound and offset the ore-bearing zones. The principal ore minerals are pyrite, chalcopyrite, and molybdenite together with minor amounts of bornite, cubanite, native gold, scheelite, and arsenopyrite. There are three types of alteration

here: quartz-tourmaline, quartz-albite-sericite, and quartz-sericite. The best ore occurs with the quartz-albite-sericite alteration (Zhukov and others, 1998).

The Varvarinskoe gold-copper deposit (fig. 1-44) is 30–40 km northeast of Bataly and is classified as a porphyry copper by Singer and others (2008). Dodd and

Thornton (2005), in an NI 43-101 technical report, classify the deposit as a skarn, and Zhukov and others (1998) classify it as a gold-copper deposit. The ores are associated with a gabbro-diorite-granodiorite intrusive complex, diorite sills and dikes, and serpentinite sills and dikes (Dodd and Thornton, 2005). The intrusions are altered to an assemblage of actinolite, pyroxene, chlorite, scapolite, and epidote. The serpentinites, formerly dunite and peridotite, are typically along fault zones.

Numerous high-angle, veinlike and low-angle stratiform ore bodies occur at Varvarinskoe along an approximately 3-km north-northeast-striking zone, and Zhukov and others (1998) note that occurrences have been identified for 2 km to the southwest of Varvarinskoe. Zhukov and others (1998) identify 12 ore types, three of which contain gold. They divide the gold-bearing ores into three subtypes: gold-chalcopryrite, gold-sulfide-arsenopyrite, and gold-niccolite-gersdorffite. The principal ore minerals are gold, chalcopryrite, pyrite, pyrrhotite, arsenopyrite, gersdorffite, and niccolite with various other iron, cobalt, nickel, and copper minerals. The principal alteration accompanying the ore is quartz, albite, chlorite, carbonate, tremolite, and talc. Pre-ore alteration consists of garnet, pyroxene, biotite, zeolites, and amphibole.

There are numerous intrusion-related replacement iron and some derivative sedimentary deposits and occurrences in overlying Mesozoic and Cenozoic rocks. Because some of the replacement intrusion-related deposits are proximal to porphyry copper type deposits in the Valerianov Arc, for example Benkala, and are typically classified as skarn deposits and occurrences, there has been speculation regarding a possible genetic link of the two deposit types.

Southeastern Tectonic Margin

In the immediate vicinity of Almalyk, Uzbekistan, there are four discrete porphyry copper deposits (fig. 1-45). The individual deposits are Kal'makyr, Dal'nee (referred to as "Central" in Shayakubov and others, 1999), Karabulak, and Northwest Balikti. Numerous skarn and polymetallic vein and replacement deposits are associated with the Almalyk group of deposits. Kal'makyr is the largest deposit in the group. Stockwork and disseminated ore mineralization is in an Upper Carboniferous to Lower Permian granodiorite porphyry intrusive complex that intruded a mid-Carboniferous monzonite-syeno-diorite intrusive complex. Although mineralization occurs in the granodiorite porphyry, most of the ore occurs in older diorite host rocks. Postmineralization faulting along the east-westerly striking, 75°–85° south-dipping Kal'makyr Fault⁴ separated the locus of ore into two blocks, Karabulak and Dal'nee to the north of the fault and Kal'makyr to the south of the fault (Korolev and Badalov, 1959; Meshchaninov and Azin, 1973).

Sarycheku (fig. 1-45) is 15–20 km southeast of Almalyk on the northern slope of the Kurama Range (Golovanov, 1978). Discovered in 1932, this deposit occurs in Lower Devonian quartz porphyries intruded by Late Carboniferous

granodiorite porphyries (Golovanov, 1978; Golovanov and others, 2005). The deposit is within a structural block bounded to the northwest by the regionally extensive northeast-striking, southwest-dipping Miskan Fault and, to the southeast, the Sargalamsk Fault (Golovanov, 1978). The ores occur in a series of subparallel, northwest-striking bodies that dip to the northeast. The ores include disseminations and stockwork veins, with the principal ore minerals being chalcopryrite, pyrite, and molybdenite. Supergene enrichment affected the upper 40 m of the deposit with chalcocite ores to 4.5 percent copper; the average grade of the 200 Mt deposit is 0.5 percent copper. Hydrothermal alteration includes quartz, K-feldspar, sericite, and chlorite. Also present are anhydrite, carbonate, and barite.

Kyzata (fig. 1-45), 5–10 km northwest of Sarycheku, is associated with granodiorite porphyry that intrudes Early Devonian alaskite, granodiorite, andesite, and quartz porphyry, Carboniferous carbonate rocks, and a Middle Carboniferous syenite-diorite complex (Zvezdov and others, 1993). The ore body is in the immediate footwall and is truncated by the northeast-striking, southwest-dipping Miskan Fault. Mineralized rock is crosscut by unmineralized granodiorite porphyry, syenite and granosyenite porphyry, and diorite porphyry dikes. The ore body consists of a northwest-trending zone of disseminated and stockwork molybdenum-copper mineralization. Ore minerals include chalcopryrite, molybdenite, bornite, chalcocite, galena, sphalerite, and tetrahedrite (Zvezdov and Migachev, 1986). The molybdenite content is greater than other deposits in the Almalyk ore field (Zvezdov and others, 1993). There are postporphyry deposit polymetallic veins. Zvezdov and others (1993) suggest that the Sarycheku and Kyzata deposits in the Saukbulak ore field originally may have been a single deposit now offset sufficiently far, 6–8 km along the Miskan Fault, to constitute two separate deposits in this assessment.

Tekeli (fig. 1-45) is an occurrence northeast of Almalyk, Uzbekistan, in the Chatkal Range. Lower to middle Carboniferous volcanic rocks consisting of dacitic tuffs, andesite and dacite lavas, and volcanogenic sedimentary deposits are intruded by a composite diorite to syenitic igneous complex with disseminated and stockwork mineralization (Golovanov, 1978).

Northeastern Tectonic Margin

Magmatic arcs built along the margin of the Turkestan Ocean have been so highly deformed and deeply eroded during late Cenozoic uplift that no Carboniferous porphyry copper occurrences of note occur in this region. Occurrences farther east along the Tian Shan trend in China attest to the possibility of porphyry copper mineralization having been present along this subduction zone at one time.

⁴See sketch maps in references cited for locations of named faults.



World topographic base from ESRI ArcGIS Online (2009). Political boundaries from U.S. Department of State (2009). Transverse Mercator Zone 42N, WGS 1984 Projection. Central meridian, 69° W., latitude of origin, 0°.

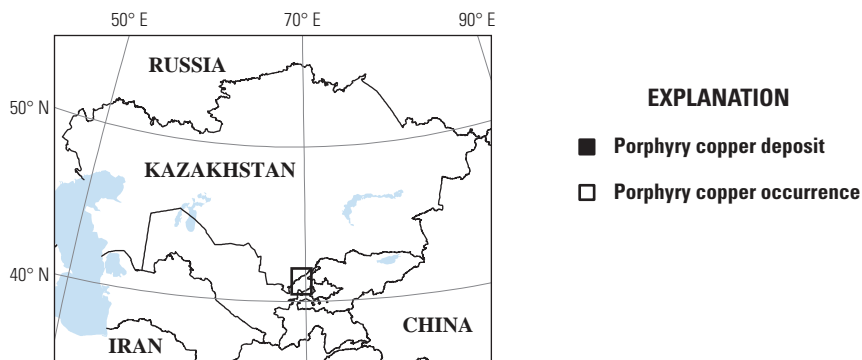
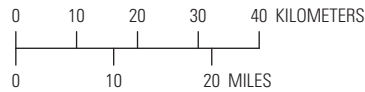


Figure 1-45. Location map of Carboniferous porphyry copper deposits and occurrences in the Chatkal-Kurama region of eastern Uzbekistan on a geographic base. Location of map area shown on inset.

Central Kazakhstan

Carboniferous mineral occurrences and deposits are widespread in the Balkhash-Ili magmatic arc, but most are north of Lake Balkhash. This is predominantly due to poor exposure of Paleozoic rocks in the Balkhash Depression to the south of the lake. In the discussions of porphyry copper deposits and occurrences that follow, those in the east limb of the orocline are described first, followed by those in the North Balkhash or northern limb, and finally those in the west limb.

East Limb of Orocline

As a consequence of low topographic relief, the depth of erosion, and areas covered by post-Carboniferous basalt, exposures of permissive Carboniferous rocks are scant in the east limb of the Balkhash-Ili orocline relative to the north limb. The Aktogai ore field (fig. 1-46) is located in the Taldy-Korgan province 55–60 km northeast of the east end of Lake Balkhash and about 380 km east of the Kounrad mine. There are two major deposits, Aktogai and Aidarly, and a smaller occurrence, Kyzylkia, in the ore field. Zhukov and others (1998) refer to other stockwork style occurrences in the Koldar batholith—Western, Promezhutochny, and Eastern—but no additional information is provided. All are associated with the Carboniferous Koldar batholith, a composite body that varies from gabbro-diorite to granodiorite-granite (Zhukov and others, 1998). Owing to their close proximity, Singer and others (2008) report copper resources for Aktogai and Aidarly combined.

The Aktogai copper-molybdenum porphyry deposit (fig. 1-46) is along the west-northwest–striking Aktogai Fault Zone and occurs in diorite and porphyritic granodiorite intruded by plagiogranite porphyry and granodiorite porphyry dikes, all within Koldar diorite, quartz diorite, and granodiorite (Zhukov and others, 1998; Seltmann and Porter, 2005). There are large roof pendants of Middle to Late Carboniferous andesitic to dacitic volcanic and sedimentary rocks (Zvezdov and others, 1993) that are also found in the deposit. The zone of stockwork veins occurs within an area approximately 2,500 by 830 m (Zhukov and others, 1998). Hydrothermal alteration includes quartz, K-feldspar, biotite, sericite, pyrite, magnetite, tourmaline, chlorite, epidote, prehnite, carbonate, and albite. Pipe-form quartz-biotite matrix breccias and sericite-tourmaline matrix breccias are prominent in the deposit (Zvezdov and others, 1993). Ore mineralization occurs predominantly in stockwork veins and ore minerals include chalcopyrite, bornite, and molybdenite with accessory chalcocite, galena, sphalerite, and tennantite (Zvezdov and others, 1993; Seltmann and Porter, 2005).

Aidarly (fig. 1-46), located about 2–4 km west-northwest of Aktogai, straddles the Aktogai Fault, where it intersects the northeast-striking Aidarly Fault. Zhukov and others (1998) report that there may be as much as 1,000 meters of vertical offset of the ore zone by the Aidarly Fault. The deposit is associated with a granodiorite porphyry stock intrusive into

diorite and quartz diorite of the Koldar pluton. Hydrothermal alteration includes quartz, pyrite, K-feldspar, biotite, sericite, tourmaline, magnetite, anhydrite, chlorite, epidote, zeolites, and carbonate (Seltmann and others, 2005). Silicification is prominent in the Aidarly deposit. Ore minerals include chalcopyrite and molybdenite with accessory sphalerite and galena. Pipe-form breccia bodies contain mineralized fragments cemented by finely comminuted rock material.

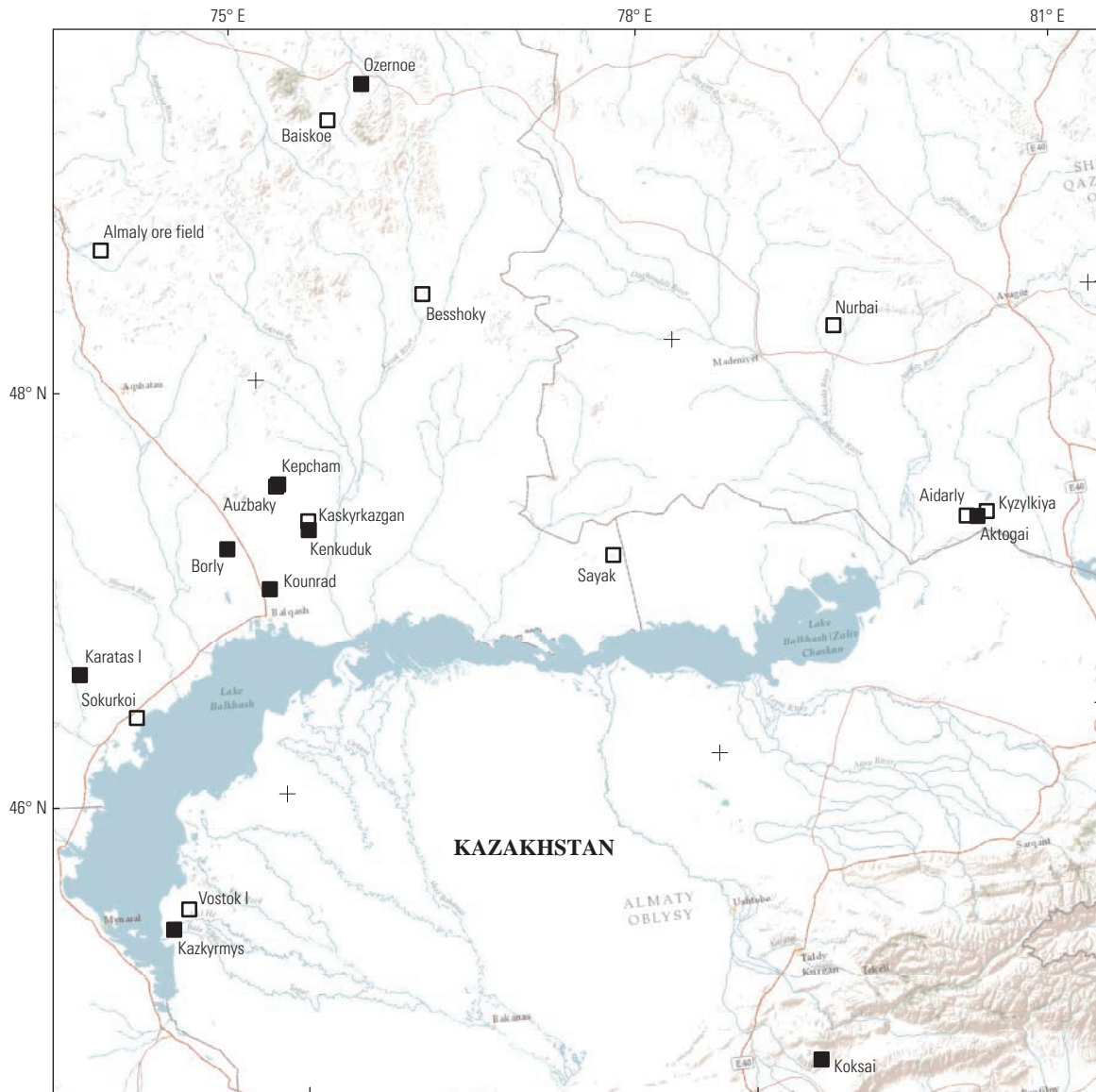
Kyzylkia (fig. 1-46) is a small porphyry copper-molybdenum occurrence located about 4 kilometers northeast of the Aktogai deposit. It lies along a north-northwest–striking fault zone and is associated with a granodiorite porphyry stock intrusive into the Koldar complex (Seltmann and Porter, 2005). Hydrothermal alteration minerals include quartz, biotite, K-feldspar, pyrite, sericite, tourmaline, magnetite, albite, carbonate, and zeolites (Zhukov and others, 1998). Ore minerals include chalcopyrite, bornite, chalcocite, and molybdenite with accessory sphalerite. This small-size occurrence consists of en echelon zones of stringer-like stockwork veining.

The Nurbai porphyry copper occurrence (fig. 1-46) is located ~120 kilometers north-northwest of the Aktogai deposit in the Semipalatinsk province. The occurrence is associated with Carboniferous monzonites and monzonite porphyritic plutons and monzonite porphyry and diorite porphyry dikes intrusive into Middle Devonian lavas, tuffs, and volcanoclastic rocks (Zhukov and others, 1998). A widespread area around the occurrence is altered by quartz-diaspore-andalusite and quartz-sericite metasomatic assemblages. The best copper mineralization occurs along a northwest-striking zone of stockwork-fractured rock altered to quartz, sericite, and pyrite with accessory arsenopyrite. Ore mineralization occurs as disseminations and stockworks with chalcopyrite and molybdenite with accessory bornite, galena, sphalerite, chalcocite, and covellite (Zhukov and others, 1998).

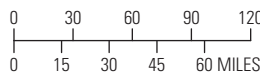
North Limb of Orocline

The Carboniferous stratigraphy is best preserved in the north limb of the Balkhash-Ili orocline. Porphyry copper occurrences are widespread and Seltmann and others (2009) show a large number of permissively linked deposit types such as copper skarn, polymetallic veins, and epithermal veins. Advanced argillic alteration, which elsewhere has a sometimes spatial association with porphyry copper deposits, is also present in many areas. For the majority of occurrences shown by Seltmann and others (2009), there is no descriptive information available. The descriptions that follow are largely from Zhukov and others (1998) although the literature on the Kounrad deposit is extensive.

The economically most significant deposit in the Balkhash-Ili magmatic arc is situated near the northern margin of Lake Balkhash at Kounrad (fig. 1-46) in the Dzhezkazgan province. Copper-molybdenum mineralization at Kounrad is associated with the porphyritic phases of a suite of intrusions



World topographic base from ESRI ArcGIS Online (2009).
 Political boundaries from U.S. Department of State (2009).
 Transverse Mercator Zone 42N, WGS 1984 Projection.
 Central meridian, 69° W., latitude of origin, 0°.



EXPLANATION

- Porphyry copper deposit
- Porphyry copper occurrence

Figure 1-46. Location map of Carboniferous porphyry copper deposits and occurrences in Central Kazakhstan on a geographic base. Location of map area shown on inset.

that include quartz diorite, granodiorite, plagiogranite, and granite (Zhukov and others, 1998). Disseminated and stockwork mineralization is predominantly in granodiorite porphyry with associated alteration that includes biotite, K-feldspar, sericite, magnetite, tourmaline, and a propylitic assemblage that includes chlorite and albite (Seltmann and Porter, 2005). Ore minerals include pyrite, chalcopyrite, molybdenite, enargite, tetrahedrite, and chalcocite with accessory sphalerite, galena, and bornite. An advanced argillic assemblage of alteration with associated ore minerals occurs within the deposit. The alteration includes corundum, andalusite, diaspore, alunite, and kaolinite. Associated sulfosalts include enargite, tennantite, and famatinite, together with gold-silver tellurides (see Seltmann and Porter, 2005).

Borly (fig. 1-46) is located about 30 km northwest of the Kounrad deposit in the Dzhezkazgan province. It occurs in association with granodiorite porphyry that intrudes the Borlinksy pluton, which is a three-phase complex consisting of quartz diorite, granodiorite, and leucogranite (Zhukov and others, 1998). Brecciation of the Borlinksy rocks accompanied emplacement of the granodiorite porphyry and localized hydrothermal alteration and stockwork sulfide mineralization. Hydrothermal alteration minerals include quartz, K-feldspar, sericite, pyrite, magnetite, chlorite, epidote, carbonate, and zeolites. Ore bodies strike north-northwest and ore minerals include chalcopyrite and molybdenite with accessory bornite, chalcocite, sphalerite, tetrahedrite, tennantite, and galena.

Thirty to 45 km northeast of the Kounrad deposit, a group of 4 occurrences in relatively close proximity to each other includes Kepcham, Kazkyrkazgan, Kenkuduk, and Auzbaky (Zhukov and others, 1998) (fig. 1-46). Zhukov and others (1998) discuss these as a group, but note that the Kazkyrkazgan occurrence has been studied in the most detail. The host rocks are granites, granite porphyries, and granodiorite porphyries of the Balkhash and Kaldirminsky intrusive complexes. Kostitsyn (1996) reports a K-Ar date for Kenkuduk of 309 ± 16 Ma. Hydrothermal alteration minerals include quartz, K-feldspar, sericite, pyrite, magnetite, and hematite. Ore minerals occur in stockwork veins and include chalcopyrite and molybdenite with accessory sphalerite and galena.

The Almaly ore field (fig. 1-46) is located ~210 kilometers northwest of Kounrad in the Dzhezkazgan province. Copper occurs as an important commodity in a number of different deposit types associated with the Almalinsky intrusive complex in this ore field, but the most valuable of these is the Akbiik porphyry copper occurrence. Kostitsyn (1996) reports a K-Ar date of 317 Ma on a small stock in the intrusive complex. The Akbiik stockwork mineralization occurs along the southeast margin of the Almalinsky complex. Hydrothermal alteration minerals include quartz, K-feldspar, pyrite, and chlorite. Ore minerals include chalcopyrite and molybdenite with accessory galena, tetrahedrite, and native gold.

Besshoky (fig. 1-46) is located about 160–170 km northeast of Kounrad in the Dzhezkazgan province.

This copper molybdenum occurrence is associated with granodiorites of the Carboniferous Toparsky intrusive complex (Zhukov and others, 1998). Extensive areas of silica-alunite alteration surround the occurrence. Other advanced argillic alteration minerals include andalusite and diaspore. Porphyry copper mineralization consists of disseminations and stockworks in quartz-sericite-pyrite and propylitically altered rock. Ore minerals include chalcopyrite and molybdenite with accessory enargite, tetrahedrite, and famatinite (Zhukov and others, 1998).

The Ozernoe porphyry copper occurrence (fig. 1-46) is located about 270 km north-northeast of Kounrad in the Karaganda province. It is associated with porphyritic granodiorites in the Carboniferous Oziorny intrusive rock complex (Zhukov and others, 1998). Hydrothermal alteration includes quartz, sericite, pyrite, and chlorite. Stockwork vein and disseminated ore minerals include chalcopyrite with accessory molybdenite, bornite, sphalerite, enargite, bismuthinite, and tetrahedrite.

Baiskoe (fig. 1-46) is located about 30–35 km southwest of the Ozernoe occurrence in Karaganda province. The deposit is associated with a granodiorite porphyry body interpreted, but not known, to be an apophysis of the Konstantinovsky granitoid intrusive complex (Zhukov and others, 1998). Although the granitic rocks intrude Late Devonian sedimentary rocks, given the uncertainty of the K-Ar date and the possibility that the mineralization-related intrusive rocks may not correlate with the Konstantinovsky complex, the occurrence is included here. The mineralization has the form of steeply dipping lenses. Hydrothermal alteration includes quartz, K-feldspar, pyrite, tourmaline, magnetite, hematite, arsenopyrite, chlorite, and carbonate. Ore minerals include chalcopyrite and molybdenite with accessory sphalerite, galena, tetrahedrite, and native gold.

The Sayak ore field (fig. 1-46) is located ~175 kilometers east of Kounrad in the Dzhezkazgan province. The ore field is a major producer of skarn copper ores, but occurrences of copper-molybdenum stockwork mineralization are noted by Zhukov and others (1998). Mineralization is associated with a predominantly quartz diorite and granodiorite intrusive suite. Dike swarms of plagiogranite and granodiorite porphyry crosscut the large intrusions and adjacent country rock. The most prominent area of stockwork-style mineralization is at Berkara where copper-molybdenum mineralization occurs as linear zones of stockwork veins and disseminations. Hydrothermal alteration includes quartz, K-feldspar, sericite, and epidote (Zhukov and others, 1998). Ore minerals include chalcopyrite and molybdenite. Other noted by Zhukov and others (1998), but not described, porphyry-style occurrences are Sayak II and Oriolnoe.

West Limb of Orocline

Most of the western limb of the Balkhash-Ili orocline is covered by Cenozoic sedimentary rocks in the Balkhash Depression. Therefore, known deposits and occurrences are

restricted to the exposed parts of the limb in the vicinity of Lake Balkhash or in the far southeast of the limb towards the Tian Shan ranges.

The Karatas ore field (fig. 1-46) in the North Balkhash region is located about 120 km southwest of the Kounrad deposit in the Dzhezkazgan province. There are a number of deposits and occurrences in the ore field, and historical production has largely come from copper skarn deposits. Known mineralization includes Karatas I-IV, Northwest Karatas, Mynshukur, Koskuduk, Kokzaboi, and Kokzaboi Medni. The mineralization is associated with small bodies of Carboniferous dacite porphyry (Zhukov and others, 1998). Zhukov and others (1998) report reserves of copper-molybdenum ores occur at Karatas I, Karatas II, and Karatas IV. The ores at I and II are associated with zones of skarn and skarn-related rocks and included are zones of massive magnetite. Breccia, disseminated, and stockwork ores occur at Karatas IV. Hydrothermal alteration includes quartz, K-feldspar, pyrite, sericite, magnetite, and hematite. Ore minerals include chalcopyrite and molybdenite with accessory galena and sphalerite. Disseminated ores are also reported (Zhukov and others, 1998) from Karatas III.

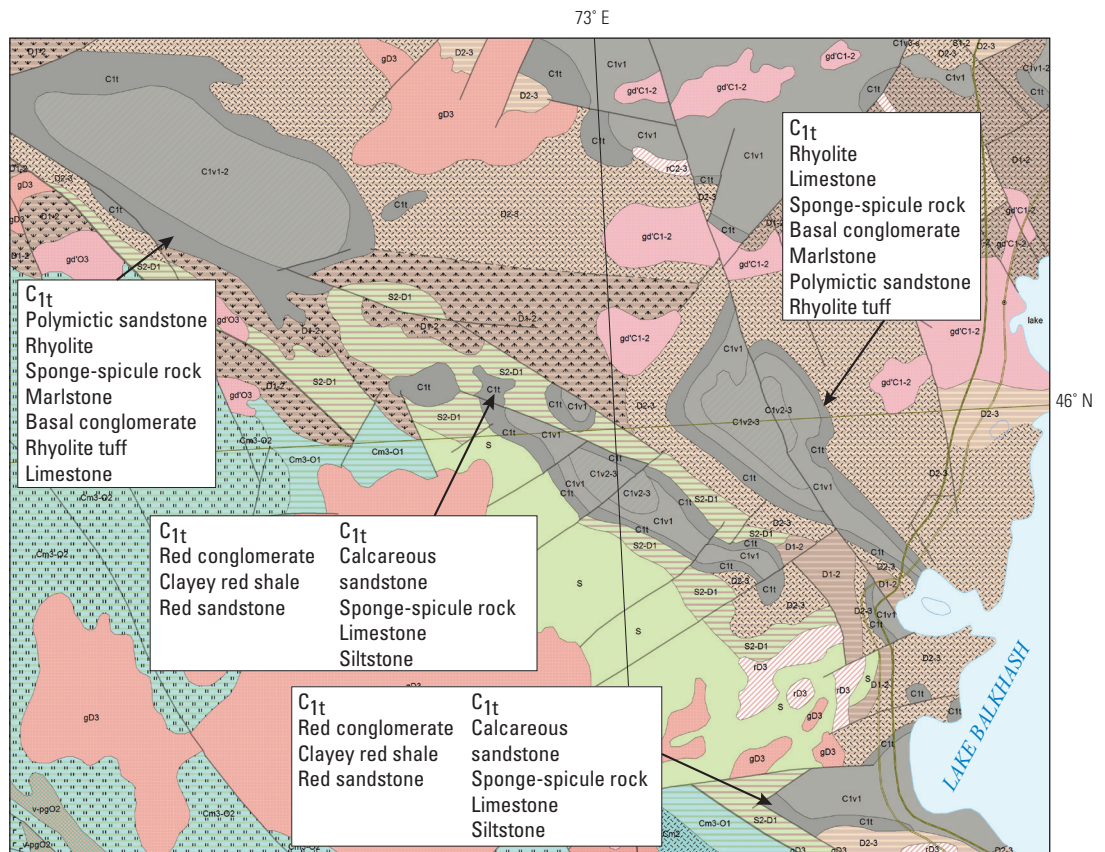
Sokurkoi (fig. 1-46) is located ~50 kilometers southeast of the Karatas ore field in Northwestern Pribalkhash. The mineralization is associated with Carboniferous intrusions described by Zhukov and others (1998) as microgranites and felsite porphyries. Hydrothermal alteration is intense and

consists of silica-alunite masses with kaolinite surrounding them and propylitic alteration in the perimeter. At depth, the silica-alunite-kaolinite gives way to quartz-sericite-pyrite alteration within which the “primary” ore occurs (Zhukov and others, 1998). Ore minerals in the quartz-sericite-pyrite alteration include chalcopyrite, chalcocite, and bornite with accessory tetrahedrite, enargite, and molybdenite.

About 200 km south-southwest of Kounrad (fig. 1-46) in Almatinskaya province is an area of mineralization known as the Kuigan-Maibulak ore region. It is located near the southwesternmost tip of Lake Balkhash along its eastern shore. There are different mineral deposit types in this region including several porphyry copper occurrences. Intense quartz stockworks occur at Kazkymys (fig. 1-47), Vostok I, II, III, IV, and V (Zhukov and others, 1998). Hydrothermal alteration includes quartz, K-feldspar, pyrite, sericite, and magnetite. Ore minerals include chalcopyrite and molybdenite with accessory bornite, sphalerite, native gold, tennantite, and galena. Silica-alunite alteration occurs at Vostok I and II and the ore mineral assemblage includes enargite.

Koksai (fig. 1-46) is located in the southeastern part of the Carboniferous magmatic arc about 390 kilometers southeast of Kounrad in the Taldy-Korgan province. The deposit occurs in a Silurian granodioritic intrusion crosscut by Carboniferous (?) plagiogranite porphyry dikes (Zhukov and others, 1998). Hydrothermal alteration includes quartz, K-feldspar, biotite, sericite, pyrite, magnetite, chlorite,

Figure 1-47. Geologic map from Seltmann and others (2009) for an area to the west of Lake Balkhash in central Kazakhstan showing the lithologies within the indicated map units of Early Carboniferous (C_{1t}) Tournasian rocks illustrating the mixtures of lithologies from different geologic environments that may be with any given mapped age unit.



hematite, and arsenopyrite. Ore minerals include chalcopyrite, bornite, and molybdenite with accessory sphalerite, galena, tetrahedrite, and native gold.

Challenges to Quantitatively Assessing Undiscovered Porphyry Copper Deposits in Western Central Asia

Consistency with Descriptive Model

The assessment of undiscovered porphyry copper deposits is based on models of the probable geologic attributes of a deposit, probable sizes, and probable grades. These models are based on the tabulation of data according to sets of mutually consistent standards from hundreds of well-explored deposits worldwide. The models used in the assessment of western Central Asia (refer to appendixes) were those of Singer and others (2008) and Berger and others (2008), and all known deposits in western Central Asia were analyzed according to the same standards and tested as to their consistency with the models. Underlying these models are two first-order assumptions—(1) the descriptive attributes, grades, and tonnages of the porphyry copper deposits that are yet to be discovered can be represented by the grades and tonnages of those already found worldwide, and (2) the lithotectonic terranes in which the deposits occur in western Central Asia are analogous to magmatic-arc environments hosting deposits and occurrences worldwide. A statistical test of the grades and tonnages of known porphyry copper deposits in the study area showed that they are consistent with the general porphyry copper model of Singer and others (2008). With respect to 2 above, however, there are challenges in applying the descriptive deposit model *vis-à-vis* the coherence of the requisite lithotectonic environment in the complex and highly deformed geologic terranes of western Central Asia, and most available geologic information does not adequately elucidate the structural elements controlling the complexity.

Identifying geologic terranes within a study area that are analogous to those in which porphyry copper deposits are known to occur—magmatic arcs formed in subduction boundary zones—and the outer boundaries of these “permissive” terranes is one of the first steps in effecting an assessment. Descriptive mineral-deposit models document the necessary information essential to discriminating between possible mineralized environments and nonpermissive environments (Singer and Menzie, 2010), and tectonic/structural models provide the spatial arrangement of environment attributes. Therefore, the geologic map-based undertaking of permissive tract delineation requires that the maps used clearly identify the lithologies indicative of a permissive terrane, the age(s) of these lithologies, and the structural relations of the permissive lithologies. That is, in addition to identifying permissive lithologies in a terrain, it

must be discernible from the map the degree to which there is still continuity or coherence of the potential mineralizing environment. Thus, challenges to delineating terranes related to magmatic arcs above Paleozoic subduction zones in western Central Asia include (1) knowing where permissive rocks occur, (2) determining the present-day continuity of the paleo-magmatic arcs, and (3) knowing the proportion of a permissive terrane that is actually representative of the original environment in a highly deformed setting.

The permissive tracts that are delineated in an assessment are tied to available geologic maps. Geologic maps are prepared for different purposes, at different scales, and with different paradigms of geologic processes. For regional-scale assessments, the availability of digital geologic maps, such as the 1:1,500,000-scale geologic map compiled by Seltmann and others (2009), greatly facilitates the initial stages of permissive tract delineation. Using GIS tools, permissive rocks may be selected by age range from the digital map. For example, the digital map compilation used in our assessment of western Central Asia differentiates ages of rocks and whether they are stratified or intrusive. In the digital version, each map unit can be queried as to the included lithologies. The quality and consistency of digital map unit attributes may be insufficient to determine whether or not to include a particular map polygon in a permissive tract. For example, Russian geologic maps typically consider sedimentary and volcanic rocks to be stratified map units; often, it is difficult to discern the proportions of the two rock types if both are present in a map unit. For small-scales, the map may not include formal or informal map unit names, which make it difficult to relate the geology to larger-scale maps and site-specific studies. Map units with the same age designation in any given area may not contain the same classes of lithologic information or lithologies representative of a single geologic environment (for example, back-arc sedimentary basin, carbonate platform, and other environments) (fig. 1-47). In addition, some map units in the digital map used for the assessment combine stratigraphic sections of different aged rocks. When discrete magmatic-arc systems are combined into a single map unit, additional information is needed to evaluate the likely differences in mineral-resource potential. Larger-scale maps, such as the 1:200,000-scale Russian map series used to supplement the digital geology in this study, and topical studies typically are required to refine the permissive tracts.

Structural information is difficult to attribute in digital geologic map compilations, which can affect the evaluation of different fault types and preclude evaluation of differences between stratigraphic units with regard to styles and intensities of deformation. Thus, regional-scale digital geologic maps typically are insufficient to use as the sole source for interpreting the tectonics and structural geology of a map area and, therefore, assessing undiscovered mineral-resource potential. An example of these types of challenges is illustrated in figure 1-48, which shows the geology of a small area in the Kyrgyz Range (fig. 1-22) in the western Tian Shan ranges. Figure 1-48A is based on the geologic map from

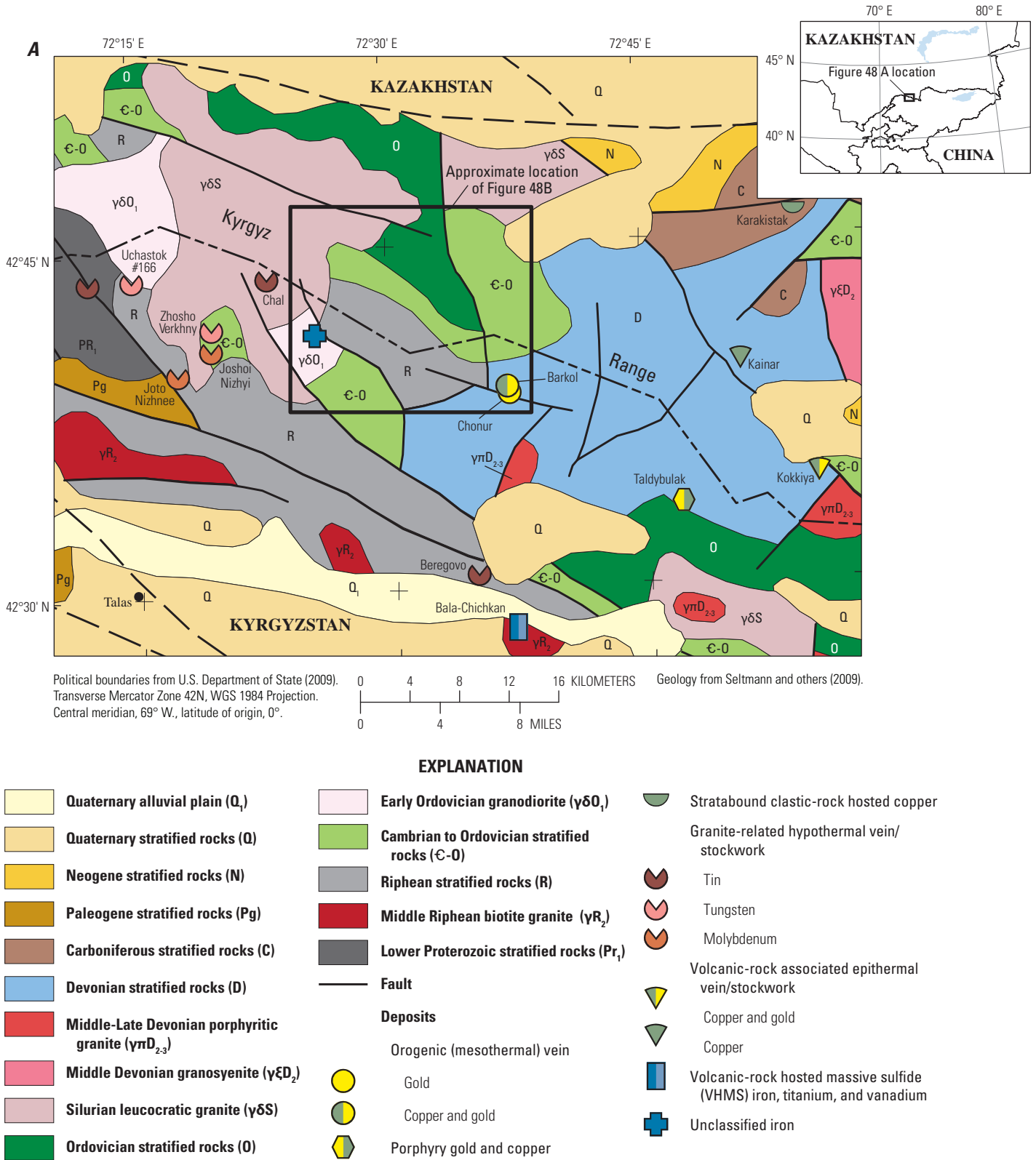
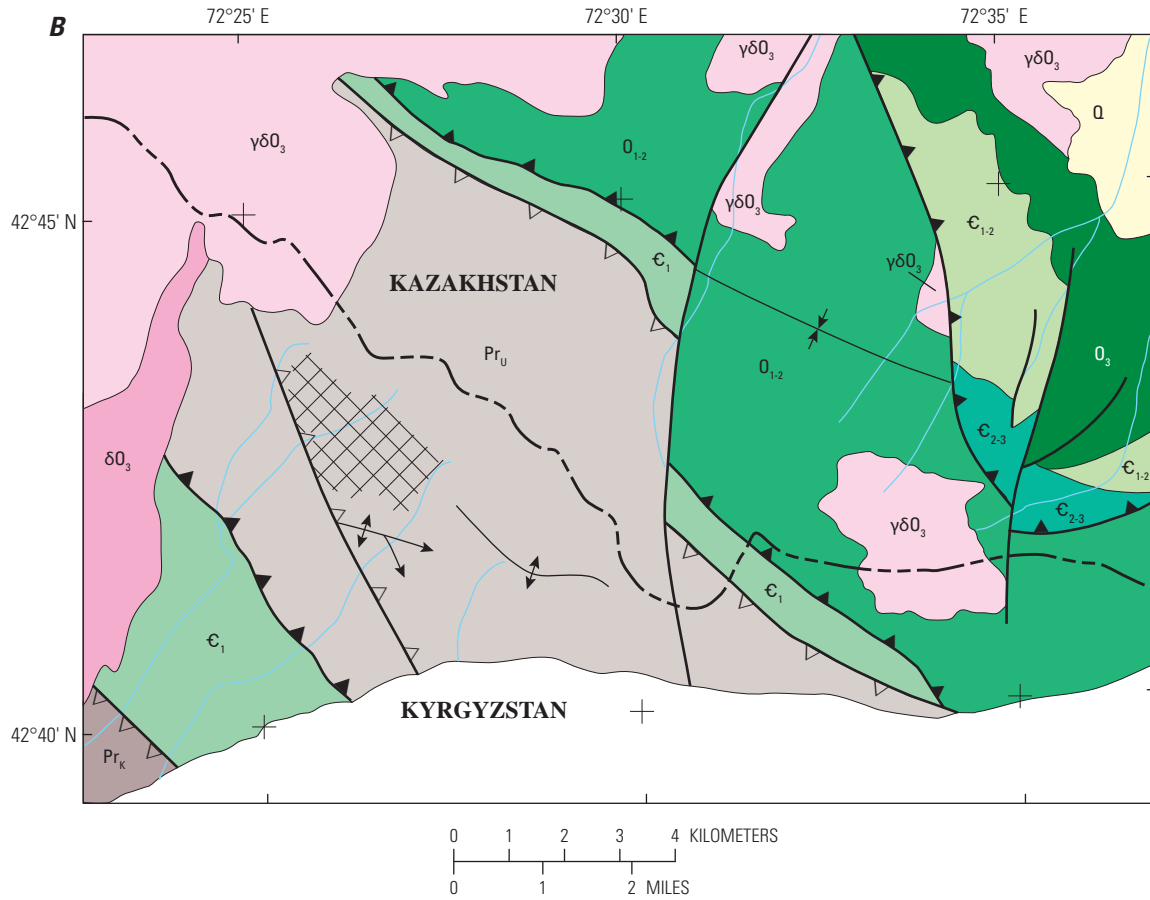


Figure 1-48. Geologic maps of a part of the Kyrgyz Range in northwest Kyrgyzstan and adjacent Kazakhstan in the western Tian Shan ranges. *A*, Main geologic map (after Seltmann and others, 2009). The city of Talas and location of figure 1-48B are shown for reference. *B*, Geologic map (after Stepanenko, 1959) for the location shown in figure 1-48A illustrating the differences between detailed geologic mapping and the map compiled by Seltmann and others (2009). The thrust and reverse faults are inferred from stratigraphic, dip, and strike data in Stepanenko (1959). Location of map area shown on inset.



EXPLANATION
















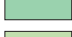
- | | |
|--|---|
|  Quaternary stratified rocks (Q) |  Late Proterozoic Kenkol' Formation (Pr _k) |
|  Late Ordovician granodiorite (γδO ₃) |  Skarn with magnetite |
|  Late Ordovician diorite (δO ₃) |  Axis of antiform |
|  Late Ordovician magmatic-arc volcanic rocks (O ₃) |  Axis of synform |
|  Lower to Middle Ordovician non-marine sedimentary rocks (O _{1,2}) |  Plunging antiform |
|  Middle to Late Cambrian volcanic and sedimentary rocks (ε _{2,3}) |  Thrust faults; teeth on upper plate |
|  Early Cambrian spilitic volcanic rocks (ε ₁) |  High-angle reverse faults; teeth on upthrown block |
|  Early to Late Cambrian rocks (ε _{1,2}) | |
|  Late Proterozoic Uchkoshoy Formation limestone, shale, sandstone, and quartzite (Pr _u) | |

Figure 1-48.—Continued

Seltmann and others (2009) and figure 1-48B shows a more detailed map of part of the area by Stepanenko (1959) on which thrust and reverse faults have been inferred based on the stratigraphic and dip and strike data provided in Stepanenko (1959). Aside from some stratigraphic age assignment differences that are important for determining what proportion of the area contains permissive magmatic-arc-related rocks, the smaller-scale Seltmann and others' (2009) map lacks fault and fold information essential to evaluating the stratigraphic coherence of permissive map units as well as evaluating the timing and evolution of deformation that may increase or decrease the mineral-resource potential. It is evident that the tectonic uplift of Precambrian blocks as well as thrust tectonics that affected Lower to Mid-Ordovician stratigraphic units preceded emplacement of the Late Ordovician intrusions with which many copper occurrences in the region are spatially associated.

The map area shown in figure 1-6 for the Akbastau-Chingiz-Arnalyk area northeast of Lake Balkhash is another example of a site where additional geologic and tectonic information are required to use a digital geologic map in a quantitative mineral-resource assessment. The tectonic terranes of Windley and others (2007) are needed to understand that the geosyncline margins are major tectonic boundaries juxtaposing unrelated lithotectonic terranes.

Additional Data Needed

Updated geologic maps that include fault types are needed, and it would be helpful if compilations included fault types as well as the separation of different lithotectonic groups of rocks in addition to age distinctions. In covered terrains, structural contours on the depth to pre-Cenozoic basement would also benefit resource assessment and exploration studies.

Although a considerable amount of thermochronological dating (principally K-Ar) was done by former Soviet Union scientists (for example, Kostitsyn, 1996), as well as in some Pb-Pb studies, and more recent studies are in progress (for example, Alexeiev and others, 2010), there is a need for many more studies that include zircon dates along with detailed thermochronologic information (for example, ^{39}Ar - ^{40}Ar) and a particular focus on the timing of key tectonic and structural events (for example, accretion, thrust faulting), metamorphism, and hydrothermal alteration. Additional paleomagnetic and paleoclimatological studies carried out in conjunction with geochronologic investigations are also needed.

The science of understanding fold and thrust belts has grown substantially in recent years (for example, Nemcok and others, 2005), and field work leading to a reinterpretation of much of western Central Asia in this modern context, such as is being done in eastern Central Asia and northwestern China (for example, Cunningham, 2010), is needed within the study area.

Acknowledgments

This overview of the tectonic and porphyry copper metallogeny of western Central Asia was made possible by the contributions of many scientists within and outside of the U.S. Geological Survey (USGS) and was supported by the Mineral Resources Program of the USGS. Particular acknowledgment is made to the participants in the assessments including USGS scientists Jane M. Hammarstrom, Michael L. Zientek, Jeffrey D. Phillips, John L. Mars, Lawrence J. Drew, David M. Sutphin, Gilpin Robinson, Mark Mihalasky, Walter Bawiec, and Connie L. Dicken; our cooperating partners including Reimar Seltmann, Dmitriy Alexeiev, and Richard Herrington; and experts on the geology and resources of the region including Vitaly Shatov, Victor Popov, and Andrei Chitalin. Helpful technical reviews were provided by USGS colleagues Donald Singer and James Jones.

References Cited

- Abduln, A.A., and Kaiulov, A.K., 1978, [Metallogeny of Kazakhstan—Ore formation—Copper ore deposits]: Alma-Ata, Kazakhstan, Academy of Sciences, 191 p. [In Russian.]
- Abrajevitch, A., Van der Voo, R., Bazhenov, M.L., Levashova, N.M., and McCausland, P.J.A., 2008, The role of Kazakhstan orocline in the late Paleozoic amalgamation of Eurasia: *Tectonophysics*, v. 455, p. 61–76.
- Abrajevitch, A., Van der Voo, R., Levashova, N.M., and Bazhenov, M.L., 2007, Paleomagnetic constraints on the paleogeography and oroclinal bending of the Devonian volcanic arc in Kazakhstan: *Tectonophysics*, v. 441, p. 67–84.
- Ageyeva, S.T., Volchkov, A.G., and Minina, O.V., 1984, The porphyry copper mineralization of the Urals and its geotectonic environment: *International Geology Review*, v. 26, p. 690–701.
- Alexeiev, D., 2008, Paleozoic tectonics and evolution of Kazakhstan continent [abs.]: CERCAMS 12 Workshop on Metallogeny of Central Asia, 25–26 November, 2008.
- Alexeiev, D.V., Ryazantsev, A.V., Kroner, A., Tretyakov, A.A., Xia, X., and Liu, D.Y., 2010, Geochemical data and zircon ages for rocks in a high-pressure belt of Chu-Yili Mountains, southern Kazakhstan—Implications for the earliest stages of accretion in Kazakhstan and the Tianshan: *Journal of Asian Earth Sciences*, v. 42, no. 5, p. 805–820.
- Ayarza, P., Brown, D., Alvarez-Marron, J., and Juhlin, C., 2000, Contrasting tectonic history of the arc-continent suture in the Southern and Middle Urals—Implications for the evolution of the orogeny: *Journal of the Geological Society of London*, v. 157, p. 1065–1076.

- Bakhteyev, M.K., and Filatova, N.I., 1969, On the distinctive features of the concluding stage of geosynclinal development of the Dzhungarian-Balkhash geosynclinal system: *Geotectonics*, v. 3, p. 179–185.
- Bea, F., Fershtater, G.B., and Montero, P., 2002, Granitoids of the Uralides—Implications for the evolution of the orogeny: *American Geophysical Union Geophysical Monograph* 132, p. 211–232.
- Belousov, V.V., 1970, Against the hypothesis of ocean-floor spreading: *Tectonophysics*, v. 9, p. 489–512.
- Berger, B.R., Ayuso, R.A., Wynn, J.C., and Seal, R.R., 2008, Preliminary model of porphyry copper deposits: U.S. Geological Survey Open-File Report 2008–1321, 55 p., accessed May 15, 2009, at <http://pubs.usgs.gov/of/2008/1321/>.
- Bertrand, M., 1887, La chaîne des Alpes et le formation du continent Européen: *Bulletin de la Société Géologique de France*, sér. 3, v. 15, p. 423–447.
- Bogdanovich, K.I., 1906, [The Dibrar system in the southeastern Caucasus]: *Geolkom, Trudy*, no. 26, 179 p. [In Russian.]
- Brown, D., Juhlin, C., Ayala, C., Tryggvason, A., Bea, F., Alvarex-Marron, J., Carbonell, R., Seward, D., Glasmacher, U., Puchkov, V., and Perez-Estaun, A., 2008, Mountain building processes during continent-continent collision in the Uralides: *Earth-Science Reviews*, v. 89, p. 177–195.
- Buslov, M.M., Zhimulev, F.I., and Travin, A.V., 2010, New data on the structural setting and $^{40}\text{Ar}/^{39}\text{Ar}$ age of the MP-LP metamorphism of the Daulet Formation, Kokchetav Metamorphic Belt, northern Kazakhstan, and their tectonic implication: *Doklady Earth Sciences*, v. 434, p. 1147–1151.
- Bykadorov, V.A., Bush, V.A., Fedorenko, O.A., Filippova, I.B., Miletenko, N.V., Puchkov, V.N., Smirnov, A.V., Uzhkenov, B.S., and Volozh, Y.A., 2003, Ordovician-Permian palaeogeography of Central Eurasia—Development of Paleozoic petroleum-bearing basins: *Journal of Petrology*, v. 26, p. 325–350.
- Chen, Z.Q., and Shi, G.R., 2003, Late Paleozoic depositional history of the Tarim basin, northwest China—An integration of biostratigraphic and lithostratigraphic constraints: *American Association of Petroleum Geologists*, v. 87, p. 1323–1354.
- Chitalin, A.F., 1996, Variscan structural evolution of Central Kazakhstan, in Shatov, V., Seltmann, R., Kremenetsky, A., Lehmann, B., Popov, V., and Ermolov, P., eds., *Granite-related ore deposits of Central Kazakhstan and adjacent areas*: St. Petersburg, GLAGOL Publishing House, p. 93–102.
- Cierny, J., and Weisgerber, G., 2003, The Bronze Age tin mines in Central Asia, in Giunlia-Mair, A., and Lo Schiavo, F., eds., *The problem of early tin*: Oxford, Archaeopress, p. 23–31.
- Cunningham, D., 2010, Tectonic setting and structural evolution of the Late Cenozoic Gobi Altai orogeny: *Geological Society of London Special Publication*, v. 338, p. 361–387.
- Dana, J.D., 1873, On some results of the earth's contraction from cooling, including a discussion of the origin of mountains, and the nature of the Earth's interior: *American Journal of Science*, v. 5, p. 423–443.
- Davis, P.S., 2002, Jerooy gold project—Audited mining and development report: Wardell Armstrong, NI 43–101 technical report prepared for Norox Mining Company, 218 p. (Also available at <http://www.sedar.com>, under Conquest Resources Limited.)
- Degtyarev, K.E., and Ryazantsev, A.V., 2007, Cambrian arc-continent collision in the Paleozooids of Kazakhstan: *Geotectonics*, v. 41, p. 63–86.
- Dodd, D., and Thornton, J.C., 2005, Varvarinskoye gold-copper project, northern Kazakhstan: NI 43-101 technical report prepared for European Minerals Corporation, 45 p. (Also available at <http://www.sedar.com>.)
- Filippova, I.B., Bush, V.A., and Didenko, A.N., 2001, Middle Paleozoic subduction belts—The leading factor in the formation of the Central Asian fold-and-thrust belt: *Russian Journal of Earth Sciences*, v. 3, p. 405–426.
- Gerdes, A., Montero, P., Bea, F., Fershtater, G., Borodina, N., Osipova, T., and Shardakova, G., 2002, Peraluminous granites frequently with mantle-like isotope compositions—The continental-type Murzonka and Dzhabyk batholiths of the western Urals: *International Journal of the Earth Sciences*, v. 91, p. 3–19.
- Golovonov, I.M., 1978, Copper deposits of the western Tian Shan: Ministry of Geology of Uzbekistan, Tashkent, Institute of the Geology of Mineral Raw Materials, 239 p.
- Golovonov, I.M., Seltmann, R., and Kremenetsky, A.A., 2005, The porphyry Cu-Au/Mo deposits of Central Eurasia—2. The Almalyk (Kal'Makyr-Dalnee) and Saukbulak Cu-Au porphyry systems, Uzbekistan, in Porter, T.M., ed., *Super porphyry copper & gold deposits—A global perspective*: Adelaide, PGC Publishing, v. 2, p. 513–523.
- Görz, I., Buschmann, B., Kroner, U., Hauer, R., and Henning, D., 2009, The Permian emplacement of granite-gneiss complexes in the East Uralian Zone and implications on the geodynamics of the Uralides: *Tectonophysics*, v. 467, p. 119–130.

- Great Western Exploration Limited, 2012, Spasskaya JV: Great Western Exploration Limited Web site, accessed November 15, 2012, at: <http://greatwesternexploration.com.au/projects/international/spasskaya-jv-kazakhstan-project.html>.
- Hall, J., 1859, Palaeontology of New York: New York Natural History Survey no. 3, part 1, 533 p.
- Haug, E., 1900, Les géosynclinaux et les aires continentales—Contribution à l'étude des regressions et des transgressions marines: Bulletin of the Geological Society of France, 3rd Series, v. 28, p. 617–711.
- Herrington, R.J., Puchkov, V.N., and Yakubchuk, A.S., 2005, A reassessment of the tectonic zonation of the Uralides—Implications for metallogeny: Geological Society of London Special Publication 248, p. 153–166.
- Heubeck, C., 2001, Assembly of central Asia during the middle and late Paleozoic, in Hendrix, M.S., and Davis, G.A., eds., Paleozoic and Mesozoic tectonic evolution of central Asia—From continental assembly to intracontinental deformation: Geological Society of America Memoir 194, p. 1–22.
- Jenchuraeva, R.J., 1997, Tectonic settings of porphyry-type mineralization and hydrothermal alteration in Paleozoic island arcs and active continental margins, Kyrghyz Range, (Tien Shan) Kyrghyzstan: Mineralium Deposita, v. 32, p. 434–440.
- John, D.A., Ayuso, R.A., Barton, M.D., Blakely, R.J., Bodnar, R.J., Dilles, J.H., Gray, Floyd, Graybeal, F.T., Mars, J.C., McPhee, D.K., Seal, R.R., Taylor, R.D., and Vikre, P.G., 2010, Porphyry copper deposit model, chap. B of Mineral deposit models for resource assessment: U.S. Geological Survey Scientific Investigations Report 2010–5070–B, 169 p., accessed September 8, 2010, at <http://pubs.usgs.gov/sir/2010/5070/b/>.
- Khain, V.E., 1970, [Is there a scientific revolution going on in geology?]: Priroda, v. 1, p. 719. [In Russian.]
- Khain, V. Ye., and Sheynmann, Yu. M., 1962, Hundredth anniversary of the geosynclinals theory: International Geology Review, v. 4, p. 166–198.
- Khain, V.E., and Ryabukhin, A.G., 2002, Russian geology and the plate tectonics revolution, in Oldroyd, D.R., ed., The Earth inside and out—Some major contributions to geology in the twentieth century: Geological Society of London, Special Publication 192, p. 185–198.
- Kheraskova, T.N., Didenko, A.N., Bush, V.A., and Volozh, Y.A., 2003, The Vendian-Early Paleozoic history of the continental margin of eastern Paleogondwana, Paleasian Ocean, and Central Asian foldbelt: Russian Journal of Earth Sciences, v. 5, p. 165–184.
- Kolb, J., Sindern, S., Kisters, A.F.M., Meyer, F.M., Hoernes, S., and Schneider, J., 2005, Timing of Uralian orogenic gold mineralization at Kochkar in the evolution of the East Uralian granite-gneiss terrane: Mineralium Deposita, v. 40, p. 473–491.
- Korolev, A.V., and Badalov, S.T., 1959, Zoning in the Amalyk ore field: Geology of Ore Deposits, no. 5, p. 31–38.
- Kostitsyn, Yu. A., 1996, K-Ar dates for the Kazakhstan granites—An overview, in Shatov, V., Seltmann, R., Kremenetsky, A., Lehmann, B., Popov, V., and Ermolov, P., eds., Granite-related ore deposits of Central Kazakhstan and adjacent areas: St. Petersburg, GLAGOL Publishing House, p. 287–299.
- Kreiter, V.M., 1956, [Structures of ore fields and deposits]: Gosgeoltekhizdat, Moscow, 270 p. [In Russian.]
- Kudryavtsev, Yu. K., 1996, The Cu-Mo deposits of Central Kazakhstan, in Shatov, V., Seltmann, R., Kremenetsky, A., Lehmann, B., Popov, V., and Ermolov, P., eds., Granite-related ore deposits of Central Kazakhstan and adjacent areas: St. Petersburg, GLAGOL Publishing House, p. 119–144.
- Letnikov, F.A., Kotov, A.B., Degtyarev, K.E., Levchenkov, O.A., Shershakova, M.M., Shershakov, A.V., Rizvanova, N.G., Makeev, A.F., and Tolkachev, M.D., 2009, Late Ordovician granitoids of northern Kazakhstan—U-Pb age and tectonic setting: Doklady Earth Sciences, v. 424, p. 24–28.
- Levashova, N.M., Van der Voo, R., Abrajevitch, A.V., and Bazhenov, M.L., 2008, Paleomagnetism of mid-Paleozoic subduction-related volcanics from the Chingiz Range in NE Kazakhstan—The evolving paleogeography of the amalgamating Eurasian composite continent: Geological Society of America Bulletin, v. 121, p. 555–573.
- Markova, N.G., 1948, Tectonics of Central Kazakhstan, in Shatski, N.S., ed., Tectonics of the U.S.S.R., Volume 1, Part L: Moscow, Academy of Sciences of the U.S.S.R., Institute of Geology, p. 1–78.
- Meshchaninov, Ye. Z., and Azin, V.N., 1973, Distribution of gold in a copper porphyry deposit, Almalıy region: International Geology Review, v. 15, no. 6, p. 660–663.
- Mossakovsky, A.A., Ruzhentsev, S.V., Samygin, S.G., and Kheraskova, T.N., 1993, Central Asian fold belt—Geodynamic evolution and formation: Geotectonics, v. 27, no. 6, p. 3–32.
- Nalivkin, D.V., 1973, Geology of the U.S.S.R.: Buffalo, New York, University of Toronto Press, 855 p.

- Nekrasoff, B., 1935, Copper-ore regions of the Union of Soviet Socialist Republics, *in* Anonymous, ed., *Copper Resources of the World*, v. 2: 16th International Geological Congress, Menasha, Wisconsin, George Banta Publishing Company, p. 649–662.
- Nemcok, M., Schamel, S., and Gayer, R., 2005, Thrust belts—Structural architecture, thermal regimes and petroleum systems: New York, Cambridge University Press, 554 p.
- Obruchev, V.A., 1926, [New trends in tectonics]: *Geolkom, Izvestiya*, no. 3. [In Russian.]
- Orlov, I.V., Sinev, O.A., Taranushich, F.F., Shul'ga, V.M., and Shchibrik, V.I., 1981, [Location and the value of volcanically induced and volcanogenic sedimentary ore genesis before the metallogeny of central Kazakhstan], *in* Abdulin, A.A., ed., [Volcanogenic sediments—Lithology and ore genesis]: Almaty, National Academy of Sciences of Kazakhstan, p. 68–80. [In Russian.]
- Peive, A.V., 1945, Deep-seated faults in geosynclinal areas: *Izvestiya, National Academy of Sciences, Geology Series*, no. 5, p. 23–46.
- Petrov, O., Shatov, V., Kondian, O., Markov, K., Guriev, G., Seltmann, R., and Armstrong, R., 2006, Mineral deposits of the Urals, explanatory notes: Centre for Russian and Central EurAsian Mineral Studies (CERCAMS), London, Natural History Museum, 91 p.
- Popov, L.E., Bassett, M.G., Zhemchuzhnikov, V.G., Holmer, L.E., and Klishevich, I.A., 2009, Gondwanan faunal signatures from Early Paleozoic terranes of Kazakhstan and Central Asia—Evidence and tectonic implications: *Geological Society of London Special Publication 325*, p. 23–64.
- Predtechenskii, A.A., 1960, An ancient uplift of southern Siberia: *Proceedings, Siberian Scientific Institute of Geophysics and Mineral Resources*, v. 13, p. 65–77.
- Safonov, Y.G., Gorbunov, G.I., Pek, A.A., Volkov, A.V., Zlobina, T.M., Kravchenko, G.G., and Malinovsky, E.P., 2007, Structure of ore fields and deposits—Current status and outlook for further development: *Geology of Ore Deposits*, v. 49, p. 343–371.
- Savelieva, G.N., and Nesbitt, R.W., 1996, A synthesis of the stratigraphic and tectonic setting of the Uralian ophiolites: *Journal of the Geological Society of London*, v. 153, p. 525–537.
- Savelieva, G.N., Sharaskin, A.Y., Saveliev, A.A., Spadea, P., Pertsev, A.N., and Babarina, I.I., 2002, Ophiolite and zoned mafic-ultramafic massifs of the Urals—A comparative analysis and some tectonic implications: *American Geophysical Union Geophysical Monograph 132*, p. 135–153.
- Seltmann, R., and Porter, T.M., 2005, The porphyry Cu-Au/Mo deposits of Central Eurasia—1. Tectonic, geologic, and metallogenic setting, and significant deposits, *in* Porter, T.M., ed., *Super porphyry copper & gold deposits—A global perspective: Adelaide*, PGC Publishing, v. 2, p. 467–512.
- Seltmann, R., Shatov, V., and Yakubchuk, A., 2009, Mineral deposits database and thematic maps of Central Asia—ArcGIS 9.2, Arc View 3.2, and MapInfo 6.0(7.0) GIS packages: London, Natural History Museum, Centre for Russian and Central EurAsian Mineral Studies (CERCAMS), scale 1:1,500,000, and explanatory text, 174 p. [Commercial dataset available at <http://www.nhm.ac.uk/research-curation/research/projects/cercams/products.html>.]
- Şengör, A.C., Natal'in, B.A., and Burtman, V.S., 1993, Evolution of the Altaid tectonic collage and Palaeozoic crustal growth in Eurasia: *Nature*, v. 364, p. 299–306.
- Şengör, A.C., and Natal'in, B.A., Paleotectonics of Asia: Fragments of a synthesis, *in* Yin, A., and Harrison, Mark, eds., *The tectonic evolution of Asia: Cambridge*, Cambridge University Press, p. 486–640.
- Shayakubov, T., Islamov, F., Kremenetsky, A. and Seltmann, R., eds., 1999, Au, Ag, and Cu deposits of Uzbekistan: International field conference of IGCP-373, London, Tashkent, Excursion B6 of the Joint SGA-IAGOD Symposium, 27 August–4 September, 1999, 112 p.
- Singer, D.A., Berger, V.I., and Moring, B.C., 2008, Porphyry copper deposits of the world: U.S. Geological Survey Open-File Report 2008–1155, 45 p., accessed August 10, 2009, at <http://pubs.usgs.gov/of/2008/1155/>.
- Singer, D.A., and Menzie, W.D., 2010, Quantitative mineral resource assessments: New York, Oxford University Press, 219 p.
- Smirnov, V.I., 1977, Ore deposits of the U.S.S.R., v. III: London, Pitman Publishing, p. 479–492.
- Spiridonov, E.M., 1995, The inversional plutogenic gold-quartz association of the northern Kazakhstan Caledonides: *Geology of Ore Deposits*, v. 37, p. 149–175.
- Stepanenko, A.F., 1959, New data on Precambrian (Sinian) and lower Paleozoic deposits in the western part of the Kirghiz Range (Northern Tyan-Shan): *Izvestiya, Geologic Series, U.S.S.R. Academy of Sciences*, no. 9, p. 58–70.
- Strokin, Y.A., and Filatova, L.I., 1977, An ancient structural suture in the Precambrian metamorphic complex of the Ulu-tau, Central Kazakhstan: *Geotectonics*, v. 11, p. 277–285.
- Suess, E., 1908, [The face of the earth, v. 3]: Oxford, Clarendon Press, 400 p. [In German.]

- Thomas, J.C., Cobbold, P.R., Shein, V.S., and Le Douaran, S., 1999, Sedimentary record of late Paleozoic to Recent tectonism in central Asia—Analysis of subsurface data from the Turan and south Kazak domains: *Tectonophysics*, v. 313, p. 243–263.
- Tryggvason, A., Brown, D., and Perez-Estaun, A., 2001, Crustal architecture of the southern Uralides from true amplitude processing of the Urals Seismic Experiment and Integrated Studies (URSEIS) vibroseis profile: *Tectonics*, v. 20, p. 1040–1052.
- Wang, B., Shu, L.S., Cluzel, D., Faure, M., and Charvet, J., 2007, Geochemical constraints on Carboniferous volcanic rocks of the Yili Block (Xinjiang, NW China)—Implication for the tectonic evolution of western Tianshan: *Journal of Asian Earth Sciences*, v. 29, p. 148–159.
- Wardell Armstrong International, 2010, Updated technical report on the Taldybulak property, Kyrgyzstan: Orsu Metals Corporation, Taldybulak Project NI 43-101 Technical Report, prepared for Orsu Metals Corporation, 205 p. (Also available at <http://www.sedar.com>.)
- Windley, B.F., Alexeiev, D., Xiao, W., Kröner, A., and Badarch, G., 2007, Tectonic models for accretion of the Central Asian orogenic belt: *Journal of the Geological Society of London*, v. 164, p. 31–47.
- Wolfson, F.I., 1962, [Study of hydrothermal ore deposits]: Gosgeoltekhizdat, Moscow. [In Russian.]
- Xiao, W.J., Windley, B.F., Huang, B.C., Han, C.M., Yuan, C., Chen, H.L., Sun, M., Sun, S., and Li, J.L., 2009, End-Permian to mid-Triassic termination of the accretionary processes of the southern Altaids—Implications for the geodynamic evolution, Phanerozoic continental growth, and metallogeny of Central Asia: *International Journal of Earth Science*, v. 98, p. 1189–1217.
- Yakubchuk, A.S., 1990, Tectonic setting of ophiolite zones in the structure of the Central Kazakhstan Paleozooids: *Geotectonics*, v. 24, p. 415–425.
- Yakubchuk, A., 2004, Architecture and mineral deposit settings of the Altaid orogenic collage—A revised model: *Journal of Asian Earth Sciences*, v. 23, p. 761–779.
- Yakubchuk, A., Cole, A., Seltmann, R., and Shatov, V.V., 2002, Tectonic setting, characteristics, and regional exploration criteria for gold exploration in the Altaid tectonic collage—The Tian Shan province as a key example, *in* Goldfarb, R.J., and Nielsen, R.L., eds., *Society of Economic Geologists Special Publication*, no. 9: Boulder, Colorado, Johnson Printing, p. 177–201.
- Zhukov, N.M., Kolesnikov, V.V., Miroshnichenko, L.M., Egembaev, K.M., Pavlova, Z.N., and Bakarsov, 1998, Copper deposits of Kazakhstan: Ministry of Ecology and Natural Resources of the Republic of Kazakhstan, p. 99–102.
- Zonenshain, L.P., 1973, The evolution of central Asiatic geosynclines through sea-floor spreading: *Tectonophysics*, v. 19, p. 213–232.
- Zvezdov, V.S., and Migachev, I.F., 1986, Stroenie i uslovia formirovaniya ne vykhodiashego na poverhnost medno-porfirovogo mestorozhdeniya Kyzata [Geology and conditions of formation of the Kyzata non-exposed porphyry copper deposit]: *Geologia Rudnih Mestorozhdenii*, v. 1, p. 73–80. [In Russian.]
- Zvezdov, V.S., Migachev, I.F., and Girfanov, M.M., 1993, Porphyry copper deposits of the CIS and the models of their formation: *Ore Geology Reviews*, v. 7, p. 511–549.

Chapter 2. Alteration Mapping of Potential Porphyry Copper Sites Using Advanced Spaceborne Thermal Emission and Reflection Radiometer (ASTER) Data in Central Asia

By John C. Mars¹

Introduction

Hydrothermal alteration is associated with many different types and ages of mineral deposits. The distinctive patterns of hydrothermal alteration associated with porphyry copper and related deposit types typically are identified by detailed geologic mapping. Remote sensing techniques, including Advanced Spaceborne Thermal Emission and Reflection Radiometer (ASTER), also can be used to identify such alteration patterns over large areas provided that vegetation and snow cover are not too extensive. Thus, ASTER data were used to map patterns that are consistent with the alteration signature of known porphyry copper deposits as a tool for estimating numbers of undiscovered deposits for parts of the Western Central Asia porphyry copper assessment.

This chapter describes the application of ASTER satellite data and alteration mapping in western Central Asia and the results of the remote sensing data analysis. The tract-by-tract application of ASTER alteration mapping is described in appendixes A–H, with references to the tables, figures, and plates described here. The permissive tracts for porphyry copper deposits in the Central Asia study area are primarily in central and southeastern Kazakhstan, with limited extension into northern and western Kyrgyzstan, eastern Uzbekistan, and northern Tajikistan (fig. 2-1). Permissive tracts are referred to by a coded_id number (142 for Asia, pCu for porphyry copper, and a 4 digit number); sub-tracts are designated with a letter following the number and a tract-id (for example, CA01PC). See table 2-1 (available online only as a .xlsx file at <http://pubs.usgs.gov/sir/2010/5090/n/>) for a listing of tract names with correlative coded-id and tract-id numbers.

Argillic and phyllic hydrothermally altered rocks were mapped using 225 scenes of ASTER data at 30-meter (m) spatial resolution, and hydrothermal silica-rich rocks (silicic altered rocks) were mapped in 150 scenes at 90-m spatial resolution (fig. 2-2). ASTER data are collected from an imaging spaceborne sensor flying on Terra, a satellite launched in December 1999 as part of NASA's Earth Observing System (EOS). The sensor captures high spatial resolution data in

14 bands from the visible to the thermal infrared wavelengths and provides stereo viewing capability. ASTER data consist of three bands in the 0.52–0.86 micrometer (μm) wavelength region (VNIR); six bands in the 1.6–2.43 μm wavelength region (SWIR); and five bands of emitted radiation in the 8.125–11.65 μm wavelength region (thermal infrared radiation, TIR) with 15-m, 30-m, and 90-m resolution, respectively (Fujisada, 1995). ASTER also has a backward-looking VNIR telescope with 15-m resolution and a swath width is 60 kilometers (km) (Fujisada, 1995).

Mineral composition was determined by mapping VNIR, SWIR and TIR spectral absorption features using ASTER data (Mars and Rowan, 2007; John and others, 2010). An ASTER hydrothermal alteration map consisting of phyllic, argillic, and silicic units overlaid on a 30-m resolution Landsat TM band 7 gray-scaled mosaic image of southeastern Kazakhstan was used for identification of potential porphyry copper sites (plates 1–4; plates are available only online at <http://pubs.usgs.gov/sir/2010/5090/n/>). Potential porphyry copper sites are sites that have ASTER-derived hydrothermal alteration signatures that are consistent with alteration styles and patterns associated with known porphyry copper deposits. The likelihood that these sites are associated with porphyry copper systems can be evaluated further by considering the local geology, proximity to known porphyry copper deposits and prospects, any available mapped alteration or geochemical and geophysical exploration data, and ultimately by field work.

Spectral Characteristics of Porphyry Copper Deposits

Porphyry copper deposits typically consist of a core of quartz and potassium-bearing minerals (mostly potassium feldspar (K-feldspar) and biotite) surrounded by multiple zones of hydrous alteration minerals (fig. 2-3; Lowell and Guilbert, 1970; John and others, 2010). The hydrous zones are characterized by mineral assemblages, which contain at least one mineral that exhibits diagnostic spectral absorption features in the visible near-infrared (VNIR) through the short-wave infrared (SWIR; 0.4–2.5 μm) and (or)

¹U.S. Geological Survey, Reston, Virginia.

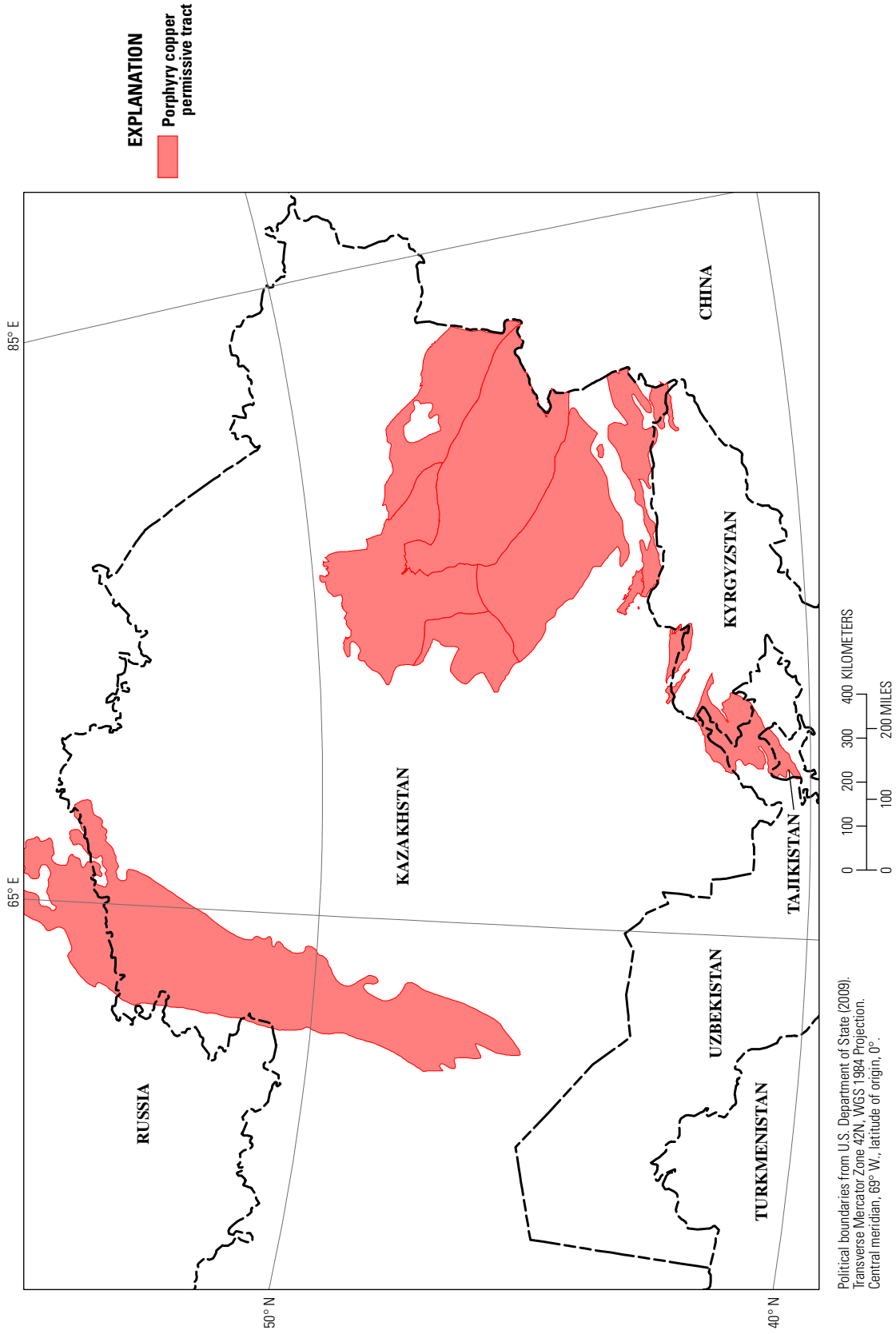


Figure 2-1. Location map of permissive porphyry copper tracts in western Central Asia.

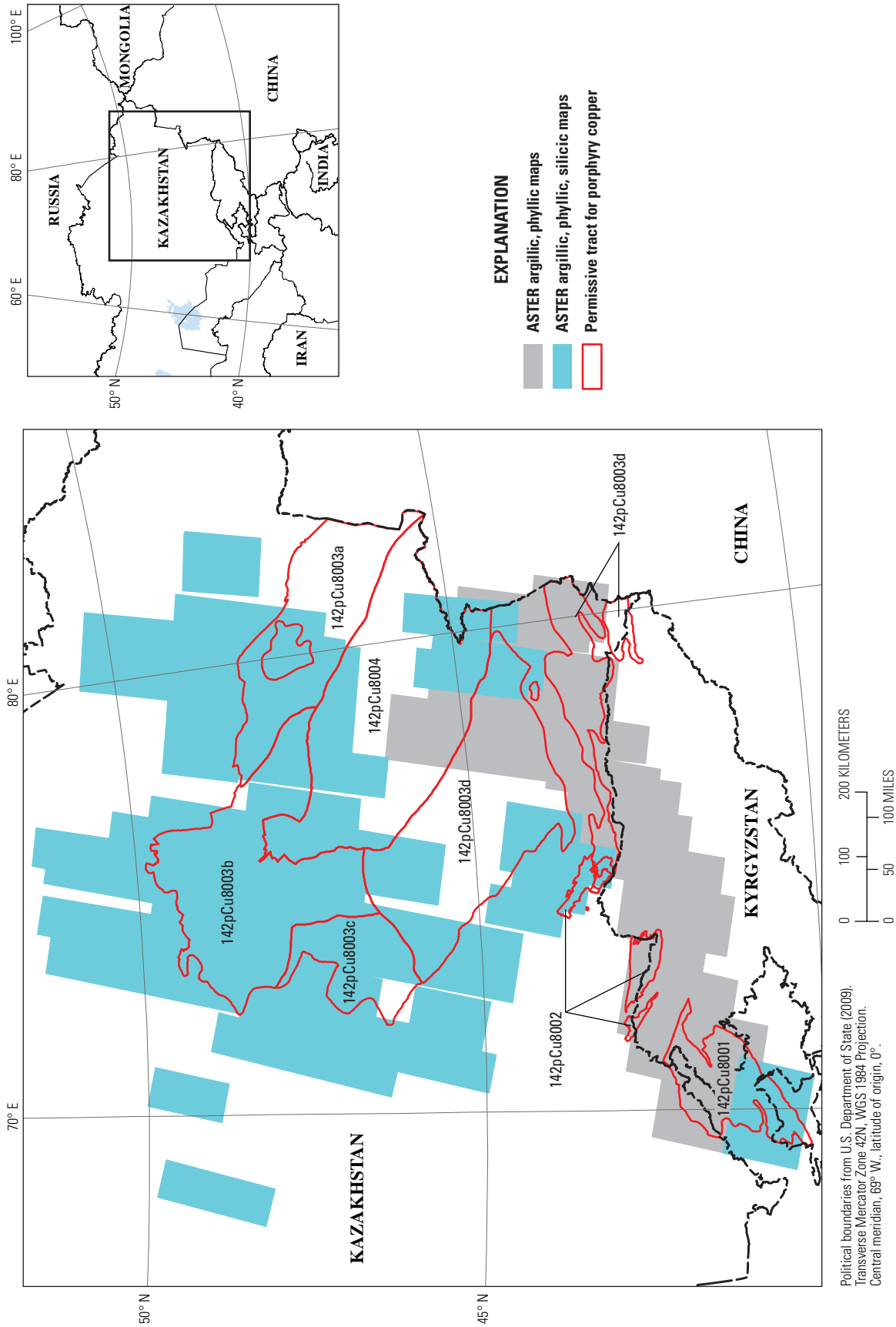


Figure 2-2. Advanced Spaceborne Thermal Emission and Reflection Radiometer (ASTER) argillic, phyllic, and silicic alteration map coverage of permissive tracts in western Central Asia. Location of map area shown on inset.

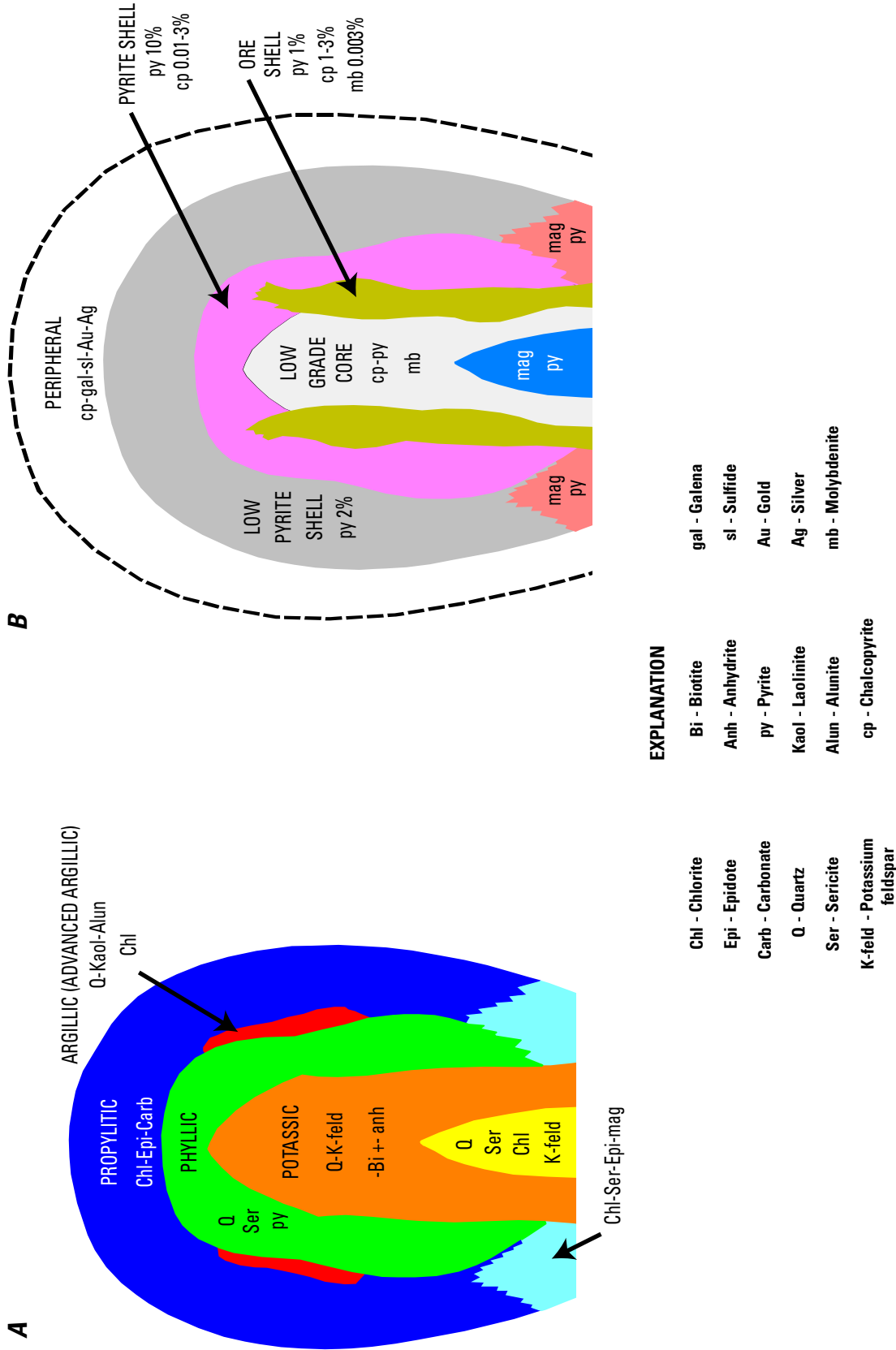


Figure 2-3. Illustrated deposit model of a porphyry copper deposit (modified from Lowell and Guilbert, 1970). *A*, Schematic cross section of hydrothermal alteration minerals and types, which include propylitic, sericitic, argillic, and potassic alteration. *B*, Schematic cross section of ores associated with each alteration type. %, percent.

the thermal-infrared (TIR; 8.0–14.0 μm) wavelength regions (Abrams and others, 1983; Hunt and Ashley, 1979; Spatz and Wilson, 1995).

Phyllic alteration typically forms in a hydrous zone adjacent to the potassic-altered core of porphyry copper deposits (fig. 2-3; Lowell and Guilbert, 1970; John and others, 2010). Phyllic-altered rocks primarily contain sericite, a fine-grained form of muscovite that has a distinct Al-OH spectral absorption feature at 2.2 μm and a less intense absorption feature at 2.35 μm (fig. 2-4; Abrams and others, 1983; Spatz and Wilson, 1995). Argillic-altered rocks typically form in a hydrous zone adjacent to, or above, phyllic-altered rocks (Lowell and Guilbert, 1970; John and others, 2010; Sillitoe, 2010). Kaolinite and alunite are characteristic minerals of advanced argillic alteration and exhibit Al-OH 2.165- and 2.2- μm spectral absorption features (fig. 2-4; Hunt, 1977; Hunt and Ashley, 1979; Rowan and others, 2003). Although less common than alunite or kaolinite, advanced argillic-altered rocks can also contain pyrophyllite, which has an intense 2.165 Al-O-H absorption feature. As shown in the Lowell and Guilbert (1970) model, argillic alteration includes what has come to be recognized as both intermediate- and advanced-argillic alteration. Intermediate argillic alteration is characterized by montmorillonite, illites, hydromicas, and chlorite with or without kaolinite (Beane and Titley, 1981).

Hydrothermally altered silica-rich rocks typically consist of quartz, opal, and chalcedony and exhibit a prominent 9.1- μm restrahten feature in TIR emissivity spectra (figs. 2-2–2-5). Hydrothermally altered silica-rich rocks associated with porphyry copper deposits consist primarily of quartz veins, silica lithocaps, or silicified deposits (Titley, 1972). Stockworks of quartz veins tend to be situated throughout the porphyry deposit, silica lithocaps tend to be associated with argillic-altered rocks, and silicified rocks typically occur in the outer hydrous argillic and propylitic zones (Lowell and Guilbert, 1970; John and others, 2010). Thus, depending on the depth of erosion or structural deformation of porphyry copper deposits, elliptical to circular patterns of phyllic-, argillic- and hydrothermally altered silica-rich rocks can indicate the location of potential porphyry copper deposits.

Data and Methods of Study

ASTER Level_1B Visible near-infrared (VNIR) through the short-wave infrared (SWIR) radiance data were used to map argillic- and phyllic- rock alteration. A crosstalk algorithm and radiance correction factors were applied to ASTER Level_1B data to correct SWIR band anomalies (Biggar and others, 2005; Iwasaki and Tonooka, 2005; Mars and Rowan, 2006; Mars and Rowan, 2010). The ASTER VNIR (3 bands) and SWIR (6 bands) Level_1B data were converted to reflectance using ACORN atmospheric correction software and Moderate Imaging Spectrometer (MODIS) water

vapor data (ImSpec, 2004, Mars and Rowan, 2010). The MODIS MOD_05 water vapor and ASTER data are acquired at the same time aboard the Terra Space Platform (Mars and Rowan, 2010). A mean water vapor value was derived for each ASTER scene from the MODIS data.

ASTER scenes used in this study were recorded at 4 different viewing angles, ranging from nadir to 8.2 degrees off nadir, which causes misregistration of scenes by as much as 600 m in high relief terrain (Mars and Rowan, 2006). To correct for this misregistration, each nine-band image was georegistered to an orthorectified Landsat Thematic Mapper (TM) mosaic using a second order polynomial warp algorithm and at least nine ground control points for each scene (National Aeronautics and Space Administration (NASA), 2003). The Landsat mosaic data has a spatial resolution of 28 m and spatial accuracy of ± 50 m and ASTER georegistration to the Landsat TM mosaic produced root-mean-square errors of less than 2.0 (60 m). A mosaic of Landsat 4 and 5 TM band 7 data was also used as a base map for the ASTER data (plates 1–8). Argillic and phyllic alteration units were converted to vector data, exported from the ASTER scenes, and overlaid on the Landsat band 7 mosaic (plates 1–8).

ASTER data have sufficient spectral resolution to identify the 2.165- and 2.200- μm Al-O-H spectral absorption features in argillic minerals such as alunite and kaolinite, and the 2.2- μm Al-O-H spectral absorption feature in the primary phyllic mineral, sericite (figs. 2-2–2-5). Thus, Interactive Data Language (IDL) logical operator algorithms (A-argillic and B-phyllic) were used to map argillic, and phyllic absorption features using ASTER data based on the following two equations (ITT, 2008; John and others, 2010; Mars and Rowan, 2006):

$$(A) ((\text{float } (b3)/b2) \text{ le } 1.35) \text{ and } (b4 \text{ gt } 2600) \text{ and } ((\text{float } (b4)/b6) \text{ gt } 1.37) \text{ and } ((\text{float } (b5)/b6) \text{ le } 1.089) \text{ and } ((\text{float } (b7)/b6) \text{ ge } 1.03),$$

and

$$(B) ((\text{float } (b3)/b2) \text{ le } 1.35) \text{ and } (b4 \text{ gt } 2600) \text{ and } ((\text{float } (b4)/b6) \text{ gt } 1.37) \text{ and } ((\text{float } (b5)/b6) \text{ gt } 1.089) \text{ and } ((\text{float } (b7)/b6) \text{ ge } 1.03),$$

where

ge is greater than or equal to,
gt is greater than;
le is less than or equal to, and
float is floating point.

The logical operator algorithms use a series of band ratios and user-defined thresholds to map spectral absorption features and mask out low-reflectance, noisy pixels, respectively. Threshold numbers for band ratios and band thresholds were determined by compiling ASTER argillic and phyllic mineral

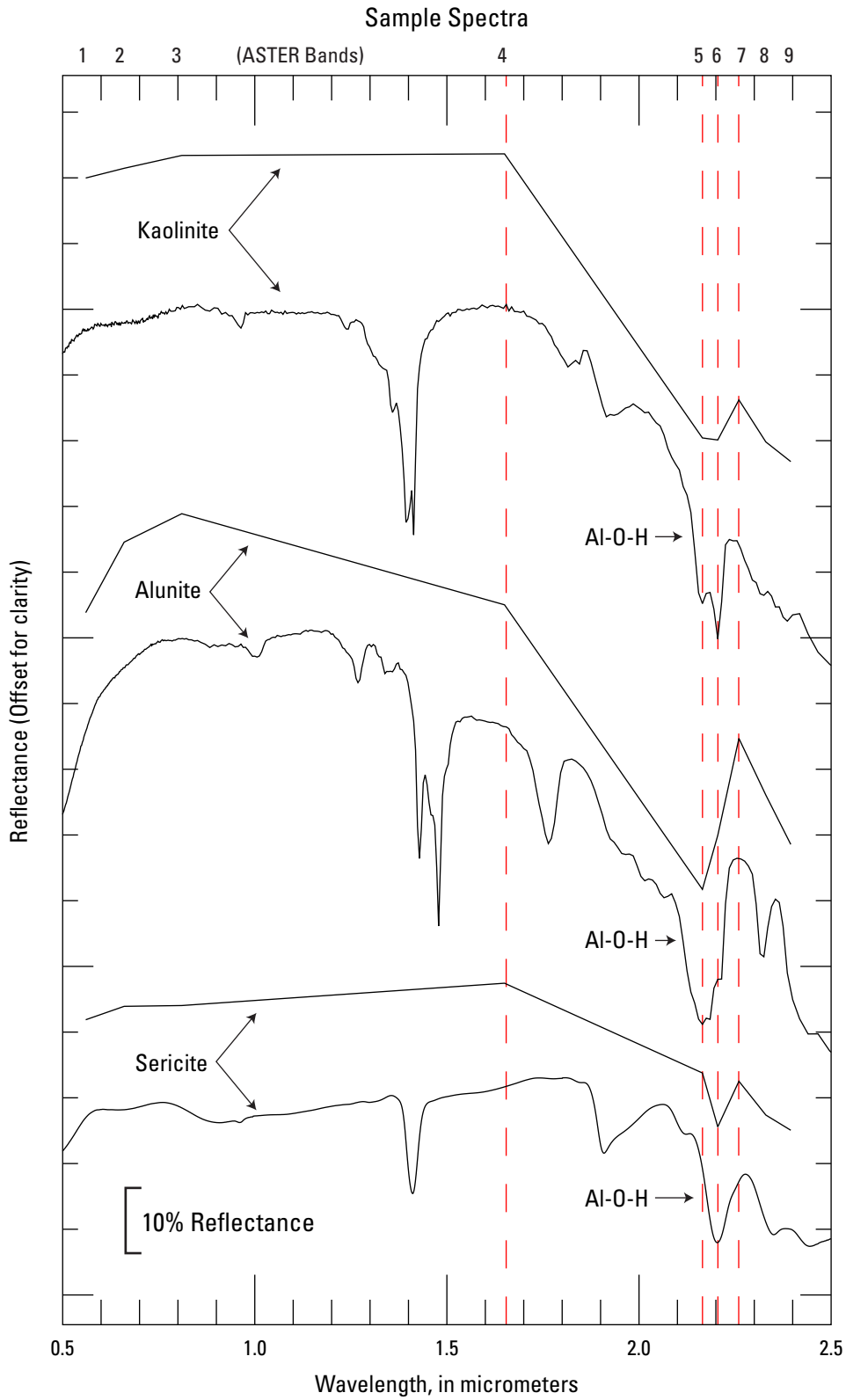


Figure 2-4. Visible near-infrared (VNIR) through the short-wave infrared (SWIR) reflectance sample spectra and Advanced Spaceborne Thermal Emission and Reflection Radiometer (ASTER) resampled sample spectra of kaolinite, alunite, and sericite. ASTER center-band positions illustrated at top of graph. Al-O-H absorption features are positioned at 2.165 and 2.2 micrometers. Red dotted lines illustrate location of ASTER band centers relative to spectral absorption features.

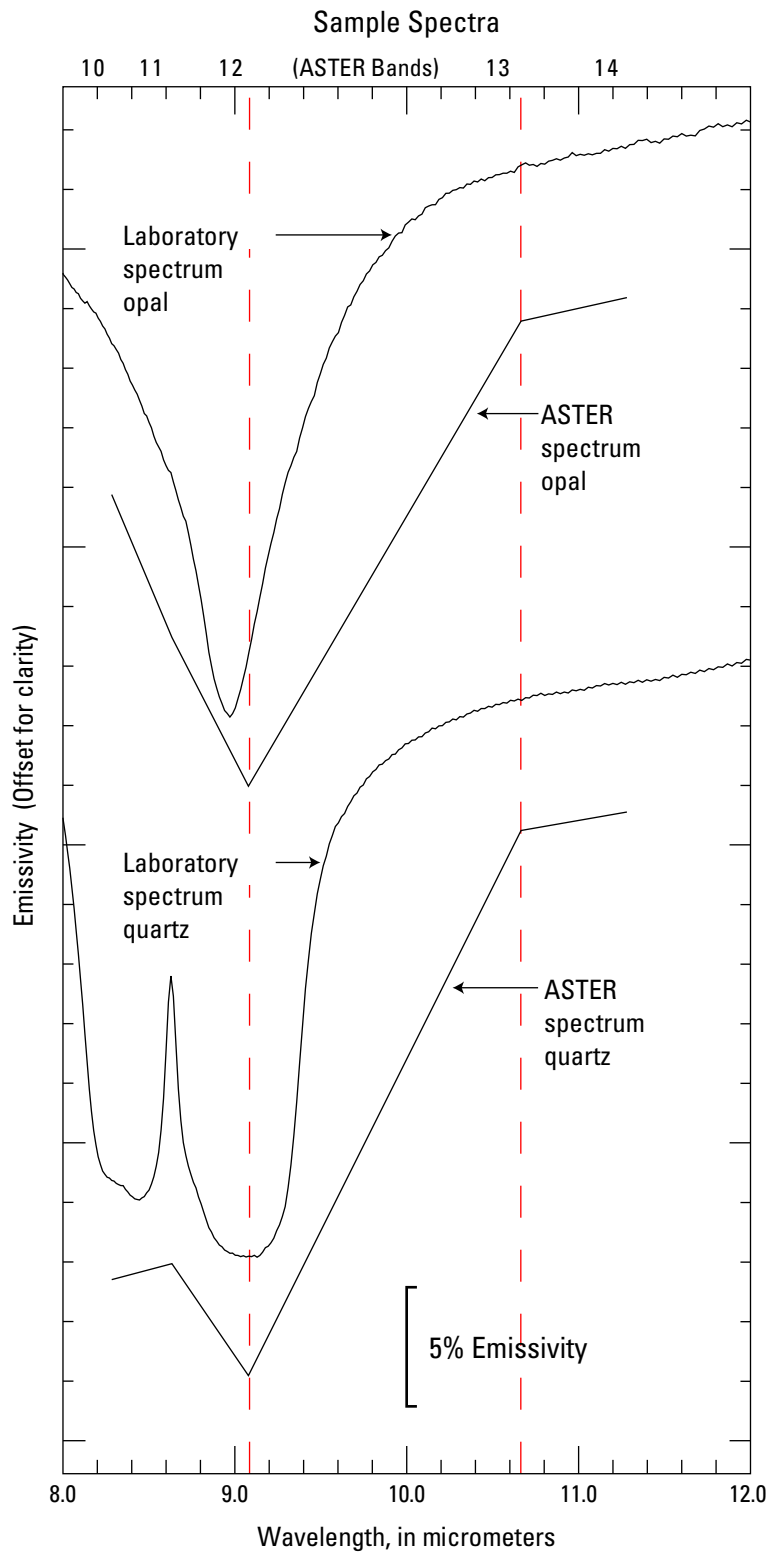


Figure 2-5. Thermal infrared radiation (TIR) emissivity sample spectra and Advanced Spaceborne Thermal Emission and Reflection Radiometer (ASTER) resampled sample spectra of opal and quartz. ASTER center-band positions illustrated at top of graph. Red dotted lines illustrate location of ASTER band centers relative to spectral absorption features.

maps for Cuprite, Nevada, that best match hyperspectral and field mineral maps from previous studies (Ashley and Abrams, 1980; Rowan and Mars, 2003; Mars and Rowan, 2006). The logical operator algorithms mask out green vegetation by utilizing the chlorophyll absorption feature at 0.65 μm using an ASTER 3/2 band ratio (fig. 2-6). Noisy pixels are eliminated in argillic and phyllic logical operators by using a threshold of ASTER band 4 centered at 1.65 μm . The argillic and phyllic logical operators (A and B) map the 2.165- and 2.2- μm Al-O-H absorption features exhibited by argillic-altered rocks and the 2.2- μm Al-O-H absorption feature illustrated by phyllic-altered rocks using 4/6, 5/6 and 7/6 ASTER ratios, respectively (fig. 2-4).

ASTER AST_05 thermal infrared (TIR) emissivity and SWIR reflectance data were used together to map silicic-altered rocks. The ASTER AST_05 TIR emissivity data consist of five emissivity bands spanning the 8.125–11.65 μm region with 90-m spatial resolution. The ASTER SWIR data consist of six bands at 30-m spatial resolution and is part of the ASTER reflectance VNIR- SWIR data (see above) processed from ASTER_level 1B radiance data. The TIR data have sufficient spectral resolution to map the quartz reststralen spectral absorption feature at 9.1 μm , which is typical in hydrothermal silica-rich rocks, such as vuggy siliceous sinter and quartz hydrothermal veins, and nonhydrothermal silica-rich rocks and sediment, such as quartz-rich rhyolite, sandstone, quartzite, and quartz-rich sand (fig. 2-7A). Hydrothermal silica-rich rocks that contain hydrous quartz, opal, and chalcedony may also exhibit Si-O-H SWIR spectral absorption features centered at 2.26 μm (fig. 2-7B). In addition, spectra of samples and spectra of samples convolved to simulate ASTER spectra from Cuprite, Goldfield, and Gemfield, Nevada, illustrate that hydrothermal silica-rich rocks typically exhibit lower SWIR reflectance in the 2–2.5- μm region than nonhydrothermal silica-rich rocks (fig. 2-7B). ASTER bands 4 and 7 are centered at 1.65 and 2.26 μm , respectively (fig. 2-7B). Thus, ASTER 4/7 band ratio values are typically higher for hydrothermal silica-rich rocks than non-hydrothermal silica-rich rocks.

Interactive Data Language (IDL) logical operators consisting of an ASTER TIR band ratio 13/12 to map silica rich rocks (C) and an ASTER SWIR 4/7 band ratio to mask nonhydrothermal silica-rich rocks (D) were developed to map hydrothermal silica-rich rocks, based on the following two equations:

$$(C) ((\text{float}(b13)/b12) \text{ ge } 1.085),$$

and

$$(D) ((\text{float}(b4)/b7) \text{ ge } 1.45),$$

where

ge is greater than or equal to, and
float is floating point.

The IDL logical operators were tested at validation sites in Cuprite, Gemfield, and Goldfield, Nevada, using sample spectra from field investigations and a hydrothermal alteration map from a previous study (Ashley and Abrams, 1980). Ashley and Abrams mapped two highly silicified centers consisting of silicified and opalized rocks at Cuprite, Nevada (fig. 2-8; Ashley and Abrams, 1980). A hydrothermal silica-rich rock map compiled using the hydrothermal silica-rich logical operator, mapped the east and west silicified centers and did not map the nonhydrothermal silica rich alluvial fans located north and south of the hydrothermal deposits (fig. 2-8; Ashley and Abrams, 1980). Field investigations at Gemfield and Goldfield, Nevada, indicate that silicified rocks consisting of opal, chalcedony and hydrothermally deposited quartz were also successfully mapped using the hydrothermal silica-rich logical operator. Thus, based on successful validation tests in Nevada, the logical operators were used to map hydrothermal silica-rich rocks in the assessment area (fig. 2-8; plates 1–4).

Muscovite (sericite) and kaolinite, which were mapped as phyllic- and argillic- altered rocks, are also associated with sedimentary rocks and sediments. To eliminate these deposits as potential porphyry copper sites, a geologic map and assessment of landforms identified on ASTER and Landsat TM imagery were used to evaluate each potential site (Seltmann and others, 2009; NASA, 2003).

Logical Operator Mapping Results

Tectonic studies indicate that the study area consists of multiple faulted and folded Paleozoic magmatic arcs (chapter 1; Abdrakhmanov and others, 1997). Geology of the Kounrad (Konyrat) mine area consists of faulted and folded Devonian-, Carboniferous-, and Permian-age granite, granodiorite, andesite, rhyolite, and limestone (Seltmann and others, 2009). The Kounrad mine, located north of the Balkhash City, Kazakhstan (fig. 1-2), is the largest porphyry copper mine in the former Soviet Union and is hosted in Carboniferous granodiorite (Abdrakhmanov and others, 1997). An alteration map compiled from field mapping shows that the mine consists of laterally extensive quartz sericitic- (phyllic) and potassic altered rocks with less extensive argillic altered rocks covering the southern part of the mine (fig. 2-9; Abdrakhmanov and others, 1997). In addition, the alteration map illustrates that quartz stock works extend over the central and southern parts of the mine site (fig. 2-9). The ASTER derived alteration map of Kounrad shows laterally extensive phyllic alteration, and less extensive argillic alteration primarily covering the southern part of the mine site with minor amounts of silicic-altered rocks (fig. 2-10). The quartz stockworks are most probably mapped as silicic-altered rocks in the ASTER alteration map. Thus, the mine alteration map exhibits good correlation to the ASTER alteration map (figs. 2-9 and 2-10).

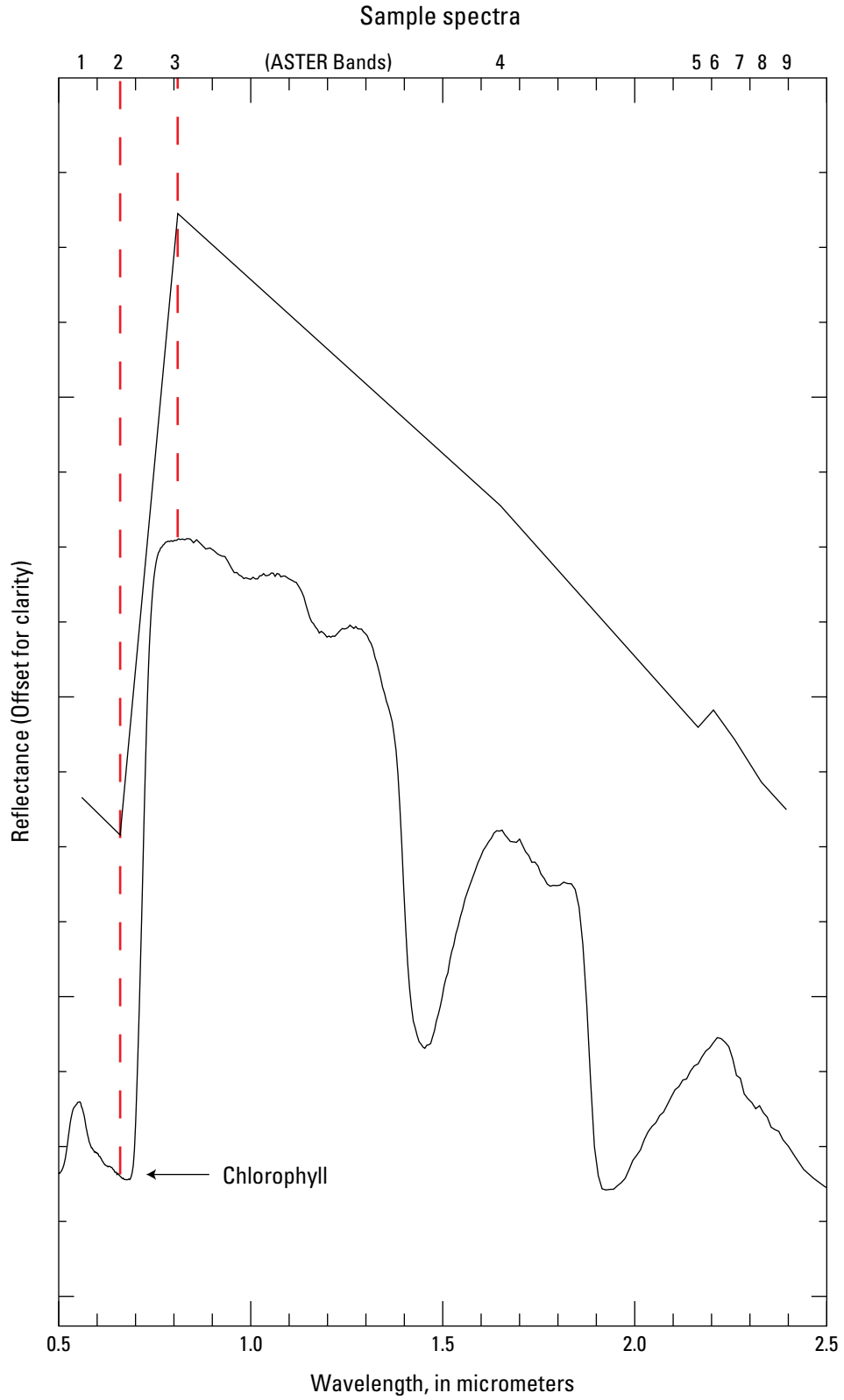


Figure 2-6. Visible near-infrared (VNIR) through the short-wave infrared (SWIR) reflectance sample spectra and Advanced Spaceborne Thermal Emission and Reflection Radiometer (ASTER) resampled sample spectra of green vegetation (green aspen leaf) illustrating the chlorophyll spectral absorption feature positioned at 0.68 micrometers. ASTER center-band positions illustrated at top of graph. Red dotted lines illustrate location of ASTER band centers relative to spectral absorption features.

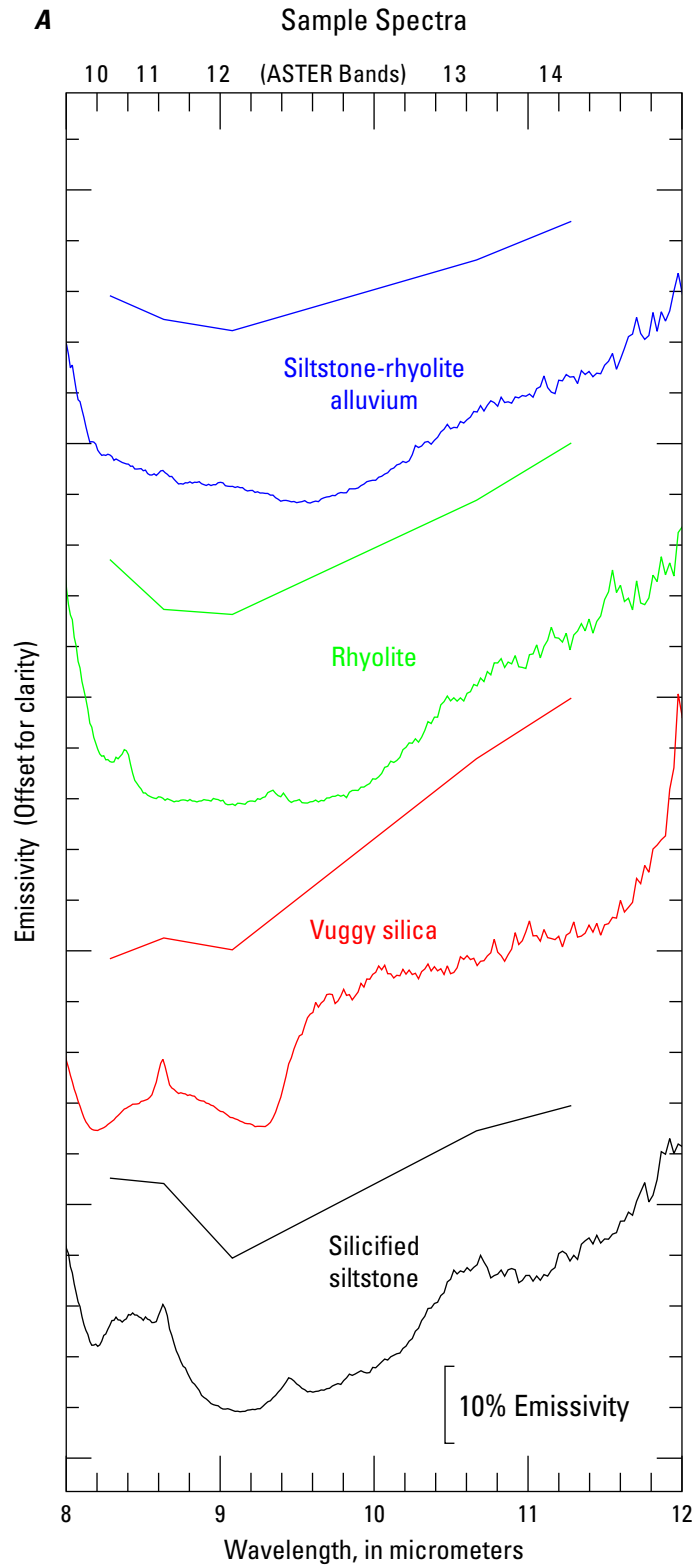


Figure 2-7. Sample spectra from Cuprite and Gemfield, Nevada. *A*, Thermal infrared radiation (TIR) emissivity sample spectra and Advanced Spaceborne Thermal Emission and Reflection Radiometer (ASTER) resampled sample spectra of siltstone-rhyolite alluvium, rhyolite, vuggy silica sinter, and silicified siltstone. ASTER center-band positions illustrated at top of graph. Quartz restralen absorption features are located in the 8- to 9.1-micrometer region. *B*, Visible near-infrared (VNIR) through the short-wave infrared (SWIR) reflectance sample spectra and ASTER resampled sample spectra of siltstone-rhyolite alluvium, rhyolite, vuggy silica sinter, and silicified siltstone. ASTER band-center positions illustrated at top of graph. The vuggy silica sinter Si-O-H absorption feature is centered at 2.26 micrometers. ASTER band centers 4 and 7 are highlighted (dotted line) to illustrate high band 4:7 ratio values for the hydrothermal silica-rich rocks silicified siltstone and vuggy silica sinter, and low 4:7 ratio values for the non-hydrothermal silica-rich rock rhyolite and siltstone and rhyolite sediment.

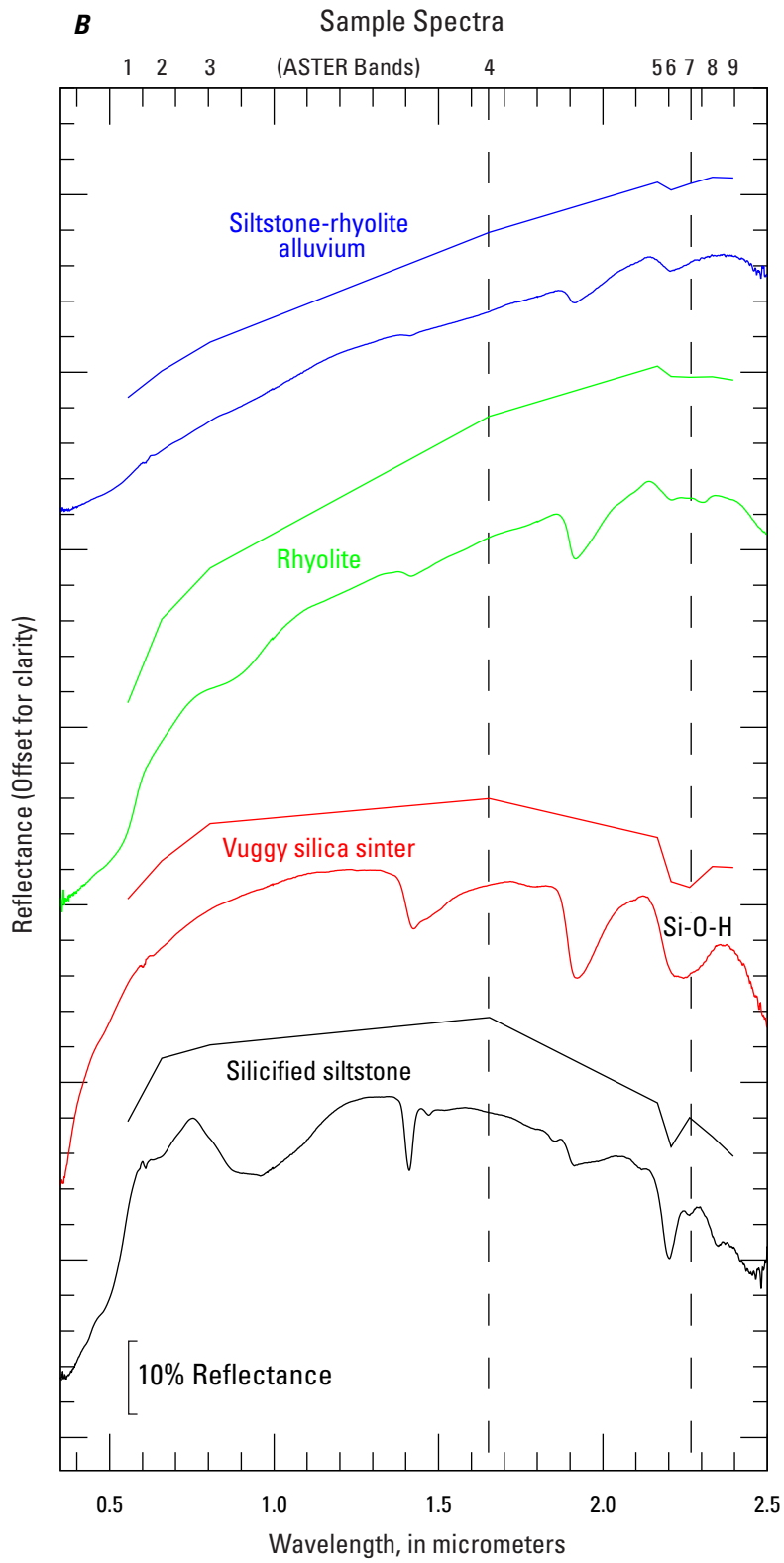


Figure 2-7.—Continued.

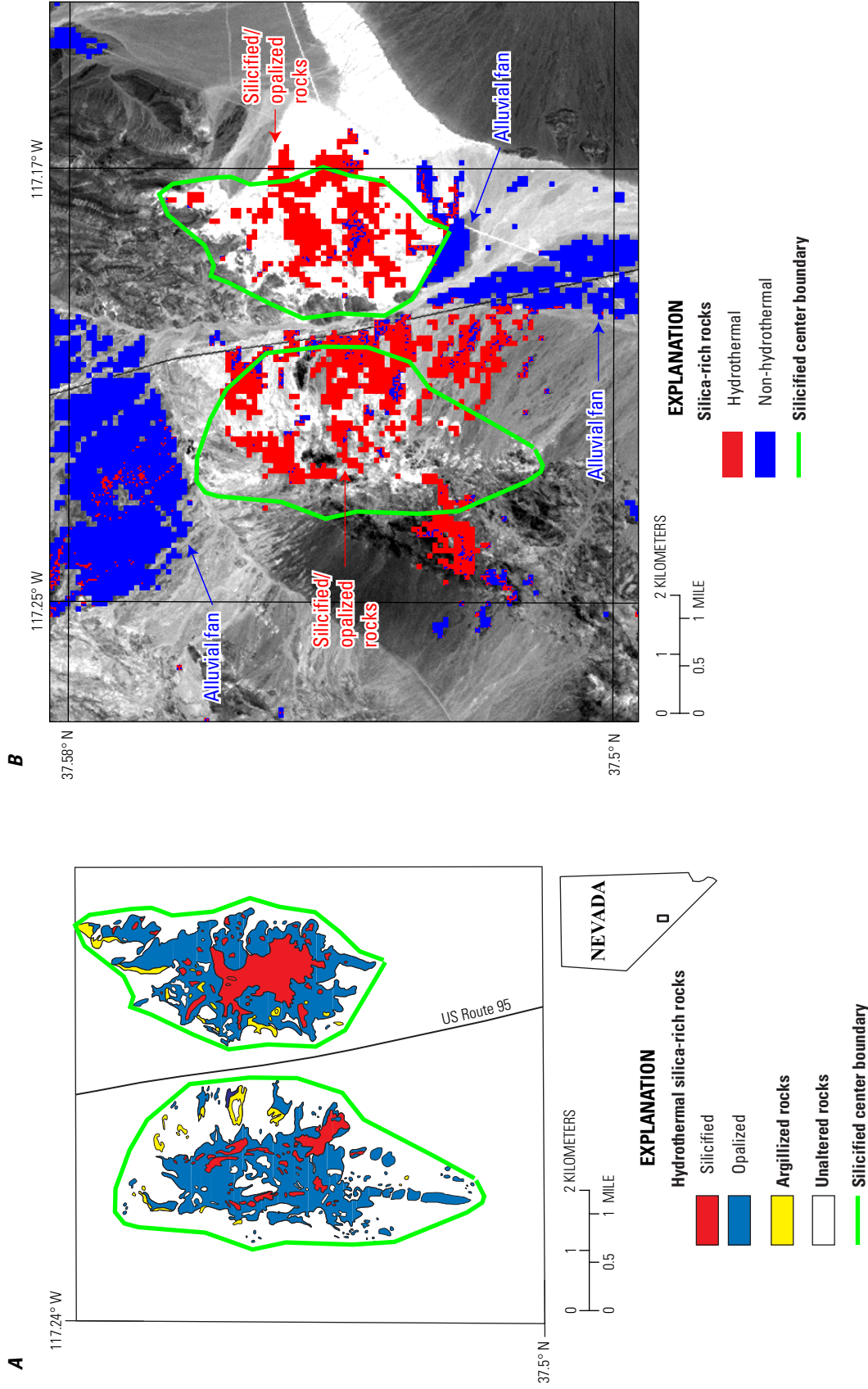


Figure 2-8. Comparison of mapped altered rock and Advanced Spaceborne Thermal Emission and Reflection Radiometer (ASTER) data for Cuprite, Nevada. *A*, Alteration map from Ashley and Abrams (1980) and *B*, hydrothermal and nonhydrothermal silica-rich rocks compiled from ASTER Interactive Data Language (IDL) logical operators. Boundaries of silicified centers are outlined in bold green line. Background image is ASTER band 3. Location of map area shown on inset of Nevada.



Figure 2-9. Alteration map of the Kounrad mine, Kazakhstan (modified from Abdrakhmanov and others, 1997).

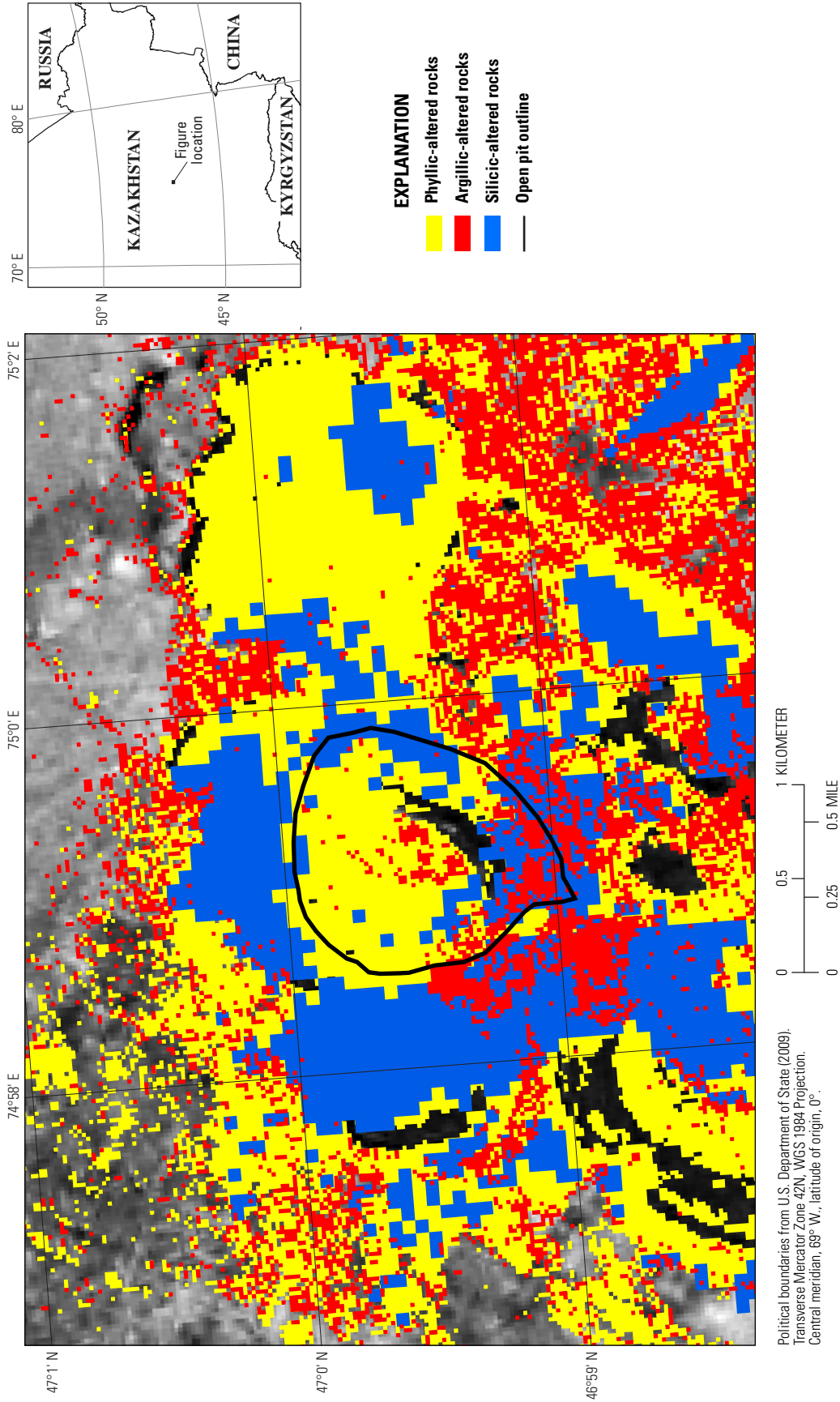


Figure 2-10. Advanced Spaceborne Thermal Emission and Reflection Radiometer (ASTER) alteration map of the Kounrad mine, Kazakhstan. Background image is Landsat TM band 7.

The ASTER hydrothermal alteration mineral map of Kazakhstan typically illustrates elliptical to circular patterns of argillic- and phyllic-altered rocks with minor amounts (less than 10 percent of the total altered-rock cover) of silicic-altered rocks (fig. 2-11: sites 3, 4, 5, 6, 7, and 14; plates 1–4). The circular to elliptical argillic and phyllic alteration patterns in Kazakhstan are similar to hydrothermal alteration patterns of known porphyry copper deposits in Iran mapped using ASTER data (Mars and Rowan, 2006; John and others, 2010). The elliptical to circular patterns of hydrothermal alteration in Kazakhstan and Iran match predicted patterns from exhumed porphyry copper deposit models which would exhibit circular to elliptical patterns of zoned phyllic and argillic altered rocks with varying amounts hydrothermal silica-rich rocks (fig. 2-1; Lowell and Guilbert, 1970; John and others, 2010). Due to the high degree of structural deformation, some areas that contained irregular patterns of argillic, phyllic, and silicic rocks were also selected as potential porphyry copper sites provided the alteration was situated in, or adjacent to, igneous rocks. The alteration maps in some areas, particularly around playas and lakes, show argillic and phyllic units that are actually detrital muscovite and kaolinite in sediments and sedimentary rocks (plates 1–8).

Linear patterns of phyllic and argillic alteration were also mapped in Kazakhstan using ASTER data. Linear patterns of phyllic and argillic rocks have been shown to be associated with epithermal deposits in other permissive tracts in Iran and Afghanistan (Mars and Rowan, 2006; 2007). Although epithermal systems are not porphyry systems, some epithermal systems overlie or border porphyry systems, and are thus included as potential, concealed, porphyry-related deposit sites (John and others, 2010).

A total of 302 potential porphyry copper-related sites were identified within the ASTER hydrothermal alteration map on the basis of alteration types and patterns similar to those of known deposits in Iran, and Afghanistan (fig. 2-12; table 2-1; plates 1–8). The ASTER hydrothermal alteration map shows that 240 potential porphyry copper sites are situated in permissive tracts (fig. 2-12; table 2-1; plates 5–8). The 62 potential porphyry copper-related sites outside of the permissive tracts were not assessed in this study and none of the 302 potential sites were used to determine permissive tract boundaries. Tract 142pCu8003b with 104 potential porphyry copper-related sites contains the greatest number of sites in a tract and is also where the largest porphyry copper deposit (Kounrad) in Kazakhstan is located (fig. 2-2; plates 5 and 6; appendix D). Tracts 142pCu8001, 142pCu8003c, 142pCu8003d contain 59, 38, and 20 potential porphyry copper sites, respectively (fig. 2-2; plates 5 and 7; appendixes A, C, and E). Tracts 142pCu8002, 142pCu8003a, 142pCu8004 each contain less than 10 potential porphyry copper sites (fig. 2-2; plates 5–8; appendixes B, D, and F). Thus, the tracts with the greatest potential for undiscovered deposits on the basis of hydrothermal alteration are tracts 142pCu8003b and 142pCu8001. Additional detail on descriptions of altered sites for each tract can be found in the appendix sections.

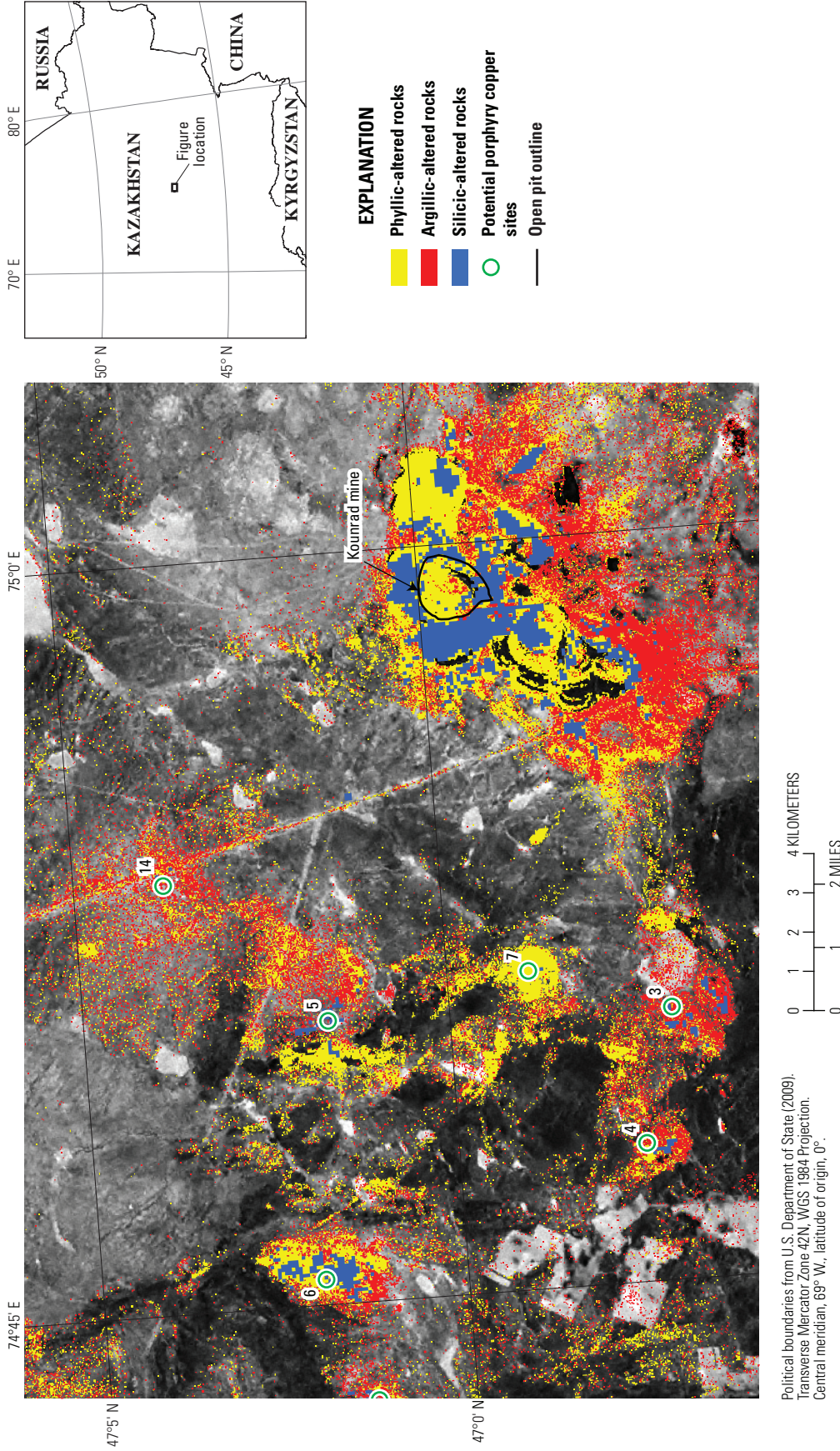
Physical Characteristics of Potential Porphyry Copper Alteration Sites

The physical characteristics of each potential porphyry copper-related site were compared to the physical characteristics of known occurrences and deposits. Thus, in addition to the total number of potential sites, the number of potential sites that had characteristics similar to those of known deposits was also provided to the assessment panel for assistance in estimating undiscovered deposits for each permissive tract.

Physical descriptions of potential porphyry copper sites, occurrences, and deposits were recorded in an ARC GIS database using the ASTER hydrothermal alteration map, an ASTER false color composite image (R=4, G=6, B=8), a database of porphyry copper deposits, and a 1:1,500,000-scale geologic map (table 2-1; plates 1–4; Seltmann and others, 2009; Singer and others, 2008). The ASTER hydrothermal alteration map was used to assess the shape of alteration patterns, types and percentages of alteration, diameter of alteration pattern along the long axis, and hydrothermal alteration density. Hydrothermal alteration density was determined by using a low pass filter on argillic and phyllic alteration data and is illustrated as contours in a low pass filter image (figs. 2-11 and 2-13). The total number of contour levels for each potential porphyry copper site in the low pass filter image is indicated as the contour level density in table 2-1. For example, the low pass filter illustrates 7 contour levels for the Kounrad mine site (fig. 2-13). The ASTER false color composite image was used to identify structures such as faults or lineaments and landforms such as hills. The porphyry copper database and geologic map were used to identify known deposits and occurrences at potential alteration sites and to indicate rocks types and ages.

Outcrop exposure is strongly controlled by vegetation and snow cover, which can affect the remotely sensed physical characteristics of a potential deposit site. Thus, physical characteristics of a potential deposit site were compared to a known deposit that had similar vegetation cover and outcrop exposure. A Landsat TM false color composite (R=7, G=4, B=2) image was used to determine the extent of vegetation and snow cover on a potential porphyry copper site, (fig. 2-14).

Tracts 142pCu8003b and 142pCu8001 with 104 and 59 potential porphyry copper sites, respectively, contain the highest number of potential porphyry copper sites that have similar physical characteristic to deposits. Tract 142pCu8001 has 34 potential porphyry copper sites that have similar physical characteristics to known deposits located within the tract. Tract 142pCu8003b has nine potential porphyry copper sites that have similar physical characteristics to Kounrad, the largest porphyry copper deposit within the tract. Additional detail on physical characteristics of potential porphyry copper sites, deposits and occurrences for each permissive tract can be found in the appendix sections.



Political boundaries from U.S. Department of State (2009).
 Transverse Mercator Zone 42N, WGS 1984 Projection.
 Central meridian, 69° W., latitude of origin, 0°.

Figure 2-11. Advanced Spaceborne Thermal Emission and Reflection Radiometer (ASTER) alteration map and potential porphyry copper sites of the Kounrad mine area in Kazakhstan. Numbered locations (in green) 3, 4, 5, 6, 7, and 14 are potential porphyry copper sites based on circular to elliptical alteration patterns. Numbered location 1 is the known porphyry copper deposit at Kounrad mine. Background image is Landsat TM band 7.

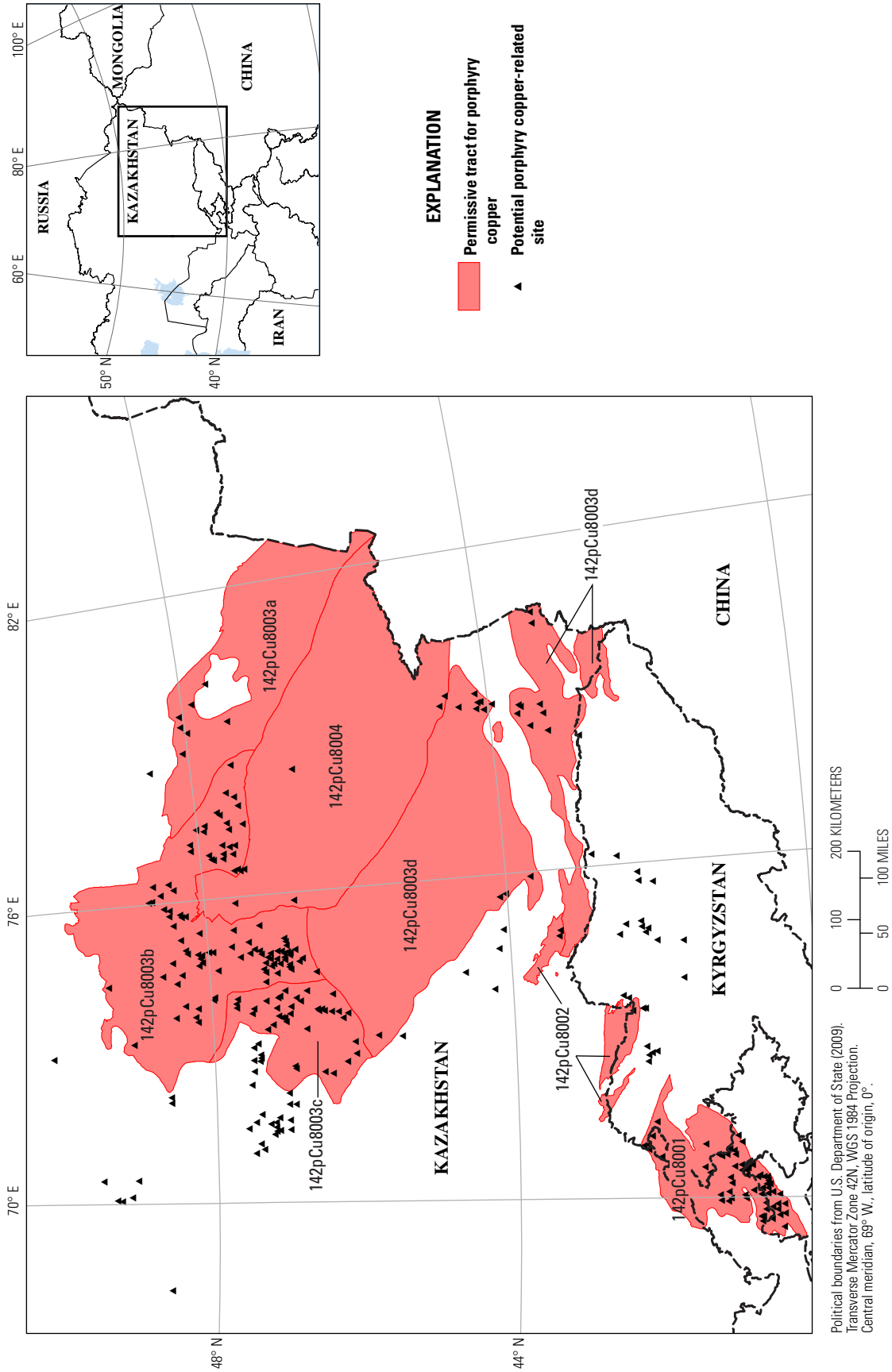


Figure 2-12. Permissive tracts and potential deposit sites in western Central Asia. Location of map area shown on inset.

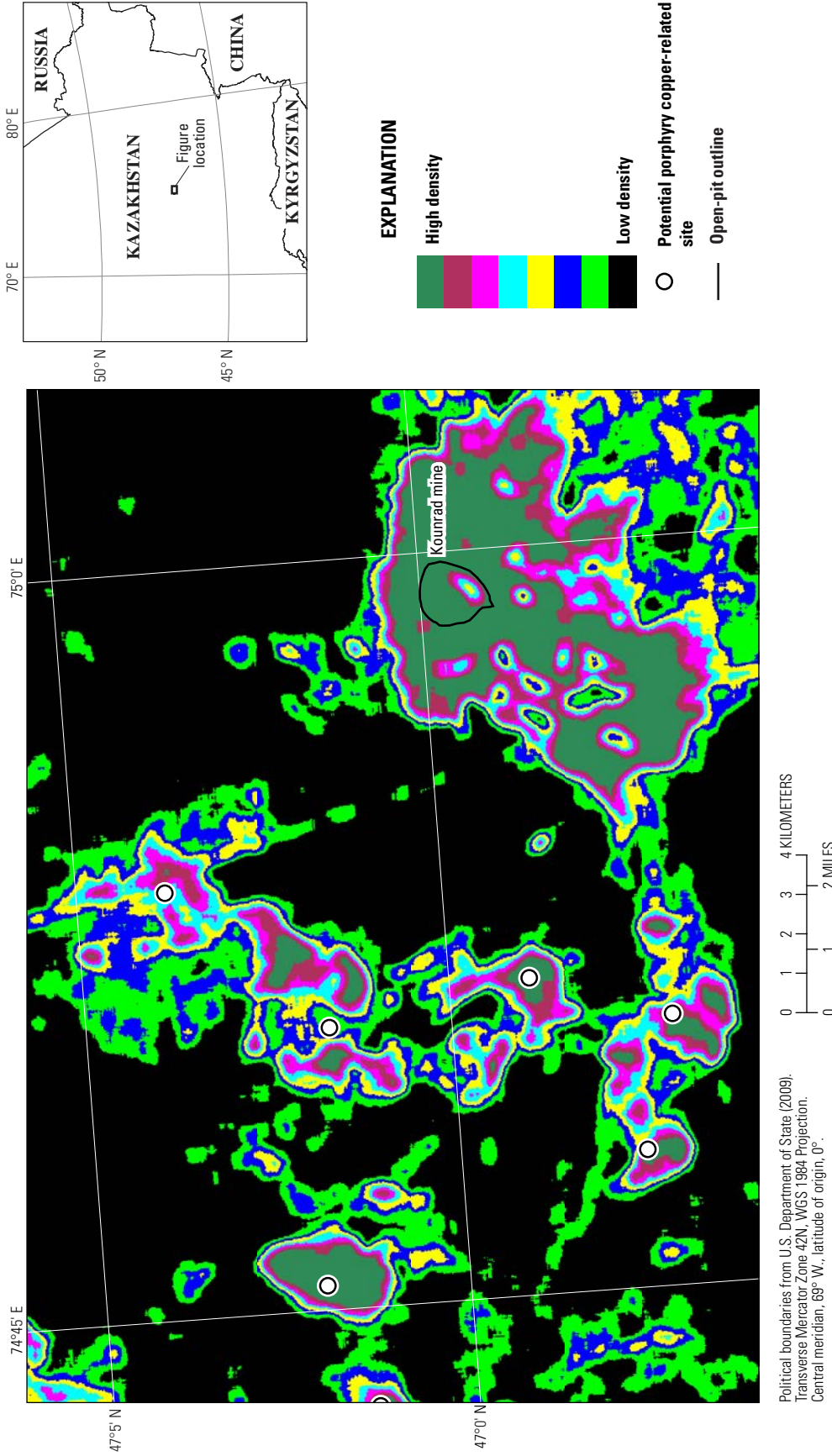
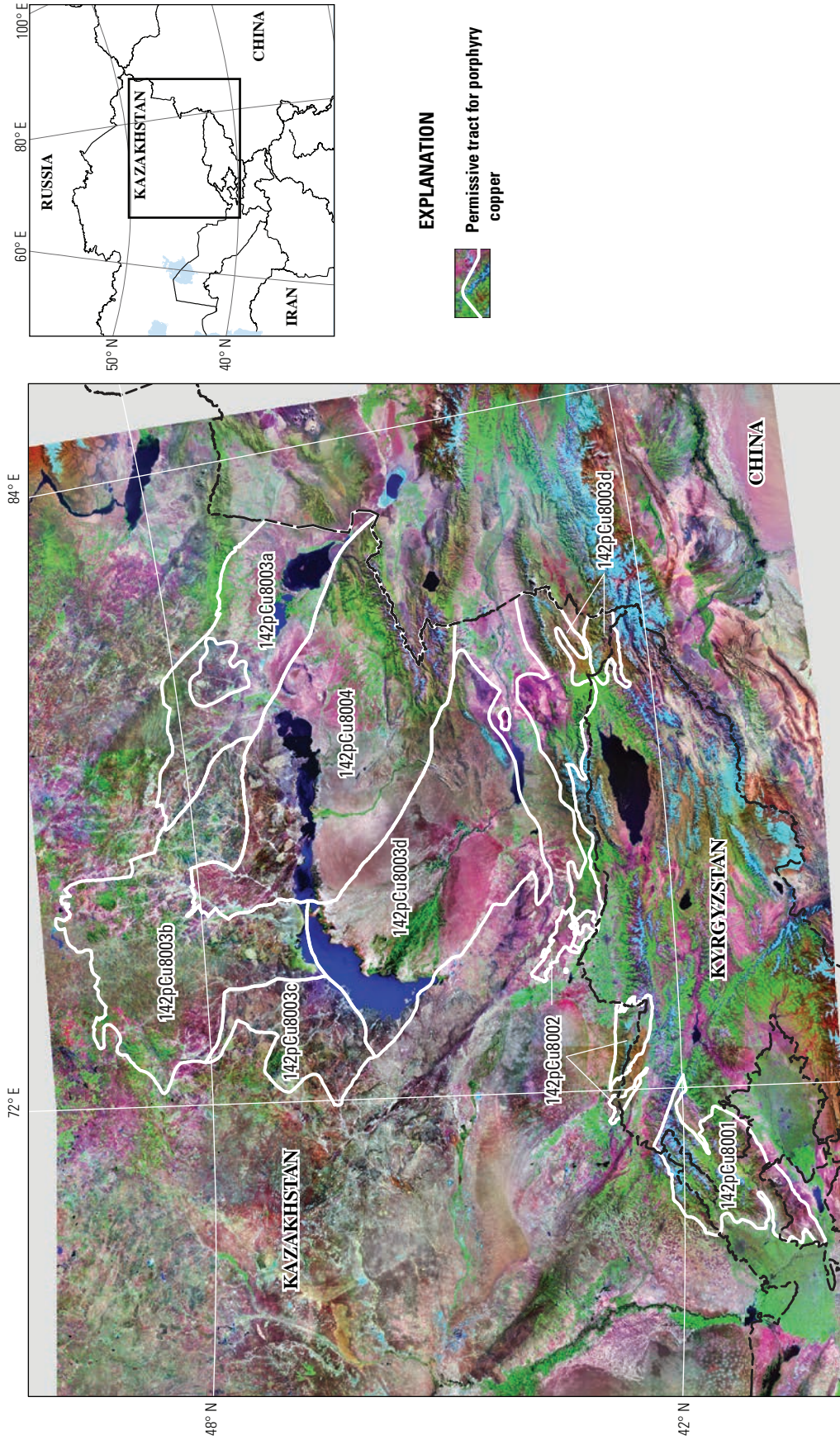


Figure 2-13. Advanced Spaceborne Thermal Emission and Reflection Radiometer (ASTER) low-pass filter map compiled from argillic and phyllic alteration in the Kounrad mine area in Kazakhstan used to determine alteration density of each potential porphyry copper site in western Central Asia.



Political boundaries from U.S. Department of State (2009).
 Transverse Mercator Zone 42N, WGS 1984 Projection.
 Central meridian, 69° W.; latitude of origin, 0°.

Figure 2-14. Landsat TM false color composite image of southeastern Kazakhstan and Kyrgyzstan and permissive tracts (band 7 = red, band 4 = green, band 2 = blue). Green illustrates green vegetation, magenta, pink, light red, gray browns, and light cyan illustrates rocks and sediments, dark blues and black illustrate water, and cyan on mountains are ice and snow. Location of map area shown on inset.

Summary

Argillic, phyllic and hydrothermal silica-rich rocks were mapped using ASTER Level_1B radiance data converted to VNIR-SWIR ASTER reflectance data (nine bands), ASTER AST_05 emissivity data, and logical operator algorithms. Validation of ASTER alteration maps was assessed at Cuprite, Goldfield, and Gemfield, Nevada, and at the Kounrad mine, Kazakhstan. Circular to elliptical patterns of argillic-, phyllic- and silicic-altered rocks are similar to ASTER mapped argillic and phyllic alteration patterns of known porphyry copper deposits in Iran. On the basis of the presence of minerals associated with argillic, phyllic and silicic alteration types and patterns, 302 potential and known porphyry sites were chosen in western Central Asia.

A list of physical characteristics for each potential site, including the shape of alteration patterns, types and percentages of alteration, diameter of alteration pattern along the long axis, argillic and phyllic alteration density, age, lithology, observed structure or landforms in the ASTER image, associated occurrences and deposits, and permissive tract defined were compiled in a geographic database. The physical characteristics of each potential site were compared to sites that contained known deposits. Thus, for each permissive tract, the total number of potential porphyry copper-related sites and the number of potential sites that had similar characteristics to known deposits were provided to the assessment panel for estimating undiscovered deposits. Permissive tracts 142pCu8003b and 142pCu8001 contain the largest number of potential porphyry copper sites and potential sites with similar physical characteristics to known deposits within their associated tracts (plates 5 and 8).

References Cited

- Abdrakhmanov, K., Zhautikov, T., Kulishkin, H., and Poletaev, A., 1997, Part II—Field trip in Kazakhstan, *in* Bekzhanov, G.R., Dudich, G., G., and Jenchuraeva, R., J., ed., Paleozoic granite-related Au, Cu, Mo, W, REE deposits and epithermal gold deposits: IUGS/UNESCO Deposit Modeling Program Workshop, Kazakhstan and Kyrgyzstan, p. 65–73.
- Abrams, M.J., Brown, L., Lepley, R., and Sadowski, P., 1983, Remote sensing for porphyry copper deposits in Southern Arizona: *Economic Geology* v. 78, p. 591–604.
- Ashley, R.P., and Abrams, M.J., 1980, Alteration mapping using multispectral images—Cuprite mining district, Esmeralda County, Nevada: U.S. Geological Survey Open-File Report 80–367, scale 1:24,000.
- Beane, R.E., and Titley, S.R., 1981, Porphyry copper deposits—Part II. Hydrothermal alteration and mineralization, *in* Skinner, B.J., ed., *Economic Geology 75th Anniversary Volume*, p. 235–269.
- Biggar, S.F., Thome, K.J., McCorkel, J.T., and D’Amico, J.M., 2005, Vicarious calibration of the ASTER SWIR sensor including crosstalk correction: *Proceedings International Society Optical Engineering*, v. 5882, p. 588217.
- Fujisada, H., 1995, Design and performance of ASTER instrument: *Proceedings, International Society Optical Engineering*, v. 2583, p. 16–25.
- Hunt, G.R., 1977, Spectral signatures of particulate minerals in the visible and near infrared: *Geophysics*, v. 42, no. 3, p. 501–513.
- Hunt, G.R., and Ashley, R.P., 1979, Spectra of altered rocks in the visible and near infrared: *Economic Geology*, v. 74, no. 7, p. 1613–1629.
- ImSpec LLC, 2004, ACORN 5.0 user’s manual, 122 p.: ImSpec LLC, accessed August 15, 2011, at <http://www.imspec.com>.
- ITT, 2008, The Environment for Visualizing Images (ENVI) software: ITT Visual Information Solutions, Boulder, Colorado, accessed August 15, 2011, at <http://www.itvis.com/ProductServices/ENVI.aspx>.
- Iwasaki, A., and Tonooka, H., 2005, Validation of a crosstalk correction algorithm for ASTER/SWIR: *Geoscience and Remote Sensing, IEEE Transactions*, v. 43, no. 12, p. 2747–2751.
- John, D.A., Ayuso, R.A., Barton, M.D., Blakely, R.J., Bodnar, R.J., Dilles, J.H., Gray, Floyd, Graybeal, F.T., Mars, J.C., McPhee, D.K., Seal, R.R., Taylor, R.D., and Vikre, P.G., 2010, Porphyry copper deposit model, chapter B of Mineral deposit models for resource assessment: U.S. Geological Survey Scientific Investigations Report 2010–5070–B, 169 p., accessed January 15, 2011, at <http://pubs.usgs.gov/sir/2010/5070/b/>.
- Lowell, J.D., and Guilbert, J.M., 1970, Lateral and vertical alteration-mineralization zoning in porphyry ore deposits: *Economic Geology*, v. 65, no. 4, p. 373–408.
- Mars, J.C., and Rowan, L.C., 2006, Regional mapping of phyllic- and argillic-altered rocks in the Zagros magmatic arc, Iran, using Advanced Spaceborne Thermal Emission and Reflection Radiometer (ASTER) data and logical operator algorithms: *Geological Society of America, Geosphere*, v. 2, p. 161–186, 2 plates.

- Mars, J.C., and Rowan, L.C., 2007, Mapping phyllic and argillic-altered rocks in southeastern Afghanistan using Advanced Spaceborne Thermal Emission and Reflection Radiometer (ASTER) data: U.S. Geological Survey Open-File Report 2007–1006, 1 plate (Also available at <http://pubs.usgs.gov/of/2007/1006/>.)
- Mars, J.C., and Rowan, L.C., 2010, Spectral assessment of new ASTER SWIR surface reflectance data products for spectroscopic mapping of rocks and minerals: *Remote Sensing of Environment*, v. 114, p. 2011–2025.
- National Aeronautics and Space Agency (NASA), 2003, Applied Sciences Directorate: National Aeronautics and Space Administration, accessed August 15, 2011, at <https://zulu.ssc.nasa.gov/mrsid/>.
- Rowan, L.C., Hook, S.J., Abrams, M.J., and Mars, J.C., 2003, Mapping hydrothermally altered rocks at Cuprite, Nevada, using the Advanced Spaceborne Thermal Emission and Reflection Radiometer (ASTER), a new satellite-imaging system: *Economic Geology*, v. 98, no. 5, p. 1019–1027.
- Rowan, L.C., and Mars, J.C., 2003, Lithologic mapping in the Mountain Pass, California area using Advanced Spaceborne Thermal Emission and Reflection Radiometer (ASTER) data: *Remote Sensing of Environment*, v. 84, no. 3, p. 350–366.
- Seltmann, R., Shatov, V., and Yakubchuk, A., 2009, Mineral deposits database and thematic maps of Central Asia—ArcGIS 9.2, Arc View 3.2, and MapInfo 6.0(7.0) GIS packages: London, Natural History Museum, Centre for Russian and Central EurAsian Mineral Studies (CERCAMS), scale 1:1,500,000, and explanatory text, 174 p. [Commercial dataset available at <http://www.nhm.ac.uk/research-curation/research/projects/cercams/products.html>.]
- Sillitoe, R.H., 2010, Porphyry copper systems: *Economic Geology*, v.105, p. 3–41.
- Singer, D.A., Berger, V.I., and Moring, B.C., 2008, Porphyry copper deposits of the world: U.S. Geological Survey Open-File Report 2008–1155, 45 p., accessed August 10, 2009, at <http://pubs.usgs.gov/of/2008/1155/>.
- Spatz, D.M., and Wilson, R.T., 1995, Remote sensing characteristics of porphyry copper systems, western America Cordillera, in Pierce, F. W. and Bolm, J. G., eds.: *Arizona Geological Society Digest*, v. 20, p. 94–108.
- Titley, S.R., 1972, Intrusion and wallrock porphyry copper deposits: *Economic Geology*, v. 67, p. 122–123.

This page intentionally left blank.

Chapter 3. Porphyry Copper Assessment of Western Central Asia—Kazakhstan, Uzbekistan, Kyrgyzstan, Tajikistan, and Parts of Russia

By Jane M. Hammarstrom¹, Byron R. Berger², Paul D. Denning², Connie L. Dicken¹, Lawrence D. Drew¹, John C. Mars¹, Jeffrey D. Phillips², and Michael L. Zientek³, with contributions from Dmitriy Alexeiev⁴, Reimar Seltmann⁵, and Richard Herrington⁵

Introduction

Areas reflecting magmatic-arc activity for two time periods, the Ordovician and the Carboniferous, were selected for the quantitative assessment of the numbers of undiscovered porphyry copper deposits in western Central Asia. The tectonic, geologic, and alteration framework discussed in chapters 1 and 2 of this report provided the basis for the assessment. This chapter describes the assessment process, an overview of the assessed areas, and a summary of results. Detailed descriptions of the eight assessed permissive tracts, the rationale for the estimates of numbers of undiscovered deposits, and estimates of amounts of undiscovered resources associated with each permissive tract are given in appendixes A through H. The assessment was done using the three-part form of quantitative mineral resource assessment developed by Singer (1993), as summarized in the Introduction to this report and described by Singer and Menzie (2010).

The selected areas (fig. 3-1) include (1) the Middle to Late Ordovician North Tian Shan magmatic arc in Kazakhstan and Kyrgyzstan, (2) the Late Paleozoic Balkash-Ili magmatic arc in Kazakhstan and Kyrgyzstan and the Central Balkash-Ili magmatic arc in Kazakhstan, (3) the Late Paleozoic magmatic arc and postcollisional igneous complexes in the Chatkal and Kurama Ranges of Kazakhstan, Kyrgyzstan, Tajikistan, and Uzbekistan, and (4) the Carboniferous Valerianov Arc in the southern Urals in Kazakhstan, Uzbekistan, and Russia.

Selecting Tracts for Assessment

The quantitative mineral-resource assessment method used in western Central Asia is based on a general mineral-deposit model (see Berger and others, 2008) that is consistent with global grade and tonnage models for porphyry copper deposits (Singer and others, 2008). Therefore, only those areas for which a substantial proportion of a magmatic-arc terrane is still intact within the study area were chosen for assessment. This does not preclude the likelihood that porphyry copper deposits may be found in permissive magmatic arcs that were not quantitatively assessed. Areas known to contain porphyry copper deposits or occurrences or permissive rocks were not assessed if the degree of tectonic deformation or depth of erosion were deemed too extensive for the models to be meaningfully applied. See chapter 1 for a discussion of porphyry copper possibilities in these highly deformed areas that were not assessed, including Cambrian magmatic arcs and western parts of the Valerianov Arc in the Urals. The permissive tracts were delineated as geographic areas that include volcanic, volcanism-related, and intrusive rocks of a specific time interval that were previously related (for example, Windley and others, 2007) to a particular magmatic-arc or magmatic-arc belt. In this assessment, the tracts were based on geologic map units in Petrov and others (2006) and Seltmann and others (2009). This report does not extend across the eastern border of Kazakhstan into China; central and eastern parts of the Central Asian Orogenic Belt are assessed in a separate report (Mihalasky and others, in press).

Assessment Data

The principal data used in the assessment were geologic, tectonic, aeromagnetic, and remote sensing data, and databases of mineral occurrences. Electronic versions of the geologic

¹U.S. Geological Survey, Reston, Virginia, United States.

²U.S. Geological Survey, Denver, Colorado, United States.

³U.S. Geological Survey, Spokane, Washington, United States.

⁴Russian Academy of Science, Moscow, Russia.

⁵Centre for Russian and Central EurAsian Mineral Studies (CERCAMS), Natural History Museum, London, United Kingdom.

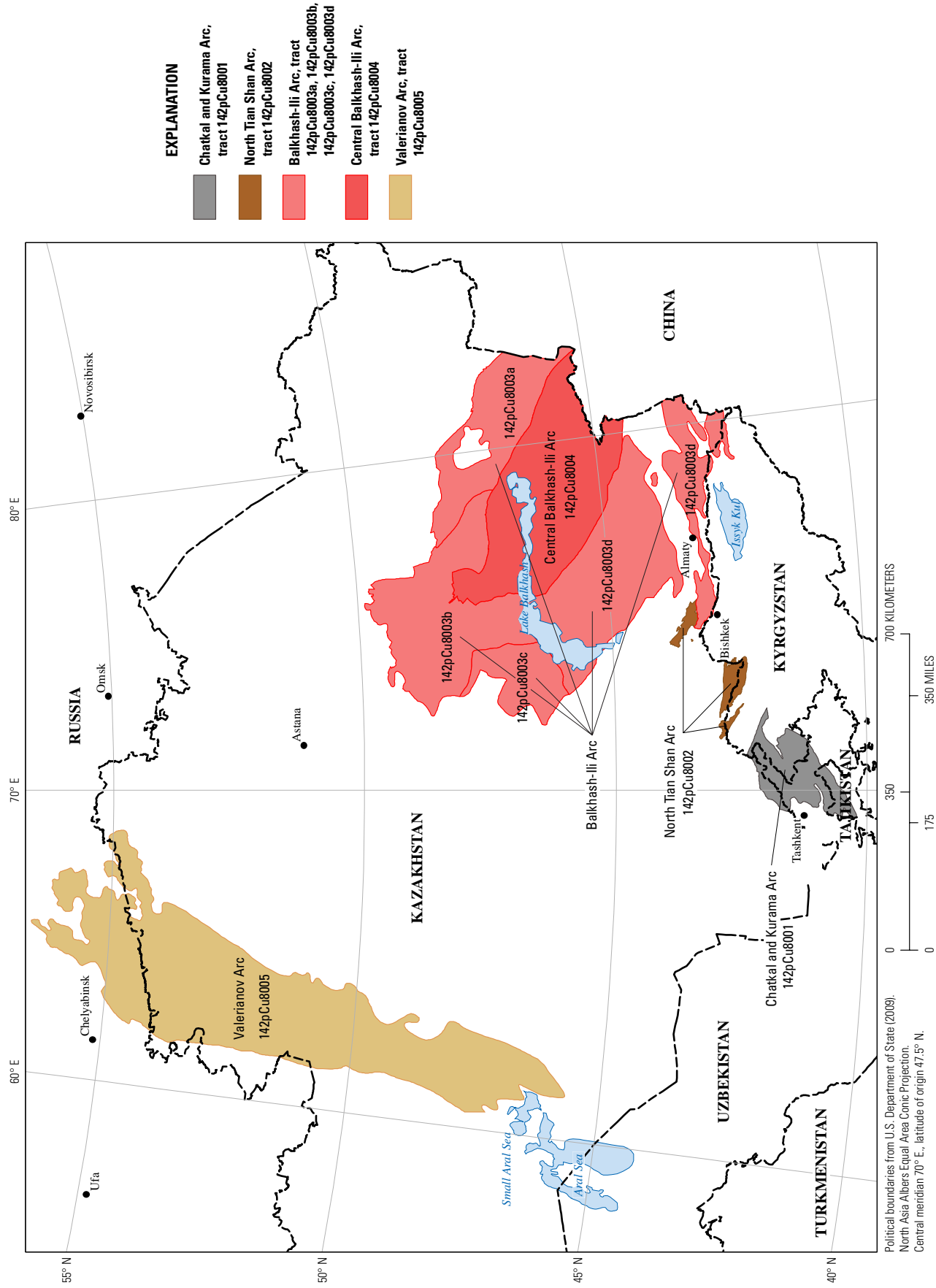


Figure 3-1. Map of permissive tracts for porphyry copper deposits in western Central Asia. See table 3-2 for description of tracts. Different colors represent different magmatic arcs: Valerianov Arc, tan; Balkhash Ili Arc, red; North Tian Shan Arc, brown; Chatkal and Kurama Arc, gray.

maps of Petrov and others (2006) and Seltmann and others (2009) were used and supplemented to the extent possible by publicly available geologic maps at various spatial scales (typically 1:200,000-scale), regional aeromagnetic data, published journal articles, books and symposia proceedings, Russian language government publications, and information obtained from various Internet Web sites. A bibliography of specific references used is included in each of the tract discussions in the appendixes.

An aeromagnetic data set for the former Soviet Union (U.S.S.R.) is available in digital form on CD-ROM from the NOAA's National Geophysical Data Center (1997). At the highest resolution, these data are sampled in a 2,500-meter (m) grid, so they are useful for examining the longer wavelength components of the aeromagnetic field. These data were used to produce a grid of long-wavelength aeromagnetic anomalies for the Central Asia study area.

The aeromagnetic grid was reduced to the pole using proprietary software. Reduction-to-the pole (RTP) is a filtering process that removes the effect of geomagnetic latitude and repositions magnetic anomalies directly over their sources (Blakely, 1995). As a first step toward interpretation, the horizontal gradient magnitude of the RTP aeromagnetic grid was calculated, and the lines of maximum horizontal gradient were extracted. These lines define potential locations of vertical (steeply dipping) magnetic contacts within the crust (Cordell and Grauch, 1985; Blakely and Simpson, 1986; Grauch and Cordell, 1987). The lines were superimposed on the RTP aeromagnetic map to aid in geologic interpretation and the selection of tract boundaries.

Chapter 2 describes Advanced Spaceborne Thermal Emission and Reflection Radiometer (ASTER) data, data processing algorithms, and results of the hydrothermal alteration mapping done for the assessment. Applications of the ASTER data to the assessment are described in the appendixes.

Known Deposits, Occurrences, and Linked Deposit Types

In this assessment, a “known” porphyry copper deposit was defined as one for which grade and tonnage data are listed in Singer and others (2008). All other porphyry coppers are referred to as “occurrences” irrespective of their chance of being classified as a deposit upon further exploration. The principal resources used regarding porphyry copper deposits, prospects, and occurrences were Petrov and others (2006), Seltmann and others (2009), and Zhukov and others (1998). Whenever possible, regardless of the source of data, the proper classification of deposits and occurrences was independently verified. Any discrepancies in deposit locations between the various sources used were adjudicated using Russian geologic map information, Russian language books, Google Earth images, or expert advice.

Spatial Rules for Grouping Deposits and Occurrences

Spatial rules are used to define the sampling unit that represents a deposit to ensure consistency in mineral resource assessment (Singer and Menzie, 2010). For porphyry copper deposits, two operational rules are applied in constructing the grade and tonnage models: (1) all mineralized or altered rock within 2 km is combined as a single deposit, and (2) grade and tonnage data are compiled for these single deposits based on total production, reserves, and resources at the lowest reported cutoff grade. On the basis of these rules, 18 porphyry copper deposits having published grade and tonnage figures are present in the study area (table 3-1).

Deposit types known to be commonly associated with porphyry copper deposits, such as copper skarns and polymetallic veins, were used as evidence for the possibility of the occurrence of a porphyry copper deposit.

The assessment data and results for each permissive tract are presented in a standardized format in the appendixes. Permissive tract boundaries and point locations of significant deposits and occurrences are included in a geographic information system (GIS) that accompanies this report (appendix I). The GIS attribute table for porphyry copper deposits and significant occurrences includes locations, descriptive information, permissive tract designations, and references. Selected attributes and references for each site are included in the tables in the appendixes. The political boundaries used are the small-scale international boundary files (SSIB) maintained by the U.S. Department of State (2009).

Permissive Tracts

The principal litho-tectonic terrane concept used to delineate tracts was that of a magmatic arc that formed in the subduction boundary zone above a subducting plate; in some cases postcollisional volcanic-plutonic complexes are included along with arc-related rocks. Eight permissive tracts were delineated within four magmatic arcs (fig. 3-1, table 3-2). Criteria for delineation of each tract, maps, and tables of deposits and occurrences are listed in the appendixes. See chapter 1 for a discussion of the geodynamic context and deposit characteristics of the magmatic arcs.

Chatkal and Kurama Arc

The 25,100 square kilometer (km²) tract in the Chatkal and Kurama Ranges of Kazakhstan, Kyrgyzstan, Tajikistan, and Uzbekistan, tract 142pCu8001, delineates Late Carboniferous to Permian magmatic-arc and postcollisional rocks (fig. 1-37) of the Chatkal-Kurama Arc (Windley and others, 2007). Four deposits are known within the tract, including the world class deposits of the Almalyk Group, which contain about 24 million metric tons (Mt) of copper and 2,250 metric tons (t) of gold (table 3-1).

Table 3-1. Porphyry copper deposits of western Central Asia.

[Mt, million metric tons; t, metric ton; %, percent; g/t, grams per metric ton; n.d., no data. Deposits and prospects within about 2 kilometers of each other are grouped]

Name	Country	Tonnage (Mt)	Copper (%)	Molybdenum (%)	Gold (g/t)	Silver (g/t)	Contained Cu (t)	Contained Au (t)
Late Carboniferous-Permian Chatkal and Kurama Ranges (142pCu8001)								
Almalyk Group (Almalyk, Dal'nee, Kal'makyr, Karabulak, Northwest Balikti)	Uzbekistan	6,080	0.39	0.002	0.37	2.20	23,712,000	2,250
Kuru Tegerek	Kyrgyzstan	10	0.53	n.d.	1.51	n.d.	53,000	15
Kyzata	Uzbekistan	700	0.85	n.d.	n.d.	n.d.	5,950,000	n.d.
Sarycheku	Uzbekistan	200	0.50	n.d.	0.10	n.d.	1,000,000	20
Ordovician North Tian Shan magmatic arc (142pCu8002)								
Chatyrkul	Kazakhstan	90.7	0.60	n.d.	n.d.	n.d.	544,200	n.d.
Taldy-Bulak Talas	Kyrgyzstan	540	0.27	0.008	0.50	n.d.	1,458,000	270
Late Paleozoic Balkhash-Ili magmatic arc (142pCu8003)								
142pCu8003a								
Aktogai-Aidarly	Kazakhstan	2,636	0.39	0.01	0.03	1.43	10,280,400	69
142pCu8003b								
Borly	Kazakhstan	94.4	0.34	0.011	0.30	3.40	320,960	28
Kenkuduk	Kazakhstan	23.7	0.34	0.017	n.d.	n.d.	80,580	n.d.
Kepcham	Kazakhstan	35.8	0.34	0.018	n.d.	n.d.	121,720	n.d.
Kounrad	Kazakhstan	637	0.59	0.011	0.19	6.28	3,751,930	121
Ozerno	Kazakhstan	194	0.36	0.005	0.02	2.90	698,400	4
142pCu8003c								
Karatas Group	Kazakhstan	29	0.44	0.024	n.d.	n.d.	127,600	n.d.
Saryshagan	Kazakhstan	324	0.27	0.007	0.024	n.d.	874,800	8
142pCu8003d								
Kazkymys	Kazakhstan	375	0.41	0.007	0.059	0.79	1,537,500	22
Koksai	Kazakhstan	320	0.55	0.049	0.12	1.24	1,760,000	38
Carboniferous Valerianov magmatic arc (142pCu8005)								
Benkala North	Kazakhstan	309	0.42	0.003	0.07	n.d.	1,297,800	22
Varvarinskoe	Kazakhstan	117.62	0.66	n.d.	1.01	0.50	776,292	119

North Tian Shan Magmatic Arc

Tract 142pCu8002 outlines a belt within the Middle to Late Ordovician North Tian Shan magmatic-arc where lithologies, evidence for copper mineralization, and levels of exposure are compatible with porphyry copper deposit characteristics as defined in descriptive models (Berger and others, 2008). Deeply eroded parts of the arc are excluded from the tract. The Chatyrkul deposit in Kendyktas Ridge in Kazakhstan (544,200 t copper) and the Taldy-Bulak Talas deposit in the western Kyrgyz Mountains, Kyrgyzstan (1.5 Mt copper) lie within the tract.

Balkhash-Ili Magmatic Arc

Five tracts represent parts of the Late Paleozoic Balkhash-Ili magmatic arc; differences in levels of exposure, deformation, fault boundaries, and expected distributions

of deposits throughout the arc led to subdivisions of the arc into sub-tracts for assessment. Sub-tracts 142pCu8003a–d represent different limbs of the arc along the orocline; each sub-tract contains one or more known deposits. Tract 142pCu8004 represents a 100,000 km² area of permissive rocks, largely under Neogene and Quaternary cover, ringed by tract 142pCu8003a–d (fig. 3-1). No deposits are known within tract 142pCu8004.

Valerianov Magmatic Arc, Southern Urals

The Carboniferous to Permian magmatic-arc rocks referred to as the Valerianov volcano-plutonic arc in the southern Urals is interpreted to link to the south into the Bel'tau–Kurama Arc in Uzbekistan (Herrington and others, 2005; Plotinskaya and others, 2006; Windley and others, 2007). Tract 142pCu8005 delineates the eastern part of the Valerianov Arc, which hosts two porphyry copper deposits

Table 3-2. Permissive tracts for porphyry copper deposits in western Central Asia.[km², square kilometers. See tract map on figure 3.1.]

Coded_ID	Appendix	Tract name	Countries	Age	Geologic feature assessed	Tract area (km²)
142pCu8001	A	Chatkal and Kurama Ranges	Kazakhstan-Kyrgyzstan Tajikistan-Uzbekistan	Late Carboniferous-Permian	Late Carboniferous to Permian magmatic arc and post-collisional volcanic-plutonic complexes	25,100
142pCu8002	B	Ordovician North Tian Shan magmatic arc	Kazakhstan-Kyrgyzstan	Middle to Late Ordovician	Middle to Late Ordovician North Tian Shan magmatic-arc	8,140
142pCu8003a	C	Late Paleozoic Balkhash-Ili magmatic arc	Kazakhstan	Early Carboniferous-Permian	Early Carboniferous to Permian magmatic arc and post-collisional rocks	47,240
142pCu8003b	D	Late Paleozoic Balkhash-Ili magmatic arc	Kazakhstan	Early Carboniferous-Permian	Early Carboniferous to Permian magmatic arc and post-collisional rocks	79,040
142pCu8003c	E	Late Paleozoic Balkhash-Ili magmatic arc	Kazakhstan	Early Carboniferous-Permian	Early Carboniferous to Permian magmatic arc and post-collisional rocks	23,800
142pCu8003d	F	Late Paleozoic Balkhash-Ili magmatic arc	Kazakhstan-Kyrgyzstan	Early Carboniferous-Permian	Early Carboniferous to Permian magmatic arc and post-collisional rocks	112,150
142pCu8004	G	Late Paleozoic Central Balkhash-Ili magmatic arc	Kazakhstan	Late Carboniferous-Permian	Late Carboniferous to Permian magmatic-arc rocks	100,820
142pCu8005	H	Carboniferous Valerianov magmatic arc	Kazakhstan-Uzbekistan Russia	Carboniferous	Carboniferous Valerianov magmatic arc	213,240

(table 3-1) and a number of copper skarn and magnetite bodies. The more complex Trans Urals zone to the west of the tract was not assessed. See Herrington and others (2005) for a discussion of the metallogeny of the Urals.

Selection of Grade and Tonnage Models

The global grade and tonnage models for porphyry copper deposits from Singer and others (2008) were evaluated for use in the simulation of undiscovered resources. Available models include a global porphyry Cu-Au-Mo model based on data from 422 deposits, a Cu-Au subtype model based on data from 115 deposits, and a Cu-Mo subtype model based on data from 51 deposits. Grades and tonnages of deposits within the tracts were tested against global models using statistical tests (*t*-test or analysis of variance (ANOVA)). Table 3-3 summarizes the results of the testing of known deposits in each permissive tract or sub-tract against the global porphyry Cu-Au-Mo model. The tests indicated that this model is appropriate for the assessment of all the tracts. Graphical comparison of the distribution of tonnage and metal grades for all 18 known deposits in the Central Asia region with the deposits in the global model further supports the model selection (fig. 3-2).

The Assessment Process

The porphyry assessment of western Central Asia began with a preliminary workshop sponsored by the Centre for Russian and Central Eurasian Mineral Studies (CERCAMS) and the U.S. Geological Survey (USGS) in Almaty, Kazakhstan in 2004. USGS assessment participants attended CERCAMS workshops in 2007 and 2008 at the Natural History Museum, London, and an assessment workshop was held in conjunction with the CERCAMS 11 meeting in 2008. Further discussions with cooperators were held at a meeting at the USGS in Vancouver, Washington, in October 2009. Cooperators contributed expertise in regional geology, porphyry copper deposits, mineral deposits and mineral exploration and provided input on tract delineation at the workshops in Almaty, in London, and in Vancouver. Contributors presented talks at a session on “Copper in Central Eurasia and Russia: Linking Mineral Resource Assessment, Tectonics, and Metallogeny” at the 2009 Geological Society of America Annual Meeting in Portland, Oregon, which was held prior to the Vancouver assessment workshop⁶. The USGS was responsible for assessment methodology, including the probabilistic assessment. The estimates of undiscovered

deposits were done by the USGS in 2009 and 2010 following data compilation and evaluation. Assessment results were vetted by an internal USGS assessment review committee and modified prior to preparation of the final report.

Estimates of Numbers of Undiscovered Deposits

Prior to making estimates of numbers of undiscovered deposits, the assessment team first reviewed the geologic framework and aeromagnetic data with particular attention paid to the (1) correctness of the tract boundary with respect to depth of covered areas, (2) permissiveness of included rock formations, (3) the proportion of the mapped geologic units that are permissive and what proportion of these are intrusive, and (4) variations in the depth of exposure of the permissive rocks within the tract and whether or not the tract should be subdivided into several sub-tracts. Second, the assessment team discussed the known deposits and occurrences, discussed the distribution of the known deposits and occurrences, and evaluated the deposit type distribution as an indicator of depth of exposure in the arc terrane as well as what the distribution implied about the uniformity of the depth of exposure across the tract. Third, the team examined alteration information as interpreted from ASTER and Landsat satellite data and discussed the possible meaning and size of altered areas. Fourth, the team speculated on the likely thoroughness with which the region had been explored.

The assessors considered the available data and made individual, subjective estimates of the numbers of undiscovered porphyry copper deposits. Estimates are expressed in terms of different levels of certainty. Estimators are asked to indicate the least number of deposits of a given type that they believe could be present at three specified levels of certainty (90 percent, 50 percent, and 10 percent). For example, on the basis of all the available data, a team member might estimate that there was a 90-percent chance (or better) of at least 1; a 50-percent chance of at least 3; and a 10-percent chance of at least 5 undiscovered porphyry copper deposits in a permissive tract. Individual estimators used different strategies to arrive at estimates. Some estimators start with their mean expected number of deposits in mind and look for a distribution that captures that mean and uncertainty. Others consider the tract area and analogies with distributions of deposits in other settings that they are familiar with. Another strategy is to consider the number of prospects and exploration history of the tract, and the likelihood of prospects becoming deposits, if fully explored.

The individual estimates were recorded and then discussed as a group, and estimators were asked to elaborate on their rationale for their numbers. After discussion, a single team estimate was agreed upon for each tract. The estimates are converted to a mean number of deposits and standard deviation based on an algorithm developed by Singer and Menzie (2005). The algorithm can be described by the following general equations to calculate an expected (mean) number of deposits (λ) and a standard deviation (s_x) based on estimates of numbers

⁶Session abstracts are available online at https://gsa.confex.com/gsa/2009AM/finalprogram/session_23983.htm.

Table 3-3. Statistical test results, porphyry copper assessment, western Central Asia.

[Pooled *t*-test or analysis of variance (ANOVA) results assuming equal variances; $p > 0.01$ indicates that the deposits in the tract are not significantly different from those in the model at the 1-percent level; $p < 0.01$ would indicate that the deposits in the tract are significantly different from those in the model at the 1-percent level. See table 3-1 for data used in tests against models of Singer and others (2008). N_{known} , number of known porphyry copper deposits. Cu, copper; Mo, molybdenum; Ag, silver; Au, gold. n.d., no data]

Coded_ID	Tract name	N_{known}	Global porphyry Cu-Au-Mo model (p values)				
			Tons	Cu	Mo	Ag	Au
142pCu8001	Chatkal and Kurama Ranges	4	0.73	0.32	n.d.	0.92	0.37
142pCu8002	Ordovician North Tian Shan magmatic arc	2	0.96	0.82	0.68	n.d.	0.38
142pCu8003a	Late Paleozoic Balkhash-Ili magmatic arc	1	0.11	0.82	0.85	0.67	0.17
142pCu8003b	Late Paleozoic Balkhash-Ili magmatic arc	5	0.20	0.56	0.88	0.17	0.59
142pCu8003c	Late Paleozoic Balkhash-Ili magmatic arc	2	0.41	0.48	0.92	n.d.	0.15
142pCu8003d	Late Paleozoic Balkhash-Ili magmatic arc	2	0.71	0.77	0.55	0.23	n.d.
142pCu8005	Carboniferous Valerianov magmatic arc	2	0.85	0.55	0.17	0.1	0.57

of undiscovered deposits predicted at different quantile levels⁷ (N_{90} = 90 percent level, N_{50} = 50 percent level, etc.):

$$0.233 N_{90} + 0.4 N_{50} + 0.225 N_{10} + 0.045 N_{05} + 0.04 N_{01} \quad (1)$$

$$s_x = 0.121 - 0.237 N_{90} - 0.093 N_{50} + 0.183 N_{10} + 0.073 N_{05} + 0.123 N_{01} \quad (2)$$

These equations were programmed in a simple spreadsheet to allow the team to quickly evaluate estimates. The spread in the number of deposits associated with the 90th percentile to the 10th percentile or 1 percentile reflects uncertainty; large differences in number suggest great uncertainty. The expected number of deposits for the permissive tract, or the numbers associated with a given probability level, reflect favorability. Another useful parameter for reporting uncertainty associated with an estimate is the coefficient of variation (C_v), defined as:

$$C_v = s_x / \lambda \quad (3)$$

The coefficient of variation is often reported as percent relative variation:

$$\% C_v = 100 \times C_v \quad (4)$$

The rationales for individual tract estimates are discussed in the appendixes. In some cases, the number of significant porphyry copper prospects within a tract served as the primary basis for estimates at the 90th and 50th quantiles. Final (consensus) team estimates of undiscovered deposits

are summarized in table 3-4 along with statistics that describe expected (mean) numbers of undiscovered deposits, the standard deviation and coefficient of variation associated with the estimate, the number of known deposits, and the implied deposit density for each tract. The consensus estimate for a tract reflects both the uncertainty in what may exist and the favorability of the tract (Singer, 1993). The assessment predicts an expected (mean) total of 25 undiscovered porphyry copper deposits in the four tracts that were assessed, which is more than the number of known deposits (18) in the four assessed tracts.

The estimates are combined with appropriate grade and tonnage models in a Monte Carlo simulation using the EMINERS computer program (Bawiec and Spanski, 2012; Duval, 2012), based on the original Mark 3 computer program described by Root and others (1992), to provide probabilistic estimates of amounts of resources that could be associated with undiscovered deposits. No economic filters are applied, so results must be viewed with the realization that deposits, if discovered, might not be developed.

Summary of Probabilistic Assessment Results

The assessment indicates that 25 undiscovered deposits could be present in the eight permissive tracts that host 18 known porphyry copper deposits (table 3-4). Mean estimates of numbers of undiscovered deposits range from about 1 to 6, with coefficients of variation ranging from a low of 61 (relatively certain) to a high of 103 (relatively uncertain). Most of the undiscovered deposits (15) are associated with parts of the Late Paleozoic Balkash-Ili magmatic arc.

Mean estimated copper in undiscovered deposits, 95 Mt, represents almost twice the 54 Mt of copper in identified resources (table 3-5). Mean, median, and identified copper and gold resources are compared on a tract-by-tract basis in figure 3-3.

⁷To use the equation in cases where three non-zero quantiles (90-50-10) are estimated, use the N_{10} values for N_{05} and N_{01} ; where four quantiles (90-50-10-5) are estimated, use the N_{05} value for N_{01} .

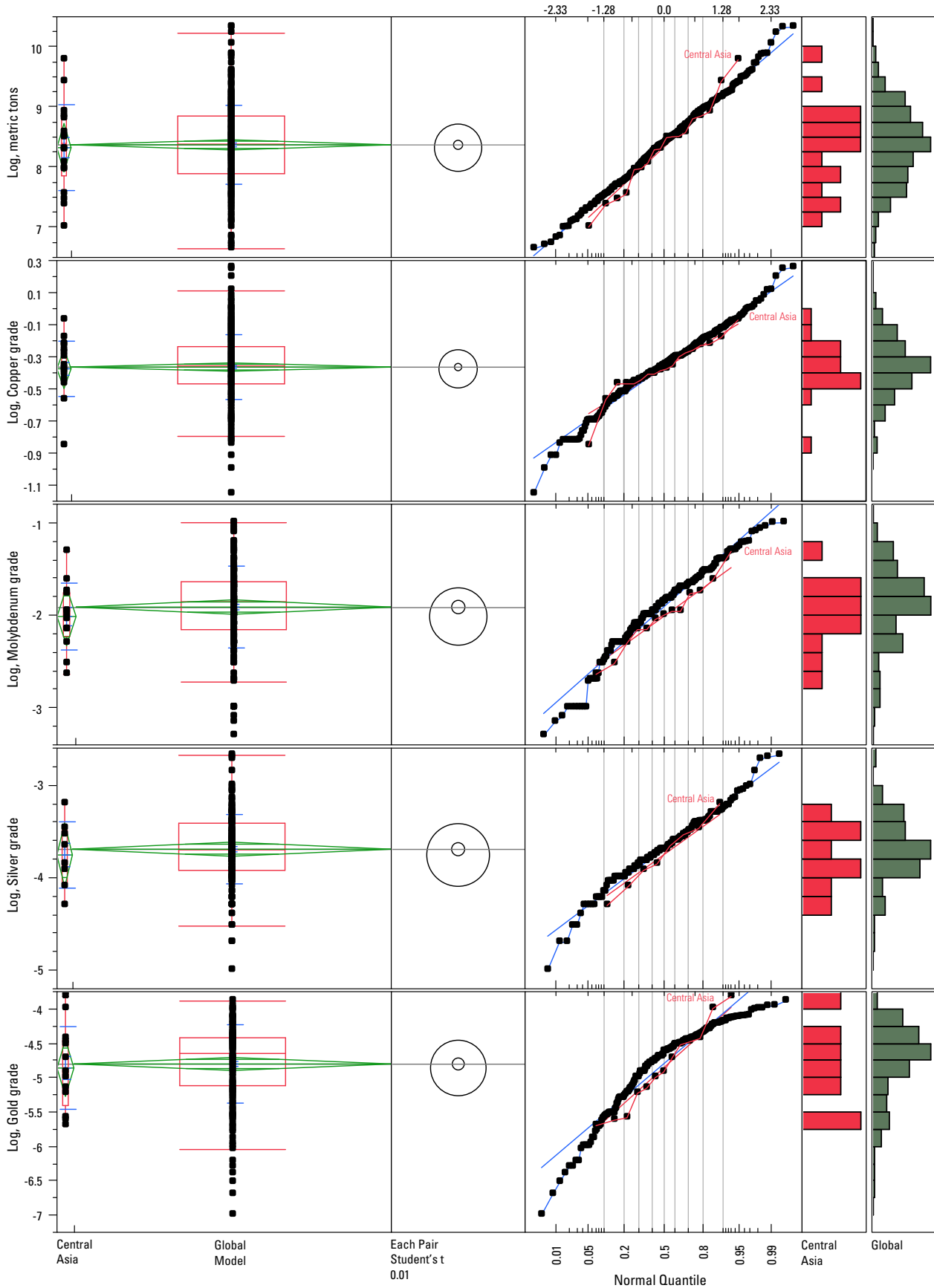


Figure 3-2. Distribution of log tonnage and log grade data for porphyry copper deposits in western Central Asia ($n=18$) compared with deposits in the global porphyry Cu-Au-Mo model of Singer and others (2008). Data are shown as box and whisker plots, Student's t -tests at the 99-percent confidence level, normal quantile plots, and histograms.

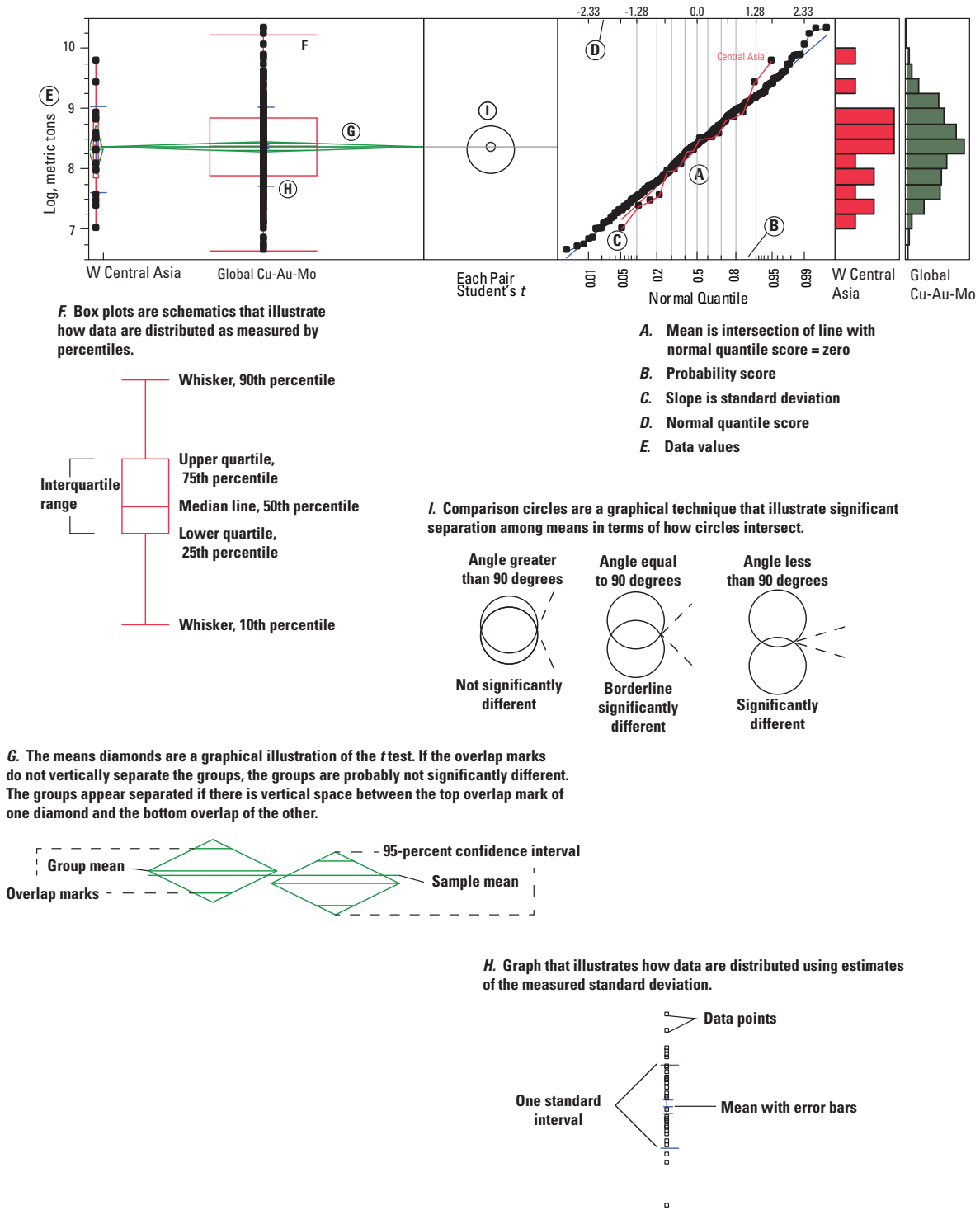


Figure 3-2.—Continued

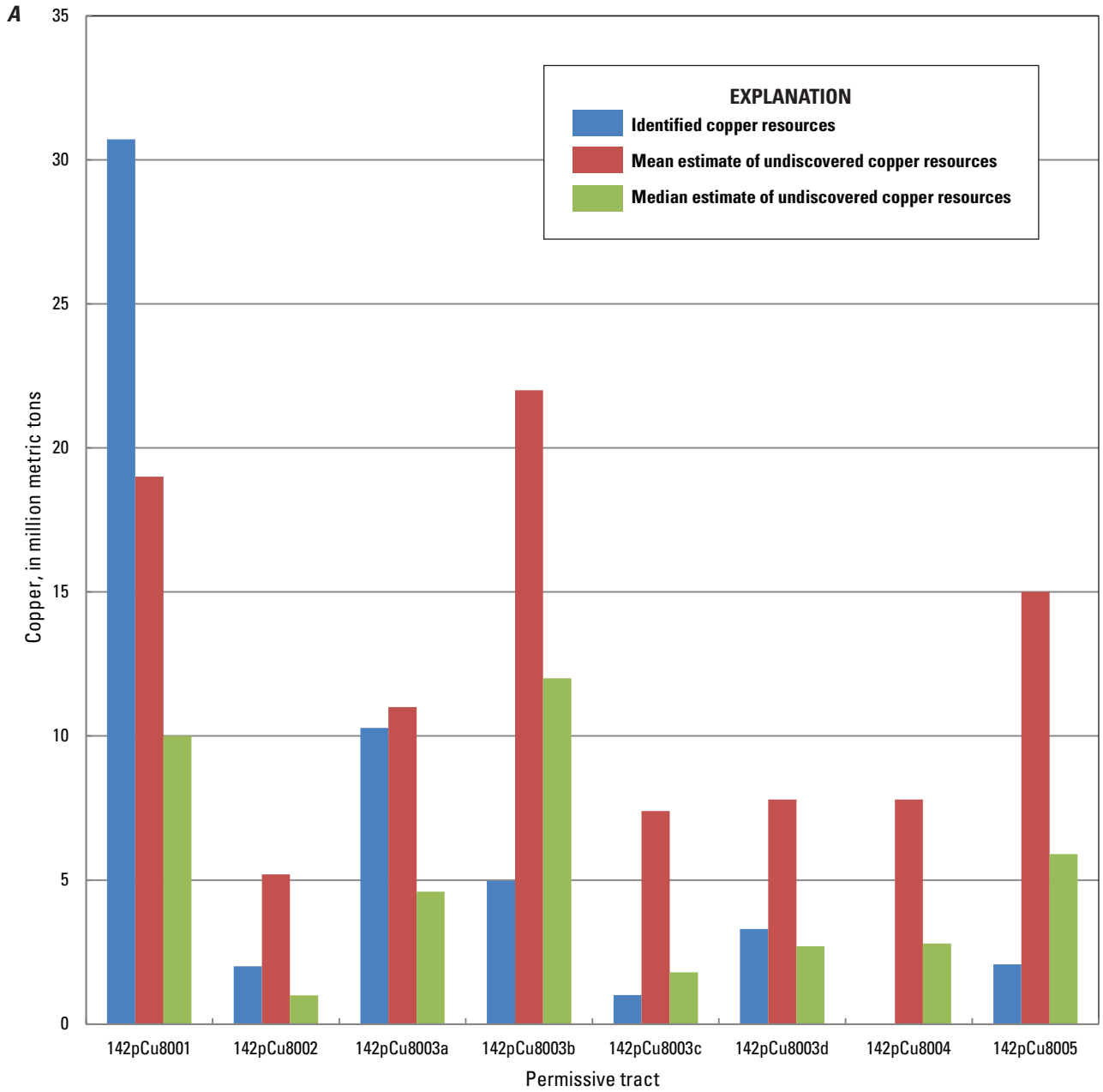


Figure 3-3. Bar charts comparing identified copper and gold resources in known deposits (table 3-1) with mean and median estimates of undiscovered resources (table 3.5) for each tract in western Central Asia. *A*, Copper. *B*, Gold.

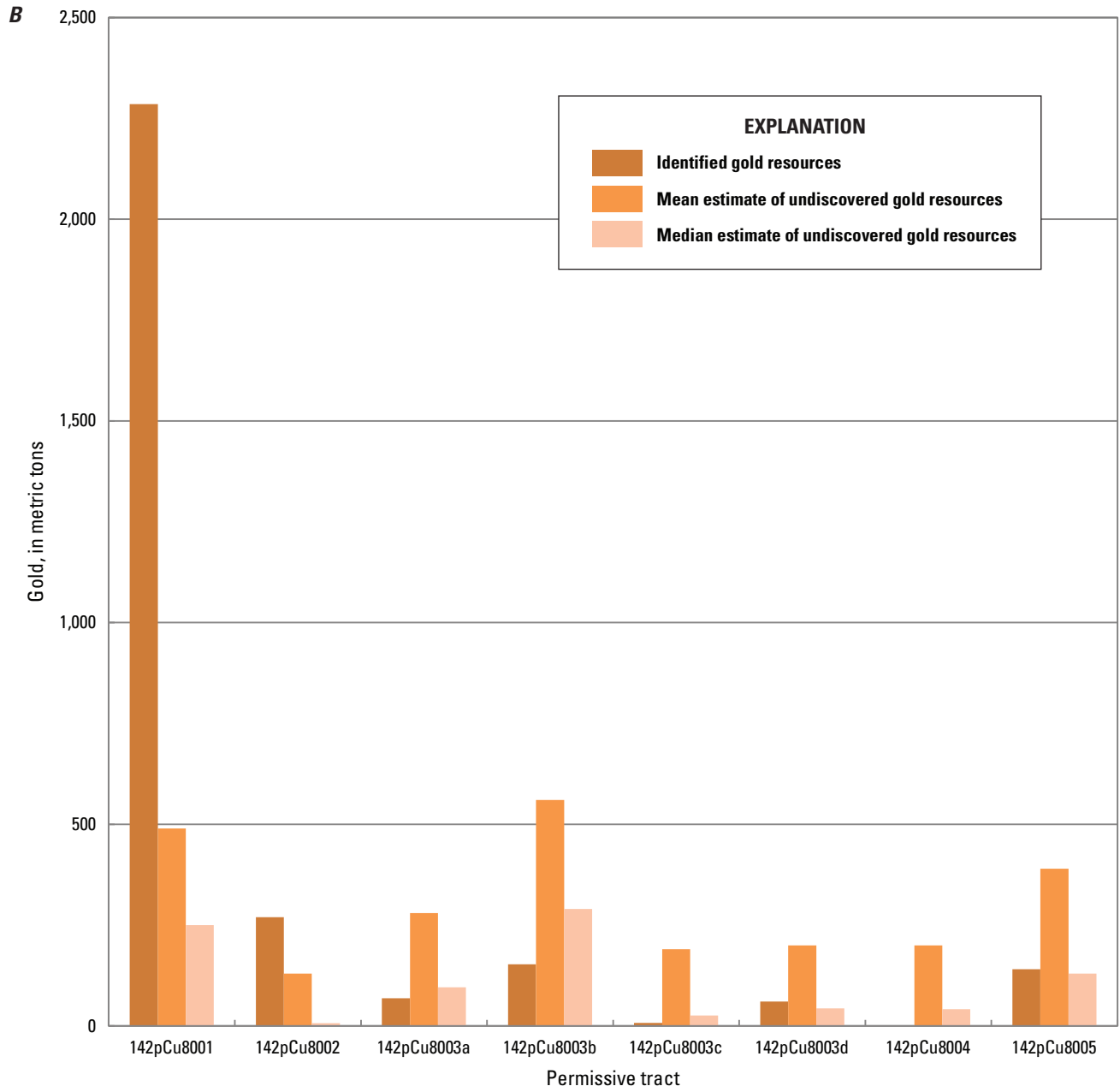


Figure 3-3.—Continued

Table 3-4. Summary of estimates of undiscovered deposits, numbers of known deposits, tract areas, and deposit densities for the porphyry copper assessments of western Central Asia.

[N_{xx} estimated number of deposits associated with the xxth percentile; N_{und} expected number of undiscovered deposits; s , standard deviation; C_v , coefficient of variance; N_{known} number of known deposits; N_{total} total of expected number of deposits plus known deposits; area, area of permissive tract in square kilometers (km^2); NA, not applicable; density, deposit density reported as the total number of deposits per 100,000 km^2]

Coded_ID	Tract name	Consensus estimates of numbers of undiscovered deposits							Summary statistics				Area (km^2)	Deposit density ($N_{total}/100k km^2$)
		N_{90}	N_{50}	N_{10}	N_{05}	N_{01}	N_{und}	s	C_v	N_{known}	N_{total}			
142pCu8001	Chatkal and Kurama Ranges	1	5	10	10	10	5.2	3.2	61	4	9.2	25,100	37	
142pCu8002	Ordovician North Tian Shan magmatic arc	0	1	3	3	3	1.3	1.2	90	2	3.3	8,140	41	
142pCu8003a	Late Paleozoic Balkhash-IIi magmatic arc	1	2	6	6	6	2.8	2	70	1	3.8	47,240	8	
142pCu8003b	Late Paleozoic Balkhash-IIi magmatic arc	1	5	12	12	12	5.8	4	68	5	10.8	79,040	14	
142pCu8003c	Late Paleozoic Balkhash-IIi magmatic arc	0	1	5	5	5	1.9	1.9	100	2	3.9	23,800	16	
142pCu8003d	Late Paleozoic Balkhash-IIi magmatic arc	0	2	4	4	4	2	1.5	73	2	4	112,150	4	
142pCu8004	Late Paleozoic Central Balkhash-IIi magmatic arc	0	2	4	4	4	2.1	1.6	79	0	2.1	100,820	2	
142pCu8005	Carboniferous Valerianov magmatic arc	0	3	8	15	15	4.1	4.25	103	2	6.1	213,240	3	
	Total	NA	NA	NA	NA	NA	25	NA	NA	18	43.2	609,530	NA	

Table 3-5. Summary of simulations of undiscovered resources in porphyry copper deposits and comparison with identified copper and gold resources in porphyry copper deposits within each permissive tract, western Central Asia.

[t, metric tons; Mt, million metric tons; *, rounded to 2 significant figures; NA, not applicable (only means are additive)]

Coded_Id	Tract name	Identified copper resources* (t)		Median estimate of undiscovered copper resources (t)		Identified gold resources* (t)		Mean estimate of undiscovered gold resources (t)		Median estimate of undiscovered gold resources (t)		Mean estimate of undiscovered silver resources (t)		Mean estimate of rock of rock (Mt)
		resources*	resources	estimate of undiscovered copper resources	resources (t)	resources (t)	resources (t)	estimate of undiscovered gold resources	resources (t)	estimate of undiscovered gold resources	resources (t)	estimate of undiscovered silver resources	resources (t)	
142pCu8001	Chatkal and Kurama Ranges	31,000,000	19,000,000	10,000,000	2,300	2,300	490	250	520,000	6,400	3,900	3,900		
142pCu8002	Ordovician North Tian Shan magmatic arc	2,000,000	5,200,000	1,000,000	270	270	130	7	140,000	1,600	1,000	1,000		
142pCu8003a	Late Paleozoic Balkhash-IIi magmatic arc	10,000,000	11,000,000	4,600,000	68	68	280	96	290,000	3,800	2,200	2,200		
142pCu8003b	Late Paleozoic Balkhash-IIi magmatic arc	5,000,000	22,000,000	12,000,000	150	150	560	290	590,000	6,900	4,500	4,500		
142pCu8003c	Late Paleozoic Balkhash-IIi magmatic arc	1,000,000	7,400,000	1,800,000	8	8	190	26	210,000	2,500	1,500	1,500		
142pCu8003d	Late Paleozoic Balkhash-IIi magmatic arc	3,300,000	7,800,000	2,700,000	61	61	200	44	220,000	2,400	1,600	1,600		
142pCu8004	Late Paleozoic Central Balkhash-IIi magmatic arc	7,800,000	7,800,000	2,800,000	0	0	200	42	210,000	2,500	1,600	1,600		
142pCu8005	Carboniferous Valerianov magmatic arc	2,000,000	15,000,000	5,900,000	120	120	390	130	410,000	5,200	3,000	3,000		
	Total	54,000,000	95,200,000	NA	3,000	3,000	2,440	NA	2,590,000	31,300	19,300	19,300		

Identified copper resources in the Chatkal and Kurama Ranges (tract 142pCu8001), dominated by the supergiant Almalyk deposit group, exceed estimated undiscovered resources within the tract. For all other tracts, mean estimated amounts of undiscovered copper equal or exceed identified resources (table 3-5). Many of the known deposits in the Balkash-Ili tract are covered by poorly consolidated sedimentary rocks of Quaternary or Neogene age. Parts of the Balkash-Ili tract that are largely covered may contain undiscovered deposits at depth. Mean estimated copper for sub-tracts c and d, as well as for 142pCu8004 which lacks identified resources, are all comparable (fig. 3-3A).

Mean estimates for other commodities that may be present in undiscovered porphyry copper deposits in the assessed area are as follows: 2,440 t of gold, 2.6 Mt of molybdenum, and 31,300 t of silver.

World production of copper (all deposit types) in 2010 was estimated at 16.2 Mt (Edelstein, 2011). Based on this figure, identified copper resources in porphyry copper deposits in the assessed tracts within the Central Asia study area represent about 3 years of global production; mean estimated undiscovered resources represent about 6 years of global production. Similarly, world production of gold in 2010 was estimated to be 2,500 t (George, 2011). The total identified gold resources in Central Asia porphyry copper deposits represent more than a year of global production; estimated mean gold resources in undiscovered porphyry copper deposits are comparable to annual global production (table 3-5). Note that significant porphyry copper deposits are present outside the assessed areas, such as the Bozshakol' deposit in the Cambrian Bozshakol'-Chingiz magmatic-arc terrane in northern Kazakhstan (see fig. 1-1).

As of 2001, the porphyry copper deposits at Almalyk, the main copper producer in Uzbekistan, had adequate copper reserves for 50 years, with byproduct selenium, tellurium, and indium (Levine and Wallace, 2010). Trends in rising gold and copper prices in recent years have resulted in renewed interest in exploration and development for porphyry copper deposits throughout the world, including western Central Asia.

Acknowledgments

Preliminary results of the assessment were evaluated by USGS assessment oversight committee members. Michael DeMarr assisted with figure preparation. The authors are grateful to Donald A. Singer (USGS emeritus) and Jamey Jones (USGS, Alaska Science Center) for their reviews of the assessment. Pam Cossette (USGS, Spokane) reviewed the GIS. Jeff Doebrich (USGS, Reston) served as coordinator for Central Asia and the Middle East at the beginning of the global assessment, established contacts with cooperators, and participated in the Almaty meeting. The authors are grateful to Kathleen Johnson (USGS, Reston) for her unwavering support for the project as USGS Mineral Resources Program coordinator.

References Cited

- Bawiec, W.J., and Spanski, G.T., 2012, Quick-start guide for version 3.0 of EMINERS—Economic Mineral Resource Simulator: U.S. Geological Survey Open-File Report 2009–1057, 26 p., accessed July 15, 2012, at <http://pubs.usgs.gov/of/2009/1057/>. (This report supplements USGS OFR 2004–1344.)
- Berger, B.R., Ayuso, R.A., Wynn, J.C., and Seal, R.R., 2008, Preliminary model of porphyry copper deposits: U.S. Geological Survey Open-File Report 2008–1321, 55 p., accessed May 15, 2009, at <http://pubs.usgs.gov/of/2008/1321/>.
- Blakely, R.J., 1995, Potential theory in gravity and magnetic applications: Cambridge, Cambridge University Press, 441 p.
- Blakely, R.J., and Simpson, R.W., 1986, Approximating edges of source bodies from magnetic or gravity anomalies: *Geophysics*, v. 51, no. 7, p. 1494–1498.
- Cordell, Lindrith, and Grauch, V.J.S., 1985, Mapping basement magnetization zones from aeromagnetic data in the San Juan basin, New Mexico, *in* Hinze, W.J., ed., *The utility of regional gravity and magnetic anomaly maps*: Society of Exploration Geophysicists, p.181–197.
- Cox, D.P., and Singer, D.A., eds., 1986, Mineral deposit models: U.S. Geological Survey Bulletin 1693, 379 p. (Also available at <http://pubs.usgs.gov/bul/b1693/>.)
- Duval, J.S., 2012, Version 3.0 of EMINERS—Economic Mineral Resource Simulator: U.S. Geological Survey Open-File Report 2004–1344, accessed July 15, 2012, at <http://pubs.usgs.gov/of/2004/1344/>.
- Edelstein, D.L., 2011, Copper [advance release], *in* Metals and minerals: U.S. Geological Survey Minerals Yearbook 2009, v. I, p. 20.1–20.29, accessed August 1, 2011, at <http://minerals.usgs.gov/minerals/pubs/commodity/copper/myb1-2009-coppe.pdf>.
- George, M.W., 2011, Gold, *in* Mineral commodity summaries: Reston, Va., U.S. Geological Survey, p. 66–67, accessed June 25, 2011, at <http://minerals.usgs.gov/minerals/pubs/commodity/gold/mcs-2011-gold.pdf>.
- Grauch, V.J.S., and Cordell, Lindrith, 1987, Limitations on determining density or magnetic boundaries from the horizontal gradient of gravity or pseudogravity data: *Geophysics*, v. 52, no. 1, p. 118–121.
- Herrington, R.J., Zaykov, V.V., Maslennikov, V.V., Brown, Dennis, and Puchkov, V.N., 2005, Mineral deposit of the Urals and links to geodynamic evolution, *in* Hedenquist, J.W., Thompson, J.F.H., Goldfarb, R.J., and Richards, J.P., eds., *Economic Geology: One-hundredth anniversary volume*, p. 1069–1095.

- Levine, R.M., and Wallace, G.J., 2010, Countries of the Baltic region (Estonia, Latvia, Lithuania), Caucasus region (Armenia, Azerbaijan, Georgia), Central Asia region (Kazakhstan, Kyrgyzstan, Tajikistan, Turkmenistan, Uzbekistan), and Eurasia region (Belarus, Moldova, Russia): U.S. Geological Survey 2008 Minerals Yearbook, p. 4.1–4.63, accessed August 15, 2011, <http://minerals.usgs.gov/minerals/pubs/country/europe.html>.
- National Geophysical Data Center, 1997, Magnetic Anomaly Data of the Former Soviet Union: National Geophysical Data Center CD-ROM.
- Petrov, O., Shatov, V., Kondian, O., Markov, K., Guriev, G., Seltmann, R., and Armstrong, R., 2006, Mineral deposits of the Urals, explanatory notes: Centre for Russian and Central EurAsian Mineral Studies (CERCAMS), Natural History Museum, London, 91 p.
- Plotinskaya, O. Yu., Kovalenker, V.A., Seltmann, R., and Stanley, C.J., 2006, Te and Se mineralogy of the high-sulfidation Kochbulak and Kairagach epithermal gold telluride deposits (Kurama Ridge, Middle Tien Shan, Uzbekistan): *Mineralogy and Petrology*, v. 87, p. 187–207.
- Root, D.H., Menzie, W.D., and Scott, W.A., 1992, Computer Monte Carlo simulation in quantitative resource estimation: *Natural Resources Research*, v. 1, no. 2, p. 125–138.
- Seltmann, R., Shatov, V., and Yakubchuk, A., 2009, Mineral deposits database and thematic maps of Central Asia—ArcGIS 9.2, Arc View 3.2, and MapInfo 6.0(7.0) GIS packages: London, Natural History Museum, Centre for Russian and Central EurAsian Mineral Studies (CERCAMS), scale 1:1,500,000, and explanatory text, 174 p. [Commercial dataset available at <http://www.nhm.ac.uk/research-curation/research/projects/cercams/products.html>.]
- Singer, D.A., 1993, Basic concepts in three-part quantitative assessments of undiscovered mineral resources: *Nonrenewable Resources*, v. 2, no. 2, p. 69–81.
- Singer, D.A., Berger, V.I., and Moring, B.C., 2008, Porphyry copper deposits of the World: U.S. Geological Survey Open-File Report 2008-1155, accessed June 10, 2010, at <http://pubs.usgs.gov/of/2008/1155/>.
- Singer, D.A., and Menzie, W.D., 2005, Statistical guides to estimating the number of undiscovered mineral deposits—An example with porphyry copper deposits, *in* Cheng, Qiuming, and Bonham-Carter, Graeme, eds., *Proceedings of IAMG—The annual conference of the International Association for Mathematical Geology*: Toronto, Canada, Geomatics Research Laboratory, York University, p. 1028–1033.
- Singer, D.A., and Menzie, W.D., 2010, *Quantitative mineral resource assessments—An integrated approach*: New York, Oxford University Press, 219 p.
- U.S. Department of State, 2009, Small-scale digital international land boundaries (SSIB)—Lines, edition 10, and polygons, beta edition 1, *in* *Boundaries and sovereignty encyclopedia (B.A.S.E.)*: U.S. Department of State, Office of the Geographer and Global Issues.
- Windley, B.F., Alexeiev, D., Xiao, W., Kröner, A., and Badarch, G., 2007, Tectonic models for accretion of the Central Asian orogenic belt: *Journal of the Geological Society of London*, v. 164, p. 31–47.
- Zhukov, N.M., Kolesnikov, V.V., Miroshnichenko, L.M., Egembayev, K.M., Pavlova, Z.N., and Bakarasov, 1998, *Copper deposits of Kazakhstan*: Ministry of Ecology and Natural Resources of the Republic of Kazakhstan, p. 99–102.

Appendixes A–K

Appendix A. Porphyry Copper Assessment for Tract 142pCu8001, Chatkal and Kurama Ranges—Uzbekistan, Kyrgyzstan, and Tajikistan

By Byron R. Berger¹, Paul D. Denning¹, Connie L. Dicken², Jane M. Hammarstrom², John C. Mars², Jeffrey D. Phillips¹, and Michael L. Zientek³

Deposit Type Assessed: Porphyry Copper

Descriptive model: Porphyry copper (Cox, 1986; Berger and others, 2008)

Grade and tonnage model: Global Cu-Au-Mo porphyry copper model (Singer and others, 2008)

Table A1 summarizes selected assessment results.

Table A1. Summary of selected resource assessment results for tract 142pCu8001, Chatkal and Kurama Ranges—Uzbekistan, Kyrgyzstan, and Tajikistan.

[km, kilometers; km², square kilometers; t, metric tons]

Date of assessment	Assessment depth (km)	Tract area (km ²)	Known copper resources (t)	Mean estimate of undiscovered copper resources (t)	Median estimate of undiscovered copper resources (t)
2009	1	25,100	30,715,000	19,000,000	10,000,000

Location

The tract is located in the Chatkal and Kurama ranges in eastern Uzbekistan, western Kyrgyzstan, and northwestern Tajikistan at the southwestern end of the Tian Shan mountain ranges (fig. A1). The area is located about 60 km southeast of Tashkent, Uzbekistan. Almalyk (lat 40.8° N., long 69.6° E.), Uzbekistan, is the largest city within permissive tract 142pCu8001.

Geologic Feature Assessed

The permissive tract encompasses Late Carboniferous to Permian magmatic-arc and postcollisional rocks (fig. A2) referred to variously as the Bel'tau–Kurama volcano-plutonic belt (Plotinskaya and others, 2006), the Zharna-Saur-Valerianov-Bel'tau-Kurama Arc (Yakubchuk, 2004), and the Chatkal-Kurama Arc (Windley and others, 2007). The name “Chatkal-Kurama Arc” is used in this report, but is inclusive of postcollisional volcanic-plutonic complexes (see fig. 1-22⁴).

¹U.S. Geological Survey, Denver, Colorado.

²U.S. Geological Survey, Reston, Virginia.

³U.S. Geological Survey, Spokane, Washington.

⁴Refer to chapter 1 of this report.

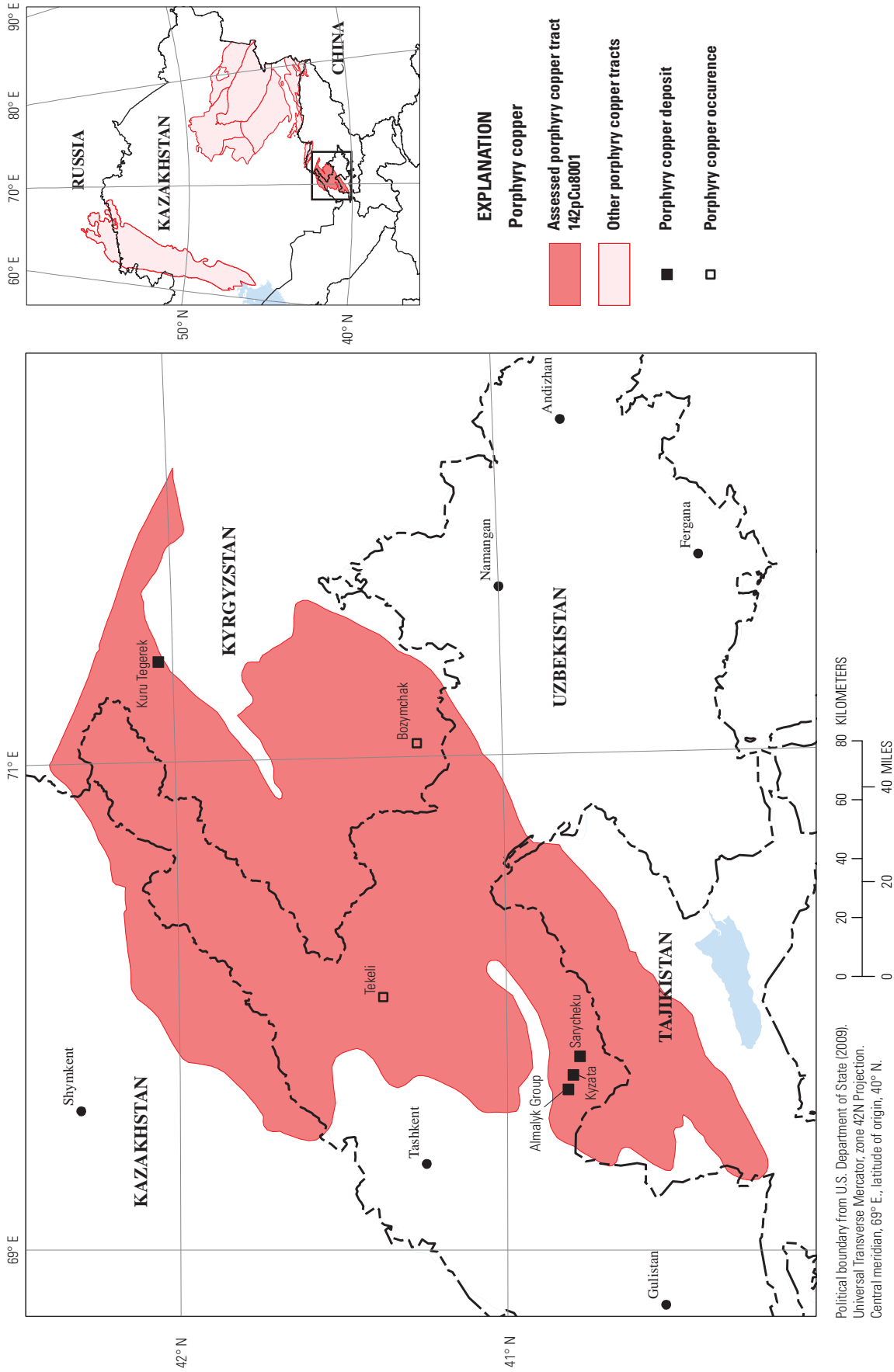


Figure A1. Map showing the location, known deposits, and significant prospects and occurrences for tract 142pCu8001, Chatkal and Kurama Ranges—Uzbekistan, Kyrgyzstan, and Tajikistan. Location of map area shown on inset.

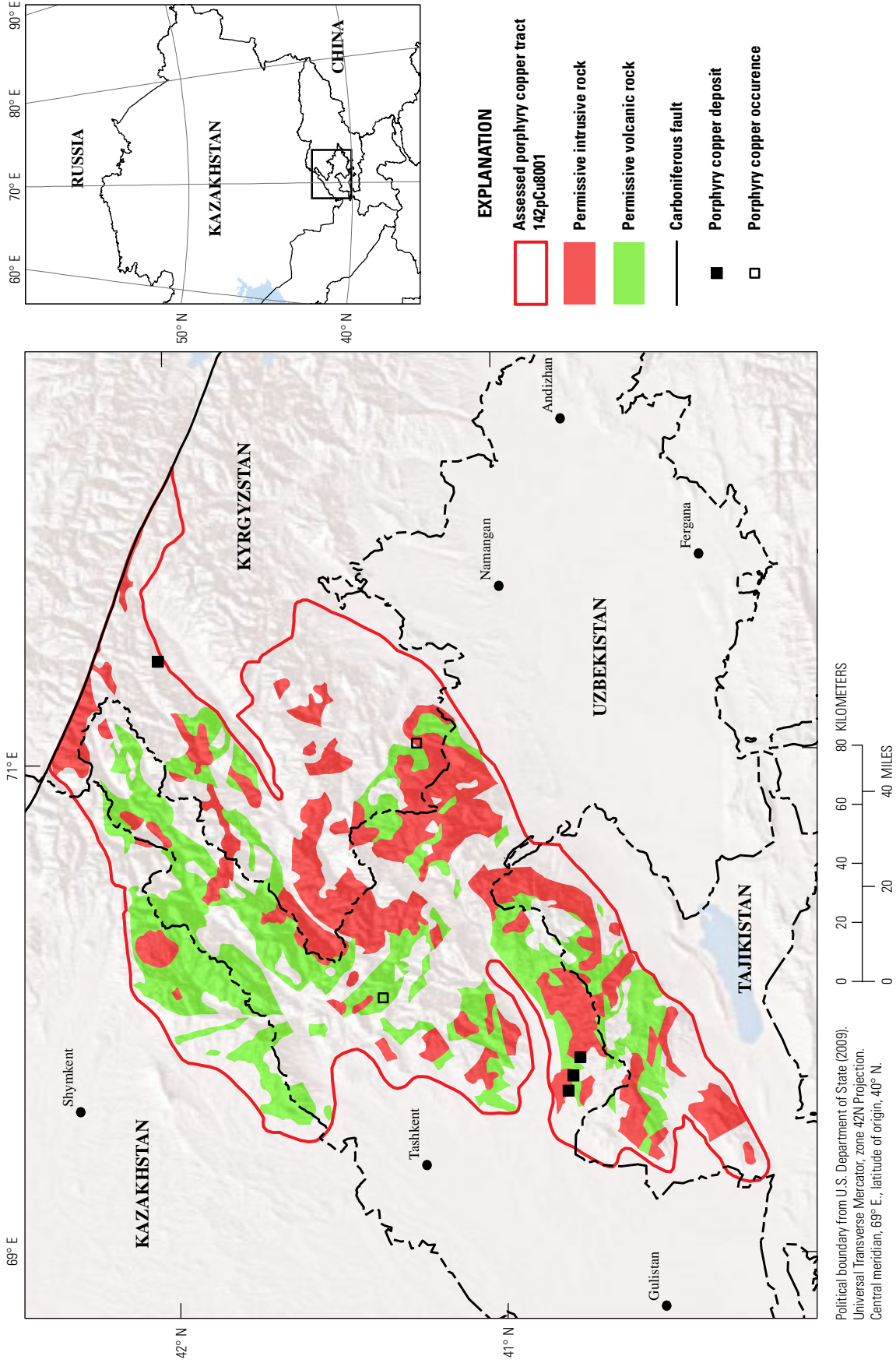


Figure A2. Map of permissive Carboniferous volcanic and volcanoclastic rocks (green) and intrusive (red) rocks in tract 142pCu8001, Chatkal and Kurama Ranges—Uzbekistan, Kyrgyzstan, and Tajikistan, on a digital elevation base. The northeast boundary of the tract is the Talas-Fergana Fault Zone.

Delineation of the Permissive Tract

Geologic Criteria

The principal litho-tectonic terrane concept used to delineate this tract was that of a magmatic arc that formed in the subduction boundary zone above a subducting plate. Four principal sources of information, supplemented by numerous published journal and symposium papers, were used to delineate this tract. The primary sources were the mineral deposits map of Central Asia on a geologic base edited by Seltmann and others (2009) and supplemented by 1:200,000-scale geologic maps originally published by the U.S.S.R. government, a reduced-to-pole aeromagnetic map prepared by J.D. Phillips from the Magnetic Anomaly Map of the World (Korhonen and others, 2007), the interpretation of Advanced Spaceborne Thermal Emission and Reflection Radiometer (ASTER) satellite imagery of hydrothermal alteration minerals or suites of minerals by J.C. Mars, and tectonic terrane maps published by Yakubchuk (2004) and Windley and others (2007).

Geographic and tectonic terminology commonly used in published papers regarding southern Central Asia can be confusing. “Tian Shan” is a term widely used to refer to the present-day high-standing, geomorphic block with many individual mountain ranges that extends across southern Central Asia from Uzbekistan to Northwest China. Geologically, the Tian Shan geomorphic unit is divided into three east-west-trending tectonic units: the North Tian Shan, Central Tian Shan, and South Tian Shan (see fig. 1-28). Each was a separate crustal terrane that became sutured together, first the South block to the Central block, and later the combined South and Central blocks to the North block. Suturing of the South and Central blocks occurred during a Late Devonian to Early Carboniferous collision event (Bullen and others, 2003). This composited terrane subsequently collided with the conjoined Kurama-Teresky–North Tian Shan block during the Late Carboniferous to Early Permian.

Central Asia is an amalgamation of Precambrian basement fragments, microcontinents, and overlying Paleozoic magmatic arcs (Windley and others, 2007) (see fig. 1-7). The permissive Late Carboniferous (C_3) to Permian (P_{1-2}) volcanic- and plutonic-rock complexes that make up the Chatkal-Kurama magmatic arc of southeastern Uzbekistan, southwestern Kyrgyzstan, and northwest Tajikistan were built on a base of Cambrian through Early Carboniferous rocks (C_1), predominantly sedimentary, although there was widespread Early to Middle Devonian andesitic volcanism (1:200,000-scale geologic maps of the U.S.S.R., sheets K-42-XVIII (Artemova and Kalabina, 1972), K-42-XXII (Artemova and others, 1958), K-42 XXIII (Doronkin and Makarov, 1974).

Tkachev (1969) defined two stages of magmatism in the permissive tract on the basis of composition and age. An early stage consisting predominantly of magmatic-arc-related

andesitic to dacitic volcanism was followed by a second stage of more siliceous and porphyritic magmas that may, in all or part, be postcollisional. The early stage began during the late Early Carboniferous (C_1^3) with interfingering of marine sedimentary and marine to nonmarine volcanic units that continued through the lower Middle Carboniferous (C_2^1). Andesitic to dacitic magmatism then predominated and lasted into the upper Late Carboniferous. During the uppermost Late Carboniferous (C_3^3), the second stage of magmatism ensued and continued through the Permian (P_{1-2}) and, perhaps, into the Lower Triassic (T).

Fault displacements and strikes and dips on the referenced maps indicate that the pre-magmatic-arc rocks were thrust faulted and folded prior to the beginning of uppermost Early Carboniferous magmatic-arc activity. Fault trends active during arc magmatism may be deduced from the orientation of pluton boundaries as inferred from geophysical data, dikes, and hydrothermal veins. Although dikes of many orientations occur in the arc-related intrusive complexes, the predominant trend is northeast-southwest. Using reduced-to-pole aeromagnetic data, the delineation of interpreted intrusive-rock boundaries shows them also to follow predominantly northeast-southwest trends that crosscut all older structures and fabrics in the pre-Chatkal-Kurama Arc rocks. Thus, taken together, the dike and magnetic lineaments indicate that a northeast-southwest structural grain dominated the localization of magmas in the first stage of volcanism. The style of faulting is not made clear on geologic maps, but Meshcheryakova (1960) documented synvolcanic, but pre-Late Carboniferous, vertical displacements on one east-west fault in the Kurama Range, the Bashtavak Fault near the Kal'makyr porphyry copper deposit, that are as much as 1 kilometer (km), and Late Carboniferous left lateral-oblique slip with vertical throws of 600–700 meters (m).

From published geologic information, closing of the Turkestan ocean basin on the south side of the arc and subsequent collision of the Tarim Plate does not appear to have severely deformed the Chatkal-Kurama Arc. Significant vertical displacements may have taken place across some faults that transect volcanic complexes, and this may mean that some domains within the permissive tract have differing favorableness although the availability of detailed geologic maps for the whole of the permissive tract limits our ability to thoroughly test the possibility. The principal deformation events were the (1) Permian suturing of the subduction-boundary terrane, including the arc along its southern boundary to the Middle Tian Shan (Windley and others, 2007) or Karakum (Yakubchuk, 2004) terrane, and (2) Alpine-age Cenozoic tectonism related to the collision of the Indian Plate with the Central Asian collage, deformation that continues to the present day. The Permian suture zone is typically drawn at a distance of 30 to 40 km or greater south of the permissive tract boundary (for example, Windley and others, 2007) and strikes east-northeast along the southern margin of the

Fergana Valley (see fig. 1-7). The trend of the suture zone is parallel to faults that were active during arc magmatism and that localized centers of volcanic eruptions as well as dikes of both stages of arc magmatism. Alpine-related tectonism occurred along the northwest-southeast-striking Talas-Fergana Fault (see fig. 1-28) that truncates the permissive rocks at the northeast end of the permissive tract (fig. A2). This fault zone is currently active (Trifonov and others, 1992). Some Alpine-age tectonism has been partitioned onto reactivated arc- and suture-related faults in the permissive tract. Near the Talas-Fergana Fault, arc-related northeast-striking faults are dragged into northwest-southeast orientations by right-lateral displacement along the fault zone. In the Kurama Range near the western end of the permissive tract, Meshcheryakova (1960) attributed the brecciation of altered rocks and quartz veins along east-west faults to Alpine stresses, and the sense of displacement appears to be right-lateral-reverse with vertical throws of as much as several hundred meters.

Tract Delineation

The tract was delineated in two stages. First, a preliminary delineation of the tract boundary was based on a combined analysis of different types of geologic information: (1) Using lithotectonic terrane boundaries in Windley and others (2007) as a guide, digitized and digital image geologic maps in GIS format were used to identify areas within which Late Carboniferous to Permian arc-related volcanic and intrusive rocks occur (fig. A2). Lithologies and ages were used as selection criteria, not formal geologic names. (2) Terrains with postpermissive rocks were analyzed for unexposed extensions of permissive rocks using geologic cross-sections and reduced-to-pole aeromagnetic data interpretations. (3) Geologic cross-sections were used to determine the 1-km depth cutoff for permissive rocks, with permissive rocks deeper than that not included in the permissive tract. (4) Mines and mineral occurrence maps and published reports were used to discriminate permissive arc and nonpermissive postarc volcano-plutonic complexes wherever possible. (5) Interpreted hydrothermal alteration maps derived from Landsat and ASTER satellite data were used to identify areas outside of permissive rocks that might conceal permissive rocks. Finally, (6) anecdotal information obtained from geologists with on-the-ground experience, published minerals exploration reports, and data and information posted on the Internet were used to refine boundaries where appropriate. The second stage was to review and revise the preliminary tract boundaries in a workshop format with experts drawn from other countries and international mining companies.

Using the various sources of information available, numerous decisions were made in the course of drawing the peripheral boundary of the tract outside of which the probability of an undiscovered porphyry copper deposit is considered negligible (less than or equal to 1:100,000 chances). The following paragraph summarizes some of the

decisions made, beginning at the southwesternmost tip of the Kurama Range and progressing clockwise around the periphery of the tract.

Permissive rocks at the southwestern tip of the Kurama Range are covered to the west by nonpermissive Quaternary and younger deposits. Because Carboniferous and Permian intrusive rocks are mapped to the Quaternary contact and a large number of copper and other base-metal-containing deposits are present at this end of the range, the margin of the permissive tract is drawn where the thickness of the Cenozoic rocks is judged to exceed 1 km. The tract margin, an approximation based on geologic cross sections, is placed about 2 km away from the outcropping permissive rocks. The tract boundary swings east up the Angren Valley, through which the Akhanghagan River flows, owing to an average thickness of 1 km of Mesozoic through Neogene rocks in the valley. The north side of the Angren Valley is the Chatkal Range. To the northwest of the Angren Valley around the west margin of the Chatkal Range, geologic cross sections indicate that, where mapped, the Cenozoic rocks are approximately 1 km thick, so the boundary was drawn close to the Cenozoic-pre-Cenozoic contact along the length of the western margin of the tract. The northwest boundary of the tract is problematic. A fault zone that localizes a string of mercury deposits is interpreted as a significant tectonic boundary separating two disparate terranes, the Carboniferous arc to the southeast and a terrane with Mississippi Valley type deposits to the northwest. Postcollisional intrusive complexes occur in both terranes, so are not useful for establishing the boundary of the permissive tract. Thus, the mercury deposit-localizing fault zone was chosen as the tract boundary and it was followed east-northeast to the Talas-Fergana strike-slip fault zone. At the Talas-Fergana Fault Zone, the tract boundary follows this zone to the southeast to the interpreted location of the North Tian Shan/Middle Tian Shan suture zone. Through a combination of following aeromagnetic lineaments and geologic contacts, the tract boundary follows the suture zone to the southwest along the southern margin of the Chatkal-Kurama ranges.

Known Deposits

Four known porphyry copper deposits occur in this tract (fig. A1, table A2), Almalyk, Kyzata, and Sarycheku in Uzbekistan and Kuru Tegerek in Kyrgyzstan. Almalyk is near the city of Almalyk. Kyzata is about 12 km east-southeast of Almalyk city, and Sarycheku deposit is about 18 km southeast of Almalyk city.

Almalyk, as used herein, is a general reference to five discrete porphyry copper deposits (shown as the Almalyk Group on fig. A1) the alteration haloes of which are not separated by 2 km or more (compare with Korolev and Badalov, 1959; Movesian and Isaenko, 1974) and are thus grouped as a single deposit for assessment purposes. The individual mines are Kal'makyr ("Bolshoi"), Kal'makyr ("Maly"), Dal'nee (referred to as "Central" in Shayakubov and

Table A2. Porphyry copper deposits in tract 142pCu8001, Chatkal and Kurama Ranges—Uzbekistan, Kyrgyzstan, and Tajikistan.

[Data for grouped deposits in boldface. Ma, mega-annum (10^6 years); km², square kilometers; t, metric tons; Mt, million metric tons, %, percent; g/t, grams per metric ton; Cu, copper; Mo, molybdenum; Au, gold; and Ag, silver; n.d., no data; NA, not applicable]

Name	Deposits included	Latitude	Longitude	Subtype	Age (Ma)	Tonnage (Mt)	Cu (%)	Mo (%)	Au (g/t)	Ag (g/t)	Contained Cu (t)	Reference
Almalyk Group	Amalyk	40.814	69.646	Cu-Au	289.5	6,080	0.39	0.0023	0.37	2.2	23,712,000	Golovanov (1978), Golovanov and others (2005), Krivtsov and others (1986), Meshchaninov and Azin (1973), Pavlova (1978), Zvezdov and others (1993)
	Kal'makyr (Bolshoi and Maly)	40.817	69.641									Singer and others (2008), Seltmann and others (2009)
	Dal'nee	40.816	69.612									Seltmann and others (2009)
	Karabulak	40.834	69.631									Singer and others (2008), Seltmann and others (2009)
	Northwest Balikti	40.797	69.635									Seltmann and others (2009)
Kyzata	NA	40.799	69.705	NA	289.5	700	0.85	n.d.	n.d.	n.d.	5,950,000	Sokolov (1999), Zvezdov and Migachev (1986), Zvezdov and others (1987, 1993)
Kuru Tegerek	NA	42.044	71.412	Cu-Au	n.d.	10	0.53	n.d.	1.51	n.d.	53,000	Seltmann and others (2009)
Sarycheku	NA	40.778	69.779	NA	289.5	200	0.5	n.d.	0.1	n.d.	1,000,000	Golovanov (1978), Golovanov and others (2005), Krivtsov and others (1986), Zvezdov and others (1993)

others, 1999), Karabulak, and Northwest Balikti. Kal'makyr (Bolshoi) is the largest locus of ore among the centers of porphyry-style mineralization in the combined Almalyk Group deposit. Stockwork and disseminated ore mineralization is in a Late Carboniferous to Early Permian granodiorite porphyry intrusive complex that intruded a mid-Carboniferous monzonite–syeno-diorite intrusive complex (K-42-XXVIII). Postmineralization faulting along the east-westerly striking, 75°–85° south-dipping Kal'makyr Fault separated the locus of ore into two blocks, “small” Kal'makyr and Dal'nee to the north of the fault and “large” Kal'makyr to the south of the fault (Korolev and Badalov, 1959; Meshchaninov and Azin, 1973).

Sarycheku is 15–20 km southeast of Amalyk, and Kyzata is 5–10 km to its east. Zvezdov and others (1993) suggest that the Sarycheku and Kyzata deposits in the Saukbulak ore field originally may have been a single deposit now offset sufficiently far, 6–8 km along the Miskan Fault, to constitute two separate deposits in this assessment.

Kuru Tegerek, Kyrgyzstan, is in the Chatkal Valley approximately 300 km south-southwest of Bishkek, Kyrgyzstan. Discovered in the 1960s, copper-gold skarn ores have been delineated in Lower Carboniferous limestone at the contact of Carboniferous quartz diorite porphyry, although no ores have been produced (Arne, 2004).

Porphyry Copper Occurrences and Related Deposit Types

The tract hosts porphyry copper and copper-gold skarn occurrences (table A3).

Bozymchak is a copper-gold skarn developed in Lower Carboniferous limestones along the contact of Middle Carboniferous granodiorites and diorites (U.N. Economic and Social Commission for Asia and the Pacific, 2000). Kazakhmys PLC (2011) was developing the skarn for copper and gold production to begin in 2012 as an open pit mine; construction of an underground mine is scheduled for 2014.

Tekeli is an occurrence northeast of Almalyk, Uzbekistan, in the Chatkal Range. Lower to middle Carboniferous volcanic rocks consisting of dacitic tuffs, andesite and dacite lavas, and volcanogenic sedimentary deposits are intruded by a composite diorite to syenitic igneous complex with disseminated and stockwork mineralization (Golovanov, 1978).

Hydrothermal Alteration Mapping (ASTER)⁵

Approximately 95 percent of tract 142pCu8001 is covered by argillic and phyllic ASTER hydrothermal alteration mapping and approximately 40 percent is covered

by silicic ASTER hydrothermal alteration mapping (see figs. 2-1 and 2-2). Using the ASTER argillic, phyllic, and silicic hydrothermal alteration map, 59 potential deposit sites were identified based on alteration patterns that were similar to known economic deposits (see fig. 2-3 and plates 1–8). Most of the sites (55) are located in the central and southwestern parts of the tract (see fig. 2-3). Four potential deposit sites are located in the northern part of the tract (see fig. 2-3). The mineral databases indicate that fifteen sites are associated with copper mineralization of which there are 5 deposits and 10 occurrences (table 2-1, Seltmann and others, 2009; Singer and others, 2008). The 1:1,000,000-scale geologic map indicates that granodiorite, andesite-dacite, trachyandesite-dacite, and rhyolite are the most common rock types associated with potential deposit sites and sites that contain copper-mineralized rocks (see table 2-1).

Sites 206 and 207 in Almalyk are associated with developed porphyry copper deposits; these sites were selected for matching potential deposit sites with similar physical alteration characteristics (see table 2-1 and plates 1–8; Seltmann and others, 2009; Singer and others, 2008). Physical characteristics from sites 206 and 207 that were used to identify other potential deposit sites with similar alteration characteristics include size diameter greater than or equal to 2.5 km, argillic and phyllic alteration density greater than 3.9, and a greater than 89 percent phyllic alteration cover. The GIS database matched 34 potential deposit sites with physical characteristics similar to those at sites 206 and 207 (see table 2-1). All but one of the 34 sites are in the central and southwestern parts of tract 142pCu8001 (see plates 5–8). The ASTER hydrothermal alteration map and mineral databases show that 6 of the sites with similar alteration characteristics to sites 206 and 207 are associated with known copper deposits, and 2 sites are associated with copper occurrences (see table 2-1 and plates 5–8; Seltmann and others, 2009; Singer and others, 2008).

Exploration History

The exploration history of the tract region was not documented.

Sources of Information

Principal sources of information used by the assessment team for delineation of 142pCu8001 are listed in table A4.

⁵Refer to figures, tables, and plates in chapter 2 of this report.

Table A3. Significant occurrences of porphyry copper and copper-gold skarn in tract 142pCu8001, Chatkal and Kurama Ranges—Uzbekistan, Kyrgyzstan, and Tajikistan.

[Ma, mega-annum (10^6 years); t, metric tons; Mt, million metric tons, %, percent; g/t, grams per metric ton; m, meters; km², square kilometers; Cu, copper; Mo, molybdenum; Au, gold; Ag, silver; n.d., no data]

Name	Country	Latitude	Longitude	Age (Ma)	Comments	Reference
Bozymchak	Kyrgyzstan	41.262	71.054	n.d.	Skarn lens (garnet-wollastonite-pyroxene); 2,000 m long, average thickness 27 m; traced to depth of 500 m; along contact of granodiorites and diorites (Middle Carboniferous) with Lower Carboniferous limestones. Grade: 1.14% Cu, 1.96 g/t Au, 13.2 g/t Ag. Tonnage: 203,000 t Cu.	U.N. Economic and Social Commission for Asia and the Pacific (1998)
Tekeli	Uzbekistan	41.377	70.027	295	Ore-bearing stock, 6 km ² , exposed from 1,700 m to 2,450 m elevation; 0.002–8% Cu, 0.001–0.3% Mo. Location: Possible trenching, some roads on Google Earth (3/2/10) close to CERCAMS location (Seltmann and others, 2009)	Golovanov (1978), Seltmann and others (2009)

Table A4. Principal sources of information used in the assessment of tract 142pCu8001, Chatkal and Kurama Ranges—Kazakhstan, Uzbekistan, Kyrgyzstan, and Tajikistan.

Theme	Name or title	Scale	Citation
Geology	Mineral deposits database and thematic maps of Central Asia	1:1,500,000	Seltmann and others (2009)
	Tectonic map of the Paleozoic folded areas of Kazakhstan and adjacent territories	1:1,500,000	Abduln and Zaitseb (1976)
	K-42-XXII (1958)	1:200,000	Artemova and others (1958)
	K-42 XXIII (1974)	1:200,000	Doronkin and Makarov (1974)
	K-42-XXVIII (1972)	1:200,000	Artemova and Kalabina (1972)
	K-43-XIII (1963)	1:200,000	Medvedev and Kislyakova (1963)
Mineral occurrences	Mineral deposits database and thematic maps of Central Asia	1:1,500,000	Seltmann and others (2009)
Geophysics	Magnetic anomaly data of the former U.S.S.R.	1:1,500,000	National Oceanic and Atmospheric Administration (1996)

Grade and Tonnage Model Selection

The general porphyry copper deposit model published by Singer and others (2008) was used on the basis of known deposits in the tract being statistically consistent with the model.

Estimate of the Number of Undiscovered Deposits

Rationale for the Estimate

Following discussion and evaluation of the available data, the assessment team consensus was that (1) there was no basis for subdividing the Chatkal-Kurama Range into sub-tracts, (2) the ratio of porphyry copper occurrences and possible linked deposit types to the number of known deposits was high and therefore a favorable indication of undiscovered deposits, (3) the depth of erosion of the terrane was not a concern, and (4) owing to the rugged terrain and remoteness of much of the area, there were many plays left despite considerable Soviet-era exploration investment in the region.

On the basis of these considerations and the occurrence of four known porphyry copper deposits and two prospect areas within the tract, the team estimated a 90-percent chance of 1 or more deposits, a 50-percent chance of 5 or more deposits and a 10-percent chance of 10 or more deposits, for a mean of 5 undiscovered deposits (table A5).

Probabilistic Assessment Simulation Results

Undiscovered resources for the tract were estimated by combining consensus estimates for numbers of undiscovered porphyry copper deposits with the global grade and tonnage model for porphyry Cu-Au-Mo deposits of Singer and others (2008) using the EMINERS program (Root and others, 1992; Bawiec and Spanski, 2012; Duval, 2012). Selected simulation results are reported in table A6. Results of the Monte Carlo simulation are presented as a cumulative frequency plot (fig. A3). The cumulative frequency plot shows the estimated resource amounts associated with cumulative probabilities of occurrence, as well as the mean, for each commodity and for total mineralized rock.

Table A5. Undiscovered deposit estimates, deposit numbers, tract area, and deposit density for tract 142pCu8001, Chatkal and Kurama Ranges—Uzbekistan, Kyrgyzstan, and Tajikistan.

[N_{xx} , estimated number of deposits associated with the xxth percentile; N_{und} , expected number of undiscovered deposits; s , standard deviation; $C_v\%$, coefficient of variance; N_{known} , number of known deposits in the tract that are included in the grade and tonnage model; N_{total} , total of expected number of deposits plus known deposits; area, area of permissive tract in square kilometers (km^2); density, deposit density reported as the total number of deposits per 100,000 km^2 . N_{und} , s , and $C_v\%$ are calculated using a regression equation (Singer and Menzie, 2005)]

Consensus undiscovered deposit estimates					Summary statistics					Tract area (km^2)	Deposit density ($N_{total}/100\text{k km}^2$)
N_{90}	N_{50}	N_{10}	N_{05}	N_{01}	N_{und}	s	$C_v\%$	N_{known}	N_{total}		
1	5	10	10	10	5.2	3.2	61	4	9.2	25,100	37.0000

Table A6. Results of Monte Carlo simulations of undiscovered resources for tract 142pCu8001, Chatkal and Kurama Ranges—Uzbekistan, Kyrgyzstan, and Tajikistan.

[Cu, copper; Mo, molybdenum; Au, gold; and Ag, silver; in metric tons. Rock, in million metric tons]

Material	Probability of at least the indicated amount						Probability of	
	0.95	0.9	0.5	0.1	0.05	Mean	Mean or greater	None
Cu	0	460,000	10,000,000	45,000,000	72,000,000	19,000,000	0.3	0.07
Mo	0	0	180,000	1,300,000	2,100,000	520,000	0.25	0.14
Au	0	0	250	1,200	1,700	490	0.31	0.13
Ag	0	0	1,900	15,000	27,000	6,400	0.24	0.2
Rock	0	110	2,300	9,200	15,000	3,900	0.32	0.07

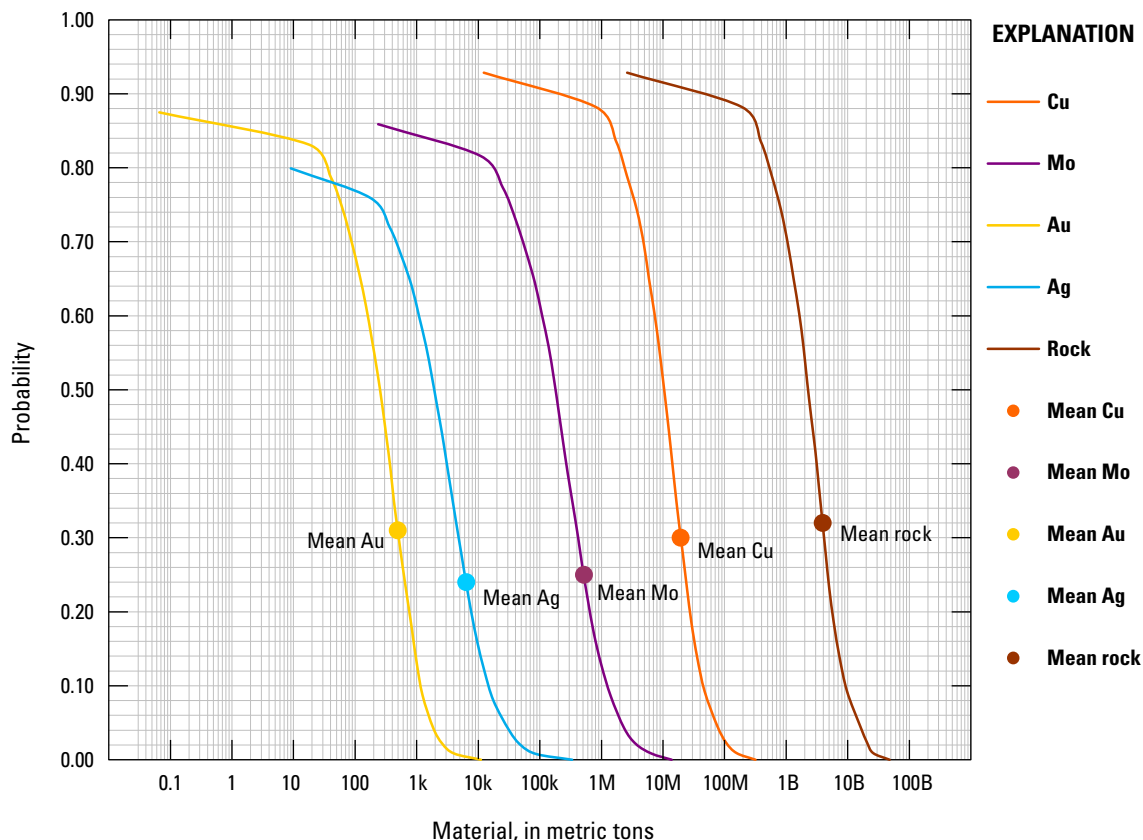


Figure A3. Cumulative frequency plot showing the results of Monte Carlo computer simulation of undiscovered resources, tract 142pCu8001, Chatkal and Kurama Ranges—Uzbekistan, Kyrgyzstan, and Tajikistan. k=thousands, M=millions, B=billions.

References Cited

- Abdulin, A.A., and Zaitseb, Yu. A., eds., 1976, [Tectonic map of the Paleozoic folded belts of Kazakhstan and adjacent territories]: Ministry of Geology of the U.S.S.R., VSEGEI, 1 map on 6 sheets, scale 1:1,500,000. [In Russian.]
- Arne, K.G., 2004, Kuru Tegerek copper-gold property, Chatkal Valley, Kyrgyz Republic: Behre Dolbear & Company, Kuru Tegerek Project NI-43-101 Technical Report, prepared for Eurasian Minerals Inc. and Altyn Minerals, Ltd., 104 p. (Also available at <http://www.sedar.com>.)
- Artemova, Z.P., Belen'ki, G.A., and Vasil'kovski, N.P., 1958, [Geological map of the U.S.S.R., Tashkent series, Sheet K-42-XXII]: Ministry of Geology and Mineral Resources Protection of the U.S.S.R., Main Management of Geology and Mineral Resources Protection of Uzbek S.S.R., scale 1:200,000. [In Russian.]
- Artemova, Z.P., and Kalabina, M.G., 1972, [Geological map of the U.S.S.R., Pritashkeniskaya Series, Sheet K-42-XXVIII]: Ministry of Geology of the U.S.S.R., scale 1:200,000. [In Russian.]
- Bawiec, W.J., and Spanski, G.T., 2012, Quick-start guide for version 3.0 of EMINERS—Economic Mineral Resource Simulator: U.S. Geological Survey Open-File Report 2009-1057, 26 p., accessed July 15, 2012, at <http://pubs.usgs.gov/of/2009/1057/>. (This report supplements USGS OFR 2004-1344.)
- Berger, B.R., Ayuso, R.A., Wynn, J.C., and Seal, R.R., 2008, Preliminary model of porphyry copper deposits: U.S. Geological Survey Open-File Report 2008-1321, 55 p., accessed May 15, 2009, at <http://pubs.usgs.gov/of/2008/1321/>.
- Bullen, M.E., Burbank, D.W., and Garver, J.I., 2003, Building the northern Tien Shan—Integrated thermal, structural, and topographic constraints: *The Journal of Geology*, v. 111, p. 149–165.
- Cox, D.P., 1986, Descriptive model of porphyry Cu (Model 17), in Cox, D.P., and Singer, D.A., eds., 1986, Mineral deposit models: U.S. Geological Survey Bulletin 1693, p. 76. (Also available at <http://pubs.usgs.gov/bul/b1693/>.)

- Doronkin, I.D., and Makarov, A.S., 1974, [Geological map of the U.S.S.R., Tashkent series, Sheet K-42-XXIII]: Ministry of Geology of the U.S.S.R., scale 1:200,000. [In Russian.]
- Duval, J.S., 2012, Version 3.0 of EMINERS—Economic Mineral Resource Simulator: U.S. Geological Survey Open-File Report 2004–1344, accessed July 15, 2012, at <http://pubs.usgs.gov/of/2004/1344/>.
- Golovanov, I.M., 1978, [Copper mineralization in the western Tian Shan]: Tashkent, Fan, 239 p. [In Russian.]
- Golovanov, I.M., Seltmann, R., and Kremenetsky, A.A., 2005, The porphyry Cu-Au/Mo deposits of central Eurasia. 2. The Almalyk (Kal'makyr-Dalnee) and Saukbulak Cu-Au porphyry systems, Uzbekistan, *in* Porter, T.M., ed., Superporphyry copper and gold deposits—A global perspective: Adelaide, PGC Publishing, v. 2, p. 513–523.
- Kazakhmys PLC, 2011, Kazakhmys PLC half-yearly report for the period ended 30 June 2011: Kazakhmys Web page, accessed November 1, 2011, at http://www.kazakhmys.com/en/investors_media/investor_library.
- Korhonen, J.V., Fairhead, J.D., Hamoudi, M., Hemant, K., Lesur, V., Manda, M., Maus, S., Purucker, M., Ravat, D., Sazonova, T., and Thébault, E., 2007, Magnetic anomaly map of the world (and associated DVD): Commission for the Geological Map of the World, scale: 1:50,000,000, DVD. (Also available at http://ccgm.free.fr/index_gb.html.)
- Korolev, A.V., and Badalov, S.T., 1959, Zoning in the Amalyk ore field: *Geology of Ore Deposits*, no. 5, p. 31–38.
- Krivtsov, A.I., Migachev, I.F., and Popov, V.S., 1986, [Porphyry copper deposits of the world]: Moscow, Nedra, 236 p. [In Russian.]
- Medvedev, V.Y., and Kislyakova, N.I., 1963, [Map of mineral resources of the U.S.S.R., North Tian Shan series, Sheet K-43-XIII]: Ministry of Geology and Mineral Resources Protection, scale 1:200,000. [In Russian.]
- Meshchaninov, Ye. Z., and Azin, V.N., 1973, Distribution of gold in a copper porphyry deposit, Almalyk region: *International Geology Review*, v. 15, p. 660–663.
- Meshcheryakova, V.B., 1960, Structural characteristics and origins of faults in northern Karamazar: *Izvestiya, Geologic Series*, no. 4, April, p. 28–32.
- Movsesian, S.A., and Isaenko, M.P., 1974, Complex copper-molybdenum mineral deposits: Moscow, Nedra, 343 p.
- National Oceanic and Atmospheric Administration, 1996, Magnetic anomaly data of the former U.S.S.R.: Boulder, Colorado, National Geophysical Data Center, accessed August 1, 2009, at <http://www.ngdc.noaa.gov>.
- Pavlova, I.G., 1978, [Porphyry copper deposits]: Leningrad, Nedra, 275 p. [In Russian.]
- Plotinskaya, O.Y., Kovalenker, V.A., Seltmann, R., and Stanley, C.J., 2006, Te and Se mineralogy of the high-sulfidation Kochbulak and Kairagach epithermal gold telluride deposits (Kurama Ridge, Middle Tian Shan, Uzbekistan): *Mineralogy and Petrology*, v. 87, p. 187–207.
- Root, D.H., Menzie, W.D., and Scott, W.A., 1992, Computer Monte Carlo simulation in quantitative resource estimation: *Natural Resources Research*, v. 1, no. 2, p. 125–138.
- Seltmann, R., Shatov, V., and Yakubchuk, A., 2009, Mineral deposits database and thematic maps of Central Asia—ArcGIS 9.2, Arc View 3.2, and MapInfo 6.0(7.0) GIS packages: London, Natural History Museum, Centre for Russian and Central EurAsian Mineral Studies (CERCAMS), scale 1:1,500,000, and explanatory text, 174 p. [Commercial dataset available at <http://www.nhm.ac.uk/research-curation/research/projects/cercams/products.html>.]
- Shayakubov, T., Islamov, F., Kremenetsky, A. and Seltmann, R., eds., 1999, Au, Ag, and Cu deposits of Uzbekistan: International field conference of IGCP-373, London, Tashkent, Excursion B6 of the Joint SGA-IAGOD Symposium, 27 August–4 September, 1999, 112 p.
- Singer, D.A., and Menzie, W.D., 2005, Statistical guides to estimating the number of undiscovered mineral deposits—An example with porphyry copper deposits, *in* Cheng, Qiuming, and Bonham-Carter, Graeme, eds., *Proceedings of IAMG—The annual conference of the International Association for Mathematical Geology*: Toronto, Canada, York University, Geomatics Research Laboratory, p. 1028–1033.
- Singer, D.A., Berger, V.I., and Moring, B.C., 2008, Porphyry copper deposits of the world: U.S. Geological Survey Open-File Report 2008–1155, 45 p., accessed August 10, 2009, at <http://pubs.usgs.gov/of/2008/1155/>.
- Sokolov, A.L., 1999, Regional and local controls on gold and copper mineralization in central Asia and Kazakhstan, *in* Porter, T.M., ed., *Porphyry and hydrothermal copper & gold deposits—A global perspective*, Conference Proceedings: Glenside, South Australia, Australian Mineral Foundation, p. 181–190.
- Tkachev, V.N., 1969, The late Paleozoic volcanism of the Kuraminsk volcanic-plutonic province, *in* *Theoretical problems of volcanic-plutonic associations and their ore resources*: Moscow, Nauka Press, p. 214–218.
- Trifonov, V.G., Makarov, V.I., and Skobolev, S.F., 1992, The Talas-Fergana active right-lateral fault: *Annales Tectonicae*, v. 6, Supplement, p. 224–237.

- U.N. Economic and Social Commission for Asia and the Pacific (ESCAP), 1998, *Geology and mineral resources of Kyrgyzstan*: New York, United Nations, 153 p.
- U.N. Economic and Social Commission for Asia and the Pacific (ESCAP), 2000, *Atlas of mineral resources of the ESCAP region*, v. 15, *Geology and mineral resources of Azerbaijan*: New York, United Nations, 216 p.
- Windley, B.F., Alexeiev, D., Xiao, W., Kroner, A., and Badarch, G., 2007, Tectonic models for accretion of the Central Asian Orogenic Belt: London, *Journal of the Geological Society*, v. 164, p. 31–47.
- Yakubchuk, A., 2004, Architecture and mineral deposit settings of the Altaid orogenic collage—A revised model: *Journal of Asian Earth Sciences*, v. 23, p. 761–779.
- Zvezdov, V.S., and Migachev, I.F., 1986, [Structure and origin of the blind Kyzata porphyry copper deposit]: *Geology of Ore Deposits*, v. 28, no. 1, p. 73–80. [In Russian.]
- Zvezdov, V.S., Migachev, I.F., and Girfanov, M.M., 1993, Porphyry copper deposits of the CIS and the models of their formation: *Ore Geology Reviews*, v. 7, p. 511–549.
- Zvezdov, V.S., Sergeeva, N.E., and Shishakov, V.B., 1987, [Geologic structure and geochemical features of the Kyzata porphyry copper deposit]: *Geology of Ore Deposits*, v. 30, no. 1, p. 109–111. [In Russian.]

Appendix B. Porphyry Copper Assessment for Tract 142pCu8002, Ordovician North Tian Shan Magmatic Arc—Kyrgyzstan and Kazakhstan

By Byron R. Berger¹, Paul D. Denning¹, Connie L. Dicken², Jane M. Hammarstrom², John C. Mars², Jeffrey D. Phillips¹, and Michael L. Zientek³

Deposit Type Assessed: Porphyry Copper

Descriptive model: Porphyry copper (Cox, 1986; Berger and others, 2008)

Grade and tonnage model: Global Cu-Au-Mo porphyry copper model (Singer and others, 2008)

Table B1 summarizes selected assessment results.

Table B1. Summary of selected resource assessment results for tract 142pCu8002, Ordovician North Tian Shan magmatic arc—Kyrgyzstan and Kazakhstan.

[km, kilometers; km², square kilometers; t, metric tons]

Date of assessment	Assessment depth (km)	Tract area (km ²)	Known copper resources (t)	Mean estimate of undiscovered copper resources (t)	Median estimate of undiscovered copper resources (t)
2009	1	8,140	2,000,000	5,200,000	1,000,000

Location

The tract consists of two separate Ordovician magmatic-arc segments in the North Tian Shan magmatic arc of Windley and others (2007), one located at the west end of the Kyrgyz Range, Kyrgyzstan, and the other on Kendyktas Ridge in southern Kazakhstan (see fig. 1-2C⁴, fig. B1). The city of Bishkek, Kyrgyzstan, is 80 km west of the southeast end of Kendyktas Ridge.

Geologic Feature Assessed

The permissive tract consists of part of the Middle to Late Ordovician North Tian Shan magmatic-arc that was built on the composite Kokchetav-North Tian Shan litho-tectonic terrane of Windley and others (2007), as modified by Alexeiev and others (2010). The village of Talas (lat 42.50° N., long 72.24° W.) is within 142pCu8002a, and Bishkek (lat 42.88° N., long 74.77° E.), Kyrgyzstan, is approximately 10 kilometers (km) south of the southwest margin of 142pCu8002b (fig. B1).

¹U.S. Geological Survey, Denver, Colorado.

²U.S. Geological Survey, Reston, Virginia.

³U.S. Geological Survey, Spokane, Washington.

⁴Refer to chapter 1 of this report.

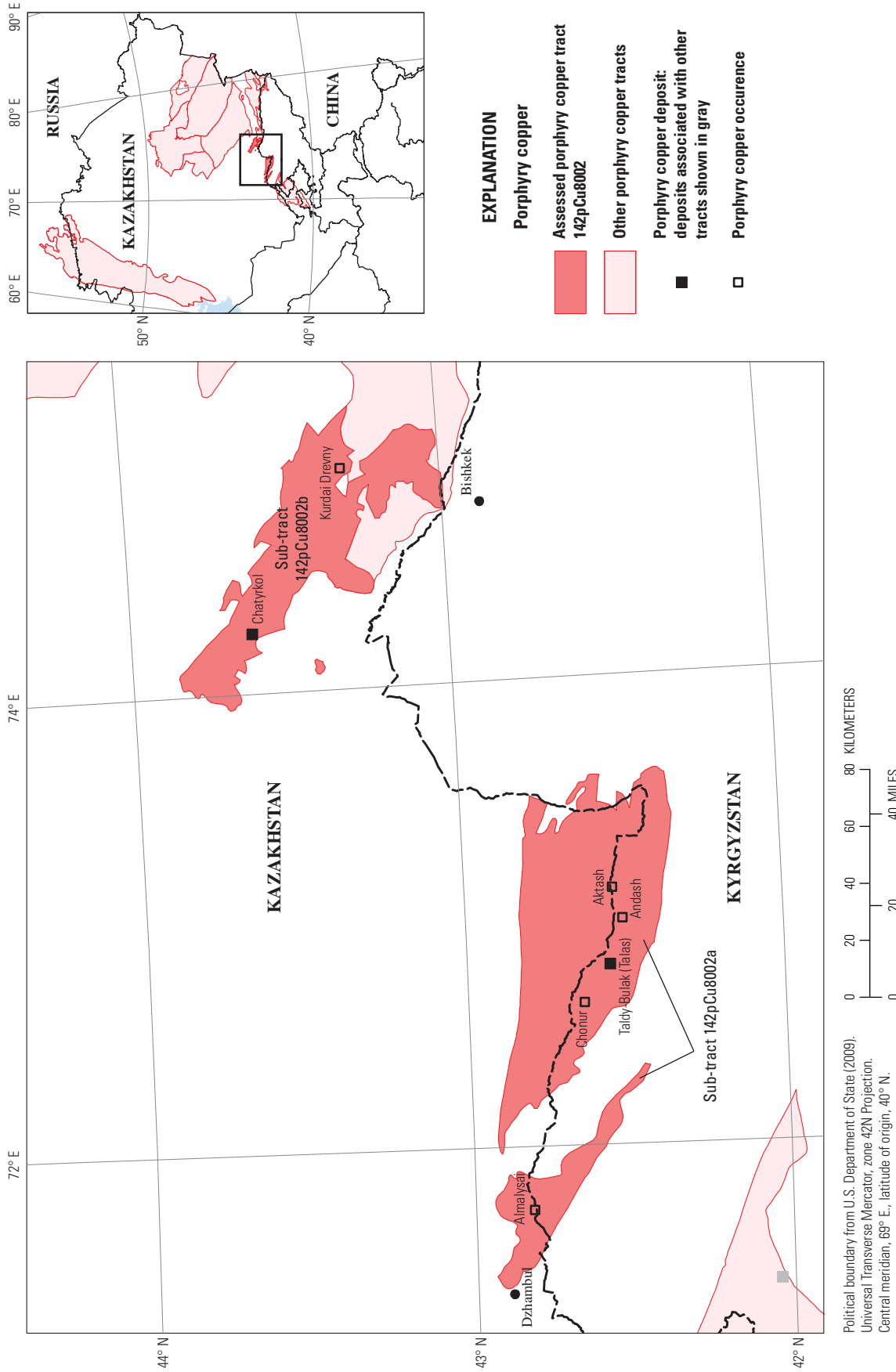


Figure B1. Map showing the location, known deposits, and significant prospects and occurrences for permissive tract 142pCu8002, Ordovician North Tian Shan magmatic arc—Kyrgyzstan and Kazakhstan. Location of map area shown on inset.

Delineation of the Permissive Tract

Geologic Criteria

The principal tectonic concept used to delineate this tract was that of a magmatic arc formed in the subduction boundary zone above a subducting plate. Five principal sources of information, supplemented by numerous published journal and symposium papers, were used to delineate this tract. The primary sources were the mineral deposits map of Central Asia on a geologic base edited by Seltmann and others (2009), supplemented by four 1:200,000-scale geologic maps originally published by the U.S.S.R. government, a reduced-to-pole aeromagnetic map prepared by J.D. Phillips from NOAA (1996), the interpretation of Advanced Spaceborne Thermal Emission and Reflection (ASTER) satellite imagery of hydrothermal alteration minerals or suites of minerals by J.C. Mars (chapter 2), the tectonic terrane map of Windley and others (2007), and stratigraphic and structural expertise provided by Dr. Dmitriy Alexeiev of the Russian Academy of Science, Moscow.

Central Asia is an amalgamation of Precambrian basement fragments, microcontinents, and overlying Paleozoic magmatic arcs (Windley and others, 2007). The permissive Upper Ordovician (O_3) North Tian Shan magmatic arc of north and central Kyrgyzstan and adjacent south-central Kazakhstan was built across two conjoined Proterozoic to mid-Ordovician litho-tectonic terranes, Kurama-Teresky and Kokchetav-North Tian Shan (Alexyutin and others, 2005; Windley and others, 2007). The Proterozoic rocks underlying both terranes are moderately to strongly metamorphosed, but differ in composition between 142pCu8002a in the western Kyrgyz Range and 142pCu8002b on Kendyktas Ridge. In western Kyrgyzstan, pelitic phyllites and schists, marble, quartzite, and quartzo-feldspathic gneiss predominate. These rocks are interpreted as having been deposited originally in continental shelf to slope environments (compare Levashova and others, 2007). On Kendyktas Ridge, the Precambrian rocks consist predominantly of schist, gneiss, amphibolite, and ophiolitic blocks, indicative of having been deposited in oceanic- to magmatic-arc environments. In the Kurama-Teresky terrane, Cambrian (Cm_{1-2}) to Ordovician (O_{1-2}) passive margin and intraplate carbonate and siliciclastic units unconformably overlie the Precambrian basement. In the Kokchetav-North Tian Shan terrane (fig. 1-7) of the western Kyrgyz Range, the Lower Cambrian to Middle Ordovician consists of volcanic, siliciclastic, and minor carbonate rocks characteristic of oceanic basin transitional to magmatic-arc environments. On Kendyktas Ridge, the lowest Paleozoic units are the Kurama-Teresky and Kokchetav-North Tian Shan terranes that were likely conjoined before the onset of O_3 arc magmatism (Windley and others, 2007), which was built across the comingled terranes. On Kendyktas Ridge, the ophiolite fragments are interpreted to be Precambrian (Seltmann and others, 2009), whereas where the ridge intersects the Tian Shan in the Aktas and Dzheta-Dzhol mountains vicinity,

ophiolite blocks are mapped as Cambrian (Seltmann and others, 2009). A late O_3 or Lower Silurian collisional event terminated arc magmatism, and Silurian leucocratic granites imply that postorogenic magmatism ensued after cessation of subduction-related magmatism. Devonian (D_{2-3}) and Carboniferous (C_{1-3}) rocks overlie the permissive Ordovician rocks. These stratigraphically younger rocks contain facies and intrusions that are typical of magmatic-arc environments.

Multiple deformation events have affected the rocks in the O_3 magmatic-arc tract (distribution shown in fig. B2), and this deformation history influenced the analysis and interpretation of the permissive terrane as well as being a source of uncertainty in our estimation of undiscovered porphyry copper deposits in this tract. The oldest deformation events occurred during the Precambrian. Proterozoic rocks in the permissive areas, indicate at least two major periods of deformation (Stepanenko, 1959), including the uplift of ultra-high pressure eclogites to the surface in the western Kyrgyz Range before unconformable deposition of Paleozoic sediments on them. The angularity of the Ordovician-Cambrian unconformity is greater between the Lower Cambrian (Cm_1) and the Middle to Late Ordovician rocks (O_{2-3}) (compare Stepanenko, 1959) than it is between the Upper Cambrian (Cm_2) and the O_{2-3} rocks. This tilting likely accompanied a change in tectonic setting from the Lower to Upper Cambrian. A gentle folding of the entire Cambrian section at the close of or during O_1 implies an additional Early Paleozoic deformation event, perhaps a consequence of the amalgamation of the Kurama-Teresky and North Tian Shan litho-tectonic terranes. A later and more intense deformation of the O_3 magmatic arc occurred towards the end of the Ordovician but before the cessation of arc magmatism; for example, O_3 plutons intrude folded Ordovician rocks (Stepanenko, 1959).

The two most important attributes used to delineate the permissive tract boundaries were outcrops of rock suites that contain O_3 and O_{2-3} volcanic- and plutonic-rock complexes and porphyry copper-style occurrences and deposits. Although permissive age intrusive rocks occur throughout the Tian Shan mountain ranges of Kyrgyzstan, for reasons discussed below, the most likely areas for the occurrence of undiscovered porphyry copper deposits with a 50:50 chance of being above or below the median grade and tonnage in the general porphyry copper model are in the western Kyrgyz Range of northern Kyrgyzstan and adjacent Kazakhstan, and nearby on Kendyktas Ridge in south-central Kazakhstan.

Magmatic-arc plutons are more widespread in the northern Tian Shan mountain ranges than are here delineated for assessment; however, the western Kyrgyz Range are deemed the only Ordovician magmatic-arc-related rocks appropriate for assessment because of their depth of erosion, which is interpreted to not exceed 4–5 km. Elsewhere in the Kyrgyz Tian Shan mountain ranges, multiple deformation events through time have exposed rocks of progressively deeper levels in the crust such that the environment suitable for the formation of porphyry-style copper deposits has

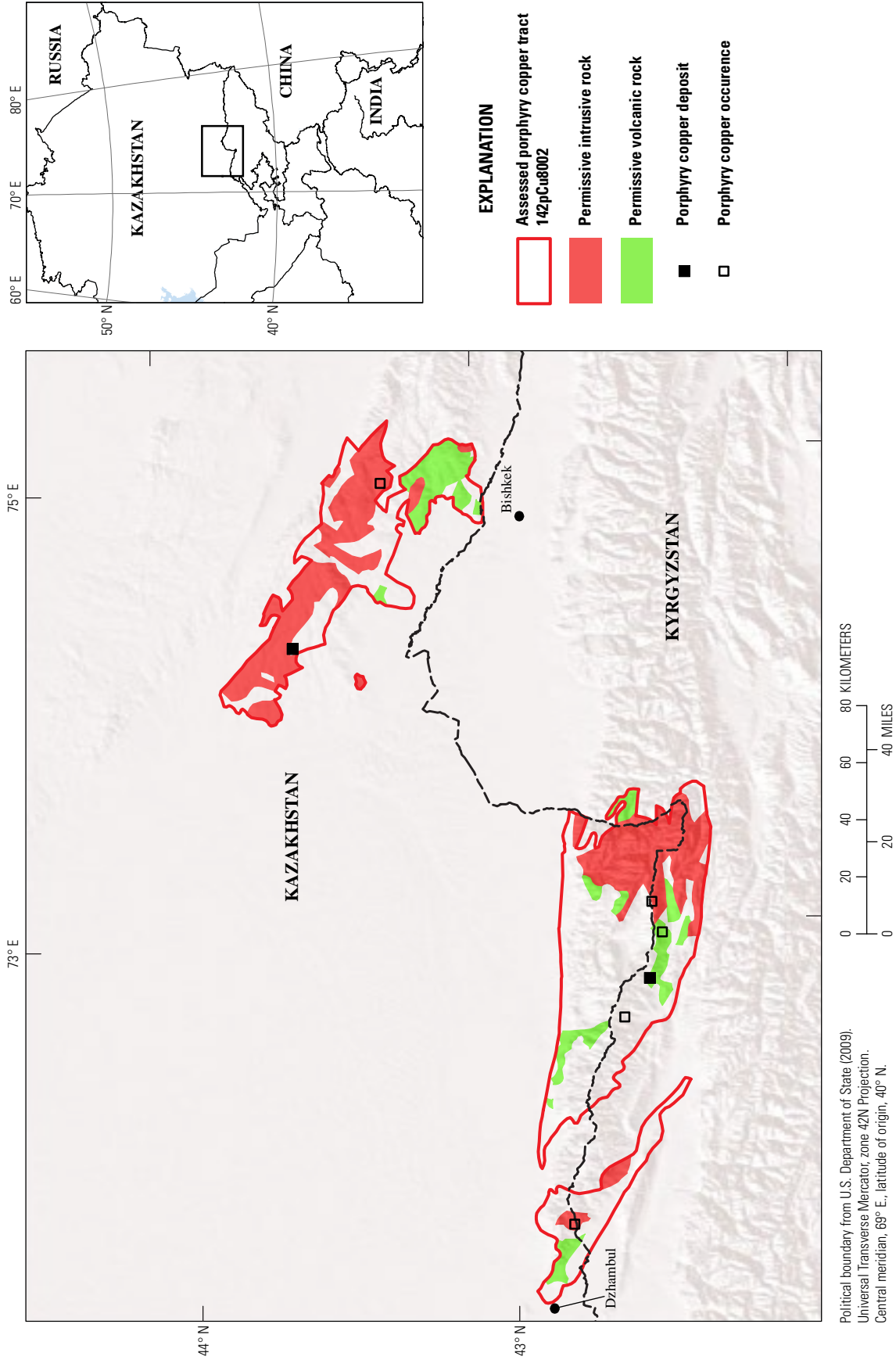


Figure B2. Map showing the distribution of permissive Ordovician volcanic and volcanoclastic (green) and intrusive (red) rocks in tract 142pCu8002, Ordovician North Tian Shan magmatic arc—Kyrgyzstan and Kazakhstan, on a digital elevation base. Location of map area shown on inset.

been removed. The primary evidence for this is the lack of verifiable porphyry copper deposits in the excluded areas, the lack of widespread hydrothermal alteration of the types typically found within and around porphyry-style deposits, and the occurrence of mesothermal (orogenic) gold deposits along regional fault zones interpreted to have formed at 5 or more kilometers depth.

In part of the tract, the lowermost Cambrian rocks include mafic marine lavas with capping limestone in addition to cherts, siliceous black shales, and sandstone. This Early Cambrian assemblage is suggestive of an oceanic sequence made up of a mixture of deep water and continental slope depositional environments. The Middle to Late Cambrian rocks are predominantly coarse clastics with carbonate cement and lenses of limestone, but a sequence of tuffs and volcanoclastic rocks make up the youngest part of the Cambrian (Stepanenko, 1959). Both assemblages of Cambrian rocks indicate a Late Cambrian near-arc environment that is not extensively exposed and is poorly dated. There are no identified porphyry copper occurrences or possibly porphyry-related deposits such as skarn and (or) polymetallic deposits of this age. We view the likelihood of Cambrian porphyry copper deposits to be negligible.

The backbone of the northwest-southeast-trending Kendyktas Ridge in Kazakhstan consists of O_3 intrusions associated with deposits and occurrences. From the northwest end of the ridge where the pre-Tertiary rocks are covered beneath Chu Basin sedimentary rocks and to the southeast, the O_3 intrusions are flanked on the northeast and southwest by metamorphosed Precambrian rocks including probable ophiolite fragments and O_1 and O_2 rocks that are predominantly siliciclastic and metamorphosed, including schist (Seltmann and others, 2009). Along this part of the ridge, there are numerous copper-molybdenum and copper-gold vein-style deposits, although a porphyry-style deposit has been delineated at the Chatyrkul mine (fig. B1), where vein ores predominate. Midway along the ridge towards the Tian Shan mountain ranges, the Ordovician rock suites include O_3 rocks that include volcanic rocks. Porphyry-style occurrences and skarns are more common in this part of the ridge.

On the north, a reverse fault separates the Kyrgyz Range from younger Chu-Sarysu basin fill, and the permissive rocks are buried beneath the basin sediments. On its southwest side, permissive Kendyktas Ridge rocks are in fault contact with the same basin fill. The northeast boundary of the Kendyktas Ridge is an Upper Cambrian to Lower Ordovician suture zone that separates the permissive rocks from the Dzhalaïr-Naiman litho-tectonic terrane (fig. 1-7) to the east (Windley and others, 2007).

During the Devonian, there was renewed intermediate to siliceous calc-alkaline volcanism and intrusions as well as some alkaline composition intrusions (see Seltmann and others, 2009). Although Windley and others (2007) classify these Devonian and associated Carboniferous rocks as part of an epicontinental marine basin, the siliceous volcanic and related intrusive rocks suggest that a Devonian magmatic

arc was built in western Kyrgyzstan on the deformed Late Ordovician arc and its postcollisional Ordovician to Silurian complexes. Early Devonian lavas were mafic to andesitic (Frasnian [370–364 mega-annum, Ma] according to Levashova and others, 2007) and were succeeded in the latest Devonian by silicic volcanic rocks and intrusions (Levashova and others, 2007). Although we are not aware of any reported Devonian porphyry copper deposits in this tract, some mineralized areas could be associated with the Upper Devonian siliceous volcanism, so the possibility cannot be dismissed.

The Tian Shan mountain ranges are typically divided into three east-west-trending tectonic units—North, Central, and South. The tectonic boundary between the southern and central blocks resulted from a Late Devonian to Early Carboniferous collision (Bullen and others, 2003). This accreted terrane subsequently collided with the accreted Kyrgyz-Teresky–North Tian Shan block upon final closing of the Tarim ocean basin during the Late Carboniferous to Early Permian. This latter accretionary event affected the permissive terrane rocks because a significant proportion of the collisional strains were accommodated on high-angle reverse and thrust faults as well as strike-slip faults in the northern block.

Distal plate margin stresses led to foreland basin formation to the north (Chu-Sarysu and Ili basins) and south (Tarim Basin) of the Tian Shan during the Jurassic to Early Cretaceous as well as some intermontane basin development within the Tian Shan (Sobel and others, 2006). Major, regional tectonic activity, however, did not begin until the collision of Eurasia and India (~55–50 Ma, Bullen and others, 2003). Shortening began about the Oligocene-Miocene boundary and propagated south to north (Sobel and others, 2006), but most of the range-wide uplift of the Tian Shan occurred during the late Miocene to early Pliocene (Bullen and others, 2003). Most of the uplift is accommodated through north-vergent thrust faults. Present-day topographic relief in the Tian Shan is extreme, with the highest elevations in central Kyrgyzstan, where the greatest amount of exhumation also took place.

Within the North Tian Shan terrane block along the northern flank of the Tian Shan mountain ranges, ultra high-pressure (UHP) eclogites (20–25 kilobar, kbar, pressure) are exposed in at least two localities, one in the western Kyrgyz Range (Makbal complex), the other in the western Zaili Range (Aktyuz Group) (Tagiri and others, 1995). The former is in rocks considered to be lower Proterozoic, and yields an Ordovician K-Ar date, and the rocks are contact metamorphosed by Ordovician intrusions, whereas the latter is Neoproterozoic and is unconformably overlain by Devonian rocks (Tagiri and others, 1995). Thus, both of these northern Tian Shan ranges eclogites are Precambrian and were uplifted by the Phanerozoic. In contrast, an eclogite formed at 15–30 kbar pressure is exposed along the “Nikolaev Line” that juxtaposes the North and Central Tian Shan blocks in the highest part of the Tian Shan. Its radiometric age is Early Permian (Tagiri and others, 1995). Inferences that may be drawn that are pertinent to this assessment are (1) not all rocks

shown on the geologic map as Precambrian age are, in fact, Precambrian, (2) the time of uplift of highly metamorphosed rocks is not all relatable to a single tectonic event and time throughout the Tian Shan ranges, and (3) the highest elevations in the Tian Shan expose deeper parts of the orogen than rocks in the northern, western, and eastern parts of the Tian Shan.

The late Miocene to early Pliocene tectonic uplift of the Tian Shan mountain ranges reactivated many faults formed during earlier tectonic events in the northern Tian Shan. Vertical displacement on these reactivated faults not only help in defining the boundaries of similar, but temporally or spatially different magmatic-arc terranes, they also brought to the surface mesothermal (“orogenic”) type low-sulfide vein deposits formed along these faults, principally economic for their gold contents. The inferred depths of formation of these deposits provide clues as to the level of exposure now observed in the permissive magmatic-arc terrane. Along the southern boundary at the western end of tract 142pCu8002a, the Jerooy low-sulfide gold deposit occurs along faults that are part of a northwest-striking system of south-dipping, strike-slip reverse faults in an Ordovician intrusive complex that is regionally part of a magmatic-arc environment. Aplite dikes and inliers of volcanoclastic sediments in the intrusive complex (Oakes and others, 1998) support an interpreted shallow level of emplacement for the intrusions. The age of the deposit is unknown, but it is clearly younger than the intrusive complex and vein orientations indicate that it was formed during active reverse faulting. Because the reverse fault brings Late Devonian to Early Carboniferous rocks over Precambrian and Ordovician rocks, the Jerooy deposit-controlling faulting is unrelated to the Ordovician arc and end-of-Ordovician deformation. The deposit is likely Late Carboniferous to Early Permian. The fault zone juxtaposes the Kyrgyz-Teresky magmatic-arc terrane and the North Tian Shan magmatic-arc terrane. There are several mesothermal gold occurrences to the south in the Kyrgyz-Teresky terrane, whereas to the north in the North Tian Shan terrane, the deposits are porphyry-style copper-gold. Although there are no laboratory data available from which to estimate a depth of formation of Jerooy and the other mesothermal deposits, their clear mesothermal character, in contrast to the porphyry copper-gold deposits and occurrences to the north and typical depths of formation of mesothermal vein deposits of greater than or equal to 5 km, leads us to assume it likely that the Kyrgyz-Teresky terrane has been uplifted and eroded down to a depth of 5–10 km depth in contrast to the rocks to the north of the fault zone. Along the south-central boundary of the permissive rocks, geochemical data from the Kumtor gold deposit indicates that it was formed at depths well in excess of 5 km, likely at 10–15 km. This is consistent with the occurrence of Permian UPH eclogites in this region. Thus, in this region, although the map of Seltmann and others (2009) show permissive rocks, the inferred depth is well below the depth interval within which porphyry copper deposits are known to form.

The first step in tract delineation was to identify all geologic units on the Seltmann and others (2009) geologic map that do or could consist of Middle and Late Ordovician arc-related volcanic and intrusive rocks (fig. B2). The region was then subdivided into the tectonic blocks as interpreted from Windley and others (2007). Permissive terrane boundaries were determined from the permissive geologic units on the geologic map in conjunction with other sources of information (such as journal articles, geophysical data, and mineral-deposit studies). Wherever available, geologic cross-sections were used to determine the 1-km depth cutoff for permissive rocks, with permissive rocks deeper than that not included in the permissive tract. Mines and mineral occurrence maps and published reports were used to discriminate permissive arc and nonpermissive postarc volcano-plutonic complexes wherever possible. Interpreted hydrothermal alteration maps derived from Landsat and ASTER satellite data were used to refine permissive tract boundaries. Anecdotal information obtained from geologists with on-the-ground experience, published minerals exploration reports, and data and information posted on the Internet also were used where appropriate. The second step was to review and revise the preliminary tract boundaries in a workshop format with experts drawn from other countries and international mining companies.

Known Deposits

There are two known porphyry copper-style deposits in this tract, Taldy Bulak (Talas) in the northwestern Kyrgyz Range, Kyrgyzstan, and Chatyrkul on Kendyktas Ridge, Kazakhstan (fig. B1, table B2). A porphyry copper occurrence in Kazakhstan on the northern flank of the Kyrgyz Range in Kazakhstan is also called Taldy-Bulak (Seltmann and others, 2009), but little information on this occurrence is publically available. Taldy-Bulak (Levoberezhny), Kyrgyzstan, a mesothermal, shear-zone hosted gold deposit about 230 km to the east of the permissive tract, is frequently mistaken for the Taldy-Bulak (Talas) deposit.

Taldy-Bulak (Talas), Kyrgyzstan

Taldy-Bulak (Talas) is associated with a composite, Late Ordovician quartz diorite to dacite intrusive complex that is approximately 1,400 by 1,000 m in plan view. A porphyritic phase of the complex was dated at 444 ± 8 Ma (Jenchuraeva, 1997). Granodiorite dikes having both concentric and radial strikes surround the main intrusive complex. The igneous rocks intrude Middle to Late Ordovician andesitic volcanoclastic rocks. The mineralized complex is intruded by postmineralization gabbro, lamprophyre, granite, felsic porphyry, pyroxene diabase, syenite, and diorite dikes (Lero Gold Corporation, 2007 Annual Report). Devonian volcanic rocks cover, in part, the Ordovician igneous complex, and the postmineralization lamprophyre dikes intrude both the Ordovician and Devonian rock suites (Jenchuraeva, 1997).

Mineralization occurs in an elliptical, east-west zone approximately 1,100 by 600 m that is centered on the intrusive complex, but includes both intrusive and host volcanoclastic rocks. A potassically altered quartz-tourmaline breccia body occurs in the middle of the mineralized body of rock. Porphyry-style copper-gold mineralization is associated with both sheeted and stockwork veins. The principal ore minerals are pyrite, chalcopyrite, bornite, molybdenite, and native gold. Total pit-constrained indicated and inferred resources are reported as 423 Mt at 0.17 percent copper, 0.01 percent molybdenum, and 0.5 grams per ton (g/t) gold (Orsu Metals Corporation, 2012).

Chatyrkul, Kazakhstan

Chatyrkul is associated with a granitic rock complex that varies from Middle Ordovician syenites and diorites to Late Ordovician biotite and biotite-hornblende granites together with dikes of the same range in composition (Zhukov and others, 1998). Vein- and stockwork-form veins cross cut all of the intrusive igneous rock types. The mining of veins dates to prehistoric times, but more recent operations date from the 1950s, when extraction of magnetite-chalcopyrite-molybdenite ores in quartz-carbonate veins began. Common accessory minerals include hematite, pyrite, and galena; less common ore minerals include sphalerite, bornite, cassiterite, and native gold. Mineable veins are as much as 30 m wide, to 5 km along strike, and to 800 m down dip. Stockworks of quartz and disseminated sulfides occur within the granitic rocks between the major veins. Zhukov and others (1998) consider the deposit to be under-explored both along strike and down dip.

Porphyry Copper Occurrences and Related Deposit Types

Although permissive rocks extend across the whole of northern Kyrgyzstan, porphyry-style mineralization is known to occur only in the western half of the tract. In this region, widespread hydrothermal alteration is associated with the Middle to Late Ordovician magmatic-arc intrusive complexes, with one of which the Taldy-Bulak (Talas) porphyry copper-gold deposit is associated. Both ancient and historical mining have occurred throughout this region, particularly along the south slope of the range facing the Talas River valley, and farther west near the Kyrgyzstan-Kazakhstan border east of the town of Taraz, Kazakhstan.

There are several porphyry-style and copper skarn prospects at the northwesternmost tip of the Kyrgyz Range, about 35–40 km east-southeast of Taraz (Dzhambul), Kazakhstan (see fig. 1-2A, fig. B1, table B3). One can see what appear to be trenching and drill sites on Google Earth

images for two areas, suggesting that in these areas, at least, a concerted exploration effort has been made, most likely during the Soviet era. The prospects are in an Ordovician arc sequence that is separated by an uplifted block of Precambrian rocks from the main zone of copper-gold exploration and mining about 60 km to the east-southeast in the Talas River valley area.

In the main copper-gold zone on the north slope of the Talas River valley, from west to east, Jenchuraeva (1997) lists the sites of porphyry-style mineralization as Chonur, Taldy-Bulak (discussed above), Andash, and Karakol. In a NI 43-101 technical report, Wardell Armstrong International (2008) also lists Dzhangyztal and Kentash as locations with porphyry-style mineralization. Mineralization in the western half of this tract is discussed in the following paragraphs using the city of Talas (lat 42° 31'09" N., long 72° 15'44" E.) as a point of geographic reference.

Andash is an advanced exploration project. Feasibility studies and open-pit mine plans for a 6-year mine were developed for one of the several zones on the property. Total reserve estimates (for zone 1 of 6), including proven and probable resources, and oxide and sulfide ore types are 16 million metric tons (Mt) at 0.40 percent copper and 1.05 g/t gold (Kentor Gold, Ltd., 2011). At Andash Zones 2 and 3, the best drill intersection from the Soviet-era exploration returned 120.7 meters (m) of core grading 2.14 g/t gold and 0.28 percent copper. Other zones on the property have similar characteristics, but are likely offset by thrust faults that have dissected the deposit. Ore is hosted in a monzodiorite-granite complex of Late Devonian age in a 400 by 200 m area of flat stockwork connected with eruptive breccias. Gold-rich copper prospects define a 30-km-long mineralized zone. Copper is confined to quartz-sericite-chlorite alteration; gold mainly is hosted in zones of argillic alteration (O.L. Chubko, written commun., 2012). Chonur is a copper-gold-molybdenum prospect approximately 30–35 km northeast of Talas.

Chonur is associated with a granodioritic intrusive complex that is within a northwest-trending belt of intrusions and associated quartz-gold vein occurrences. Much of the area is covered by postmineralization, Devonian volcanic rocks that may conceal additional copper-gold mineralization, although the Devonian rocks may approach 1 km in thickness in some locations (Lero Gold Corporation, 2007 Annual Report; www.orsumetals.com).

The Korgontash prospect area, approximately 28 km east-southeast of the Taldy-Bulak deposit, is in the Karakol district, which has been primarily explored for copper-gold skarn mineralization. The area includes the Aktash and Tokhtonnisai skarn deposits. The skarns are in calcareous Cambrian and Ordovician sedimentary rocks on the north side of a Late Ordovician intrusive complex (Lero Gold Corporation, 2007 Annual Report; <http://www.orsumetals.com>).

Table B2. Identified porphyry copper resources in tract 142pCu8002, Ordovician North Tian Shan magmatic arc—Kyrgyzstan and Kazakhstan.[Ma, mega-annum (10^6 years); km², square kilometers; t, metric tons; Mt, million metric tons; %, percent; g/t, grams per metric ton; Cu, copper; Mo, molybdenum; Au, gold; Ag, silver; n.d., no data]

Name	Country	Latitude	Longitude	Subtype	Age (Ma)	Tonnage (Mt)	Cu (%)	Mo (%)	Au (g/t)	Ag (g/t)	Contained Cu (t)	Reference
Taldy-Bulak (Talas)	Kyrgyzstan	42.551	72.768	Cu-Au	420	540	0.27	0.008	0.50	n.d.	1,458,000	Djenchuraeva (2005), Jenchuraeva (1997), Jenchuraeva and Maksumova (1993), Orsu Metals Corporation (2012), Seltmann and Porter (2005), Wardell Armstrong International (2010)
Chatyrkul	Kazakhstan	43.620	74.262	NA	401	90.7	0.60	n.d.	n.d.	n.d.	544,200	Kolesnikov and others (1986), Pavlova (1978), Plyushchev (1993), Sokolov (1999)

Table B3. Significant occurrences of porphyry-style and copper skarn prospects in tract 142pCu8002, Ordovician North Tian Shan magmatic arc—Kyrgyzstan and Kazakhstan.[Ma, mega-annum (10^6 years); km², square kilometers; t, metric tons; Mt, million metric tons; %, percent; g/t, grams per metric ton; km, kilometers; km², square kilometers; NE, northeast; Cu, copper; Mo, molybdenum; Au, gold; Ag, silver; Co, cobalt; Fe, iron; U, uranium; AuEq, gold equivalent; JORC, Joint Ore Reserves Committee; n.d., no data]

Name	Country	Latitude	Longitude	Age (Ma)	Comments	Reference
Aktash	Kazakhstan	42.534	73.094	n.d.	Skarn associated with Late Ordovician intrusive complex in the Karakol district. Exploration target under JORC guidelines for 2–5 Mt of ore, 0.3–0.7% Cu, 2–3.5 g/t Au, 8–12 g/t Ag. Explored 1990–1993; 59 drill holes. May be developed with nearby (8 km) Andash project processing plant. Cu-Au prospect area; also known as Karakol ore field, with Cu skarn production.	Proactive Investors (2010)
Almalyasai	Kazakhstan	42.817	71.729	n.d.	Small porphyry. Major Cu, Au. Minor Ag, Co.	Seltmann and others (2009)
Andash	Kyrgyzstan	42.505	72.961	n.d.	In development as an open pit (Kentor Gold, 2011). JORC-compliant measured, indicated, and inferred resources of 19.6 Mt at 0.40% Cu, 1.10 g/t Au (cutoff 1.25 g/t AuEq). Late Ordovician granodiorite and diorite porphyries intruding Lower and Middle Ordovician volcanic sedimentary rocks. Alteration types: argillic, propylitic, phyllic, quartz-feldspar, quartz tourmaline. Copper ore in quartz-sericite chlorite alteration zones; economic gold in argillic alteration zones. Two ore bodies within an area of 9.23 km ² . Location: Towards west end of >1 km wide exploration zone on Google Earth (3/3/10)	Kentor Gold (2011), Newall (2005), Seltmann and Jenchuraeva (2001), U.N. Economic and Social Commission for Asia and the Pacific (1998)
Chonur	Kazakhstan	42.636	72.608	n.d.	Cu-Au-Mo prospect associated with a granodiorite complex. Approximate location from Google Earth image after Orsu Metals Corporation Web site, excavations on hillslope and old trenches on GoogleEarth (3/3/10) Called mesothermal vein stockwork type deposit; mine (Seltmann and others, 2009)	Jenchuraeva (1997), Orsu Metals Corporation (2011)
Kurdai Drevny	Kazakhstan	43.310	74.952	n.d.	Small porphyry with major Cu and Mo; minor Au, Fe, and U associated with Middle Ordovician host rocks Location: Small prospect pits/old mines(?) on Google Earth (3/4/10); about 2.7 km NE of Kurdai open pit	Seltmann and others (2009)

Exploration History

Mining activity goes back to ancient times and a considerable amount of work was done during the Soviet era, particularly between the 1960s and 1980s. It was during this latter interval that the Taldy Bulak (Talas) Cu-Au deposit was drilled and a resource established. Beginning in the 1990s, joint ventures between Kyrgyz and foreign interests reevaluated the region, particularly for its low-grade gold potential.

Hydrothermal Alteration Mapping (ASTER)⁵

Argillic and phyllic ASTER hydrothermal alteration mapping covers all of tract 142pCu8002a (see fig. 2-1); however, ASTER silicic hydrothermal alteration mapping does not cover the tract.

Sub-tract 142pCu8002a

One potential porphyry-type alteration site (site number 170) is defined in the southeastern part of tract sub-tract 142pCu8002a based on ASTER argillic and phyllic alteration patterns (see fig. 2-3 and plates 1–8). The geologic map of Seltmann and others (2009) shows that altered rocks at site 170 are subporphyritic granodiorites (see table 2-1). Available mineral databases do not indicate any copper mineralization associated with the site (Seltmann and others, 2009; Singer and others, 2008).

Sub-tract 142pCu8002b

Two potential deposit sites (site number 249 and 250) are defined in the southeastern part of sub-tract 142pCu8002a using ASTER argillic and phyllic alteration patterns (see fig. 2-3 and plates 1–8). The altered rocks are associated with subporphyritic granodiorites and copper, molybdenum, and uranium occurrences (see table 2-1 and plates 5–8). No deposits or significant prospects are known to be associated with the defined alteration sites.

Sources of Information

Principal sources of information used by the assessment team for delineation of 142pCu8002 are listed in table B4.

⁵Refer to figures, tables, and plates in chapter 2 of this report.

Grade and Tonnage Model Selection

The general porphyry copper deposit model published by Singer and others (2008) was used based on the known deposits in the tract being statistically consistent with the model.

Estimate of the Number of Undiscovered Deposits

Rationale for the Estimate

The consensus was that (1) it was not necessary to subdivide the Ordovician North Tian Shan tract into sub-tracts, (2) there are plays to be made, particularly in areas of known porphyry copper-related deposit types such as copper skarns and polymetallic veins, (3) the depth of erosion of the terrane was not a limiting factor excepting near tectonic boundaries, and (4) owing to the rugged terrain and remoteness of some of the area, plays were left despite considerable Soviet-era exploration investment in the region. A mitigating factor is that the average grade of the Taldy-Bulak is less than a median deposit in the general porphyry copper model, and the tonnage at Chatyrkul is considerably below the median tonnage in the general model.

The tract contains two known deposits (table B2), five significant occurrences (table B3), and three additional areas that could be associated with porphyry-style occurrences based on alteration patterns. The team estimated a 50-percent chance of 1 or more undiscovered deposits and a 10-percent chance of 3 or more deposits, for a mean of 1.3 expected undiscovered deposits (table B5).

Probabilistic Assessment Simulation Results

Undiscovered resources for the tract were estimated by combining consensus estimates for numbers of undiscovered porphyry copper deposits with the general porphyry copper grade and tonnage model of Singer and others (2008), using the EMINERS program (Root and others, 1992; Bawiec and others, 2012; Duval, 2012). Selected simulation results are reported in table B6. Results of the Monte Carlo simulation are presented as a cumulative frequency plot (fig. B3). The cumulative frequency plot shows the estimated resource amounts associated with cumulative probabilities of occurrence, as well as the mean, for each commodity and for total mineralized rock.

The median estimate of undiscovered copper resources (1 Mt copper) is comparable to the identified resources in the two known deposits in the tract (1.5 Mt copper); the mean amount of undiscovered copper, 5.2 Mt copper, exceeds the identified resources (table B6).

Table B4. Principal sources of information used for the delineation of tract 142pCu8002, Ordovician North Tian Shan magmatic arc—Kyrgyzstan and Kazakhstan.

Theme	Name or title	Scale	Citation
Geology	Mineral deposits database and thematic maps of Central Asia	1:1,500,000	Seltmann and others (2009)
	Tectonic map of the Paleozoic folded areas of Kazakhstan and adjacent territories	1:1,500,000	Abdulin and Zaitseb (1976)
	K-43-IV (1987)	1:200,000	Paretseki and Akhamatullin (1987)
	K-43-VII (1963)	1:200,000	Stepanenko and others (1963)
	K-43-XIII (1963)	1:200,000	Medvedev and Kislyakova (1963)
	K-43-XIV (1960)	1:200,000	Burtman and others (1960)
Mineral occurrences	Mineral deposits database and thematic maps of Central Asia	1:1,500,000	Seltmann and others (2009)
Geophysics	Magnetic anomaly data of the former U.S.S.R.	1:1,500,000	National Oceanic and Atmospheric Administration (1996)

Table B5. Undiscovered deposit estimates, deposit numbers, tract area, and deposit density for tract 142pCu8002, Ordovician North Tian Shan magmatic arc—Kyrgyzstan and Kazakhstan.

[N_{xx} , estimated number of deposits associated with the xxth percentile; N_{und} , expected number of undiscovered deposits; s , standard deviation; $C_v\%$, coefficient of variance; N_{known} , number of known deposits in the tract that are included in the grade and tonnage model; N_{total} , total of expected number of deposits plus known deposits; area, area of permissive tract in square kilometers (km^2); density, deposit density reported as the total number of deposits per 100,000 km^2 . N_{und} , s , and $C_v\%$ are calculated using a regression equation (Singer and Menzie, 2005)]

Consensus undiscovered deposit estimates					Summary statistics					Tract area (km^2)	Deposit density ($N_{total}/100\text{k km}^2$)
N_{90}	N_{50}	N_{10}	N_{05}	N_{01}	N_{und}	s	$C_v\%$	N_{known}	N_{total}		
0	1	3	3	3	1.3	1.2	90	2	3.3	8,140	41

Table B6. Results of Monte Carlo simulations of undiscovered resources for tract 142pCu8002, Ordovician North Tian Shan magmatic arc—Kyrgyzstan and Kazakhstan.

[Cu, copper; Mo, molybdenum; Au, gold; and Ag, silver; in metric tons. Rock, in million metric tons]

Material	Probability of at least the indicated amount					Probability of		
	0.95	0.9	0.5	0.1	0.05	Mean	Mean or greater	None
Cu	0	0	1,000,000	11,000,000	20,000,000	5,200,000	0.23	0.3
Mo	0	0	0	290,000	580,000	140,000	0.17	0.51
Au	0	0	7	320	560	130	0.22	0.46
Ag	0	0	0	3,500	6,800	1,600	0.16	0.58
Rock	0	0	250	2,300	4,000	1,000	0.24	0.3

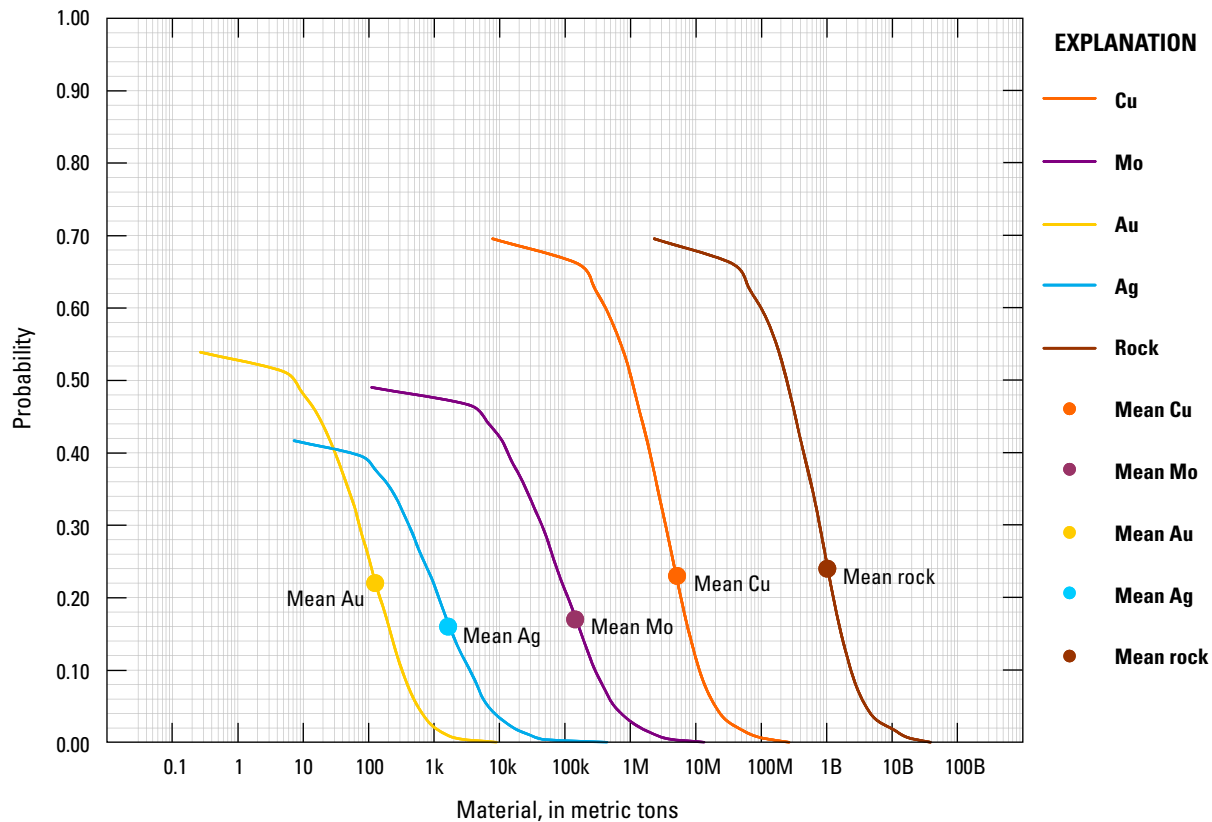


Figure B3. Cumulative frequency plot showing the results of Monte Carlo computer simulation of undiscovered resources in permissive tract 142pCu8002, Ordovician North Tian Shan magmatic arc—Kyrgyzstan and Kazakhstan. k = thousands, M = millions, B = billions.

References Cited

- Abduln, A.A., and Zaitseb, Yu.A., eds., 1976, [Tectonic map of the Paleozoic folded belts of Kazakhstan and adjacent territories]: Ministry of Geology of the U.S.S.R., VSEGEI, 1 map on 6 sheets, scale 1:1,500,000. [In Russian.]
- Alexeiev, D.V., Ryazantsev, A.V., Kroner, A., Tretyakov, A.A., Xia, X., and Liu, D.Y., 2010, Geochemical data and zircon ages for rocks in a high-pressure belt of Chu-Yili Mountains, southern Kazakhstan—Implications for the earliest stages of accretion in Kazakhstan and the Tianshan: *Journal of Asian Earth Sciences*, v. 42, no. 5, p. 805–820.
- Alexyutin, M.V., Bachtadse, V., Alexeiev, D.V., and Nikitina, O., 2005, Paleomagnetism of Ordovician and Silurian rocks from the Chu-Ili and Kendyktas mountains, south Kazakhstan: *Geophysical Journal International*, v. 162, p. 321–331.
- Bawiec, W.J., and Spanski, G.T., 2012, Quick-start guide for version 3.0 of EMINERS—Economic Mineral Resource Simulator: U.S. Geological Survey Open-File Report 2009–1057, 26 p., accessed July 15, 2012, at <http://pubs.usgs.gov/of/2009/1057/>. (This report supplements USGS OFR 2004–1344.)
- Berger, B.R., Ayuso, R.A., Wynn, J.C., and Seal, R.R., 2008, Preliminary model of porphyry copper deposits: U.S. Geological Survey Open-File Report 2008–1321, 55 p., accessed May 15, 2009, at <http://pubs.usgs.gov/of/2008/1321/>.
- Bullen, M.E., Burbank, D.W., and Garver, J.I., 2003, Building the northern Tien Shan: Integrated thermal, structural, and topographic constraints: *Journal of Geology*, v. 111, p. 149–165.
- Burtman, V.S., Katkova, N.S., Kordun, B.M., and Medvedev, V.Y., 1960, [Geological map of the U.S.S.R., North Tian Shan series, Sheet K-43-XIV]: Ministry of Geology and Mineral Resources Protection, scale 1:200,000. [In Russian.]
- Cox, D.P., 1986, Descriptive model of porphyry Cu (Model 17), in Cox, D.P., and Singer, D.A., eds., 1986, *Mineral deposit models*: U.S. Geological Survey Bulletin 1693, p. 76. (Also available at <http://pubs.usgs.gov/bul/b1693/>.)
- Djenchuraeva, R.D., 2005, Geodynamics and metallogeny of active continental margins of the Kyrgyz Tien Shan, in Mao, J., Bierlein, F.P., eds., *Mineral deposits research—Meeting the global challenge*, v. 2: Springer, p. 1309–1311.

- Duval, J.S., 2012, Version 3.0 of EMINERS—Economic Mineral Resource Simulator: U.S. Geological Survey Open-File Report 2004–1344, accessed July 15, 2012, at <http://pubs.usgs.gov/of/2004/1344/>.
- Jenchuraeva, R.J., 1997, Tectonic settings of porphyry-type mineralization and hydrothermal alteration in Paleozoic island arcs and active continental margins, Kyrgyz Range, (Tien Shan) Kyrgyzstan: *Mineralium Deposita*, v. 32, p. 434–440.
- Jenchuraeva, R.J., and Maksumova, R.A., 1993, Porphyry copper-gold mineralization in the ancient active continental margins of the Tien Shan: Proceedings of the 29th International Geological Congress 1992, Mineral Resources Symposia Volume A, Resource Geology Special Issue, no. 15, Tokyo, p. 241–252.
- Kentor Gold, 2011, Andash gold-copper project: Kentor Gold Web page, accessed October 10, 2011, at <http://www.kentorgold.com/andash-gold-copper-project>.
- Kolesnikov, V.V., Zhukov, N.M., Solodilova, V.V., and Filimonova, L.E., 1986, [Porphyry copper deposits of the Balkhash region]: Nauka, Alma Ata, 199 p. [In Russian.]
- Lero Gold Corporation, 2007 Annual Report: Lero Gold Corporation, 13 p. (Also available at <http://www.sedar.com>.)
- Levashova, N.M., Mikolaichuk, A.V., McCausland, P.J.A., Baxhenov, M.L., and Van der Voo, R., 2007, Devonian paleomagnetism of the north Tien Shan—Implications for the middle-late Paleozoic paleogeography of Eurasia: *Earth and Planetary Science Letters*, v. 257, p. 104–120.
- Medvedev, V.Y., and Kislyakova, N.I., 1963, [Map of mineral resources of the U.S.S.R., North Tian Shan series, Sheet K-43-XIII]: Ministry of Geology and Mineral Resources Protection, scale 1:200,000. [In Russian.]
- National Oceanic and Atmospheric Administration, 1996, Magnetic anomaly data of the former U.S.S.R.: National Geophysical Data Center, Boulder, Colorado, accessed August 1, 2010, at <http://www.ngdc.noaa.gov>.
- Newall, Phil, 2005, Resource audit of the Andash project, northwest Kyrgystan: Wardell Armstrong International Limited, prepared for Aurum Mining, accessed October 15, 2011, at http://www.aurummining.net/documents/da6m67fq_1160663453.doc.
- Oakes, B., Kay, B.D., and Arifiev, V., 1998, The Jerooy gold deposit, Kyrgyz Republic, in Porter, T.M., ed., Porphyry and hydrothermal copper and gold deposits, a global perspective: Glenside, South Australia, Conference Proceedings, Australian Mineral Foundation, p. 191–196.
- Orsu Metals Corporation, 2011, Barkol license—North West Kyrgyzstan: Orsu Metals Corp. Web site, accessed October 11, 2011, at <http://www.orsumetals.com/barkol.aspx>.
- Orsu Metals Corporation, 2012, Orsu Metals Corporation—A base & precious metal exploration & development company—March 2012: Orsu Metals Corp., Accessed August 12, 2013, at http://minesite.com/media/pub/var/conference_presenter_presentation_file/126.pdf.
- Paretseki, I.I., and Akhamatullin, A.K., 1987, [State geological map of the U.S.S.R., Betpakdala series, Sheet K-43-IV]: Ministry of Geology of the U.S.S.R., scale 1:200,000. [In Russian.]
- Pavlova, I.G., 1978, [Porphyry copper deposits]: Leningrad, Nedra, 275 p. [In Russian.]
- Plyushchev, E.V., 1993, Map of hydrothermal-metasomatic formations of Kazakhstan fold area: St. Petersburg, VSEGEI, 4 sheets, scale 1:1,500,000.
- Proactive Investors, 2010, Kentor Gold gains exclusive window to acquire Aktash gold-copper deposit: Proactive Investors Web page, accessed October 1, 2011, at <http://www.proactiveinvestors.com.au/companies/news/8793/kentor-gold-gains-exclusive-window-to-acquire-aktash-gold-copper-deposit-8793.html>.
- Root, D.H., Menzie, W.D., and Scott, W.A., 1992, Computer Monte Carlo simulation in quantitative resource estimation: *Natural Resources Research*, v. 1, no. 2, p. 125–138.
- Seltmann, R., and Jenchuraeva, R., eds., 2001, Paleozoic geodynamics and gold deposits in the Kyrgyz Tien Shan: Excursion Guidebook of IGCP-373 International Field Conference in Bishkek and the Kyrgyz Tien Shan, Kyrgyz Republic, 16–25 August 2001, IAGOD Guidebook series 9, Natural History Museum, London, 183 p.
- Seltmann, R., and Porter, T.M., 2005, The porphyry Cu-Au/Mo deposits of Central Eurasia. 1. Tectonic, geologic and metallogenic setting, and significant deposits, in Porter, T.M., ed., Superporphyry copper and gold deposits—A global perspective: Adelaide, PGC Publishing, v. 2, p. 467–512.
- Seltmann, R., Shatov, V., and Yakubchuk, A., 2009, Mineral deposits database and thematic maps of Central Asia—ArcGIS 9.2, Arc View 3.2, and MapInfo 6.0(7.0) GIS packages: London, Natural History Museum, Centre for Russian and Central EurAsian Mineral Studies (CERCAMS), scale 1:1,500,000, and explanatory text, 174 p. [Commercial dataset available at <http://www.nhm.ac.uk/research-curation/research/projects/cercams/products.html>.]

- Singer, D.A., Berger, V.I., and Moring, B.C., 2008, Porphyry copper deposits of the world: U.S. Geological Survey Open-File Report 2008-1155, 45 p., accessed August 10, 2009, at <http://pubs.usgs.gov/of/2008/1155/>.
- Singer, D.A., and Menzie, W.D., 2005, Statistical guides to estimating the number of undiscovered mineral deposits—An example with porphyry copper deposits, *in* Cheng, Qiuming, and Bonham-Carter, Graeme, eds., Proceedings of IAMG—The annual conference of the International Association for Mathematical Geology: Toronto, Canada, York University, Geomatics Research Laboratory, p. 1028–1033.
- Sobel, E.R., Oskin, M., Burbank, D., and Mikolaichuk, A., 2006, Exhumation of basement-cored uplifts—Example of the Kyrgyz Range quantified with fission track thermochronology: *Tectonics*, v. 25, no. 2, 17 p.
- Sokolov, A.L., 1999, Regional and local controls on gold and copper mineralization in central Asia and Kazakhstan, *in* Porter, T.M., ed., Porphyry and hydrothermal copper and gold deposits—A global perspective, Conference Proceedings: Australian Mineral Foundation, Glenside, South Australia, p. 181–190.
- Stepanenko, A.F., 1959, New data on the Sinian and lower Paleozoic deposits in the western Kyrgyz Range, northern Tian Shan: *Izvestiya, Academy of Sciences, U.S.S.R., B., Geologic Series* no. 9, p. 58–70.
- Stepanenko, A.F., Medvedev, I.E., and Stepanenko, M.A., 1963, [Geological map of the U.S.S.R., North Tian Shan series, Sheet K-43-VII]: Ministry of Geology and Mineral Resources Protection, scale 1:200,000. [In Russian.]
- Tagiri, M., Yano, T., Bakirov, A., Nakajima, T., and Uchiumi, S., 1995, Mineral parageneses and metamorphic P-T paths of ultrahigh-pressure eclogites from Kyrgyzstan Tien Shan: *Island Arc*, v. 4, p. 280–292.
- U.N. Economic and Social Commission for Asia and the Pacific, 1998, Atlas of mineral resources of the ESCAP region, v. 13, Geology and mineral resources of Kyrgystan: New York, United Nations, 153 p.
- Wardell Armstrong International, 2010, Updated technical report on the Taldybulak property, Kyrgyzstan: Orsu Metals Corporation, NI 43-101 Technical Report, prepared for Orsu Metals Corporation, 205 p.
- Windley, B.F., Alexeiev, D., Xiao, W., Kroner, A., and Badarch, G., 2007, Tectonic models for accretion of the Central Asian Orogenic Belt: *Journal of the Geological Society, London*, v. 164, p. 31–47.
- Zhukov, N.M., Kolesnikov, V.V., Miroshnichenko, L.M., Egembaev, K.M., Pavlova, Z.N., and Bakarasov, E.V., compilers, 1998, Copper deposits of Kazakhstan—Reference book: Almaty, Ministry of Ecology and Natural Resources of the Republic of Kazakhstan, 136 p.

Appendix C. Porphyry Copper Assessment for Sub-tract 142pCu8003a, Late Paleozoic Balkhash-Ili Magmatic Arc (East)—Kazakhstan

By Byron R. Berger¹, Paul D. Denning¹, Connie L. Dicken², Jane M. Hammarstrom², John C. Mars², Jeffrey D. Phillips¹, and Michael L. Zientek³

Deposit Type Assessed: Porphyry Copper

Descriptive model: Porphyry copper (Cox, 1986; Berger and others, 2008)

Grade and tonnage model: Global Cu-Au-Mo porphyry copper model (Singer and others, 2008)

Selected results are summarized in table C1.

Table C1. Summary of selected resource assessment results for sub-tract 142pCu8003a, Late Paleozoic Balkhash-Ili magmatic arc (east)—Kazakhstan.

[km, kilometers; km², square kilometers; t, metric tons]

Date of assessment	Assessment depth (km)	Tract area (km ²)	Known copper resources (t)	Mean estimate of undiscovered copper resources (t)	Median estimate of undiscovered copper resources (t)
2009	1	47,240	10,280,400	11,000,000	4,600,000

Location

Tract 142pCu8003 comprises four permissive Carboniferous arc terrains (sub-tracts a, b, c, and d) that surround the eastern part of the Balkhash Depression (see fig. 1-2⁴). Permissive sub-tract 142pCu8003a (fig. C1) is located in east-central Kazakhstan, the eastern part of a generally horseshoe-shaped area (see figs. 1-29 and 1-30) of Carboniferous magmatic-arc activity. The region is made up of low-relief, hilly countryside east of the Balkhash geographic depression. In general, it is within the Balkhash-Ili tectonic terrane (see fig. 1-22) of Windley and others (2007). The area extends from northeast of Lake Balkhash southeast to the China border. The city of Ucharal (lat 46.18° N., long 80.95° E.) is near the southwest boundary of the tract about 125 kilometers (km) northwest of the China border. The assessment does not include that part of the permissive terrane that extends into China.

Geologic Feature Assessed

The permissive sub-tract encompasses latest Early Carboniferous (C₂) to Permian (P₁) magmatic-arc and postcollisional rocks. The distribution of permissive volcanic, volcanoclastic, and intrusive rocks in tract 142pCu8003a is shown in fig. C2.

¹U.S. Geological Survey, Denver, Colorado.

²U.S. Geological Survey, Reston, Virginia.

³U.S. Geological Survey, Spokane, Washington.

⁴Refer to chapter 1 of this report.

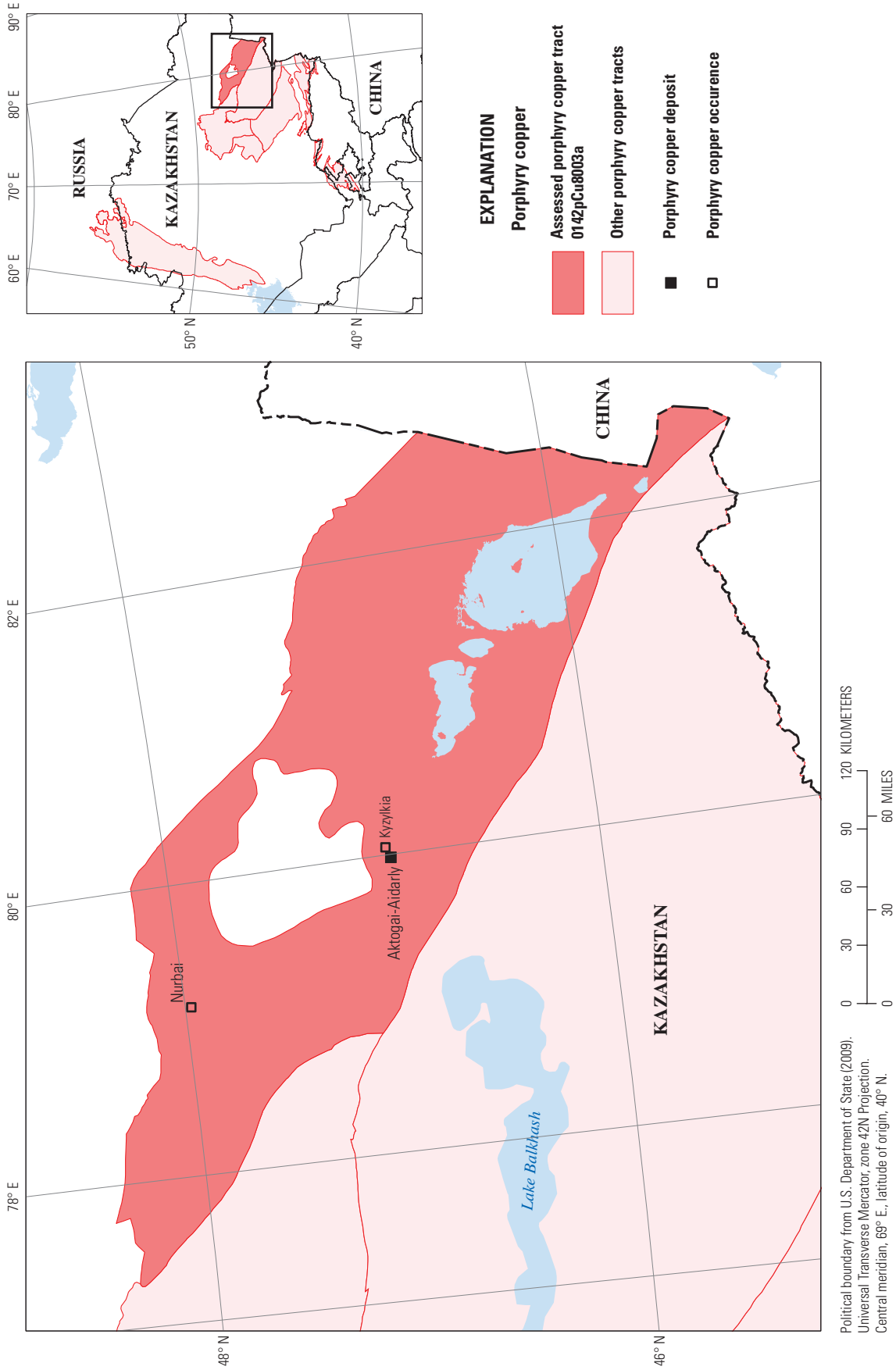


Figure C1. Map showing the location, known deposits, and significant prospects and occurrences for sub-tract 142pCu8003a, Late Paleozoic Balkhash-Ili magmatic arc (east)—Kazakhstan. Location of map area shown on inset.

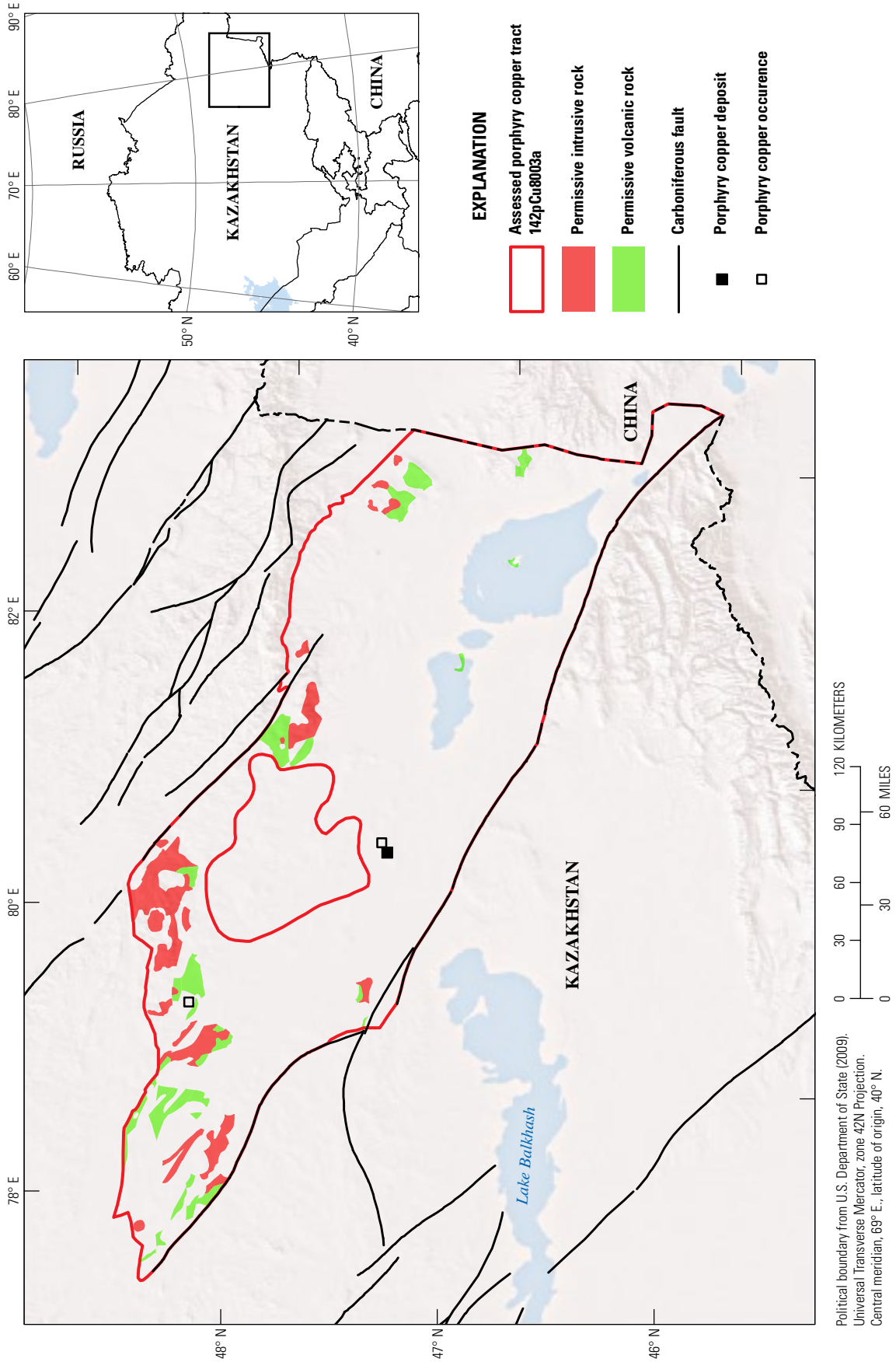


Figure C2. Map of permissive Carboniferous volcanic and volcaniclastic rocks (green) and intrusive rocks (red) in sub-tract 142pCu8003a, Late Paleozoic Balkhash-Ili magmatic arc (east)—Kazakhstan, on a digital elevation base. Location of map area shown on inset.

Delineation of the Permissive Tract

Geologic Criteria

The principal tectonic concept used to delineate sub-tract 142pCu8003a was that of a magmatic arc formed in the subduction boundary zone above a subducting plate. Five principal sources of information, supplemented by numerous published journal and symposium papers, were used to delineate this tract. The primary sources were the mineral deposits map of Central Asia on a geologic base edited by Seltmann and others (2009), supplemented by four 1:200,000-scale geologic maps originally published by the former Soviet (U.S.S.R.) government, a reduced-to-pole aeromagnetic map prepared by J.D. Phillips from NOAA (1996), the interpretation of Advanced Spaceborne Thermal Emission and Reflection Radiometer (ASTER) satellite imagery of hydrothermal alteration minerals or suites of minerals by J.C. Mars (chapter 2 of this report), the tectonic terrane map of Windley and others (2007), and stratigraphic and structural expertise provided by Dr. Dmitriy Alexeiev of the Russian Academy of Science, Moscow.

Central Asia is an amalgamation of Precambrian basement fragments, accreted Paleozoic terranes, and overlying Early to Middle Paleozoic magmatic arcs (Windley and others, 2007). The permissive Carboniferous magmatic arc was built on this complex basement that had been deformed one or more times prior to arc-related magmatism. Further, the present distribution of permissive rocks has been structurally rearranged since arc magmatism, largely through strike-slip tectonics (D. Alexeiev, Russian Academy of Science, unpublished data, 2008).

Tract 142pCu8003a adjoins permissive tract 142pCu8003b to the northwest, permissive tract 142pCu8004 to the south of 142pCu8003b, nonpermissive terrain to the east and the China border to the southeast. Permissive ground persists into China, but that area was not assessed in this study.

The two most important attributes used to delineate the permissive tract boundaries were outcrops of rock suites that are one or more of the following: C₁₋₃ volcanic, volcanogenic, and volcanoclastic rocks, C₃ plutonic-rock complexes, and (or) Middle to Late Carboniferous porphyry copper-type deposits and occurrences. Although the ages of different rock groups are relatively well documented by Seltmann and others (2009), there is uncertainty as to the ages of known deposits and occurrences. This raises the uncertainty level in the assessment of this tract.

The first step in tract delineation was to identify all geologic units on the Seltmann and others (2009) geologic map that do, or are interpreted to, consist of Middle and Late Carboniferous arc-related volcanic and intrusive rocks (fig. C2). This initial delineation included the region now delineated as tract 142pCu8004 in the Balkhash Depression. The area that is now 142pCu8004 was put into a separate permissive

tract from 142pCu8003a due to the significant difference in the magnetic susceptibility of the rocks in this one area vis-à-vis the rest of the Carboniferous terrane, extensive postmineralization cover in the Balkhash Depression, and the lack of any known porphyry copper deposits, although occurrences are known to the north of Lake Balkhash. Sub-tract 142pCu8003a is one of four permissive Carboniferous arc terrains that surround the eastern part of the Balkhash Depression. The subdividing was done owing to regional-scale geologic differences between the sub-tracts with respect to levels of exposure and numbers of known porphyry copper deposits and (or) occurrences. The criteria for delineation of each sub-tract are discussed in separate appendixes.

Sub-tract 142pCu8003a makes up the easternmost part of the permissive Carboniferous magmatic-arc terrane. It contains a considerable amount and spatial continuity of postcollisional Permian rocks, including flood basalts that in some places exceed 1 km in thickness and have been removed from consideration within the tract, and arc-related Middle to Late Carboniferous volcanic rocks have been largely eroded away. The northern and eastern boundaries of 142pCu8003a were drawn to include mapped outcrops of C₂ and C₃ permissive rocks. Wherever the boundaries of these permissive units were interpreted to be major fault zones with large displacements, the boundary was placed along the fault zone. The southeastmost boundary was placed at the Kazakhstan-China border. The southwestern boundary that adjoins sub-tract 142pCu8004 is drawn along a structural boundary, northeast of which the rocks are predominantly Permian, southwest of which, in permissive tract 142pCu8004, the rocks are predominantly Devonian to Carboniferous, and there is a marked change in the aeromagnetic patterns as already noted. To the southwest of the boundary, rocks of lower magnetic susceptibility predominate.

Known Deposits

Singer and others (2008) show one known deposit in this sub-tract, the Aktogai deposit (fig. C1, includes Aidarly in Singer and others, 2008; table C2).

Aktogai-Aidarly

Aktogai, as used by Singer and others (2008), refers to the combined resources of the nearby Aktogai and Aidarly deposits because their outermost hydrothermal alteration zones are separated by less than 2 km. The deposits are part of a Late Carboniferous to Lower Permian intrusive complex known as the Koldarsky Massif (Zhukov and others, 1998) that was emplaced into a sequence of Early to Late Carboniferous volcanic and volcanoclastic rocks. The 75 square kilometers (km²) exposure of intrusive rocks includes gabbro, diorite, granodiorite, and granite along with quartz and dacite porphyry, plagiogranite porphyry, and granodiorite porphyry dikes.

Table C2. Porphyry copper deposits in sub-tract 142pCu8003a, Late Paleozoic Balkhash-Ili magmatic arc (east)—Kazakhstan.

[Ma, mega-annum (10^6 years); km², square kilometers; t, metric tons; Mt, million metric tons, %, percent; g/t, grams per metric ton; Cu, copper; Mo, molybdenum; Au, gold; Ag, silver]

Name	Latitude	Longitude	Subtype	Age (Ma)	Tonnage (Mt)	Cu (%)	Mo (%)	Au (g/t)	Ag (g/t)	Contained Cu (t)	Reference
Aktogai-Aidarly	46.970	79.979	Cu-Mo	333	2,636	0.39	0.01	0.03	1.43	10,280,400	Berzina and others (2005), Cooke and others (2005), Kolesnikov and others (1986), Krivtsov and others (1986), Mutschler and others (2000), Pavlova (1978), Seltmann and Porter (2005), Sokolov (1999), Zhukov and Filimonova (1982), Zvezdov and others (1993)

The Aktogai deposit is hosted by diorites and granodiorites that intrude into a suite of volcanoclastic rocks of dacite to rhyolite composition (Zhukov and others, 1998). The copper-molybdenum ore zone is elliptical in plan view, extending for 2,500 meters (m) west-northwest and is as much as 850 m wide. It extends down dip for greater than 800 m. The principal ore minerals are bornite, chalcocopyrite, chalcocite, and pyrite. There are small amounts of sphalerite and galena in the outer parts of the alteration sequence.

The Aidarly deposit is associated with diorite, granodiorite and granite along with numerous dikes of granodiorite porphyry, plagiogranite porphyry, and microgranite (Zhukov and others, 1998). Aidarly is elliptical in plan view with a long axis elongated northwest-southeast. The deposit has been deformed with the northwest end of the deposit displaced more than 1 km to the west-southwest by a left-lateral strike-slip fault.

Porphyry Copper Occurrences and Related Deposit Types

In addition to the known deposits in the Aktogai ore field, several porphyry-style copper occurrences have been identified and explored to varying extents (table C3). The most completely explored and described is Kyzylkia, 2–3 km northeast of the Aktogai deposit. Other porphyry-style occurrences include Western, Promezhutochny, and Eastern (Zhukov and others, 1998). Seltmann and others (2009) indicate that the prospects are copper-molybdenum, molybdenum-copper, and copper-gold.

Nurbai

Nurbai (fig. C1) is in the Shubartau District, Semipalatinsk Province (Zhukov and others, 1998). The

deposit is in Middle Devonian porphyritic lavas, tuffs, and volcanoclastic sandstones intruded by Middle to Late Carboniferous monzonite and monzonite porphyry. There is extensive siliceous alteration of the metavolcanic and metasedimentary rocks characterized by quartz with abundant diaspore and andalusite. The intrusive rocks are extensively altered to quartz + sericite. The mineralization is controlled by northwest-striking faults. The higher grade mineralization occurs along the fault zone for as long as 1,400 m with widths to 200 m. Hydrothermal alteration along the fault zone is intermittent over a 10-km strike length.

Kyzylkia

The Kyzylkia molybdenum-copper occurrence (fig. C1) is associated with a small granodiorite porphyry stock that intrudes Late Carboniferous granodiorites (Zvezdov and others, 1993). It is part of the Aktogai-Aidarly group. Ore minerals in stockwork veins include chalcocite, bornite, and chalcocopyrite in a potassic and sericitic gangue. Zvezdov and others (1993) consider Kyzylkia to be deeply eroded.

About 70–90 km west-northwest of Aktogai, Seltmann and others (2009) show several porphyry-style occurrences. There are several more occurrences about 100 km north of Aktogai, including those containing copper, copper-molybdenum, copper-gold, and gold-molybdenum. About 75–110 km to the northeast of Aktogai are several porphyry-style occurrences including copper-gold, copper-molybdenum, and molybdenum.

Exploration History

No historical record of exploration was compiled for this tract.

Table C3. Significant porphyry copper occurrences in sub-tract 142pCu8003a, Late Paleozoic Balkhash-Ili magmatic arc (east)—Kazakhstan.

[Ma, mega-annum (10^6 years); t, metric tons; Mt, million metric tons, %, percent; g/t, grams per metric ton; km, kilometers; NW, northwest; Cu, copper; Mo, molybdenum; Au, gold; and Ag, silver; Re, rhenium; Se, selenium; n.d., no data]

Name	Country	Latitude	Longitude	Age (Ma)	Comments	Reference
Kyzylkia	Kazakhstan	46.987	80.053	n.d.	Eroded Cu-Mo prospect associated with a granodiorite porphyry stock in the Aktogai district. Location based on grid road pattern, trenches on Google Earth (3/5/10); 14 km NW of Singer and others (2008) location. Grade: 0.36% Cu (?), 0.01% Mo, 0.24 g/t Re, 1.8 g/t Se, 0.007–0.40g/t Au, 1.8 g/t Ag. Location spelled “Qyzylkiya” in Seltmann and others (2009) is located ~ 1 km NW of location from Google Earth; evidence of exploration activity on Google Earth (3/5/10), but most of road grid pattern is to south	Seltmann and others (2009), Zvezdov and others (1993)
Nurbai	Kazakhstan	47.972	79.157	n.d.	Grades reported: average 0.5% Cu, 0.001 0.03% Mo. Location: Grid road pattern, trenches on Google Earth (3/5/10); 14 km NW of Singer and others (2008) location	Zhukov and others (1998)

Hydrothermal Alteration Mapping (ASTER)⁵

Argillic, phyllic and silicic ASTER hydrothermal alteration mapping covers approximately 60 percent of sub-tract 142pCu8003a (see figs. 2-1 and 2-2). Using the ASTER hydrothermal alteration map, 7 sites having alteration patterns consistent with porphyry copper or epithermal deposits were defined in the northeastern part of the tract (see fig. 2-13 and plates 1–8). Copper occurrences are located at 4 of the sites (see table 2-1). The geologic map indicates that altered rocks at the sites include trachydacite tuff, dacite, granite, and rhyolite (see table 2-1). No significant deposits or prospects are associated with the mapped alteration sites, based on comparison of the ASTER hydrothermal alteration map with point data from mineral databases.

Sources of Information

Principal sources of information used by the assessment team for delineation of 142pCu8003a are listed in table C4 and in the bibliography.

Grade and Tonnage Model Selection

The general porphyry copper deposit model published by Singer and others (2008) was used based on the known deposits in the tract being statistically consistent with the model.

Estimate of the Number of Undiscovered Deposits

Rationale for the Estimate

Following discussion and evaluation of the available data, the assessment team concluded that (1) the ratio of porphyry copper occurrences and possible linked deposit types to the number of known deposits was moderate and therefore a positive indication of undiscovered deposits, (2) the depth of erosion of the terrane was not a concern although high-strain deformation is a concern along and adjacent to suture zones, and (3) owing to the low relief, remoteness of much of the area, and partial cover by post-Carboniferous volcanic rocks, there were plays left despite Soviet-era exploration investment in the region.

The sub-tract hosts the Aktogai-Aidarly porphyry copper deposit (table C2), two partially characterized significant porphyry copper occurrences (table C3), and seven additional

⁵Refer to figures, tables, and plates in chapter 2 of this report.

Table C4. Principal sources of information used for delineation of sub-tract 142pCu8003a, Late Paleozoic Balkhash-Ili magmatic arc (east)—Kazakhstan.

Theme	Name or title	Scale	Citation
Geology	Mineral deposits database and thematic maps of Central Asia	1:1,500,000	Seltmann and others (2009)
	Tectonic map of the Paleozoic folded areas of Kazakhstan and adjacent territories	1:1,500,000	Abdulin and Zaitseb (1976)
	L-44-I (1962)	1:200,000	Rosenkrantse and others (1962)
	L-44-II (1963)	1:200,000	Rosenkrantse and others (1963)
	L-44-III (1962)	1:200,000	Rosenkrantse and others (1962)
	L-44-VI (1959)	1:200,000	Bespalov (1959)
	L-44-VII (1955)	1:200,000	Galitsekitse (1955)
	L-44-VIII (1957)	1:200,000	Staal (1957)
	L-44-IX (1962)	1:200,000	Rosenkrantse (1962)
	L-44-XIV (1960)	1:200,000	Ponomarev and Davydov (1960)
	L-44-XV (1959)	1:200,000	Gendlev and others (1959)
	M-44-XXXI (1960)	1:200,000	Mychekin and Reshaetov (1960)
	M-44-XXXII (1960)	1:200,000	Borikaev and others (1960)
	M-44-XXXIII (1960)	1:200,000	Mychenik and Reshaetov (1960)
Mineral occurrences	Mineral deposits database and thematic maps of Central Asia	1:1,500,000	Seltmann and others (2009)
Geophysics	Magnetic anomaly data of the former U.S.S.R.	1:1,500,000	National Oceanic and Atmospheric Administration (1996)

Table C5. Undiscovered deposit estimates, deposit numbers, tract area, and deposit density for tract 142pCu8003a, Late Paleozoic Balkhash-Ili magmatic arc (east)—Kazakhstan.

[N_{xx} , estimated number of deposits associated with the xx th percentile; N_{und} , expected number of undiscovered deposits; s , standard deviation; $C_v\%$, coefficient of variance; N_{known} , number of known deposits in the tract that are included in the grade and tonnage model; N_{total} , total of expected number of deposits plus known deposits; area, area of permissive tract in square kilometers (km^2); density, deposit density reported as the total number of deposits per 100,000 km^2 . N_{und} , s , and $C_v\%$ are calculated using a regression equation (Singer and Menzie, 2005)]

Consensus undiscovered deposit estimates					Summary statistics					Tract area (km^2)	Deposit density ($N_{total}/100k km^2$)
N_{90}	N_{50}	N_{10}	N_{05}	N_{01}	N_{und}	s	$C_v\%$	N_{known}	N_{total}		
1	2	6	6	6	2.8	2	70	1	3.8	47,240	8

sites with permissive alteration patterns. The team estimated a 90-percent chance of 1 or more undiscovered deposits, a 50-percent chance of 2 or more, and a 10-percent chance of 6 or more deposits. The mean number of deposits associated with this distribution is 2.8 undiscovered deposits (table C5).

Probabilistic Assessment Simulation Results

Undiscovered resources for the tract were estimated by combining consensus estimates for numbers of undiscovered porphyry copper deposits with the general porphyry copper

grade and tonnage model of Singer and others (2008) using the EMINERS program (Root and others, 1992; Bawiec and others, 2012; Duval, 2012). Selected simulation results are reported in table C6. Results of the Monte Carlo simulation are presented as a cumulative frequency plot (fig. C3). The cumulative frequency plot shows the estimated resource amounts associated with cumulative probabilities of occurrence, as well as the mean, for each commodity and for total mineralized rock.

Based on the simulation, the expected (mean) amount of copper in undiscovered deposits, 11 million metric tons (Mt), is comparable to the identified resources, 10 Mt (table C6).

Table C6. Results of Monte Carlo simulations of undiscovered resources for sub-tract 142pCu8003a, Late Paleozoic Balkhash-Ili magmatic arc (east)—Kazakhstan.

[Cu, copper; Mo, molybdenum; Au, gold; and Ag, silver; in metric tons. Rock, in million metric tons]

Material	Probability of at least the indicated amount						Probability of	
	0.95	0.9	0.5	0.1	0.05	Mean	Mean or greater	None
Cu	0	160,000	4,600,000	25,000,000	42,000,000	11,000,000	0.28	0.07
Mo	0	0	56,000	680,000	1,200,000	290,000	0.22	0.25
Au	0	0	96	700	1,100	280	0.26	0.21
Ag	0	0	560	7,900	15,000	3,800	0.2	0.34
Rock	0	43	1,000	5,300	8,100	2,200	0.29	0.07

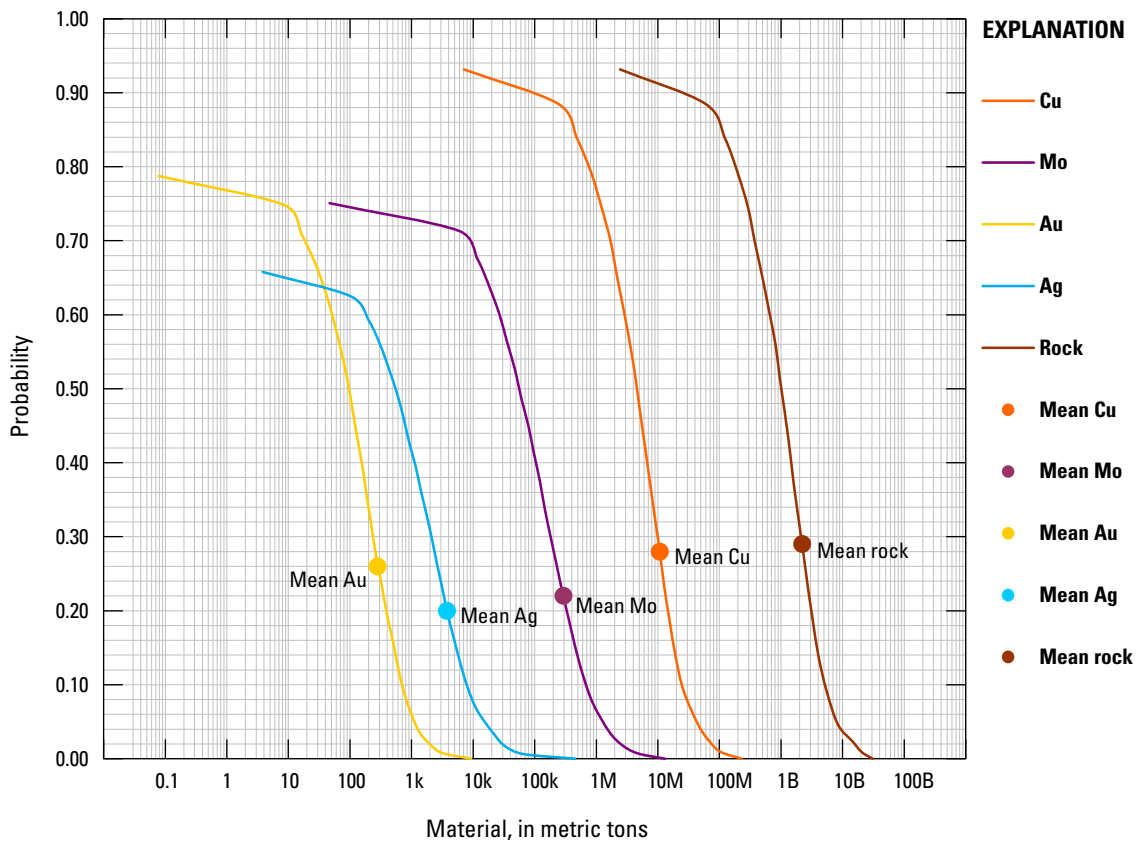


Figure C3. Cumulative frequency plot showing the results of Monte Carlo computer simulation of undiscovered resources in sub-tract 142pCu8003a, Late Paleozoic Balkhash-Ili magmatic arc (east)—Kazakhstan. k=thousands, M=millions, B=billions.

References Cited

- Abduln, A.A., and Zaitseb, Yu.A., eds., 1976, [Tectonic map of the Paleozoic folded belts of Kazakhstan and adjacent territories]: Ministry of Geology of the U.S.S.R., VSEGEI, 1 map on 6 sheets, scale 1:1,500,000. [In Russian.]
- Bawiec, W.J., and Spanski, G.T., 2012, Quick-start guide for version 3.0 of EMINERS—Economic Mineral Resource Simulator: U.S. Geological Survey Open-File Report 2009–1057, 26 p., accessed July 15, 2012, at <http://pubs.usgs.gov/of/2009/1057/>. (This report supplements USGS OFR 2004–1344.)
- Berger, B.R., Ayuso, R.A., Wynn, J.C., and Seal, R.R., 2008, Preliminary model of porphyry copper deposits: U.S. Geological Survey Open-File Report 2008–1321, 55 p., accessed May 15, 2009, at <http://pubs.usgs.gov/of/2008/1321/>.
- Berzina, A.N., Sotnikov, V.I., Economou-Eliopoulos, M., and Eliopoulos, D.G., 2005, Distribution of rhenium in molybdenite from porphyry Cu-Mo and Mo-Cu deposits of Russia (Siberia) and Mongolia: *Ore Geology Reviews*, v. 26, p. 91–113.
- Bespalov, V.F., 1959, [Geological map of the U.S.S.R., Balkhash series, Sheet L-43-VI]: Ministry of Geology and Mineral Resources Protection, scale 1:200,000. [In Russian.]
- Borikaev, R.A., Ergalinev, G.H., Karagodin, P.F., and Tseai, D.T., 1960, [Map of mineral resources of the U.S.S.R., Chingiz-Saur Series, Sheet M-44-XXXII]: Ministry of Geology and Mineral Resources Protection, scale 1:200,000. [In Russian.]
- Cooke, D.R., Hollings, P., and Walshe, J.L., 2005, Giant porphyry deposits—Characteristics, distribution, and tectonic controls: *Economic Geology*, v. 100, p. 801–818.
- Cox, D.P., 1986, Descriptive model of porphyry Cu (Model 17), in Cox, D.P., and Singer, D.A., eds., 1986, *Mineral deposit models*: U.S. Geological Survey Bulletin 1693, p. 76. (Also available at <http://pubs.usgs.gov/bul/b1693/>.)
- Duval, J.S., 2012, Version 3.0 of EMINERS—Economic Mineral Resource Simulator: U.S. Geological Survey Open-File Report 2004–1344, accessed July 15, 2012, at <http://pubs.usgs.gov/of/2004/1344>.
- Galitsekits, V.V., 1955, [Geological map of the U.S.S.R., eastern Circum-Balkhash Series, Sheet L-44-VII]: Ministry of Geology and Mineral Resources Protection, scale 1:200,000 [In Russian.]
- Gendlev, V.E., Sonin, I.I., and Lisovskaya, E.V., 1959, [Geological map of the U.S.S.R., Dzungar Series, Sheet L-44-XV]: Ministry of Geology and Mineral Resources Protection, scale 1:200,000. [In Russian.]
- Kolesnikov, V.V., Zhukov, N.M., Solodilova, V.V., and Filimonova, L.E., 1986, [Porphyry copper deposits of the Balkhash region]: Nauka, Alma Ata, 199 p. [In Russian.]
- Krivtsov, A.I., Migachev, I.F., and Popov, V.S., 1986, [Porphyry copper deposits of the world]: Moscow, Nedra, 236 p. [In Russian.]
- Mutschler, F.E., Ludington, S., and Bookstrom, A.A., 2000, Giant porphyry-related metal camps of the world—A database: U.S. Geological Survey Open-File Report 99–556, accessed September 9, 2012, at <http://pubs.er.usgs.gov/usgspubs/ofr/ofr99556/>.
- Mychekin, M.B., and Reshaetov, R.N., 1960, [Map of mineral resources of the U.S.S.R., Chingiz-Saur Series, Sheet M-44-XXXI]: Ministry of Geology and Mineral Resources Protection, scale 1:200,000. [In Russian.]
- Mychenik, M.B., and Reshetov, R.N., 1960, [Geological map of the U.S.S.R., Chingiz-Saur Series, Sheet M-44-XXXIII]: Ministry of Geology and Mineral Resources Protection, scale 1:200,000. [In Russian.]
- National Oceanic and Atmospheric Administration, 1996, *Magnetic anomaly data of the former U.S.S.R.*: National Geophysical Data Center, Boulder, Colorado, accessed August 1, 2010, at <http://www.ngdc.noaa.gov>.
- Pavlova, I.G., 1978, [Porphyry copper deposits]: Leningrad, Nedra, 275 p. [In Russian.]
- Ponomarev, B.Y., and Davydov, N.M., 1960, [Geological map of the U.S.S.R., Circum-Balkhash Series, Sheet L-44-XIV]: Ministry of Geology and Mineral Resources Protection, scale 1:200,000. [In Russian.]
- Root, D.H., Menzie, W.D., and Scott, W.A., 1992, Computer Monte Carlo simulation in quantitative resource estimation: *Natural Resources Research*, v. 1, no. 2, p. 125–138.
- Rosenkrantse, A.A., 1962, [Map of mineral resources of the U.S.S.R., Chingiz-Saur Series, Sheet L-44-IX]: Ministry of Geology and Mineral Resources Protection, scale 1:200,000. [In Russian.]
- Rosenkrantse, A.A., Gushchain, A.V., and Kovaleva, V.V., 1962, [Map of mineral resources of the U.S.S.R., Circum-Balkhash Series, Sheet L-44-I]: Ministry of Geology and Mineral Resources Protection, scale 1:200,000. [In Russian.]

- Rosenkrantse, A.A., Gushchain, A.V., Kovaleva, V.V., Kozitskaya, E.A., Lebedeva, L.I., and Staal, M.B., 1963, [Geological map of the U.S.S.R., Chingiz-Saur Series, Sheet L-44-II]: Ministry of Geology and Mineral Resources Protection, U.S.S.R., scale 1:200,000. [In Russian.]
- Rosenkrantse, A.A., Gushchain, A.V., Kovaleva, V.V., and Tverdislov, Y.A., 1962, [Map of mineral resources of the U.S.S.R., Chingiz-Saur Series, Sheet L-44-III]: Ministry of Geology and Mineral Resources Protection, scale 1:200,000. [In Russian.]
- Seltmann, R., and Porter, T.M., 2005, The porphyry Cu-Au/Mo deposits of Central Eurasia. 1. Tectonic, geologic and metallogenic setting, and significant deposits, *in* Porter, T.M., ed., Superporphyry copper and gold deposits—A global perspective: Adelaide, PGC Publishing, v. 2, p. 467–512.
- Seltmann, R., Shatov, V., and Yakubchuk, A., 2009, Mineral deposits database and thematic maps of Central Asia—ArcGIS 9.2, Arc View 3.2, and MapInfo 6.0(7.0) GIS packages: London, Natural History Museum, Centre for Russian and Central EurAsian Mineral Studies (CERCAMS), scale 1:1,500,000, and explanatory text, 174 p. [Commercial dataset available at <http://www.nhm.ac.uk/research-curation/research/projects/cercams/products.html>.]
- Singer, D.A., Berger, V.I., and Moring, B.C., 2008, Porphyry copper deposits of the world: U.S. Geological Survey Open-File Report 2008–1155, 45 p., accessed August 10, 2009, at <http://pubs.usgs.gov/of/2008/1155/>.
- Singer, D.A., and Menzie, W.D., 2005, Statistical guides to estimating the number of undiscovered mineral deposits—An example with porphyry copper deposits, *in* Cheng, Qiuming, and Bonham-Carter, Graeme, eds., Proceedings of IAMG—The annual conference of the International Association for Mathematical Geology: Toronto, Canada, York University, Geomatics Research Laboratory, p. 1028–1033.
- Sokolov, A.L., 1999, Regional and local controls on gold and copper mineralization in central Asia and Kazakhstan, *in* Porter, T.M., ed., Porphyry and hydrothermal copper and gold deposits—A global perspective, Conference Proceedings: Glenside, South Australia, Australian Mineral Foundation, p. 181–190.
- Staal, M.B., 1957, [Geological map of the U.S.S.R., Circum-Balkhash Series, Sheet L-44-VIII]: Ministry of Geology and Mineral Resources Protection, scale 1:200,000. [In Russian.]
- Windley, B.F., Alexeiev, D., Xiao, W., Kroner, A., and Badarch, G., 2007, Tectonic models for accretion of the Central Asian Orogenic Belt: London, Journal of the Geological Society, v. 164, p. 31–47.
- Zhukov, N.M., and Filimonova, L.E., 1982, [Metasomatites and hypogene mineralization in the Aktogai porphyry copper deposit]: *Geology of Ore Deposits*, v. 24, no. 2, p. 102–110. [In Russian.]
- Zhukov, N.M., Kolesnikov, V.V., Miroshnichenko, L.M., Egembayev, K.M., Pavlova, Z.N., and Bakarasov, E.V., compilers, 1998, Copper deposits of Kazakhstan—Reference book: Almaty, Ministry of Ecology and Natural Resources of the Republic of Kazakhstan, 136 p.
- Zvezdov, V.S., Migachev, I.F., and Girfanov, M.M., 1993, Porphyry copper deposits of the CIS and the models of their formation: *Ore Geology Reviews*, v. 7, p. 511–549.

Appendix D. Porphyry Copper Assessment for Sub-tract 142pCu8003b, Late Paleozoic Balkhash-Ili Magmatic Arc (North)—Kazakhstan

By Byron R. Berger¹, Paul D. Denning¹, Connie L. Dicken², Jane M. Hammarstrom², John C. Mars², Jeffrey D. Phillips¹, and Michael L. Zientek³

Deposit Type Assessed: Porphyry Copper

Descriptive model: Porphyry copper (Cox, 1986; Berger and others, 2008)

Grade and tonnage model: Global Cu-Au-Mo porphyry copper model (Singer and others, 2008)

Table D1 summarizes selected assessment results.

Table D1. Summary of selected resource assessment results for sub-tract 142pCu8003b, Late Paleozoic Balkhash-Ili magmatic arc (north)—Kazakhstan.

[km, kilometers; km², square kilometers; t, metric tons]

Date of assessment	Assessment depth (km)	Tract area (km ²)	Known copper resources (t)	Mean estimate of undiscovered copper resources (t)	Median estimate of undiscovered copper resources (t)
2009	1	79,040	5,000,000	22,000,000	12,000,000

Location

Tract 142pCu8003 comprises four permissive Carboniferous arc terrains (sub-tracts a, b, c, and d) that surround the eastern part of the Balkhash Depression (fig. 1-2⁴). Subtract 142pCu8003b (fig. D1) is in north-central Kazakhstan, the northern part of a generally horseshoe-shaped area of Carboniferous magmatic-arc activity (see figs. 1-29 and 1-30). The region is made up of low-relief, hilly countryside north of Lake Balkhash. It is within the Balkhash-Ili tectonic terrane of Windley and others (2007). The area extends from the Spassky tectonic zone north of Lake Balkhash (fig. 1-2) south to the north margins of permissive sub-tract 142pCu8003d and tract 142pCu8004 on the south. Sub-tract 142pCu8003c borders 142pCu8003b on the west and 142pCu8003a is on the east.

Geologic Feature Assessed

The permissive tract encompasses latest Early Carboniferous (C₁) to Permian (P₁) magmatic-arc and postcollisional rocks. The city of Balkhash is located on the northwest shoreline of Lake Balkhash approximately 425 kilometers (km) north-northwest of Almaty, the largest city in Kazakhstan.

¹U.S. Geological Survey, Denver, Colorado.

²U.S. Geological Survey, Reston, Virginia.

³U.S. Geological Survey, Spokane, Washington.

⁴Refer to chapter 1 of this report.

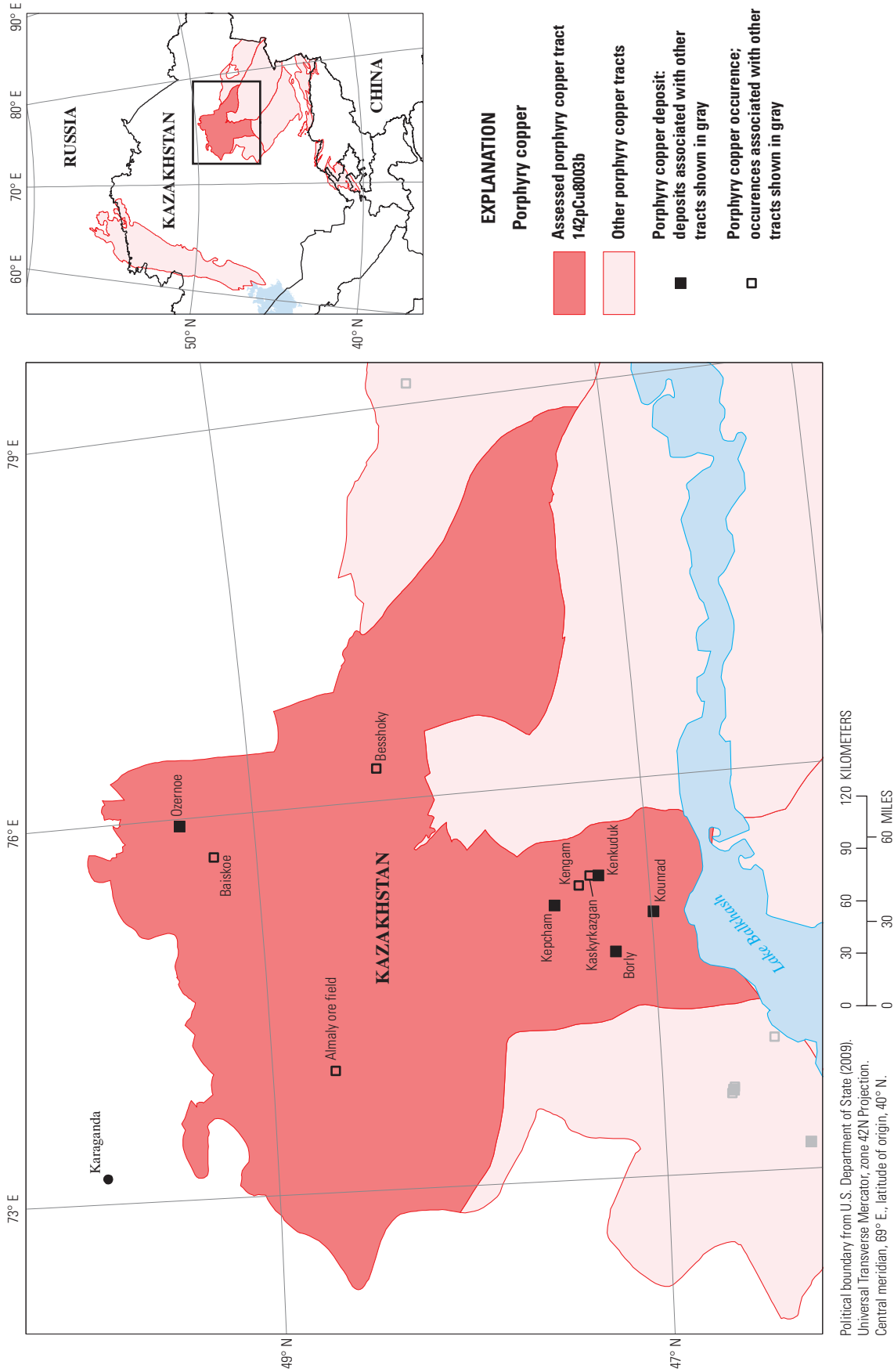


Figure D1. Map showing the location, known deposits, and significant prospects and occurrences for permissive sub-tract 142pCu8003b, Late Paleozoic Balkhash-Ili magmatic arc (north)—Kazakhstan. Location of map area shown on inset.

Delineation of the Permissive Tract

Geologic Criteria

The principal tectonic concept used to delineate tract 142pCu8003b was that of a magmatic arc formed in the subduction boundary zone above a subducting plate. Five principal sources of information, supplemented by numerous published journal and symposium papers, were used to delineate this tract. The primary sources were the mineral deposits map of Central Asia on a geologic base edited by Seltmann and others (2009), supplemented by four 1:200,000-scale geologic maps originally published by the former Soviet (U.S.S.R.) government, a reduced-to-pole aeromagnetic map prepared by J.D. Phillips from NOAA (1996), the interpretation of Advanced Spaceborne Thermal Emission and Reflection Radiometer (ASTER) satellite imagery of hydrothermal alteration minerals or suites of minerals by J.C. Mars (chapter 2 of this report), the tectonic terrane map of Windley and others (2007), and stratigraphic and structural expertise provided by Dr. Dmitriy Alexeiev of the Russian Academy of Science, Moscow.

Central Asia is an amalgamation of Precambrian basement fragments, accreted Paleozoic terranes, and overlying Early to Middle Paleozoic magmatic arcs (Windley and others, 2007). The permissive Carboniferous magmatic arc in 142pCu8003b was built on this complex basement that had been deformed one or more times prior to arc-related magmatism. Further, the present distribution of permissive rocks has been structurally rearranged since arc magmatism, largely through strike-slip tectonics (D. Alexeiev, unpublished data, 2008). The distribution of Carboniferous volcanic, volcanoclastic, and intrusive rocks is shown in fig. D2.

The two most important attributes used to delineate the permissive tract boundaries were outcrops of rock suites that are one or more of the following: C_{1-3} volcanic, volcanogenic, and volcanoclastic rocks, C_3 plutonic-rock complexes, and (or) Middle to Late Carboniferous porphyry copper-type deposits and occurrences. Although the ages of different rock groups are relatively well documented by Seltmann and others (2009), there is uncertainty as to the ages of many deposits and occurrences. This raises the uncertainty level in the assessment of this tract, particularly owing to the likely overlap of Carboniferous and Devonian magmatic-arc deposits to the north.

The first step in tract delineation was to identify all geologic units on the geologic map (Seltmann and others, 2009) that do, or are interpreted to consist of Middle and Late Carboniferous arc-related volcanic and intrusive rocks (see figs. 1-29 and 1-30). Sub-tract 142pCu8003b is one of four permissive Carboniferous arc terrains that surround the Balkhash Depression. The subdividing was done owing to regional-scale geologic differences between the sub-tracts with respect to levels of exposure and numbers of known porphyry copper deposits and (or) occurrences. The criteria

for delineation of each sub-tract are discussed in separate appendices.

Sub-tract 142pCu8003b makes up the northernmost subdivision of the permissive tract. Within this region, there are extensive outcrops of Middle to Late Carboniferous arc-related volcanic and volcanoclastic rocks and coeval intrusions. The northern boundary of the tract, the Spassky zone, is a generally east-west tectonic terrane boundary along which the permissive rocks are strongly deformed and stratigraphy intermittently inverted. The eastern and western sides of this sub-tract are where mapped outcrops of Carboniferous arc-related volcanic and related rocks greatly diminish in outcrop. The southern sub-tract boundary is primarily a common boundary with permissive tract 142pCu8004 and sub-tract 142pCu8003d.

Known Deposits

Singer and others (2008) show there to be five deposits in this sub-tract for which grade and tonnage data could be compiled. These known deposits, described below in alphabetical order, are Borly, Kenkuduk, Kepcham, Kounrad⁵, and Ozernoe (fig. D1, table D2).

Borly

Borly is in the Priozirny District of the Dzhezkazgan Province about 45 km north of the Kounrad deposit (Zhukov and others, 1998). The deposit is in a suite of Middle to Late Carboniferous intermediate to siliceous volcanic rocks intruded by quartz diorites, granodiorites, and leucocratic granites. The mineralization is most directly associated with granodiorite porphyry dikes. There are two ore-bearing areas in the ore field. The “Central” zone is 800 meters (m) long, to 340 m wide, and extends to a depth of 460 m. The “Eastern” zone is 260 m long, to 150 m wide, and extends to 120 m deep. Quartz-tourmaline breccia pipes occur in the district, but are not specifically associated with porphyry-style mineralization. Hydrothermal alteration minerals (Zhukov and others, 1998) include quartz, biotite, chlorite, sericite, K-feldspar, anhydrite, epidote, apatite, tourmaline, hematite, and alunite, kaolinite, and diaspore. The principal ore-stage minerals (Zhukov and others, 1986) are pyrite, chalcocopyrite, molybdenite, and sphalerite. Less abundant are pyrrotite, chalcocite, and galena. Also present are marcasite, bornite, and enargite.

Kenkuduk

Kenkuduk consists of six lens-shaped bodies. The principal ore-stage minerals (Zhukov and others, 1998) are pyrite, chalcocopyrite, and molybdenite. Also occurring are magnetite, sphalerite, and galena. The deposit contains anomalous concentrations of tungsten.

⁵Also known as Konyrat.

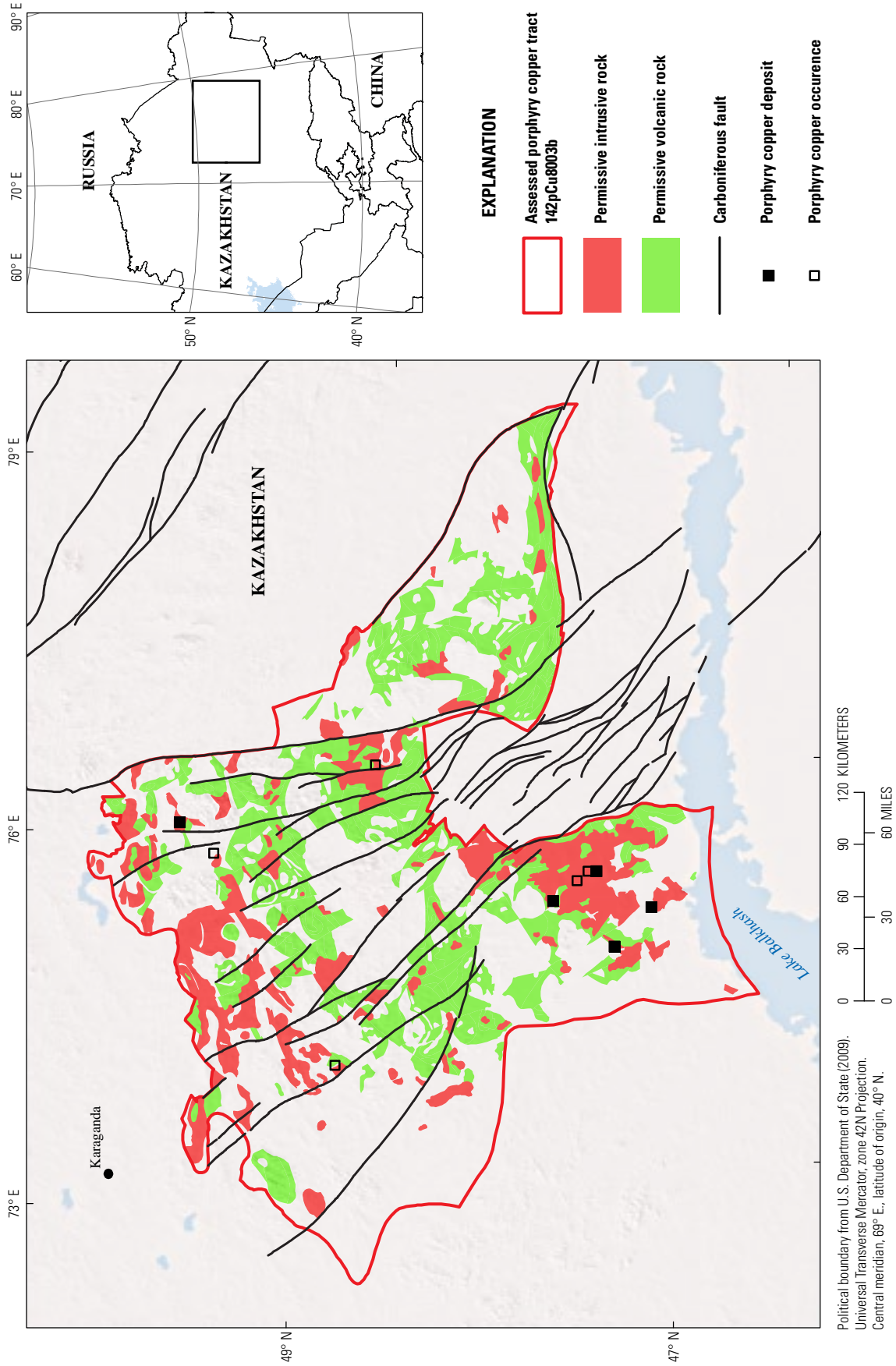


Figure D2. Map of permissive Carboniferous volcanic and volcanoclastic rocks (green) and intrusive rocks (red) in sub-tract 142pCu8003b, Late Paleozoic Balkhash-Ili magmatic arc (north)—Kazakhstan, on a digital elevation base. Location of map area shown on inset.

Table D2. Porphyry copper deposits in sub-tract 142pCu8003b, Late Paleozoic Balkhash-Ili magmatic arc (north)—Kazakhstan.

[Ma, mega-annum (10^6 years); km², square kilometers; t, metric tons; Mt, million metric tons, %, percent; g/t, grams per metric ton; Cu, copper; Mo, molybdenum; Au, gold; Ag, silver; n.d., no data; NA, not applicable]

Name	Latitude	Longitude	Subtype	Age (Ma)	Tonnage (Mt)	Cu (%)	Mo (%)	Au (g/t)	Ag (g/t)	Contained Cu (t)	Reference
Borly	47.197	74.709	NA	329	94.4	0.34	0.011	0.30	3.40	320,960	Kolesnikov and others (1986), Krivtsov and others (1986), Kudryavtsev (1996), Zhukov and others (1998)
Kenkuduk	47.258	75.291	NA	309	23.7	0.34	0.017	n.d.	n.d.	80,580	Kolesnikov and others (1986), Krivtsov and others (1986), Kudryavtsev (1996), Plyushchev (1993), Zhukov and others (1998)
Kepcham	47.495	75.090	NA	n.d.	35.8	0.34	0.018	n.d.	n.d.	121,720	Kudryavtsev (1996), Zhukov and others (1998)
Kounrad	46.991	74.987	NA	330	637	0.59	0.011	0.19	6.28	3,751,930	Krivtsov and others (1986), Kudryavtsev (1996), Pavlova (1978), Plyushchev (1993), Seltmann and Porter (2005), Sokolov (1999), Yudin (1969), Zhukov and others (1998), Zvezdov and others (1993)
Ozernoe	49.379	75.945	NA	315	194	0.36	0.005	0.02	2.90	698,400	Kolesnikov and others (1986), Kudryavtsev (1996), Zhukov and others (1998)

Kepcham

At Kepcham, the stockwork zone is 2,060 m long and as wide as 500 m. The principal ore-stage minerals (Zhukov and others, 1998) are pyrite, chalcopyrite, and molybdenite.

Kounrad

Kounrad is in the Prioziorny District in the Dzhezkazgan Province, about 15 km north of Lake Balkhash (Zhukov and others, 1998). It is associated with a late Early Carboniferous intrusive complex including gabbro, diorite, granodiorite, and granite. Porphyritic intrusions predominate, and breccia bodies are also important components of the ore deposit. The deposit is elliptical, measuring 1,000 m in the long direction and as much as 800 m wide. Hydrothermal alteration minerals (Zhukov and others, 1998) include quartz, sericite, chlorite, actinolite, epidote, calcite, siderite, tourmaline, alunite, kaolinite, diaspore, and barite. The principal ore-stage minerals (Zhukov and others, 1998) are pyrite, chalcopyrite, enargite, and molybdenite. Less abundant are magnetite, pyrrhotite, bornite, sphalerite, and galena. Also present are luzonite, tennantite, tetrahedrite, and arsenopyrite.

Ozernoe

Ozernoe is in the Karkaralinsky District in the Karaganda Province (Zhukov and others, 1998). It is within an Early to Middle Carboniferous igneous complex intrusive into Devonian sedimentary and volcanic rocks. The igneous rocks include quartz diorite, granodiorite, and granite. The overall zone within which hydrothermal alteration occurs is about 7 km long and as wide as 500 m. Within this extensive zone are smaller areas of intense quartz-sericite-pyrite alteration and sulfide mineralization. The main hydrothermal alteration minerals are quartz, sericite, and chlorite. The largest intensely altered areas contain lenses of stockwork veins with pyrite and chalcopyrite. Less abundant minerals include molybdenite, sphalerite, arsenopyrite, enargite, tetrahedrite, and bornite.

Porphyry Copper Occurrences and Related Deposit Types

There are numerous porphyry-style occurrences shown in this area on the map of Seltmann and others (2009), but there is little or no publically available information on them. Significant prospects are listed in table D3 and plotted on figure D1.

Table D3. Significant occurrences of porphyry-style copper in sub-tract 142pCu8003b, Late Paleozoic Balkhash-Ili magmatic arc (north)—Kazakhstan.

[Ma, mega-annum (10^6 years); t, metric tons; Mt, million metric tons, %, percent; g/t, grams per metric ton; km, kilometers; E, east; NE, northeast; Cu, copper; Mo, molybdenum; Au, gold; and Ag, silver; Pb, lead; Bi, bismuth; Re, rhenium; n.d., no data]

Name	Latitude	Longitude	Age (Ma)	Comments	Reference
Almaly ore field	46.987	80.053	n.d.	Medium size deposit, small mining operations at the start of 20th century. Grades: 0.3–0.9% Cu, 0.001–0.006% Mo, up to 0.7 g/t Au; 0.15% Pb, 0.03% Bi. Exposed. Location: Akbiik; best guess from Google Earth (3/9/10) using geology as guide; faults discernible on satellite image; 18 km E of Singer and others (2008) location. Singer and others (2008) use Almaly as collective name for two nearby deposits, Akbiik and Oginskoe; at the given location, there is no evidence of exploration activity on Google Earth (3/8/10)	Kolesnikov and others (1986), Zhukov and others (1998)
Baiskoe	49.219	75.677	310	Small deposit with average grades: 0.43–0.53% Cu and 0.004–0.007% Mo; 946–980 g/t Re in molybdenite from concentrate. Location: Pits, trenches, open cuts, and mine dumps evident on Google Earth (3/8/10); 8.5 km NE of Singer and others (2008) location	Kolesnikov and others (1986), Zhukov and others (1998)
Besshoky	48.346	76.250	310	Resource: 138 Mt at 0.52% Cu and 0.002% Mo. Exposed. Location: Altered appearing area on Google Earth (3/5/10); some cuts trenches on hill; topography fits geologic map (compare to Zhukov and others, 1998), but location should be considered approximate	Kolesnikov and others (1986), Kudryavtsev (1996), Pavlova (1978), Zhukov and others (1998)
Kaskyrkazgan	47.3028	75.2955	n.d.	Location: Grid road pattern on Google Earth (3/10/10); 1.7 km of Seltmann and others (2009) location	Seltmann and others (2009)
Kengam	47.363	75.229	n.d.	Road grid visible on Google Earth (3/10/10); about 2.3 km S of Singer and others (2008) Kenkuduk location	Seltmann and others (2009)

Almaly Ore Field

Almaly is in the Shetsky District of the Dzhezkazgan Province (Zhukov and others, 1998); it is an ore field within which there is more than a single zone of alteration and more than a single deposit type. The ore field is localized in Late Silurian siliciclastic and volcanic rocks and Lower to Middle Carboniferous andesitic to dacitic volcanic rocks intruded by Middle to Late Carboniferous diorite, quartz diorite, and granodiorite. There are two main zones of phyllic alteration within which there are quartz-sulfide stockworks. The western of the two alteration zones is elliptical in plan, measuring 2 by 1.5 km. Zhukov and others (1998) identify three quartz-sulfide stockworks within the broader alteration zone that are localized along northwest-striking faults. The stockwork zones measure between 500 m and 750 m along strike and are on the order of 250 m wide. These are the Malaya Zhila, Novaya Zhila, and Zhaman Koitas occurrences. To the east is a second zone of phyllic alteration that is irregular in shape and elongated northeast-southwest (Zhukov and others, 1998). The maximum length of this zone is about 4 km; its greatest width is about 1.5 km. Within the phyllic zone, an extensive zone of quartz-sulfide stockworks is about 2,250 m long and as great as 300 to 400 m wide. Three prospects are identified

by Zhukov and others (1998) within this stockwork zone. Olginskoe at the southwest end consists of fault-controlled, vein-form ore bodies. Akbiik is a mineralized stockwork zone that measures 1,900 m along strike, is as much as 260 m wide, and extends to a depth as much as 400 m depth, and Severniy Tantau-Nangan is an undescribed occurrence at the northeast end of the stockwork zone. Hydrothermal alteration minerals (Zhukov and others, 1998) include quartz, sericite, chlorite, and K-feldspar. The principal ore-stage minerals (Zhukov and others, 1998) are pyrite, chalcopyrite, molybdenite, and pyrrhotite. Less abundant are sphalerite, galena, and magnetite.

Baiskoe

Baiskoe is in the Taldinsky District of the Karaganda Province (Zhukov and others, 1998). The deposit is in Devonian siliciclastic and tuffaceous rocks intruded by diorite, granodiorite, and felsite porphyries. The deposit consists of three steeply dipping lens-form ore zones associated with granodiorite porphyry. Hydrothermal alteration minerals (Kolesnikov and others, 1986) include quartz, K-feldspar, biotite, chlorite, epidote, and ankerite. The principal ore-stage minerals (Zhukov and others, 1998) are pyrite,

chalcopyrite, and molybdenite. Also occurring are sphalerite, galena, magnetite, arsenopyrite, pyrrhotite, tetrahedrite, and native gold.

Besshoky (Besshoki)

Besshoky is in the Prioziorny District of the Dzhezkazgan Province (Zhukov and others, 1998). The deposit is localized in Middle Carboniferous intermediate volcanic rocks intruded by Middle Carboniferous granodiorite. Large areas of alunite, diaspore, and andalusite alteration occur in the ore field. The porphyry-style ores are in phyllically altered rocks surrounded by propylitically altered rock. The principal ore-stage minerals are pyrite, chalcopyrite, and molybdenite. Also occurring, but uncommon, are enargite, tetrahedrite, and famatinite.

Exploration History

No historical record of exploration was compiled for this tract.

Hydrothermal Alteration Mapping (ASTER)⁶

Argillic, phyllic, and silicic ASTER hydrothermal alteration mapping covers approximately 95 percent of tract 142pCu8003b (see figs. 2-1 and 2-2). Using the ASTER

hydrothermal alteration map, 104 alteration sites compatible with porphyry-style deposits were defined in the central and southern parts of the tract (see fig. 2-3 and plates 1–8). Tract 142pCu8003b contains more ASTER mapped alteration and potential deposit sites than any other tract in the study area (see chapter 2, plates 1–8 and table 2-1). Mineral databases show that copper mineralization is associated with 27 of the sites and 3 sites contain economic deposits of copper (see table 2-1). The 1:1,500,000-scale geologic map of Seltmann and others (2009) indicates that rhyolite, granodiorite, biotite granite, dacite, and granite underlie the alteration (see table 2-1).

The Kounrad mine, the largest porphyry copper deposit in the region, is within the sub-tract. Altered rock characteristics of the area around the Kounrad deposit were used to identify other potential sites with similar alteration characteristics. Altered rock characteristics include size diameter of alteration pattern greater than or equal to 1.7 km, phyllic and argillic alteration density greater than or equal to 7, and at least 80 percent phyllic alteration coverage. A total of 9 sites have alteration characteristics similar to Kounrad within subtract 142pCu8003b (see table 2-1). The ASTER hydrothermal alteration map and mineral databases suggest that none of the sites with similar alteration characteristics to Kounrad (site 1) are associated with known copper mineralized rocks (see table 2-1).

⁶Refer to figures, tables, and plates in chapter 2 of this report.

Table D4. Principal sources of information used for the delineation of sub-tract 142pCu8003b, Late Paleozoic Balkhash-Ili magmatic arc (north)—Kazakhstan.

Theme	Name or title	Scale	Citation
Geology	Mineral deposits database and thematic maps of Central Asia	1:1,500,000	Seltmann and others (2009)
	Tectonic map of the Paleozoic folded areas of Kazakhstan and adjacent territories	1:1,500,000	Abdulin and Zaitseb (1976)
	L-43-III (1959)	1:200,000	Vurovym and Vokan (1959)
	L-43-VI (1955)	1:200,000	Bespalov (1959)
	L-43-IX (1968)	1:200,000	Gaek and Cheurkin (1968)
Mineral occurrences	Mineral deposits database and thematic maps of Central Asia	1:1,500,000	Seltmann and others (2009)
Geophysics	Magnetic anomaly data of the former U.S.S.R.	1:1,500,000	National Oceanic and Atmospheric Administration (1996)

Sources of Information

Principal sources of information used by the assessment team for delineation of 142pCu8003b are listed in table D4 and in the bibliography.

Grade and Tonnage Model Selection

The general porphyry copper deposit model published by Singer and others (2008) was used based on the known deposits in the tract being statistically consistent with the model.

Estimate of the Number of Undiscovered Deposits

Rationale for the Estimate

The consensus of the assessment team was that (1) the ratio of porphyry copper occurrences and possible linked deposit types to the number of known deposits was high and therefore a favorable indication of undiscovered deposits, (2) the depth of erosion of the terrane is the most favorable

of all the Carboniferous sub-tracts, and (3) owing to low relief, complex geologic structure, and remoteness of much of the area, there were many plays left despite considerable Soviet-era exploration investment in the region.

On the basis of discussions of known deposits, occurrences, and mapped alteration, the team estimated a 90-percent chance of 1, a 50-percent chance of 5, and a 10-percent chance of 12 or more undiscovered deposits within the 79,000 km² tract area, for a mean of 5.8 undiscovered deposits (table D5).

Probabilistic Assessment Simulation Results

Undiscovered resources for the tract were estimated by combining consensus estimates for numbers of undiscovered porphyry copper deposits with the global grade and tonnage model for porphyry Cu-Au-Mo deposits of Singer and others (2008) using the EMINERS program (Root and others, 1992; Bawiec and Spanski, 2012; Duval, 2012). Selected simulation results are reported in table D6. Results of the Monte Carlo simulation are presented as a cumulative frequency plot (fig. D3). The cumulative frequency plot shows the estimated resource amounts associated with cumulative probabilities of occurrence, as well as the mean, for each commodity and for total mineralized rock.

Table D5. Undiscovered deposit estimates, deposit numbers, tract area, and deposit density for sub-tract 142pCu8003b, Late Paleozoic Balkhash-Ili magmatic arc (north)—Kazakhstan.

[N_{xx} , estimated number of deposits associated with the xxth percentile; N_{und} , expected number of undiscovered deposits; s , standard deviation; $C_v\%$, coefficient of variance; N_{known} , number of known deposits in the tract that are included in the grade and tonnage model; N_{total} , total of expected number of deposits plus known deposits; area, area of permissive tract in square kilometers (km²); density, deposit density reported as the total number of deposits per 100,000 km². N_{und} , s , and $C_v\%$ are calculated using a regression equation (Singer and Menzie, 2005)]

Consensus undiscovered deposit estimates					Summary statistics					Tract area (km ²)	Deposit density ($N_{total}/100k\text{ km}^2$)
N_{90}	N_{50}	N_{10}	N_{05}	N_{01}	N_{und}	s	$C_v\%$	N_{known}	N_{total}		
1	5	12	12	12	5.8	4	68	5	10.8	79,040	14

Table D6. Results of Monte Carlo simulations of undiscovered resources for sub-tract 142pCu8003b, Late Paleozoic Balkhash-Ili magmatic arc (north)—Kazakhstan.

[Cu, copper; Mo, molybdenum; Au, gold; and Ag, silver; in metric tons. Rock, in million metric tons]

Material	Probability of at least the indicated amount						Probability of	
	0.95	0.9	0.5	0.1	0.05	Mean	Mean or greater	None
Cu	0	540,000	12,000,000	54,000,000	83,000,000	22,000,000	0.32	0.06
Mo	0	0	220,000	1,500,000	2,400,000	590,000	0.27	0.15
Au	0	0	290	1,400	2,100	560	0.32	0.11
Ag	0	0	2,300	18,000	29,000	6,900	0.26	0.19
Rock	0	130	2,700	11,000	18,000	4,500	0.33	0.06

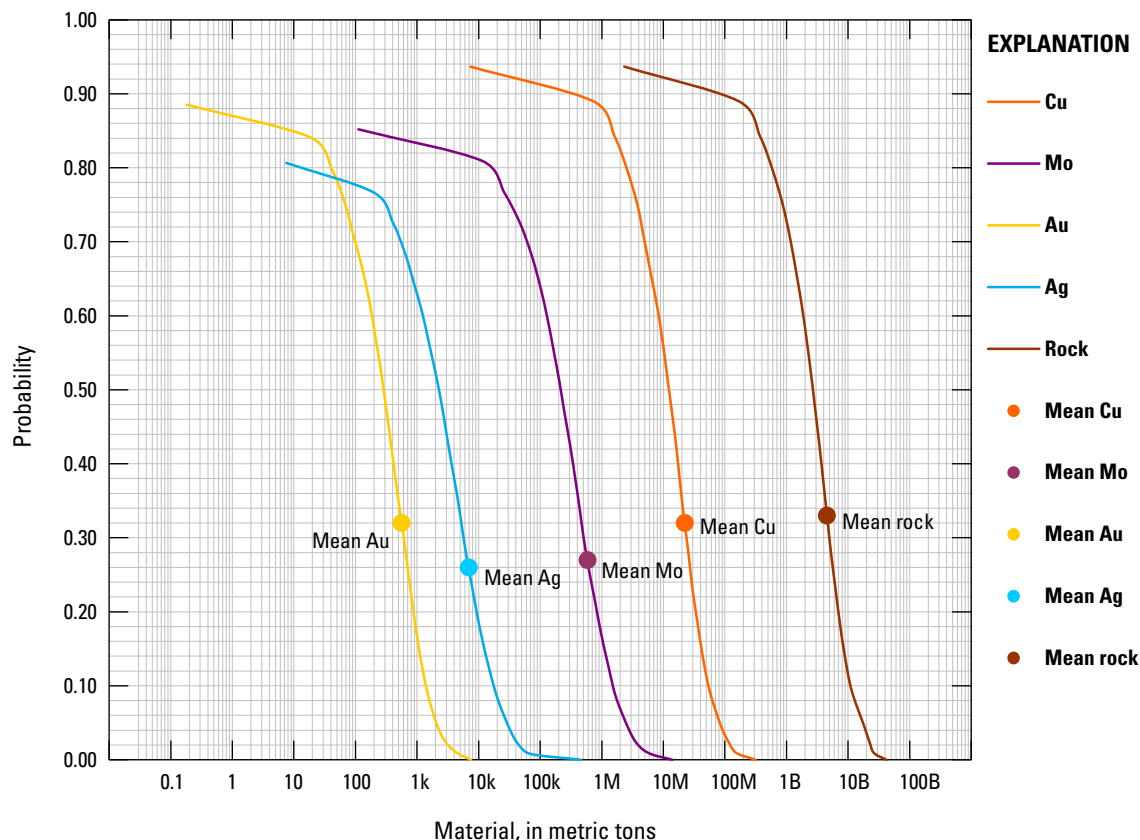


Figure D3. Cumulative frequency plot showing the results of Monte Carlo computer simulation of undiscovered resources in sub-tract 142pCu8003b, Late Paleozoic Balkhash-Ili magmatic arc (north)—Kazakhstan. k=thousands, M=millions, B=billions.

Mean estimated amounts of undiscovered copper, 22 million metric tons (Mt), are about 4.4 times the amount of identified copper resources in known deposits (table D1).

References Cited

- Abduln, A.A., and Zaitseb, Yu.A., eds., 1976, [Tectonic map of the Paleozoic folded belts of Kazakhstan and adjacent territories]: Ministry of Geology of the U.S.S.R., VSEGEI, 1 map on 6 sheets, scale 1:1,500,000. [In Russian.]
- Bawiec, W.J., and Spanski, G.T., 2012, Quick-start guide for version 3.0 of EMINERS—Economic Mineral Resource Simulator: U.S. Geological Survey Open-File Report 2009–1057, 26 p., accessed July 15, 2012, at <http://pubs.usgs.gov/of/2009/1057/>. (This report supplements USGS OFR 2004–1344.)
- Bespalov, V.F., 1959, [Geological map of the U.S.S.R., Balkhash series, Sheet L-43-VI]: Ministry of Geology and Mineral Resources Protection, scale 1:200,000. [In Russian.]
- Berger, B.R., Ayuso, R.A., Wynn, J.C., and Seal, R.R., 2008, Preliminary model of porphyry copper deposits: U.S. Geological Survey Open-File Report 2008–1321, 55 p., accessed May 15, 2009, at <http://pubs.usgs.gov/of/2008/1321/>.
- Cox, D.P., 1986, Descriptive model of porphyry Cu (Model 17), in Cox, D.P., and Singer, D.A., eds., 1986, Mineral deposit models: U.S. Geological Survey Bulletin 1693, p. 76. (Also available at <http://pubs.usgs.gov/bul/b1693/>.)
- Duval, J.S., 2012, Version 3.0 of EMINERS—Economic Mineral Resource Simulator: U.S. Geological Survey Open-File Report 2004–1344, accessed July 15, 2012, at <http://pubs.usgs.gov/of/2004/1344/>.
- Gaek, O.M., and Cheurkin, I.I., 1968, [Geological map of the U.S.S.R., Balkhash series, Sheet L-43-IX]: Ministry of Geology of the U.S.S.R., scale 1:200,000. [In Russian.]
- Kolesnikov, V.V., Zhukov, N.M., Solodilova, V.V., and Filimonova, L.E., 1986, [Porphyry copper deposits of the Balkhash region]: Nauka, Alma Ata, 199 p. [In Russian.]

- Krivtsov, A.I., Migachev, I.F., and Popov, V.S., 1986, [Porphyry copper deposits of the world]: Moscow, Nedra, 236 p. [In Russian.]
- Kudryavtsev, Y.K., 1996, The Cu-Mo deposits of Central Kazakhstan, *in* Shatov V., Seltmann, R., Kremenetsky, A., Lehman, B., Popov, V., and Ermolov, P., eds., Granite-related ore deposits of Central Kazakhstan and adjacent areas: St. Petersburg, IAGOD, Working Group on Tin and Tungsten Deposits (WGTT), p. 119–144.
- National Oceanic and Atmospheric Administration, 1996, Magnetic anomaly data of the former U.S.S.R.: National Geophysical Data Center, Boulder, Colorado, accessed August 1, 2010, at <http://www.ngdc.noaa.gov>.
- Pavlova, I.G., 1978, [Porphyry copper deposits]: Leningrad, Nedra, 275 p. [In Russian.]
- Plyushchev, E.V., 1993, Map of hydrothermal-metasomatic formations of Kazakhstan fold area: St. Petersburg, VSEGEI, 4 sheets, scale 1:1,500,000.
- Root, D.H., Menzie, W.D., and Scott, W.A., 1992, Computer Monte Carlo simulation in quantitative resource estimation: *Natural Resources Research*, v. 1, no. 2, p. 125–138.
- Seltmann, R., and Porter, T.M., 2005, The porphyry Cu-Au/Mo deposits of Central Eurasia. 1. Tectonic, geologic and metallogenic setting, and significant deposits, *in* Porter, T.M., ed., Superporphyry copper and gold deposits—A global perspective: Adelaide, PGC Publishing, v. 2, p. 467–512.
- Seltmann, R., Shatov, V., and Yakubchuk, A., 2009, Mineral deposits database and thematic maps of Central Asia—ArcGIS 9.2, Arc View 3.2, and MapInfo 6.0(7.0) GIS packages: London, Natural History Museum, Centre for Russian and Central EurAsian Mineral Studies (CERCAMS), scale 1:1,500,000, and explanatory text, 174 p. [Commercial dataset available at <http://www.nhm.ac.uk/research-curation/research/projects/cercams/products.html>.]
- Singer, D.A., Berger, V.I., and Moring, B.C., 2008, Porphyry copper deposits of the world: U.S. Geological Survey Open-File Report 2008–1155, 45 p., accessed August 10, 2009, at <http://pubs.usgs.gov/of/2008/1155/>.
- Singer, D.A., and Menzie, W.D., 2005, Statistical guides to estimating the number of undiscovered mineral deposits—An example with porphyry copper deposits, *in* Cheng, Qiuming, and Bonham-Carter, Graeme, eds., Proceedings of IAMG—The annual conference of the International Association for Mathematical Geology: Toronto, Canada, York University, Geomatics Research Laboratory, p. 1028–1033.
- Sokolov, A.L., 1999, Regional and local controls on gold and copper mineralization in central Asia and Kazakhstan, *in* Porter, T.M., ed., Porphyry and hydrothermal copper and gold deposits—A global perspective, Conference Proceedings: Glenside, South Australia, Australian Mineral Foundation, p. 181–190.
- Vurovym, V.G., and Vokan, V.V., 1959, [Geological map of the U.S.S.R., Balkhash series, Sheet L-43-III]: Ministry of Geology and Mineral Resources Protection, scale 1:200,000. [In Russian.]
- Windley, B.F., Alexeiev, D., Xiao, W., Kroner, A., and Badarch, G., 2007, Tectonic models for accretion of the Central Asian Orogenic Belt: London, *Journal of the Geological Society*, v. 164, p. 31–47.
- Yudin, I.M., 1969, [The Kounrad copper deposit]: Moscow, Moscow University Publishing Company, 150 p. [In Russian.]
- Zhukov, N.M., Kolesnikov, V.V., Miroshnichenko, L.M., Egembaev, K.M., Pavlova, Z.N., and Bakarasov, E.V., comps., 1998, Copper deposits of Kazakhstan—Reference book: Almaty, Ministry of Ecology and Natural Resources of the Republic of Kazakhstan, 136 p.
- Zvezdov, V.S., Migachev, I.F., and Girfanov, M.M., 1993, Porphyry copper deposits of the CIS and the models of their formation: *Ore Geology Reviews*, v. 7, p. 511–549.

Appendix E. Porphyry Copper Assessment for Sub-tract 142pCu8003c, Late Paleozoic Balkhash-Ili Magmatic Arc (West)—Kazakhstan

By Byron R. Berger¹, Paul D. Denning¹, Connie L. Dicken², Jane M. Hammarstrom², John C. Mars², Jeffrey D. Phillips¹, and Michael L. Zientek³

Deposit Type Assessed: Porphyry Copper

Descriptive model: Porphyry copper (Cox, 1986; Berger and others, 2008)

Grade and tonnage model: Global Cu-Au-Mo porphyry copper model (Singer and others, 2008)

Table E1 summarizes selected assessment results.

Table E1. Summary of selected resource assessment results for sub-tract 142pCu8003c, Late Paleozoic Balkhash-Ili magmatic arc (west)—Kazakhstan.

[km, kilometers; km², square kilometers; t, metric ton]

Date of assessment	Assessment depth (km)	Tract area (km ²)	Known copper resources (t)	Mean estimate of undiscovered copper resources (t)	Median estimate of undiscovered copper resources (t)
2009	1	23,800	1,000,000	7,400,000	1,800,000

Location

Tract 142pCu8003 comprises four permissive Carboniferous arc terrains (sub-tracts a, b, c, and d) that surround the eastern part of the Balkhash Depression (see fig. 1-2⁴). Sub-tract 142pCu8003c delineates a region in west-central Kazakhstan wherein the surficial permissive Carboniferous magmatic-arc rocks are largely eroded and overlap with Devonian magmatic-arc rocks is considerable. The area that makes up the tract and its relation to other permissive tracts in Central Asia is shown in figure E1.

Geologic Feature Assessed

The permissive tract encompasses Late Carboniferous to Permian magmatic-arc rocks that are a part of the Balkhash-Ili volcanic arc (see fig. 1-22) of Windley and others (2007). The tract lacks widespread preservation of Carboniferous lavas and volcanoclastic rocks and a paucity of geochronologic data on mineral deposits and intrusions makes it highly uncertain as to which deposits and intrusions are Devonian and which are Carboniferous. There are known Carboniferous porphyry copper occurrences in the tract, but there are more occurrences of uncertain age and affinity as well as some considered to be Devonian. The tract also contains intrusive complexes of probable Carboniferous to Permian age with which porphyry molybdenum deposits are associated.

¹U.S. Geological Survey, Denver, Colorado.

²U.S. Geological Survey, Reston, Virginia.

³U.S. Geological Survey, Spokane, Washington.

⁴Refer to chapter 1 of this report.

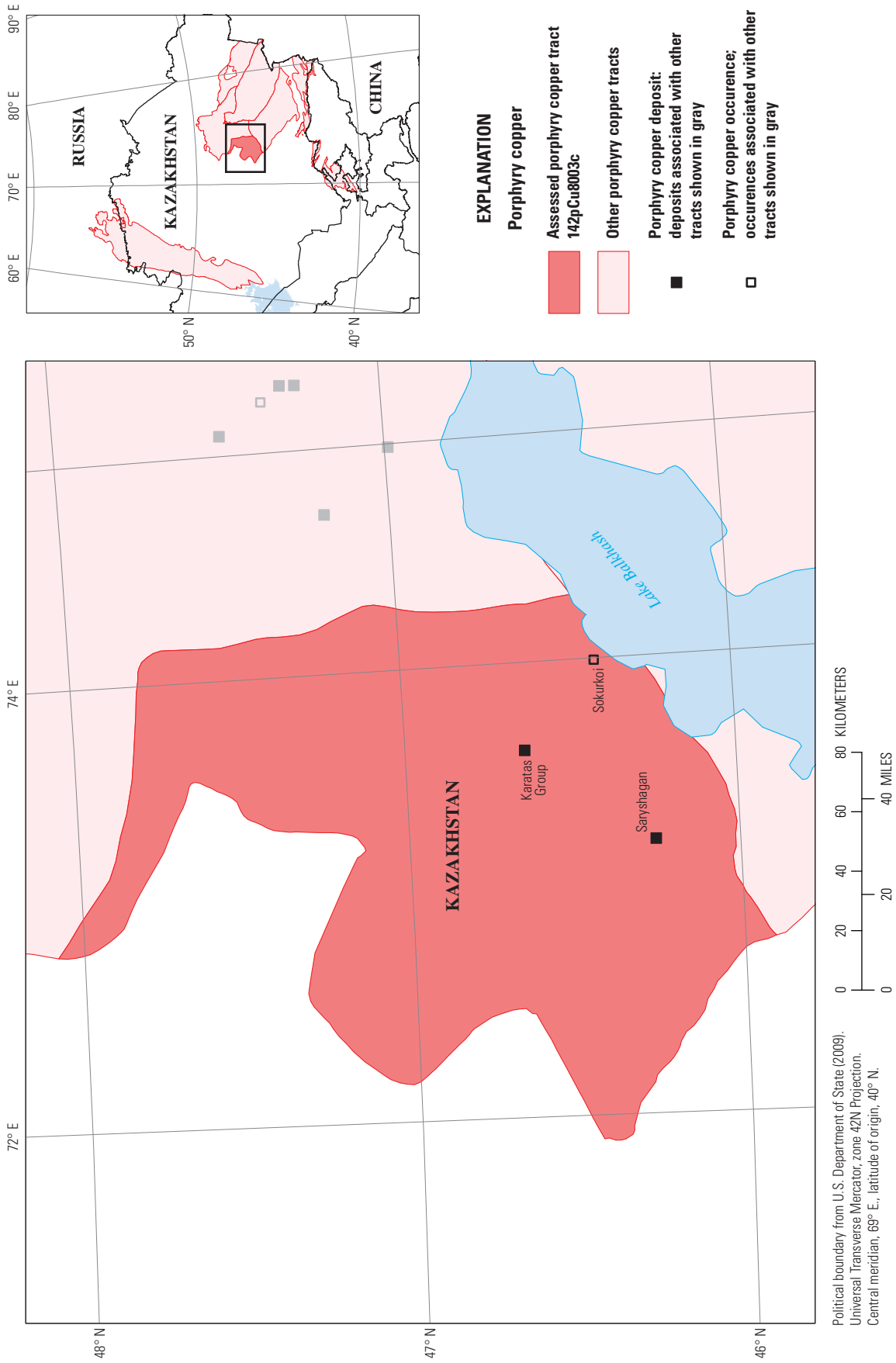


Figure E1. Map showing the location, known deposits, and significant occurrences for sub-tract 142pCu8003c, Late Paleozoic Balkhash-Ili magmatic arc (west)—Kazakhstan. Location of map area shown on inset.

Delineation of the Permissive Tract

Geologic Criteria

The principal litho-tectonic terrane concept used to delineate this sub-tract was that of a magmatic arc that formed above a subduction zone. Sub-tract 142pCu8003c includes rocks interpreted to be part of the Late Paleozoic Balkhash-Ili Arc. It is a relatively small area along the west boundary of permissive region 148pCu8003b. It is characterized and differentiated from 148pCu8003b by the presence of only sparse outcrops (fig. E2) of Middle to Late Carboniferous arc-related volcanic and volcanoclastic rocks, but abundant permissive intrusive rock complexes (see figs. 1-29 and 1-30). In addition, there is complete overlap of the underlying Devonian magmatic arc rocks. Four principal sources of information, supplemented by numerous published journal and symposium papers, were used to delineate this tract. The primary sources were the mineral deposits map of Central Asia on a geologic base edited by Seltmann and others (2009), supplemented by 1:200,000-scale geologic maps originally published by the former Soviet (U.S.S.R.) government, a reduced-to-pole aeromagnetic map prepared by J.D. Phillips from the Magnetic Anomaly Map of the World (2007), the interpretation of Advanced Spaceborne Thermal Emission and Reflection Radiometer (ASTER) satellite imagery of hydrothermal alteration minerals or suites of minerals by J.C. Mars, and tectonic terrane maps published by Abdulin and Zaitseb (1976), Yakubchuk (2004), and Windley and others (2007).

Of most importance in the delineation of the boundaries of this tract are (1) Carboniferous and Permian magmatic-arc-related volcanic and intrusive rocks as shown on the mineral deposits map of Central Asia (Seltmann and others, 2009) and (2) the age and composition of the arc-hosting rocks. The east boundary of the tract is permissive tract 148pCu8003a, the south boundary is permissive tract 148pCu8003d, and

the west boundary was determined subjectively based on the occurrence farther west of Middle to Late Carboniferous rocks that are not arc related as well as an area within which there are no presently identified Middle to Late Carboniferous intrusions. The whole of sub-tract 142pCu8003c is located to the north of Lake Balkhash and the south boundary of the tract is the inferred north structural margin of the Balkhash Depression.

The greatest proportion of nonintrusive rocks in this sub-tract are pre-Carboniferous, predominantly Devonian, although there are moderate areas of Permian late-collisional andesite-dacite and postcollisional alkali rhyolites, but the relative proportions of these differing rock suites cannot be determined directly from Seltmann and others (2009). Seltmann and others (2009) show a cluster of Carboniferous intrusive rocks in a small area northwest of Lake Balkhash, but deposits elsewhere known to be Carboniferous and associated with intrusive rocks suggest that the actual proportion of Carboniferous intrusive rocks in the tract is highly uncertain but likely a greater proportion than shown on Seltmann and others (2009).

Throughout the permissive tract, thrust and related faults and folding deformed the pre-Carboniferous arc sequences prior to the onset of C₂₋₃ magmatism. During C₃-P₁ arc magmatism, strike-slip faulting predominated, but the most through-going faults on Seltmann and others (2009) are to the east of sub-tract 142pCu8003c in permissive sub-tract 148pCu8003b.

Known Deposits

Singer and others (2008) show there to be two known deposits in sub-tract 142pCu8003c, that is, two deposits for which they were able to document grade and tonnage data. These known deposits are Karatas and Saryshagan (fig. E1, table E2).

Table E2. Porphyry copper deposits in sub-tract 142pCu8003c, Late Paleozoic Balkhash-Ili magmatic arc (west)—Kazakhstan.

[Ma, mega-annum (10⁶ years); km², square kilometers; t, metric tons; Mt, million metric tons; %, percent; g/t, grams per metric ton; Cu, copper; Mo, molybdenum; Au, gold; Ag, silver; n.d., no data; NA, not applicable]

Name	Latitude	Longitude	Subtype	Age (Ma)	Tonnage (Mt)	Cu (%)	Mo (%)	Au (g/t)	Ag (g/t)	Contained Cu (t)	Reference
Karatas I	46.639	73.613	NA	Late Carboniferous (~310)	29	0.44	0.024	n.d.	n.d.	127,600	Kudryavtsev (1996), Pavlova (1978), Plyushchev (1993), Zhukov and others (1998)
Saryshagan	46.257	73.199	NA	Late Carboniferous (~310)	324	0.27	0.007	0.024	n.d.	874,800	Kolesnikov and others (1986), Kudryavtsev (1996), Zhukov and others (1998)

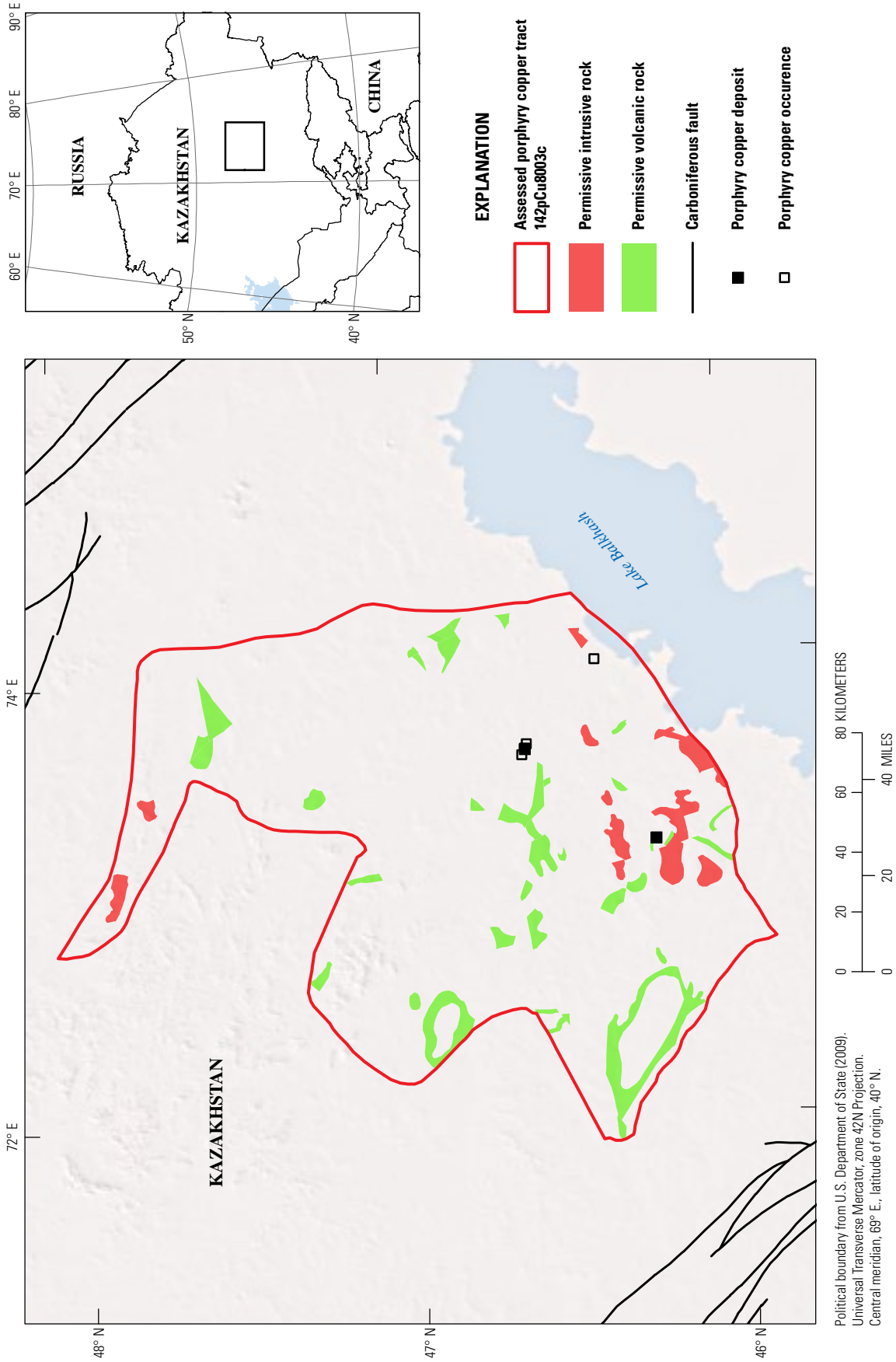


Figure E2. Map of permissive Carboniferous volcanic and volcanoclastic rocks (green) and intrusive rocks (red) in sub-tract 142pCu8003c, Late Paleozoic Balkhash-Ili magmatic arc (west)—Kazakhstan, on a digital elevation base. Location of map area shown on inset.

Karatas

The Karatas ore field is in the North Balkash region. There are three mineralized areas along a north-northeast–striking zone, Karatas I, Karatas II, Karatas IV, one in the northwest part of the ore field (Northwest Karatas), and occurrences in the eastern part of the ore field (fig. E1; see fig. 1-47). Identified resources for Karatas I are listed in table E2; information on other sites in the Karatas ore field is listed in table E3.

Saryshagan

Saryshagan is located in the Western Pribalkhash District near the western end of Lake Balkhash (fig. 1-38) (Zhukov and others, 1998). It is in a series of mid-Silurian sedimentary rocks interbedded with tuffs and Late Devonian (?) intermediate to siliceous volcanic rocks. Both Silurian and Devonian rocks were intruded by presumed Middle to Late Carboniferous plagiogranite porphyry dikes that vary from quartz diorite to granite in composition. The principal hydrothermal alteration includes quartz, sericite, chlorite, titanite, rutile, and albite. The principal ore-stage minerals (Zhukov and others, 1988) include pyrite, chalcopyrite, and molybdenite. Less abundant are magnetite, pyrrhotite, sphalerite, and galena. Also present are bornite and chalcocite.

Porphyry Copper Occurrences and Related Deposit Types

Although not as numerous as in sub-tract 142pCu8003b, several porphyry copper-style occurrences (table E3) are shown by Seltmann and others (2009).

Sokurkoi

The Sokurkoi porphyry copper prospect is in a series of Carboniferous (C_{1-3}) rocks consisting of C_1 porphyritic volcanic rocks, granodiorite, granosyenite, and granite intrusions ($g\sigma C_1$), sandstone, siltstone, and shale, C_{2-3} eruptive volcanic breccias, C_3 siliceous tuffs, and P_{2-3} granite porphyries and granophyre.

Garnet-epidote skarn is developed locally in the C_1 sedimentary rocks as stratiform zones near the $g\sigma C_1$ intrusions. Advanced argillic to argillic alteration, primarily alunite and dickite, and secondary linear masses of fault-controlled silica, are prominent in the ore field and affect, to varying extents, all of the Carboniferous formations. Although alunite and kaolinite are predominant, these altered zones also contain sericite, zunyite, and iron- and copper-sulfide minerals. Propylitic alteration occurs outside of the advanced argillic and argillic zones and quartz-sericite-pyrite alteration predominates at depth.

Hydrothermal Alteration Mapping (ASTER)⁵

Argillic, phyllic and silicic ASTER hydrothermal alteration mapping covers approximately 90 percent of sub-tract 142pCu8003c (see figs. 2-1 and 2-2). Using the ASTER hydrothermal alteration map, 38 potential deposit sites were defined in the tract (see fig. 2-3 and plates 1–8). Mineral databases indicate that there are 8 copper occurrences and 2 copper mines that are associated with potential deposit sites in the sub-tract (table 2-1). Based on the geologic map of Seltmann and others (2009), the most common altered rocks at the sites include rhyolite tuff, granodiorite, and trachyrhyolite (see table 2-1).

The Kounrad mine, the largest porphyry copper deposit in the region, is located in sub-tract 142pCu8003b. Alteration characteristics of the Kounrad mine were used to identify other potential sites with similar alteration characteristics in tract 142pCu8003c due to the similarities of rock exposure and vegetation of sub-tracts 142pCu8003b and 142pCu8003c (see fig. 2-4). Altered rock characteristics include size diameter of alteration pattern greater than or equal to 1.7 km, phyllic and argillic alteration density greater than or equal to 7 km, and at least 80 percent phyllic alteration coverage. A total of 12 sites have alteration characteristics similar to Kounrad in sub-tract 142pCu8003b (see table 2-3). The ASTER hydrothermal alteration map and mineral databases show that 4 of the sites with similar alteration characteristics to Kounrad (site1) were associated with known copper occurrences (see table 2-3 and plates 5–8).

Exploration History

An historical record of exploration within this tract has not been compiled.

Sources of Information

Principal sources of information used by the assessment team for delineation of 142pCu8003c are listed in table E4 and in the bibliography.

⁵Refer to figures, tables, and plates in chapter 2 of this report.

Table E3. Significant porphyry copper occurrences in sub-tract 142pCu8003c Late Paleozoic Balkhash-Ili magmatic arc (west)—Kazakhstan.

[Ma, mega-annum (10^6 years); t, metric tons; Mt, million metric tons; %, percent; g/t, grams per metric ton; m, meters; N, north; NE, northeast; SE, southeast; Cu, copper; Mo, molybdenum; Au, gold; and Ag, silver; Re, rhenium; Se, selenium; Te, tellurium; In, indium; n.d., no data]

Name	Includes	Country	Latitude	Longitude	Age (Ma)	Contained Cu (t)	Reference
Karatas Ore Field	Karatas II	Kazakhstan	46.639	73.618	n.d.	Mineralized area along N-NE-striking zone that hosts Karatas I,III, and IV. Mine workings on Google Earth (3/11/10); estimated location	Seltmann and others (2009)
	Karatas III	Kazakhstan	46.633	73.637	n.d.	Mineralized area along N-NE-striking zone that hosts Karatas I, II, and IV. Skarn occurrence; location estimated on Google Earth (3/11/10)	Zhukov and others (1998)
	Karatas IV	Kazakhstan	46.640	73.619	n.d.	Grade: 0.24% Cu and 0.11% Mo; 0.16 g/t Re, 4.35 g/t Se, 0.23 g/t Te, 9.8 g/t Co, 27.0 g/t In. Dacite porphyries of the Keregetass suite (Middle Upper Carboniferous); granitoids of the Kokdombaksky complex (Upper Carboniferous) Minor granodiorite porphyries of the Kounradsky complex (Upper Carboniferous-Permian), with feldspathization, quartz alteration and sericitization. Cu-Mo ores at Karatas IV are within explosive breccias. Ore stockwork measures 360–400 m in diameter, dipping steeply to the northwest. Ore styles include disseminated, vein disseminated, and locally brecciated. Mine workings on Google Earth (3/11/10); estimated location; classified as porphyry-style deposit; extensive network of exploration roads; discoloration	Seltmann and others (2009)
	Northwest Karatas	Kazakhstan	46.648	73.591	n.d.	Deposit area characterized by biotite and biotite amphibolite gneiss granites, plagiogranites, and granodiorites of the Riphaen Mynshukursky complex; meta-limestones and dolomites, biotite-amphibole shales and amphibolites. Skarns and skarn-related rocks contain most of the ores. Daciteporphyries, granodiorites, small bodies of diorites and quartz diorites. Garnet, and pyroxene skarnoids. The copper magnetite ores are contained in the northwest-trending skarn zones, which are 600–700 m long by 50–100 m wide. Copper magnetite ores up to 50 m thick have also been intercepted in the skarns by drill holes. SE part of the Tasaral Kyzylespinskiy anticlinorium. Explored 1930–1952. Skarn occurrence; location estimated on Google Earth (3/11/10)	Seltmann and others (2009)
Sokurkoi	NA	Kazakhstan	46.413	73.991	Late Carboniferous (~310)	Small deposit with reported average grades 0.66% Cu and 0.005% Mo; and 0.1–10 g/t Au. Exposed. Location: Located in middle of road grid pattern; west of vein mines(?)	Zhukov and others (1998)

Grade and Tonnage Model Selection

The general porphyry copper deposit model published by Singer and others (2008) was used based on the known deposits in the tract being statistically consistent with the model.

Estimate of the Number of Undiscovered Deposits

Rationale for the Estimate

For sub-tract 142pCu8003c, after evaluation of available data the consensus was that (1) the ratio of porphyry copper occurrences and possible linked deposit types to the number

of known deposits was high and therefore a favorable indication of undiscovered deposits, (2) the depth of erosion of the terrane was not a concern, and (3) owing to the rugged terrain and remoteness of much of the area, there were plays left despite considerable Soviet-era exploration investment in the region.

The consensus estimate of the assessment team, a 50-percent chance of 1 or more deposits and a 10-percent chance of 5 or more deposits, results in an expected mean of 2 undiscovered deposits (table E5).

Probabilistic Assessment Simulation Results

Undiscovered resources were estimated by combining consensus estimates for numbers of undiscovered porphyry

Table E4. Principal sources of information used for the delineation of sub-tract 142pCu8003c, Late Paleozoic Balkhash-Ili magmatic arc (west)—Kazakhstan.

Theme	Name or title	Scale	Citation
Geology	Mineral deposits database and thematic maps of Central Asia	1:1,500,000	Seltmann and others (2009)
	Tectonic map of the Paleozoic folded areas of Kazakhstan and adjacent territories	1:1,500,000	Abdulin and Zaitseb (1976)
	Map of the ore fields and oil and gas fields of the Kazakh S.S.R. and adjacent territories of the Union Republics	1:500,000	Abdulin and others (1982)
	L-43-III (1959)	1:200,000	Vurovym and Vokan (1959)
	L-43-VII (1962)	1:200,000	Koshakin and others (1962)
	L-43-IX (1968)	1:200,000	Gaek and Cheurkin (1968)
	L-43-XIV (1966)	1:200,000	Nikolaenko and others (1966)
Mineral occurrences	Mineral deposits database and thematic maps of Central Asia	1:1,500,000	Seltmann and others (2009)
Geophysics	Magnetic anomaly data of the former U.S.S.R.	1:1,500,000	National Oceanic and Atmospheric Administration (1996)

Table E5. Undiscovered deposit estimates, deposit numbers, area, and deposit density for sub-tract 142pCu8003c, Late Paleozoic Balkhash-Ili magmatic arc (west)—Kazakhstan.

[N_{xx} , estimated number of deposits associated with the xxth percentile; N_{und} , expected number of undiscovered deposits; s , standard deviation; $C_v\%$, coefficient of variance; N_{known} , number of known deposits in the tract that are included in the grade and tonnage model; N_{total} , total of expected number of deposits plus known deposits; area, area of permissive tract in square kilometers (km^2); density, deposit density reported as the total number of deposits per 100,000 km^2 . N_{und} , s , and $C_v\%$ are calculated using a regression equation (Singer and Menzie, 2005)]

Consensus undiscovered deposit estimates					Summary statistics					Tract area (km^2)	Deposit density ($N_{total}/100k km^2$)
N_{90}	N_{50}	N_{10}	N_{05}	N_{01}	N_{und}	s	$C_v\%$	N_{known}	N_{total}		
0	1	5	5	5	1.9	1.9	100	2	3.9	23,800	16

copper deposits with the global grade and tonnage model for porphyry Cu-Au-Mo deposits of Singer and others (2008) using the EMINERS program (Root and others, 1992; Bawiec and Spanski, 2012; Duval, 2012). Selected simulation results are reported in table E6. Results of the Monte Carlo simulation are presented as a cumulative frequency plot (fig. E2). The cumulative frequency plot shows the estimated resource amounts associated with cumulative probabilities of

occurrence, as well as the mean, for each commodity and for total mineralized rock fig. E3).

Mean estimated copper resources in undiscovered deposits for tract 142pCu8003c, 7.4 Mt, greatly exceeds the 1 Mt of identified resources whereas the median estimate, 1.8 Mt, for the estimate of 2 undiscovered deposits is more comparable with the identified resources in the 2 known deposit in the tract (tables E1 and E6).

Table E6. Results of Monte Carlo simulations of undiscovered resources for sub-tract 142pCu8003c, Late Paleozoic Balkhash-Ili magmatic arc (west)—Kazakhstan.

[Cu, copper; Mo, molybdenum; Au, gold; and Ag, silver; in metric tons. Rock, in million metric tons]

Material	Probability of at least the indicated amount						Probability of	
	0.95	0.9	0.5	0.1	0.05	Mean	Mean or greater	None
Cu	0	0	1,800,000	18,000,000	31,000,000	7,400,000	0.26	0.3
Mo	0	0	9,700	480,000	900,000	210,000	0.2	0.45
Au	0	0	26	500	830	190	0.25	0.41
Ag	0	0	0	5,700	11,000	2,500	0.2	0.52
Rock	0	0	420	3,800	6,300	1,500	0.27	0.3

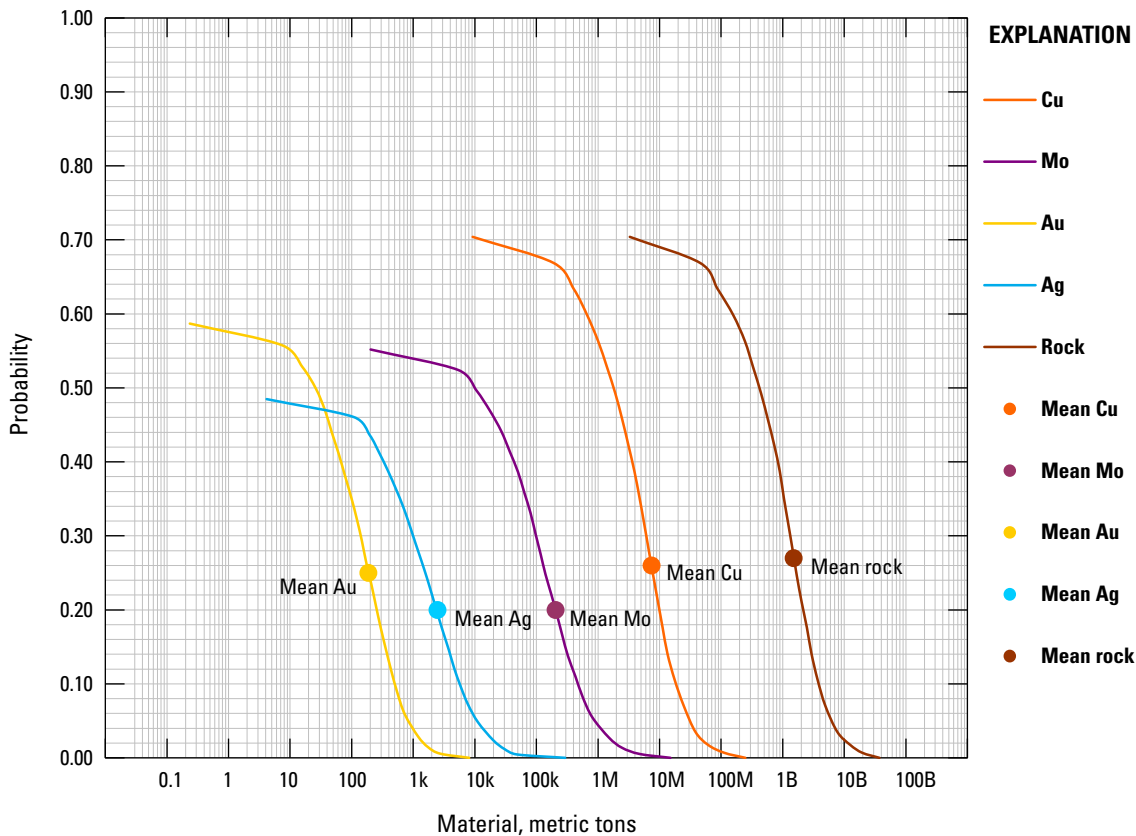


Figure E3. Cumulative frequency plot showing the results of Monte Carlo computer simulation of undiscovered resources in sub-tract 142pCu8003c, Late Paleozoic Balkhash-Ili magmatic arc (west)—Kazakhstan. k=thousands, M=millions, B=billions.

References Cited

- Abduln, A.A., and Zaitseb, Yu. A., 1976, [Tectonic map of the Paleozoic folded areas of Kazakhstan and adjacent territories]: Moscow, Aerogeologiya, scale 1:1,500,000. [In Russian.]
- Abduln, A.A., Bespalov, V.F., Volkov, V.M., Nikitchenko, I.I., Chakabaev, S.E., and Chimbulatov, M.A., 1982, [Map of the ore fields and oil and gas fields of the Kazakh S.S.R. and adjacent territories of the Union Republics]: St. Petersburg, VSEGEI, scale 1:500,000. [In Russian.]
- Bawiec, W.J., and Spanski, G.T., 2012, Quick-start guide for version 3.0 of EMINERS—Economic Mineral Resource Simulator: U.S. Geological Survey Open-File Report 2009–1057, 26 p., available at <http://pubs.usgs.gov/of/2009/1057/>. (This report supplements USGS OFR 2004–1344.)
- Berger, B.R., Ayuso, R.A., Wynn, J.C., and Seal, R.R., 2008, Preliminary model of porphyry copper deposits: U.S. Geological Survey Open-File Report 2008–1321, 55 p. (Also available at <http://pubs.usgs.gov/of/2008/1321/>.)
- Cox, D.P., 1986, Descriptive model of porphyry Cu (Model 17), in Cox, D.P., and Singer, D.A., eds., 1986, Mineral deposit models: U.S. Geological Survey Bulletin 1693, p. 76. (Also available at <http://pubs.usgs.gov/bul/b1693/>.)
- Duval, J.S., 2012, Version 3.0 of EMINERS—Economic Mineral Resource Simulator: U.S. Geological Survey Open-File Report 2004–1344, available at <http://pubs.usgs.gov/of/2004/1344/>.
- Gaek, O.M., and Cheurkin, I.I., 1968, [Geological map of the U.S.S.R., Balkhash series, Sheet L-43-IX]: Ministry of Geology of the U.S.S.R., scale 1:200,000. [In Russian.]
- Kolesnikov, V.V., Zhukov, N.M., Solodilova, V.V., and Filimonova, L.E., 1986, [Porphyry copper deposits of the Balkhash region]: Alma Ata, Nauka, 199 p. [In Russian.]
- Koshakin, V.Y., Koshakina, S.D., and Sklyarenko, L.M., 1962, [Geological map of the U.S.S.R., Balkhash series, Sheet L-43-XII]: Ministry of Geology and Mineral Resources Protection, scale 1:200,000. [In Russian.]
- Kudryavtsev, Y.K., 1996, The Cu-Mo deposits of Central Kazakhstan, in Shatov V., Seltmann, R., Kremenetsky, A., Lehman, B., Popov, V., and Ermolov, P., eds., Granite-related ore deposits of Central Kazakhstan and adjacent areas: St. Petersburg, IAGOD, Working Group on Tin and Tungsten Deposits (WGTT), p. 119–144.
- National Oceanic and Atmospheric Administration, 1996, Magnetic anomaly data of the former U.S.S.R.: Boulder, Colorado, National Geophysical Data Center, accessed August 1, 2009, at <http://www.ngdc.noaa.gov>.
- Nikolaenko, B.A., Nikolaenko, T.S., and Gonchearuk, A.F., 1966, [Geological map of the U.S.S.R., Balkhash series, Sheet L-43-XIV]: Ministry of Geology of the U.S.S.R., scale 1:200,000. [In Russian.]
- Pavlova, I.G., 1978, [Porphyry copper deposits]: Leningrad, Nedra, 275 p. [In Russian.]
- Plyushchev, E.V., 1993, Map of hydrothermal-metasomatic formations of Kazakhstan fold area: St. Petersburg, VSEGEI, 4 sheets, 1:1,500,000.
- Root, D.H., Menzie, W.D., and Scott, W.A., 1992, Computer Monte Carlo simulation in quantitative resource estimation: Natural Resources Research, v. 1, no. 2, p. 125–138.
- Seltmann, R., Shatov, V., and Yakubchuk, A., 2009, Mineral deposits database and thematic maps of Central Asia—ArcGIS 9.2, Arc View 3.2, and MapInfo 6.0 (7.0) GIS packages: London, Natural History Museum, Centre for Russian and Central EurAsian Mineral Studies (CERCAMS), scale 1:1,500,000, and explanatory text, 174 p. [Commercial dataset available at <http://www.nhm.ac.uk/research-curation/research/projects/cercams/products.html>.]
- Singer, D.A., and Menzie, W.D., 2005, Statistical guides to estimating the number of undiscovered mineral deposits—An example with porphyry copper deposits, in Cheng, Qiuming, and Bonham-Carter, G., eds., Proceedings of IAMG—The annual conference of the International Association for Mathematical Geology: Toronto, Canada, Geomatics Research Laboratory, York University, p. 1028–1033.
- Singer, D.A., Berger, V.I., and Moring, B.C., 2008, Porphyry copper deposits of the world: U.S. Geological Survey Open-File Report 2008–1155, 45 p., accessed August 10, 2009, at <http://pubs.usgs.gov/of/2008/1155/>.
- Vurovym, V.G., and Vokan, V.V., 1959, [Geological map of the U.S.S.R., Balkhash series, Sheet L-43-III]: Ministry of Geology and Mineral Resources Protection, scale 1:200,000. [In Russian.]
- Windley, B.F., Alexeiev, D., Xiao, W., Kroner, A., and Badarch, G., 2007, Tectonic models for accretion of the Central Asian Orogenic Belt: London, Journal of the Geological Society, v. 164, p. 31–47.
- Yakubchuk, A., 2004, Architecture and mineral deposit settings of the Altaid orogenic collage—A revised model: Journal of Asian Earth Sciences, v. 23, p. 761–779.
- Zhukov, N.M., Kolesnikov, V.V., Miroshnichenko, L.M., Egembayev, K.M., Pavlova, Z.N., and Bakarasov, E.V., compilers, 1998, Copper deposits of Kazakhstan—Reference book: Almaty, Ministry of Ecology and Natural Resources of the Republic of Kazakhstan, 136 p.

Appendix F. Porphyry Copper Assessment for Sub-tract 142pCu8003d, Late Paleozoic Balkhash-Ili Magmatic Arc (Northwest)—Kazakhstan and Kyrgyzstan

By Byron R. Berger¹, Paul D. Denning¹, Connie L. Dicken², Lawrence J. Drew², Jane M. Hammarstrom², John C. Mars², Jeffrey D. Phillips¹, and Michael L. Zientek³

Deposit Type Assessed: Porphyry Copper

Descriptive model: Porphyry copper (Cox, 1986; Berger and others, 2008)

Grade and tonnage model: Global Cu-Au-Mo porphyry copper model (Singer and others, 2008)

Table F1 summarizes selected assessment results.

Table F1. Summary of selected resource assessment results for sub-tract 142pCu8003d, Late Paleozoic Balkhash-Ili magmatic arc (northwest)—Kazakhstan and Kyrgyzstan.

[km, kilometers; km², square kilometers; t, metric tons]

Date of assessment	Assessment depth (km)	Tract area (km ²)	Known copper resources (t)	Mean estimate of undiscovered copper resources (t)	Median estimate of undiscovered copper resources (t)
2009	1	112,150	3,300,000	7,800,000	2,700,000

Location

The tract is a region in central Kazakhstan to the southeast of western Lake Balkhash within the Balkhash Depression (fig. F1). In this region, the permissive Carboniferous magmatic-arc rocks are largely unexposed owing to cover by Late Cenozoic sedimentary deposits. The city of Balkhash on the north shore of Lake Balkhash (see fig. 1-2⁴) in permissive sub-tract 142pCu8003b is located approximately 20 kilometers (km) due north of the north boundary of permissive sub-tract 142pCu8003d, and the village of Mynaral is located on the west shore of Lake Balkhash near the west boundary of sub-tract 142pCu8003d.

Geologic Feature Assessed

The permissive tract encompasses Late Carboniferous to Permian magmatic-arc rocks that are a part of the Balkhash-Ili volcanic arc (see fig. 1-22) of Windley and others (2007), most of which is concealed beneath Cenozoic fill in the Balkhash Depression. Geologic cross sections based on drill hole data in the Mesozoic to Cenozoic sediments show that the fill across much of the depression is less than 1 km thick. In the cross sections as well as regional-scale geologic maps of the basement, maps show the basement to the fill to be predominantly a Devonian magmatic-arc sequence although some thin stratigraphic sections of Carboniferous magmatic arc rocks are also shown. Some intrusive rocks, largely undated, are mapped as Devonian, others as Carboniferous. There are known Carboniferous porphyry copper occurrences in the sub-tract.

¹U.S. Geological Survey, Denver, Colorado.

²U.S. Geological Survey, Reston, Virginia.

³U.S. Geological Survey, Spokane, Washington.

⁴Refer to chapter 1 of this report.

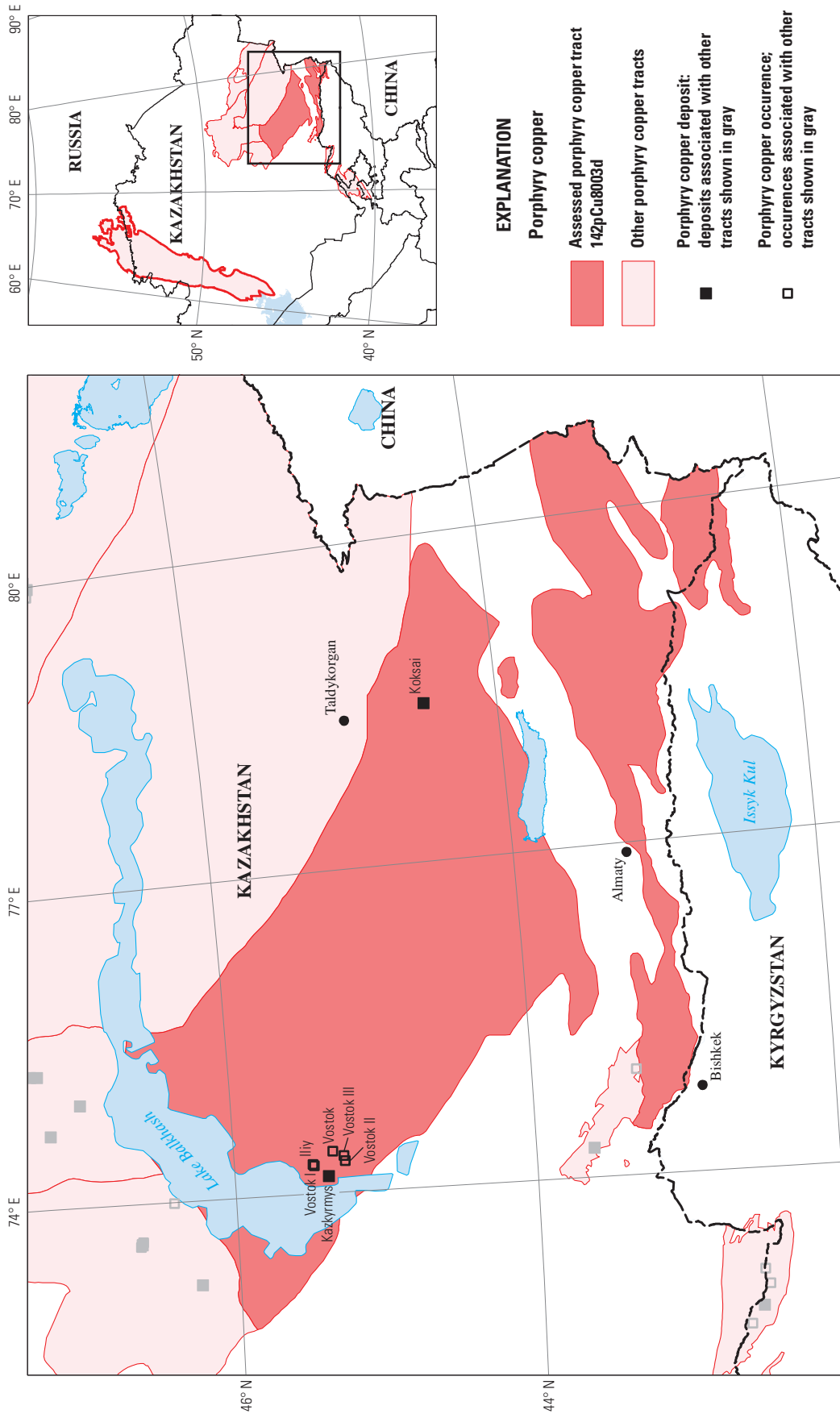


Figure F1. Map showing the location, known deposits, and significant occurrences for sub-tract 142pCu8003d, Late Paleozoic Balkhash-Il'i magmatic arc (northwest)—Kazakhstan and Kyrgyzstan. Location of map area shown on inset.

Delineation of the Permissive Tract

Geologic Criteria

The principal litho-tectonic terrane concept used to delineate this sub-tract was that of a magmatic arc that formed above a subduction zone. Sub-tract 142pCu8003d adjoins sub-tracts 142pCu8003b and 142pCu8003c on the north at Lake Balkhash and extends south to the Tian Shan mountain ranges and adjacent terrains. Nonpermissive rocks form the west and south boundaries, and permissive sub-tract 142pCu8004 forms the east boundary. To the south, in the vicinity of the Tian Shan mountain ranges, the continuity of the sub-tract is interrupted by a series of Cenozoic basins that exceed 1 km in depth and parallel the north margin of the Tian Shan. The southernmost area of this segmented permissive sub-tract is within the Tian Shan mountain ranges. The northern boundary of this southernmost segment is along the frontal fault zone for the Tian Shan uplift. The southern boundary is drawn to include permissive Middle to Late Carboniferous rocks and associated intrusions that are part of the North Tian Shan tectonic block. The eastern boundary of the southern segment is placed at the Kazakhstan-China border the distribution of permissive Carboniferous rocks in the tract are shown in fig. F2.

Sub-tract 142pCu8003d includes rocks interpreted to be part of the Late Paleozoic Balkhash-Ili Arc. It is a large area characterized and differentiated from adjoining sub-tracts by extensive Mesozoic to Cenozoic cover within the Balkhash Depression, a distinct aeromagnetic anomaly pattern dominated by numerous and closely spaced positive magnetic anomalies, and a considerable uncertainty as to the age and source of the magnetic susceptibility observed owing to the complete overlap of Devonian and Carboniferous magmatic-arc sequences.

Four principal sources of information, supplemented by numerous published journal and symposium papers, were used to delineate this tract. The primary sources were the mineral deposits map of Central Asia on a geologic base edited by Seltmann and others (2009), supplemented by 1:200,000-scale geologic maps originally published by the former Soviet (U.S.S.R.) government, a reduced-to-pole aeromagnetic map prepared by J.D. Phillips from the Magnetic Anomaly Map of the World (2007), the interpretation of Advanced Spaceborne Thermal Emission and Reflection Radiometer (ASTER) satellite imagery of hydrothermal alteration minerals or suites of minerals wherever possible by J.C. Mars, and tectonic terrane maps published by Abdulin and Zaitseb (1976), Yakubchuk (2004), and Windley and others (2007).

In geologic map cross sections, the greatest proportion of nonintrusive rocks beneath the Mesozoic to Cenozoic cover in this sub-tract are pre-Carboniferous, predominantly Devonian. However, many of the assigned ages on the published geologic maps are visual interpretations based on drill cuttings that are subject to question and many more of the intrusive rocks in this tract than the mapping implies may be Carboniferous

(D. Alexeiev, Russian Academy of Sciences, oral commun., 2009). Throughout the permissive tract, geologic mapping indicates that thrust and related faults and folding deformed the Devonian arc suites prior to the onset of Carboniferous arc magmatism. During C_2 - P_1 arc magmatism, strike-slip faulting predominated along the margins of the sub-tract, although Seltmann and others (2009) show some buried, inferred regional strike-slip faults within the sub-tract.

Known Deposits

Two porphyry copper deposits are known within sub-tract 142pCu8003d, Kazkymys and Koksai (fig. F1, table F2).

Kazkymys

Although listed by Singer and others (2008) as Devonian, the Kazkymys porphyry copper deposit is likely Carboniferous (D. Alexeiev, oral commun., 2009). The deposit is located near the southwest margin of Lake Balkhash. Kazkymys is a complex of discrete, but nearby deposits known as Vostok I-V. Zhukov and others (1998) list pyrite, chalcopyrite, molybdenite, and gold as primary ore minerals. Singer and others (2008) also include bornite, chalcocite, and enargite. Gangue minerals include quartz, biotite, sericite, magnetite, and pyrrhotite (Zhukov and others, 1998). Singer and others (2008) include alunite as an alteration mineral.

Koksai

The Koksai porphyry copper deposit is located in the southeast part of this sub-tract. Although it was interpreted by Singer and others (2008) as Silurian, our own reanalysis of data in Toloiev and others (1986) shows that the deposit is most likely C_3 - P_1 . Toloiev and others (1986) describe quartz-sericite-chlorite-sulfide alteration of Silurian and Carboniferous country rocks as well as alteration of dikes within the deposit and, outside of the deposit, texturally and compositionally similar dikes cross cut Carboniferous rocks. Toloiev and others (1986) interpret the dikes to be Permian.

The Koksai deposit is associated with a swarm of Permian (?) granodiorite porphyry dikes that intrude a Silurian (?) granodiorite to diorite stock. Host rocks to the stock are Early Silurian siliciclastic and carbonate rocks. Lying unconformably on this sequence are Early to Late Carboniferous volcanoclastic and volcanic rocks of the Balkhash-Ili Arc complex. The quartz-biotite plagiogranite to granodiorite dikes, with which the porphyry copper mineralization appears to be related, intrude Carboniferous rocks as young as C_3 . Disseminated and stockwork vein ores developed within the dikes and the Silurian (?) stock. Ore minerals include chalcopyrite, molybdenite, bornite, digenite, and pyrite (Zhukov and Filimonova, 1986). Alteration minerals include quartz, sericite, K-feldspar, chlorite, apatite, calcite, dolomite, albite, titanite, anhydrite, barite, and ankerite (Zhukov and Filimonova, 1986).

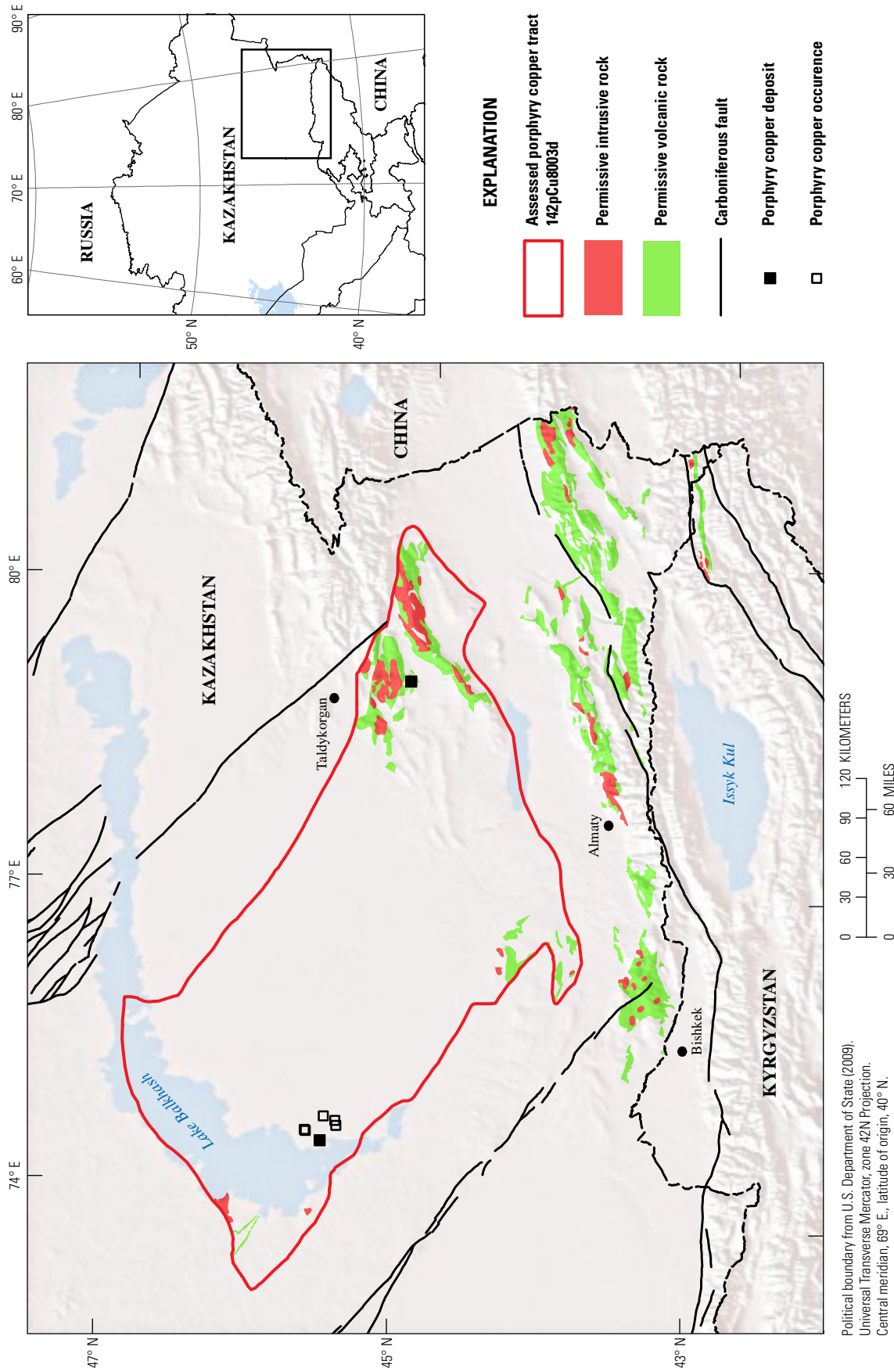


Figure F2. Map showing the distribution of permissive Carboniferous volcanic and volcanoclastic rocks (green) and intrusive rocks (red) in sub-tract 142pCu8003d, Late Paleozoic Balkhash-Ili magmatic arc (northwest)—Kazakhstan and Kyrgyzstan, on a digital elevation base. Location of map area shown on inset.

Table F2. Porphyry copper deposits in sub-tract 142pCu8003d, Late Paleozoic Balkhash-Ili magmatic arc (northwest)—Kazakhstan and Kyrgyzstan.

[Ma, mega-annum (10^6 years); t, metric tons; Mt, million metric tons; %, percent; g/t, grams per metric ton; Cu, copper; Mo, molybdenum; Au, gold; Ag, silver; Cu-Mo subtype, deposits that have Au/Mo ratios less than 3 or average Mo grades greater than 0.03%; NA, not applicable]

Name	Country	Latitude	Longitude	Subtype	Age (Ma)	Tonnage (Mt)	Cu (%)	Mo (%)	Au (g/t)	Ag (g/t)	Contained Cu (t)	Reference
Kazkymys	Kazakhstan	45.383	74.158	NA	375	375	0.41	0.007	0.059	0.79	1,537,500	D.P. Cox (U.S. Geological Survey, written commun., 2001), Zhukov and others (1998)
Koksai	Kazakhstan	44.482	78.450	Cu-Mo	422	320	0.55	0.049	0.12	1.24	1,760,000	Kolesnikov and others (1986), Krivtsov and others (1986), Metal Mining Agency of Japan (1997), Pavlova (1978), Plyushchev (1993), Sokolov (1999), Zhukov and others (1998)

Porphyry Copper Occurrences, and Related Deposit Types

Seltmann and others (2009) show occurrences near the southwestern shoreline of Lake Balkhash, as well as occurrences about 210 km west-southwest of Koksai, several occurrences scattered from near Koksai to about 40 km northwest, and several others scattered from about 30 to 75 km southeast of Koksai (table F3).

As of 2008, Vale S.A. had an 85 percent interest in the Vostok advanced copper exploration project; the other 15 percent was held by Cape Lambert Resources Limited. The project includes five prospect areas, primarily focused on two porphyry exploration targets, Vostok I and III, which had Soviet era resource estimates; the prospects are covered by about 100 meters (m) of Neogene and Quaternary sediments. Supergene zones (chalcocite, copper oxides) overlie chalcopyrite at some prospects. The deposits were drilled in 2004 and 2005, with estimates of about 2 million metric tons (Mt) of copper to 500 m depth (Scarborough Minerals plc, 2006). Results of subsequent exploration are unknown.

Hydrothermal Alteration Mapping (ASTER)⁵

Argillic and phyllic ASTER hydrothermal alteration mapping covers approximately 50 percent of tract 142pCu8003d; silicic alteration mapping covers approximately

30 percent of the tract (see figs. 2-1 and 2-2). Using the ASTER hydrothermal alteration map, 20 potential deposit sites were defined in the tract (see fig. 2-3 and plates 1–8). Mineral databases indicate the existence of 4 copper occurrences associated with potential deposit sites in the tract (see table 2-1). The geologic map indicates that the most common altered rocks at the sites include intermediate tuff, and granodiorite (see table 2-1; Seltmann and others, 2009).

The Kounrad mine, the largest porphyry copper deposit in the region, is located in tract 142pCu8003b. Alteration characteristics of the Kounrad mine were used to identify other potential sites with similar alteration characteristics in sub-tract 142pCu8003d due to the similarities of rock exposure and vegetation of tracts the two tracts (see fig. 2-4). Altered rock characteristics include size diameter of alteration pattern greater than or equal to 1.7 km, phyllic and argillic alteration density greater than or equal to 7 km, and at least 80 percent phyllic alteration coverage. A total of 6 sites have alteration characteristics similar to Kounrad (see table 2-1). The ASTER hydrothermal alteration map and mineral databases show that 1 of the sites with similar alteration characteristics to Kounrad (see table 2-1, site1) was associated with a known copper occurrence.

Exploration History

An historical record of exploration within this sub-tract has not been compiled.

⁵Refer to figures, tables, and plates in chapter 2 of this report.

Table F3. Significant porphyry copper occurrences in sub-tract 142pCu8003d, Late Paleozoic Balkhash-Ili magmatic arc (northwest)—Kazakhstan and Kyrgyzstan.

[Ma, mega-annum (10^6 years); %, percent; g/t, grams per metric ton; m, meters; SE, southeast; Cu, copper; Co, cobalt; Au, gold; Ag, silver; Bi, bismuth; n.d., no data]

Name	Country	Latitude	Longitude	Age (Ma)	Comments	Reference
Iliy	Kazakhstan	45.482	74.276	n.d.	Occurrence	Seltmann and others (2009)
Vostok	Kazakhstan	45.347	74.391	n.d.	Vostok exploration project includes Vostok I-V; Soviet era resource estimates of grade: 0.7% Cu; 0.25 g/t Au, 5 g/t Ag, 5 g/t Bi, 0.005% Co. Secondary alunite quartzites.	Seltmann and others (2009), Scarborough Minerals (2006), Mineral Securities Ltd. (2007)
Vostok I	Kazakhstan	45.476	74.266	n.d.	Cluster of small porphyry occurrences SE of Kaskyrmys; estimated locations for I, II, and III are after Zhukov and others (1998) using Google Earth (3/11/10); roads evident at all locations sited. Chalcocite and pyrite; chalcopyrite at depth. Porphyry copper prospect beneath 100 m Quaternary cover; Soviet era discovery.	Seltmann and others (2009), Scarborough Minerals (2006), Mineral Securities Ltd. (2007), Zhukov and others (1998)
Vostok II	Kazakhstan	45.269	74.292	n.d.	Cluster of small porphyry occurrences SE of Kaskyrmys; estimated locations for I, II, and III are after Zhukov and others (1998) using Google Earth (3/11/10); roads evident at all locations sited	Seltmann and others (2009), Zhukov and others (1998)
Vostok III	Kazakhstan	45.274	74.343	n.d.	Cluster of small porphyry occurrences SE of Kaskyrmys; estimated locations for I, II, and III are after Zhukov and others (1998) using Google Earth (3/11/10); roads evident at all locations sited	Seltmann and others (2009), Scarborough Minerals (2006), Mineral Securities Ltd. (2007), Zhukov and others (1998)

Sources of Information

Principal sources of information used by the assessment team for delineation of 142pCu8003d are listed in table F4 and in the references cited.

Grade and Tonnage Model Selection

The general porphyry copper deposit model published by Singer and others (2008) was used based on the known deposits in the tract being statistically consistent with the model.

Estimate of the Number of Undiscovered Deposits

Rationale for the Estimate

Prior to making estimates of undiscovered deposits (table F5), the assessment team first reviewed the geologic framework and aeromagnetic data with particular attention paid to the (1) correctness of the tract boundary with respect to depth of covered areas, (2) permissiveness of included rock formations, (3) the proportion of the mapped geologic units

that are permissive and what proportion of these are intrusive, and (4) variations in the depth of exposure of the permissive rocks within the tract and whether or not the tract or whether the tract should be subdivided into several sub-tracts. Second, the assessment team discussed the known deposits and occurrences, discussed the distribution of the known deposits and occurrences, and evaluated the deposit type distribution as an indicator of depth of exposure in the arc terrane as well as what the distribution implied about the uniformity of the depth of exposure across the tract. Third, the team examined alteration information as interpreted from ASTER and Landsat satellite data and discussed the possible meaning and size of altered areas. Fourth, the team speculated on the likely thoroughness with which the region had been explored. The consensus was that less than a tenth of the delineated tract was of the correct age and (or) the correct igneous rock types to host porphyry copper deposits but maps were not available to subdivide the tract. The consensus was that (1) there was no basis for further subdividing the sub-tract, (2) the ratio of porphyry copper occurrences and possible linked deposit types to the number of known deposits was high and therefore a favorable indication of undiscovered deposits, (3) the depth of erosion of the terrane was not a concern, and (4) owing to the rugged terrain and remoteness of much of the area, many plays were left despite considerable Soviet-era exploration investment in the region.

Table F4. Principal sources of information used for the delineation of sub-tract 142pCu8003d, Late Paleozoic Balkhash-Ili magmatic arc (northwest)—Kazakhstan and Kyrgyzstan.

Theme	Name or title	Scale	Citation
Geology	Mineral deposits database and thematic maps of Central Asia	1:1,500,000	Seltmann and others (2009)
	Tectonic map of the Paleozoic folded areas of Kazakhstan and adjacent territories	1:1,500,000	Abduln and Zaitseb (1976)
	K-44-I (1964)	1:200,000	Cheabdarov (1964)
	K-44-II (1965)	1:200,000	Cheabdarov and Bazheanov (1965)
	K-44-III (1965)	1:200,000	Kashakarov and others (1965)
	L-43-XIV (1966)	1:200,000	Nikolaenko and others (1966)
	L-43-XXI (1981)	1:200,000	Samigullin (1981a)
	L-43-XXVII (1981)	1:200,000	Samigullin (1981b)
	L-43-XXVIII (1978)	1:200,000	Karagodin (1978)
	L-43-XXXIV (1979)	1:200,000	Gokhashatein and Prokopenko (1979)
	L-44-XXV (1965)	1:200,000	Mairin and Nikitchenko (1965)
	L-44-XXXII (1965)	1:200,000	Sterkin and others (1965a)
L-44-XXXIII (1965)	1:200,000	Sterkin and others (1965b)	
Mineral occurrences	Mineral deposits database and thematic maps of Central Asia	1:1,500,000	Seltmann and others (2009), Zvezdov and others (1993)
Geophysics	Magnetic anomaly data of the former U.S.S.R.	1:1,500,000	National Oceanic and Atmospheric Administration (1996)

Table F5. Undiscovered deposit estimates, deposit numbers, sub-tract area, and deposit density for sub-tract 142pCu8003d, Late Paleozoic Balkhash-Ili magmatic arc (northwest)—Kazakhstan and Kyrgyzstan.

[N_{xx} , estimated number of deposits associated with the xxth percentile; N_{und} , expected number of undiscovered deposits; s , standard deviation; $C_v\%$, coefficient of variance; N_{known} , number of known deposits in the tract that are included in the grade and tonnage model; N_{total} , total of expected number of deposits plus known deposits; area, area of permissive tract in square kilometers (km^2); density, deposit density reported as the total number of deposits per 100,000 km^2 . N_{und} , s , and $C_v\%$ are calculated using a regression equation (Singer and Menzie, 2005)]

Consensus undiscovered deposit estimates					Summary statistics					Tract area (km^2)	Deposit density ($N_{total}/100k km^2$)
N_{90}	N_{50}	N_{10}	N_{05}	N_{01}	N_{und}	s	$C_v\%$	N_{known}	N_{total}		
0	2	4	4	4	2	1.5	73	2	4	112,150	4

The team considered the 2 known deposits in the sub-tract area (table F2), the significant occurrences in the Vostok project area (table F3), and the 6 alteration sites compatible with porphyry-style occurrences for a consensus estimate of a 50-percent chance of 2 undiscovered deposits and a 10-percent chance of 4 deposits; the result is a mean of 2 undiscovered deposits.

Probabilistic Assessment Simulation Results

Undiscovered resources for the tract were estimated by combining consensus estimates for numbers of undiscovered porphyry copper deposits with the global grade and tonnage

model for porphyry Cu-Au-Mo deposits of Singer and others (2008) using the EMINERS program (Root and others, 1992; Bawiec and Spanski, 2012; Duval, 2012). Selected simulation results are reported in table F6. Results of the Monte Carlo simulation are presented as a cumulative frequency plot (fig. F3). The cumulative frequency plot shows the estimated resource amounts associated with cumulative probabilities of occurrence, as well as the mean, for each commodity and for total mineralized rock.

Mean estimated copper (7.8 Mt copper) associated with undiscovered deposits in the tract is about twice the identified resources (3.3 Mt); the median from the simulation (2.7 Mt) is slightly less than identified resources (table F1).

Table F6. Results of Monte Carlo simulations of undiscovered resources for sub-tract 142pCu8003d, Late Paleozoic Balkhash-Ili magmatic arc (northwest)—Kazakhstan and Kyrgyzstan.

[Cu, copper; Mo, molybdenum; Au, gold; and Ag, silver; in metric tons. Rock, in million metric tons]

Material	Probability of at least the indicated amount						Probability of	
	0.95	0.9	0.5	0.1	0.05	Mean	Mean or greater	None
Cu	0	0	2,700,000	17,000,000	31,000,000	7,800,000	0.25	0.2
Mo	0	0	24,000	520,000	960,000	220,000	0.2	0.36
Au	0	0	44	510	820	200	0.26	0.32
Ag	0	0	150	5,500	11,000	2,400	0.2	0.45
Rock	0	0	610	3,700	6,200	1,600	0.26	0.2

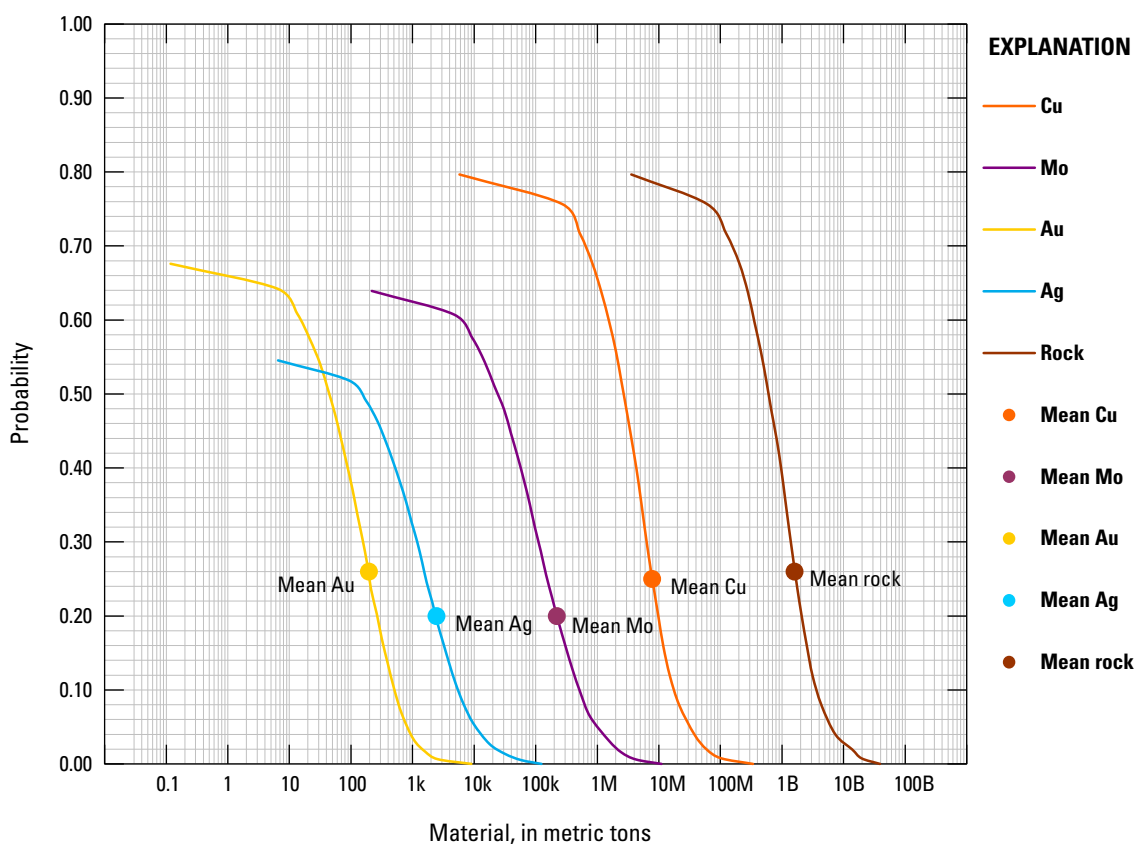


Figure F3. Cumulative frequency plot showing the results of Monte Carlo computer simulation of undiscovered resources for sub-tract 142pCu8003d, Late Paleozoic Balkhash-Ili magmatic arc (northwest)—Kazakhstan and Kyrgyzstan. k=thousands, M=millions, B=billions.

References Cited

- Abdulin, A.A., and Zaitseb, Yu. A., 1976, [Tectonic map of the Paleozoic folded areas of Kazakhstan and adjacent territories]: Moscow, Aerogeologiya, scale 1:1,500,000. [In Russian.]
- Abdulin, A.A., Bepalov, V.F., Volkov, V.M., Nikitchenko, I.I., Chakabaev, S.E., and Chimbulatov, M.A., 1982, [Map of the ore fields and oil and gas fields of the Kazakh S.S.R. and adjacent territories of the Union Republics]: St. Petersburg, VSEGEI, scale 1:500,000. [In Russian.]
- Bawiec, W.J., and Spanski, G.T., 2012, Quick-start guide for version 3.0 of EMINERS—Economic Mineral Resource Simulator: U.S. Geological Survey Open-File Report 2009–1057, 26 p., accessed July 15, 2012, at <http://pubs.usgs.gov/of/2009/1057/>. (This report supplements USGS OFR 2004–1344.)
- Berger, B.R., Ayuso, R.A., Wynn, J.C., and Seal, R.R., 2008, Preliminary model of porphyry copper deposits: U.S. Geological Survey Open-File Report 2008–1321, 55 p., accessed May 15, 2009, at <http://pubs.usgs.gov/of/2008/1321/>.
- Cheabdarov, N.M., 1964, [Map of mineral resources of the U.S.S.R., Dzungar Series, Sheet K-44-I]: State Geological Committee of the U.S.S.R., scale 1:200,000. [In Russian.]
- Cheabdarov, N.M., and Bazheanov, O.V., 1965, [Geological map of the U.S.S.R., Dzungar Series, Sheet K-44-II]: State Geological Committee of the U.S.S.R., scale 1:200,000. [In Russian.]
- Cox, D.P., 1986, Descriptive model of porphyry Cu (Model 17), in Cox, D.P., and Singer, D.A., eds., 1986, Mineral deposit models: U.S. Geological Survey Bulletin 1693, p. 76. (Also available at <http://pubs.usgs.gov/bul/b1693/>.)
- Duval, J.S., 2012, Version 3.0 of EMINERS—Economic Mineral Resource Simulator: U.S. Geological Survey Open-File Report 2004–1344, accessed July 15, 2012, at <http://pubs.usgs.gov/of/2004/1344>.
- Gokhashatein, V.I., and Prokopenko, T.A., 1979, [State geological map of the U.S.S.R., Betpakdala series, Sheet L-43-XXXIV, Aydarly]: Ministry of Geology U.S.S.R., scale 1:200,000. [In Russian.]
- Karagodin, P.F., 1978, [State geological map of the U.S.S.R., Balkhash series, sheet L-43-XXIII Zharkudun Village]: Ministry of Geology of the U.S.S.R., VSEGEI, scale 1:200,000. [In Russian.]
- Kashakarov, B.F., Grigoriev, S.I., and Blinov, B.P., 1965, [Map of mineral resources of the U.S.S.R., Dzungar Series, Sheet K-44-III]: State Geological Committee of the U.S.S.R., scale 1:200,000. [In Russian.]
- Kolesnikov, V.V., Zhukov, N.M., Solodilova, V.V., and Filimonova, L.E., 1986, [Porphyry copper deposits of the Balkhash region]: Alma Ata, Nauka, 199 p. [In Russian.]
- Krivtsov, A.I., Migachev, I.F., and Popov, V.S., 1986, [Porphyry copper deposits of the world]: Moscow, Nedra, 236 p. [In Russian.]
- Mairin, S.E., and Nikitchenko, I.I., 1965, [Geological map of the U.S.S.R., Dzungar Series, Sheet L-44-XXV]: State Geological Committee of the U.S.S.R., scale 1:200,000. [In Russian.]
- Metal Mining Agency of Japan, 1997, Non-ferrous metal deposits of C.I.S. countries and Mongolia: Metal Mining Agency of Japan, 20 p.
- Mineral Securities Limited, 2007, Annual report 2007: Mineral Securities Limited, 80 p.
- National Oceanic and Atmospheric Administration, 1996, Magnetic anomaly data of the former U.S.S.R.: Boulder, Colorado, National Geophysical Data Center, accessed August 1, 2009, at <http://www.ngdc.noaa.gov>.
- Nikolaenko, B.A., Nikolaenko, T.S., and Gonchearuk, A.F., 1966, [Geological map of the U.S.S.R., Balkhash series, Sheet L-43-XIV]: Ministry of Geology of the U.S.S.R., scale 1:200,000. [In Russian.]
- Pavlova, I.G., 1978, [Porphyry copper deposits]: Nedra, Leningrad, 275 p. [In Russian.]
- Plyushchev, E.V., 1993, Map of hydrothermal-metasomatic formations of Kazakhstan fold area: St. Petersburg, VSEGEI, 4 sheets, 1:1,500,000.
- Root, D.H., Menzie, W.D., and Scott, W.A., 1992, Computer Monte Carlo simulation in quantitative resource estimation: Natural Resources Research, v. 1, no. 2, p. 125–138.
- Samigullin, F.A., 1981a, [State geological map of the U.S.S.R., Balkhash series, Sheet L-43-XXI, Karan]: Ministry of Geology U.S.S.R., scale 1:200,000. [In Russian.]
- Samigullin, F.A., 1981b, [State geological map of the U.S.S.R., Betpakdala series, Sheet L-43-XXVII, Balatopar]: Ministry of Geology U.S.S.R., scale 1:200,000. [In Russian.]
- Scarborough Minerals plc, 2006, Annual report 2006: Scarborough Minerals plc, 72 p.

- Seltmann, R., Shatov, V., and Yakubchuk, A., 2009, Mineral deposits database and thematic maps of Central Asia—ArcGIS 9.2, Arc View 3.2, and MapInfo 6.0(7.0) GIS packages: London, Natural History Museum, Centre for Russian and Central EurAsian Mineral Studies (CERCAMS), scale 1:1,500,000, and explanatory text, 174 p. [Commercial dataset available at <http://www.nhm.ac.uk/research-curation/research/projects/cercams/products.html>.]
- Singer, D.A., and Menzie, W.D., 2005, Statistical guides to estimating the number of undiscovered mineral deposits—An example with porphyry copper deposits, *in* Cheng, Q., and Bonham-Carter, G., eds., *Proceedings of IAMG—The annual conference of the International Assoc. for Mathematical Geology*: Toronto, Canada, Geomatics Research Laboratory, York University, p. 1028–1033.
- Singer, D.A., Berger, V.I., and Moring, B.C., 2008, Porphyry copper deposits of the world: U.S. Geological Survey Open-File Report 2008–1155, 45 p., accessed August 15, 2011, at <http://pubs.usgs.gov/of/2008/1155/>.
- Sokolov, A.L., 1999, Regional and local controls on gold and copper mineralization in central Asia and Kazakhstan, *in* Porter, T.M., ed., *Porphyry and hydrothermal copper & gold deposits—A global perspective*, Conference Proceedings: Glenside, South Australia, Australian Mineral Foundation, p. 181–190.
- Sterkin, V.D., Sklyarenko, L.M., and Il'yasov, M.A., 1965a, [Map of mineral resources of the U.S.S.R., Dzungar Series, Sheet L-44-XXXII]: State Geological Committee of the U.S.S.R., scale 1:200,000. [In Russian.]
- Sterkin, V.D., Sklyarenko, L.M., and Il'yasov, M.A., 1965b, [Geological map of the U.S.S.R., Dzungar Series, Sheet L-44-XXXIII]: State Geological Committee of the U.S.S.R., scale 1:200,000. [In Russian.]
- Toloev, A.N., Kukareka, M.V., Zhukov, N.M., and Filimonova, L.E., 1986, Koksai deposit, *in* Abdulina, A.A., and Chakabaev, S.E., eds., *Balkhash segment: Kazakhstan S.S.R.*, Nauka, p. 35–44.
- Windley, B.F., Alexeiev, D., Xiao, W., Kroner, A., and Badarch, G., 2007, Tectonic models for accretion of the Central Asian Orogenic Belt: *Journal of the Geological Society*, London, v. 164, p. 31–47.
- Yakubchuk, A., 2004, Architecture and mineral deposit settings of the Altaid orogenic collage—A revised model: *Journal of Asian Earth Sciences*, v. 23, p. 761–779.
- Zhukov, N.M., and Filimonova, L.E., 1982, [Metasomatites and hypogene mineralization in the Aktogai porphyry copper deposit]: *Geology of Ore Deposits*, v. 24, no. 2, p. 102–110. [In Russian.]
- Zhukov, N.M., and Filimonova, L.E., 1986, Mineralogical and petrographical characteristics of the hypogene mineralization and hydrothermally altered rocks, *in* Abdulina, A.A., and Chakabaev, S.E., eds., *Balkhash segment: Kazakhstan S.S.R.*, Nauka, p. 111–115.
- Zhukov, N.M., Kolesnikov, V.V., Miroshnichenko, L.M., Egembaev, K.M., Pavlova, Z.N., and Bakarasov, E.V., comps., 1998, *Copper deposits of Kazakhstan—Reference book*: Almaty, Ministry of Ecology and Natural Resources of the Republic of Kazakhstan, 136 p.
- Zvezdov, V.S., Migachev, I.F., and Girfanov, M.M., 1993, Porphyry copper deposits of the CIS and the models of their formation: *Ore Geology Reviews*, v. 7, p. 511–549.

Appendix G. Porphyry Copper Assessment for 142pCu8004, Late Paleozoic Central Balkhash-Ili Magmatic Arc—Kazakhstan

By Byron R. Berger¹, Paul D. Denning¹, Connie L. Dicken², Lawrence J. Drew², Jane M. Hammarstrom², John C. Mars², Jeffrey D. Phillips¹, and Michael L. Zientek³

Deposit Type Assessed: Porphyry Copper

Descriptive model: Porphyry copper (Cox, 1986; Berger and others, 2008)

Grade and tonnage model: Global Cu-Au-Mo porphyry copper model (Singer and others, 2008)

Table G1 summarizes selected assessment results.

Table G1. Summary of selected resource assessment results for tract 142pCu8004, Late Paleozoic Central Balkhash-Ili magmatic arc—Kazakhstan.

[km, kilometers; km², square kilometers; t, metric tons; n.d., no data]

Date of assessment	Assessment depth (km)	Tract area (km ²)	Known copper resources (t)	Mean estimate of undiscovered copper resources (t)	Median estimate of undiscovered copper resources (t)
2010	1	100,820	n.d.	7,800,000	2,800,000

Location

The tract is a region in central-eastern Kazakhstan wherein the permissive Carboniferous magmatic-arc rocks are largely not exposed, and there is less areal continuity to the positive magnetic anomalies indicative of magmatic activity than is the case for equivalent-age arc rocks in the adjacent permissive sub-tract 142pCu8003d. The area that makes up 142pCu8004 and its relation to other permissive tracts in Central Asia is shown in figure G1.

Geologic Feature Assessed

The permissive tract encompasses largely concealed Late Carboniferous to Permian magmatic-arc rocks that are a part of the Balkhash-Ili volcanic arc (see fig. 1-22⁴) of Windley and others (2007). The tract has different composition and, in some regions, different age rocks in which arc-related mineral deposits occur in comparison to the adjacent sub-tracts 142pCu8003a, 142pCu8003b, and 142pCu8003d. In addition, there are fewer positive magnetic anomalies in the reduced-to-pole aeromagnetic database, yet there are known porphyry-style copper-bearing occurrences (compare Seltmann and others, 2009). Regions of higher magnetic intensity are presumed to reflect the presence of arc-related rocks in the subsurface. It is possible that some positive magnetic anomalies could reflect the presence of Permian mafic lavas and (or) ophiolites in the basement, but on the basis of published tectonic and geologic information, such occurrences are more likely to occur on the east and west margins of the tract rather than within its core.

¹U.S. Geological Survey, Denver, Colorado.

²U.S. Geological Survey, Reston, Virginia.

³U.S. Geological Survey, Spokane, Washington.

⁴Refer to chapter 1 of this report.

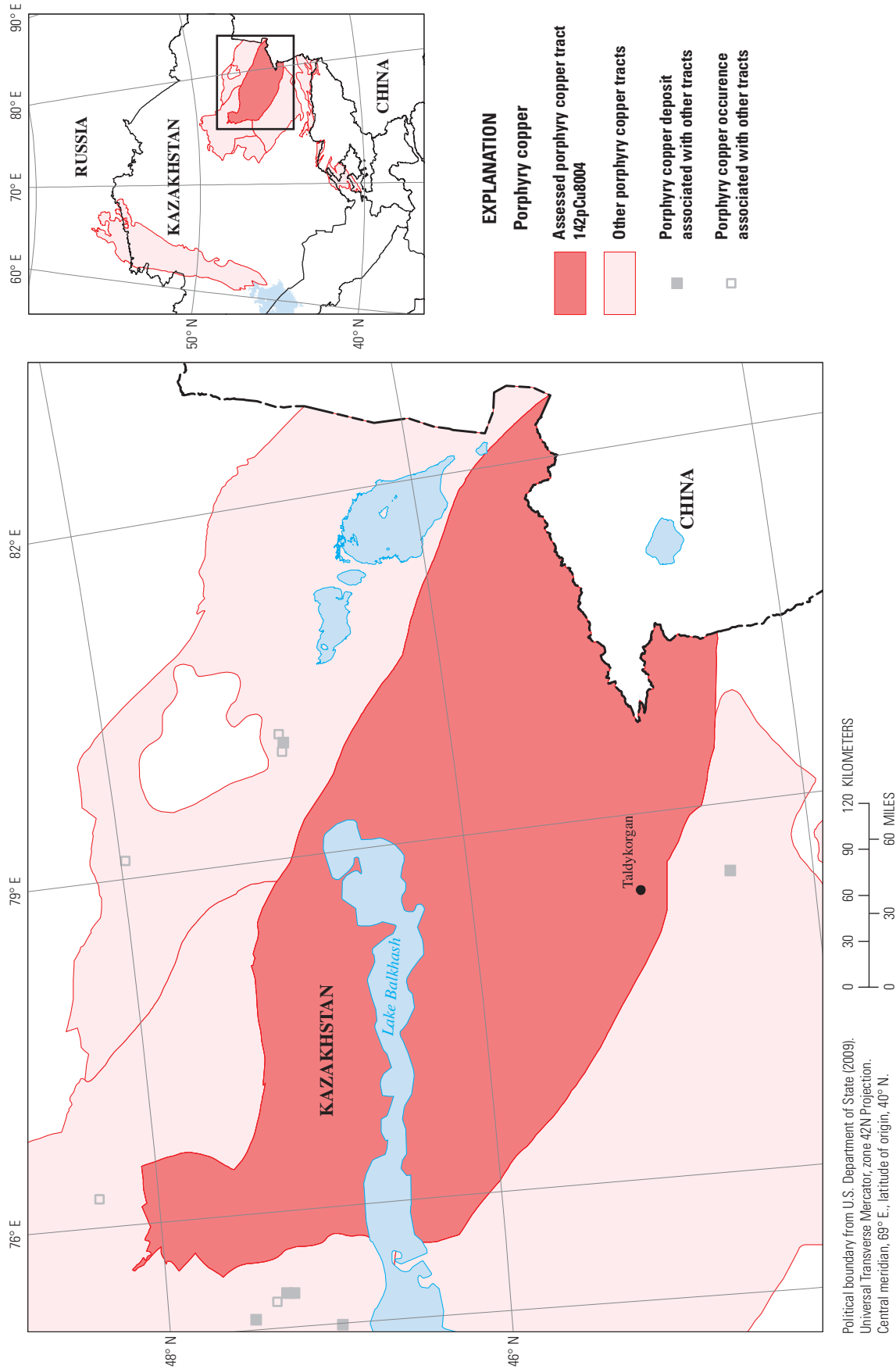


Figure G1. Map showing the location, known deposits, and significant occurrences for tract 142pCu8004, Late Paleozoic Central Balkhash-Ili magmatic arc—Kazakhstan. Location of map area shown on inset.

Delineation of the Permissive Tract

Geologic Criteria

The principal litho-tectonic terrane concept used to delineate this tract was that of a magmatic arc that formed above a subduction zone. The tract consists of those rocks interpreted to be that part of the Late Paleozoic Balkhash-Ili Arc where the aeromagnetic data indicate a lack of lateral continuity of volcano-plutonic centers in contrast to the adjacent parts of the Balkhash-Ili Arc (permissive tract 142pCu8003). Four principal sources of information, supplemented by numerous published journal and symposium papers, were used to delineate this tract. The primary sources were the mineral deposits map of Central Asia on a geologic base edited by Seltnann and others (2009), supplemented by 1:200,000-scale geologic maps originally published by the former Soviet (U.S.S.R.) government, a reduced-to-pole aeromagnetic map prepared by J.D. Phillips from NOAA (1996), the interpretation of Advanced Spaceborne Thermal Emission and Reflection Radiometer (ASTER) satellite imagery of hydrothermal alteration minerals or suites of minerals by J.C. Mars, and tectonic terrane maps published by Abdulin and Zaitseb (1976), Yakubchuk (2004), and Windley and others (2007).

Of most importance in the delineation of the boundaries of this tract are (1) Carboniferous and Permian magmatic-arc-related volcanic and intrusive rocks as shown on the mineral deposits map of Central Asia (Seltnann and others, 2009), (2) the age and composition of the arc-hosting rocks, and (3) that part of the arc with extensive nonpermissive cover rocks as well as fewer positive aeromagnetic anomalies interpreted as indicating the possible occurrence of permissive arc rocks. The distribution of permissive rocks in the tract is shown in figure G2. The southeasternmost end of the tract is a political, not geologic, boundary and is drawn along the Kazakhstan-China border. All of the other boundaries to this permissive tract are geological, generally structural and tectonic, and in common with boundaries around the mostly circumscribing sub-tracts of permissive region 142pCu8003.

Approximately one-third of permissive tract 142pCu8004 is located to the north of Lake Balkhash, a 600-kilometer (km) long, 5- to 70-km-wide lake at the north end of the Balkhash geographic depression. This northern region of the tract was drawn to include stratigraphic sections that are predominantly sedimentary, but within which are Carboniferous to Permian intrusions and numerous associated mineral occurrences including significant copper skarn deposits in the Sayak ore field and associated porphyry-copper occurrences (fig. G3). Interpreted by Glukhan and Serykh (1996) to have a Neoproterozoic basement, the oldest rocks in this part of the tract are Early Paleozoic, probably Ordovician, marine basalts (Glukhan and Serykh, 1996; Kudryavtsev, 1996), Silurian greywacke, and Devonian (D_1) marine deposits, including carbonate rocks. In the contiguous permissive

sub-tract 142pCu8003d, the sedimentary sequences are overlain by D_1 andesitic to dacitic magmatic-arc rocks, but these arc rocks do not crop out in this part of the permissive area and all documented Devonian mineralization is beyond the permissive tract boundary. During the Late Devonian (D_3 ; Kudryavtsev, 1996) and into the Early Carboniferous, magmatic-arc activity began in the region, but arc magmatism in the tract was most prevalent during the Late Carboniferous (C_3) and into the Permian (P_1).

Along the southwestern margin of permissive tract 142pCu8004, there is a marked change in the character of the aeromagnetic anomalies. This change generally corresponds to a fault-controlled tectonic boundary mapped by Abdulin and Zaitseb (1976) and Abdulin and others (1982) beneath the post-Mesozoic cover rocks in the Balkhash geographic depression. Along this fault zone, predominantly Carboniferous rocks and intrusions to the west in 142pCu8003d are juxtaposed against predominantly Devonian rocks with some Carboniferous sedimentary and Carboniferous and Permian intrusions to the east in 142pCu8004. Although the tract boundary corresponds to a clear tectonic boundary north of the Ili Basin and the Tian Shan mountain ranges, the boundary is wholly subjective within the basin and into the mountains. In this area, the boundary is drawn to correspond to a zone of west-northwest-striking faults that separate a domain with different styles of mineralization (see Seltnann and others, 2009) to the northeast relative to the southwest across these faults.

As with the southwestern margin of tract 142pCu8004, the northeastern margin also corresponds to a change in the aeromagnetic data patterns. The patterns generally reflect a change in the predominant bedrock geology on which the Carboniferous arc was built. The bedrock geology change is owing to a number of different fault zones. To the northeast of the boundary in permissive tract 142pCu8003a, the rocks are predominantly Permian, whereas to the southwest within the permissive tract, the rocks are predominantly Devonian to Carboniferous. This bedrock change is followed as a tract boundary southeast to the Kazakhstan-China border.

Throughout the permissive tract, thrust and related faults and folding deformed the pre-Carboniferous arc sequences prior to the onset of C_{2-3} magmatism. During C_3 - P_1 arc magmatism, strike-slip faulting was widespread in the permissive terrane concurrent with the intrusive activity, and played a critical role in the localization of mineralization. On some faults, there are postmineralization offsets of a few kilometers.

Although tract 142pCu8004 has a lower density of positive magnetic anomalies relative to the sub-tracts that make up tract 142pCu8003, the wide spacing of flight lines and extensive postmineralization cover leave considerable uncertainty as to just how much of the permissive region is likely to contain undiscovered porphyry copper deposits. Small, but significant, anomalies could easily be missed.

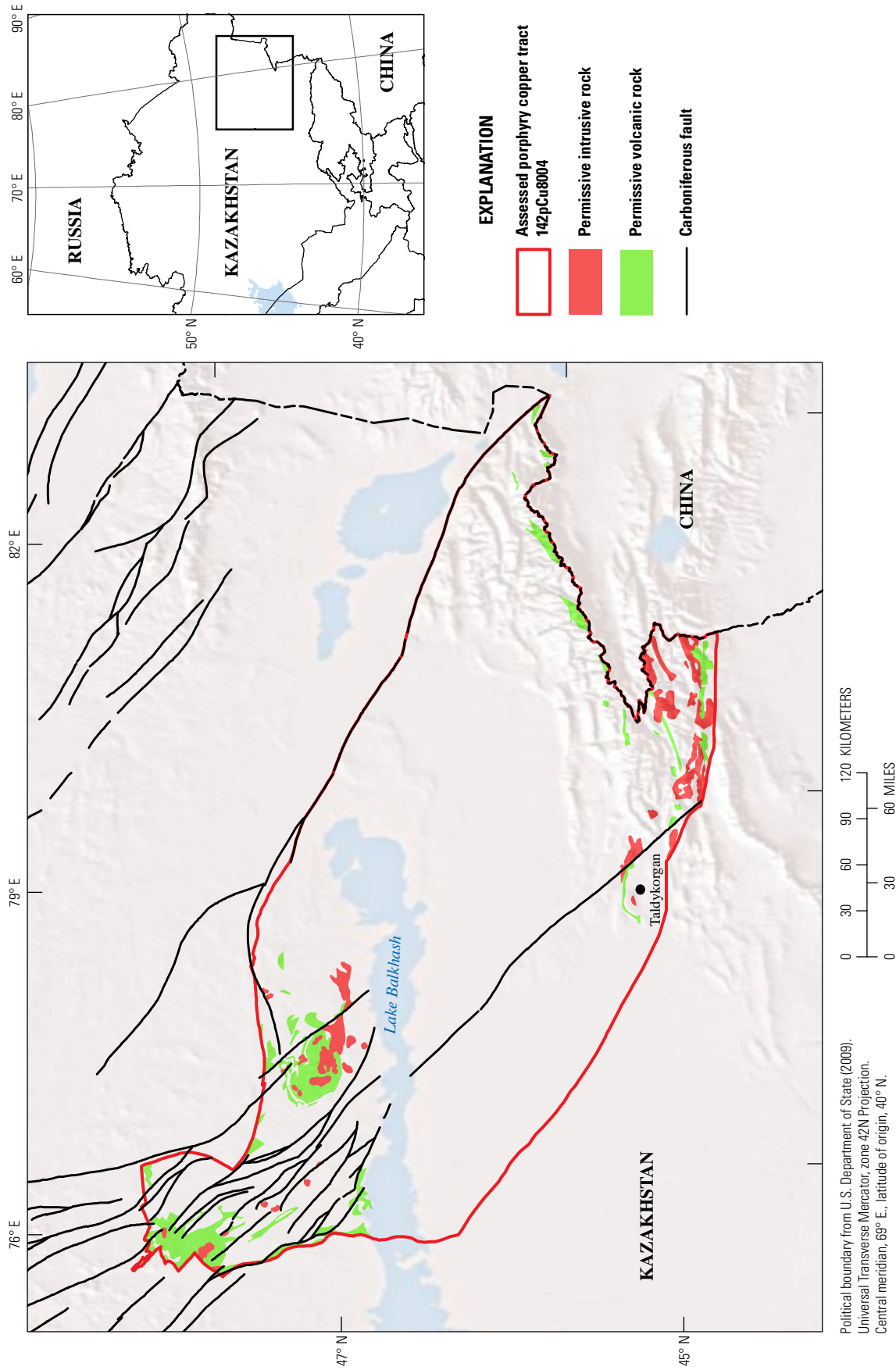


Figure G2. Map showing distribution of permissive Carboniferous volcanic and volcanoclastic rocks (green) and intrusive rocks (red) in tract 142pCu8004, Late Paleozoic Central Balkhash-Ili magmatic arc—Kazakhstan, on a digital elevation base. Location of map area shown on inset.

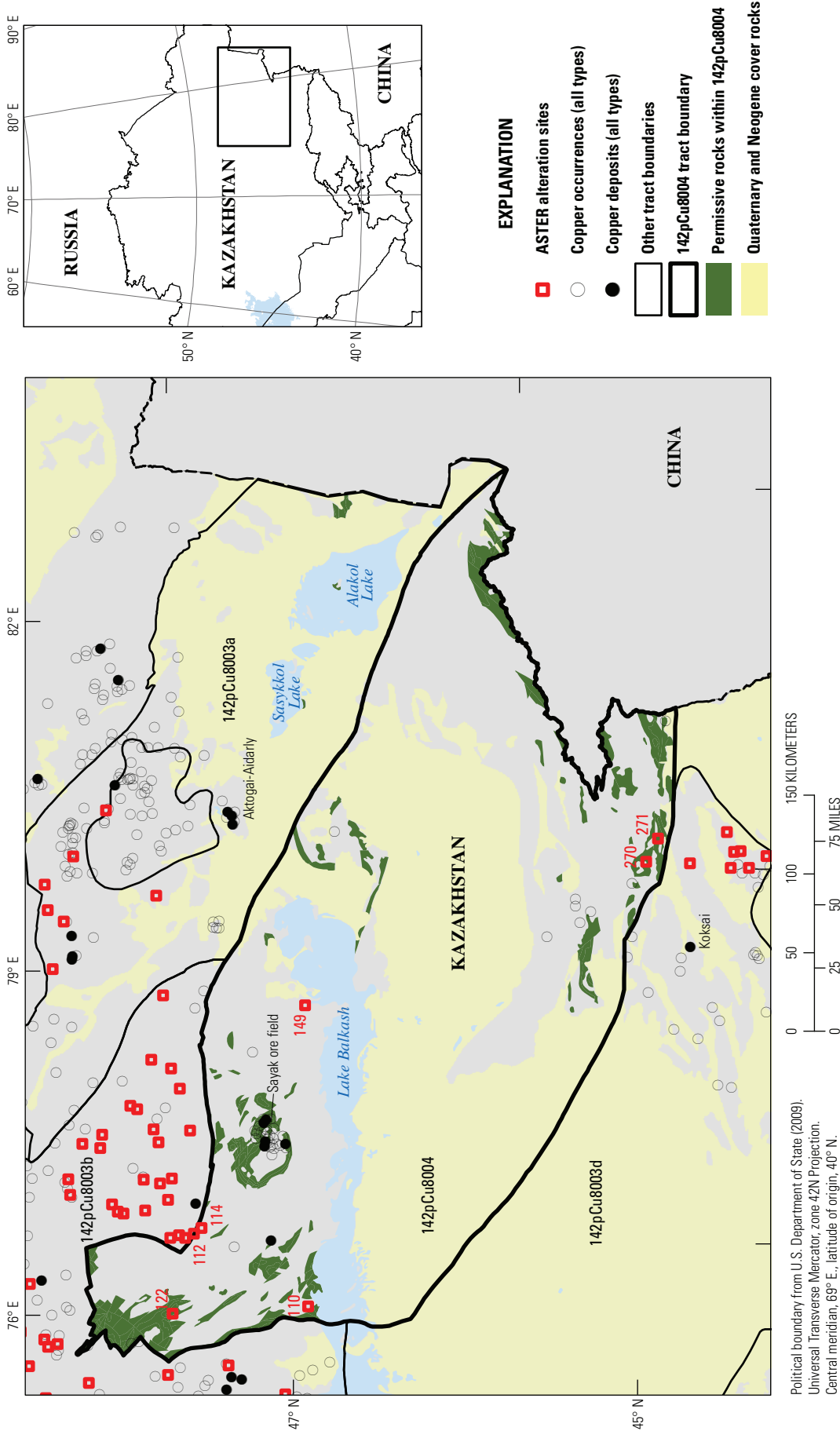


Figure G3. Map showing the extent of permissive rock, Quaternary and Neogene cover, copper deposits and occurrences from Seltmann and others (2009), and ASTER alteration sites in tract 142pCu8004, Late Paleozoic Central Balkhash-Ili magmatic arc—Kazakhstan. Location of map area shown on inset.

The aeromagnetic data derived from widely spaced flight lines could only be coarsely gridded relative to the typical size of a porphyry copper deposit; thus there is considerable question whether or not all potential intrusive targets are recognizable as magnetic highs. Therefore, even areas within the tract of low magnetic intensity are assumed to have a greater than 1:100,000 chance to contain a porphyry copper deposit and are, therefore, considered permissive for the purposes of this assessment.

Because a considerable proportion of the permissive rocks in this tract lie beneath postmineralization cover in the Balkhash geographic depression (fig. G2), interpretive maps of the pre-Tertiary tectonic setting by Abdulin and Zaitseb (1976) and pre-Tertiary geology by Abdulin and others (1984) were used, together with depths to bedrock derived from drill-hole controlled cross sections on 1:250,000-scale geologic maps, to delineate the permissive area boundaries.

Known Deposits

For this tract, the Singer and others (2008) database contains neither porphyry copper deposits with published grades and tonnages nor any occurrences. Therefore, although Seltmann and others (2009) report porphyry-style copper occurrences within the permissive tract boundaries, little information is available on classification and locations. Therefore, for the purposes of this assessment none of the identified occurrences in Seltmann and others (2009) are classified herein as “known” deposits or occurrences.

Porphyry Copper Occurrences and Related Deposit Types

According to Seltmann and others (2009), the largest grouping of porphyry-style copper, copper-molybdenum, and copper-gold occurrences, approximately 12 altogether, is in the Sayak ore field about 40 km north of Lake Balkhash (fig. G3). Primarily copper-bearing skarn deposits have been mined from a sequence of Late Devonian to Early Carboniferous carbonate and volcanoclastic and minor andesitic rocks intruded by Late Carboniferous igneous rocks. Pyroxene-biotite-plagioclase hornfels and wollastonite-pyroxene-garnet skarn formed adjacent to the boundaries of most intrusions. High magnesium skarns constitute magnetite resources at some localities. The skarn sulfide ores locally overprint the early-phase skarn rocks with bornite and chalcopyrite as the predominant copper-bearing minerals of economic importance. Molybdenite, which is an important accessory mineral in the sulfide ores, occurs in extensive zones of stockwork-like veinlets in some areas. Low-grade copper-molybdenum porphyry-style ores have been explored, but have been found to date to be economic only if mineable in conjunction with the mining of a different, but nearby, deposit type (compare Zhukov and others, 1998).

Seltmann and others (2009) show another cluster of six porphyry-style occurrences, not all of which are shown to contain copper as a primary commodity, northeast of the Sayak ore field. It is uncertain how many of these occurrences correspond to a porphyry-style copper deposit as used in this report. Other than primary and secondary commodity information, no other information about these occurrences is available. Seltmann and others (2009) show a third area with six porphyry-style deposits widely scattered near the southwestern boundary in the southeastern part of the tract (fig. G3). The degree to which any of these occurrences correspond to the porphyry copper model used in this assessment is unknown.

Hydrothermal Alteration Mapping (ASTER)⁵

Approximately 50 percent of tract 142pCu8004 is covered by ASTER data (see fig. 2-1). Assessment of Landsat TM 742 false color composite images shows that lakes and unconsolidated sediments constitute most of the tract not covered by ASTER scenes (see fig. 2-2). Five potential deposit sites were defined on the basis of argillic, phyllic, and silicic alteration patterns (see table 2-1 and plates 1–8; fig. 2-3). The mineral databases indicate that potential deposit sites are not associated with known copper-mineralized rocks (compare Singer and others, 2008; Seltmann and others, 2009). The geologic and alteration maps illustrate that altered rocks at sites in tract 142pCu8004 include quartzite, granite, plagiogranite, granodiorite, basalt, and some altered sandstones (see table 2-1 and plates 1–4; Seltmann and others, 2009).

Assessment of Landsat TM 742 false color composite data of tract 142pCu8004 indicates vegetation cover and rock exposure similar to adjacent tract 142pCu8003b (see fig. 2-4). The Kounrad mine, the largest porphyry copper deposit in the region, is located in tract 142pCu8003c. Altered rock characteristics of the Kounrad mine area were used to identify potential deposit sites in tract 142pCu8004 with similar alteration characteristics. Altered rock characteristics include diameter of alteration pattern greater than or equal to 1.7 km, phyllic and argillic alteration density greater than or equal to 7, and at least 80 percent phyllic alteration coverage. Site 122 contains alteration characteristics similar to the Kounrad mine area (see table 2-1; fig. G3). Although part of the altered rocks for site 122 are situated in sandstone (see table 2-1), a significant amount of the altered rocks are associated with an adjacent granodiorite suggesting that the clays were deposited in a hydrothermal system.

⁵Refer to figures, tables, and plates in chapter 2 of this report.

Exploration History

An historical record of exploration within this tract has not been compiled.

Sources of Information

Principal sources of information used by the assessment team for delineation of 142pCu8004 are listed in table G2 and in the references cited.

Grade and Tonnage Model Selection

The general porphyry copper deposit model published by Singer and others (2008) was used based on the known deposits in the tract being statistically consistent with the model.

Estimate of the Number of Undiscovered Deposits

Rationale for the Estimate

Prior to making estimates of undiscovered deposits, the assessment team first reviewed the geologic framework, aeromagnetic, and remotely sensed data with particular attention paid to the (1) correctness of the tract boundary with respect to depth of covered areas, (2) permissiveness of included rock formations, (3) the proportion of the mapped geologic units that are intrusive, and (4) depth of erosion of the permissive arc terrane and whether or not the depth of erosion was uniform across the tract or whether the tract should be considered for subdivision into two or more sub-tracts for the assessment. Second, the assessment team discussed the known occurrences, discussed the distribution of

Table G2. Principal sources of information used to delineate tract 142pCu8004, Late Paleozoic Central Balkhash-Ili magmatic arc—Kazakhstan.

[NA, not applicable]

Theme	Name or title	Scale	Citation
Geology	Mineral deposits map of Central Asia	1:1,500,000	Seltmann and others (2009)
	Tectonic map of the Paleozoic folded areas of Kazakhstan and adjacent territories	1:1,500,000	Abdulin and Zaitseb (1976)
	Tectonic terrane maps	NA	Windley and others (2007), Yakubchuk (2004)
	Mineral deposits database and thematic maps of Central Asia	1:1,500,000	Seltmann and others (2009)
	Tectonic map of the Paleozoic folded areas of Kazakhstan and adjacent territories	1:1,500,000	Abdulin and Zaitseb (1976)
	Tectonic terrane maps	NA	Windley and others (2007), Yakubchuk (2004)
	L-43-XII (1962)	1:200,000	Koshakin and others (1962)
	L-44-VII (1955)	1:200,000	Galitsekii (1955)
	L-44-VIII (1957)	1:200,000	Staal (1957)
	L-44-XIII (1960)	1:200,000	Ponomarev and Davydov (1960a)
	L-44-XIV (1960)	1:200,000	Ponomarev and Davydov (1960b)
	L-44-XV (1959)	1:200,000	Gendler and others (1959)
	L-44-XX (1985)	1:200,000	Samigullin (1985)
	L-44-XXV (1965)	1:200,000	Mairin and Nikitchenko (1965)
	L-44-XXVI (1966)	1:200,000	Busha (1966)
	L-44-XXXI (1961)	1:200,000	Mairin and Sterkin (1961)
	L-44-XXXII (1965)	1:200,000	Sterkin and others (1965a)
Mineral occurrences	Mineral deposits map of Central Asia	1:1,500,000	Seltmann and others (2009)
Geophysics	Magnetic anomaly data of the former U.S.S.R.	1:2,500,000	NOAA, National Geophysical Data Center (1996), http://www.ngdc.noaa.gov

the known occurrences and linked deposit types, considered the density of occurrence of altered areas as determined from remotely sensed data, and evaluated the deposit type distribution as an indicator of depth of exposure in the arc terrane as well as what the distribution implied about the uniformity of the depth of exposure across the tract. Third, the team examined the “type locality” of remotely sensed alteration information as interpreted from ASTER and Landsat satellite data and discussed the possible meaning and size of altered areas. Fourth, the team speculated on the likely thoroughness with which the region had been explored. The consensus was that less than a twentieth of the delineated tract was of the correct age and (or) the correct igneous rock types to host porphyry copper deposits but maps were not available to subdivide the tract.

Figure G2 illustrates the extent of Quaternary and Neogene cover in the tract area based on the geologic map of Seltmann and others (2009), as well as the distribution of copper occurrences that may or may not be associated with porphyry copper deposits in the Balkash-Ili magmatic arc and the locations of alteration sites identified in the analysis of ASTER data. Exposed permissive rocks represent a very small part of the tract area. On the basis of available data, the team estimated a 50-percent chance of 2 undiscovered deposits, a 10-percent chance of 4, and a 5-percent chance of 5 or more (table G3). The expected (mean) number of deposits based on this distribution is 2.1 deposits.

Probabilistic Assessment Simulation Results

Undiscovered resources for the tract were estimated by combining consensus estimates for numbers of undiscovered porphyry copper deposits with the global grade and tonnage model for porphyry Cu-Au-Mo deposits of Singer and others (2008) using the EMINERS program (Root and others, 1992; Bawiec and Spanski, 2012; Duval, 2012). Selected simulation results are reported in table G4. Results of the Monte Carlo simulation are presented as a cumulative frequency plot (fig. G4). The cumulative frequency plot shows the estimated resource amounts associated with cumulative probabilities of occurrence, as well as the mean, for each commodity and for total mineralized rock.

The expected (mean) number of undiscovered deposits, as well as the and median amounts of copper for the tract (table G4) are comparable to the results for adjacent tract 142pCu8003d in the Balkash-Ili Arc, which contains 2 known deposits and an estimate of 2 undiscovered deposits (see table 3-4⁶). Tract areas (about 100,000 km²) are comparable as well (see table 3-3).

⁶See chapter 3 of this report.

Table G3. Undiscovered deposit estimates, deposit numbers, tract area, and deposit density for tract 142pCu8004, Late Paleozoic Central Balkhash-Ili magmatic arc—Kazakhstan.

[N_{xx} , estimated number of deposits associated with the xxth percentile; N_{und} , expected number of undiscovered deposits; s , standard deviation; $C_v\%$, coefficient of variance; N_{known} , number of known deposits in the tract that are included in the grade and tonnage model; N_{total} , total of expected number of deposits plus known deposits; area, area of permissive tract in square kilometers (km²); density, deposit density reported as the total number of deposits per 100,000 km². N_{und} , s , and $C_v\%$ are calculated using a regression equation (Singer and Menzie, 2005)]

Consensus undiscovered deposit estimates					Summary statistics					Tract area (km ²)	Deposit density ($N_{total}/100k\ km^2$)
N_{90}	N_{50}	N_{10}	N_{05}	N_{01}	N_{und}	s	$C_v\%$	N_{known}	N_{total}		
0	2	4	5	5	2.1	1.6	79	0	2.1	100,820	21

Table G4. Results of Monte Carlo simulations of undiscovered resources for tract 142pCu8004, Late Paleozoic Central Balkhash-Ili magmatic arc—Kazakhstan.

[Cu, copper; Mo, molybdenum; Au, gold; and Ag, silver; in metric tons. Rock, in million metric tons]

Material	Probability of at least the indicated amount					Probability of		
	0.95	0.9	0.5	0.1	0.05	Mean	Mean or greater	None
Cu	0	0	2,800,000	18,000,000	31,000,000	7,800,000	0.26	0.21
Mo	0	0	25,000	490,000	910,000	210,000	0.21	0.36
Au	0	0	42	510	850	200	0.26	0.33
Ag	0	0	150	5,700	11,000	2,500	0.2	0.46
Rock	0	0	620	3,800	6,000	1,600	0.26	0.21

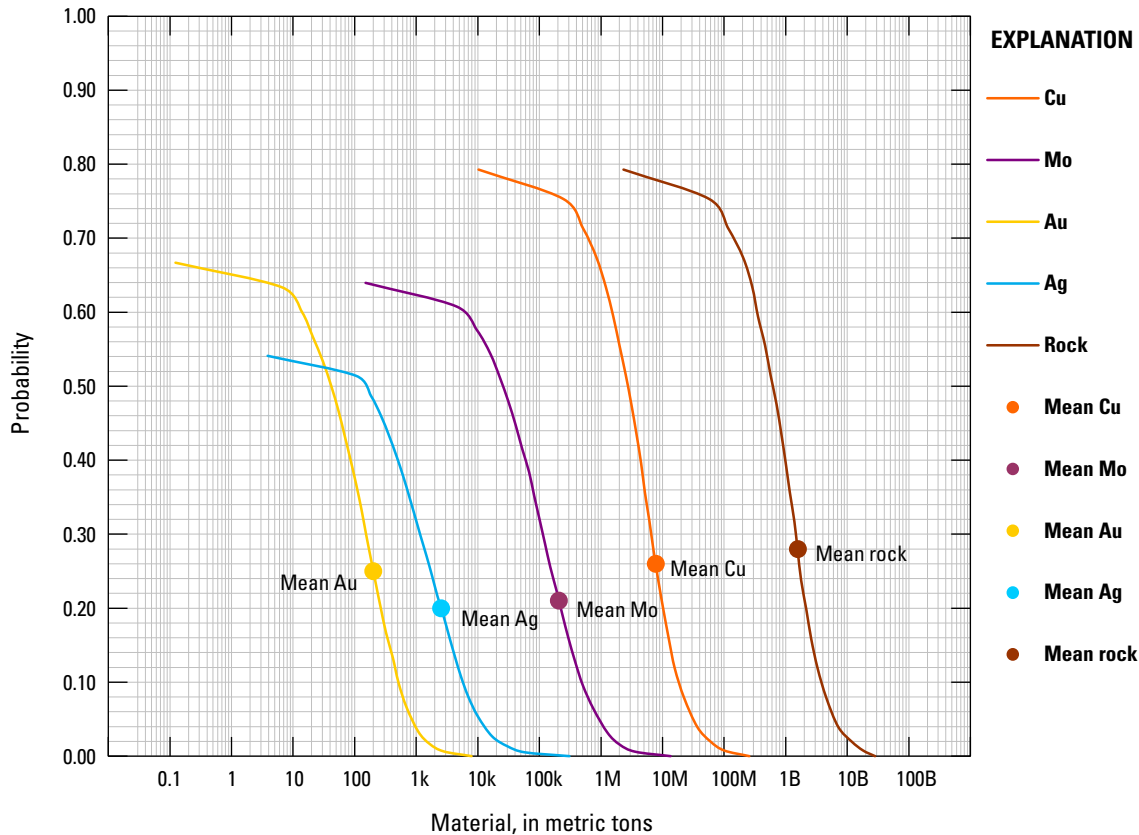


Figure G4. Cumulative frequency plot showing the results of Monte Carlo computer simulation of undiscovered resources in tract 142pCu8004, Late Paleozoic Central Balkhash-Ili magmatic arc—Kazakhstan. k=thousands, M=millions, B=billions.

References Cited

- Abduln, A.A., and Zaitseb, Yu. A., 1976, [Tectonic map of the Paleozoic folded areas of Kazakhstan and adjacent territories]: Moscow, Aerogeologiya, scale 1:1,500,000. [In Russian.]
- Abduln, A.A., Besimalov, V.F., Volkov, V.M., Nikitchenko, I.I., Chakabaev, S.E., and Chimbulatov, M.A., 1982, [Map of the ore fields and oil and gas fields of the Kazakh S.S.R. and adjacent territories of the Union Republics]: St. Petersburg, VSEGEI, scale 1:500,000. [In Russian.]
- Abduln, A.A., Zaitsev, Yu.A., and Rozanov, S.B., 1984, On the “Atlas of paleotectonic maps of the Paleozooids of Kazakhstan and adjacent territories”: Moscow University Geology Bulletin, v. 39, no. 6, p. 61–65.
- Bawiec, W.J., and Spanski, G.T., 2012, Quick-start guide for version 3.0 of EMINERS—Economic Mineral Resource Simulator: U.S. Geological Survey Open-File Report 2009–1057, 26 p., accessed July 15, 2012, at <http://pubs.usgs.gov/of/2009/1057/>. (This report supplements USGS OFR 2004–1344.)
- Berger, B.R., Ayuso, R.A., Wynn, J.C., and Seal, R.R., 2008, Preliminary model of porphyry copper deposits: U.S. Geological Survey Open-File Report 2008–1321, 55 p., accessed May 15, 2009, at <http://pubs.usgs.gov/of/2008/1321/>.
- Busha, V.A., 1966, [Map of mineral resources of the U.S.S.R., Dzungar Series, Sheet L-44-XXVI]: Ministry of Geology of the U.S.S.R., scale 1:200,000. [In Russian.]
- Cox, D.P., 1986, Descriptive model of porphyry Cu (Model 17), in Cox, D.P., and Singer, D.A., eds., 1986, Mineral deposit models: U.S. Geological Survey Bulletin 1693, p. 76. (Also available at <http://pubs.usgs.gov/bul/b1693/>.)
- Duval, J.S., 2012, Version 3.0 of EMINERS—Economic Mineral Resource Simulator: U.S. Geological Survey Open-File Report 2004–1344, accessed July 15, 2012, at <http://pubs.usgs.gov/of/2004/1344/>.
- Galitsekii, V.V., 1955, [Geological map of the U.S.S.R., eastern Circum-Balkhash Series, Sheet L-44-VII]: Ministry of Geology and Mineral Resources Protection, scale 1:200,000 [In Russian.]

- Gendler, V.E., Sonin, I.I., and Iisovskaya, E.V., 1959, [Geological map of the U.S.S.R., Dzungar Series, Sheet L-44-XV]: Ministry of Geology and Mineral Resources Protection, scale 1:200,000. [In Russian.]
- Glukhan, I.V., and Serykh, V.I., 1996, Geology and tectonic evolution of central Kazakhstan, *in* Shatov, V., Seltmann, R., Kremenetsky, A., Lehmann, B., Popov, V., and Ermolov, P., eds., Granite-related ore deposits of central Kazakhstan and adjacent areas: St. Petersburg, Glagol Publishing House, p. 11–24.
- Koshakin, V.Y., Koshakina, S.D., and Sklyarenko, L.M., 1962, [Geological map of the U.S.S.R., Balkhash series, Sheet L-43-XII]: Ministry of Geology and Mineral Resources Protection, scale 1:200,000. [In Russian.]
- Kudryavtsev, Y.K., 1996, The Cu-Mo deposits of central Kazakhstan, *in* Shatov, V., Seltmann, R., Kremenetsky, A., Lehmann, B., Popov, V., and Ermolov, P., eds., Granite-related ore deposits of central Kazakhstan and adjacent areas: St. Petersburg, Glagol Publishing House, p. 119–144.
- Mairin, S.E., and Nikitchenko, I.I., 1965, [Geological map of the U.S.S.R., Dzungar Series, Sheet L-44-XXV]: State Geological Committee of the U.S.S.R., scale 1:200,000. [In Russian.]
- Mairin, S.E., and Sterkin, V.D., 1961, [Map of mineral resources of the U.S.S.R., Dzungar Series, Sheet L-44-XXXI]: Ministry of Geology and Mineral Resources Protection, scale 1:200,000. [In Russian.]
- National Oceanic and Atmospheric Administration, 1996, Magnetic anomaly data of the former U.S.S.R.: Boulder, Colorado, National Geophysical Data Center, accessed August 1, 2009, at <http://www.ngdc.noaa.gov>.
- Ponomarev, B.Y., and Davydov, N.M., 1960a, [Geological map of the U.S.S.R., Circum-Balkhash Series, Sheet L-44-XIII]: Ministry of Geology and Mineral Resources Protection, scale 1:200,000. [In Russian.]
- Ponomarev, B.Y., and Davydov, N.M., 1960b, [Geological map of the U.S.S.R., Circum-Balkhash Series, Sheet L-44-XIV]: Ministry of Geology and Mineral Resources Protection, scale 1:200,000. [In Russian.]
- Root, D.H., Menzie, W.D., and Scott, W.A., 1992, Computer Monte Carlo simulation in quantitative resource estimation: *Natural Resources Research*, v. 1, no. 2, p. 125–138.
- Samigullin, F.A., 1985, [Geological map of the U.S.S.R., Dzungar Series, Sheet L-44-XX]: Ministry of Geology of the U.S.S.R., scale 1:200,000. [In Russian.]
- Seltmann, R., Shatov, V., and Yakubchuk, A., 2009, Mineral deposits database and thematic maps of Central Asia—ArcGIS 9.2, Arc View 3.2, and MapInfo 6.0(7.0) GIS packages: London, Natural History Museum, Centre for Russian and Central EurAsian Mineral Studies (CERCAMS), scale 1:1,500,000, and explanatory text, 174 p. [Commercial dataset available at <http://www.nhm.ac.uk/research-curation/research/projects/cercams/products.html>.]
- Singer, D.A., Berger, V.I., and Moring, B.C., 2008, Porphyry copper deposits of the world: U.S. Geological Survey Open-File Report 2008–1155, 45 p., accessed August 15, 2009, at <http://pubs.usgs.gov/of/2008/1155/>.
- Singer, D.A., and Menzie, W.D., 2005, Statistical guides to estimating the number of undiscovered mineral deposits—An example with porphyry copper deposits, *in* Cheng, Q., and Bonham-Carter, G., eds., Proceedings of IAMG—The annual conference of the International Assoc. for Mathematical Geology: Toronto, Canada, Geomatics Research Laboratory, York University, p. 1028–1033.
- Staal, M.B., 1957, [Geological map of the U.S.S.R., Circum-Balkhash Series, Sheet L-44-VIII]: Ministry of Geology and Mineral Resources Protection, scale 1:200,000. [In Russian.]
- Sterkin, V.D., Sklyarenko, L.M., and Il'yasov, M.A., 1965a, [Map of mineral resources of the U.S.S.R., Dzungar Series, Sheet L-44-XXXII]: State Geological Committee of the U.S.S.R., scale 1:200,000. [In Russian.]
- Sterkin, V.D., Sklyarenko, L.M., and Il'yasov, M.A., 1965b, [Geological map of the U.S.S.R., Dzungar Series, Sheet L-44-XXXIII]: State Geological Committee of the U.S.S.R., scale 1:200,000. [In Russian.]
- Windley, B.F., Alexeiev, D., Xiao, W., Kroner, A., and Badarch, G., 2007, Tectonic models for accretion of the Central Asia orogenic belt: *Journal of the Geological Society*, v. 164, p. 31–47.
- Yakubchuk, A., 2004, Architecture and mineral deposit settings of the Altaid orogenic collage—A revised model: *Journal of Asian Earth Sciences*, v. 23, p. 761–779.
- Zhukov, N.M., Kolesnikov, V.V., Miroshnichenko, L.M., Egembayev, K.M., Pavlova, Z.N., and Bakarasov, E.V., comps., 1998, Copper deposits of Kazakhstan—Reference book: Almaty, Ministry of Ecology and Natural Resources of the Republic of Kazakhstan, 136 p.

Appendix H. Porphyry Copper Assessment for 142pCu8005, Carboniferous Valerianov Arc—Kazakhstan and Russia

By Byron R. Berger¹, Paul D. Denning¹, Connie L. Dicken², Jane M. Hammarstrom², John C. Mars², Jeffrey D. Phillips¹, and Michael L. Zientek³

Deposit Type Assessed: Porphyry Copper

Descriptive model: Cox, 1986; Berger and others, 2008

Grade and tonnage model: Global Cu-Au-Mo porphyry copper model (Singer and others, 2008)

Table H1 summarizes selected assessment results.

Table H1. Summary of selected resource assessment results for tract 142pCu8005, Carboniferous Valerianov Arc—Kazakhstan and Russia.

[km, kilometers; km², square kilometers; t, metric tons]

Date of assessment	Assessment depth (km)	Tract area (km ²)	Known copper resources (t)	Mean estimate of undiscovered copper resources (t)	Median estimate of undiscovered copper resources (t)
2010	1	213,240	2,100,000	15,000,000	5,900,000

Location

This tract is located along the northwest margin of the Kazakhstan composite tectonic plate south of about latitude 56° N. in Russia and east of the main Ural Mountains and continues to the south in Kazakhstan to just north of the Aral Sea (fig. H1 and fig. 1-2). Much of the tract is covered by post-Carboniferous materials.

Geologic Feature Assessed

The permissive tract encompasses Carboniferous to Permian magmatic-arc rocks referred to as the Valerianov volcano-plutonic arc (fig. 1-33; Herrington and others, 2005). It is interpreted to link to the south into the Bel'tau–Kurama Arc in Uzbekistan (Herrington and others, 2005; Plotinskaya and others, 2006; Windley and others, 2007).

¹U.S. Geological Survey, Denver, Colorado.

²U.S. Geological Survey, Reston, Virginia.

³U.S. Geological Survey, Spokane, Washington.

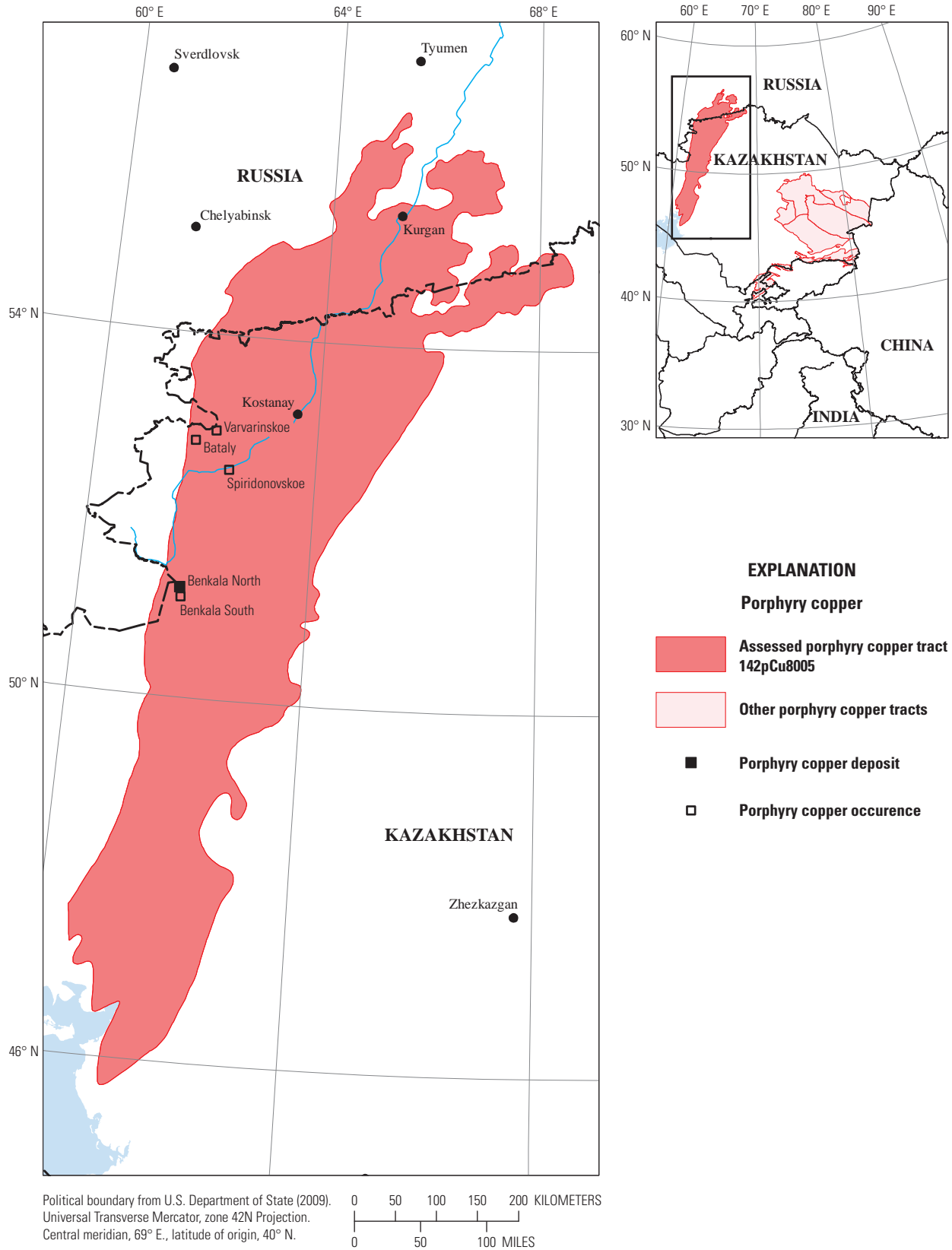


Figure H1. Map showing the location, known deposits, and significant occurrences for tract 142pCu8005, Carboniferous Valerianov Arc—Kazakhstan and Russia. Location of map area shown on inset.

Delineation of the Permissive Tract

Geologic Criteria

The principal litho-tectonic terrane concept used to delineate this tract was that of a magmatic arc that formed in the subduction boundary zone above a subducting plate. The arc terrane was identified and delineated using five principal sources of information supplemented by numerous published journal and symposium papers. The principal sources of information are (1) Mineral Deposits of the Urals on a geologic base edited by Petrov and others (2006), (2) the mineral deposits map of Central Asia on a geologic base edited by Seltmann and others (2009), (3) 1:200,000-scale geologic maps originally published by the former Soviet (U.S.S.R.) government, (4) a reduced-to-pole aeromagnetic map prepared by J.D. Phillips from NOAA (1996), and (5) a tectonic terrane map published by Ayarza and others (2000) in conjunction with a discussion of the terranes by Herrington and others (2005) and Windley and others (2007). The depth of cover along the eastern side of the tract was estimated from depth to basement contours on regional geologic maps of Russia, Kazakhstan, and Uzbekistan (Nalivkin, 1968), as well as estimated from cross sections on 1:200,000-scale geologic maps. The distribution of permissive Carboniferous rocks for that part of the tract within Kazakhstan is shown in figure H2.

The permissive tract is along the eastern margin of the southern Ural Mountains. The Urals are a geographic expression of the tectonic boundary between the eastern European craton and associated accreted terranes to its east and the composite Kazakhstan-Tarim tectonic plate and the Siberian craton farther east. The suture zone bounding the Kazakhstan-Tarim Plate is generally along the boundary between the East Uralian tectonic zone and the Trans Uralian tectonic zone (compare Ayarza and others, 2000; Herrington and others, 2005; Brown and others, 2006). The East Uralian zone is composed of deformed and metamorphosed fragments of oceanic island-arc rocks as well as Precambrian and Paleozoic continental rocks (Brown and others, 2006) that Herrington and others (2005) consider an accretionary complex that accumulated in front of the Valerianov Arc. The arc formed above a subduction zone beneath the Kazakhstan Plate to the east of the European Plate. Herrington and others (2005) separate the East Uralian zone from the Trans Uralian zone to the east along the Troitsk Fault Zone (fig. 1-33).

The late Early to middle Carboniferous Valerianov Arc formed on the Kazakhstan plate owing to subduction of Trans-Uralian basin rocks to the east (Herrington and others, 2005). Orogenesis related to the collision of the European Uralides and the Trans-Urals zone began during the middle (early Late (?)) Carboniferous, thereby ending arc activity; postcollisional magmatism and transpressional deformation continued into the Permian. Outcrops of the permissive arc rocks are sparse owing to extensive cover by Mesozoic and

younger rocks, with the best exposures being found in the southeastern Ural Mountains in Kazakhstan. Yakubchuk and others (2005) delineate the width and length of the arc on the basis of aeromagnetic patterns, and through this evidence they link the Valerianov Arc of the South Urals with the Kurama Arc in eastern Uzbekistan.

The northern, eastern, and southern segments of the permissive tract boundary are wholly subjective and were delineated through a combination of thickness of postmineralization cover as determined from cross sections of published geologic maps, structural contours published by Nalivkin (1968), and trends on the reduced-to-pole aeromagnetic map of the tract. Areas of known post-Carboniferous basalt were also excluded. The western boundary is an interpretation of the boundary between the Trans Urals and East Urals tectonic zones, but is subjective because no single fault defines the zone boundary; rather, the tectonic boundary is a system of generally north-northeast-striking faults. Wherever practicable, Precambrian rock exposures within the tectonic contact zone were not included in the permissive tract.

Known Deposits

Two known deposits listed in Singer and others (2008) are within this permissive tract (table H2). One is known as Benkala, and the other is known as Varvarinskoe.

Benkala, Kazakhstan

Benkala (Singer and others, 2008), also known as Benkala North (Seltmann and others, 2009), is located in northernmost, west-central Kazakhstan. The deposit is in late Early Carboniferous volcanogenic sedimentary and volcanic rocks intruded by Early to middle Carboniferous stocks and dikes (Zhukov and others, 1998). The sedimentary rocks are tuffaceous sands and silts. The volcanic rocks are dacite, andesite, andesitic basalt, and basalt porphyries. Intrusive rocks associated with the deposit are porphyritic quartz diorites and granodiorites.

Zhukov and others (1998) show the Benkala mineralization as oval in plan with the long axis more than 1 kilometer (km) long and the short axis 500–700 meters (m) wide. A thin supergene blanket overlies the deposit. Magnetite replacement deposits occur 1–2 km to the southeast of the Benkala porphyry copper-molybdenum deposit.

The Benkala ores occur as disseminations and stockwork veins with alteration assemblages that include quartz, biotite, K-feldspar, sericite, chlorite, epidote, tourmaline, and albite (Zhukov and others, 1988). The ore occurs as stockworks and disseminations, and the principal ore minerals are pyrite, chalcopyrite, and magnetite, with lower contents of molybdenite, bornite, chalcocite, and digenite. Alteration minerals include quartz, biotite, K-feldspar, sericite, chlorite, epidote, tourmaline, and carbonate.

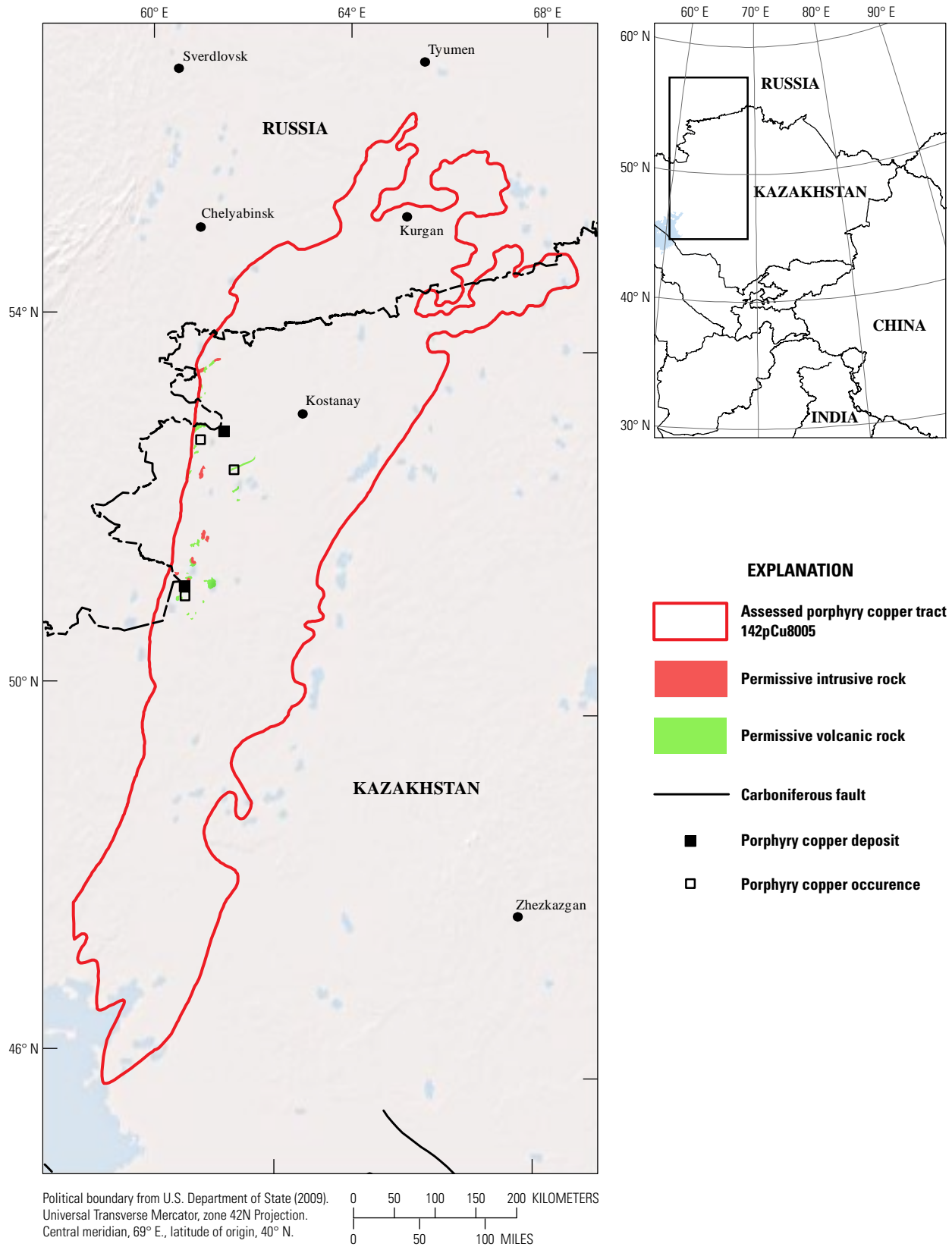


Figure H2. Distribution of permissive Carboniferous volcanic and volcanoclastic rocks (green) and intrusive rocks (red) in part of tract 142pCu8005, Carboniferous Valerianov Arc—Kazakhstan and Russia, on a digital elevation base. Location of map area shown on inset.

Varvarinskoe, Kazakhstan

Singer and others (2008) classify the Varvarinskoe deposit, which is a few kilometers north-northeast of the Bataly porphyry copper-molybdenum occurrence, as a porphyry copper-gold deposit. Zhukov and others (1998) note that Varvarinskoe has been classified in various ways by different investigators, including as a porphyry copper, but prefer a nonspecific classification as a gold-copper deposit owing to the variety of styles and ore assemblages in the deposit. Owing to the presence of garnet and pyroxene as alteration minerals in calcareous volcanic rocks that contain sulfides and magnetite, Dodd and others (2005) in an NI 43-101 report classify Varvarinskoye as a skarn-type deposit.

According to Dodd and others (2005), Varvarinskoe occurs in a Paleozoic sequence made up of Middle Devonian basaltic pillow lavas, andesite, tuff, and flysch-like siliciclastic sedimentary rocks. These rocks are altered to an assemblage of chlorite, albite, and epidote. Middle Devonian to Early Carboniferous rocks are siliciclastic rocks that are strongly altered and typically schistose. Unconformable on these rocks is another volcanic-siliciclastic sequence with basalt predominating. The Devonian to Carboniferous rocks are intruded by a gabbro to granodiorite complex in the form of plutons, dikes, and sills. Serpentinite dikes and sills, once dunites and pyroxenites, are common along faults. All of the intrusive rocks have been metamorphosed.

The main hydrothermal alteration minerals are garnet, diopside, calcite, chlorite, and quartz in skarn rocks, and muscovite, magnetite, rutile, K-feldspar, chlorite, calcite, quartz, and clay in volcanic rocks (Dodd and others, 2005). The primary ore has two predominant forms (Dodd and others, 2005). Stratiform massive and disseminated sulfides occur as alterations of garnet-pyroxene skarn in calcareous volcanic rocks, marbled limestone, and volcanic breccias. A second ore type consists of vein and disseminated sulfides and stockworks at the contacts of porphyritic diorite and serpentinite intrusions and tectonic breccias. Ore minerals include chalcopyrite, pyrite, and pyrrhotite with associated gold. Less common are marcasite, arsenopyrite, sphalerite, magnetite, hematite, pentlandite, gersdorffite, and niccolite. The deposit is oxidized at the surface and some supergene mineralization occurs. Dodd and others (2005) note the potential for an additional reserve at depth beyond what has already been delineated (compare Singer and others, 2008), but a mentioned possible relationship to an underlying granodiorite stock is apparently wholly speculative.

The Varvarinskoe deposit was discovered in 1981 and was developed as an open-pit mine by European Minerals Corporation, and it was subsequently developed by Orsu Metals. Mining started in 2006. The mine was acquired by Polymetal International plc in 2009 and is in production as the Varvara Mine with mine life projected to 2021. The deposit produced 6,900 metric tons (t) of copper in 2011 (Polymetal International plc, 2012).

Occurrences and Related Deposit Types

Possible porphyry copper-related occurrences are present in the tract within Kazakhstan (table H3).

Bataly (Singer and others, 2008) is located north of the Benkala deposit in northernmost, west-central Kazakhstan. Zhukov and others (1998) describe the copper-molybdenum occurrence as being located in a paleovolcanic structure wherein two neck-like zones of intrusive rock coalesce at depth into a single, larger composite intrusion of regional dimensions (14 by 6–9 km). The volcanogenic rocks are Early Carboniferous andesite and andesitic basalt porphyries and related tuffs.

The Bataly copper-molybdenum mineralization is in a complex of granodiorite and granodiorite porphyry intrusions. Vein and disseminated mineralization occurs in a zone elongated northwest-southeast. Zhukov and others (1998) note three principal alteration assemblages—quartz-tourmaline, quartz-albite-sericite, and quartz-sericite. The principal ore minerals are chalcopyrite, molybdenite, and pyrite with lower amounts of bornite, cubanite, galena, arsenopyrite, tetrahedrite, native gold, scheelite, magnetite, and hematite. Zhukov and others (1998) note that the deposit is not completely drilled at depth and warrants further exploration.

The Spiridonovskoe (Spiridonov on fig. 1-33) porphyry copper-molybdenum occurrence (Singer and others, 2008), Kazakhstan, is located between the Benkala deposit and the Bataly occurrence near the western boundary of the permissive tract (fig. 1-44). Its age is equivocal. Zhukov and others (1998) place the deposit in association with the Denisov massif, tuffs and diorite to granodiorite intrusive rocks, to which they assign a Late Silurian to Early Devonian date. This assignment is based on mineralized, fossiliferous Silurian rocks. Herrington and others (2005) show the Denisov Arc to have been active during the Late Devonian and located west of the Valerianov trench in the subducting plate. Therefore, either age interpretation places the Spiridonovskoe deposit within accreted rocks and not part of the Valerianov magmatic arc. Another deposit associated with the Denisov Arc is known as Mikheyev (fig. 1-33) (Girfanov and others, 1991). It is west of the tract boundary in Russia and serves to illustrate the complex nature of the tectonic boundary between the East Urals and Trans Urals zones and the challenge the Denisov Arc presents to estimating undiscovered porphyry copper deposits associated with the Valerianov Arc.

Magnetite is a common accessory mineral in Trans Urals porphyry copper deposits and occurrences, and many have magnetite-copper skarn deposits in association with the intrusive complexes that host the porphyry copper deposits and occurrences. Consequently, iron skarn deposits have been considered as a favorable indication for the possibility of an undiscovered porphyry-style deposit in the same intrusive complex in which the skarns occur (compare Herrington and others, 2005).

Table H2. Porphyry copper deposits in tract 142pCu8005, Carboniferous Valerianov Arc—Kazakhstan and Russia.

[Ma, mega-annum (10^6 years); t, metric tons; Mt, million metric tons; %, percent; g/t, grams per metric ton; Cu, copper; Mo, molybdenum; Au, gold; Ag, silver; n.d., no data; NA, not applicable]

Name	Country	Latitude	Longitude	Subtype	Age (Ma)	Tonnage (Mt)	Cu (%)	Mo (%)	Au (g/t)	Ag (g/t)	Contained Cu (t)	Reference
Benkala North	Kazakhstan	51.206	61.771	NA	312	309	0.42	0.003	0.07	n.d.	1,297,800	Grabezhev (2007)
Varvarinskoe	Kazakhstan	52.945	62.152	Cu-Au	310	117.62	0.66	n.d.	1.01	0.50	776,292	European Minerals Corporation (2005), Kazakhstan Minerals Corporation (2000), Polymetal International plc (2012), Zhukov and others (1998)

Table H3. Significant porphyry copper-related occurrences in tract 142pCu8005, Carboniferous Valerianov Arc—Kazakhstan and Russia.

[Ma, mega-annum (10^6 years); Mt, million metric tons; %, percent; g/t, grams per metric ton; km, kilometers; Cu, Copper; Mo, molybdenum; Au, gold; Ag, silver; n.d., no data]

Name	Country	Latitude	Longitude	Age (Ma)	Comments	Reference
Bataly	Kazakhstan	52.822	61.795	301	100% of the deposit area is covered by Mesozoic-Cenozoic sediments.	Grabezhev and Borovikov (1993), Kolesnikov and others (1986), Krivtsov and others (1986), Zhukov and others (1998)
Benkala South	Kazakhstan	51.099	61.800	n.d.	Located 10 km south of Benkala North deposit; C2 reserve estimate based on Soviet drilling in 1979: 151.5 Mt primary ore average grade 0.34% Cu, 0.008% Mo, 0.17 g/t Ag, with 23.62 Mt secondary ore at 0.4% (cutoff grade 0.25%). Source of additional ore for the main Benkala North deposit.	Frontier Mining, Ltd. (2011)
Spiridonovskoe	Kazakhstan	52.532	62.449	n.d.	Drilling data indicate small resources at 0.3–1.5% Cu, 0.01–0.05% Mo, and ≤ 0.2 g/t Au. 100% of the deposit area is covered by un lithified sediments.	Zhukov and others (1998)

Benkala South, located 10 km from the Benkala project, has preliminary resource estimates of 95,000 t of oxide copper and 515,000 t of sulfide copper (Frontier Mining, Ltd., 2011). The data are based on 1979 Soviet estimates at a copper cutoff grade of 0.25 percent.

Exploration History

Data on the history of exploration in this region was not acquired during this assessment.

Sources of Information

Principal sources of information used by the assessment team for delineation of 142pCu8005 are listed in table H4 and in the references cited.

Grade and Tonnage Model Selection

The general porphyry copper deposit model published by Singer and others (2008) was used based on the known deposits in the tract being statistically consistent with the model.

Estimate of the Number of Undiscovered Deposits

Rationale for the Estimate

Prior to making estimates of undiscovered deposits, the assessment team first reviewed the geologic framework and aeromagnetic data with particular attention paid to the (1) correctness of the tract boundary with respect to depth of covered areas, (2) permissiveness of included rock formations, (3) the proportion of the mapped geologic units that are permissive and what proportion of these are intrusive, and (4) variations in the depth of exposure of the permissive rocks within the tract and whether or not the tract should be subdivided into several sub-tracts. Second, the assessment team discussed the known deposits and occurrences, discussed the distribution of the known deposits and occurrences, and evaluated the deposit type distribution as an indicator of depth of exposure in the arc terrane as well as what the distribution implied about the uniformity of the depth of exposure across the tract. Third, the team speculated on the likely thoroughness with which the region had been explored. The consensus was that (1) only the modestly deformed part of the Valerianov Arc was suitable for quantitative estimations of undiscovered deposits, (2) the ratio of porphyry copper occurrences and possible linked

Table H4. Principal sources of information used for tract 142pCu8005, Carboniferous Valerianov Arc—Kazakhstan and Russia.

Theme	Name or title	Scale	Citation
Geology	Mineral deposits map of Central Asia	1:1,500,000	Seltmann and others (2009)
	Mineral deposits of the Urals	1:1,000,000	Petrov and others (2006)
	Tectonic map of the Paleozoic folded areas of Kazakhstan and adjacent territories	1:1,500,000	Abdulin and Zaitseb (1976)
	Tselinograd Akmola M41-42	1:1,000,000	Grigaytis and others (1994)
	M-41-IX (1967)	1:200,000	Mukashev (1967)
	M-41-X (1967)	1:200,000	Nakhatigal (1967)
	M-41-XV (1979)	1:200,000	Dragun (1979)
	M-41-XVI (1974)	1:200,000	Semyanov and Feigus (1974)
	M-41-XVII (1979)	1:200,000	Sukhaov (1979)
	N-41-XX (1974)	1:200,000	Spiridonva (1974)
	N-41-XXI (1965)	1:200,000	Dugnistaya and Maksimenko (1965)
	N-41-XXII (1966)	1:200,000	Semyanov (1966)
	N-41-XXIII (1966)	1:200,000	Feigus (1966)
	N-41-XXIV (1966)	1:200,000	Dragun (1966)
Mineral occurrences	Mineral deposits map of Central Asia	1:1,500,000	Seltmann and others (2009)
	Mineral deposits of the Urals	1:1,000,000	Petrov and others (2006)
Geophysics	Magnetic anomaly data of the former U.S.S.R.	1:1,500,000	National Oceanic and Atmospheric Administration (1996)

deposit types to the number of known deposits was high and therefore a favorable indication of undiscovered deposits, (3) the depth of erosion of the terrane was not excessive, and (4) owing to low relief, poor bedrock exposures and remoteness of much of the area, there were many plays left despite some Soviet-era exploration investment in the region. The consensus was that less than a tenth of the delineated tract was of the correct age and (or) the correct igneous rock types to host porphyry copper deposits but maps were not available to subdivide the tract.

The team estimated a mean of 4 undiscovered deposits, based on a 50-percent chance of 3 deposits, a 10-percent chance of 8 deposits, and a 5-percent chance of 15 or more deposits (table H5). The high coefficient of variation, 103 percent, associated with the probability distribution for undiscovered deposit within the tracts reflects a relatively high degree of uncertainty.

Probabilistic Assessment Simulation Results

Undiscovered resources for the tract were estimated by combining consensus estimates for numbers of undiscovered porphyry copper deposits with the global grade and tonnage model for porphyry Cu-Au-Mo deposits of Singer and others (2008) using the EMINERS program (Root and others, 1992; Bawiec and Spanski, 2012; Duval, 2012). Selected simulation results are reported in table H6). Results of the Monte Carlo simulation are presented as a cumulative frequency plot (fig. H3). The cumulative frequency plot shows the estimated resource amounts associated with cumulative probabilities of occurrence, as well as the mean, for each commodity and for total mineralized rock.

The mean amount of copper from the simulation, 15 million metric tons (Mt), exceeds the identified copper resources, 2 Mt (table H6).

Table H5. Undiscovered deposit estimates, deposit numbers, tract area, and deposit density for tract 142pCu8005, Carboniferous Valerianov Arc—Kazakhstan and Russia.

[N_{xx} , estimated number of deposits associated with the xxth percentile; N_{und} , expected number of undiscovered deposits; s , standard deviation; $C_v\%$, coefficient of variance; N_{known} , number of known deposits in the tract that are included in the grade and tonnage model; N_{total} , total of expected number of deposits plus known deposits; area, area of permissive tract in square kilometers (km^2); density, deposit density reported as the total number of deposits per 100,000 km^2 . N_{und} , s , and $C_v\%$ are calculated using a regression equation (Singer and Menzie, 2005)]

Consensus undiscovered deposit estimates					Summary statistics					Tract area (km^2)	Deposit density ($N_{total}/100k km^2$)
N_{90}	N_{50}	N_{10}	N_{05}	N_{01}	N_{und}	s	$C_v\%$	N_{known}	N_{total}		
0	3	8	15	15	4.1	4.25	103	2	6.1	213,240	3

Table H6. Results of Monte Carlo simulations of undiscovered resources for tract 142pCu8005, Carboniferous Valerianov Arc—Kazakhstan and Russia.

[Cu, copper; Mo, molybdenum; Au, gold; and Ag, silver; in metric tons. Rock, in million metric tons]

Material	Probability of at least the indicated amount						Probability of	
	0.95	0.9	0.5	0.1	0.05	Mean	Mean or greater	None
Cu	0	0	5,900,000	37,000,000	62,000,000	15,000,000	0.29	0.17
Mo	0	0	81,000	1,100,000	1,900,000	410,000	0.23	0.27
Au	0	0	130	1,100	1,500	390	0.28	0.25
Ag	0	0	840	13,000	22,000	5,200	0.22	0.34
Rock	0	0	1,300	7,700	13,000	3,000	0.3	0.17

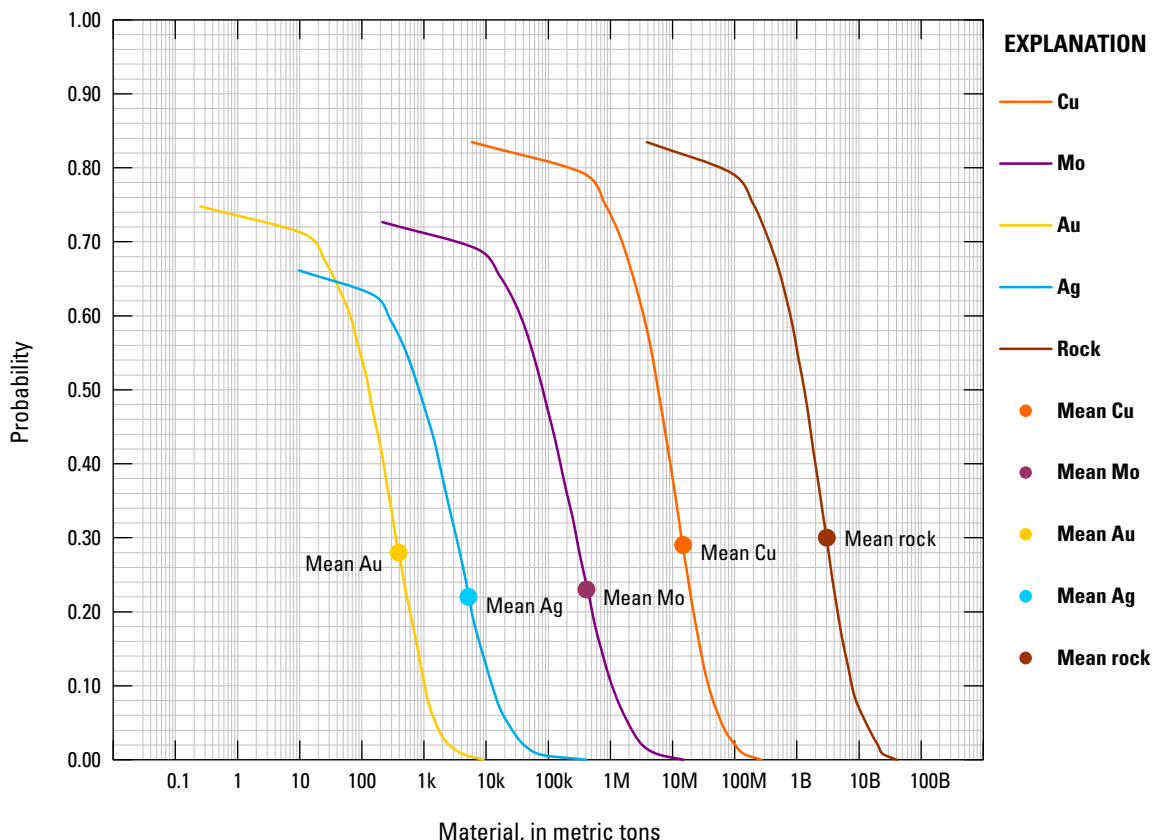


Figure H3. Cumulative frequency plot showing the results of Monte Carlo computer simulation of undiscovered resources, tract 142pCu8005, Carboniferous Valerianov Arc—Kazakhstan and Russia. k=thousands, M=millions, B=billions.

References Cited

- Abduln, A.A., and Zaitseb, Yu. A., 1976, [Tectonic map of the Paleozoic folded areas of Kazakhstan and adjacent territories]: Moscow, Aerogeologiya, scale 1:1,500,000. [In Russian.]
- Ayarza, P., Brown, D., Alvarez-Marrón, J., and Juhlin, C., 2000, Contrasting tectonic history of the arc-continent suture in the Southern and Middle Urals—Implications for the evolution of the orogen: *Journal of the Geological Society of London*, v. 157, p. 1065–1076.
- Bawiec, W.J., and Spanski, G.T., 2012, Quick-start guide for version 3.0 of EMINERS—Economic Mineral Resource Simulator: U.S. Geological Survey Open-File Report 2009–1057, 26 p., accessed July 15, 2012, at <http://pubs.usgs.gov/of/2009/1057/>. (This report supplements USGS OFR 2004–1344.)
- Berger, B.R., Ayuso, R.A., Wynn, J.C., and Seal, R.R., 2008, Preliminary model of porphyry copper deposits: U.S. Geological Survey Open-File Report 2008–1321, 55 p., accessed May 15, 2009, at <http://pubs.usgs.gov/of/2008/1321/>.
- Brown, D., Puchkov, V., Alvarez-Marron, J., Bea, F., and Perez-Estaun, A., 2006, Tectonic processes in the southern and middle Urals—An overview, *in* Gee, D.G., and Stephenson, R.A., eds., *European lithosphere dynamics: Geological Society of London Memoirs*, v. 32, p. 407–419.
- Cox, D.P., 1986, Descriptive model of porphyry Cu (Model 17), *in* Cox, D.P., and Singer, D.A., eds., 1986, *Mineral deposit models: U.S. Geological Survey Bulletin 1693*, p. 76. (Also available at <http://pubs.usgs.gov/bul/b1693/>.)

- Dodd, David, Thornton, J.C., and Arik, Abdullah, 2005, Varvarinskoe gold-copper project, northern Kazakhstan: Technical report prepared for European Minerals Corporation, 50 p.
- Dragun, A.F., 1966, [Geological map of the U.S.S.R., Turgay series, sheet N-41-XXIV]: Ministry of Geology of the U.S.S.R., scale 1:200,000. [In Russian.]
- Dragun, A.F., 1979, [Geological map of the U.S.S.R., Turgay series, sheet M-41-XV Tolybay]: Ministry of Geology of the U.S.S.R., VSEGEI, scale 1:200,000. [In Russian.]
- Dugnistaya, L.N., and Maksimenko, V.I., 1965, [Geological map of the U.S.S.R., Turgay series, sheet N-41-XXI]: State Geological Committee of the U.S.S.R., scale 1:200,000. [In Russian.]
- Duval, J.S., 2012, Version 3.0 of EMINERS—Economic Mineral Resource Simulator: U.S. Geological Survey Open-File Report 2004–1344, accessed July 15, 2012, at <http://pubs.usgs.gov/of/2004/1344/>.
- European Minerals Corporation, 2005, Varvarinskoye gold-copper project, Northern Kazakhstan, Technical Report, 150 p.
- Feigus, I.I., 1966, [Geological map of the U.S.S.R., Turgay series, sheet N-41-XXIII]: Ministry of Geology of the U.S.S.R., scale 1:200,000. [In Russian.]
- Frontier Mining, Ltd., 2011, Significant Developments: Frontier Mining, Ltd., presentation, accessed November 1, 2011, at <http://www.frontiermining.com/>.
- Girfanov, M.M., Sergeeva, N.E., and Shishakov, V.B., 1991, Ore metasomatic zoning of Mikheyev copper-porphyry deposit in the South Ural: Moscow University Geology Bulletin, v. 46, no. 5, p. 68–70.
- Grabezhev, A., and Borovikov, Y., 1993, Porphyry-copper deposits of the Urals—Proceedings of the 29th International Geological Congress, 1992, Mineral Resources Symposia, Volume A: Tokyo, Resource Geology Special Issue, no. 15, p. 275–284.
- Grabezhev, A.I., 2007, Rhenium in ores of porphyry copper deposits in the Urals: Doklady Earth Sciences, v. 413, no. 2, p. 265–268.
- Grigaytis, R.K., Sememova-Tyan-Shanskaya, E.R., Sizova, E.N., Semenov, Y.L., Kraskov, L.N., Babichev, E.A., Zavrzhnov, V.N., Kotelnikov, V.I., Rozanov, S.B., Klyushkin, V.V., and Ksenofontov, O.K., 1994, [Geological map, new series, sheet M-(41), 42 Tselinograd (Akmola), Map of the pre-Quaternary rocks]: Committee of the Russian Federation on Geology and Mineral Resources, VSEGEI, scale 1:1,000,000. [In Russian.]
- Herrington, R.J., Puchkov, V.N., and Yakubchuk, A.S., 2005, A reassessment of the tectonic zonation of the Uralides—Implications for metallogeny, in McDonald, I., Boyce, A.J., Butler, I.B., Herrington, R.J., and Poly, D.A., eds., Mineral deposits and earth evolution: Geological Society of London Special Publication 248, p. 153–166.
- Kazakhstan Minerals Corporation, 2000, Our properties: Kazakhstan Minerals Corporation Web site, accessed June 15, 2009, at <http://kazminco.com/prop/varva.html>.
- Kolesnikov, V.V., Zhukov, N.M., Solodilova, V.V., and Filimonova, L.E., 1986, [Porphyry copper deposits of the Balkhash region]: Alma Ata, Nauka, 199 p. [In Russian.]
- Krivtsov, A.I., Migachev, I.F., and Popov, V.S., 1986, [Porphyry copper deposits of the world]: Moscow, Nedra, 236 p. [In Russian.]
- Mukashev, R.A., 1967, [Geological map of the U.S.S.R., Turgay series, sheet M-41-IX]: Ministry of Geology of the U.S.S.R., scale 1:200,000. [In Russian.]
- Nakhatigal, V.Y.U., 1967, [Geological map of the U.S.S.R., Turgay series, sheet M-41-X]: Ministry of Geology of the U.S.S.R., scale 1:200,000. [In Russian.]
- Nalivkin, D.V., 1968, Geological map of the Union of Soviet Socialist Republics: The Ministry of Geology of the U.S.S.R., scale 1:2,500,000.
- National Oceanic and Atmospheric Administration, 1996, Magnetic anomaly data of the former U.S.S.R.: Boulder, Colorado, National Geophysical Data Center, accessed August 1, 2009, at <http://www.ngdc.noaa.gov>.
- Petrov, O., Shatov, V., Kondian, O., Markov, K., Guriev, G., Seltmann, R., and Armstrong, R., 2006, Mineral deposits of the Urals, scale 1:1,000,000 and database—ArcView 3.2 GIS package: London, Natural History Museum, Centre for Russian and Central EurAsian Mineral Studies (CERCAMS), scale 1:1,000,000 and explanatory text, 91 p. [Commercial dataset available at <http://www.nhm.ac.uk/research-curation/research/projects/cercams/products.html>.]
- Polymetal International plc, 2012, Varvara project: Company Web site accessed September 9, 2012, at <http://www.polymetalinternational.com/operations-landing/varvara/overview.aspx>.
- Plotinskaya, O.Y., Kovalenker, V.A., Seltmann, R., and Stanley, C.J., 2006, Te and Se mineralogy of the high-sulfidation Kochbulak and Kairagach epithermal gold telluride deposits (Kurama Range, Middle Tien Shan, Uzbekistan): Mineralogy and Petrology, v. 87, p. 187–207.
- Root, D.H., Menzie, W.D., and Scott, W.A., 1992, Computer Monte Carlo simulation in quantitative resource estimation: Natural Resources Research, v. 1, no. 2, p. 125–138.

- Seltmann, R., Shatov, V., and Yakubchuk, A., 2009, Mineral deposits database and thematic maps of Central Asia—ArcGIS 9.2, Arc View 3.2, and MapInfo 6.0(7.0) GIS packages: London, Natural History Museum, Centre for Russian and Central EurAsian Mineral Studies (CERCAMS), scale 1:1,500,000, and explanatory text, 174 p. [Commercial dataset available at <http://www.nhm.ac.uk/research-curation/research/projects/cercams/products.html>.]
- Semyanov, A.P., 1966, [Geological map of the U.S.S.R., Turgay series, sheet N-41-XXII]: Ministry of Geology of the U.S.S.R., scale 1:200,000. [In Russian.]
- Semyanov, A.P., and Feigus, I.I., 1974, [Geological map of the U.S.S.R., Turgay series, sheet M-41-XVI]: Ministry of Geology of the U.S.S.R., scale 1:200,000. [In Russian.]
- Singer, D.A., and Menzie, W.D., 2005, Statistical guides to estimating the number of undiscovered mineral deposits—An example with porphyry copper deposits, *in* Cheng, Q., and Bonham-Carter, G., eds., Proceedings of IAMG—The annual conference of the International Assoc. for Mathematical Geology: Toronto, Canada, Geomatics Research Laboratory, York University, p. 1028–1033.
- Singer, D.A., Berger, V.I., and Moring, B.C., 2008, Porphyry copper deposits of the world: U.S. Geological Survey Open-File Report 2008–1155, 45 p., accessed August 10, 2009, at <http://pubs.usgs.gov/of/2008/1155/>.
- Spiridonva, A.F., 1974, [Geological map of the U.S.S.R., Turgay series, sheet M-41-XX]: Ministry of Geology of the U.S.S.R., scale 1:200,000. [In Russian.]
- Sukhaov, A.M., 1979, [State geological map of the U.S.S.R., Turgay series, sheet M-41-XVII Kumkeshu]: Ministry of Geology of the U.S.S.R., VSEGEI, scale 1:200,000. [In Russian.]
- Windley, B.F., Alexeiev, D., Xiao, W., Kroner, A., and Badarch, G., 2007, Tectonic models for accretion of the Central Asia orogenic belt: London, Journal of the Geological Society, v. 164, p. 31–47.
- Yakubchuk, A.S., Shatov, V.V., Kirwin, D., Edwards, A., Tomurtogoo, O., Badarch, G., and Buryak, V.A., 2005, Gold and base metal metallogeny of the Central Asian orogenic supercollage, *in* Hedenquist, T.W., Thompson, J.F.H., Goldfarb, K.J., and Richards, J.P., eds., One Hundredth Anniversary Volume 1905–2005: Littleton, Colorado, Society of Economic Geologists, p. 1035–1068.
- Zhukov, N.M., Kolesnikov, V.V., Miroshnichenko, L.M., Egembayev, K.M., Pavlova, Z.N., Bakarasov, E.V., 1998, Copper deposits of Kazakhstan, *in* Abdulin, A.A., and others, eds., Reference Book: Almaty, Ministry of Ecology and Natural Resources of the Republic of Kazakhstan, 136 p.

Appendix I. Description of Spatial Data Files

A file geodatabase (.gdb) and an ESRI map document (.mxd) are included with this report. The file geodatabase contains eight feature classes and two data tables. These may be downloaded from the USGS website as zipped file **GIS_SIR2010-5090-N.zip**.

The file geodatabase is **Central_Asia_pCu** and contains the following eight feature classes and two data tables:

Central_Asia_pCu_tracts is a polygon feature class of the permissive tracts. Attributes include the tract identifiers, tract name, a brief description of the basis for tract delineation, and assessment results. Attributes are defined in the metadata that accompanies the feature class.

Central_Asia_deposits_prospects is a point feature class that represents locations for known deposits (identified resources that have well-defined tonnage and copper grade) and prospects. Feature class attributes include the assigned tract, alternate site names, information on grades and tonnages, age, mineralogy, associated igneous rocks, site status, comments fields, data sources, and references. Attributes are defined in the metadata that accompanies the feature class. Note that feature class values for tonnages listed as “-9999” represent no data available.

SSIB_Asia_Russia is a polygon feature class showing countries within and adjacent to the study area. The feature class is extracted from the country and shoreline boundaries maintained by the U.S. Department of State (2009).

Feature classes showing Advanced Spaceborne Thermal Emission and Reflection (ASTER) data described in chapter 2 of this report are as follows:

Central_Asia_argillic is a polygon feature class that represents a hydrothermal mineral group consisting primarily of alunite and or kaolinite.

Central_Asia_phyllic is a polygon feature class that represents a hydrothermal mineral consisting primarily of sericite.

Central_Asia_silicic is a polygon feature class that represents silica-rich rocks deposited in a hydrothermal system.

Central_Asia_potential_porphyry_sites is a point feature class that represents sites that contain at least one or a combination of phyllic, argillic, and hydrothermal silica-rich rocks that form surficial patterns and are associated with rock types typically found at porphyry copper deposits.

Central_Asia_ASTER_scene_index is a polygon feature class that represents the ASTER scene outlines used to create argillic, phyllic and silica feature classes.

Assessment results for each permissive tract described in chapter 3 and appendixes A–H are included in the following data tables:

Means data table – shows the mean amount for each commodity by tract in Central Asia.

Quantiles data table – shows the probabilistic assessment results as quantiles for commodity by tract.

These feature classes are included in an ESRI map document (version 10 Service Pack 5): **Central_Asia_pCu.mxd**. Probabilistic assessment results are included in two tables in the GIS package; Excel versions of these tables also are provided. Mean, shows the mean amount for each commodity by tract. Quantiles shows probabilistic assessment results as quantiles for commodity by tract.

References Cited

U.S. Department of State, 2009, Small-scale digital international land boundaries (SSIB)—Lines, edition 10, and polygons, beta edition 1, *in* Boundaries and sovereignty encyclopedia (B.A.S.E.): U.S. Department of State, Office of the Geographer and Global Issues.

Appendix J. Assessment Participants

Dmitriy Alexeiev is a research geologist with the Russian Academy of Sciences in Moscow, Russia. He is an expert on the accretionary tectonics of Central Asia. He guided the team's understanding of modern geodynamic interpretations of the study area and participated in assessment meetings.

Walter Bawiec is a geologist (retired) with the USGS in Reston, Virginia. He participated in the Almaty and London assessment workshops as a GIS specialist and implemented the computer program used for simulation of undiscovered resources.

Byron R. Berger [deceased] was a research economic geologist with the USGS in Denver, Colorado. He was an expert in porphyry copper deposits, mineral resource assessment, and porphyry- and related mineral deposits of Central Asia. He conducted field work in the study area and had an interest in structural settings of porphyry copper and epithermal vein deposits. He led the porphyry copper assessment of western Central Asia and presided over the USGS quantitative assessment.

Hugo de Boorder is a professor at the Institute of Earth Sciences at Utrecht University in the Netherlands. He is an expert on the geodynamics and metallogeny of Europe and Central Asia, and attended the London 2009 workshop.

Andrei Chitalin is a consultant based in Moscow, Russia. He has a background in porphyry copper exploration in many areas of the world, including Russia. He participated in the 2009 workshop in Vancouver, Washington.

Paul D. Denning is a GIS specialist with the USGS in Denver, Colorado. He constructed the GIS for the project, processed data, and prepared figures for the report.

Connie L. Dicken is a GIS specialist with the USGS in Reston, Virginia. She is the GIS task leader for the USGS Global Mineral Resource Assessment Project, oversaw the GIS activities of the project, and participated in the assessment meetings at the USGS.

Alla Dolgoplova is a researcher in economic and environmental mineralogy at the Natural History Museum, London, United Kingdom. Dolgoplova works on mineral deposit research studies related to consultancy projects in Kazakhstan, Kyrgyzstan, Uzbekistan, Mongolia and Russia. She helped organize the Almaty and London meetings and participated in workshops.

Lawrence J. Drew is a senior mineral economist and expert on mineral resource assessment. He participated in the quantitative assessment.

Jane M. Hammarstrom is a research geologist with the USGS in Reston, Virginia. She is co-chief of the USGS Global Mineral Resource Assessment project and task leader for the

porphyry copper assessment. She coordinated workshops with CERCAMS in the latter part of the project and participated in assessment meetings.

Richard J. Herrington is a Merit Researcher and head of mineral deposit research in the Department of Mineralogy at the Natural History Museum, London, United Kingdom. He is an expert on the mineral deposits and geodynamic evolution of the Urals and other areas of the world. He participated in the Vancouver workshop, CERCAMS-hosted meetings, and provided expertise on the Urals.

John C. Mars is a research geologist with the USGS in Reston, Virginia. He is an expert in remote sensing. He developed algorithms for processing ASTER data to map hydrothermal alteration as an assessment tool, analyzed the ASTER data for the study area, and participated in assessment meetings.

Steve McRobbie is a geology manager with the Kazakhmys Project, Ltd., in Karaganda, Kazakhstan. He participated in the 2009 London workshop.

Jeffrey D. Phillips is a geophysicist with the USGS in Denver, Colorado. He processed aeromagnetic data for the study area, provided guidance on its use for extending permissive tracts under cover, and participated in the quantitative assessment.

Victor Popov is a geologist with the Russian State Geological Prospecting University in Moscow, Russia. He is an expert on the Uralides and was a compiler of the CERCAMS mineral deposits database for Central Asia. He participated in the London 2009 workshop.

Reimar Seltmann is the director of the Centre for Russian and Central EurAsian Mineral Studies (CERCAMS) at the Natural History Museum, London, United Kingdom. As an economic geologist focused on mineral deposit studies of central Asia, he coordinates industry-funded research projects and produces research papers, monographs, metallogenic maps and reference guidebooks on metal provinces of the CERCAMS region. He provided data and expertise on the region, logistics for workshops in London and Almaty, and participated in assessment workshops.

Vitaly Shatov is a geologist with the A.P. Karpinsky Russian Geological Research Institute (VSEGEI) in St. Petersburg, Russia. He is an expert on the metallogeny of Russia, author of metallogenic maps of Central Asia, and co-author of the CERCAMS GIS of Central Asia.

Michael L. Zientek is a research geologist with the USGS in Spokane, Washington, with expertise in magmatic ore deposits and mineral resource assessment. He is co-chief of the USGS Global Mineral Resource Assessment project and participated in the quantitative assessment

Appendix K. Geologic Time Charts

Description

Geologic maps prepared using Russian, Chinese, and Mongolian standards employ stratigraphic charts that differ slightly from each other, and from standards used in other parts of the world. Figures K1 and K2 show correlations among Series-Epoch map symbols and durations for Phanerozoic and Precambrian Eons as used in Russia (Katalog Mineralov, 2005), China (Ma and others, 2002), and Mongolia (Mineral Resources Authority of Mongolia, 1998).

For comparisons with the International Stratigraphic Chart, see International Commission on Stratigraphy (2010).

References Cited

- International Committee on Stratigraphy, 2010, International stratigraphic chart: International Committee on Stratigraphy, accessed October 1, 2011, at [http://www.stratigraphy.org/column.php?id=Chart/Time Scale](http://www.stratigraphy.org/column.php?id=Chart/Time%20Scale).
- Katalog Mineralov, 2005, Gyeokhronologisheskaya skkala [geologic time scale]: Katalog Mineralov Web page and MS Excel format file, accessed September 30, 2009, at <http://www.catalogmineralov.ru/img/content/geoshkala.zip>.
- Ma, Lifang, Qiao, Xiufu, Min, Longrui, Fan, Benxian, and Ding, Xiazohong, comps., 2002, Geological atlas of China: Beijing, Geological Publishing House, 348 p., 59 map sheets.
- Mineral Resources Authority of Mongolia, Geological Survey, and Mongolian Academy of Sciences, Institute of Geology and Mineral Resources, 1998, Geological map of Mongolia: Ulaanbaatar, Mineral Resources Authority of Mongolia, Geological Survey, and Mongolian Academy of Sciences, Institute of Geology and Mineral Resources, 1 map on 14 sheets, 30 p., scale 1:1,000,000.

Division of Geologic Time, as used											
Color	Eon	Color	Russia								
			Sym.	Duration	Color	Era	Color	Sym.	Name	Duration	End date
[Dark Red]	Proterozoic	[Light Pink]	PR2	1,960±50	[Light Pink]	Riphean	[Light Pink]	V	Vendian	90±20	650±10
								R3 (PR23)	Upper/Late	350±50	1,000±50
								R2 (PR22)	Middle	350±50	1,350±20
		[Dark Red]	PR1	[Dark Red]	R1 (PR21)	Lower/Early	300±50	1,650±50			
					PR12	Upper/Late	250±50	1,900±50			
					PR11	Lower/Early	600±50	2,500±50			
[Orange]	Archean	[Orange]	AR2	1,000	[Orange]	[Orange]	[Orange]	Upper/Late	650±50	3,150±50	
			AR1					Lower/Early			
References:			Katalog Mineralov (2005)								

Figure K2. Geologic time correlations among Series-Epoch map symbols and durations (in millions of years) for Precambrian Eons as used in Russia (Katalog Mineralov, 2005), China (Ma and others, 2002), and Mongolia (Mineral Resources Authority of Mongolia, 1998). End dates are millions of years before present.

in Russia, Mongolia, and China

Mongolia					China						
Sym.	Era	Sym.	Duration	End date	Sym.	Era	Sym.	Duration	End date	Magmatic Stage	
PR	Vendian	V	40	610	Pt	Sinian	Z2	100	700	Proterozoic	Y^3_2
	Riphean	R3	1,040	1,650			Z1	100	800		
		R2				Early Late Proterozoic	Pt13	200	1,000		
		R1				Middle Proterozoic	Pt2	850	1,850		Y^2_2
	Lower Proterozoic	PR1	850	2,500		Early Proterozoic	Pt1	750	2,600		Y^1_2
AR	Upper Archean	AR2			Ar	Late Archean	Ar3	400	3,000	Archean	Y^3_1
	Lower Archean	AR1				Middle Archean	Ar2	500	3,500		Y^2_1
						Early Archean	Ar1				Y^1_1
Mineral Resources Authority of Mongolia, Geological Survey, and Mongolian Academy of Sciences, Institute of Geology and Mineral Resources (1998)					Ma and others (2002)						

This page intentionally left blank.

Menlo Park Publishing Service Center, California
Manuscript approved for publication March 26, 2013
Edited on contract and by James W. Hendley II and
Sarah Nagorsen
Layout and design by Sharon L. Wahlstrom



Berger and others—**Porphyry Copper Assessment of Western Central Asia—Scientific Investigations Report 2010–5090–N**